

Wind Resource Assessment using the Numerical Weather Prediction Model to Identify the Offshore Wind Resource in the Philippines

A thesis submitted in partial
fulfilment of the requirements of
Birmingham City University for the
degree of Doctor of Philosophy

Sherdon Niño Yu Uy

THE FACULTY OF COMPUTING, ENGINEERING AND BUILT
ENVIRONMENT
BIRMINGHAM CITY UNIVERSITY

March 2020

Abstract

Developing nations need to build their economies in order to reach the millennium goals of the world. Energy is an essential resource for economic development but the conventional fuel at present is not a sustainable energy source. Thus, these countries must seek for renewable energy sources so that they can develop in a sustainable manner. Wind energy is found to be a potential source for power generation especially, the offshore locations. There are many developing countries in the low-latitude areas that have open waters close to them. So, offshore wind energy may be a possible source for power but there are limited data available to make a reliable wind resource assessment (WRA). This study aims to develop a wind characterisation method that can be useful for coastal and small island areas with no or few in-situ wind observations. The study area is focused in Palawan Province of the Philippines because it has similar characteristics as small island nations and coastal areas in the low-latitude regions. The research found that numerical weather prediction is an alternative for in-situ wind measurements for WRA. A technique that involves coupling mesoscale model to microscale model is employed in this work in order to produce wind maps. The results found that a combination of mesoscale model and microscale model can be a good method for wind profiling areas without or few wind observations. The mesoscale model is deemed sufficient for open water areas while coastal areas are better represented by microscale models especially the low wind speed conditions.

Acknowledgements

I would like to express my gratitude to my thesis supervisors; Abed Alaswad, Venkatesh Chennam Vijay, and Noel Perera. Their generosity in sharing knowledge and wisdom are invaluable in completing this research.

I am very thankful to the Newton-Agham PhD Scholarship Programme for funding my study. This would not have been possible without the assistance of the Department of Science and Technology in the Philippines and the British Council. Thus, I am very grateful for their partnership on this programme.

To my former mentor, Gregory Tangonan, who is the progenitor of this study and always available for discussing ideas. I wish to thank him for all the time, patience, and generosity in sharing new research ideas.

I also would like to thank my friends and colleagues at the Manila Observatory who helped me in running the mesoscale model of this work, namely Faye Abigail Cruz and Julie Mae Dado. I am also thankful to Armelle Reza Remedio-Ghosh for the discussions on atmospheric dynamics and processes which aided me in numerous occasions to make sense of the model outputs.

I am very grateful to Catherine Meissner and Pablo Duran for all their help in running the microscale model. I wish to express my gratitude to the insights and technical knowledge they shared with me in performing simulations.

I wish to say thank you to my friends and colleagues at the KBE Lab, Maxim Filimonov and Guolong Zhong. Their support for this research are invaluable. I would also like to thank Sue Witton and Ian McDonald. They have always been ready to assist for any administrative matters and making the transition of moving to a new place much easier. I am also thankful to my past supervisors; Craig Chapman, Pathmeswaran Raju, William Byrne, and Mohammed Farazi. They all have provided guidance for me in doing this study.

To my family and friends for all the support throughout life that has led me into this path. I am very deeply grateful to my wife, Mariel and my daughter, Amelia. They have always inspired me to keep moving on with this research and life despite all the challenges.

Lastly, to God for all the blessings that made everything possible.

Contents

1	Introduction.....	22
1.1	Research Motives and Problem Statement	23
1.2	Aim of the Study	23
1.3	Research Gaps.....	24
1.4	Research Framework	24
1.5	Phases of the Research	25
1.5.1	Phase 1 – Review of Literature	28
1.5.2	Phase 2 – Method Development and Study Area Determination for the Research.....	28
1.5.3	Phase 3 – Wind Model Configuration and Sensitivity Testing	29
1.5.4	Phase 4 – Wind Simulation	29
1.6	Summary	30
2	Literature Review.....	32
2.1	Renewable Energy.....	32
2.2	Wind Energy Generation.....	33
2.3	Global Offshore Wind Energy Resource.....	34
2.4	Worldwide Offshore Wind Energy Developments.....	37
2.5	Grid-Connected Offshore Wind Energy Production	39
2.6	Offshore Wind Studies in Low Latitude Regions.....	40
2.6.1	South America.....	42
2.6.2	Africa	44
2.6.3	South Asia	46
2.6.4	East Asia	47
2.6.5	Southeast Asia.....	50
2.7	Techniques in Offshore Wind Resource Assessment.....	52
2.7.1	Wind Observations and Wind Map Products	52
2.7.2	Wind Modelling.....	54
2.8	Summary	59
3	Methodology	60
3.1	Study Area.....	60
3.2	Concepts of Atmospheric Science.....	63
3.2.1	Atmospheric Coordinates and Conventions	63
3.2.2	Layers of the atmosphere	64
3.2.3	Atmospheric Parameters for Thermodynamics.....	64
3.2.4	Equations of Motion	67

3.2.5	Governing Equations for Geophysical Fluid Dynamics	69
3.3	Equations for Computational Fluid Dynamics (CFD)	70
3.4	Mesoscale and Microscale Model Applications	73
3.5	Model configuration and design	73
3.6	Sensitivity test and analysis	76
3.7	WindSim Simulations	78
3.8	Summary	80
4	Implementation	82
4.1	Data gathering	82
4.2	Performing Mesoscale Wind Simulations	83
4.3	Performing Microscale Wind Simulations	88
5	Results and Analysis.....	94
5.1	Mesoscale Model	94
5.1.1	Mesoscale Model Wind Speed Results	94
5.1.2	Mesoscale Model Wind Direction Results	126
5.2	Wind Maps for Palawan Province	137
5.3	7SEAS Observation Comparison	140
5.3.1	Balabac Island	140
5.3.2	Guntao Islands	141
5.3.3	Notch Island	145
5.3.4	Tubbataha Reef	146
5.4	Microscale model.....	149
5.4.1	CFD Sensitivity Tests	149
5.4.2	Grid resolution sensitivity	151
5.4.3	Turbulence Closure Scheme	153
5.5	Mesoscale and Microscale (CFD) Model Comparison	154
5.6	Discussion.....	162
5.7	Summary	166
6	Conclusion	169
6.1	Research Outputs.....	169
6.2	Contribution to Knowledge.....	170
6.3	Recommendations for Future Work	171
	References	172
	Appendix 1: Mesoscale Model Wind Speed Scatter Plots	183
	Appendix 2: Mesoscale Model Wind Direction Charts	224

Appendix 3: PAGASA with Mesoscale Model Wind Speed and Wind Direction Data	233
Appendix 4: Mesoscale Model Wind Direction Error and Bias Tables.....	341
Appendix 5: 7SEAS Sites Wind Speed and Wind Direction Charts.....	343
Appendix 6: 7SEAS, Mesoscale Model, and Microscale Model Wind Velocity Data	360
Appendix 7: WRF Configuration Files.....	364
Appendix 8: Cray Job Submission Scripts.....	368
Appendix 9: Scripts for Wind Mapping.....	371
Appendix 10: WindSim Pre-processing and Post-processing Scripts.....	379

List of Figures

Figure 1. An illustration of the research framework.....	25
Figure 2. Work flow of the study for WRA method development.....	30
Figure 3. Wind power density (WPD) in the winter and summer months for the Earth’s ocean surface at 80m level from QuikSCAT data analysis [45]	35
Figure 4. Wind power density (WPD) for the Earth’s ocean surface at 10m level from 1988 to 2017 based on CCMP wind product [47]	36
Figure 5. Power capacities of installed offshore wind farms.....	39
Figure 6. Yearly mean wind speeds across the globe at 90m height and up to 100 nautical miles from shore [78].....	41
Figure 7. Yearly mean wind power densities for 1988 to 2007 over open waters at 10m height from WindSat [80,81]	42
Figure 8. Wind power density map from 1988 to 2007 for South America and Caribbean region from WindSat data.....	44
Figure 9. The African continent wind power density map for 1988 to 2007 using WindSat wind product dataset.....	46
Figure 10. A generated wind power density map from 1988 to 2007 using WindSat data for the Indian subcontinent	47
Figure 11. East Asia and Southeast Asia wind power density map from satellite observations of WindSat for the years of 1988 to 2007	50
Figure 12. . Average wind power densities at 80m level for different low latitude locations.....	51
Figure 13. Global wind power index that includes open waters from coastline to 30 km distance of land masses at 100 m above ground level [132]	55
Figure 14. Global wind speeds that includes open waters from ERA5 simulations at 100 m above ground level for the years of 1979 to 2018 [133].....	56
Figure 15. Map of Philippines and Palawan Island. The weather station is located within (a) Coron Island, (b) Cuyo Island, and (c) Puerto Princesa City.	61
Figure 16. The ship made observations at the locations marked by numbers on the zoomed in map. These sites are 1. Guntao Islands, 2. Notch Island, 3. Tubbataha Reef, and 4. Balabac Island	62
Figure 17. Coordinates and conventions in atmospheric science	63
Figure 18. Vertical profile of temperature, pressure, and density in the atmosphere [159]	65
Figure 19. Domains configured for WRF. Palawan Island is within Domain 3 (d03).	75
Figure 20. Sample scatter plot for simulation and measured wind speed comparison.	76
Figure 21. Flow chart for wind simulations.....	79
Figure 22. Download page for reanalysis and operational data sets from UCAR.....	83
Figure 23. Initialisation for NCL and running NCL script to generate wind maps.....	87
Figure 24. Execution of NCL script to generate wind maps	87
Figure 25. Terrain module of WindSim	88
Figure 26. Data import tool for mesoscale model results	89
Figure 27. Screenshot of saving extracted mesoscale output data into xyz file.....	89
Figure 28. Opening screen of import tool.....	90
Figure 29. Screenshot of xyz import tool requesting file path, quantity, and naming format	90
Figure 30. Screenshot of xyz import tool requesting starting coordinates of domain and terrain file	91
Figure 31. Screenshot of xyz import tool successfully converting xyz to dws file	91
Figure 32. Screenshot of Wind Field module during a simulation run	92
Figure 33. Screenshot of post-processing WindSim results with Matlab	92
Figure 34. Wind simulation flow for mesoscale and microscale model coupling	93

Figure 35. Scatter plot of different WRF model settings with PAGASA station data in Cuyo Island for January 2010.	95
Figure 36. Scatter plot of different WRF model settings with PAGASA station data in Puerto Princesa for January 2012.	96
Figure 37. Scatter plot of different WRF model settings with PAGASA station data in Coron Island for February 2011.	98
Figure 38. Scatter plot of different WRF model settings with PAGASA station data in Puerto Princesa for February 2012.	99
Figure 39. Scatter plot of different WRF model settings with PAGASA station data in Puerto Princesa for March 2010.	100
Figure 40. Scatter plot of different WRF model settings with PAGASA station data in Puerto Princesa for April 2011.	102
Figure 41. Scatter plot of different WRF model settings with PAGASA station data in Coron Island for April 2012.	103
Figure 42. Scatter plot of different WRF model settings with PAGASA station data in Cuyo Island for April 2012.	104
Figure 43. Scatter plot of different WRF model settings with PAGASA station data in Puerto Princesa for April 2012.	104
Figure 44. Scatter plot of different WRF model settings with PAGASA station data in Cuyo Island for May 2010.	106
Figure 45. Scatter plot of different WRF model settings with PAGASA station data in Puerto Princesa for May 2011.	107
Figure 46. Scatter plot of different WRF model settings with PAGASA station data in Coron Island for May 2012.	108
Figure 47. Scatter plot of different WRF model settings with PAGASA station data in Coron Island for June 2010.	109
Figure 48. Scatter plot of different WRF model settings with PAGASA station data in Puerto Princesa for June 2011.	110
Figure 49. Scatter plot of different WRF model settings with PAGASA station data in Coron Island for July 2010.	111
Figure 50. Scatter plot of different WRF model settings with PAGASA station data in Puerto Princesa for July 2012.	112
Figure 51. Scatter plot of different WRF model settings with PAGASA station data in Puerto Princesa for August 2011.	114
Figure 52. Scatter plot of different WRF model settings with PAGASA station data in Coron Island for September 2010.	115
Figure 53. Scatter plot of different WRF model settings with PAGASA station data in Cuyo Island for September 2010.	116
Figure 54. Scatter plot of different WRF model settings with PAGASA station data in Puerto Princesa for September 2010.	117
Figure 55. Scatter plot of different WRF model settings with PAGASA station data in Coron Island for October 2010.	118
Figure 56. Scatter plot of different WRF model settings with PAGASA station data in Puerto Princesa for October 2011.	119
Figure 57. Scatter plot of different WRF model settings with PAGASA station data in Cuyo Island for November 2010.	120
Figure 58. Scatter plot of different WRF model settings with PAGASA station data in Puerto Princesa for November 2010.	121

Figure 59. Scatter plot of different WRF model settings with PAGASA station data in Coron Island for December 2010.....	122
Figure 60. Scatter plot of different WRF model settings with PAGASA station data in Puerto Princesa for December 2011.....	123
Figure 61. Scatter plot of different WRF model settings with PAGASA station data in Cuyo Island for December 2012.....	124
Figure 62. Comparison of average wind direction between WRF output and observation data at (a) Coron Island, (b) Cuyo Island, and (c) Puerto Princesa for the month of January 2012.....	127
Figure 63. Comparison of average wind direction between WRF output and observation data at (a) Coron Island, (b) Cuyo Island, and (c) Puerto Princesa for the month of February 2010.....	128
Figure 64. Comparison of average wind direction between WRF output and observation data at (a) Coron Island, (b) Cuyo Island, and (c) Puerto Princesa for the month of March 2010.....	128
Figure 65. Comparison of average wind direction between WRF output and observation data at (a) Coron Island, (b) Cuyo Island, and (c) Puerto Princesa for the month of April 2011.....	129
Figure 66. Comparison of average wind direction between WRF output and observation data at (a) Coron Island, (b) Cuyo Island, and (c) Puerto Princesa for the month of May 2010.....	130
Figure 67. Comparison of average wind direction between WRF output and observation data at (a) Coron Island, (b) Cuyo Island, and (c) Puerto Princesa for the month of June 2012.....	131
Figure 68. Comparison of average wind direction between WRF output and observation data at (a) Coron Island, (b) Cuyo Island, and (c) Puerto Princesa for the month of July 2011.....	132
Figure 69. Comparison of average wind direction between WRF output and observation data at (a) Coron Island, (b) Cuyo Island, and (c) Puerto Princesa for the month of August 2012.....	133
Figure 70. Comparison of average wind direction between WRF output and observation data at (a) Coron Island, (b) Cuyo Island, and (c) Puerto Princesa for the month of September 2011.....	133
Figure 71. Comparison of average wind direction between WRF output and observation data at (a) Coron Island, (b) Cuyo Island, and (c) Puerto Princesa for the month of October 2011.....	134
Figure 72. Comparison of average wind direction between WRF output and observation data at (a) Coron Island, (b) Cuyo Island, and (c) Puerto Princesa for the month of November 2012.....	135
Figure 73. Comparison of average wind direction between WRF output and observation data at (a) Coron Island, (b) Cuyo Island, and (c) Puerto Princesa for the month of December 2011.....	136
Figure 74. Wind maps for Palawan Island showing the available offshore wind resource around the island at 80 m: (a) January and (b) April.....	138
Figure 75. Wind maps for Palawan Island showing the available offshore wind resource around the island at 80 m: (a) June and (b) September.....	138
Figure 76. Wind speeds from mesoscale model outputs and actual observations at Balabac Island on 16 September 2012.....	140
Figure 77. Wind direction values from mesoscale model results and measurements for Balabac Island on 16 September 2012.....	141
Figure 78. South Guntao Island wind speed measurements and model results for 24 September 2011.....	142
Figure 79. Modelled wind direction alongside measurements for South Guntao Island on 24 September 2011.....	143
Figure 80. South Guntao Island wind speed measurements and model results for 25 September 2011.....	144
Figure 81. Modelled wind direction alongside measurements for South Guntao Island on 25 September 2011.....	144
Figure 82. Simulated and observed wind speeds Notch Island on 21 September 2011.....	145
Figure 83. Model outputs and measured wind direction for Notch Island on 21 September 2011... 146	146

Figure 84. Tubbataha North Reef wind speeds on 22 September 2012.....	147
Figure 85. Wind directions for Tubbataha North Reef on 22 September 2012.....	147
Figure 86. CFD model runs at Balabac Island that compares (a) simulation without WRF temperature and (b) initialisation of temperature with mesoscale model results.....	150
Figure 87. CFD model runs at Guntao Islands that compares (a) simulation without mesoscale model output temperature and (b) initialisation of temperature with mesoscale model results	151
Figure 88. CFD model runs at Balabac Island that compares different grid resolutions at (a) 152m, (b) 76m, and (c) 38m	152
Figure 89. WindSim runs at Notch Island that compares different grid resolutions at (a) 152m, (b) 76m, and (c) 38m	152
Figure 90. Comparison of different turbulence model using (a) standard k- ϵ and (b) RNG k- ϵ over Balabac Island	153
Figure 91. Comparison of different turbulence model using (a) standard k- ϵ and (b) RNG k- ϵ over Notch Island	153
Figure 92. Comparison of mesoscale and microscale model wind speed results off the coast of Balabac Island on 16 September 2012.....	155
Figure 93. Comparison of mesoscale and microscale model wind direction results off the coast of Balabac Island on 16 September 2012.....	156
Figure 94. Comparison of mesoscale and microscale model wind speed results off the coast of Guntao Islands on 24 September 2011.....	157
Figure 95. Comparison of mesoscale and microscale model wind direction results off the coast of Guntao Islands on 24 September 2011.....	158
Figure 96. Comparison of mesoscale and microscale model wind speed results off the coast of Notch Island on 21 September 2011	159
Figure 97. Comparison of mesoscale and microscale model wind direction results off the coast of Notch Island on 21 September 2011	159
Figure 98. Comparison of mesoscale and microscale model wind speed results off the coast of Tubbataha Reef on 22 September 2012	160
Figure 99. Comparison of mesoscale and microscale model wind direction results off the coast of Tubbataha Reef on 22 September 2012	161
Figure 100. Scatter plot of different WRF model settings with PAGASA station data in Coron Island for January 2010.	183
Figure 101. Scatter plot of different WRF model settings with PAGASA station data in Puerto Princesa for January 2010.	183
Figure 102. Scatter plot of different WRF model settings with PAGASA station data in Coron Island for February 2010.	184
Figure 103. Scatter plot of different WRF model settings with PAGASA station data in Cuyo Island for February 2010.	184
Figure 104. Scatter plot of different WRF model settings with PAGASA station data in Puerto Princesa for February 2010.	185
Figure 105. Scatter plot of different WRF model settings with PAGASA station data in Coron Island for March 2010.	185
Figure 106. Scatter plot of different WRF model settings with PAGASA station data in Cuyo Island for March 2010.	186
Figure 107. Scatter plot of different WRF model settings with PAGASA station data in Coron Island for April 2010.	186
Figure 108. Scatter plot of different WRF model settings with PAGASA station data in Cuyo Island for April 2010.....	187

Figure 109. Scatter plot of different WRF model settings with PAGASA station data in Puerto Princesa for April 2010.	187
Figure 110. Scatter plot of different WRF model settings with PAGASA station data in Coron Island for May 2010.....	188
Figure 111. Scatter plot of different WRF model settings with PAGASA station data in Puerto Princesa for May 2010.....	188
Figure 112. Scatter plot of different WRF model settings with PAGASA station data in Cuyo Island for June 2010.	189
Figure 113. Scatter plot of different WRF model settings with PAGASA station data in Puerto Princesa for June 2010.	189
Figure 114. Scatter plot of different WRF model settings with PAGASA station data in Cuyo Island for July 2010.	190
Figure 115. Scatter plot of different WRF model settings with PAGASA station data in Puerto Princesa for July 2010.....	190
Figure 116. Scatter plot of different WRF model settings with PAGASA station data in Coron Island for August 2010.....	191
Figure 117. Scatter plot of different WRF model settings with PAGASA station data in Cuyo Island for August 2010.	191
Figure 118. Scatter plot of different WRF model settings with PAGASA station data in Puerto Princesa for August 2010.....	192
Figure 119. Scatter plot of different WRF model settings with PAGASA station data in Cuyo Island for October 2010.	192
Figure 120. Scatter plot of different WRF model settings with PAGASA station data in Puerto Princesa for October 2010.....	193
Figure 121 Scatter plot of different WRF model settings with PAGASA station data in Coron Island for November 2010.	193
Figure 122. Scatter plot of different WRF model settings with PAGASA station data in Cuyo Island for December 2010.....	194
Figure 123. Scatter plot of different WRF model settings with PAGASA station data in Puerto Princesa for December 2010.	194
Figure 124. Scatter plot of different WRF model settings with PAGASA station data in Coron Island for January 2011.	195
Figure 125. Scatter plot of different WRF model settings with PAGASA station data in Cuyo Island for January 2011.....	195
Figure 126. Scatter plot of different WRF model settings with PAGASA station data in Puerto Princesa for January 2011.	196
Figure 127. Scatter plot of different WRF model settings with PAGASA station data in Cuyo Island for February 2011.....	196
Figure 128. Scatter plot of different WRF model settings with PAGASA station data in Puerto Princesa for February 2011.	197
Figure 129. Scatter plot of different WRF model settings with PAGASA station data in Coron Island for March 2011.	197
Figure 130. Scatter plot of different WRF model settings with PAGASA station data in Cuyo Island for March 2011.....	198
Figure 131. Scatter plot of different WRF model settings with PAGASA station data in Puerto Princesa for March 2011.	198
Figure 132. Scatter plot of different WRF model settings with PAGASA station data in Coron Island for April 2011.	199

Figure 133. Scatter plot of different WRF model settings with PAGASA station data in Cuyo Island for April 2011.....	199
Figure 134. Scatter plot of different WRF model settings with PAGASA station data in Coron Island for May 2011.....	200
Figure 135. Scatter plot of different WRF model settings with PAGASA station data in Cuyo Island for May 2011.	200
Figure 136. Scatter plot of different WRF model settings with PAGASA station data in Coron Island for June 2011.	201
Figure 137. Scatter plot of different WRF model settings with PAGASA station data in Cuyo Island for June 2011.....	201
Figure 138. Scatter plot of different WRF model settings with PAGASA station data in Coron Island for July 2011.....	202
Figure 139. Scatter plot of different WRF model settings with PAGASA station data in Cuyo Island for July 2011.	202
Figure 140. Scatter plot of different WRF model settings with PAGASA station data in Puerto Princesa for July 2011.....	203
Figure 141. Scatter plot of different WRF model settings with PAGASA station data in Coron Island for August 2011.....	203
Figure 142. Scatter plot of different WRF model settings with PAGASA station data in Cuyo Island for August 2011.	204
Figure 143. Scatter plot of different WRF model settings with PAGASA station data in Coron Island for September 2011.....	204
Figure 144. Scatter plot of different WRF model settings with PAGASA station data in Cuyo Island for September 2011.....	205
Figure 145. Scatter plot of different WRF model settings with PAGASA station data in Puerto Princesa for September 2011.....	205
Figure 146. Scatter plot of different WRF model settings with PAGASA station data in Coron Island for October 2011.....	206
Figure 147. Scatter plot of different WRF model settings with PAGASA station data in Cuyo Island for October 2011.	206
Figure 148. Scatter plot of different WRF model settings with PAGASA station data in Coron Island for November 2011.....	207
Figure 149. Scatter plot of different WRF model settings with PAGASA station data in Cuyo Island for November 2011.	207
Figure 150. Scatter plot of different WRF model settings with PAGASA station data in Puerto Princesa for November 2011.....	208
Figure 151. Scatter plot of different WRF model settings with PAGASA station data in Coron Island for December 2011.....	208
Figure 152. Scatter plot of different WRF model settings with PAGASA station data in Cuyo Island for December 2011.....	209
Figure 153. Scatter plot of different WRF model settings with PAGASA station data in Coron Island for January 2012.	209
Figure 154. Scatter plot of different WRF model settings with PAGASA station data in Cuyo Island for January 2012.....	210
Figure 155. Scatter plot of different WRF model settings with PAGASA station data in Coron Island for February 2012.	210
Figure 156. Scatter plot of different WRF model settings with PAGASA station data in Cuyo Island for February 2012.....	211

Figure 157. Scatter plot of different WRF model settings with PAGASA station data in Coron Island for March 2012.	211
Figure 158. Scatter plot of different WRF model settings with PAGASA station data in Cuyo Island for March 2012.	212
Figure 159. Scatter plot of different WRF model settings with PAGASA station data in Puerto Princesa for March 2012.	212
Figure 160. Scatter plot of different WRF model settings with PAGASA station data in Cuyo Island for May 2012.	213
Figure 161. Scatter plot of different WRF model settings with PAGASA station data in Puerto Princesa for May 2012.	213
Figure 162. Scatter plot of different WRF model settings with PAGASA station data in Coron Island for June 2012.	214
Figure 163. Scatter plot of different WRF model settings with PAGASA station data in Cuyo Island for June 2012.	214
Figure 164. Scatter plot of different WRF model settings with PAGASA station data in Puerto Princesa for June 2012.	215
Figure 165. Scatter plot of different WRF model settings with PAGASA station data in Coron Island for July 2012.	215
Figure 166. Scatter plot of different WRF model settings with PAGASA station data in Cuyo Island for July 2012.	216
Figure 167. Scatter plot of different WRF model settings with PAGASA station data in Coron Island for August 2012.	216
Figure 168. Scatter plot of different WRF model settings with PAGASA station data in Cuyo Island for August 2012.	217
Figure 169. Scatter plot of different WRF model settings with PAGASA station data in Puerto Princesa for August 2012.	217
Figure 170. Scatter plot of different WRF model settings with PAGASA station data in Coron Island for September 2012.	218
Figure 171. Scatter plot of different WRF model settings with PAGASA station data in Cuyo Island for September 2012.	218
Figure 172. Scatter plot of different WRF model settings with PAGASA station data in Puerto Princesa for September 2012.	219
Figure 173. Scatter plot of different WRF model settings with PAGASA station data in Coron Island for October 2012.	219
Figure 174. Scatter plot of different WRF model settings with PAGASA station data in Cuyo Island for October 2012.	220
Figure 175. Scatter plot of different WRF model settings with PAGASA station data in Puerto Princesa for October 2012.	220
Figure 176. Scatter plot of different WRF model settings with PAGASA station data in Coron Island for November 2012.	221
Figure 177. Scatter plot of different WRF model settings with PAGASA station data in Cuyo Island for November 2012.	221
Figure 178. Scatter plot of different WRF model settings with PAGASA station data in Puerto Princesa for November 2012.	222
Figure 179. Scatter plot of different WRF model settings with PAGASA station data in Coron Island for December 2012.	222
Figure 180. Scatter plot of different WRF model settings with PAGASA station data in Puerto Princesa for December 2012.	223

Figure 205. Comparison of average wind direction between WRF output and observation data at (a) Coron Island, (b) Cuyo Island, and (c) Puerto Princesa for the month of December 2012	232
Figure 206. Wind speeds from WRF outputs and actual observations at Balabac Island on 15 September 2012.....	343
Figure 207. Wind direction values from WRF results and measurements for Balabac Island on 15 September 2012.....	343
Figure 208. Wind speeds from WRF outputs and actual observations at Balabac Island on 16 September 2012.....	344
Figure 209. Wind direction values from WRF results and measurements for Balabac Island on 16 September 2012.....	344
Figure 210. Wind speeds from WRF outputs and actual observations at Balabac Island on 17 September 2012.....	345
Figure 211. Wind direction values from WRF results and measurements for Balabac Island on 17 September 2012.....	345
Figure 212. Wind speeds from WRF outputs and actual observations at Balabac Island on 18 September 2012.....	346
Figure 213. Wind direction values from WRF results and measurements for Balabac Island on 18 September 2012.....	346
Figure 214. North Guntao Island wind speeds from WRF simulations and ship observations on 20 September 2011.....	347
Figure 215. Wind direction values from ship measurements and WRF outputs for North Guntao Island on 20 September 2011	347
Figure 216. North Guntao Island wind speeds from WRF simulations and ship observations on 8 September 2012.....	348
Figure 217. Wind direction values from ship measurements and WRF outputs for North Guntao Island on 8 September 2012	348
Figure 218. North Guntao Island wind speeds from WRF simulations and ship observations on 9 September 2012.....	349
Figure 219. Wind direction values from ship measurements and WRF outputs for North Guntao Island on 9 September 2012	349
Figure 220. Simulated and observed wind speeds Notch Island on 21 September 2011	350
Figure 221. Model outputs and measured wind direction for Notch Island on 21 September 2011.	350
Figure 222. Simulated and observed wind speeds Notch Island on 22 September 2011	351
Figure 223. Model outputs and measured wind direction for Notch Island on 22 September 2011.	351
Figure 224. South Guntao Island wind speed measurements and model results for 23 September 2011	352
Figure 225. Modelled wind direction alongside measurements for South Guntao Island on 23 September 2011.....	352
Figure 226. South Guntao Island wind speed measurements and model results for 11 September 2012	353
Figure 227. Modelled wind direction alongside measurements for South Guntao Island on 11 September 2012.....	353
Figure 228. Tubbataha North Reef wind speeds on 21 September 2012.....	354
Figure 229. Wind directions for Tubbataha North Reef on 21 September 2012.....	354
Figure 230. Tubbataha North Reef wind speeds on 22 September 2012.....	355
Figure 231. Wind directions for Tubbataha North Reef on 22 September 2012.....	355
Figure 232. Tubbataha North Reef wind speeds on 23 September 2012.....	356
Figure 233. Wind directions for Tubbataha North Reef on 23 September 2012.....	356

Figure 234. Tubbataha North Reef wind speeds on 24 September 2012..... 357
Figure 235. Wind directions for Tubbataha North Reef on 24 September 2012..... 357
Figure 236. Wind speed comparison for Tubbataha South Reef on 25 September 2012 358
Figure 237. Comparison of wind direction for Tubbataha South Reef on 25 September 2012 358
Figure 238. Wind speed comparison for Tubbataha South Reef on 26 September 2012 359
Figure 239. Comparison of wind direction for Tubbataha South Reef on 26 September 2012 359

List of Tables

Table 1. Summary of Research Phases	26
Table 2. Summary of total electricity consumption, power production from offshore wind farms, and percentage of electricity supplied by offshore wind for 2016.....	40
Table 3. List of publications and dataset used for research within the low latitude region	52
Table 4. Input Dataset Specifications.....	74
Table 5. WRF Configuration Settings	74
Table 6. Wind classification standard to determine wind potential of an area	80
Table 7. January 2010 Model Errors and Bias Quantification of Wind Speed	96
Table 8. January 2012 Model Errors and Bias Quantification of Wind Speed	97
Table 9. February 2011 Model Errors and Bias Quantification of Wind Speed	98
Table 10. February 2012 Model Errors and Bias Quantification of Wind Speed	99
Table 11. March 2010 Model Errors and Bias Quantification of Wind Speed	100
Table 12. April 2011 Model Errors and Bias Quantification of Wind Speed	102
Table 13. April 2012 Model Errors and Bias Quantification of Wind Speed	105
Table 14. May 2010 Model Errors and Bias Quantification of Wind Speed	106
Table 15. May 2011 Model Errors and Bias Quantification of Wind Speed	107
Table 16. May 2012 Model Errors and Bias Quantification of Wind Speed	108
Table 17. June 2010 Model Errors and Bias Quantification of Wind Speed	109
Table 18. June 2011 Model Errors and Bias Quantification of Wind Speed	111
Table 19. July 2010 Model Errors and Bias Quantification of Wind Speed	112
Table 20. July 2012 Model Errors and Bias Quantification of Wind Speed	112
Table 21. August 2011 Model Errors and Bias Quantification of Wind Speed	114
Table 22. September 2010 Model Errors and Bias Quantification of Wind Speed.....	117
Table 23. October 2010 Model Errors and Bias Quantification of Wind Speed	118
Table 24. October 2011 Model Errors and Bias Quantification of Wind Speed	119
Table 25. November 2010 Model Errors and Bias Quantification of Wind Speed	121
Table 26. December 2010 Model Errors and Bias Quantification of Wind Speed.....	122
Table 27. December 2011 Model Errors and Bias Quantification of Wind Speed.....	123
Table 28. December 2012 Model Errors and Bias Quantification of Wind Speed.....	124
Table 29. Summary of Best Mesoscale Model Configuration for Wind Speeds	125
Table 30. Summary of Best Mesoscale Model Configuration for Wind Direction.....	136
Table 31. Error and bias values of wind speed and direction for each mesoscale model configuration settings.....	148
Table 32. Summary of best model configuration settings at each 7SEAS site.....	149
Table 33. Summary of microscale model configurations.....	154
Table 34. Microscale Model Errors and Bias Quantification of Wind Speed and Wind Direction.....	161
Table 35. January 2010 wind data at Coron Island from onshore weather station and meoscale model output	233
Table 36. January 2010 wind data at Cuyo Island from onshore weather station and meoscale model output	234
Table 37. January 2010 wind data at Puerto Princesa from onshore weather station and meoscale model output	235
Table 38. February 2010 wind data at Coron Island from onshore weather station and meoscale model output	236

Table 39. February 2010 wind data at Cuyo Island from onshore weather station and meoscale model output	237
Table 40. February 2010 wind data at Puerto Princesa from onshore weather station and meoscale model output	238
Table 41. March 2010 wind data at Coron Island from onshore weather station and meoscale model output	239
Table 42. March 2010 wind data at Cuyo Island from onshore weather station and meoscale model output	240
Table 43. March 2010 wind data at Puerto Princesa from onshore weather station and meoscale model output	241
Table 44. April 2010 wind data at Coron Island from onshore weather station and meoscale model output	242
Table 45. April 2010 wind data at Cuyo Island from onshore weather station and meoscale model output	243
Table 46. April 2010 wind data at Puerto Princesa from onshore weather station and meoscale model output	244
Table 47. May 2010 wind data at Coron Island from onshore weather station and meoscale model output	245
Table 48. May 2010 wind data at Cuyo Island from onshore weather station and meoscale model output	246
Table 49. May 2010 wind data at Puerto Princesa from onshore weather station and meoscale model output	247
Table 50. June 2010 wind data at Coron Island from onshore weather station and meoscale model output	248
Table 51. June 2010 wind data at Cuyo Island from onshore weather station and meoscale model output	249
Table 52. June 2010 wind data at Puerto Princesa from onshore weather station and meoscale model output	250
Table 53. July 2010 wind data at Coron Island from onshore weather station and meoscale model output	251
Table 54. July 2010 wind data at Cuyo Island from onshore weather station and meoscale model output	252
Table 55. July 2010 wind data at Puerto Princesa from onshore weather station and meoscale model output	253
Table 56. August 2010 wind data at Coron Island from onshore weather station and meoscale model output	254
Table 57. August 2010 wind data at Cuyo Island from onshore weather station and meoscale model output	255
Table 58. August 2010 wind data at Puerto Princesa from onshore weather station and meoscale model output	256
Table 59. September 2010 wind data at Coron Island from onshore weather station and meoscale model output	257
Table 60. September 2010 wind data at Cuyo Island from onshore weather station and meoscale model output	258
Table 61. September 2010 wind data at Puerto Princesa from onshore weather station and meoscale model output	259
Table 62. October 2010 wind data at Coron Island from onshore weather station and meoscale model output	260

Table 63. October 2010 wind data at Cuyo Island from onshore weather station and meoscale model output	261
Table 64. October 2010 wind data at Puerto Princesa from onshore weather station and meoscale model output	262
Table 65. November 2010 wind data at Coron Island from onshore weather station and meoscale model output	263
Table 66. November 2010 wind data at Cuyo Island from onshore weather station and meoscale model output	264
Table 67. November 2010 wind data at Puerto Princesa from onshore weather station and meoscale model output	265
Table 68. December 2010 wind data at Coron Island from onshore weather station and meoscale model output	266
Table 69. December 2010 wind data at Cuyo Island from onshore weather station and meoscale model output	267
Table 70. December 2010 wind data at Puerto Princesa from onshore weather station and meoscale model output	268
Table 71. January 2011 wind data at Coron Island from onshore weather station and meoscale model output	269
Table 72. January 2011 wind data at Cuyo Island from onshore weather station and meoscale model output	270
Table 73. January 2011 wind data at Puerto Princesa from onshore weather station and meoscale model output	271
Table 74. February 2011 wind data at Coron Island from onshore weather station and meoscale model output	272
Table 75. February 2011 wind data at Cuyo Island from onshore weather station and meoscale model output	273
Table 76. February 2011 wind data at Puerto Princesa from onshore weather station and meoscale model output	274
Table 77. March 2011 wind data at Coron Island from onshore weather station and meoscale model output	275
Table 78. March 2011 wind data at Cuyo Island from onshore weather station and meoscale model output	276
Table 79. March 2011 wind data at Puerto Princesa from onshore weather station and meoscale model output	277
Table 80. April 2011 wind data at Coron Island from onshore weather station and meoscale model output	278
Table 81. April 2011 wind data at Cuyo Island from onshore weather station and meoscale model output	279
Table 82. April 2011 wind data at Puerto Princesa from onshore weather station and meoscale model output	280
Table 83. May 2011 wind data at Coron Island from onshore weather station and meoscale model output	281
Table 84. May 2011 wind data at Cuyo Island from onshore weather station and meoscale model output	282
Table 85. May 2011 wind data at Puerto Princesa from onshore weather station and meoscale model output	283
Table 86. June 2011 wind data at Coron Island from onshore weather station and meoscale model output	284

Table 87. June 2011 wind data at Cuyo Island from onshore weather station and meoscale model output	285
Table 88. June 2011 wind data at Puerto Princesa from onshore weather station and meoscale model output	286
Table 89. July 2011 wind data at Coron Island from onshore weather station and meoscale model output	287
Table 90. July 2011 wind data at Cuyo Island from onshore weather station and meoscale model output	288
Table 91. July 2011 wind data at Puerto Princesa from onshore weather station and meoscale model output	289
Table 92. August 2011 wind data at Coron Island from onshore weather station and meoscale model output	290
Table 93. August 2011 wind data at Cuyo Island from onshore weather station and meoscale model output	291
Table 94. August 2011 wind data at Puerto Princesa from onshore weather station and meoscale model output	292
Table 95. September 2011 wind data at Coron Island from onshore weather station and meoscale model output	293
Table 96. September 2011 wind data at Cuyo Island from onshore weather station and meoscale model output	294
Table 97. September 2011 wind data at Puerto Princesa from onshore weather station and meoscale model output	295
Table 98. October 2011 wind data at Coron Island from onshore weather station and meoscale model output	296
Table 99. October 2011 wind data at Cuyo Island from onshore weather station and meoscale model output	297
Table 100. October 2011 wind data at Puerto Princesa from onshore weather station and meoscale model output	298
Table 101. November 2011 wind data at Coron Island from onshore weather station and meoscale model output	299
Table 102. November 2011 wind data at Cuyo Island from onshore weather station and meoscale model output	300
Table 103. November 2011 wind data at Puerto Princesa from onshore weather station and meoscale model output	301
Table 104. December 2011 wind data at Coron Island from onshore weather station and meoscale model output	302
Table 105. December 2011 wind data at Cuyo Island from onshore weather station and meoscale model output	303
Table 106. December 2011 wind data at Puerto Princesa from onshore weather station and meoscale model output	304
Table 107. January 2012 wind data at Coron Island from onshore weather station and meoscale model output	305
Table 108. January 2012 wind data at Cuyo Island from onshore weather station and meoscale model output	306
Table 109. January 2012 wind data at Puerto Princesa from onshore weather station and meoscale model output	307
Table 110. February 2012 wind data at Coron Island from onshore weather station and meoscale model output	308

Table 111. February 2012 wind data at Cuyo Island from onshore weather station and meoscale model output	309
Table 112. February 2012 wind data at Puerto Princesa from onshore weather station and meoscale model output	310
Table 113. March 2012 wind data at Coron Island from onshore weather station and meoscale model output	311
Table 114. March 2012 wind data at Cuyo Island from onshore weather station and meoscale model output	312
Table 115. March 2012 wind data at Puerto Princesa from onshore weather station and meoscale model output	313
Table 116. April 2012 wind data at Coron Island from onshore weather station and meoscale model output	314
Table 117. April 2012 wind data at Cuyo Island from onshore weather station and meoscale model output	315
Table 118. April 2012 wind data at Puerto Princesa from onshore weather station and meoscale model output	316
Table 119. May 2012 wind data at Coron Island from onshore weather station and meoscale model output	317
Table 120. May 2012 wind data at Cuyo Island from onshore weather station and meoscale model output	318
Table 121. May 2012 wind data at Puerto Princesa from onshore weather station and meoscale model output	319
Table 122. June 2012 wind data at Coron Island from onshore weather station and meoscale model output	320
Table 123. June 2012 wind data at Cuyo Island from onshore weather station and meoscale model output	321
Table 124. June 2012 wind data at Puerto Princesa from onshore weather station and meoscale model output	322
Table 125. July 2012 wind data at Coron Island from onshore weather station and meoscale model output	323
Table 126. July 2012 wind data at Cuyo Island from onshore weather station and meoscale model output	324
Table 127. July 2012 wind data at Puerto Princesa from onshore weather station and meoscale model output	325
Table 128. August 2012 wind data at Coron Island from onshore weather station and meoscale model output	326
Table 129. August 2012 wind data at Cuyo Island from onshore weather station and meoscale model output	327
Table 130. August 2012 wind data at Puerto Princesa from onshore weather station and meoscale model output	328
Table 131. September 2012 wind data at Coron Island from onshore weather station and meoscale model output	329
Table 132. September 2012 wind data at Cuyo Island from onshore weather station and meoscale model output	330
Table 133. September 2012 wind data at Puerto Princesa from onshore weather station and meoscale model output	331
Table 134. October 2012 wind data at Coron Island from onshore weather station and meoscale model output	332

Table 135. October 2012 wind data at Cuyo Island from onshore weather station and meoscale model output	333
Table 136. October 2012 wind data at Puerto Princesa from onshore weather station and meoscale model output	334
Table 137. November 2012 wind data at Coron Island from onshore weather station and meoscale model output	335
Table 138. November 2012 wind data at Cuyo Island from onshore weather station and meoscale model output	336
Table 139. November 2012 wind data at Puerto Princesa from onshore weather station and meoscale model output	337
Table 140. December 2012 wind data at Coron Island from onshore weather station and meoscale model output	338
Table 141. December 2012 wind data at Cuyo Island from onshore weather station and meoscale model output	339
Table 142. December 2012 wind data at Puerto Princesa from onshore weather station and meoscale model output	340
Table 143. February 2010 Model Errors and Bias Quantification of Wind Speed	341
Table 144. April 2010 Model Errors and Bias Quantification of Wind Speed	341
Table 145. August 2010 Model Errors and Bias Quantification of Wind Speed	341
Table 146. January 2011 Model Errors and Bias Quantification of Wind Speed	341
Table 147. March 2011 Model Errors and Bias Quantification of Wind Speed	341
Table 148. July 2011 Model Errors and Bias Quantification of Wind Speed	341
Table 149. September 2011 Model Errors and Bias Quantification of Wind Speed	341
Table 150. November 2011 Model Errors and Bias Quantification of Wind Speed	342
Table 151. March 2012 Model Errors and Bias Quantification of Wind Speed	342
Table 152. June 2012 Model Errors and Bias Quantification of Wind Speed	342
Table 153. November 2012 Model Errors and Bias Quantification of Wind Speed	342
Table 154. Balabac Island wind speed and wind direction values on 16 September 2012	360
Table 155. Guntao Islands wind speed and wind direction values on 24 September 2011	361
Table 156. Notch Island wind speed and wind direction values on 21 September 2011	362
Table 157. Tubbataha Reef wind speed and wind direction values on 22 September 2012	363

1 INTRODUCTION

Many nations in the world, especially developing countries, are dependent on fossil fuels as the primary source for energy [1,2]. Some of these nations are located within the subtropical and tropical band which is the low latitude region of the world [3]. Market price volatility for fossil fuels pose an adverse impact to economies so, renewable energy is a solution to attain energy independence for many low latitude countries [4]. A renewable energy source, like wind, can supplant the extensive usage of costly and non-sustainable fossil fuels [1]. Winds over oceans and seas are much more stable and possess higher and more regular speeds in comparison with those over land [5]. This energy resource is immense for the entire world [6]. Development for offshore wind turbines began in Europe with pilot projects starting in 1991 with a prototype deployment in Denmark [5,7]. Significant strides have been made since that initial offshore wind farm, so that the total capacity in Europe reached 3,294 MW by the middle of 2011 [8]. Successful projects in the North Sea made offshore wind energy be viewed as one potential power source that can help address the increasing demand for energy across the globe. Although the power generation potential for offshore wind is promising, the investments required are expensive and deemed to be risky [9], therefore, a thorough wind resource assessment (WRA) is required to enable strategic planning prior to the wind energy project commencement [10,11]. There are different WRA techniques classified as preliminary area identification, area wind resource evaluation, and micro-siting [12]. Each of these classifications are generally analyzed in terms of short or long periods time scales through statistical methods [13]. The breadth of available approaches in undertaking WRA is wide and it is essential to seek the appropriate method for the conditions in low latitude regions. Accurate and sufficient WRA data can help decision makers to determine the suitable locations for offshore wind farm development [14].

This study focuses on the Philippines which is a country situated in the low latitude region of the world. Wind resource in offshore locations have greater available energy for exploitation in comparison with sites found on land [15]. It is this potential that research on offshore wind energy are being undertaken in different parts of the world. The Philippines has the potential to generate power from offshore wind but a thorough wind resource assessment (WRA) must be made for wind energy prospecting [16]. WRA is essential for any wind energy development in order to minimise risks in investments [11]. This study aims to use numerical weather prediction (NWP) method in making a WRA for offshore regions around Palawan Island, Philippines. Results of the study demonstrate how NWP can be used for offshore WRA on the different islands in the country as well as low latitude regions. This will help in guiding offshore wind projects in the Philippines for the stakeholders on wind energy.

1.1 Research Motives and Problem Statement

Vulnerability to fossil fuel prices and dependence on such fuels necessitates developing countries and small island nations in the low latitudes to foster their locally available renewable energy sources. There are vast bodies of water in this region that may have high wind energy potential thus, offshore wind energy can be a viable option for local power generation in these locations. However, offshore wind farm projects are significantly costly in terms of capital investment, on-site measurements for wind resource assessment (WRA), operations, and maintenance [17]. Therefore, a meticulous WRA must be made before considering any offshore wind project to avoid unnecessary costs and failures.

This study focuses on the Philippines as it is a developing nation in the low latitude area of the world and it is an archipelago. Due to the Philippines' need to power its numerous islands with minimal environmental impact, offshore wind energy is a promising sustainable energy resource for the country. Presently, there are limited offshore wind observations in the country with available data insufficient for determining the wind potential over its waters. Alternatively, using numerical wind prediction, an initial offshore wind resource assessment can be carried out. Thus, the question that this study aims to answer is:

How can wind assessment be done for offshore locations with limited wind profile data and topography data?

1.2 Aim of the Study

The research aims to develop an offshore wind resource assessment method that is suitable for low latitudes and small islands in order to aid in decision-making for siting wind farms over coastal and open waters.

The aim will be achieved via the following objectives:

O1: Investigate state of the art in offshore WRA method

O2: Determine the applicable WRA for locations with limited wind data availability

O3: Adapt and modify the WRA method according to the physical dynamics and topography of the Philippines

O4: Produce a high resolution wind field map to identify areas with wind power generation potential over the surrounding waters of an island

1.3 Research Gaps

Most of the developments for offshore wind power generation have been at the mid or high latitudes. It is found that research on offshore wind energy in the low latitudes have been on preliminary WRA that involved coarse spatial resolution wind data analysis. There are few efforts for in depth research in this part of the world that can enable adoption and deployment of the technology since only China and Taiwan are actively pursuing the technology. So, the physical dynamics of the atmosphere in the subtropical and tropical regions must be studied to determine the wind characteristics at offshore locations. Then, WRA methods that are suited for the sea and atmospheric conditions in low latitudes have to be known. Although there are efforts to address these gaps, new techniques and knowledge must still be sought since the literature acknowledges the inadequateness of the current findings.

1.4 Research Framework

In this study, the need of renewable energy sources for developing countries so that their economies can grow in a sustainable manner has been determined from the literature. Many developing nations are located within the low latitude and that region have plenty of open waters thus, offshore wind energy should be considered as a renewable source for power production. Although offshore winds can be a good resource for local power production, availability of data for WRA is limited especially in open water areas. An alternative solution would be to use wind simulations to produce data that can be utilised for WRA in regions with few or no data. These are the premise of this research and it is illustrated in the following figure.

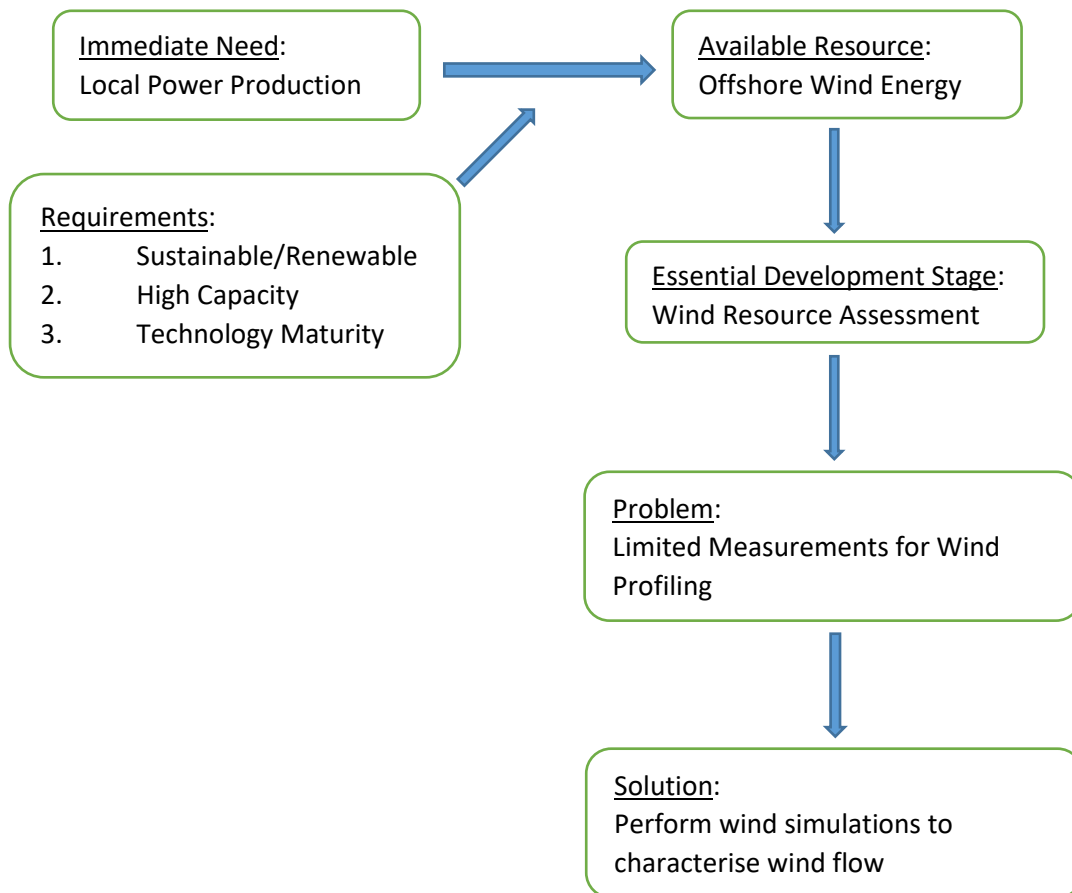


Figure 1. An illustration of the research

The research will focus on the Palawan Province as a study area since it is within the low latitude region and composed of several small islands with varying sizes. Wind simulations will be done within this domain to generate wind maps. Since wind profiling or wind characterisation is the important initial step before determination of potential wind power production thus, it is the main focus of the research. Validation of the winds is also possible for the area at 10 m level but not at typical wind turbine heights from 30 m – 80 m. To validate any power production approximations, actual measurements at these altitudes are necessary to produce meaningful wind power generation estimates. Thus, the potential wind velocities are the only factors considered since it is the one that may be validated with data observations.

1.5 Phases of the Research

This research is broken down into six phases and an outline is presented in Table 1 that lists significant research milestones. The outputs and objectives outlined in Section 1.2 are to be met by each phase are also found in Table 1. They are broken down into tasks to make up the complete work which are to be discussed in this chapter.

The literature review in Phase 1 is necessary in order to determine the techniques used for wind resource assessment and find which methods are applicable for the study. Among all the information gathered, the methods are to be improved to fit the needs of the research. Techniques in wind analysis will be applied for wind characterisation of each station to enable site selection in Phase 2. This is needed to locate areas with potential for extracting energy from the wind. The selected sites will serve as the primary areas for validating wind simulation and will be chosen as region of study in running the computational fluid dynamics model to produce a higher resolution wind field of a good wind turbine site. It is necessary to streamline the study area since CFD is computationally intensive and the computing resources available are limited.

Prior to running wind simulations, the appropriate model for the study area must be known. This is done in Phase 3 by running sensitivity tests and preliminary simulations that are compared with the selected sites in Phase 2. The models that can capture wind pattern trends and able to yield wind speed values with the least discrepancy to measured values are to be chosen. Phase 1 can aid in determining the model that performs well based on the previous studies found in the literature. Even when a model is selected by performance comparison in the literature review, that chosen model must go through the sensitivity tests for appropriate configuration to the study area. Wind simulations in Phase 4 can be done after that and generate fine resolution wind field maps from the selected mesoscale model and CFD model. These wind simulations shall provide the wind patterns over the study area where wind data observations are unavailable. Each of the work packages are expounded in the following sections.

Table 1. Summary of Research Phases

Research Phase	Outputs	Objectives
Phase 1: Review of Literature 1.1 Wind energy generation 1.2 Offshore wind resource and technologies 1.3 Wind resource assessment methods for offshore sites	A review document on the following: <ol style="list-style-type: none"> 1. energy conversion methods 2. offshore wind power potential and technologies 3. wind assessment techniques 	O1 O1
Phase 2: Method Development and Study Area Determination for the Research		

<p>2.1 Identifying offshore wind data availability and study area selection</p> <p>2.2 Observed meteorological data preparation</p> <p>2.3 Choose the suitable WRA technique for the study area</p>	<p>Select study area based on onshore and open water wind observations</p> <p>Inventory of quality checked and quality controlled wind data Wind profile of each station</p> <p>Preprocess for wind model validation</p> <p>Select WRA method to modify for study area</p> <p>Present findings at a conference</p>	<p>O2</p> <p>O3</p>
<p>Phase 3: Wind Model Configuration and Sensitivity Testing</p> <p>3.1 Identify appropriate model</p> <p>3.2 Validation of chosen model with observed data</p>	<p>Compilation of regional scale and mesoscale models as well as the microscale and computational fluid dynamics (CFD) models currently in use from literature</p> <p>Sensitivity test results on various model for the location</p> <p>Name the regional scale/mesoscale model and CFD model combination for simulation</p>	<p>O3, O4</p>
<p>Phase 4: Wind Simulation</p> <p>4.1 Mesoscale Modelling</p> <p>4.2 Produce monthly wind maps</p> <p>4.3 Identify areas with power generation potential</p> <p>4.4 Microscal Modelling</p>	<p>Simulate entire study area domain</p> <p>Compilation of wind field maps over surrounding waters of Palawan Island</p> <p>A directory of locations that have power production potential from wind</p>	<p>O4</p>

4.5 Comparison between Mesoscale and Microscale Model Performance	Simulate selected locations from wind maps for fine spatial resolution scale Performance improvement determination in the usage of microscale model	
-------------------------------------------------------------------	------------------------------------------------------------------------------------------------------------------------------------------------------------	--

1.5.1 Phase 1 – Review of Literature

This study reviews existing research papers and reports on power generation from wind energy, current technology on offshore wind energy, the methods and techniques utilised for wind resource assessment, and wind maps. This overview is used in the analysis of available meteorological wind data so that a wind resource profile can be formed on observed data. It will also serve as a survey of the recent technology developments for offshore wind energy. Techniques for wind resource assessment have been evaluated in the review to find the appropriate method considering the available data and computing resource. Some of the techniques for wind analysis and wind modelling has been done to assess the viability of the research.

1.5.2 Phase 2 – Method Development and Study Area Determination for the Research

The study area is selected based on the preliminary onshore WRA for the Philippines and offshore wind observation data availability. A preliminary onshore WRA for the Philippines has been performed before which should aid in determining which islands have offshore wind potential. Weather stations close to shore or are located in small islands that are operated by the Philippine Atmospheric, Geophysical, and Astronomical Services Administration (PAGASA) are identified and the data quality are assessed. Data quality is based on the longevity of observations from a station that has quality assured continuous data by PAGASA. Observations close to the sea are valuable for making wind profiles of open waters at the vicinity of the stations in the absence of actual offshore wind measurements since such data are difficult to obtain. But meteorological observation on offshore locations from the 7 Southeast Asian Studies (7SEAS), which was conducted by the Naval Research Laboratory and Manila Observatory at Palawan Island, are available although the data spans one to four days of continuous measurements. Other wind data that can be utilized for the Philippines are reanalysis data which are a composition of ground measurements, satellite data, and global circulation models (GCM) to produce atmospheric condition maps all over the world. Given the limited wind data available for the Philippines in offshore locations, simulating wind conditions is a viable solution to form a database that can be used for WRA [18].

1.5.3 Phase 3 – Wind Model Configuration and Sensitivity Testing

To do the wind simulations, identification of suitable regional scale or mesoscale wind models for the study area will be done and will be coupled to CFD models to get high spatial resolution wind field maps from available community-developed or commercial models. Reanalysis data from GCM will provide initial and boundary conditions for the mesoscale or regional scale model. Initial conditions are needed by the model in order to give it a starting point in time for wind simulations. To avoid divergence in the computations, boundary conditions are necessary in solving the atmospheric governing equations through finite element methods. Reanalysis data are GCM interpolations of weather observations around the world. In turn, the results will be used for the microscale or CFD model. These models will be validated with observed wind data and tested for sensitivity in order to know which ones are appropriate for Palawan. From the literature review, it is found that the Weather Research and Forecasting (WRF) model is being utilised for wind resource assessment and open source so, it has been selected as the mesoscale model. On the part of the CFD model, the WindSim is found to be developed and optimized for the use of wind industry from published journal articles so it is chosen to be the CFD model for the study. Sensitivity tests will be done for evaluation purposes of the models in order to determine the suitable configuration for modelling coastal and open water areas. The tests will involve varying the planetary boundary layer values and the microphysics for both models.

1.5.4 Phase 4 – Wind Simulation

After these tests and model validation, the model combination that is able to simulate the area of interest will be used to produce high resolution wind field maps. These are deterministic models that solve the atmospheric governing equations through finite element method. This work entail running the selected regional scale or mesoscale model with data from reanalysis as input. The output of the mesoscale model are 3 km resolution grids. Downscaling the results of the mesoscale model with the chosen CFD model produces 38m – 76 m fine spatial resolution grid [19]. This fine scale is necessary since wind flow near coastlines are highly influenced by land-sea interaction and land features [20]. Thus, CFD is employed to allow wind flow analysis over complex topography and account for microscale physical dynamics where regional scale or mesoscale models are incapable of simulating. Finally, the mesoscale and microscale models are compared to find performance improvements gained from using microscale models.

All of these phases have been done in the course of the study and they are illustrated in Figure 2. The figure shows the work flow that was followed in order to achieve the objectives stated in Section 1.2.

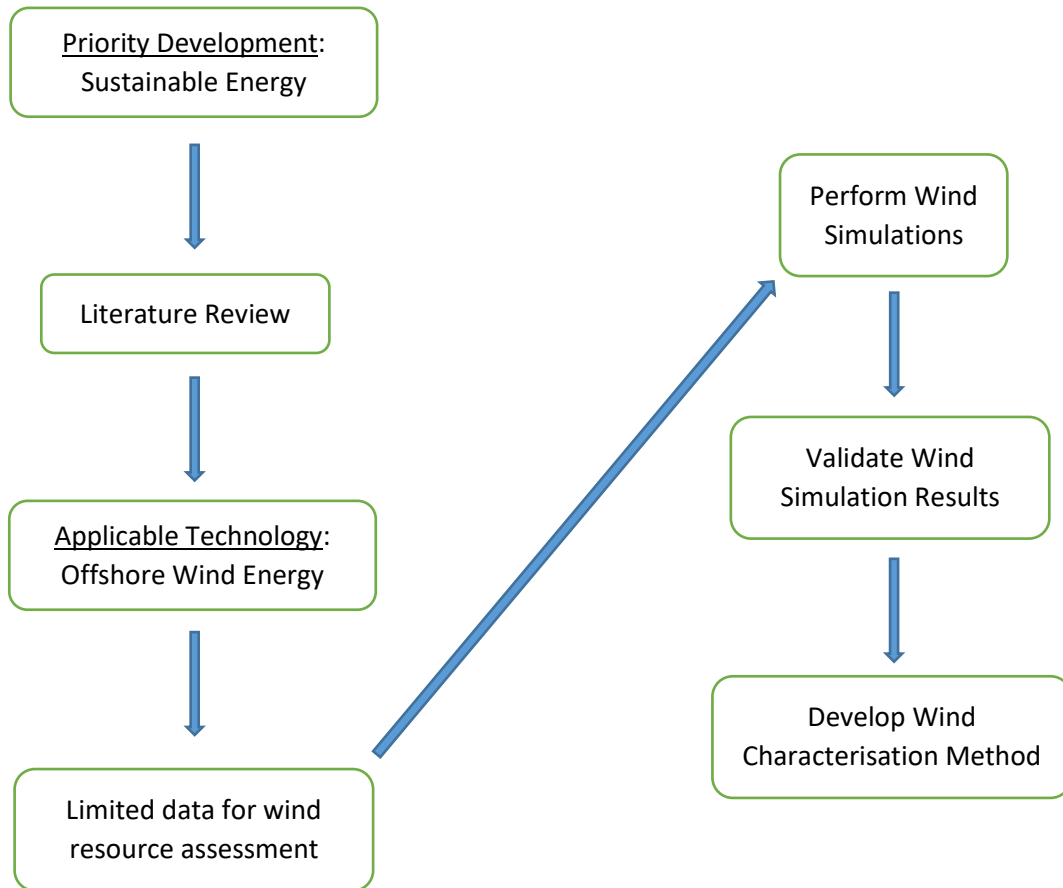


Figure 2. Work flow of the study for WRA method development

This figure describes what transpired during the research from the need that has driven this research, problems encountered, the solutions to address those problems, and the research output. The details on how these steps were worked out can be found in Chapter 4.

1.6 Summary

Energy is an essential resource for modern society and economic development but the current source of energy has proven to be unsustainable. So, developing nations must seek renewable energy sources that will be sustainable in order to assure continuous development of their economies. A potential renewable energy source can be wind since it is a mature technology and abundant. In the course of wind energy development, it has been determined that the offshore wind resource are more consistent and wind speeds are higher than onshore locations. Thus, the wind industry has expanded into the deployment of wind turbines in offshore wind farms.

Many developing countries are located in the low latitude regions and most of them have oceans or seas within their territories. Therefore, these nations have potential wind resources over the open waters that are close to them. Any wind energy development project must begin with a good WRA in order to ensure its success in power generation [11] but there are limited data available in developing

countries that will allow for a meaningful WRA [21]. In addition to that, much of the research and development on offshore wind energy are in Europe which is located in the high to mid-latitude. Wind patterns can differ between locations depending on the local topography, weather, and climate. So, there is a need to develop WRA methods for low latitude areas because the climate and weather effects in those regions are different from high and mid-latitude areas.

2 LITERATURE REVIEW

This section looks at the published literature regarding renewable energy and wind energy generation. Then, the offshore wind resources and offshore wind energy in the world are explored to see the current state of the technology and find the learnings in the course of development. It then proceeds with a review of methods in performing WRA for offshore locations. These are performed in order to find the appropriate WRA techniques for the Philippines.

2.1 Renewable Energy

An energy source is renewable if it can be quickly replenished by nature like sunlight, wind, sea tides or waves, biomass, hydro, and geothermal heat. Renewable energy is deemed beneficial because it has little or no impact to the environment [22]. This type of energy source is being slowly adopted because many technologies are still under development, the mature ones are not deployable in all locations, and the intermittency of many sources [23]. But the intermittency or variability are only applicable to solar, ocean current, tidal, wave, and wind as determined in the study of Tran and Smith [24]. In their work, they found that all the other renewables like biomass, geothermal, and hydro are actually dispatchable. The existing power generation structure is not compatible to the way renewable energy systems operate [25]. Thus, opponents to the renewable energy transition use this reasoning by stating that the variability of renewable energy would be detrimental to the electrical grid [24]. This mindset is rooted on the concept of a rigid power system concept that is prevalent called base-load [25]. Given the variability of some renewable energy sources, Diesendorf and Elliston [25] argues that it is necessary to shift towards a flexible power system that have dispatchable power stations and energy storage.

At present, 80% of power generated on the planet use fossil fuels that is comprised of petroleum, coal, and natural gas [26]. But the market price volatility of fossil fuels offer an opportunity for investments to be made for renewable energy systems [4]. In fact, there are studies [25,27,28] that show it is possible for the world to transition to a fully renewable power generation system. Both the publications of Jacobson and Delucchi [27] and Diesendorf and Elliston [25] have stated that the obstacle towards a full transition to renewable energy are political and institutional reasons. The political reasons are due to the incumbent industries from fossil fuels, nuclear, and electricity who are very influential to energy planning while institutional reasons are the incompatibility of renewable energy to the market regulations [25]. To enable renewable energy to make a significant penetration into the energy market, careful planning and effective policies must be in place [29]. Lund [30] has stated that energy policies can have a great impact on the development of local industries for sustainable energy. In that paper, the results show that the gains from the policies outweigh the public

expenditure as evidenced by the increase in income and corporate tax revenues from sustainable energy industries. Even if fossil fuel resource is abundant in a region, it must invest in sustainable and renewable energy because fossil fuel reserves will be depleted [31]. But there is a difference when using renewable energy because several sources must be exploited at a location to be able to optimise power production instead of relying with a single technology [24].

There are feasibility studies [25,27,28] that show it is possible to source the majority of the world's energy requirements from renewable sources. One of those feasibilities was carried out by Jacobson et al. [28] where they determined that it is possible to produce the global power needs from solar, water, and wind sources. In fact, there are countries such as Bhutan, Iceland, New Zealand, Norway, and Tasmania that produce 80% - 100% of their energy from dammed hydro systems [25]. But there are publications [27,28] that have shown the global potential for solar and wind to supply the entire power demand of the world between 2030 - 2050. This has been achieved by certain locations that lack hydro power systems like South Australia, Denmark, Northern Germany, and Scotland for a few days at a time [25]. Countries such as Denmark and Scotland are able to achieve this primarily with wind energy [25,32] which is a renewable energy that has a potential power production of 40 – 85 TW within locations that can be developed into wind farms worldwide [27]. This potential of wind power has been acknowledged in recent times which allowed its rapid growth in the power industry [23,33]. Its power has an extensive history since it is one of the oldest renewable energy known to humans [34]. The next section will be a brief narration of wind energy history and the emergence of the modern wind power technology.

2.2 Wind Energy Generation

Wind energy has been known to humans for a very long time. The earliest known machine is dated at around 7th century B.C. and it was used for milling grain in Afghanistan [35]. Early wind powered machines used the concept of drag but were later modified into using lift concepts where more wind energy can be converted into mechanical work. These were widely used for grinding or pumping water, and improved through the centuries. Development for the technology slowed down by the late 19th century but improvements were still being made and in 1891, the first wind turbine for electric generation was completed [34].

A resurgence in research for wind turbines came when an oil crisis occurred in the 1970s and environmental concerns paved the way for renewable sources to be utilized in place of fossil fuels [34,36]. The initial turbines produced had power capacities of around 50 kW that increased to about 200 kW by late 1980s [35]. In the early 1990s, these turbines have reached 500 kW range which further increased to (750 kW- 1000 kW) power capacities [37]. By the end of that decade, wind turbines with

1.5 MW to 2.5 MW were in production, and have attained power capacities of 3.5 MW in the late 2000s [35,37].

Improvements on wind turbine technology enabled the construction of wind farms for large-scale power production. It is the fastest growing renewable energy source and the demand for it continues to increase [36,38]. Wind power generation is the most advanced technology among new and renewable energy sources [39]. Installations started in the U.S. during the late 1970s until the early part of 1990s[35]. When interests in the U.S. began to dwindle, European countries rapidly built wind farms with Germany, Denmark, and Spain at the forefront [36,37]. At the end of 1995, Europe had an installed capacity of about 2.5 GW [35]. Then, this quickly increased to 33.6 GW by the end of 2004 [37]. In fact, Europe had three-quarters of the installed wind power capacity in the world by 2002 [36]. In 2004, Europe maintained this huge share while Asia has achieved a global share of 12.4% with India and Japan as the leading nations in wind farm construction [36]. For the worldwide perspective, total installation has increased from 6 GW in 1996 to 370 GW in 2014 [40]. This unprecedented growth was unforeseen and wind energy is expected to keep increasing its share in power production [38,40].

These studies have shown that wind machines are in use since the ancient times and continued development to suit the needs of societies through time. Recent developments have been focused on electric power generation from onshore wind farms. As more power is needed while de-carbonizing the energy sector, wind power is now expanding to other sites such as forested areas, urban, and offshore. Pursuing wind energy generation earlier will make it more cost-effective since this will reduce the greenhouse gas (GHG) emissions and may prevent effect of decreasing wind resource if the world becomes warmer [41]. For high capacity power generation, offshore wind farms can be a solution and its availability and development are the topic for the following section.

2.3 Global Offshore Wind Energy Resource

Published research [42–44] on available offshore wind resource on the planet are showing that it is a promising option for high power production. Advancement in atmospheric observations and computational technology have enabled progress in offshore wind research to be possible [42]. Measuring instruments mounted on satellites have allowed the determination of offshore wind speeds across the world such as the maps generated by Quik Scatterometer (QuikSCAT) [45] as can be seen in Figure 3. The utilisation of scatterometer data can be considered as preliminary WRA because of the coarse spatial resolution and the coarse time intervals between scans from satellites.

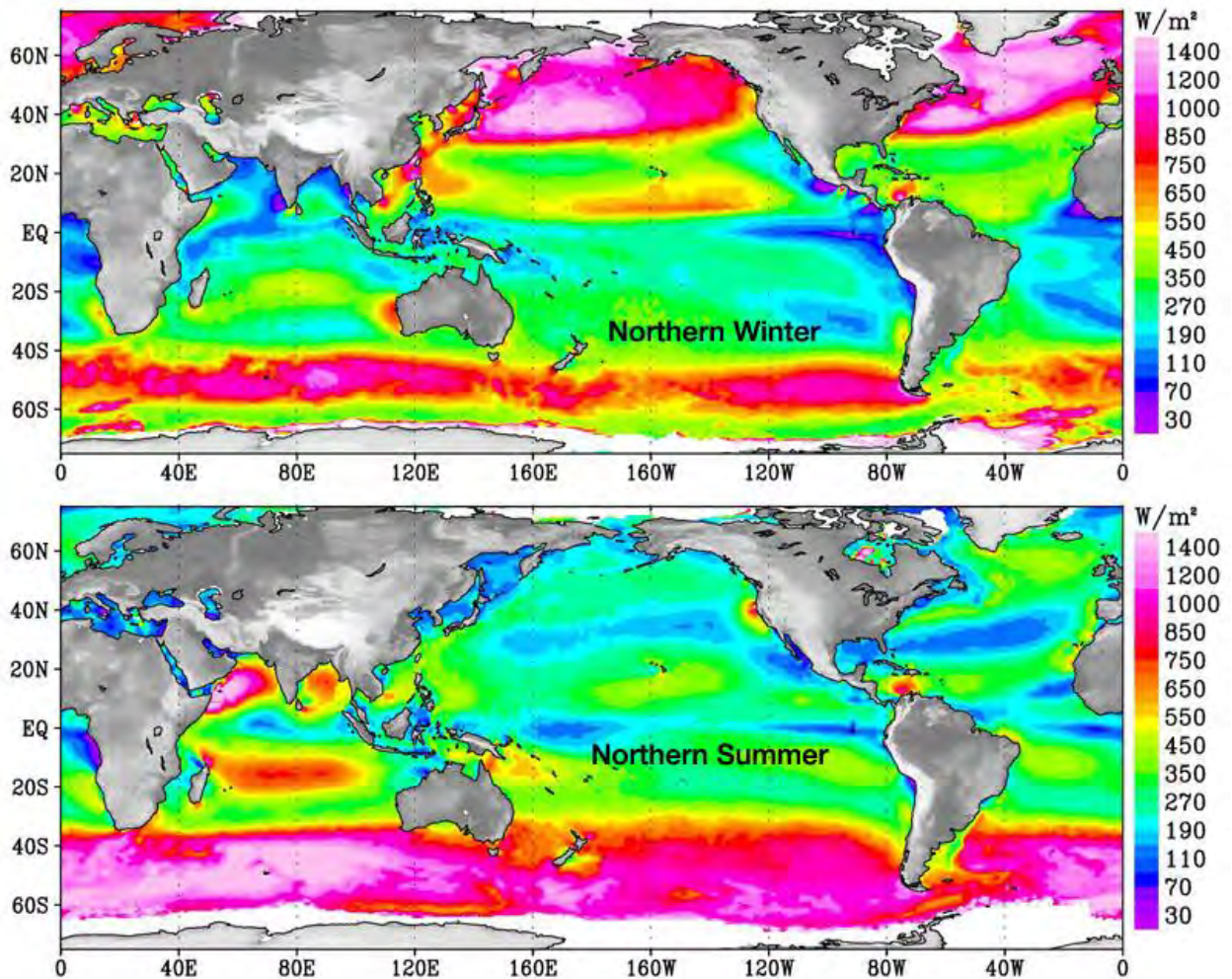


Figure 3. Wind power density (WPD) in the winter and summer months for the Earth's ocean surface at 80m level from QuikSCAT data analysis [45]

Better wind profiles over waters is possible by studying the wind and wave interaction such as Jiang and Chen [46] who complimented satellite-based wind and sea surface wave observations with other wind data sources. The authors were able to produce seasonal mean wind speeds over the oceans of the world using wind data from Jason Microwave Radiometer (JMR) aboard the Jason-1 satellite. Such analysis, that combines multiple datasets, was made possible because of the advances in scientific computing which enables the calculation of vital offshore wind resource parameters. In fact, wind datasets such as the Cross-Calibrated Multi-Platform (CCMP) wind product are the outputs of such combined data analysis [43]. Carvalho et al. [18] have compared various offshore wind datasets, concluding that CCMP is a viable option in performing WRA when in situ data is not available or resources are limited to perform numerical wind modelling. An offshore wind power density map of the world using the CCMP wind product, is shown in Figure 4.

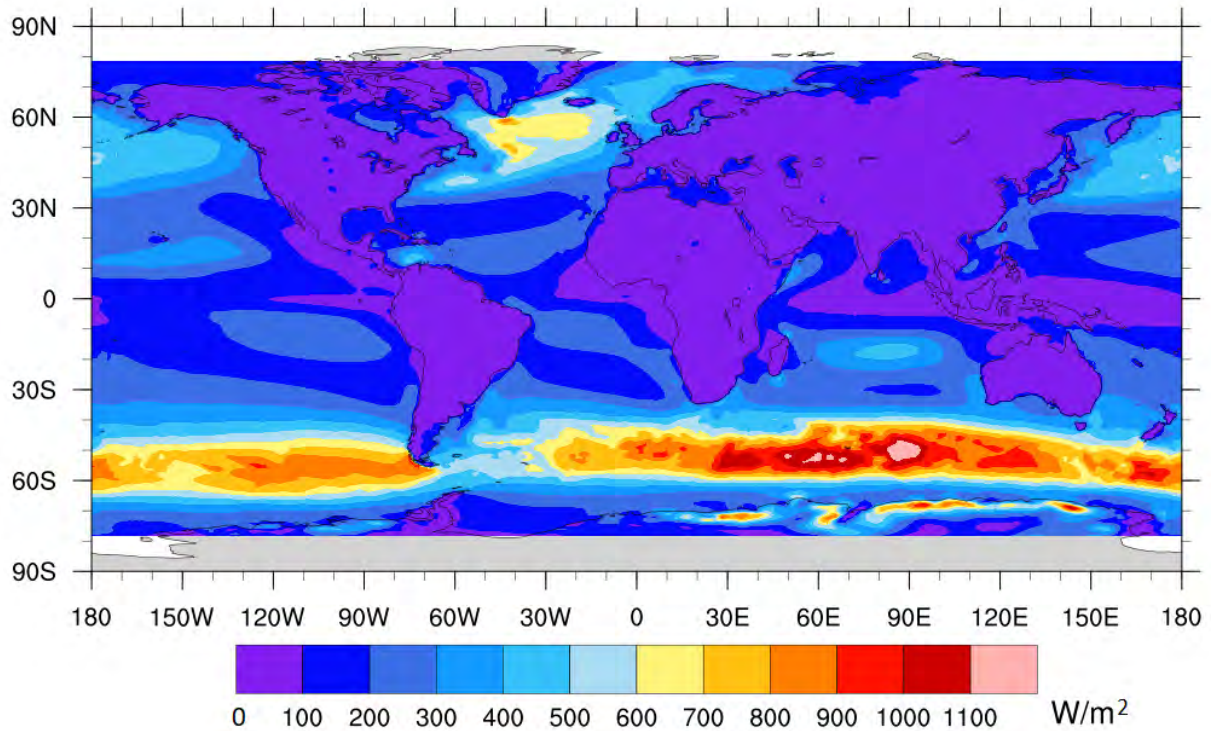


Figure 4. Wind power density (WPD) for the Earth's ocean surface at 10m level from 1988 to 2017 based on CCMP wind product [47]

Due to their wind vector representation, the utilisation of multiple wind data products in the analysis of wind profiles has been employed in research such as wind power density (WPD) for the world's oceans. The method of using combined observation data, reanalysis, and satellite observations, like CCMP dataset, has been employed for further offshore WRA as demonstrated by Zheng and Pan [48]. Their computed worldwide wind speed estimates that in most ocean surfaces there are high wind speeds over open waters for a cumulative period of eight months in a year, and over 50W/m^2 WPD for nine and a half months cumulatively in a year. In another study, the same authors investigated climate trends of the world's ocean wind speeds and found that there is a 3.35 cm/s increase every year from 1988 to 2011 globally [43]. Thus showing that the offshore wind energy has promising potential for power generation. A practical approach in studying the global WPD by Eureka et al. [49] calculated the wind power density by taking into account the exclusive economic zone (EEZ) of each country and identifying the suitable areas for offshore wind energy development within the EEZ. From their research, authors concluded that the global average WPD is 31.13 W/m^2 for the height of 90 m above ground. Recent developments [43,44,50,51] have even considered global offshore wind power prediction which is essential for wind farm planning. Sasaki [44] demonstrated the possibility of a 5-day wind power production forecast thereby, encouraging more research to gain better reliability on wind power predictions. In addition to improving wind forecasting capabilities, Zheng et al. [52] suggested that grade division by wind turbine classes and production of a wind energy

development index is necessary to aid offshore wind project proposal and feasibility studies. Following that recommendation, Zheng et al. [53] refined the WRA method implemented by Zheng and Pan [48] through the addition of cost and environmental impact risks. Their analysis [53] yielded similar results to the latter work [48] except in the region between 30° N and 30° S where they found that there are potential offshore wind resource available within that band of latitude. These efforts are indeed useful for the development of offshore wind farms for the different nations since they offer preliminary WRA. It is interesting to find that some of the areas identified to possess good wind energy resource from the global WRA results are currently the active areas of OWF deployments which will be the next topic to be discussed.

2.4 Worldwide Offshore Wind Energy Developments

Wind farms located at offshore sites have been growing by 40% per annum for the entire world [54]. In the report of WindEurope for 2017 [55], it was shown that there have been significant offshore wind farm capacity installations in the United Kingdom, Germany, Denmark, Netherlands, and Belgium. The cumulative installed capacities for the countries respectively are 6,835 MW, 5,355 MW, 1,266 MW, 1,118 MW, and 877 MW [55]. There is also growing interests in developing offshore wind farms in the Adriatic Sea and Mediterranean Sea [54,56]. A WRA at 90m height carried out by Soukissian, Karathanasi, and Axaopoulos [57] has located suitable sites that have good potential wind resource within the Mediterranean Sea such as in the Gulf of Lions where WPD can be as high as 1,600 W/m² and in the Aegean Sea where its Northeastern region can potentially have 1,150 W/m². Presently, the hurdle for offshore wind farm projects in the Mediterranean is that the sea depths are beyond 30m while the current capabilities for offshore foundation construction are for depths less than 30m [54]. Since open waters at depths greater than 30m offer higher wind power potential, there are research and development on floating platforms for offshore wind turbines across Europe [6,58–61] especially on deep sea deployment [62]. Beyond the North Sea, areas such as the Baltic Sea, Irish Sea, and the Atlantic Ocean have offshore wind farm developments from Finland, Sweden, Norway, Ireland, and Portugal [63]. In addition to these countries, there are test offshore wind turbine installations in Spain and France over the Atlantic Ocean [55]. Other large bodies of water in Europe such as the Black Sea and Caspian Sea have been studied for their potential wind resource by Onea and Rusu [64] and showed that the WPD over the Black Sea can range from 387 W/m² – 542 W/m² while the Caspian Sea can have between 437 W/m² – 532 W/m² at the height of 80m. The determination of WPD through WRA on both the Black Sea and Caspian Sea shows that even inland seas have good potential for offshore wind development. All these successful deployments and learning experiences from Europe have been the foundation of other OWF projects around the globe thus, low latitude nations could also benefit from the exploits of their European counterparts.

Across the Atlantic Ocean, the idea of offshore wind turbines has been brought about in a conference at Massachusetts back in 1972 [6]. However, offshore wind farm projects in Canada and U.S. are mostly at the planning and evaluation phase [8]. There are four Canadian projects that are being evaluated where the two that have power production capacities of 414 MW and 300 MW are situated in the Great Lakes [7,8]. In the U.S., both the Atlantic Ocean and Great Lakes are being considered for offshore wind projects [6, 8]. The most promising is the Block Island project that has a 30 MW power production capability and commissioned in December 2016 [63,65]. The state of Massachusetts has also approved the Vineyard Wind project which will have 800 MW capacity and the construction begins in 2019 [66]. Developments in the Great Lakes have been agreed upon to be a collaborative effort between the countries of U.S. and Canada [67]. Although the OWF deployments in the U.S. and Canada are in the early stages, their proposed projects in the Great Lakes is unique because these are inland freshwater OWF projects [67]. These projects will yield techniques and practices for OWF projects in lakes and will be useful for inland waters in the low latitudes such as those in Africa or South America.

In East Asia, Japan began the research and development of offshore wind turbine technology in the region with two 600-kW turbines back in 2003 [68]. This initial effort was revitalised after the dangers of nuclear power became apparent in Fukushima for earthquake prone regions [63]. In fact, Japan has 49.6 MW offshore wind power and is actively developing floating platforms for wind turbines [69]. Despite the recent progress in Japan, China is the leading investor in the wind turbine technology in the Asia-Pacific region in terms of manufacturing and deployment [63,65]. China has surpassed Denmark in terms of total capacity installed with 1,627 MW in 2016 [65]. This gap widened in 2017 when China added more capacity giving a total of 1,796 MW [70] while Denmark decommissioned one of its pilot installations [55]. South Korea has started developing its offshore wind turbine capabilities with a 5-MW installation in Cheju Island during 2011 and 2012 [69]. In 2017, South Korea increased its offshore wind energy capacity to 35 MW [70], while initial offshore wind turbine deployments were carried out by Taiwan in 2016 with two offshore turbines located off the coast of Miaoli County having 8 MW production capacity [71]. These OWF development have involved islands as study areas within the East Asian region thus, their findings can benefit small islands or archipelagic nations within the low latitudes when pursuing their own respective OWF projects. Figure 5 summarizes the power production of operational offshore wind farms around the world.

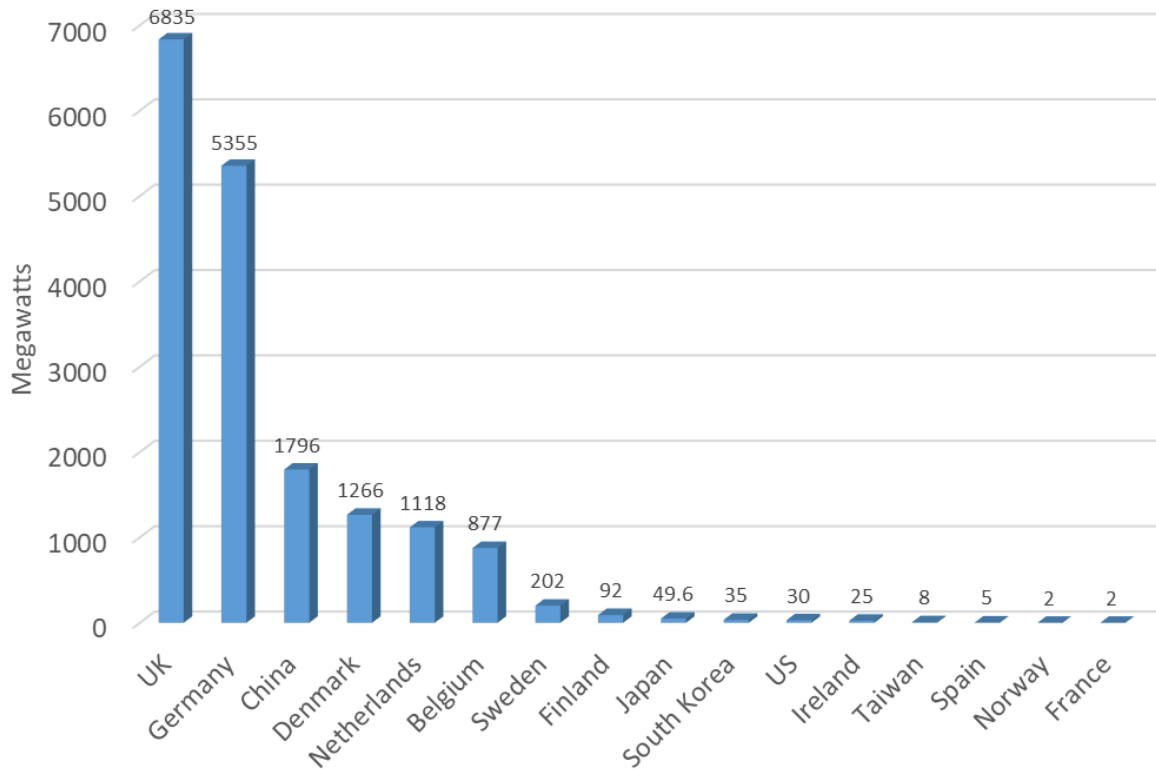


Figure 5. Power capacities of installed offshore wind farms

The OWF power generation capabilities of each country in Figure 5 is a composition of operational wind farms and pilot testing projects. Thus, not all nations that have OWF are producing electricity that are supplied to consumers because some are still in the trial stage. The following section discusses the countries that feed their OWF generated energy to the electrical grid.

2.5 Grid-Connected Offshore Wind Energy Production

When considering the overall energy consumption of the world, electricity is only a fifth of the total energy consumed [72]. This study focuses on OWFs' potential contribution to electrical power generation and does not discuss other forms of energy used by each country. Having these OWF installations around the world, the electrical energy needs of some countries that made significant investments on the technology are being met sustainably. The following table shows the electrical consumption and annual OWF production of each country with offshore wind farm installations. The percentage of electricity supplied by offshore wind farms to the total consumption is also indicated.

Table 2. Summary of total electricity consumption, power production from offshore wind farms, and percentage of electricity supplied by offshore wind for 2016

Country	Consumption (GWh)	OWF Production (GWh)	Supplied Electricity by OWF (%)
United Kingdom	303903	16406	5.40
Germany	517377	12274	2.37
China	5101661	2409	0.05
Denmark	31154	4650	14.93
Netherlands	105628	2269	2.15
Belgium	81848	2390	2.92
Sweden	127496	608	0.48

From the table above, it is apparent that there is varying success on OWF deployments at first glance. However it is notable that countries that have invested in the technology are able to obtain at least 2% of their electrical energy needs from offshore wind energy. Despite China having similar OWF production levels as Belgium and Netherlands, the supplied electricity percentage from OWF is low because the energy consumption in China is at least one order of magnitude higher than any country listed in Table 2. The low percentage contribution in Sweden shows that it is at the initial stages in deploying OWF. These developments show the viability of offshore wind energy for developed countries and demonstrate that offshore wind power may supplant conventional fossil fuel power plants [9]. In fact, some of the offshore wind farms have been decommissioned or due for decommissioning after being operational for more than a decade [73]. The present status of offshore wind energy development prove that the technology has advanced to the point where component costing can be quantified [74] and the complete life cycle of wind farms can be assessed for financing [75]. Successful deployments of OWFs have sown interests from different countries to determine the potential of OWFs for local power generation [76]. Having seen the worldwide status for offshore wind, the focus now shifts to the main interest of this paper which is the region of low latitudes.

2.6 Offshore Wind Studies in Low Latitude Regions

Many developing countries are found in the low latitude region and there are plenty of open waters in these locations [77]. Offshore wind energy is a potential choice for power production in these areas as they have wind speed average at around 7 m/s to 9 m/s throughout the year [46]. Unfortunately, many published work are about OWFs in Europe and there is very little attention given to developing nations [21]. Rusu and Onea [21] investigated the marine energy resource of developing nations where they had compiled the WPDs available from the different countries. This section will use a similar treatment by making a compilation of determined WPDs available within 23.5°N and 23.5°S latitude band from published literature but will focus on the offshore wind energy. In selected regions where Rusu and Onea analysed wind data, they found that Somalia has a WPD of 1,073 W/m² while Vietnam has 695.5 W/m² for the 80 m height above the surface. These conditions are suitable

for offshore wind development indicating that it may be a viable sustainable energy source for the future [21]. Areas close to Angola, Brazil, Guinea-Bissau, Madagascar, Mexico, Myanmar, Peru, Papua New Guinea, Timor, and Venezuela were examined [21] demonstrating moderate wind resource reserves ranging from 67 W/m^2 - 315 W/m^2 . The WPD values from all the countries in Rusu and Onea's publication are well above the global average WPD of 50 W/m^2 determined by Zheng and Pan [48] which suggest that there is a potential for offshore wind power generation in these countries. Interestingly, some of the sites that Rusu and Onea [21] identified as good sites such as Madagascar, Peru and Somalia are categorised as possessing rich offshore wind resource by Zheng et al. [53]. This agreement confirms that wind energy is available over the open seas in these latitudes and must be seriously considered for power production development.

Satellite observations has enabled initial WRA on oceans for different locations where wind map products, such as in Figure 4, can be used for analysis [52]. However, this remote sensing method has limits since each satellite scan can only cover a portion of the planet at a particular time so, its spatial and temporal resolution is not sufficient for a complete offshore WRA [52]. There are developments in combining different satellite observations as a remedy which allow the production of better offshore wind maps like in the work of the National Renewable Energy Laboratory (NREL) [78]. To produce offshore wind maps, NREL used the Blended Sea Winds dataset where wind speeds have been extrapolated to the 90m level and covered the open waters within 100 nautical miles from coastlines [79] as shown in Figure 6.

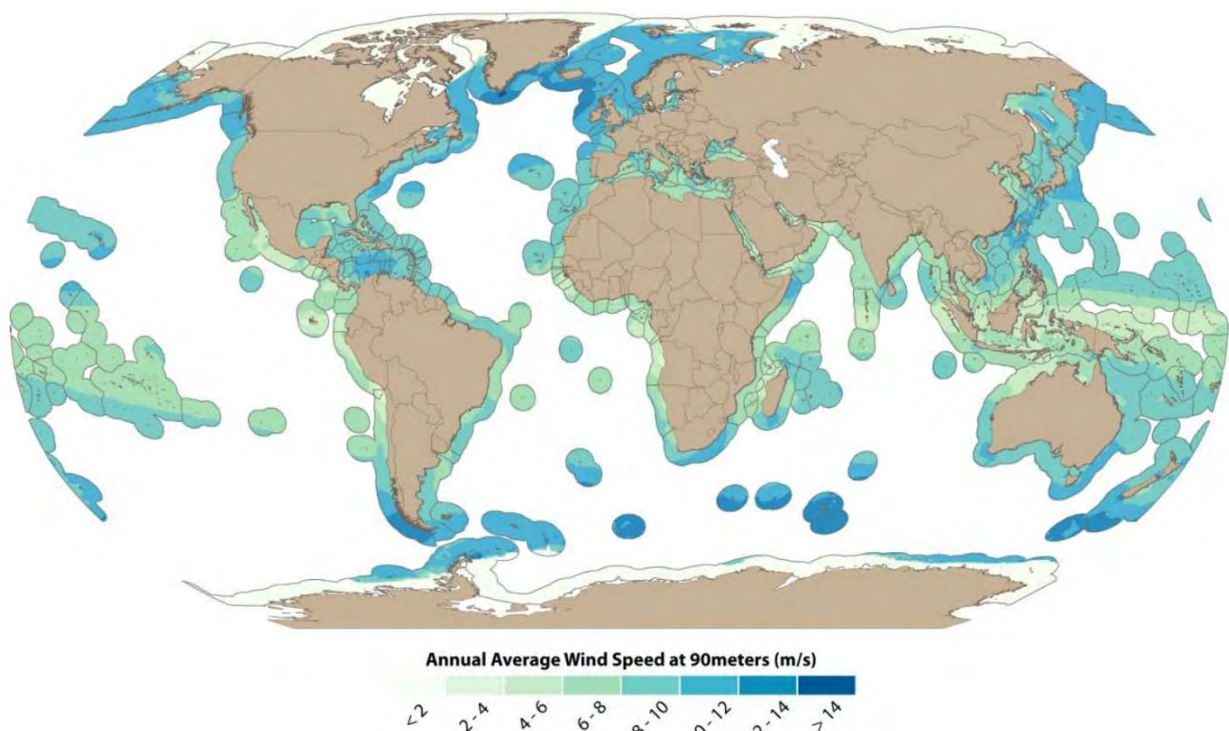


Figure 6. Yearly mean wind speeds across the globe at 90m height and up to 100 nautical miles from shore [78]

An improved satellite-based wind dataset is the WindSat Spaceborne Polarimetric Microwave Radiometer [80] where ocean wind maps can be produced utilising the dataset as shown in Figure 7. Even though WindSat is a new generation satellite observation system, it still possesses the inherent spatial and temporal limitation of satellites scans [52] mentioned earlier.

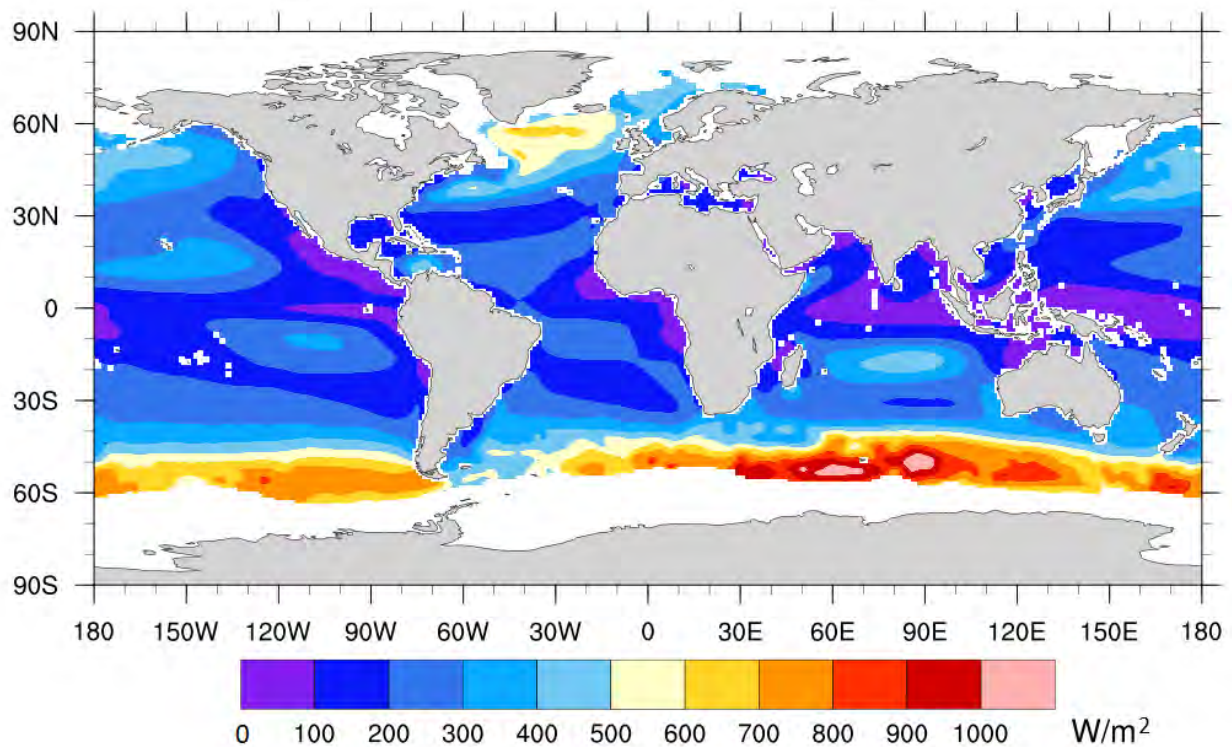


Figure 7. Yearly mean wind power densities for 1988 to 2007 over open waters at 10m height from WindSat [80,81]

Although combination of satellite measurements yields improvements for WRA, they are still coarse in terms of spatial resolution and a finer resolution WRA is necessary to take into account local atmospheric dynamics [18]. A careful evaluation is needed to better understand the wind energy reserves for each country thus, there have been efforts to do this that can be found in the literature.

2.6.1 South America

A zoomed in WPD map for the Caribbean and South American region, which was produced using WindSat dataset, can be viewed in Figure 8. It shows that winds near coastal areas are not available with WindSat as depicted by the white pixels on the image which is a limitation for satellite-based wind observations [18,82]. Areas of Latin America facing the Atlantic were investigated by Pimenta, Kempton, and Garvine [83] where they reported that Brazil has $300 \text{ W/m}^2 - 550 \text{ W/m}^2$ WPD between $19^\circ\text{S} - 23^\circ\text{S}$ latitude at 80 m level. Their results showed that offshore wind energy in Brazil is promising since the highly populated cities are close to shore and may complement the existing hydro power in the country [83]. Another study covered the entire coast of Brazil where Ortiz and Kampel [84]; obtained similar results to Pimenta, Kempton, and Garvine; discovered that there are richer

offshore wind resource off the coasts between 1°S – 12°S latitude at 80 m level where WPDs range from 550 W/m² – 968 W/m². In a more recent study for the state of Ceará in Brazil, Lima et al. [85] found that WPD can reach 750 W/m² in that region alone by simulating winds using a mesoscale atmospheric model which shows that Brazil may have greater potential than previously determined [85]. These findings from the work of Ortiz and Kampel [84] and study of Lima et al. [85] give credence to the selected site for the planned 12 MW offshore wind farm pilot project off the coast of Ceará called Asa Branca [63]. On the other hand, Soler-Bientz et al. [86] studied the offshore wind at the Yucatan Peninsula in Mexico using wind observations at 10 m and 25 m above ground level and characterised the wind profile in the area [86] but has not been able to relate their output in terms of wind energy potential. The region of the Caribbean Sea is also identified as a location for good wind resource in the analysis of Zheng et al. [53] having a WPD of 250 W/m² – 300 W/m² at a 10m height from the ground. Therefore, based on the findings of Zheng et al. [53], the Yucatan Peninsula has good potential for offshore wind energy development. This also demonstrates that the results of Zheng et al. is in agreement with Rusu and Onea [21] as both publications found the Caribbean Sea region of Venezuela to possess an average WPD of 315.3 W/m². This WPD value also reflects the estimated WPD from offshore satellite measurements such as the WindSat data in Figure 7. It is apparent that this Caribbean Sea region has been detected by WindSat to possess high WPD despite the instrument having a coarse data resolution. On the Western side of the South American continent, Zheng et al. [53] have confirmed that Peru has a rich wind resource off the Pacific with similar values as the Caribbean Sea. Further West in the Pacific, they also pointed out that Hawaii has good wind potential in the Southern waters of the island which has 200 W/m² – 250 W/m² at 10m height. Therefore, these determined WPDs in the Caribbean Sea, Atlantic and West Pacific show the potential offshore wind resource surrounding the Americas.

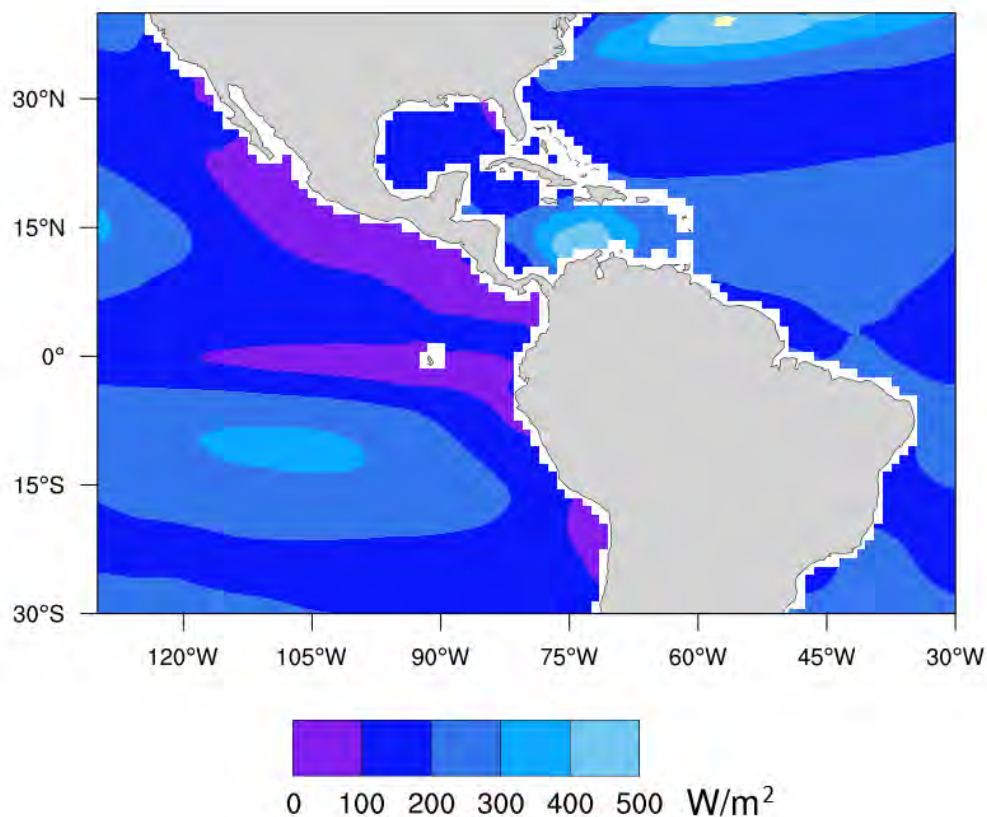


Figure 8. Wind power density map from 1988 to 2007 for South America and Caribbean region from WindSat data

2.6.2 Africa

Research on offshore wind energy in the African continent has been surveyed as part of the global WRA as shown by Rusu and Onea [21] and later by Zheng et al. [53] but few publications are focused on Africa itself. In both published research [21,53], many of the covered areas are in the low latitudes of Africa. Rusu and Onea have focused on the assessment for Angola, Guinea-Bissau, Madagascar, and Somalia, and they found that these countries have WPDs at 73.3 W/m^2 , 137.6 W/m^2 , 181.7 W/m^2 , and $1,073 \text{ W/m}^2$, respectively. These predictions give a picture of the potential offshore wind available on the Atlantic Ocean and Indian Ocean shores, and it is worth noting that these values are in line with the global wind map generated by Zheng et al. [53]. Offshore wind power is promising in Africa with renewable energy studies in the region acknowledging that it is a potential energy source for the coastal and island nations. Using the WindSat data, the climatological scale WPD map in Figure 9 surrounding the continent illustrates the vast wind resource that is available. Renewable energy policy and development research for Mauritius have recommended that the offshore wind energy must be considered for future planning [87,88]. A WRA for Mauritius in the preliminary stages has estimated that the WPD to be 350 W/m^2 and above for heights of 100m [89]. That assessment has located Flic en Flac, Mahebourg, and Rodrigues to be possible sites for offshore wind development in

the country. Further studies on the wind potential of Mauritius are planned for the future as the government's national budget has an allocation for such purposes [90]. Analysis on offshore wind project viability in Africa has also been done such as finding an appropriate technique for Nigeria in terms of project costing for potential offshore wind farm development projects [91]. The case study by Effiom, Nwankwojike, and Abam [91] proposed an offshore wind project in Calabar, near Cameroon, where they stated that their model is suited for initial analysis of offshore wind farm costing, and that offshore wind projects are feasible in Nigeria. The latest WRA study in Africa by Olaofe [92] encompassed the entire continent and found similar results as the global offshore wind maps. In that study, most of the coastal nations facing the Atlantic were reported to have around 50 W/m² or less WPD at 10 m level, but can reach up to 200 W/m² in the Southern Atlantic area. Olaofe [92] also showed that there are regions in the Indian Ocean where the WPD are similar to those on the Atlantic side. However, the South of Madagascar can have as much as 523 W/m² with the Horn of Africa having a WPD as high as 350 W/m² [92]. At 160m above ground level, Olaofe's findings show that countries that are facing the Atlantic Ocean have around 200 W/m², while WPD in the Indian Ocean locations range from 810 W/m² – 1,705 W/m² [92]. These global and continental scale WRA are preliminary assessments for Africa and show that the African Nations have a promising offshore wind energy resource. However, a thorough WRA is needed for each member country in this continent in order to refine these initial WRAs.

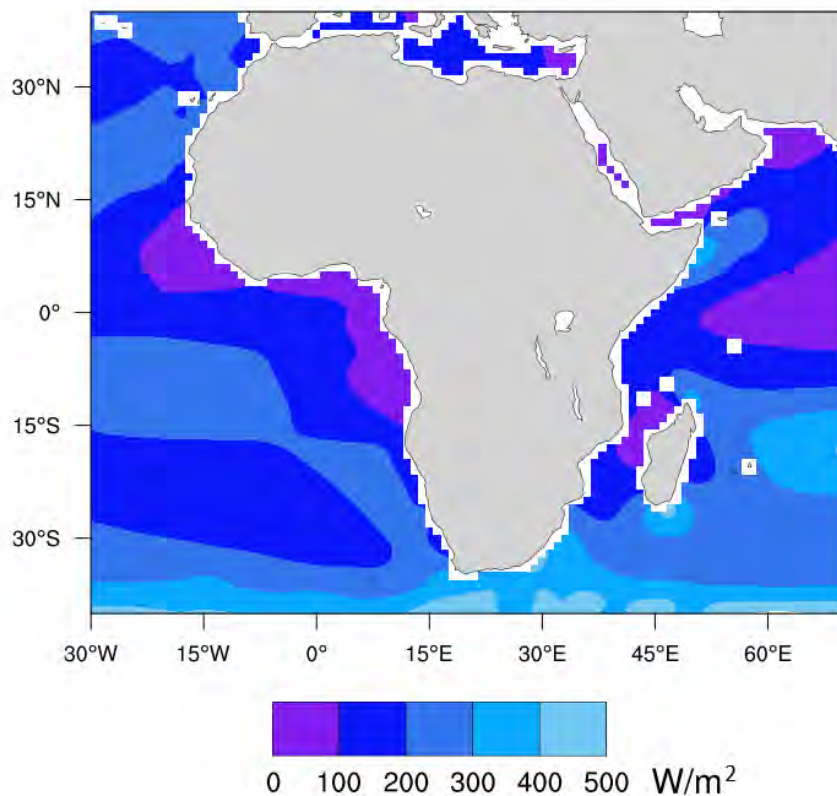


Figure 9. The African continent wind power density map for 1988 to 2007 using WindSat wind product dataset

2.6.3 South Asia

Similar WRA methods used in the studies for Africa have been carried out in South Asia aiming to investigate the EEZ of India. Nagababu et al. [93] has reported that there is 437 W/m^2 of wind power density at 80 m height in the Indian EEZ. The authors claim that investing in this area can supply 41% of the nation's annual energy requirement [93]. Extending past the Indian EEZ; Kulkarni, Deo, and Ghosh [94] studied the areas of the Arabian Sea and Bay of Bengal. They highlighted that at least 60% of the area, covered by both bodies of water, have WPDs that range from 250 W/m^2 to greater than 400 W/m^2 at the height of 80 m. Although India does invest in renewable energy, the country requires a policy to begin concrete offshore wind farm development and be implemented in its national energy planning [95]. Concerns with changes on government policies have been echoed by a later study of Kota, Bayne, and Nimmagadda [96]. The authors drew comparisons on the offshore wind development between UK, US, and India where they found that the learning experience in the UK could aid offshore wind development for the latter two nations. In that part of the world, even small island nations such as Maldives have potential offshore wind resource with power densities ranging from 72 W/m^2 to 104 W/m^2 at 10m level that could contribute in making the country self-sufficient in its energy needs [97]. This range of WPD values are also found in the climatological WindSat data

derived WPD as shown in Figure 10. The scope and breadth of research in the Indian subcontinent have covered the technical requirements and policies necessary for OWF projects in the region. In situ wind measurements like buoy observations must be deployed in the offshore areas identified to have good wind resource before proceeding with pilot testing offshore wind turbines.

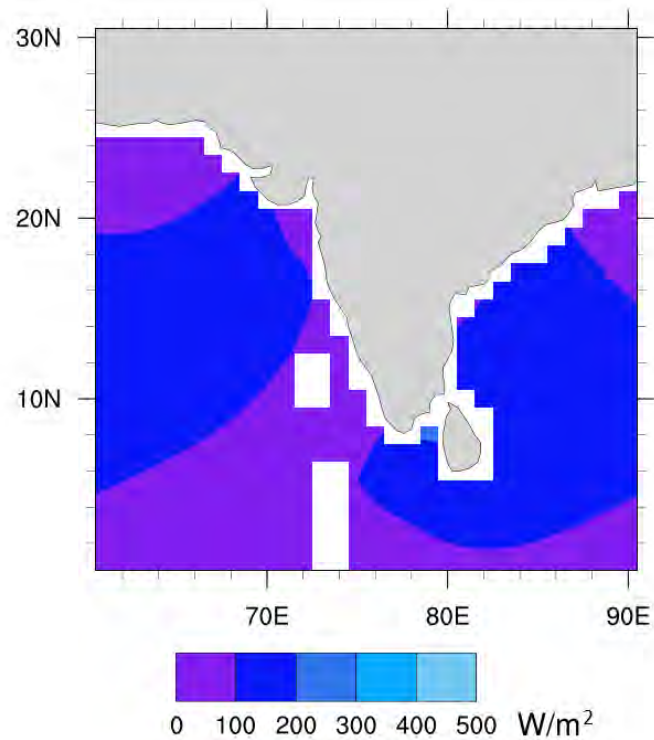


Figure 10. A generated wind power density map from 1988 to 2007 using WindSat data for the Indian subcontinent

2.6.4 East Asia

Offshore wind research is more active within the South China Sea, as evident from the deployments in China [65]. The first operational offshore wind farm outside Europe is found in Donghai Bridge [69]. Since then, the Chinese planned for other offshore projects that are currently under construction or in the commissioning phase [63], while other projects are being developed by Taiwan, Hong Kong, Vietnam, and Thailand. A study by Chang et al. [98] involved analysing the wind resource around the Hainan Island. Their results show that the surrounding waters of that island have 400 W/m^2 to 600 W/m^2 WPD at 100 m height [98]. A further investigation in the area was carried out by Liu et al. [15] in a larger study domain that included East China Sea and South China Sea covering the 29 wind farm sites. They were comparing the performance of different vertical wind profile methods under various atmospheric stability conditions so that they may find the suitable atmospheric vertical model for extreme and normal weather conditions [15]. A more recent study by Nie and Li [99] covered the entire coastal region of China that have water depth of less than 250m. Their research uncovered that the Southeast coasts of China have significant wind resource, especially

the Taiwan Strait where WPD that is greater than 900 W/m^2 can be obtained at 70m height. Such studies are necessary because coarse wind data resolution that is shown in Figure 11 does not suffice for the region due to the multiple islands that are relatively close to each other. This topographical layout produces a feature where coastal water regions overlap. Wind flows near the shore cannot be detected correctly by satellite instruments like radiometers thus, measurements made within such areas are deemed unreliable. Developments for offshore wind farms have been pushed forward in China because of the country's energy requirements and has influenced the marine functional zoning of its provinces near the coasts [100]. The zoning assignments that define how the marine environment is utilised in China has been studied by Ou et al. [100]. It was demonstrated that the coastal areas in China have offshore wind zoning in marine management policies, but must be improved through better marine siting methods development that enables optimal open sea area usage for offshore wind energy and other marine activities [100].

Due to having a greater wind resource potential, many studies have been carried out in the region of Taiwan with regards to offshore wind energy. One of these is the work on three offshore islands at the western part of Taiwan by Hsieh and Dai [101]. In their study, the authors employed both the Hilbert-Huang transform and the Fast Fourier transform in order to improve the statistical models used for characterising winds in terms of climate time scales in Taiwan and a tool for wind forecasting that is needed in reporting power production capacity outlook to the grid for operations [101]. A more comprehensive study on the wind resource at the western coast of Taiwan and the Penghu archipelago, which includes the three islands in the previous study, was carried out by Fang [102]. The results from that study yielded that the offshore area close to Taiwan's western coasts has a power density of approximately $1,000 \text{ W/m}^2$ while the offshore winds located in the region of Penghu can be greater than $1,400 \text{ W/m}^2$ at heights between 100m to 200m [102]. These findings have been reinforced by Chang, Yang, and Lai [103] in the western Taiwan offshore wind resource where they found for the 100 m level, the area has a power density of $1,079 \text{ W/m}^2$ to $2,665 \text{ W/m}^2$. The technical research in Taiwan is being complemented by reviews on government policies for offshore wind power development and technology development for patenting. In the perspective of acquiring patent portfolio for Taiwan; Chang, Fan, and Kao [104] analysed the available patents related to offshore wind technology that have been awarded to each country. They recommend that Taiwan should follow the lessons from China in pursuing patents for its offshore wind technology. With regards to policies, there are studies that conclude the necessity for a framework to nurture projects for offshore wind that incorporates experiences in Europe, social structure, public involvement, and proper marine area zoning [71,105,106].

In Hong Kong, a study on the wind profiles of the offshore islands of Waglan, Cheung Chau, and Sha Chau have been performed by Shu, Li, and Chan [107]. Their assessment showed that the lowest wind power density of 124.68 W/m^2 is found on Cheung Chau Island and the highest is located at Waglan Island with 275.29 W/m^2 . Shu et al. [108] concentrated at the Southeastern part of Hong Kong where they calculated the WPD based on the observations from an offshore platform. It was determined that the WPD at 27.8m height was $1,091.60 \text{ W/m}^2$ and at 160.8m was $1,811.60 \text{ W/m}^2$. Going beyond WRA for Hong Kong and into wind farm design, a few studies have been pursued by Renewable Energy Research Group (RERG) at the Hong Kong Polytechnic University on optimizing turbine layout for the case of a wind farm located in the Southeastern offshore area [109–111]. In these research, the group used multi-population genetic algorithm, and found that the total potential annual power production from the promising offshore sites may range from $39.14 \times 10^8 \text{ kWh}$ to $112.81 \times 10^8 \text{ kWh}$. All these research efforts [107–111] in the Southeastern marine area of Hong Kong should support the proposed 200 MW offshore wind project by CLP Power Hong Kong Limited located in that region [68,112].

The very active offshore wind energy research within the South China Sea comes from China, Hong Kong, and Taiwan. Their contribution to published literature is immense and has allowed them to propose OWF project sites and trial deployments [63,71]. Thus, the research efforts and learning experiences of these countries can be a model for other low latitude nations that are planning to develop their own OWF projects.

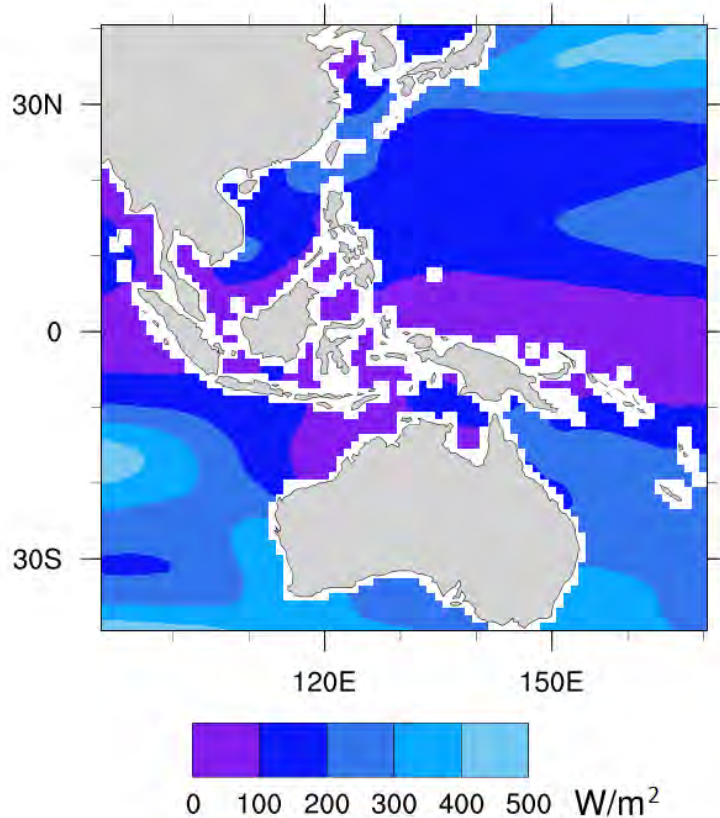


Figure 11. East Asia and Southeast Asia wind power density map from satellite observations of WindSat for the years of 1988 to 2007

2.6.5 Southeast Asia

In Southeast Asia, studies on Thailand offshore wind resource were carried out for the Gulf of Thailand [113,114]. One of the studies at Thaksin University have found that the Gulf of Thailand has an area of 3,500 km² that is appropriate for offshore wind development with a 15 TWh/year power production potential [113]. In another study by the same institution, a wind map for the Gulf of Thailand was generated and priority development sites were suggested for offshore wind plants [114]. Zheng et al. [115] surveyed the offshore wind resource in East China Sea and South China Sea where they discovered that the region of water in between Taiwan and Philippines has a rich wind resource throughout the year with around 300 W/m² average WPD at low heights of 10m. Vietnam is starting its offshore wind deployment in the region with a 99.2 MW wind farm in the Mekong Delta, and other planned upcoming projects in the area [65]. With a perspective of building a sustainable power grid for the entire Southeast Asia, the findings of Huber, Roger, and Hamacher [116] have shown that lower CO₂ emission targets would require the installation of onshore and offshore wind farms in the region. Potentially, these wind farm infrastructures can be built in Vietnam and Philippines because of their available potential wind resource and the power generated can be contributed to the grid. A later study by Ahmed et al. [117] stated that the Association of Southeast Asian Nations members possess

a high offshore wind energy potential that can be sourced for power generation. They listed Indonesia, Malaysia, Philippines, Thailand, and Vietnam as countries with potential offshore wind resource that have a combined power production of 76 TWh. All these WPDs determined in various works are summarised in Figure 12.

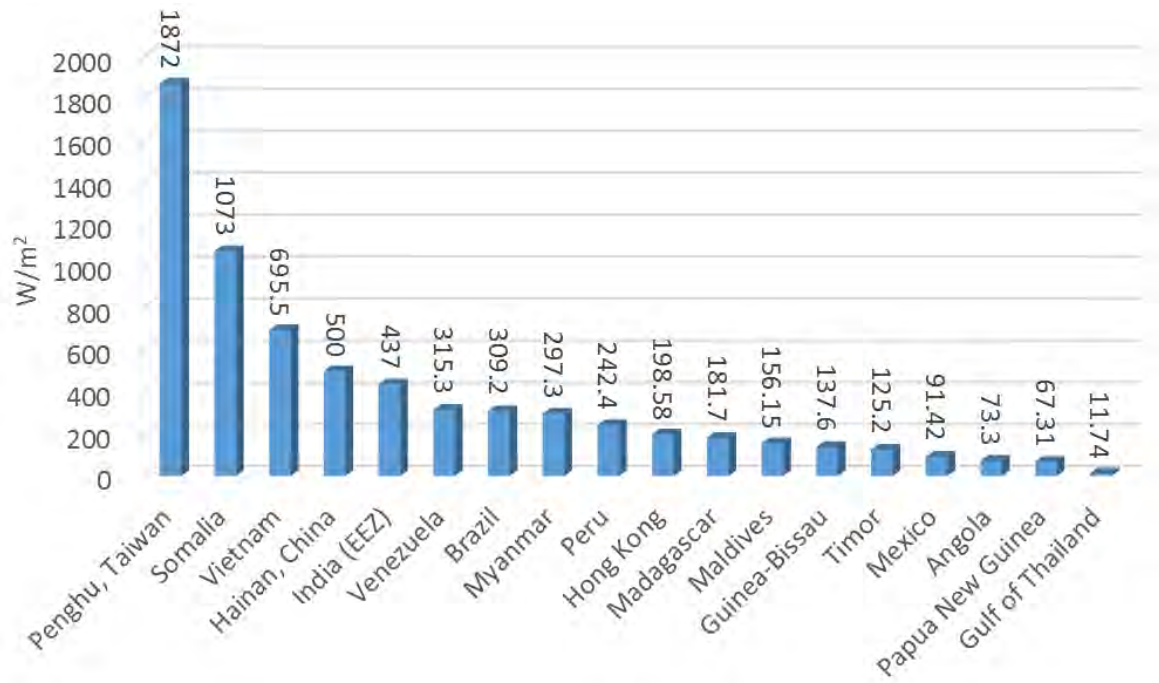


Figure 12. . Average wind power densities at 80m level for different low latitude locations

Based on all the cited offshore wind research in the low latitude region, it is apparent that it has a great energy resource potential for countries located there which can support a sustainable manner of economic development [21]. However, as the literature shows, a thorough wind resource assessment for offshore sites is necessary before proceeding with any offshore wind project. This is due to concerns with the marine environment which have to be better understood. One avenue where WRA can be improved as highlighted by Liu et al. [15] is the need for a better understanding of the atmospheric dynamics to produce an improved wind resource assessment of the region. As such, this concern for deeper comprehension of atmospheric dynamics in the region was reflected in a study for three offshore islands at the western part of Taiwan by Hsieh and Dai [101]. The authors attempted to improve wind modelling by utilizing nonlinear and nonstationary daily wind speed time series. Another room for offshore locations WRA improvement is considering sea conditions in the analysis. Nie and Li [99] carried out such an improvement through the incorporation of sea surface roughness in the computation of wind speeds at 70m and 110m height. Waves are also another parameter that can affect wind farm siting as stated by Liu et al. [118] who made wave simulations to characterize the sea waves as part of an offshore wind study for the South China Sea. Since there are many areas in the low latitude that have available offshore wind energy resource, applicable WRA techniques must

be identified in the context of the region and the succeeding section presents the available WRA found in the literature.

2.7 Techniques in Offshore Wind Resource Assessment

Many of the methods for offshore wind resource assessment have been adopted from onshore wind project developments. The use of wind measurements and analysis as well as wind simulations in the offshore WRA is very much the same for onshore ones. These have been implemented in many locations all over the world hence are applicable to low latitude parts of the globe. In this section, the various techniques employed for offshore WRA are reviewed.

2.7.1 Wind Observations and Wind Map Products

Published literature [114,119–121] have utilised wind data over the oceans from buoys, meteorological masts, ship observations, and satellite-mounted scatterometers. Performing analysis on these observations enable the researchers to generate wind resource maps. One of the widely used techniques for producing high quality wind resource maps is measure-correlate-predict (MCP) [11]. This was employed by Oh et al. [76] in determining the wind power potential at an offshore site in South Korea. Authors analysed the wind observations from a meteorological tower at sea in order to select the wind turbine class suited and the feasibility of the project based on the annual energy production (AEP) and capacity factor (CF) [76]. The use of wind observation masts was carried out in the 2016 Adriatic Sea study by Schweizer et al. [56]. Their analysis also considered wave data from buoys to complement the wind data in locating for a feasible offshore wind farm site in the Adriatic Sea. MCP method has been used for wind analysis and WRA in the low latitude region as listed in Table 3. As a guide, Table 3 lists the published research reviewed with details on the dataset or technique implemented and region of study are summarised in the table below:

Table 3. List of publications and dataset used for research within the low latitude region

Authors	Data	Study Area
Hsieh and Dai [101]	Weather Station Observations	Taiwan
Shu, Li, and Chan [107]	Weather Station Observations	Hong Kong
Nagababu et al. [122]	Scatterometer (OSCAT)	Indian EEZ
Ortiz and Kampel [84]	Scatterometer (QuikSCAT)	Brazil
Nagababu, Kachhwaha, and Saysani [123]	Reanalysis (ERA-Interim)	India
Nie and Li [99]	CCMP	China
Olaofe [92]	CCMP	Africa
Shu et al. [108]	LiDAR	Hong Kong
Chang, Yang, and Lai [103]	LiDAR	Taiwan

There are weather stations which are conveniently located on small offshore islands such as in Taiwan where Hsieh and Dai [101] studied the wind profiles of two islets in the Taiwan Strait and a further one to the North of Taiwan using the MCP technique. These small islets allow valuable wind

observations but averts the construction of expensive offshore platforms. Extending beyond the use of wind data on wind potential and wind project feasibility, both authors were able to study different wind farm design scenarios [56]. Similarly, offshore island weather stations were used by Shu, Li, and Chan who performed WRA for three islands in Hong Kong. The authors analysed the Weibull distribution of the wind data and determined that the Southeastern part of Hong Kong has potential for offshore wind farm development [107].

In other studies [82,97,124–126], remote sensing techniques were used, or in some cases, reanalysis data when in situ measurements were not available or insufficient for the requirements of the work to produce wind maps or for wind profile analysis. Although these can serve as substitutes to the actual ground measurement, validation of these data have been done and deemed necessary by researchers [121,127]. Studies have been undertaken to see the usability of such data in the absence of wind masts for offshore WRA, and it has been shown that it can serve as proxy data as long as the users know the limitations of such datasets [121,127]. A WRA for the Indian EEZ has used data from remote sensing by performing analysis with observation data from Oceansat-2 scatterometer (OSCAT) [122]. This allowed Nagababu et al. [122] to make wind classification on offshore sites surrounding India, and to identify the well-suited areas for offshore wind development. Another scatterometer dataset from QuikSCAT was used by NREL for the determination of global WPD at 10m height to define a wind classification scheme [128]. Ortiz and Kampel [84] also utilized QuikSCAT data when they studied the whole offshore region of Brazil, and they analysed the observed data from August 1999 until December 2009 with a spatial resolution of $0.5^\circ \times 0.5^\circ$. They were able to characterize the offshore winds in Brazil at 80m level with their method and can support the siting for the proposed Asa Branca project mentioned by Rodrigues et al. [63] in their review. Studies that combine several satellite data from scatterometers (ASCAT and QuikSCAT) and radiometers (WindSat) have been reported by Guo et al. [119]. They have demonstrated a better approximation of available wind resource as validated by buoy data in their findings.

In the literature, global or regional scale wind resource assessment has been carried out using reanalysis wind data from institutions such as the European Centre for Medium-Range Weather Forecasts (ECMWF), the National Centers for Environmental Prediction (NCEP) and National Center for Atmospheric Research (NCAR). One of such study by Zheng et al. [42] over the South China Sea region where they classified the wind power based on the NREL classification levels and segregated the temporal portion according to seasons [42]. The use of reanalysis data has also been utilised for determining the feasibility of wind projects on the coasts of the Indian sub-continent [123]. Nagababu, Kachhwaha, and Savsani [123] used European Reanalysis-Interim (ERA-Interim) data and implemented a geospatial information system (GIS) method to identify the offshore wind potential and potential

project investments. ERA-Interim data have also been used by Zheng et al. [53] to improve the technique of global wind classification by using the Delphi method, and they deemed that their new method is better than determination of WPDs through the analysis of QuikSCAT or CCMP datasets. A more sophisticated dataset called Cross-Calibrated Multi-Platform (CCMP) Ocean Surface Wind Velocity Project, which combines reanalysis data with microwave-based sensors from satellites, has been used for offshore wind resource studies as well [99,121]. The CCMP data enabled Nie and Li to study the offshore wind resource availability of the coastal seas along China, and determine that the locations of good sites for offshore wind power production are along the shores of Taiwan Strait [99]. Olaofe [92] also used CCMP data in producing wind resource maps for the entire African continent with a $0.5^\circ \times 0.5^\circ$ spatial resolution. Another remote sensing measuring technique using the light detection and ranging (LiDAR) was conducted for wind profiling in Hong Kong [108]. In this method, the LiDAR instrument was mounted on an offshore platform situated in Clear Water Bay, and the LiDAR measurements were compared with the meteorological mast on the same platform. Since the LiDAR data correlates well with the wind measurements from anemometers mounted on the mast, they were able to characterise the winds over the platform that included turbulence intensity. This measurement technique, in addition to tidal and buoy observations, was also carried out by Chang, Yang, and Lai [103] in their study of the West coast of Taiwan. The authors used LiDAR wind observations over the Miaoli and Tainan regions to determine the wind energy resource available in those areas.

The mentioned datasets in this section allowed many studies on offshore wind potential for different locations on the planet. Table 2 lists the details of the methods and locations where each technique has been applied for WRA. However, there were cases when high spatial and temporal resolutions were needed for WRA or there was a lack of data to perform the WRA. Additionally researchers have used computer simulations to produce wind models that address the requirements for fine resolution and wind data generation for analysis.

2.7.2 Wind Modelling

There are different scales in modelling the wind which are classified as mesoscale and microscale [19,129]. Mesoscale models are useful for preliminary WRA where coarse spatial resolution wind profile maps that have 100 km grid scales are needed [129]. Upon determination of promising locations identified from the coarse resolution maps, microscale models are necessary for wind turbine micrositing because of the fine spatial resolution wind maps that they generate within a 10 – 20 km² area [129].

2.7.2.1 Mesoscale Models

Usage of wind simulations for the study of offshore wind resource is being undertaken in many published research. Ayotte [130] noted that there has been constant development for high resolution calculations involving complex geometries on meteorological models. These improvements in meteorological models made numerical weather predictions (NWP) to be utilisable for WRA. Along with these enhancements, simulation accuracy has become better because of the rapid progress in computing technology that permits higher spatial and temporal resolutions, as well as complex algorithms processing [131]. An example of WRA using wind simulations is the Global Wind Atlas [132] that can be seen in Figure 13. This wind map is generated through the utilisation of 70-km coarse spatial resolution reanalysis data as mesoscale model input then, downscales them to a finer 1-km spatial resolution.

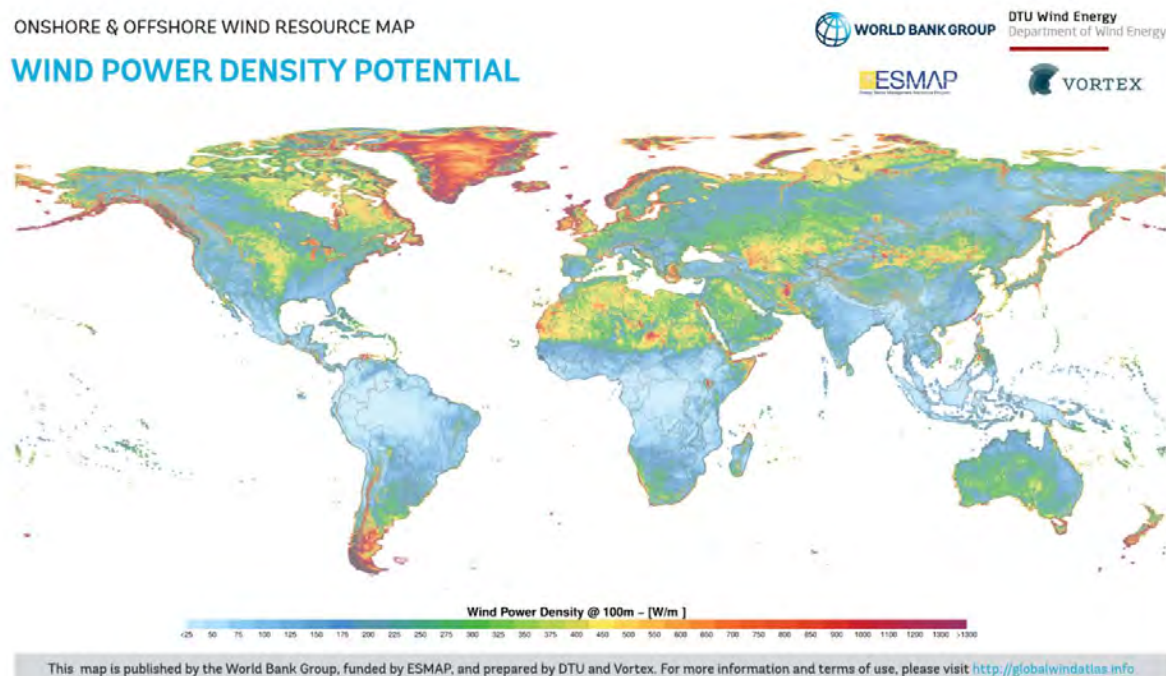


Figure 13. Global wind power index that includes open waters from coastline to 30 km distance of land masses at 100 m above ground level [132]

Such techniques may benefit from the fine resolution datasets that produce improved results from the next generation reanalysis which have smaller grids than prior datasets like the ECMWF Reanalysis 5 (ERA5) in Figure 14. These datasets have higher spatial resolution since it has improved from a 80km resolution in ERA-Interim into 31km resolution with the ERA5 [133].

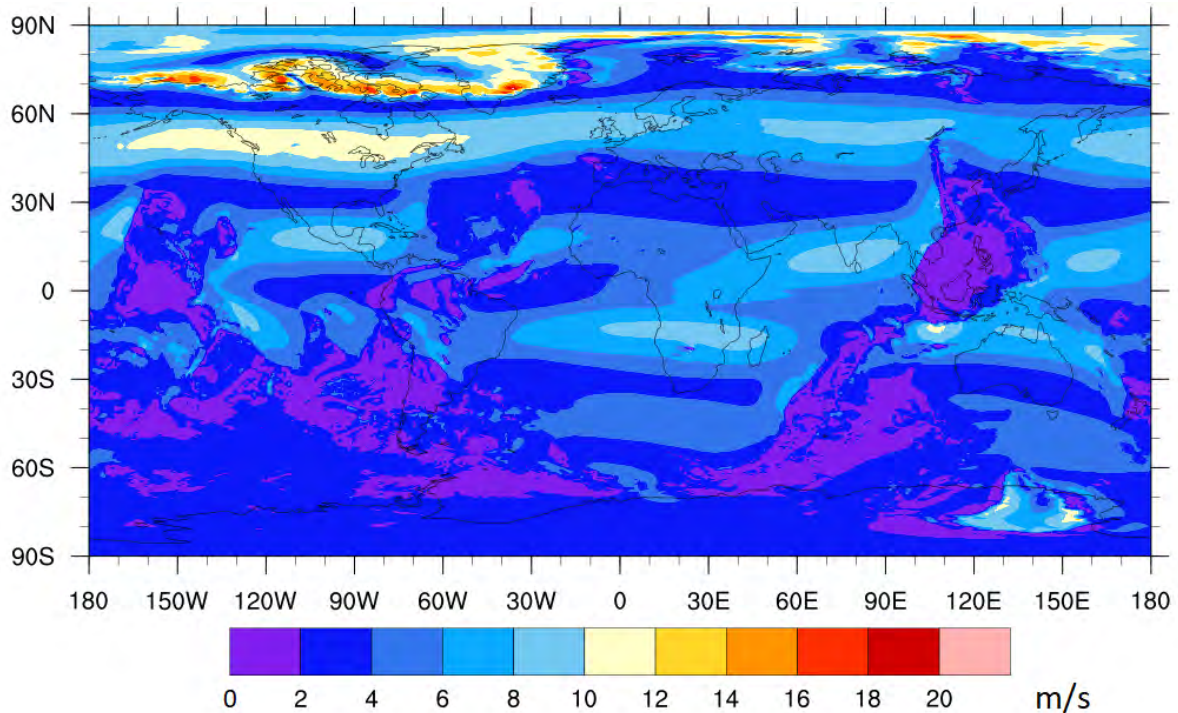


Figure 14. Global wind speeds that includes open waters from ERA5 simulations at 100 m above ground level for the years of 1979 to 2018 [133]

A review on the role of NWP in WRA by Al-Yahyai et al. [134] stated that observations have coarse spatial resolutions that require high cost investments in equipment and operations. The authors also pointed out that the recommended practice for wind observations require different vertical levels for measurements, and long observation periods making wind analysis for assessment studies an expensive endeavour. These costs can be averted by using NWP models that is able to yield high spatial resolution wind vectors with multiple atmospheric layers with the only cost incurred is the system used for the simulation [134]. By being less expensive than actual meteorological mast deployment and offering good quality data, NWP is being increasingly utilised for offshore wind research.

Various researchers [20,114,135] used NWP involving WRA where they compared the simulation results with actual measurements or assimilated wind data to improve the model output. When wind observations are lacking, data obtained through remote sensing and reanalysis data were used for comparison or as model inputs for the NWP. In a similar manner, reanalysis data and remote sensing techniques of measurement have been found to be applicable in offshore WRA. A study by Carvalho, Rocha and Gomez-Gesteira [20] employed NWP to simulate winds over the seas off the Iberian Peninsula coasts. Different reanalysis data was used to drive the Weather Research and Forecast (WRF) model which was validated with buoy wind data. Their results showed that using ERA-Interim as an input gave adequate results for offshore WRA [20]. Following this, Carvalho et al. [18] evaluated the performance of scatterometers and found that WRF simulations performed better than

other databases when studying the open seas [18]. Using a different NWP model, Lima et al. [85] used the Regional Atmospheric Modeling System (RAMS) analysed dry and wet seasons with consideration of the La Niña and El Niño phenomena in Brazil. The authors compared their wind simulations with state meteorological tower data and found that the RAMS model yielded adequate output upon validating with the 60.4m height level [85].

To determine the WRA of the seas surrounding India, a general circulation model (GCM) and a regional climate model (RCM) were analysed by Kulkarni, Deo and Ghosh [94] with reanalysis data employed for the validation. The authors used ERA-Interim, NCEP/ NCAR Reanalysis Project (NNRP), and Climate Forecast System Reanalysis (CFSR) where it was determined that the results from the Coordinated Regional Downscaling Experiment (CORDEX) RCMs were not necessarily better than their primary source GCMs. Similar WRA methods have also been carried out in other publications that studied the wind resource availability within the South China Sea region. These publications include the study of Chang et al. [103] who reported on WRF and assimilated satellite-based data into the model to determine the wind resource around Hainan Island. Offshore WRA for the Gulf of Thailand was simulated using WRF in the work of Chancham, Waewsak and Gagnon [114] where they downscaled NCEP/NCAR Reanalysis II (R2) data to obtain 9-km spatial resolution wind maps. Downscaling reanalysis data using NWP can yield improved WRA because of smaller grid resolution compared to the original reanalysis data set. However, they have limits in resolving physical dynamics that occur in less than 1 km resolution or a fraction of a second [136]. To perform wind modelling in fine spatial resolutions at short time scales, it is necessary to employ microscale models to effectively simulate the wind conditions.

2.7.2.2 *Microscale Models*

Although NWP can be useful for WRA, it has limited capabilities in simulating very high spatial and temporal resolutions [136–138]. NWP models are not designed to simulate wind flows in spatial scales that are less than 1 km, because the included turbulence model are incapable to model in very fine scales [139]. Therefore, linear models or flow models are commonly used for microscale or localized WRA [19,102,140]. This is the approach that Fang [102] applied for the 2001 WRA study in Taiwan. Fang mentioned that the Mesoscale Model ver. 5 (MM5) was used as the NWP for generating wind maps for the Taiwan. They reported that the open seas over the western side of the country have good wind potential. To make an improved local WRA in the Western Coast of Taiwan, Fang used a linear model called the Wind Atlas Analysis and Application Program (WASP). The author was able to simulate with a resolution of 100m using WASP exceeding the capabilities of NWP models. The

WASP software was also used by Chang, Yang and Lai [103] in examining the Taiwan West Coast but incorporating buoy and LiDAR data into the simulations.

A more sophisticated model using computational fluid dynamics (CFD) has wide applications for offshore wind technology that can be used for turbine component analysis and wind farm layout design [141]. CFD was used in the analysis of offshore wind farms as reported by Castellani et al. [142] where the wake effects for the Sexbierum wind farm in the Netherlands were investigated using the WindSim CFD model. Published literature by Yan and Li [140] used the ANSYS Fluent CFD model that was configured for the Reynolds Averaged Navier-Stokes (RANS) turbulence model to simulate the winds over Cheung Chau Island, Hong Kong which is a small offshore island. Their results were validated with wind tunnel experiments and data from the island's weather station. The CFD model had an 8% mean deviation to the average wind speed values of the actual wind data. This was deemed to be satisfactory by the authors and demonstrated that using both CFD simulations and actual wind measurements can generate high resolution wind maps with at least 20m per grid for WRA in complex terrain [140]. Another study that used CFD was the WRA for Mauritius by Dhunny, Lollchund and Rughooputh [143]. WindSim was utilised to solve the RANS equations for wind simulations. The generated results were validated with meteorological mast data that has four levels for wind observation, showing that the highest percentage error for the CFD model was 9.92% at the 33m level while the lowest was 1.48% at the 135m level. The authors concluded that WindSim enabled the production of accurate wind maps for Mauritius, and identified the feasible areas for wind farms which are located in the Southeast coast, lower central plateau, and Southwest regions [143]. Although CFD offers very high spatial resolution simulations for wind flow in comparison to NWP and linear models, its use must be properly tested on the study area before meaningful results can be obtained [137,144,145]. There are other extensions to WRA where CFD has been used as highlighted by Chancham, Waewsak, and Gagnon [114] where WindSim was used for the wake loss analysis of potential offshore wind farm layout design in the Gulf of Thailand. Furthermore, studies on wind and wave interaction may find CFD models to be useful as reported in Yao et al. [146] and Jiang and Chen [46], for future work because these types of models are able to incorporate the surface roughness introduced by waves to winds and the generation of waves from winds.

It can be concluded that there has been extensive use of NWP in different parts of the world for offshore wind research. Such an approach despite its limitations was found to be useful for areas that lack in situ observations [18]. In addition to that, NWP offers a solution that can avoid high capital expenditure associated with the deployment of offshore meteorological masts. Refinements to the NWP is necessary to allow it to adjust in accordance to local atmospheric conditions and input data such as the initial and boundary conditions dataset and marine atmospheric boundary layer [147–

151]. Even when wind mast data are available, NWP can complement the observed data for WRA [134]. Although NWP have coarse spatial resolution results, they are important for preliminary assessment and their simulation outputs can be improved using linear models or CFD in order to produce a better WRA [19,102,136].

NWP are based on the concepts of atmospheric science and the CFD models applied to WRA are also incorporating the characteristics and dynamics of the atmosphere. Thus, a discussion of atmospheric science is necessary to gain a better understanding of these models. These principles of atmospheric science and mathematical methods of the models are the topics for the next chapter.

2.8 Summary

Any wind farm development must begin with a precise and thorough WRA [11]. This is the essential and initial step in order to determine the wind profiles of areas. The wind profiles allow the determination of potential wind farm sites that are suited for wind farm development in order to ensure the success of wind farm projects.

WRA methods for onshore wind farms have been applied for offshore wind applications but the techniques prove to be more difficult because of deployment cost and maintenance of offshore meteorological platforms for wind observations [99]. In the context of small island countries and developing nations, such methods may limit offshore wind developments because the investments needed to perform WRA using the in situ methods introduces risks to any proposed offshore wind farm development. An alternative would be to use numerical modelling in order to generate wind maps for initial WRA that can facilitate wind energy prospecting [18].

Employing NWP has been done as an alternative WRA method to direct measurements. A mesoscale model is used to see the large-scale and long-term wind patterns over the study area while the CFD model is utilised for fine spatial resolution and short-term wind profiles. The two models are coupled for this study in order to generate monthly and daily wind patterns over the area of interest. This coupling is through the usage of mesoscale model results as input data for the microscale model simulations.

This research sought to seek a WRA method in offshore locations for low latitude regions and small island nations as these places would benefit from offshore wind power generation to address their energy requirements. Since there are limited data, the method must be able to produce high resolution wind maps that will serve as initial WRA. In the course of the literature review, it has been determined that NWP are capable of high spatial resolution data [99]. NWP are also a good substitute to wind characterisation if actual measurements are not available [18]. Thus, a mesoscale model has been chosen to perform wind simulations for this study.

3 METHODOLOGY

In this chapter, the method used in doing WRA based on the literature are discussed. The modifications and extensions of the methods gathered from the literature review in Chapter 2 are also presented here. The theoretical background of the models as well as their internal structure are to be discussed in this chapter.

3.1 Study Area

This study is focused on generating a WRA for Palawan, Philippines using NWP method. It has been selected because preliminary onshore WRA for the Philippines has shown that the province has good potential for wind energy development [16], it is composed of several small islands within the low latitude region, and good quality but short-term in-situ offshore wind measurements [152,153] have been done in the area. Since it is in the Philippines, the Asian monsoons affect the region in terms of its seasons [152,154]. The Philippines is influenced by the Northeast Monsoon from October to March which is characterised by dry and cold air that are coming from the main Asian continent [154,155]. The winds during Northeast Monsoon is strong in the months of January and February [154]. There is a shift in the season into a hot-dry one in April and May when the winds are coming from the East. These winds are blowing from the Pacific Ocean and are called Easterlies [155]. Another transition in the season happens that starts in June and ends in September which is the effect of the Southwest Monsoon [151,152]. This is characterised by winds coming from the Indian Ocean which travels across the Indochina Peninsula and arrives at the Philippines. The season is warm and wet while winds are weaker because the Indochina Peninsula slows down the winds that reaches the Philippines since it is situated downwind of the entire peninsula [154].

Palawan Island is located at the western part of the Philippines and it is in between the South China Sea and Sulu Sea. This island is a province of the Philippines where the capital is called Puerto Princesa. Figure 15 shows the location of the island within the Philippine archipelago. It is a popular tourist destination for its beaches and the underground river. There are several fishing ports around the island since fishing is one of its major industry. Given the economic activity on the island, it is suffering from an energy crisis [156,157]. Around 60% of the province have no electricity at all and areas that do, experience brown outs or black outs that can last for 10 hours every day [156]. An offshore platform is also located at the west side of this island for gas production but this is not used for energy by the island [156]. Thus, it relies on independent power producers that ship diesel and bunker oil fuels into the island to generate electricity [156,157]. Similar situation is true for the other islands in the Philippines that is why Palawan is the focus of the study in order seek for a WRA method that can be replicated to other sites. Palawan has also been selected as the study site since the island

has shown that it has a good wind resource [16]. Another reason for studying the waters around Palawan Island is because the South China Sea has been found to be rich in wind resources [15].

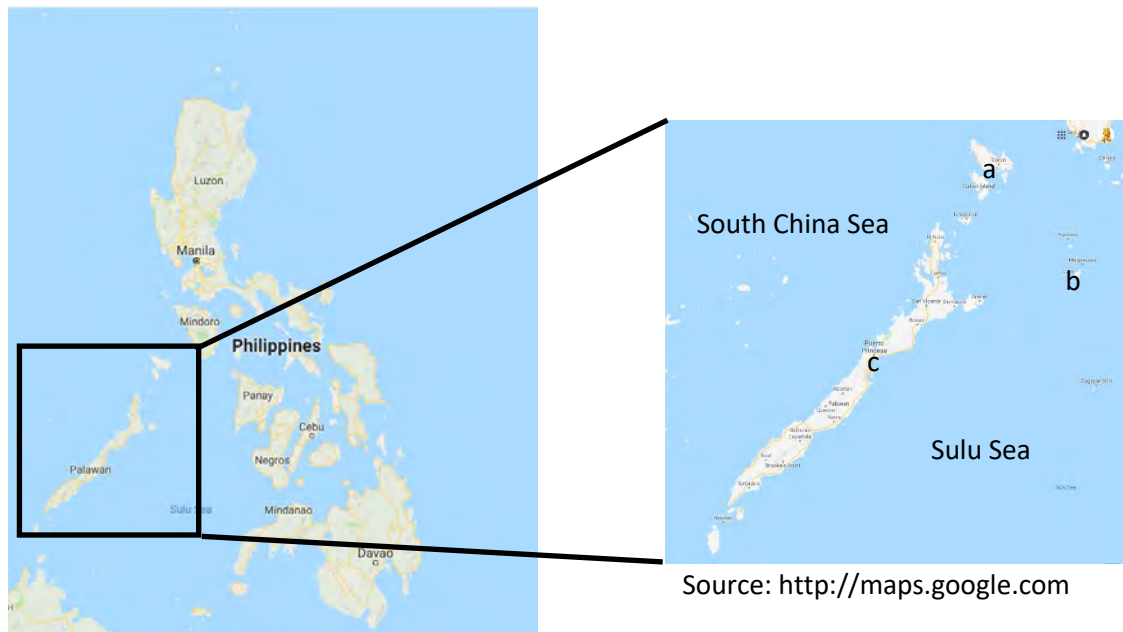


Figure 15. Map of Philippines and Palawan Island. The weather station is located within (a) Coron Island, (b) Cuyo Island, and (c) Puerto Princesa City.

The study used 2010 to 2012 weather station observation at Coron, Cuyo, and Puerto Princesa for validation of the NWP. This station is maintained by the Philippine Atmospheric, Geophysical, and Astronomical Services Administration (PAGASA) which is the official weather bureau of the country. The wind observations are done at 10 m above ground level using a cup anemometer and a wind vane. Coron Island (12°N , 120.20°E) is located at the northern part of Palawan Province which is between the South China Sea and Sulu Sea. Cuyo Island (10.85°N , 121°E) is situated in the Northwest region of the said province and within the Sulu Sea. The site for the Puerto Princesa station (9.74°N , 118.73°E) is beside the city's airport where the immediate vicinity is surrounded by suburban area. This location is a small peninsula that is facing the Sulu Sea and the city proper is towards North. The validation of the model uses onshore wind observations, despite the study focuses on offshore WRA, in order to determine the NWP configuration settings appropriate for the study area since the ground-based observations have long-term data available. The wind simulation results from the best performing NWP settings will be used as input data to the CFD simulations.

To establish the suitability of NWP, the offshore wind observations from the 7 Southeast Asian Studies (7SEAS) aerosol research cruise will also be utilised for validation. For interests in tropical meteorology phenomena and aerosol transport, this island had been selected for the 7SEAS research cruise in 2011 and 2012 [152,153]. Upon reviewing the meteorological parameters measured on the

research cruise, it has been deemed that the wind measurements can be used for preliminary offshore WRA around Palawan.



Figure 16. The ship made observations at the locations marked by numbers on the zoomed in map. These sites are 1. Guntao Islands, 2. Notch Island, 3. Tubbataha Reef, and 4. Balabac Island

Wind observations in 2011 and 2012 aboard the ship for the aerosol research cruise, that was part of the 7SEAS programme, were processed to validate the NWP. The locations chosen to be included for this validation are found in Figure 16. The 5-minute interval wind observations were recorded at 10 m above sea level using a Campbell sonic anemometer [152]. Based on the continuity of wind observations, the chosen sites for validation are the Guntao Islands, Notch Island, Balabac Island, and the Tubbataha Reef. The 2011 campaign happened in September which covered the Guntao Islands and Notch Island [152]. For the 2012 campaign, Balabac Island and Tubbataha Reef were the additional sites and the mission was done on the month of September also [153]. Guntao Islands (11.12°N , 119.26°E) and Notch Island (10.97°N , 119.24°E) are located at the northern part of Palawan Province that faces the South China Sea. Tubbataha Reef (8.85°N , 119.92°E) is situated Southeast of Palawan and within the Sulu Sea. Balabac Island (7.86°N , 116.94°E) is at the southern tip of Palawan and close to Borneo.

3.2 Concepts of Atmospheric Science

Atmospheric Science is the study of the Earth's atmosphere that encompasses the physical dynamics and chemical processes. It is classically known as meteorology. The physical dynamics of the atmosphere are based on thermodynamics and fluid mechanics [158]. Thermodynamic parameters of the air such as temperature, pressure, and density are necessary to define the state of the atmosphere. Differences in the thermodynamic parameters set the air into motion which obeys fluid mechanics. This fluid motion is commonly known as wind which enables energy and chemical transport in the atmosphere. This transport will influence the thermodynamic state of the atmosphere and may strengthen or weaken the winds. Hence, it is a complex interaction between thermodynamics, fluid mechanics, and chemical reaction. This chapter will focus on the thermodynamics and fluid mechanics of the atmosphere since atmospheric chemistry is mostly studied for air quality and radiative transfer research. Before proceeding further, some conventions are to be defined first.

3.2.1 Atmospheric Coordinates and Conventions

Before proceeding to the models used in the study of WRA, some basic concepts about the atmosphere are necessary. The Cartesian coordinate system x, y, z are translated as E-W, N-S, and altitude. Wind vectors are expressed as U, V, W which corresponds to E-W, N-S, and Up-Down. Wind direction follow the bearings in navigation convention. Thus, 0° means the wind is coming from North, 90° means wind is from the East, 180° means the wind comes from South, and 270° is when the wind is from the West. These are visualised in the following diagram:

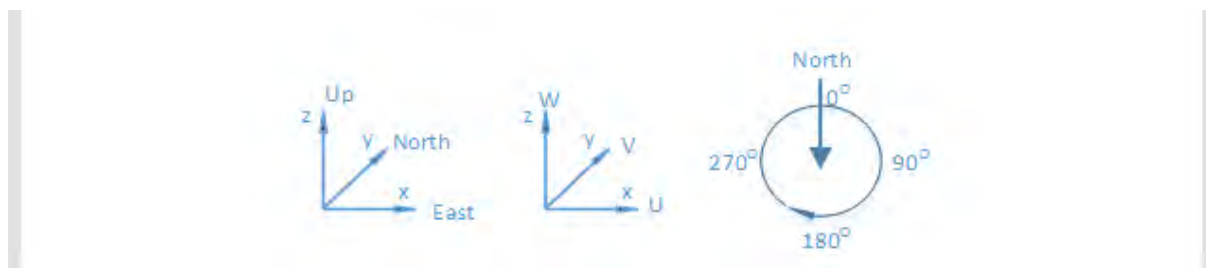


Figure 17. Coordinates and conventions in atmospheric science

The frame of reference in analysing fluid dynamics must be introduced at this point. There are two essential frame of reference which are Eulerian and Lagrangian. Eulerian frame of reference is a point of observation that is stationary on the Earth's surface. On the other hand, Lagrangian frame of reference do not have a fixed location in space and follows the designated air under observation as it travels in space.

Some quantities must be defined to facilitate discussion before proceeding to characterise atmospheric parameters. The acceleration of a body due to gravity decreases as it goes to higher altitudes. To make the value of gravitational acceleration constant when analysing the atmosphere, it is convenient to introduce a term called the geopotential height, H . This can be expressed as [158]:

$$H = \frac{R_0 z}{R_0 + z} \quad (1)$$

Where $R_0 = 6356.766\text{km}$, z is the geometric height

Another quantity that is used in atmospheric science is called the air parcel. This is the basic block that is composed of air molecules grouped together. This block is the portion of an air packet that is unaffected by external turbulence that tends to mix different air packets together. In the atmosphere, occurrence of turbulence are manifested by eddies. These eddies are responsible in mixing the difference in atmospheric parameters like pressure, humidity, temperature, and momentum so that the final state of the air is the average of all the parameter values. Heat energy input to the atmosphere is from the radiation emitted by the Sun. This energy influences the temperature and humidity changes on the Earth's surface radiative heating in the daytime and infrared radiated out to space at night.

3.2.2 Layers of the atmosphere

The atmosphere is composed of several layers and they are the following (from highest to lowest) [158]:

- Exosphere at about $(500 \text{ to } 10^3) \text{ km} \leq z$
- Thermopause or Exobase at $z = 500 - 10^3 \text{ km}$
- Thermosphere for $84.9 \leq H \leq (500 \text{ to } 10^3) \text{ km}$
- Mesopause at $H = 84.9 \text{ km}$
- Mesosphere when $47 \leq H \leq 84.9 \text{ km}$
- Stratopause at $H = 47 \text{ km}$
- Stratosphere for $11 \leq H \leq 47 \text{ km}$
- Tropopause at $H = 11 \text{ km}$
- Troposphere when $0 \leq H \leq 11 \text{ km}$

There is a layer within the Troposphere that is of special interest to atmospheric science. The layer is called the atmospheric boundary layer. This is the part of the atmosphere that is highly influenced by the Earth's surface such as introducing drag to winds and heating of its air during daytime and cooled at night. This is the layer that is very turbulent because of the interactions with the surface of the Earth.

3.2.3 Atmospheric Parameters for Thermodynamics

Thermodynamic parameters vary vertically among the different layers of the atmosphere. Pressure can be expressed by the following relation [158]:

$$P = P_0 e^{-(a/T)z} \quad (2)$$

Where $P_0 = 101.325 \text{ kPa}$, $a = 0.0342 \text{ K/m}$, and z is height

In the study of the atmosphere, pressure may be used as the substitute for height because of the one-to-one correlation of altitude to pressure value.

Similarly, the density can be expressed in the following equation [158]:

$$\rho = \rho_0 e^{-(a/T)z} \quad (3)$$

Where $\rho_0 = 1.2250 \text{ kg/m}^3$, $a = 0.040 \text{ K/m}$, and z is height at $T = 288\text{K}$

Although temperature varies with height as well, it is more complex than the other two thermodynamic parameters. Now, the variation of temperature along the vertical depends on the particular layer of the atmosphere because the solar heating from short-wave radiation affects each layer differently. Below is a diagram that shows the vertical profile of temperature along with the different atmospheric layers:

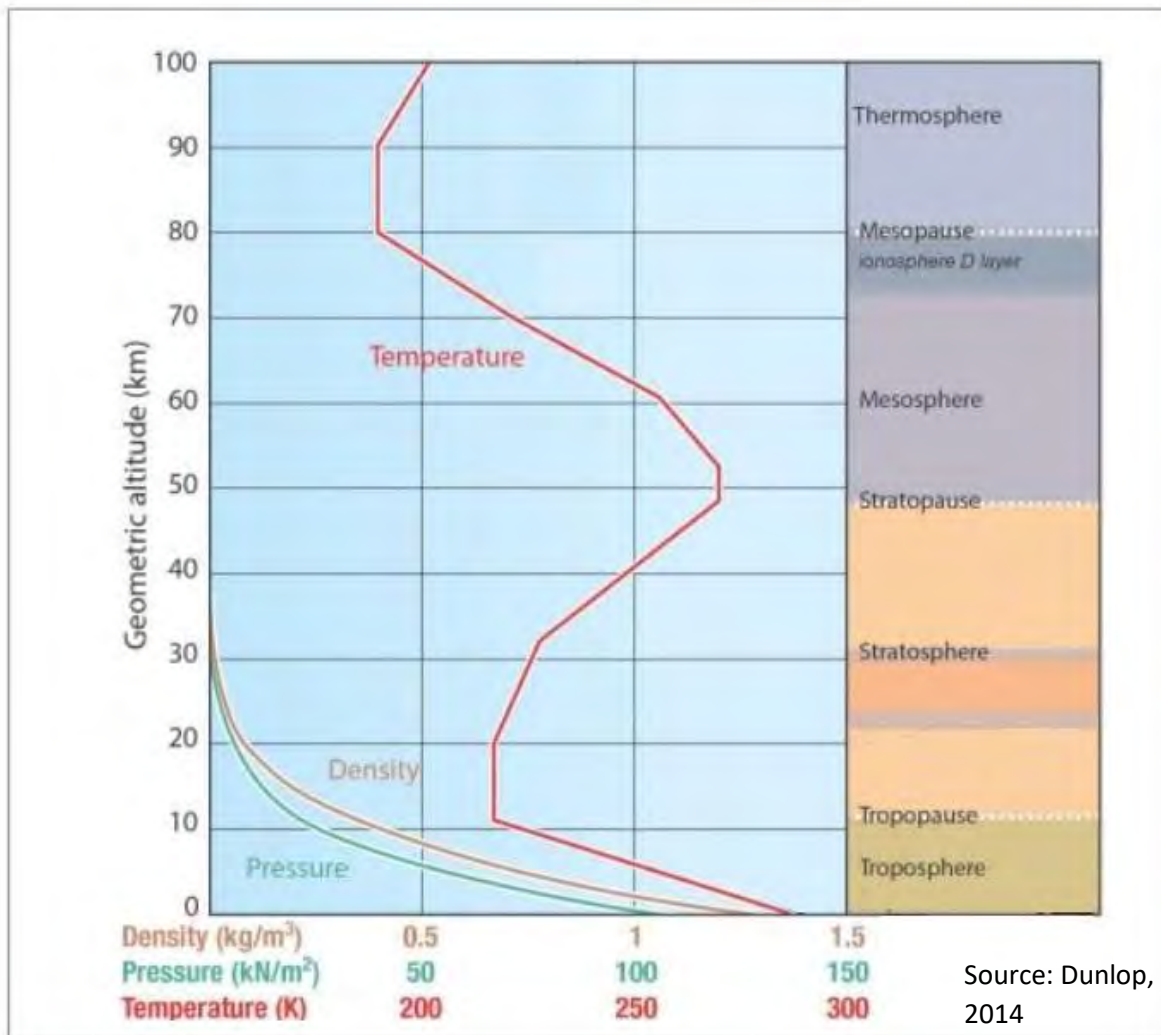


Figure 18. Vertical profile of temperature, pressure, and density in the atmosphere [159]

The temperature profile in the figure above can be expressed with the equations enumerated below:

$$T = 288.15 \text{ K} - (6.5 \text{ K/km}) \cdot H \text{ for } H \leq 11 \text{ km}$$

$$T = 216.65 \text{ K when } 11 \leq H \leq 20 \text{ km}$$

$$T = 216.65 \text{ K} + (1 \text{ K/km}) \cdot (H - 20 \text{ km}) \text{ at } 20 \leq H \leq 32 \text{ km}$$

$$T = 228.65 \text{ K} + (2.8 \text{ K/km}) \cdot (H - 32 \text{ km}) \text{ for } 32 \leq H \leq 47 \text{ km}$$

$$T = 270.65 \text{ K when } 47 \leq H \leq 51 \text{ km}$$

With the above temperature relations, the pressure values along the vertical of the atmosphere can be made more accurate by substituting them to the exponential pressure expression.

The results are listed as follows:

$$P = (101.325 \text{ kPa}) \cdot (288.15 \text{ K}/T)^{-5.255877} \text{ for } H \leq 11 \text{ km}$$

$$P = (22.632 \text{ kPa}) \cdot \exp[-0.1577 \cdot (H - 11 \text{ km})] \text{ when } 11 \leq H \leq 20 \text{ km}$$

$$P = (5.4749 \text{ kPa}) \cdot (216.65 \text{ K}/T)^{34.16319} \text{ at } 20 \leq H \leq 32 \text{ km}$$

$$P = (0.868 \text{ kPa}) \cdot (228.65 \text{ K}/T)^{12.2011} \text{ for } 32 \leq H \leq 47 \text{ km}$$

$$P = (0.1109 \text{ kPa}) \cdot \exp[-0.1262 \cdot (H - 47 \text{ km})] \text{ when } 47 \leq H \leq 51 \text{ km}$$

Since the temperature and pressure are known, the atmospheric density can be determined at any level using the Ideal Gas Law relation because the gases that comprise the atmosphere obeys it.

An atmospheric relation that is found to be important is called the hydrostatic equilibrium. This is a condition where the pressure that pushes an air parcel up and the gravity that pulls it back to the ground are equal. This is expressed by the following equation:

$$\frac{\Delta P}{\Delta z} = -\rho g \quad (4)$$

This is the vertical motion that influences the atmosphere since the pressure at low altitudes have higher pressure than the ones above while gravity is highest close to the ground and decreases as one goes up the atmosphere. The state of equilibrium is what determines the stability of the atmosphere. The stability shows if the atmosphere is turbulent or not based on parameters such as temperature, humidity, and wind along the vertical. There are three stability characteristics which are enumerated below:

1. Unstable - the air is turbulent or becoming turbulent
2. Stable - air is laminar or becoming laminar
3. Neutral - air flow conditions will persist or remain the same.

3.2.4 Equations of Motion

Winds are generated by differences in pressure in the atmosphere. The tendency to balance out the atmospheric pressure causes air to flow. The flow is from high pressure to low pressure regions of the atmosphere. The main driver for this air flow is called the pressure gradient force but there are other contributors that enable the motion. These are expressed below [158]:

$$\frac{F_{x\ net}}{m} = \frac{F_{x\ AD}}{m} + \frac{F_{x\ PG}}{m} + \frac{F_{x\ CN}}{m} + \frac{F_{x\ CF}}{m} + \frac{F_{x\ TD}}{m} \quad (5)$$

Where the subscripts denote the forces from advection (AD), pressure gradient force (PG), centrifugal force (CN), Coriolis force (CF), and turbulent drag (TD).

$$\frac{F_{y\ net}}{m} = \frac{F_{y\ AD}}{m} + \frac{F_{y\ PG}}{m} + \frac{F_{y\ CN}}{m} + \frac{F_{y\ CF}}{m} + \frac{F_{y\ TD}}{m} \quad (6)$$

Each term will be derived and discussed in the following sections. When making an observation at a stationary point (Eulerian), air parcels that passes through that point can contain a momentum value. These moving air parcels can transfer varying momentum values from winds. This phenomenon is called advection and it is shown in the following equation:

$$\frac{F_{x\ AD}}{m} = -U \frac{\Delta U}{\Delta x} - V \frac{\Delta U}{\Delta y} - W \frac{\Delta U}{\Delta z} \quad (7)$$

$$\frac{F_{y\ AD}}{m} = -U \frac{\Delta V}{\Delta x} - V \frac{\Delta V}{\Delta y} - W \frac{\Delta V}{\Delta z} \quad (8)$$

The next term to be discussed is the pressure gradient force. This is from the pressure variations in the atmosphere where the direction is from high to low pressure region and the magnitude is dictated by the pressure difference. The pressure gradient force is higher in intensity as the pressure difference is larger. Mathematically, this is shown below:

$$\frac{F_{x\ PG}}{m} = -\frac{1}{\rho} \cdot \frac{\Delta P}{\Delta x} \quad (9)$$

$$\frac{F_{y\ PG}}{m} = -\frac{1}{\rho} \cdot \frac{\Delta P}{\Delta y} \quad (10)$$

When wind flows in circular motion, the centrifugal force has to be defined to make it convenient when making calculations. This is expressed as follows:

$$\frac{F_{x\,CN}}{m} = s \cdot \frac{V \cdot M}{R} \quad (11)$$

$$\frac{F_{y\,CN}}{m} = -s \cdot \frac{U \cdot M}{R} \quad (12)$$

Where $M = \sqrt{U^2 + V^2}$, s is the sign dependent on Northern or Southern Hemisphere, and R is the radius of curvature. This term is included for special conditions where the wind flow is around circles.

Since the Earth is a rotating reference frame, the superposition of tangential velocity of the planet's surface and object being observed which is called the compound centrifugal force. Due to the ellipsoid shape of the Earth, gravity is dependent on the distance of the object from the ground and its latitudinal position. Combining this latitudinal gravity component with the compound centrifugal force yields the Coriolis force. The latitudinal dependence of this force is expressed with a Coriolis parameter which is the following equation:

$$f_c = 2\Omega \sin \phi \quad (13)$$

Where ϕ is the latitude and 2Ω is $1.458423 \times 10^{-4}/s$

So, the Coriolis force for the Northern Hemisphere are:

$$\frac{F_{x\,CF}}{m} = f_c \cdot V \quad (14)$$

$$\frac{F_{y\,CF}}{m} = -f_c \cdot U \quad (15)$$

The signs in the above expressions will interchange for the Southern Hemisphere.

There are many objects on the surface of the Earth that can influence the air flow. These are composed of topography, land features such as forests and plantations, and structures such as buildings. These introduce drag to the wind flow and they are collectively referred to as surface roughness. They affect the troposphere especially the level between 0.3m to 3km called the atmospheric boundary layer (ABL). This is where turbulence occur as the winds slowed by surface roughness mixes with the faster moving winds at higher altitudes within the ABL. The momentum transfer that happens within the ABL decreases the average wind speed of the layer. This speed reduction is called the turbulent drag force which is expressed below:

$$\frac{F_{x\,TD}}{m} = -w_T \cdot \frac{U}{z_i} \quad (16)$$

$$\frac{F_{y\,TD}}{m} = -w_T \cdot \frac{V}{z_i} \quad (17)$$

Where w_T is the turbulent transport velocity and z_i is the ABL depth

For the horizontal motion, all the derived relations can now be substituted to obtain the following relations:

$$\frac{\Delta U}{\Delta t} = -U \frac{\Delta U}{\Delta x} - V \frac{\Delta U}{\Delta y} - W \frac{\Delta U}{\Delta z} - \frac{1}{\rho} \cdot \frac{\Delta P}{\Delta x} + f_c \cdot V - w_T \cdot \frac{U}{z_i} \quad (18)$$

$$\frac{\Delta V}{\Delta t} = -U \frac{\Delta V}{\Delta x} - V \frac{\Delta V}{\Delta y} - W \frac{\Delta V}{\Delta z} - \frac{1}{\rho} \cdot \frac{\Delta P}{\Delta y} - f_c \cdot U - w_T \cdot \frac{V}{z_i} \quad (19)$$

The centrifugal force may be added in the above equations when there is an expected constant circular air flow. The turbulent drag force can be expanded to make a better representation of the term and this will be shown in the governing equations. The simple form for these equations has been derived as shown by Eqs. (18) and (19). To proceed further, it is necessary to mention that mass and energy continuity applies to the atmosphere meaning that there is conservation of mass and energy. Another parameter that has to be addressed is the density of the air. The air density varies at different layers of the atmosphere but, for adjacent layers, these variations are small and may be neglected. This assumption is called the Boussinesq Approximation which pertains to the condition where the fluid density ρ do not vary too much from the mean reference value ρ_0 [160]. This assumption is expressed below:

$$\rho = \rho_0 + \rho'(x, y, z, t) \quad \text{with} \quad |\rho'| \ll \rho_0 \quad (20)$$

3.2.5 Governing Equations for Geophysical Fluid Dynamics

A more sophisticated form of Eqs. (18) and (19) are necessary in order to express the dynamics of the wind more accurately. This subject matter is part of the field called geophysical fluid dynamics (GFD) [160]. Recall that the parameters that influence the weather and climate on the planet are the barometric pressure, wind flow, air density, Coriolis force, turbulence drag and gravity. But the turbulence drag needs to include the eddy viscosity and diffusivity for a more accurate solution. Taking into account the continuity of mass and energy as well as the Boussinesq Approximation, the governing equations of GFD may be derived. The basic unit of analysis for GFD is called air parcel which is an infinitesimal volume depicted by a cube. This basic unit is depicted in the equations by the partial derivatives. The momentum equations are expressed in each coordinate of the three dimensional rectangular system. These governing equations are expressed in the following relations:

x-momentum:

$$\frac{\partial u}{\partial t} + u \frac{\partial u}{\partial x} + v \frac{\partial u}{\partial y} + w \frac{\partial u}{\partial z} - fv = -\frac{1}{\rho_0} \frac{\partial p}{\partial x} + \frac{\partial}{\partial x} \left(\mathcal{A} \frac{\partial u}{\partial x} \right) + \frac{\partial}{\partial y} \left(\mathcal{A} \frac{\partial u}{\partial y} \right) + \frac{\partial}{\partial z} \left(v_E \frac{\partial u}{\partial z} \right) \quad (21)$$

y-momentum:

$$\frac{\partial v}{\partial t} + u \frac{\partial v}{\partial x} + v \frac{\partial v}{\partial y} + w \frac{\partial v}{\partial z} - fu = -\frac{1}{\rho_0} \frac{\partial p}{\partial y} + \frac{\partial}{\partial x} \left(\mathcal{A} \frac{\partial v}{\partial x} \right) + \frac{\partial}{\partial y} \left(\mathcal{A} \frac{\partial v}{\partial y} \right) + \frac{\partial}{\partial z} \left(v_E \frac{\partial v}{\partial z} \right) \quad (22)$$

z-momentum:

$$0 = -\frac{\partial p}{\partial z} - \rho g \quad (23)$$

Continuity:

$$\frac{\partial u}{\partial x} + \frac{\partial v}{\partial y} + \frac{\partial w}{\partial z} = 0 \quad (24)$$

Energy:

$$\frac{\partial \rho}{\partial t} + u \frac{\partial \rho}{\partial x} + v \frac{\partial \rho}{\partial y} + w \frac{\partial \rho}{\partial z} = \frac{\partial}{\partial x} \left(\mathcal{A} \frac{\partial \rho}{\partial x} \right) + \frac{\partial}{\partial y} \left(\mathcal{A} \frac{\partial \rho}{\partial y} \right) + \frac{\partial}{\partial z} \left(\kappa_E \frac{\partial \rho}{\partial z} \right) \quad (25)$$

Where ρ_0 is the reference density, g is the acceleration due to gravity, u is the north-south direction of motion, v is the east-west direction of motion, w is the vertical motion, $f = 2\Omega \sin \varphi$ (Coriolis parameter), \mathcal{A} , ν_E , and κ_E are eddy viscosity and diffusivity coefficients which may be dependent on flow variables and grid parameters.

There are varying horizontal motion scales within the troposphere. Scales would range from thousands to several hundreds of kilometres for the macroscale, between 700km to 3km for mesoscale, and less than 3km to a few meters for microscale [158]. Although the governing equations are applicable to any horizontal scale mentioned, the turbulence terms have to be expressed more accurately for scales that are less than 3km. This involves the equations of motion for computational fluid dynamics (CFD) which will be discussed next.

3.3 Equations for Computational Fluid Dynamics (CFD)

To account for the turbulence more accurately, CFD employs relations that have turbulent flow elements which may be simplified in the mesoscale model. Expressions that affect large-scale fluid flow such as the Coriolis Force may be ignored in the microscale level [161]. These are the adjustment made to produce a solution to the Navier-Stokes equation that is for the microscale.

There are three techniques in solving the Navier-Stokes equations for turbulent flow of compressible fluids. These are known as direct numerical simulation (DNS), large-eddy simulation (LES), and Reynolds-Averaged Navier-Stokes (RANS) [162]. DNS takes into account the mean flow and all turbulent velocity fluctuations in the simulations using unsteady Navier-Stokes equations. LES uses unsteady Navier-Stokes equations that includes big eddies in the flow but neglects small eddies. RANS emphasises on the mean flow and how turbulence affects the mean flow properties. The Navier-Stokes equations are time averaged where extra terms are present to express the interactions between various turbulent fluctuations. RANS is a finite volume method which is extensively used in CFD for its flexibility on the technique of discretising physical systems that avoids coordinate transformation in the computational domain. It is also capable of solving complex geometries and the

physics and conservation principles of a system are captured by this numerical method [161]. The system of equations for RANS are listed below:

Continuity:

$$\frac{\partial \bar{\rho}}{\partial t} + \nabla \cdot (\bar{\rho} \tilde{\mathbf{U}}) = 0 \quad (26)$$

Reynolds Equations (RANS):

$$\frac{\partial(\bar{\rho}\tilde{U})}{\partial t} + \nabla \cdot (\bar{\rho}\tilde{U}\tilde{\mathbf{U}}) = -\frac{\partial\bar{P}}{\partial x} + \nabla \cdot (\mu\nabla\tilde{U}) + \left[-\frac{\partial(\bar{\rho}u'^2)}{\partial x} - \frac{\partial(\bar{\rho}u'v')}{\partial y} - \frac{\partial(\bar{\rho}u'w')}{\partial z} \right] + S_{Mx} \quad (27)$$

$$\frac{\partial(\bar{\rho}\tilde{V})}{\partial t} + \nabla \cdot (\bar{\rho}\tilde{V}\tilde{\mathbf{U}}) = -\frac{\partial\bar{P}}{\partial y} + \nabla \cdot (\mu\nabla\tilde{V}) + \left[-\frac{\partial(\bar{\rho}u'v')}{\partial x} - \frac{\partial(\bar{\rho}v'^2)}{\partial y} - \frac{\partial(\bar{\rho}v'w')}{\partial z} \right] + S_{My} \quad (28)$$

$$\frac{\partial(\bar{\rho}\tilde{W})}{\partial t} + \nabla \cdot (\bar{\rho}\tilde{W}\tilde{\mathbf{U}}) = -\frac{\partial\bar{P}}{\partial z} + \nabla \cdot (\mu\nabla\tilde{W}) + \left[-\frac{\partial(\bar{\rho}u'w')}{\partial x} - \frac{\partial(\bar{\rho}v'w')}{\partial y} - \frac{\partial(\bar{\rho}w'^2)}{\partial z} \right] + S_{Mz} \quad (29)$$

Scalar transport equation:

$$\frac{\partial(\bar{\rho}\tilde{\Phi})}{\partial t} + \nabla \cdot (\bar{\rho}\tilde{\Phi}\tilde{\mathbf{U}}) = \nabla \cdot (\Gamma_{\Phi}\nabla\tilde{\Phi}) + \left[-\frac{\partial(\bar{\rho}u'\phi')}{\partial x} - \frac{\partial(\bar{\rho}v'\phi')}{\partial y} - \frac{\partial(\bar{\rho}w'\phi')}{\partial z} \right] + S_{\phi} \quad (30)$$

These terms are similar with the GFD expressions in the previous section. The extra terms in square brackets and last term, S are the added turbulent stresses called Reynolds stresses. To solve these extra terms, the k-ε model is used as a turbulence closure scheme. The k-ε model widely used in the industry and has been validated in many instances [162]. This model solves two transport equations which are the turbulent kinetic energy, k and dissipation rate of turbulent kinetic energy, ε [162]. The governing equations for the model are as follows:

Mean flow kinetic energy, K:

$$\frac{\partial(\rho K)}{\partial t} + \nabla \cdot (\rho K \mathbf{U}) = \nabla \cdot (-P\mathbf{U} + 2\mu\mathbf{U}S_{ij} - \rho\mathbf{U}\overline{u'_i u'_j}) - 2\mu S_{ij} \cdot S_{ij} + \overline{\rho u'_i u'_j} \cdot S_{ij} \quad (31)$$

The expression above relates the rate of change for K and convective transport of K to the transport by pressure of K, transport by viscous stresses of K, transport by Reynolds stress of K, viscous dissipation rate of K, and the destruction rate of K due to turbulence production.

Turbulent kinetic energy k:

$$\frac{\partial(\rho k)}{\partial t} + \nabla \cdot (\rho k \mathbf{U}) = \nabla \cdot (-\overline{p' \mathbf{u}'} + 2\mu\overline{\mathbf{u}' s'_{ij}} - \rho\frac{1}{2}\overline{u'_i \cdot u'_i u'_j}) - 2\mu\overline{s'_{ij} \cdot s'_{ij}} - \overline{\rho u'_i u'_j} \cdot S_{ij} \quad (32)$$

The expression above relates the rate of change for k and convective transport of k to the transport by pressure of k, transport by viscous stresses of k, transport by Reynolds stress of k, dissipation rate of K, and the production rate of k.

Before proceeding to the transport equation for k and ϵ , certain relations must be defined which are the following:

Rate of Dissipation:

$$\epsilon = 2\nu \overline{s'_{ij} \cdot s'_{ij}} \quad (33)$$

The above expression relates the rate of dissipation per unit volume to the density multiplied by turbulent kinetic energy dissipation rate per unit mass, ϵ .

Eddy viscosity:

$$\mu_t = C_\mu \rho \nu \ell = \rho C_\mu \frac{k^2}{\epsilon} \quad (34)$$

Now, the transport equations can be presented and they are shown in the following expression:

For k :

$$\frac{\partial(\rho k)}{\partial t} + \nabla \cdot (\rho k \mathbf{U}) = \nabla \cdot \left[\frac{\mu_t}{\sigma_k} \nabla k \right] + 2\mu_t S_{ij} \cdot S_{ij} - \rho \epsilon \quad (35)$$

For ϵ :

$$\frac{\partial(\rho \epsilon)}{\partial t} + \nabla \cdot (\rho \epsilon \mathbf{U}) = \nabla \cdot \left[\frac{\mu_t}{\sigma_\epsilon} \nabla \epsilon \right] + C_{1\epsilon} \frac{\epsilon}{k} 2\mu_t S_{ij} \cdot S_{ij} - C_{2\epsilon} \rho \frac{\epsilon^2}{k} \quad (36)$$

These relate the rate of change of k or ϵ and the convective transport of k or ϵ to the diffusive transport of k or ϵ , production rate of k or ϵ , and destruction rate of k or ϵ . The values of the constants are:

$$C_\mu = 0.09 \quad \sigma_k = 1.00 \quad \sigma_\epsilon = 1.30 \quad C_{1\epsilon} = 1.44 \quad C_{2\epsilon} = 1.92$$

The concepts and mathematical methods discussed in this section are used for NWP and CFD software applications to simulate fluid flow. For this study, the winds are simulated using the mentioned software to generate wind data that are essential for WRA. The chosen models for the research are described and discussed in the next section.

3.4 Mesoscale and Microscale Model Applications

The mesoscale model utilised for this research is the Weather Research and Forecasting (WRF) Model. It has been found to be capable of simulating wind conditions in many studies [18,98,114] so, it is the one selected for this study. The WRF is a NWP for mesoscale modelling and there are two dynamic solvers for the software namely, the Nonhydrostatic Mesoscale Model (NMM) and the Advanced Research WRF (ARW) [163]. NMM solver is used for operational applications such as weather prediction while ARW is designed for atmospheric research. The code base of WRF is open source and written in Fortran and C/C++ language. It can be compiled to run in serial or parallel computation on x86 desktop systems that can scale to supercomputer systems in a Linux environment.

It is the ARW solver that has been chosen since it is meant for research purposes. Specifically, the version of WRF used is the Advanced Research WRF Ver. 3.8. In calculations, it uses a terrain-following coordinate system and solves nonhydrostatic equations for compressible fluid [163]. It is the governing equations for GFD found in the previous section that is being calculated by the WRF-ARW solver. The implemented numerical method in integrating the system of equations is the third-order Runge-Kutta integration scheme [163].

For the microscale model, a CFD model called WindSim is used to run fine spatial resolution wind simulations. It is the WindSim 9 version that is utilised to do the wind simulations for this study. WindSim is a commercial software that has been demonstrated to perform adequately in several publications [143,164] for coastal and small island nations found in the literature. WindSim is a steady-state model that solves the RANS equations using finite volume method [165]. The turbulence model implemented are based on the $k-\epsilon$ models and have been validated with the Bolund Experiment to ensure its performance. The software is composed of several modules but only the Terrain and Wind Fields modules are used for mesoscale model coupling. WindSim runs on a Windows environment and can perform simulations in serial or multicore mode for parallel processing on an x86 workstation.

3.5 Model configuration and design

For this work, the WRF is used to make offshore wind fields around the Palawan Island. The model is configured using three different settings found to perform well in other studies in the Philippines [150,151] and Thailand [114] in order to compare each one with observed data. Reanalysis data and operational data from the National Centres for Environmental Prediction (NCEP) and European Centre for Medium-Range Weather Forecasts (ECMWF) have been used as input data for WRF. The specific datasets used are the European Reanalysis-Interim (ERA-Interim), NCEP Climate Forecasts System Reanalysis (NCEP-CFSR or NCEP-CFS), and the NCEP Final Operational Global Analysis

Data (FNL). The ERA-Interim reanalysis data encompasses the whole planet as its domain with a 79 km spatial resolution [166]. Its dataset begins in 1979 and has 60 vertical levels of the atmosphere. NCEP-CFSR is also a reanalysis data that starts its data set in 1979. It has a spatial resolution of around 100 km and has 64 vertical levels [167]. The NCEP-FNL is a global operational data set in contrast to the other two data set mentioned. It has a 1° x 1° spatial resolution and incorporates real-time weather observation data into the datasets so that it can be used for weather forecasting [150,168]. The descriptions of each one are summarised in Table 4.

Table 4. Input Dataset Specifications

Parameters \ Dataset	ERA-Interim	NCEP-FNL	NCEP-CFSR
Data Type	Reanalysis	Operational	Reanalysis
Spatial Resolution	79 km	1° (~110 km)	100 km
Common Use	Diagnostics & Validation	Weather Forecasting	Diagnostics & Validation
Origin	ECMWF	NCEP	NCEP

For the planetary boundary layer (PBL) parameter, there are also three different ones used for comparison. PBL used for the simulations are Mellor-Yamada-Janjic (MYJ), Asymmetric Convective Model ver. 2 (ACM2), and Yonsei University (YSU) along with their prescribed surface layer parameters namely, Eta similarity and revised Mesoscale Model ver. 5 (MM5). In addition, the microphysics scheme settings utilised WRF single-moment 3-class (WSM3) and 6-class (WSM6) options. These settings are summarised in Table 5.

Table 5. WRF Configuration Settings

Parameters \ Authors	Dado and Takahashi [151]	Cruz and Narisma [150]	Chancham, Waewsak, and Gagnon [114]
Input Data	ERA-Interim	NCEP-FNL	NCEP-CFSR
Planetary Boundary Layer	MYJ	ACM2	YSU
Surface Layer	Eta Similarity	Revised MM5	Revised MM5
Microphysics Scheme	WSM6	WSM6	WSM3

Although studies reported in [150,151] are focused on rainfall, similar configurations have been used for wind in other studies [114,149]. Slight modifications have been made to the referred studies in order to limit the comparison between input data and PBL. The first modification involved enabling the cumulus parameterization scheme for [151]. The second one is using NCEP-CFSR dataset as input for [114]. Model setting differences have been narrowed to these two parameters as previous studies have shown that wind simulations in WRF is highly sensitive to them [148,149]. These minor changes are similar with the configuration used for other offshore wind research in the South China Sea [98]. Differences with the microphysics scheme has been maintained according to the respective settings of the prior works as these pertain to the precipitation in the model and not essential for this study.

The surface layer option had to vary because the PBL parameter selected dictates the compatible surface layer setting. Other model parameters are kept the same in the three model configurations selected for this study. Radiation schemes use the Rapid Radiative Transfer Model (RRTM) for long wave and Dudhia for short wave. The same land use and land cover parameter using the 30 arcsec US Geological Survey (USGS) data have been set and the Noah land surface model has been activated for all simulation runs [114,150,151]. The Kain-Fritsch cumulus parametrisation scheme has been utilised for all but has been disabled at the third domain since the model explicitly calculates this parameter for fine resolutions.

There are three domains setup for this simulation in WRF where Domain 1 has the size of 2,430 km x 2,349 km with 27 km grid resolution, Domain 2 has 1,440 km x 1,602 km at 9 km grid size, and Domain 3 has 462 km x 570 km at 3 km resolution with all domains having an hourly time resolution. Palawan Island is contained within the third domain. The defined domains for the study site can be seen in Figure 19.

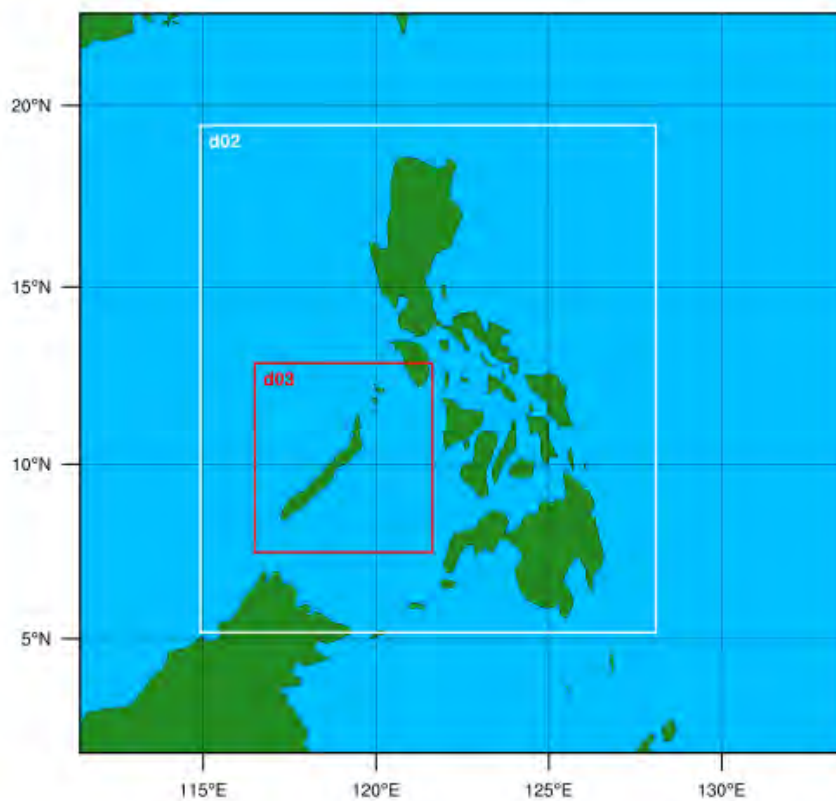


Figure 19. Domains configured for WRF. Palawan Island is within Domain 3 (d03).

Vertical resolution of the model has been increased to 50 vertical eta levels where the first 9 levels are within the 200 m height in order to enable WRF to perform better in accounting for the atmospheric dynamics within the boundary layer [169]. Two-way nesting has been enabled for all the model runs even for simulations that are configured, as reported in [150], for one-way nesting used in the study. Simulations were done on the Advanced Research Computing High End Resource

(ARCHER) supercomputing facility where a Cray XC30 is used to provide high performance computing services. Some simulations were also done at the supercomputer of ECMWF which uses Cray XC40.

3.6 Sensitivity test and analysis

The WRF has been run on three different settings used in other studies which are summarised in Table 5. PAGASA weather station in Coron, Cuyo Island, and Puerto Princesa are used for validating the results. Daily wind speed averages have been calculated from the model output since the obtained observation data are also daily averages. A scatter plot to compare the performance of each WRF configuration with measured data is made for validating the wind speeds [113,151]. This chart shows the accuracy of simulation data in determining the wind speed observed values. A sample chart for scatter plots is shown below:

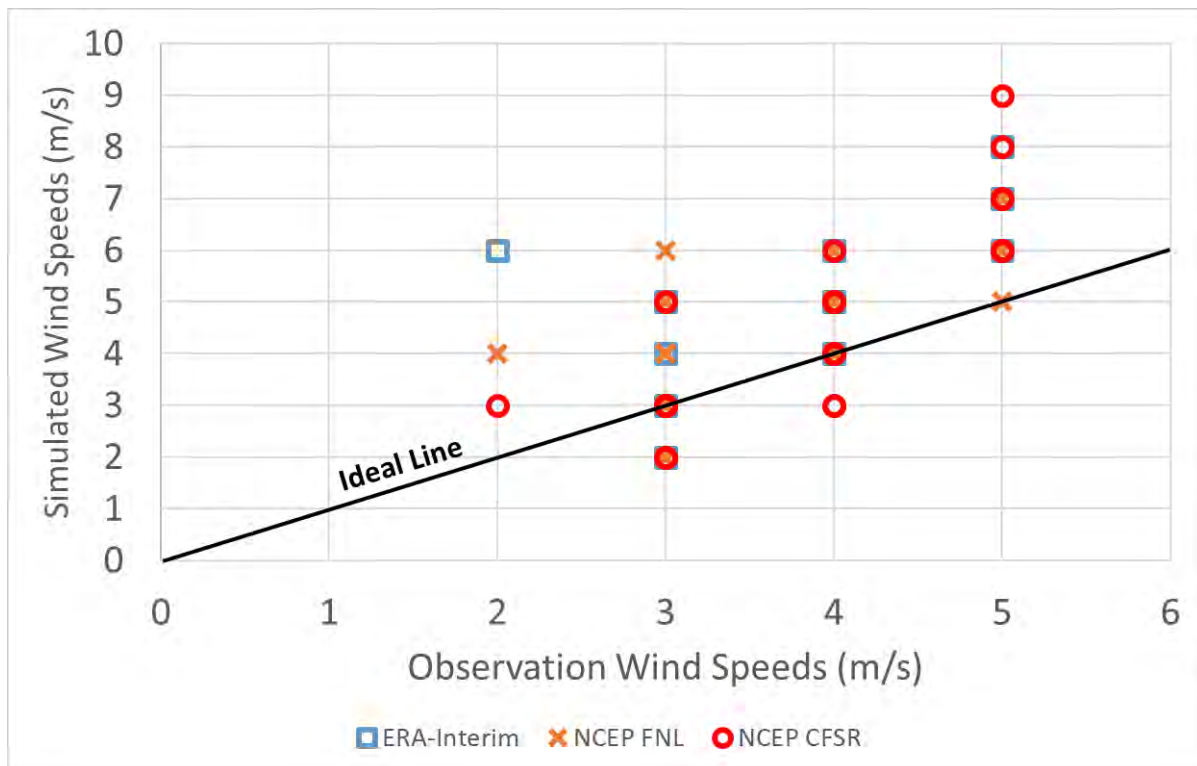


Figure 20. Sample scatter plot for simulation and measured wind speed comparison.

The sample chart found in Figure 20 gives the ideal line depicted by the black line. This ideal line corresponds to the values where the simulated wind speed values are exactly the same as the observations. Any points above this line are overestimated values generated by the model while the values below the line are underestimated values produced by the model outputs. It also presents the percentage error of the WRF simulations results in comparison with the PAGASA wind data. Scatter plots will be used extensively in Chapter 5 for the comparison and analysis of mesoscale model results from this study.

The root-mean-square error (RMSE) of wind speeds are calculated in order to know how much the model results deviates from the measured data [144,149,150]. RMSE is determined using the following equation:

$$RMSE = \sqrt{\frac{1}{N} \sum_{i=1}^N (U^{sim} - U^{obs})^2} \quad (37)$$

where U^{sim} is the simulated wind speed and U^{obs} is the measured wind speed in m/s.

The bias of the results are also to be determined to see if the model has a tendency to overestimate or underestimate the wind speeds [18,20,127,144]. This is given by the relation that follows:

$$Bias = \frac{1}{N} \sum_{i=1}^N (U^{sim} - U^{obs}) \quad (38)$$

A third quantity known as the standard deviation of the error (STDE) is also calculated to determine the error variability from the mean value of the wind [20,121,127]. This is expressed in the equation below:

$$STDE = \sqrt{RMSE^2 - Bias^2} \quad (39)$$

Wind direction are analysed with monthly averages in order to see the seasonal trends and determine the predominant wind direction which is essential for WRA of wind farms [76].

Wind maps at 80 m above ground level are generated to determine the areas with good wind resources. This is the height selected since commercial wind turbines commonly have 80-m hub heights [164]. The wind maps are to be generated using the mesoscale model results with the configuration found to be suitable to the study area based on the sensitivity and validation analyses. The WRF results are to be processed using the NCAR Command Language (NCL) for producing the maps. NCL is the supported scripting language by the WRF model at the time this research is being carried out but the model outputs may be post-processed using other languages such as Python. These wind maps will also be used to determine the sites to be downscaled for fine spatial resolution wind simulation with a microscale model.

The computational fluid dynamics (CFD) is implemented as the microscale model in this study since mesoscale models cannot resolve spatial resolutions that are smaller than 1km. Fine spatial resolution wind simulations are necessary in order to determine the wind profiles of waters near the shore since wind flow is affected by local physical dynamics and coastal topography [10]. The CFD model used is WindSim 9 and this software is developed for the wind energy industry.

3.7 WindSim Simulations

The 3km x 3km grid resolution WRF model output are further downscaled to produce fine resolution wind simulation results. Wind observations aboard a ship from the 7SEAS campaign in Palawan are analysed and categorised to select the locations for the model validation. These campaigns were carried out in the month of September in 2011 and 2012. This particular month was selected for the aerosol measurement campaign in Palawan because of the Southwest Monsoon phenomena which is of interest to atmospheric science research [152,153]. Stationary positions during the campaign that have wind measurements of at least 24-hour period and situated outside pier or bay areas are chosen for the validation. The selected sites are Balabac Island, North Guntao Island, Notch Island, South Guntao Island, Tubbataha North Reef, and Tubbataha South Reef. Statistical error analysis are to be performed to the grid of the WRF model output with the closest coordinates for each site selected. This is necessary for the determination of which simulation results from the three WRF configurations are closest to the measured wind values from the ship observations. The WRF results that have the least error value are selected as input for WindSim.

Simulation domain of WindSim is generated using the WindSim Express software. With that application, the coordinates of the domain to be simulated can be defined. The terrain and surface roughness data are also selected in this program before generating the domain for CFD simulations. In this study, the Advanced Spaceborne Thermal Emission and Reflection Radiometer Global Digital Elevation Map (ASTER GDEM) is used and the surface roughness is the Vegetation Continuous Fields (VCF) Tree Cover dataset. ASTER GDEM has a spatial resolution of 1 arc second while the spatial resolution of VCF is 500 m.

There are sensitivity test to be done for these WindSim simulations as well since there are a number of model configurations available that must be set according to the study area. A general flow of the process is to be discussed here and more details along with explanations of these sensitivity test results can be found in Chapter 5. Since the WindSim model will be used to downscale mesoscale model results, it will be configured accordingly because the default options for the model are for long-term wind observations with multiple levels. When using mesoscale models, the simulations may be initialised with the temperature from the mesoscale results. This is the first parameter to be tested for sensitivity as it has been determined that stable atmospheric conditions do not need this while moderately stable and unstable conditions would require this temperature initialization [170,171]. CFD models are also sensitive to grid resolution as they are found to change their results depending on the mesh size [143,162,164]. The spatial resolution will be varied with resolutions of 152m, 76m, and 38m by changing the number of maximum cells by 100,000, 500,000, and 1,500,000 respectively for the simulations. The boundary layer height and wind speeds above it are to be set according to the

literature. This is determined to be approximately around 1,500m for regions in the tropics [143,152]. This value for the boundary layer height was used by Dhunny, Lollchund, and Rughooputh [143] for their wind energy evaluation of Mauritius using WindSim. Experimentally, this is the boundary layer height that Reid et al. [152] found on their 2011 aerosol campaign in Palawan Island with the Navy Global Atmospheric Prediction System and the Cloud-Aerosol Lidar with Orthogonal Polarization data. The wind speed above the boundary layer height is set at 10 m/s which is the value found by Reid et al. [153] at the said altitude in their 2012 Palawan Island aerosol campaign. The last model parameter that will be part of the sensitivity test is the turbulence model. Wind energy studies that use WindSim have either found that the standard k-ε or the k-ε RNG best suits their study area [136,137,143,164]. Taking into account geographical and atmospheric conditions that are similar with the Philippines among the published studies [136,137,143,164], the standard k-ε has been used by Waewsak et al. [164] in Thailand and Dhunny, Lollchund, and Rughooputh [143] found that k-ε RNG gives the best results in Mauritius. Thus, the sensitivity tests will involve the use of standard k-ε and k-ε RNG turbulence models. The flow chart in Figure 21 summarises the flow for the wind simulations.

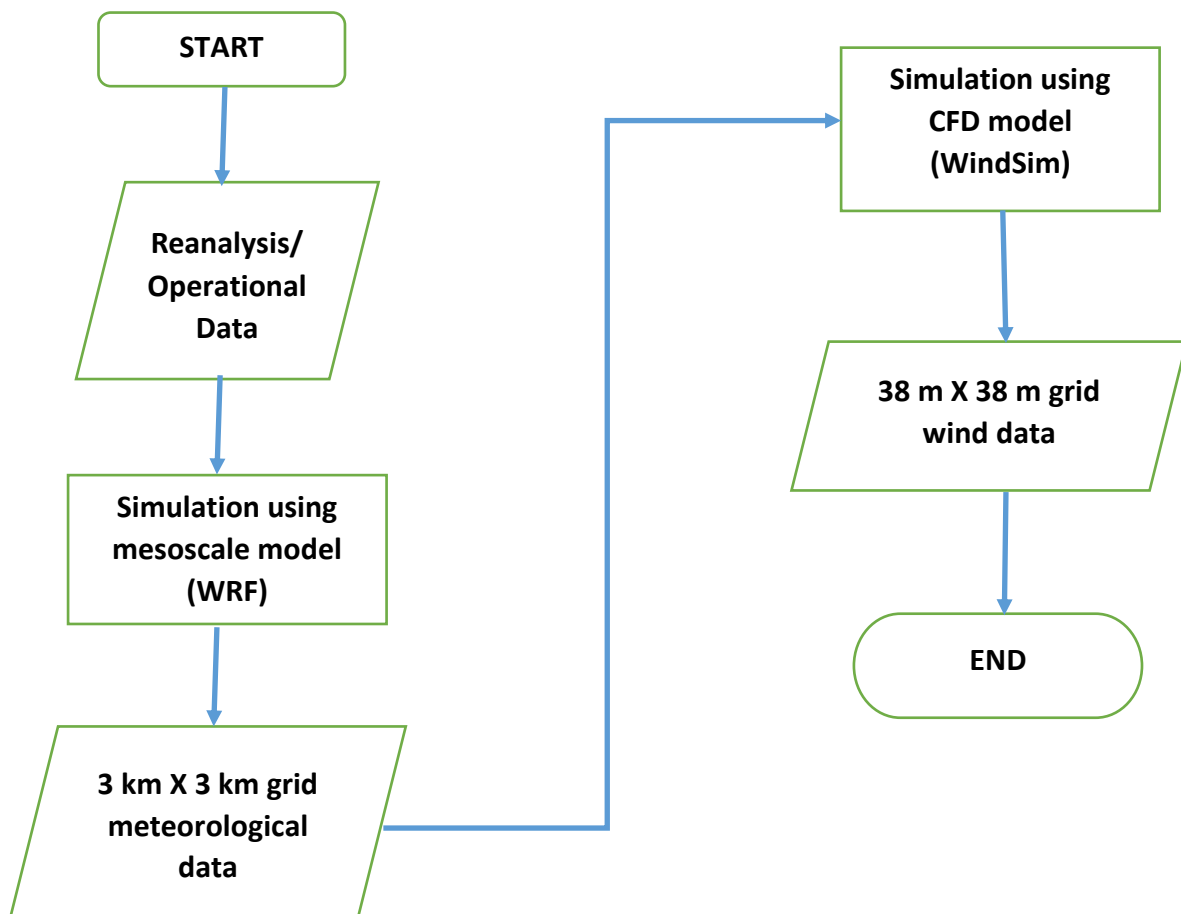


Figure 21. Flow chart for wind simulations

Figure 21 illustrates the wind simulation work flow briefly. The generated data from each simulation output are the ones being validated in this study. Comparison between the WRF results and WindSim

outputs are made in order to see the improvements in simulation from CFD models. This comparison will involve the best performing WRF configuration and WindSim configuration that is found to be best suited for each selected site from the 7SEAS aerosol campaign. The results will form the basis for the wind resource assessment of Palawan Province and present a method for wind characterisation of sites with short-term offshore wind observations.

Wind power production potential will be based on the standard classification used in wind industry [53]. A summary of the wind potential classification is given in the table below:

Table 6. Wind classification standard to determine wind potential of an area

Class	Average Wind Speed (m/s)	Wind Energy Division
1	0 – 4.4	Indigent Area
2	4.4 – 5.1	Available Area
3	5.1 – 5.6	Subrich Area
4	5.6 – 6	Rich Area
5	6 – 6.4	Rich Area
6	6.4 – 7	Rich Area
7	7 – 9.4	Rich Area

The determination of a site’s wind resource potential will be based on Table 6. These will guide the wind simulation results in identifying areas with good wind resource.

3.8 Summary

Palawan Province of the Philippines has been selected as the study area because it is located within the low latitude area and it is composed of multiple small islands. It is also situated in the South China Sea which is an area of active offshore wind development as discussed in Chapter 2 because it possesses good offshore wind resource. An onshore WRA for the Philippines has also shown that Palawan is one of the islands that has potential for wind farm development [16]. Before performing the wind simulations, observation data have been gathered because any simulation requires validation in order to determine the model performance. Three onshore weather stations from PAGASA for 2010 – 2012 have been obtained. These stations are located in Coron Island, Cuyo Island, and Puerto Princesa. For offshore wind measurements, the 7SEAS campaign has been used for the validation. The campaign deployed a ship to measure aerosols and meteorological conditions around Palawan Province in 2011 and 2012 on the month of September [152,153]. Since the ship sailed around the province, sites have been selected for validation based on the length of observation at a location. The periods when the ship was stationary and had 24-hour duration of continuous observations are the criteria for site selection for validating the wind simulations. Balabac Island, Guntao Islands, Notch Island, and Tubbataha Reef were selected based on the two criteria mentioned.

A mesoscale model, called the WRF-ARW, was used for this work as the NWP model which has been extensively used for wind profile studies as presented in Chapter 2. Three different configurations of the model were used to simulate the wind patterns over Palawan. This is necessary because models must be adjusted to the configuration that is suited for a location which can be determined by validating them with observed data. The configurations used for the research have been discussed in this chapter. The mesoscale model results were validated with the PAGASA data for the long-term performance then, with the 7SEAS observation for short-term performance.

There are limitations with the capabilities of mesoscale models because they have relatively coarse resolution and topography are simplified by smoothening [149] therefore, it experiences difficulty in simulating coastal regions. Atmospheric dynamics that occur in the microscale such as the interface of land and sea are also not modelled well with mesoscale models [20]. This necessitates a model that can simulate coastal areas such as microscale models which must be coupled with the mesoscale model. Coupling the models would involve the mesoscale model results to be used as input data to drive the microscale model simulations. A CFD model, called WindSim, has been chosen as the microscale model because it is capable of incorporating complexity in the terrain [136] and found capable of simulating wind conditions on small island nations [143]. Prior to coupling the two models, the appropriate mesoscale model configuration data have been determined through validation with offshore observations from the 7SEAS data.

4 IMPLEMENTATION

The details in doing the research are discussed in this chapter. It covers the process of seeking in-situ measurements used for validation, gathering data for driving the mesoscale model, configuration of the models, running simulations, data extraction, and wind map generation. This will serve as the documentation for performing WRA on areas that have limited data availability on wind velocity.

4.1 Data gathering

Actual measurements for Palawan Province are required for the validation of the wind simulations for this study. The 7SEAS campaign wind data is the starting point in determining the winds at offshore locations around Palawan. Dataset from the meteorological tower aboard the ship for the said campaign were obtained from the Manila Observatory. Since the 7SEAS wind measurements were only made for a few days at selected locations, these are not sufficient to validate the wind models used in this study. In order to see the performance of the model, a long-term observation is needed for validation. This required requesting data from the PAGASA for wind data from the three weather stations operated by the agency in Palawan Province. The data received are for the years of 2010 – 2012. These are the years that overlap with the 7SEAS campaign so, they were asked from PAGASA in order to allow comparisons with offshore data.

The quality of the data had to be assured so, tidying of the data received were done prior to using them for model validation. To do this, the data were reviewed in order to see their suitability for the purpose of the study. The PAGASA data had days at Cuyo Island station where there are no data available so, those days were eliminated for analysis. The ship wind data from the 7SEAS campaign had to be segregated between dates where the ship is in transit and stationary. On periods when the ship is moving from one location to the next, wind observations were not used for this study. During times when the ship is anchored, the locations where the ship is docked at ports are not used since there are features and structure on land that will influence the wind measurements. Offshore locations where the ship is stationary are filtered according to the number of days where continuous measurements were made at the site. Locations where there are less than a day of measurements were discarded because short-term observations that lasts a few to several hours will not be meaningful.

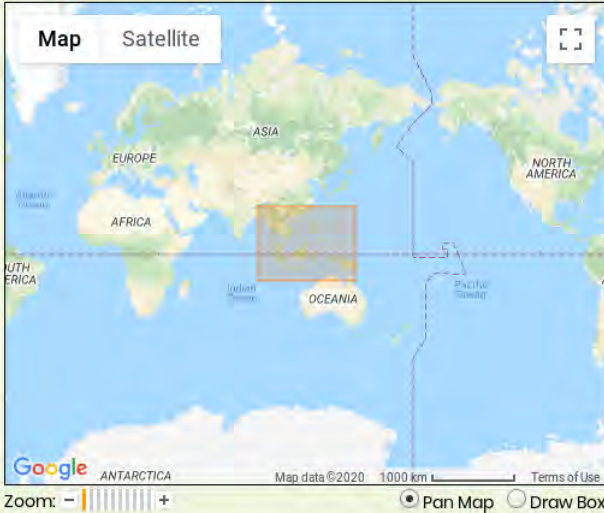
When running the WRF model, it is necessary to use reanalysis or operational data to initialise the simulations. This required downloading the datasets of ERA-Interim, NCEP-CFS, and NCEP-FNL. Downloading the datasets requires logging into the web portal and defining the region that data is to be downloaded. A sample page is shown in Figure 22.

[Description](#)
[Data Access](#)
[Documentation](#)
[Software](#)
[Metrics](#)

Get a Subset

Refine Your Selections:

- **Dataset Product:** GRIB2 6 HOURLY FILES 2007.12.06 to current
- **Input Data Format:** WMO_GRIB2
- **Output Format:** Same as input Converted to netCDF Converted to CSV
- **Valid Date Range:** 2010-12-01 00:00 to 2010-12-31 23:00
- **Parameter(s):**
 - All available
 - 5-wave geopotential height
 - 5-wave geopotential height anomaly
 - Absolute vorticity
 - Best (4 layer) lifted index
 - Cloud water
 - Cloud water mixing ratio
- **Vertical Level(s):**
 - All available
 - Convective cloud layer
 - Entire atmosphere (considered as a single layer)
 - Ground or water surface
 - Highest tropospheric freezing level
 - Isobaric surface: 1000 mbar
 - Isobaric surface: 975 mbar
- **Gridded Product:** Analysis
- **Grid:** 1° x 1° from 0E to 359E and 90N to 90S (360 x 181 Longitude/Latitude)
- **Spatial Selection:** Data within a bounding box



Interactive Map Instructions:

- Use the 'Pan Map' option to drag and center the map on your area of interest
- Use the 'Draw Box' option to drag a box around your area of interest. You can also manually enter bounding latitudes and longitudes in the text boxes.

North*: 27
 West*: 89 Reset East*: 146
 South*: -15

*Latitudes and longitudes must be specified in whole degrees

Figure 22. Download page for reanalysis and operational data sets from UCAR.

The downloaded data are stored in a workstation which are then used as input data for the mesoscale model. The reanalysis data and operational data are transferred to the high-performance computing facility of ARCHER and ECMWF.

4.2 Performing Mesoscale Wind Simulations

The WRF has three components that needs to be executed in order to generate and extract the wind data. These components are the pre-processing, simulation, and post-processing. Pre-processing involves setting up the model domain, terrain data, and initial/boundary conditions data. Simulation is the part when the model is running in order to calculate the atmospheric conditions within the chosen domain. Post-processing is the component where the simulation results are extracted for

analysis and visualisation. For simplicity, the serial processing mode on a workstation will be discussed here but the steps are the same for parallel processing in a supercomputer.

In the pre-processing, the `namelist.wps` must be configured. A complete listing of the file may be found in the Appendix. The number of domain nests, simulation dates, and dataset to be used as input data are to be indicated in the `namelist.wps` file. When this is done, the `geogrid.exe` is to be run to generate the terrain data, land-use, and domain boundaries. When in the proper directory, the following command is to be typed in the console:

```
./geogrid.exe
```

If the program runs successfully, the following message will appear:

```
Processing ALBEDO12M
Processing GREENFRAC
Processing LAI12M
Processing SNOALB
Processing SLOPECAT
Processing SLOPECAT
Processing CON
Processing VAR
Processing OA1
Processing OA2
Processing OA3
Processing OA4
Processing OL1
Processing OL2
Processing OL3
Processing OL4
Processing VAR_SSO
Processing LAKE_DEPTH

!!!!!!!!!!!!!!!!!!!!!!!!!!!!!!!!!!!!!!!!!!!!!!!!!!!!!!!!!!!!!!
!   Successful completion of geogrid.           !
!!!!!!!!!!!!!!!!!!!!!!!!!!!!!!!!!!!!!!!!!!!!!!!!!!!!!!!!!!!!!!
```

The downloaded dataset to be used for the simulation should be linked into the working directory. This is done by using the `./link_csh` command followed by the directory location of the dataset. A file named `VTable` must be a symbolic link to the proper data table that corresponds to the linked dataset to be read. This will allow the program to determine the data format of the dataset properly. After running this program, the `ungrib.exe` program must be executed in order to unpack the downloaded datasets. In the same directory, the following command is to be entered:

```
./ungrib.exe
```

When the program is finished, the message that follows should appear:

```
2016-06-21 13:23:47.482 --- -----
--
2016-06-21 13:23:47.645 --- Subroutine DATINT: Interpolating 3-d files to
fill in any missing data...
2016-06-21 13:23:47.645 --- Looking for data at time 2016-06-19_00
2016-06-21 13:23:47.645 --- Found file:      FILE:2016-06-19_00
2016-06-21 13:23:47.645 --- Looking for data at time 2016-06-19_06
2016-06-21 13:23:47.645 --- Found file:      FILE:2016-06-19_06
2016-06-21 13:23:47.645 --- Looking for data at time 2016-06-19_12
2016-06-21 13:23:47.645 --- Found file:      FILE:2016-06-19_12
2016-06-21 13:23:47.645 --- End Subroutine DATINT.
2016-06-21 13:23:47.645 --- ****   Deleting temporary files created by
ungrib...
2016-06-21 13:23:47.645 ---   Deleting file: ./PFILE:2016-06-19_00
2016-06-21 13:23:47.672 ---   Deleting file: ./PFILE:2016-06-19_06
2016-06-21 13:23:47.697 ---   Deleting file: ./PFILE:2016-06-19_12
2016-06-21 13:23:47.722 --- ****   Done deleting temporary files.
2016-06-21 13:23:47.722 --- *** Successful completion of program ungrib.exe
***
```

With the geography data and the unpacked input data, these are to be merged by the `metgrid.exe` program and convert them into the format that is compatible with WRF. The command to be entered in the console is:

```
./metgrid.exe
```

The following message should show in the console when the program is done:

```
Processing domain 1 of 2
  Processing 2016-06-19_00
    FILE
  Processing 2016-06-19_06
    FILE
  Processing 2016-06-19_12
    FILE
Processing domain 2 of 2
  Processing 2016-06-19_00
    FILE
  Processing 2016-06-19_06
    FILE
  Processing 2016-06-19_12
    FILE
!!!!!!!!!!!!!!!!!!!!!!!!!!!!!!!!!!!!!!!!!!!!!!!!!!!!!!!!!!!!
! Successful completion of metgrid. !
!!!!!!!!!!!!!!!!!!!!!!!!!!!!!!!!!!!!!!!!!!!!!!!!!!!!!!!!!!!!
```

Now, the wind simulation configuration file must be modified to the appropriate values based on the `namelist.wps` and the number of vertical levels. The generated files by the `metgrid.exe` must also be transferred or linked to the working directory. The working directory must be changed to the proper WRF directory to edit the `namelist.input` file which contains the configuration for the WRF simulation. The dates, domain boundaries, and nesting values in the `namelist.input`

must be consistent with the `namelist.wps`. The complete listing of `namelist.input` used in this study can be found in the Appendix.

The first part of the simulation run involves generating the initial conditions of the atmosphere. This is done by the `real.exe` program. To do this, the following command should be entered:

```
./real.exe
```

When the program is finished, the following message should appear on the console:

```
d01 2016-06-19_12:00:00 Timing for processing          0 s.
d01 2016-06-19_12:00:00 Timing for output            0 s.
d01 2016-06-19_12:00:00 Timing for loop #    1 =      0 s.
d01 2016-06-19_12:00:00 real_em: SUCCESS COMPLETE REAL_EM INIT
```

The initial condition files are generated when `real.exe` runs successfully and the proper WRF simulation can be started. The simulation will begin upon execution of the following command:

```
./wrf.exe
```

When the WRF runs successfully and finishes the simulation, the log files would contain the following messages:

```
Timing for main (dt= 26.58): time 2011-05-01_00:00:00 on domain   3:
0.31438 elapsed seconds
Timing for Writing wrfout_d03_2011-05-01_00:00:00 for domain
3:    3.24085 elapsed seconds
Timing for main (dt= 53.15): time 2011-05-01_00:00:00 on domain   2:
4.27884 elapsed seconds
Timing for Writing wrfout_d02_2011-05-01_00:00:00 for domain
2:    2.70046 elapsed seconds
Timing for main (dt=106.31): time 2011-05-01_00:00:00 on domain   1:
8.17225 elapsed seconds
Timing for Writing wrfout_d01_2011-05-01_00:00:00 for domain
1:    1.69815 elapsed seconds
wrf: SUCCESS COMPLETE WRF
```

From here, post-processing can be done to the output files. These can be read by several programs and the NCL language is used for this study to do the data extraction and visualisation. The scripts written for these tasks are listed in Appendix 7. These output data are used for making the wind maps and also pre-processed to become input data for the microscale model. These are all made possible by the NCL scripts that have been written for this research.

To generate the wind maps, it is important to initialise the work environment so that the NCL scripts can be executed properly. This can be done by the `WRF_init.sh` which is also listed in Appendix 7. Running this initialisation to the console is indicated at the second line in Figure 23.



Figure 23. Initialisation for NCL and running NCL script to generate wind maps.

After doing the initialisation, the target WRF output file that contains the desired wind data must be indicated into `wrf_EtaLevels_color.ncl` before running the script. When that is done, NCL script for wind mapping can be executed and generate the wind maps as shown in Figure 24.

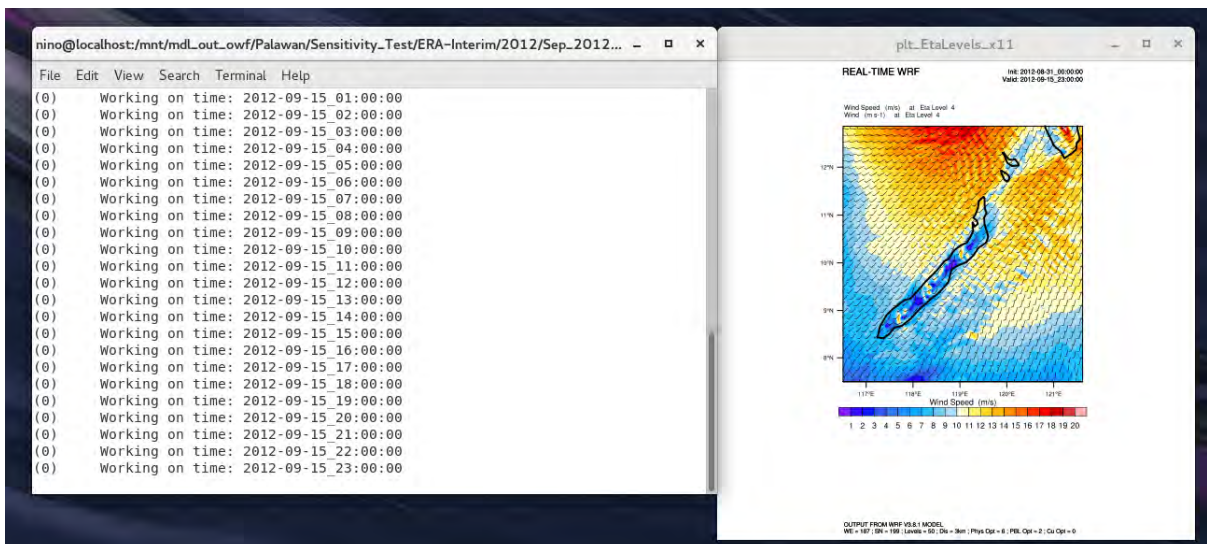


Figure 24. Execution of NCL script to generate wind maps

4.3 Performing Microscale Wind Simulations

In this work, a CFD model called WindSim has been used to produce fine spatial resolution wind simulations. To do that, the Terrain and Wind Fields module of the software has been utilised. A project must be created to begin the simulations and this can be generated from the WindSim Express software. This may be opened in the full WindSim application and the Terrain Module may be run to generate the topography of the model. A screenshot can be found in Figure 25.

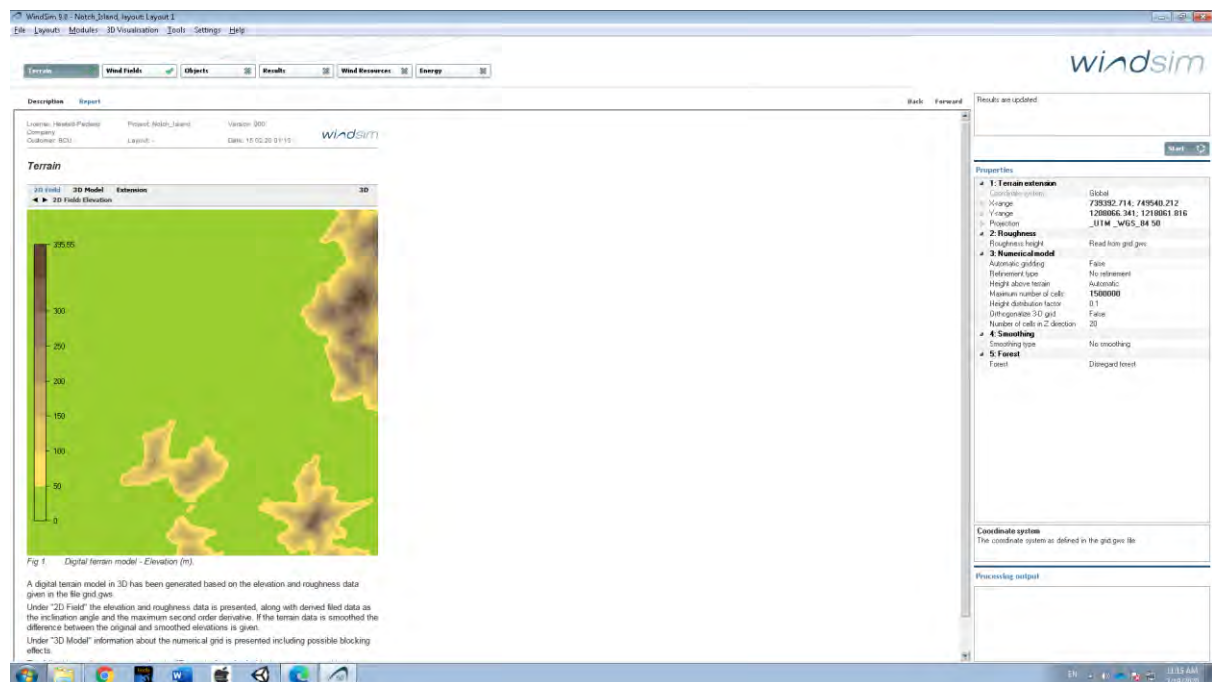


Figure 25. Terrain module of WindSim

After the Terrain module, a typical WindSim run would proceed to the Wind Field module immediately when wind observation data are available. Since the study involves coupling the mesoscale model with the CFD model, the mesoscale model results must be converted into input data for the WindSim program. A data import tool is available within the program which is shown in Figure 26.

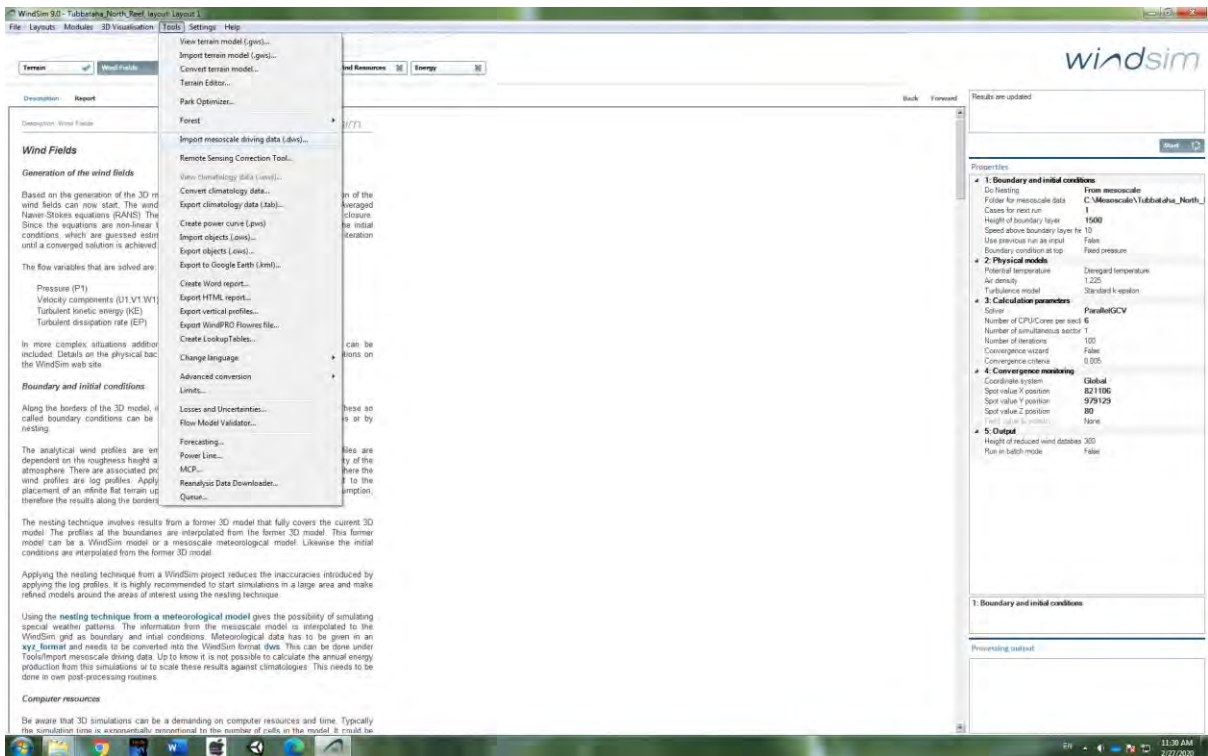


Figure 26. Data import tool for mesoscale model results

The WRF outputs that has been extracted using the NCL script are to be converted into xyz file. These are to be saved with the file name mesofieldxxx as shown in Figure 27.

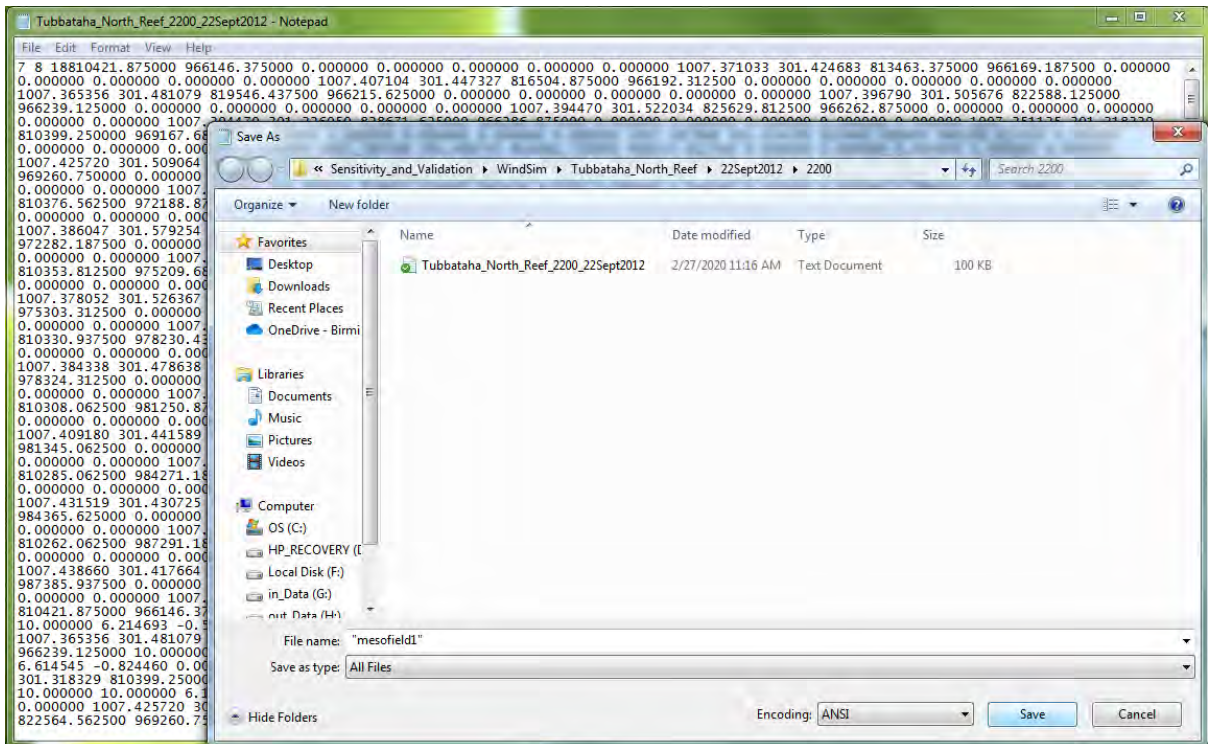


Figure 27. Screenshot of saving extracted mesoscale output data into xyz file

The import tool within WindSim, as shown in Figure 26, is to be executed which will open the console window shown in Figure 28.

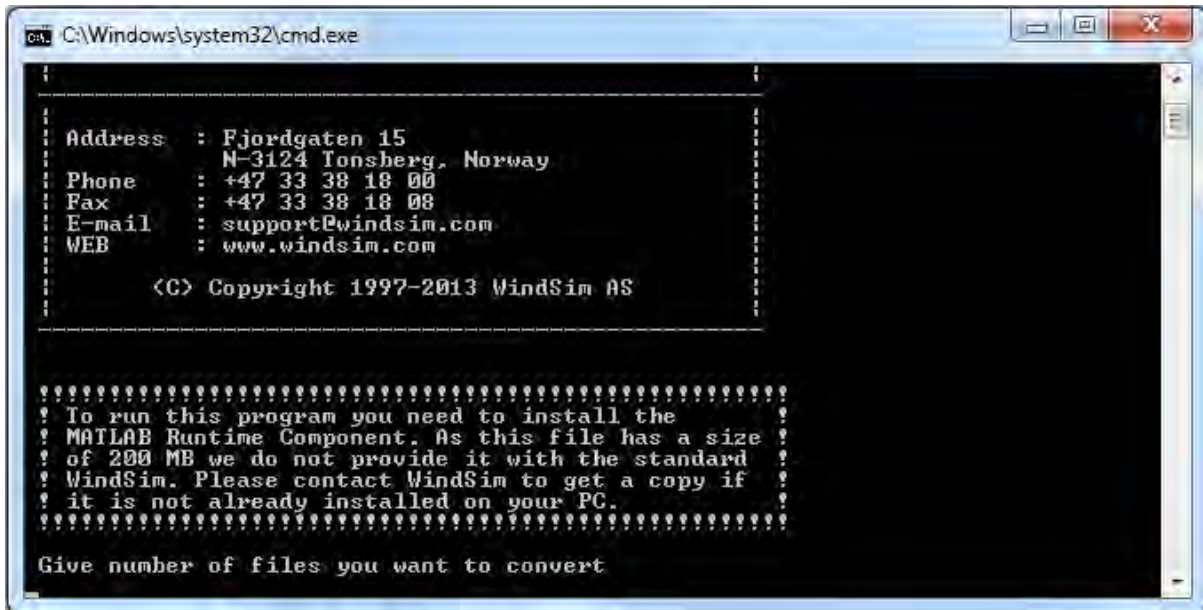


Figure 28. Opening screen of import tool

The data needed by the program are to be given through the console. These are shown in Figure 29 and Figure 30. The program asks for the number of files to be converted and the naming convention as presented in Figure 29. It also asks for the path of the folder where the xyz file is located.

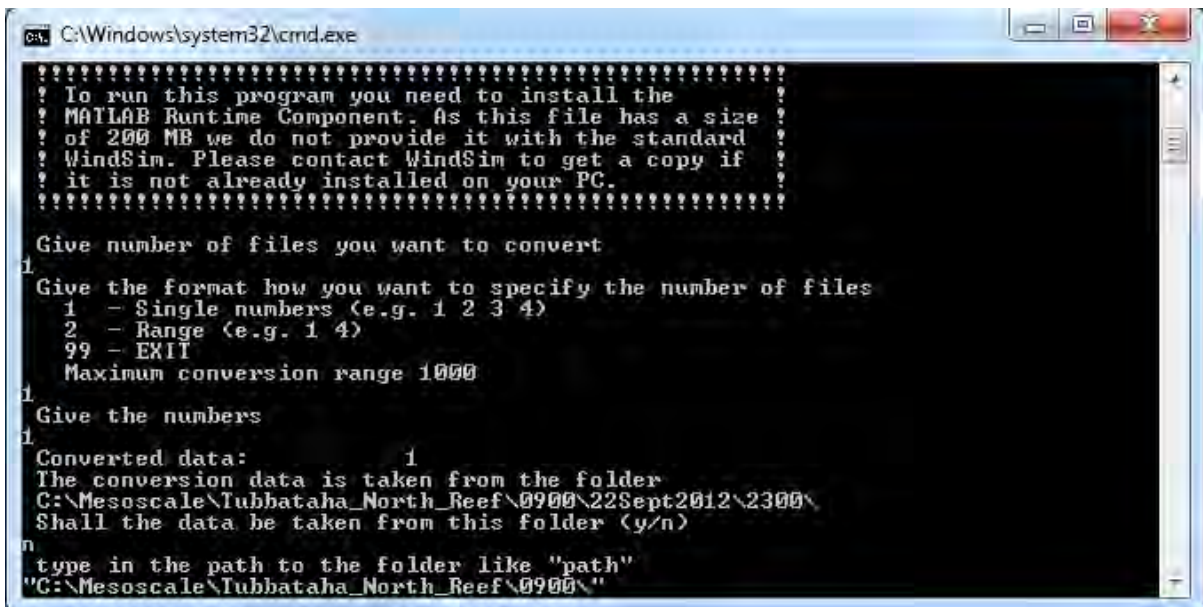


Figure 29. Screenshot of xyz import tool requesting file path, quantity, and naming format

In Figure 30, the import tool also asks for the starting x and y coordinates of the Terrain module. It also confirms which digital terrain model file it must access.

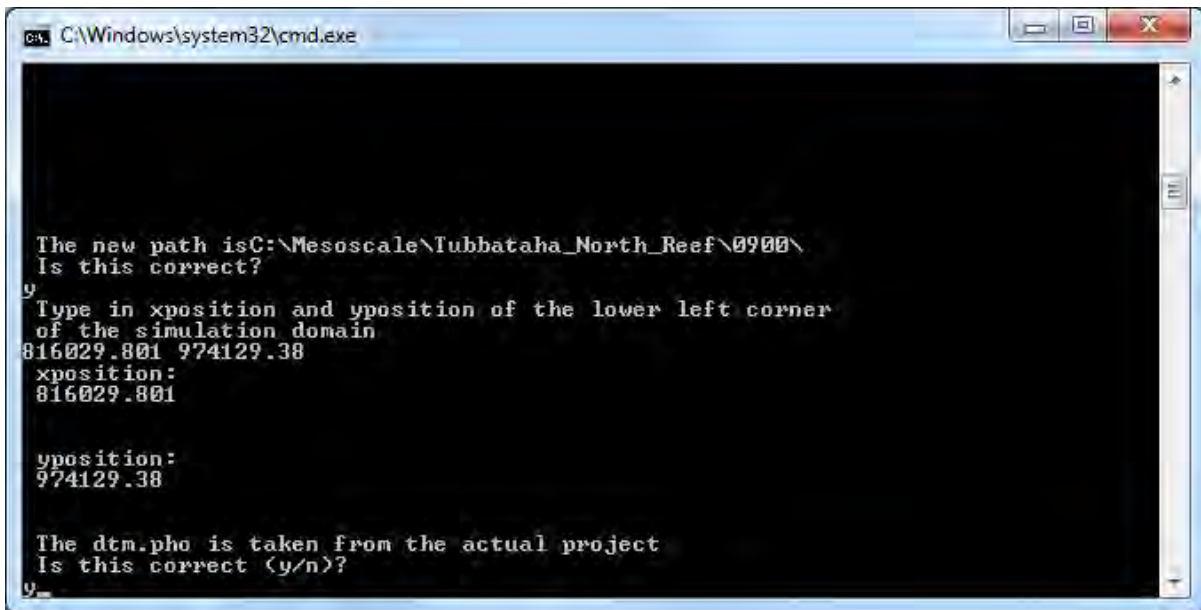


Figure 30. Screenshot of xyz import tool requesting starting coordinates of domain and terrain file

After giving all these inputs, the import tool will proceed to convert the xyz file into dws file. The dws file is the wind data that is compatible with the Wind Field module. A successful conversion will show a message such as presented in Figure 31.

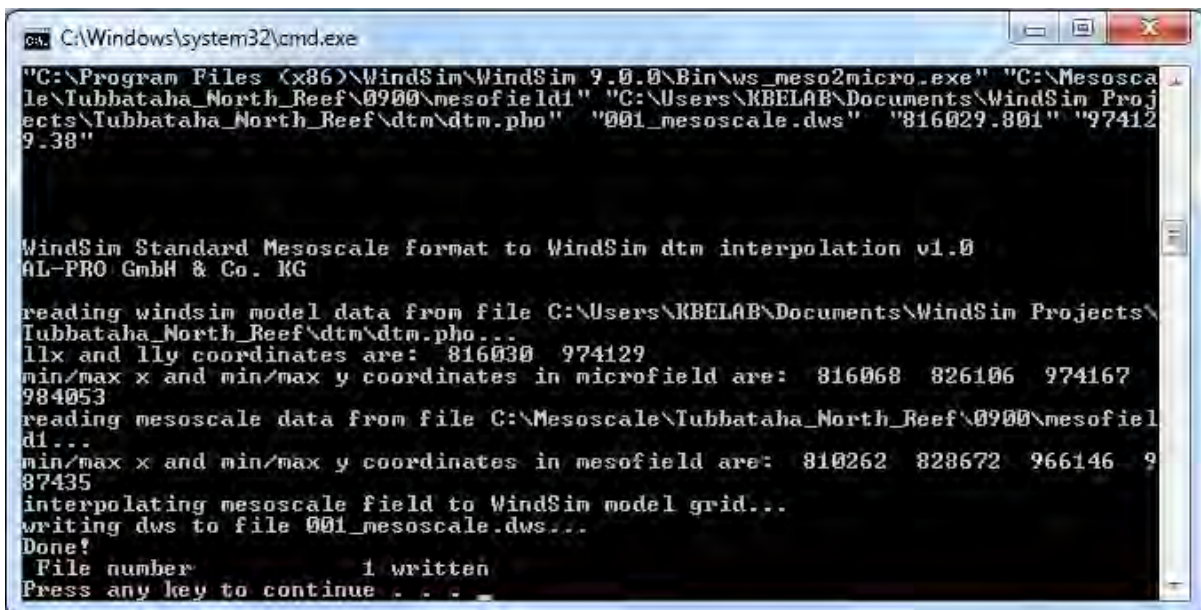


Figure 31. Screenshot of xyz import tool successfully converting xyz to dws file

Having imported the mesoscale model data, the Wind Field module can be started to perform the CFD simulation. A screenshot when the Wind Field module is running can be seen in Figure 32.

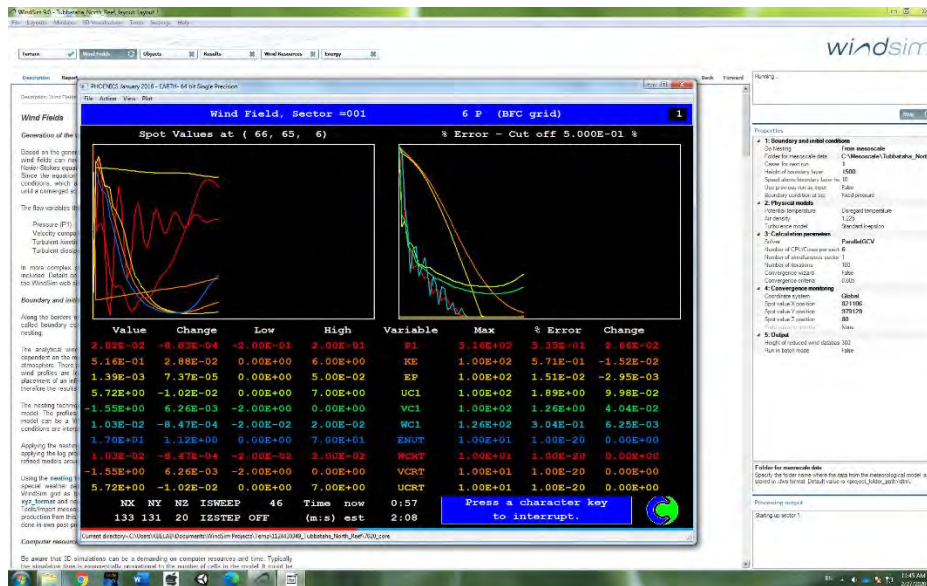


Figure 32. Screenshot of Wind Field module during a simulation run

The results of the WindSim simulations are stored in `xxx_red.phi` for the wind flow and `dtm.pho` for the topography. These are to be processed using Matlab so that the wind fields can be visualised and extracted for analysis. The Matlab scripts used are listed in the Appendix. A screenshot of the post-processing using Matlab is shown in Figure 33.

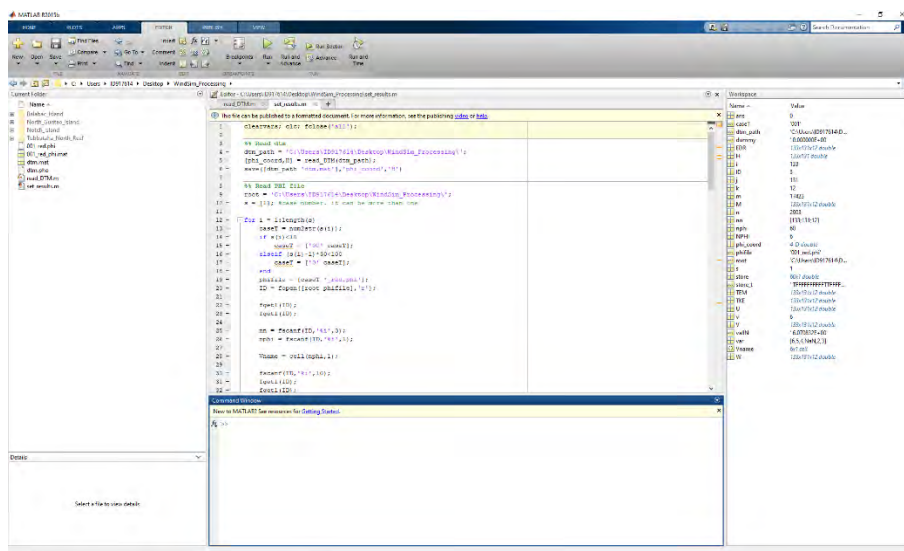


Figure 33. Screenshot of post-processing WindSim results with Matlab

The extracted data from Matlab are used to validate the WindSim results with the 7SEAS observations. All of the results from the mesoscale and microscale model are to be presented and discussed in Chapter 5.

These simulation work flow can be done for different areas and forms a guide that may be used for low latitude areas and small islands. A detailed wind simulation work flow is depicted in Figure 34. It can serve as an overview of the entire process that was done in this research.

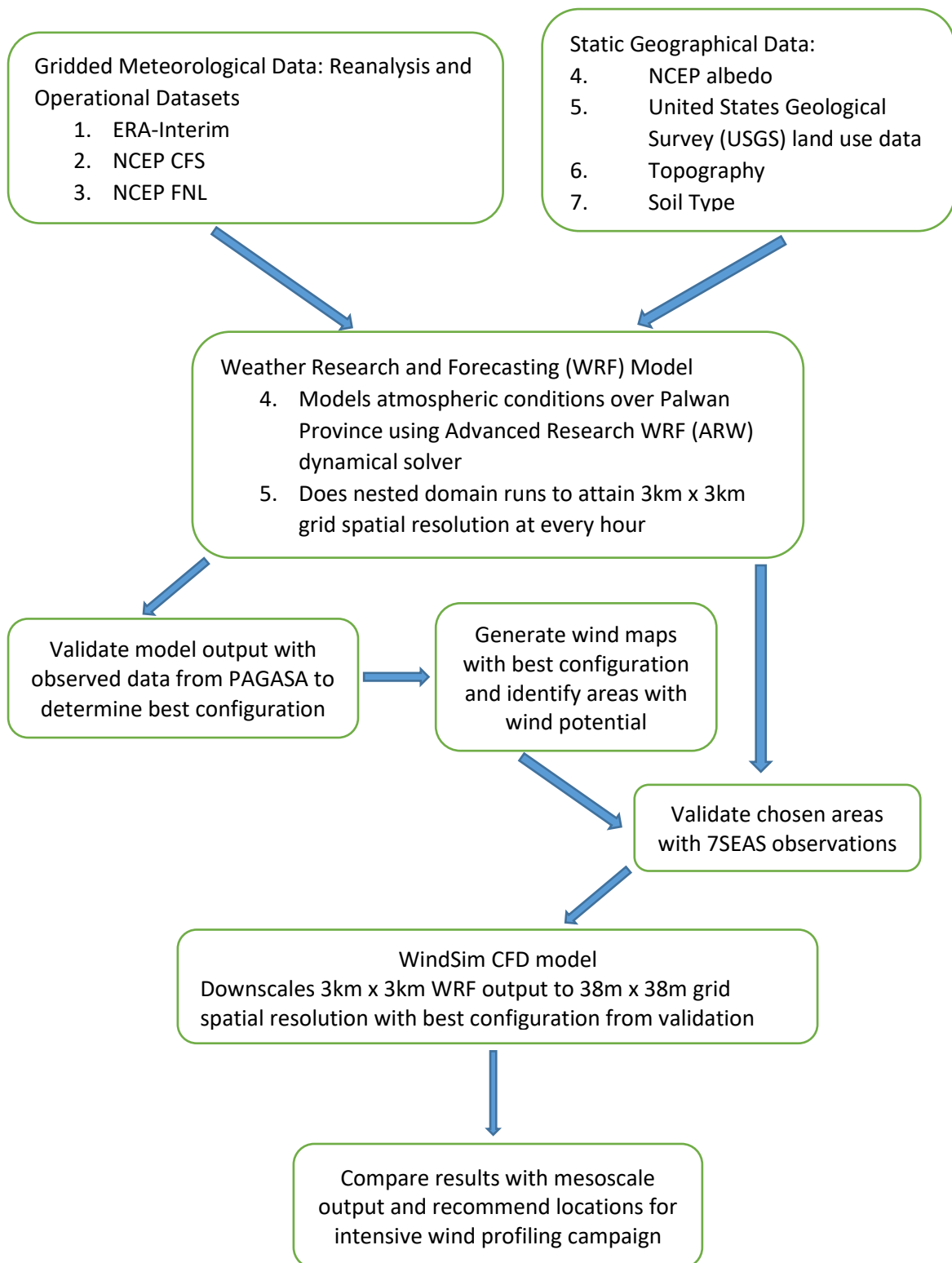


Figure 34. Wind simulation flow for mesoscale and microscale model

The necessary data for the simulations and essential observation data for validation are also outlined in Figure 34. The suitability of the generated wind data in this study are to be analysed in the next chapter.

5 RESULTS AND ANALYSIS

The mesoscale wind simulation results has undergone sensitivity tests and validation. These tests has involved varying the configuration of the model and using different reanalysis and operational data as input for the simulations. Details of these model settings have been discussed in Chapter 3. The subsequent sections show the different charts that compare the wind observations to the mesoscale results where the model used is the WRF. In another section of this chapter, the microscale model results are to be discussed. It will involve the parameter sensitivity of the WindSim CFD software that is used as the microscale model for this study. Then, a comparison in the performance between the mesoscale and microscale model are to be done to demonstrate the limitations of the mesoscale model in simulating low wind speeds in complex terrain and show that the microscale model integrated with mesoscale can be used to overcome that limitation. In turn, the limitation of microscale models for simple terrain will be discussed and how the mesoscale model is adequate in such cases.

5.1 Mesoscale Model

The wind speeds and wind direction are to be compared with the PAGASA stations in order to show the long-term and seasonal performance of the mesoscale model. This comparison will involve monthly wind speed scatter plots and monthly wind direction averages. This covers the years of 2010 to 2012 from the stations of Cuyo, Coron, and Puerto Princesa. These charts demonstrate that the WRF simulation results are capable of capturing the predominant wind flows in terms of direction but the wind speeds are generally overestimated. On the scatter plots, the black line depicts the ideal case where the simulation wind speed values are exactly equal to the measured values. Data points above the line are instances where the model results overestimate the wind speed while points below the line are model outputs that underestimate the wind speed observed. A more detailed discussion on scatter plots can be found in Section 3.6 (Page76). The errors on the simulations have also been quantified using root mean square error (RMSE), bias, and standard deviation error (STDE). These statistical tools have been discussed in Chapter 3. RMSE is needed so that the usual error value of the simulated results compared to observations can be known. Bias values allows the determination whether the errors are overestimates or underestimates of the measured wind velocities. Finally, STDE presents the deviation of simulated results from the mean which can show the long period cycle trends in the wind profile such as daily, monthly, or seasonal trends.

5.1.1 Mesoscale Model Wind Speed Results

Simulation runs on the mesoscale model has been done for the years of 2010, 2011, and 2012. The wind speeds in the simulation has been compared with the measured data from PAGASA [172].

The charts that show these model outputs in comparison with weather station data are found in the figures that follows. Charts with significant results are shown here but the rest of the figures are found in the Appendix. In the succeeding discussion, mesoscale model settings will be referred by the name of input dataset for readability and brevity but the complete settings are in Table 5 of Chapter 3.

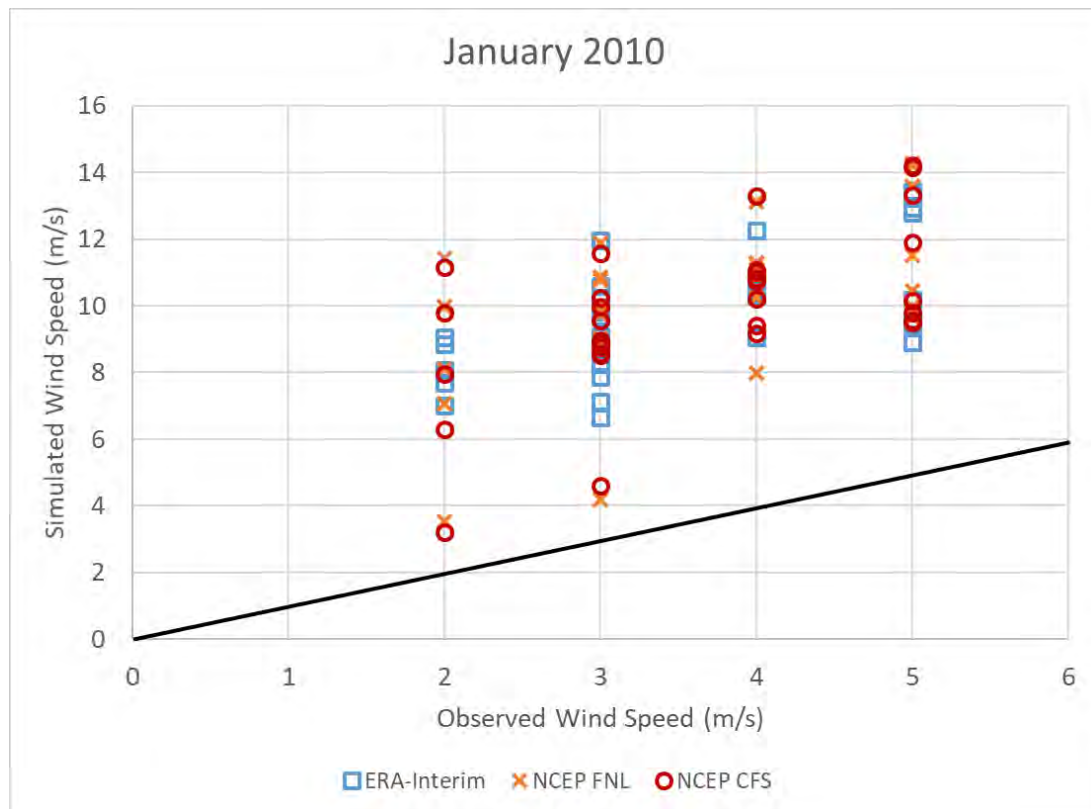


Figure 35. Scatter plot of different WRF model settings with PAGASA station data in Cuyo Island for January 2010.

For January months of 2010 – 2012, Coron and Cuyo simulations have the tendency to overestimate the wind speeds based on the scatter plots such as in Figure 35. This is also visible from the bias values of the two sites found in Table 7. NCEP-CFS and NCEP-FNL are slightly better than the ERA-Interim in Coron but majority of the model daily wind speed average are much higher than the observations. Table 7 presents that the RMSE and STDE values for ERA-Interim are higher by a small margin to the NCEP-CFS and NCEP-FNL at Coron Island. NCEP-FNL performs better than ERA-Interim and NCEP-CFS in Coron for January 2010 since it has the lowest RMSE, bias, and STDE values. For Cuyo Island, the NCEP-CFS has the smallest RMSE, bias, and STDE than the other two configurations. Overestimation can be as much as 5 – 6 m/s as shown in Table 5 for Coron and Cuyo. There are slight deviations from these values for January 2011 but not significant in terms of model performance. Thus, there is difficulty for the mesoscale model to simulate Coron and Cuyo Island for January. This is brought about by the low wind regime in the two islands since there are many days when the winds are less than 4 m/s. These low wind speeds are found to be overestimated by mesoscale models [20].

Table 7. January 2010 Model Errors and Bias Quantification of Wind Speed

Location	Configuration	ERA-Interim			NCEP-FNL			NCEP-CFS		
		RMSE	Bias	STDE	RMSE	Bias	STDE	RMSE	Bias	STDE
Coron Island		30.16	5.42	29.67	28.84	5.17	28.37	29.92	5.37	29.44
Cuyo Island		35.00	6.29	34.43	36.38	6.53	35.79	34.92	6.27	34.35
Puerto Princesa		6.64	1.19	6.53	8.13	1.46	8.00	5.33	0.96	5.24

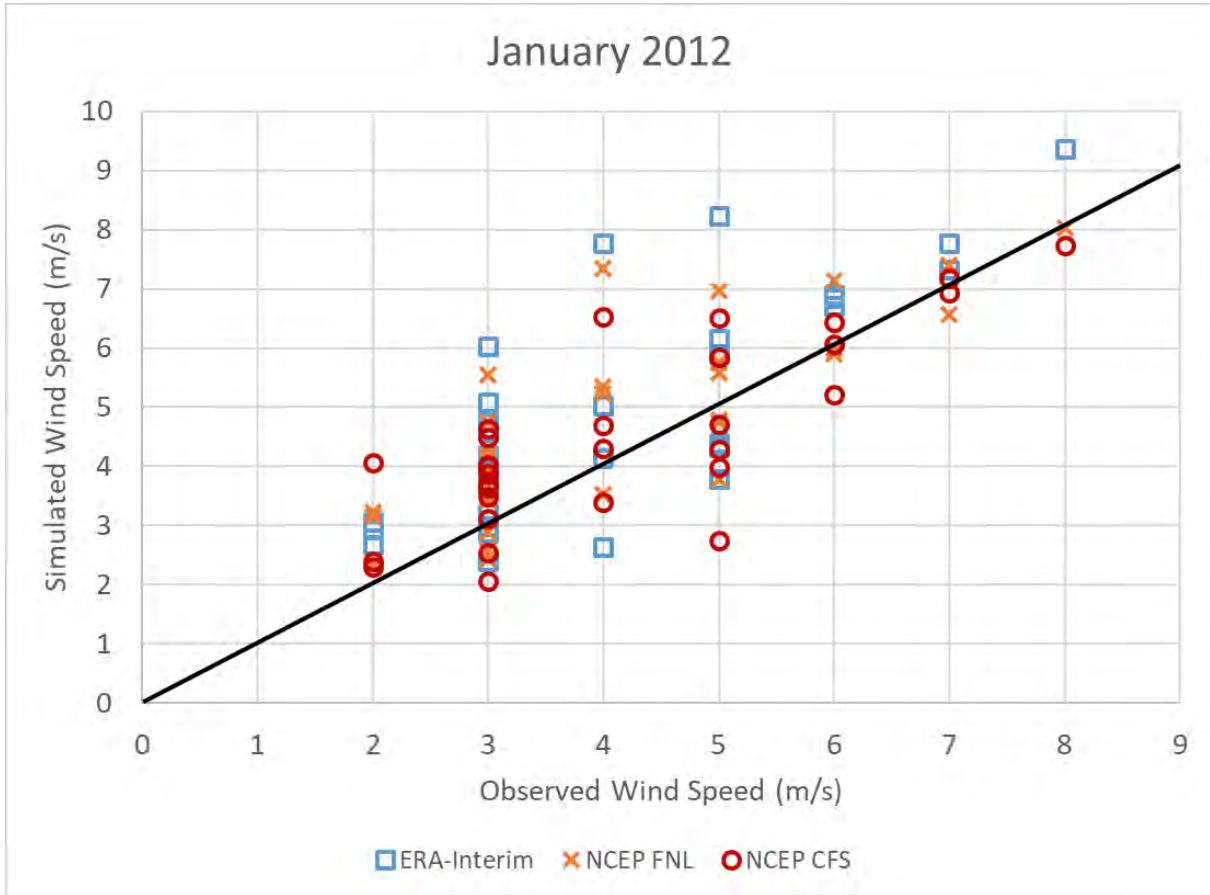


Figure 36. Scatter plot of different WRF model settings with PAGASA station data in Puerto Princesa for January 2012.

Looking at the plot in Figure 36, this presents the widest band of daily average wind speed from all the measurements obtained from PAGASA. This also yields the best simulation for Puerto Princesa on the month of January. There are still more overestimation of the wind speeds than underestimation being generated by the mesoscale model. Comparing the different model settings, it shows that ERA-Interim and NCEP-FNL produce the highest wind speed value difference to the observations. This also shows in Table 8 because ERA-Interim and NCEP-FNL have high bias values. On the other hand, the NCEP-CFS configuration have a tendency to cluster closer to the ideal line along with the least RMSE, bias, and STDE values that can be seen in Table 8. Thus, it is the NCEP CFS that gives the best wind profile of Puerto Princesa for January months.

Table 8. January 2012 Model Errors and Bias Quantification of Wind Speed

Location	Configuration	ERA-Interim			NCEP-FNL			NCEP-CFS		
		RMSE	Bias	STDE	RMSE	Bias	STDE	RMSE	Bias	STDE
Coron Island		26.54	4.77	26.11	25.06	4.50	24.65	28.16	5.06	27.70
Cuyo Island		30.57	5.49	30.07	33.37	5.99	32.82	30.73	5.52	30.23
Puerto Princesa		4.58	0.82	4.50	3.56	0.64	3.51	1.90	0.34	1.87

All three simulation results have similar wind speed value range for the three sites. When considering the model performance for Puerto Princesa, it is apparent from Figure 36 that the three models are better in simulating the area compared to Coron and Cuyo. This is also shown by the lower RMSE, bias, and STDE values calculated found in Table 7 and Table 8. Although they are still overestimating the wind speeds, the difference is smaller and at times there are underestimation. The higher wind speeds experienced in January for Puerto Princesa allowed the mesoscale model to yield a good wind profile of the area. The wind speeds between 6 – 8 m/s from the observations are modelled well since these are within the range where the mesoscale model can effectively determine wind characteristics [18]. NCEP-CFS and ERA-Interim perform well for this site on this month while NCEP-FNL have higher wind speed values overall from the bias with higher RMSE and STDE values. The dynamic range of NCEP-CFS and NCEP-FNL is better than the ERA-Interim since there are daily averages where the ERA-Interim yields twice the measured values. When looking at the range and the magnitude of daily average difference between simulation and observation, the NCEP-CFS offers the best results for Puerto Princesa.

The simulation results of February months for Coron Island and Cuyo Island are very similar with the January months. These are quantified in Table 9 and Table 10 because the values are similar in addition to the similarity between the scatter plots that can be seen in the Appendix 1. The generally overestimated values can be seen in Figure 37 where even days with zero wind are shown to have 2 m/s to almost 5 m/s. This presents the fact that the mesoscale model is always producing winds and unable to reproduce lull moments.

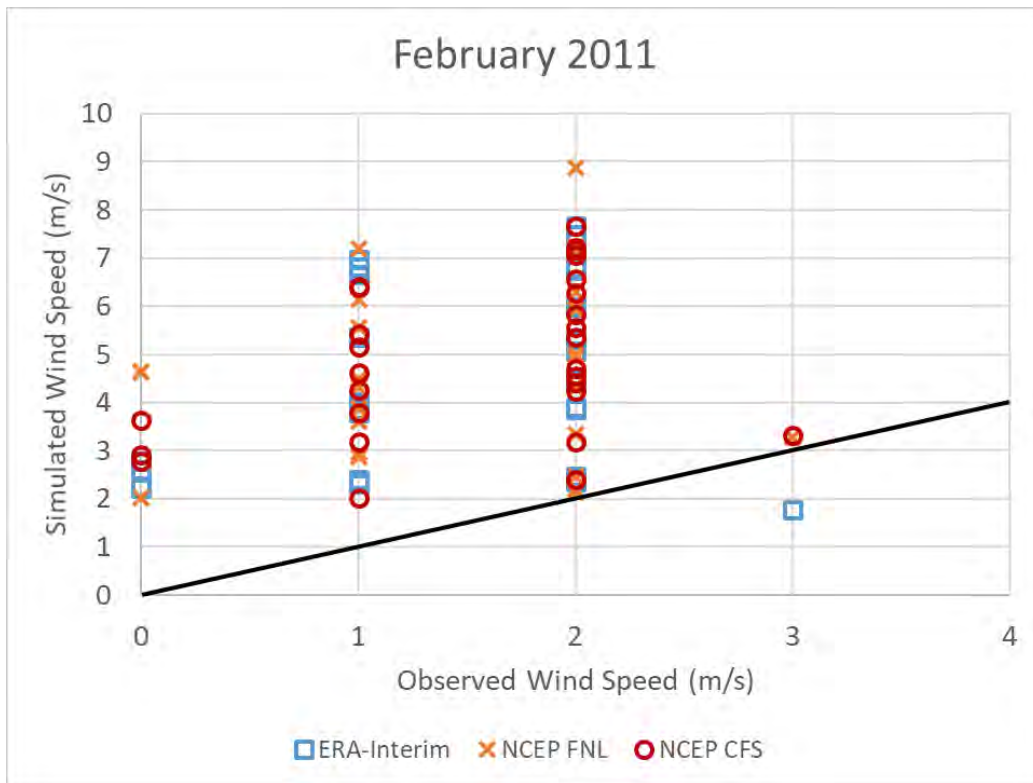


Figure 37. Scatter plot of different WRF model settings with PAGASA station data in Coron Island for February 2011.

The three model configurations have performed better than the January months simulations because there is lower RMSE, bias, and STDE across the three settings. But the overestimation by the WRF model persists here so, the mesoscale model have trouble modelling the wind at Coron and Cuyo Island for February months. This for the same reason that there are low wind speeds in the region since all are below 4 m/s and these are values that the mesoscale model overestimates which also happens in the January months. Looking at Figure 38, the simulations show a markedly better performance as the dynamic range and difference of daily averages with measurements are smaller. This is also reflected in Table 9 because the RMSE, bias, and STDE are lower than the January values especially for the Coron Island which is significantly lower.

Table 9. February 2011 Model Errors and Bias Quantification of Wind Speed

Configuration	ERA-Interim			NCEP-FNL			NCEP-CFS		
	RMSE	Bias	STDE	RMSE	Bias	STDE	RMSE	Bias	STDE
Coron Island	17.01	3.22	16.71	17.18	3.25	16.87	17.78	3.36	17.45
Cuyo Island	37.56	7.10	36.89	39.76	7.51	39.05	39.38	7.44	38.67
Puerto Princesa	9.61	1.82	9.43	7.86	1.49	7.72	6.69	1.26	6.56

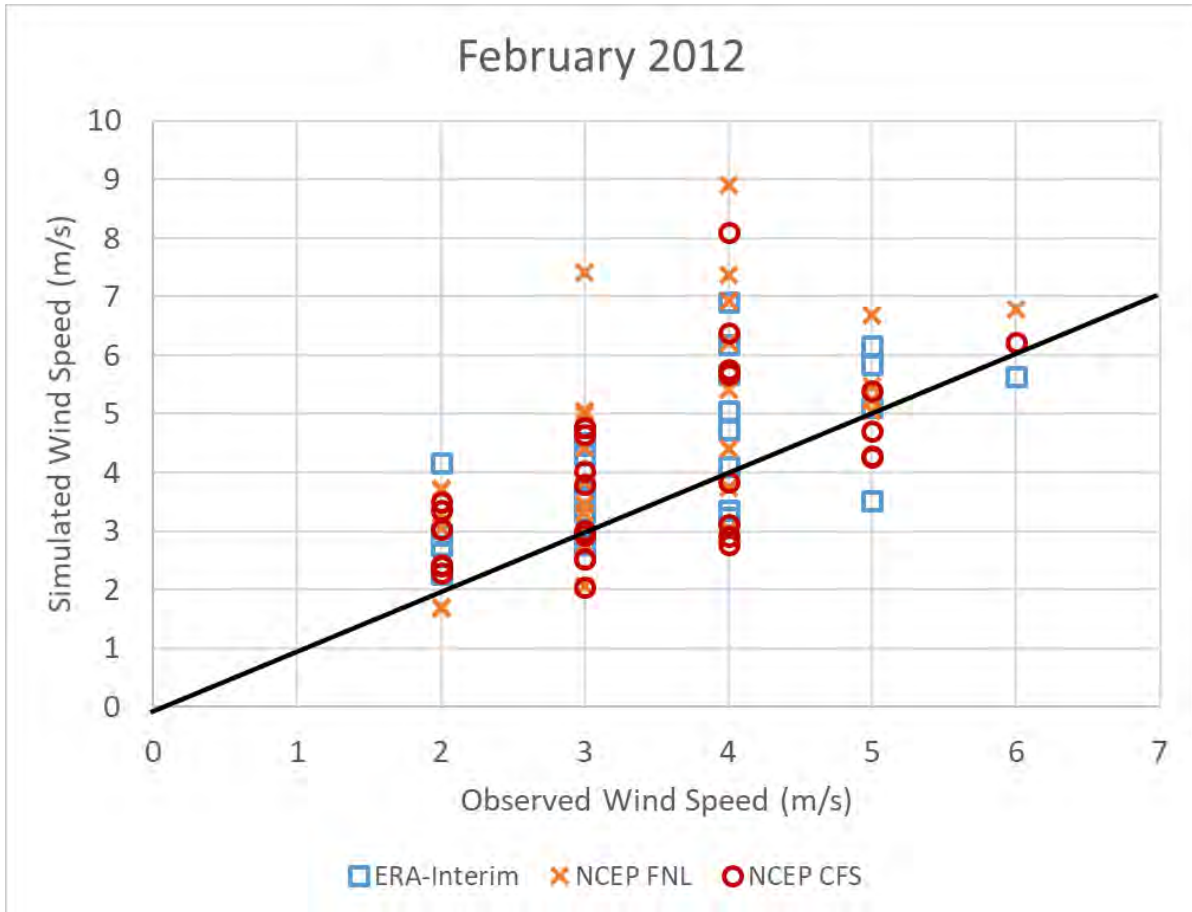


Figure 38. Scatter plot of different WRF model settings with PAGASA station data in Puerto Princesa for February 2012.

The scatter plot in Figure 38 presents that the mesoscale model is capable of simulating the Puerto Princesa site for February. This is also true in some cases when there are low wind speeds in February as can be seen in the Appendix 1. Wind speeds that are 4 m/s or below are overestimated which is also characteristic in the January months. The NCEP-CFS gives the best performance for this site since it has the smallest RMSE, bias, and STDE values compared to ERA-Interim and NCEP-FNL where the typical values are listed in Table 10. It is noticeable that there is a slightly lower maximum daily wind speed average in February compared to January. This is because of the weakening of the Northeast Monsoon which is strong in January months for the Philippines [154].

Table 10. February 2012 Model Errors and Bias Quantification of Wind Speed

Configuration	ERA-Interim			NCEP-FNL			NCEP-CFS		
	RMSE	Bias	STDE	RMSE	Bias	STDE	RMSE	Bias	STDE
Coron Island	25.26	4.69	24.82	26.78	4.97	26.31	26.33	4.89	25.88
Cuyo Island	29.21	5.42	28.70	30.55	5.67	30.02	27.44	5.10	26.96
Puerto Princesa	3.80	0.71	3.73	6.02	1.12	5.91	2.87	0.53	2.82

The month of March at Coron Island has proven to be difficult for the mesoscale model as shown by the results for 2010, 2011, and 2012. None of the model configurations is better than the other for this since they all have the same range of daily wind speed average values as shown in the

Appendix 1. The values in Table 11 are similar to the RMSE, bias, and STDE values for March 2011 and March 2012 that are quite high so, the inability of the model is evident here. There is the occurrence of overestimation in Coron Island and this overestimation is also shown in the bias values for Cuyo Island in Table 11 that ranges from 5.13 – 5.69 m/s. Thus, the simulation performance for March is no better than the results for February months for Coron and Cuyo. Once again, the low wind speed regime in Coron and Cuyo Islands are yielding the large deviation between measurements and simulations because of the tendency of the mesoscale model to overestimate these wind speed range.



Figure 39. Scatter plot of different WRF model settings with PAGASA station data in Puerto Princesa for March 2010.

Table 11. March 2010 Model Errors and Bias Quantification of Wind Speed

Configuration	ERA-Interim			NCEP-FNL			NCEP-CFS		
	RMSE	Bias	STDE	RMSE	Bias	STDE	RMSE	Bias	STDE
Coron Island	25.50	4.58	25.09	23.22	4.17	22.84	23.95	4.30	23.56
Cuyo Island	28.54	5.13	28.08	31.69	5.69	31.17	30.36	5.45	29.87
Puerto Princesa	1.70	0.31	1.67	2.80	0.50	2.75	0.06	-0.01	0.06

For Puerto Princesa, the simulations are underestimating and overestimating the daily wind speed averages in a more equal distribution as shown by Figure 39. ERA-Interim tends to overestimate observed values at 3 m/s while giving a more equal distribution of overestimates and underestimates for higher wind speeds. NCEP FNL has a more equal distribution for wind speeds at 3 – 4 m/s but overestimates winds at 5 m/s. NCEP CFS yields an equal distribution for any wind speeds at Puerto

Princesa for March so, it is the best performing mesoscale model configuration here. This good performance is also evident with RMSE, bias, and STDE to be almost zero as enumerated in Table 11. The relatively higher daily wind speed average in Puerto Princesa, compared to Coron and Cuyo, enables the mesoscale model to perform better at this location. There is a decrease in daily wind speed average in March compared to January and February since this is the time when hot-dry season begins in the Philippines and the Northeast Monsoon weakens further.

On the April months, the Coron Island simulations are slightly better when compared with the Cuyo Island results even though a few daily averages for Cuyo are close to the observed daily averages. This is because when considering Table 12 and Table 13, it can be seen that the RMSE, bias, and STDE for all configurations are lower or similar at the Coron site than at Cuyo. The Puerto Princesa simulations demonstrate similar performance as with the simulations for the month of March. The results from NCEP CFS and ERA-Interim are better than the NCEP FNL since this model setting produced some values that have the highest difference with the measured daily wind speed average. This is consistent with the RMSE, bias, and STDE values in Table 12 where it can be seen that NCEP-FNL is higher than the two settings. The RMSE, bias, and STDE are lowest for NCEP-CFS as shown in Table 12 and Table 13 thus, it is the best configuration for Puerto Princesa for the months of April. Some of the scatter plots for April are shown in the following figures to further discuss the model performance.

In the figures that follow, it shows that there is a lower average daily wind speed compared to the months of January to March. This is because the Northeast Monsoon has ended and winds are coming from the West Pacific Ocean at this time of the year which are called the Easterlies [155]. These winds are weaker compared to the winds generated by the Northeast Monsoon in the Philippines. Thus, there is a decrease in average wind speeds in all the sites under study as will be shown in the charts.

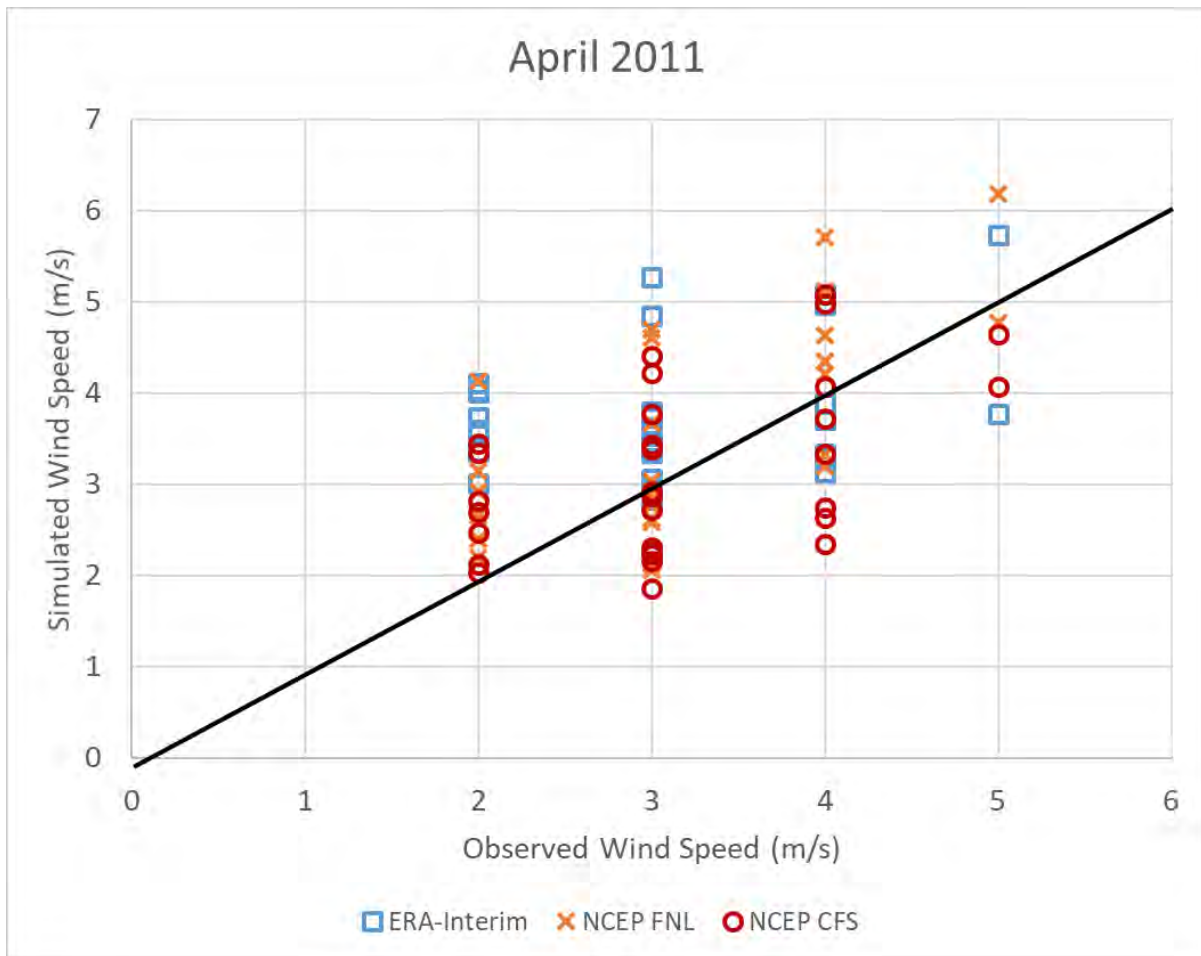


Figure 40. Scatter plot of different WRF model settings with PAGASA station data in Puerto Princesa for April 2011.

At Puerto Princesa, the wind speeds for April 2011 as seen in Figure 40 have similar dynamic range as April 2010 of 2 m/s to 5 m/s. Although the overall model performance is the same with the results from the April 2010 simulations, it is apparent that the NCEP-CFS gives better output than ERA-Interim and NCEP-FNL. This is also evident in Table 12 where it shows that the calculated RMSE, bias, and STDE values are almost zero for the NCEP-CFS.

Table 12. April 2011 Model Errors and Bias Quantification of Wind Speed

Configuration	ERA-Interim			NCEP-FNL			NCEP-CFS		
	RMSE	Bias	STDE	RMSE	Bias	STDE	RMSE	Bias	STDE
Coron Island	19.32	3.53	18.99	18.34	3.35	18.03	18.40	3.36	18.09
Cuyo Island	24.38	4.45	23.97	27.42	5.01	26.96	26.35	4.81	25.91
Puerto Princesa	3.44	0.63	3.38	1.80	0.33	1.77	0.03	0.01	0.03

There is a notable improvement in the simulations of Coron Island for April 2012 which can be seen in Figure 41. When compared with April 2010 and April 2011, NCEP-CFS and ERA-Interim have performed essentially the same but the NCEP-FNL have shown a drastic improvement. Table 13 also shows the low error and bias values for NCEP-FNL configuration that reflects the good model performance. The NCEP-FNL configuration outputs are densely bunched together near the ideal line with the lowest

RMSE, bias, and STDE values thus, it is the most suited settings for the mesoscale model in simulating Coron Island for April 2012. Another simulation result with a remarkable improvement is with the output of WRF for April 2012 at Cuyo Island that appears in Figure 42. When the April 2012 results are compared with April 2010 and April 2011, it shows that all the three configurations for 2012 gave better results because of lower overestimation magnitude than the 2010 and 2011 model output for April. All three configurations also have lower RMSE, bias, and STDE values compared to the April 2010 and April 2011 values. NCEP-CFS is the better configuration than ERA-Interim because the data points from ERA-Interim gives higher difference between the observations and simulations. The NCEP-FNL is the best configuration for April 2012 at the Cuyo Island site because it is heavily clustered near the ideal line of the scatter plot along with the fact that the RMSE, bias, and STDE values are smallest among the three model settings.

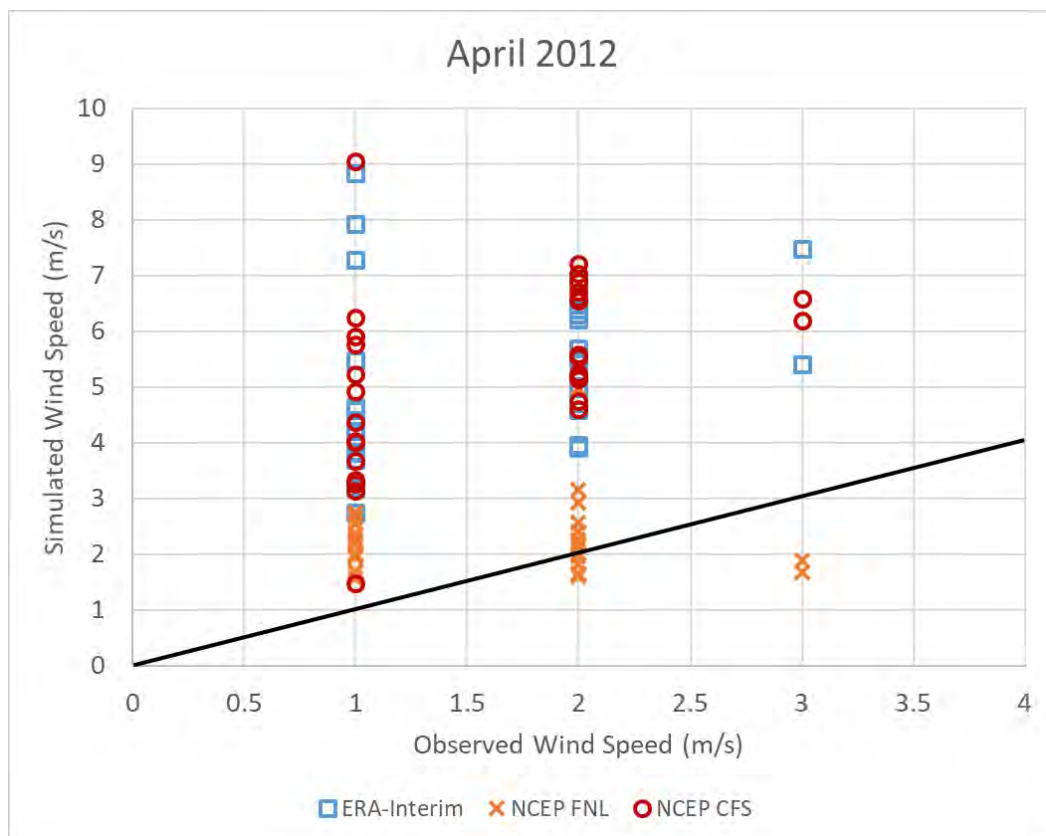


Figure 41. Scatter plot of different WRF model settings with PAGASA station data in Coron Island for April 2012.

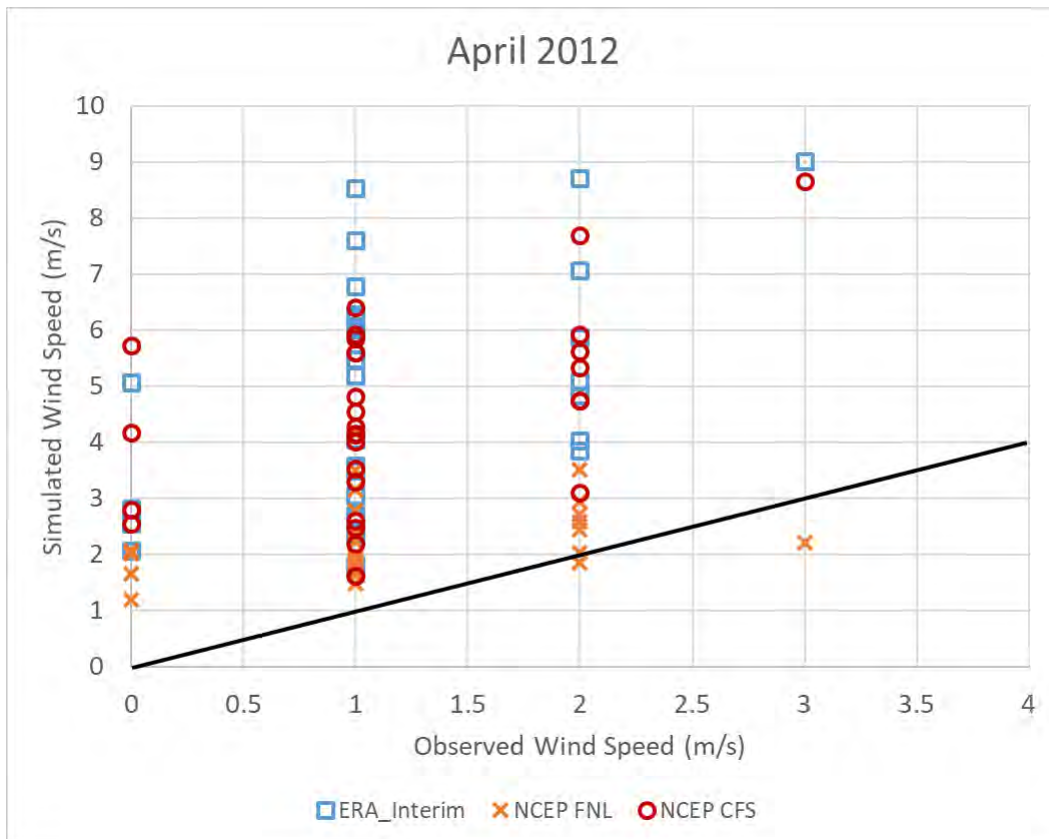


Figure 42. Scatter plot of different WRF model settings with PAGASA station data in Cuyo Island for April 2012.

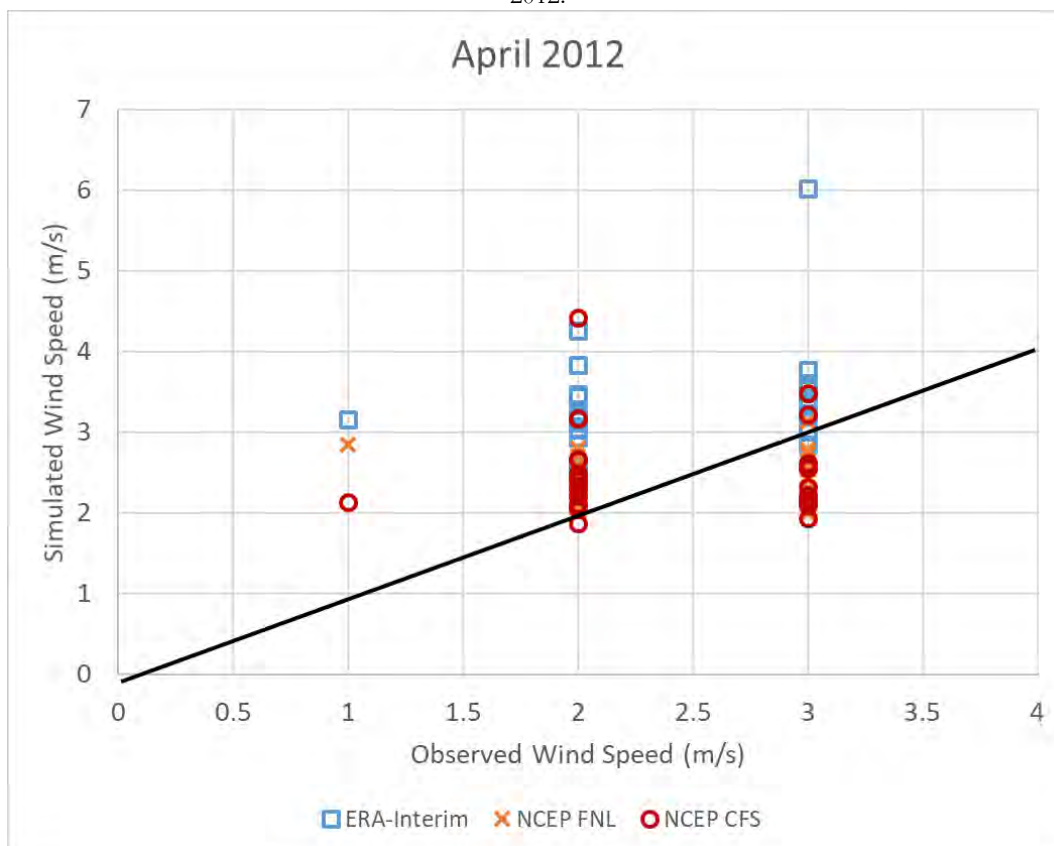


Figure 43. Scatter plot of different WRF model settings with PAGASA station data in Puerto Princesa for April 2012.

Measured daily wind speed averages at the Puerto Princesa station have decreased for April 2012, found in Figure 43, compared to April 2010 and April 2011. The Aprils of 2010 and 2011 have wind speed ranges of 2 – 5 m/s while April 2012 has dropped down to the 1 – 3 m/s range. There is also an improvement in the WRF modelling performance with the NCEP FNL configuration for April 2012. The NCEP-FNL model settings have generated daily wind speed average values that are grouped together close to the ideal line. It also has the least RMSE, bias, and STDE values among the three configurations enumerated in Table 13. Therefore, NCEP-FNL is capable of simulating the wind profile at Puerto Princesa for April 2012.

The generally low wind speeds for April months show that limits of the mesoscale model in simulating winds below 4 m/s again especially for the Coron and Cuyo Islands. The daily average wind speeds in those areas have a maximum of 3 m/s which are below the wind speed range that the mesoscale model is capable of simulating. So, the model performance and yielded results are expected to produce high bias and error values as listed in Table 13.

Table 13. April 2012 Model Errors and Bias Quantification of Wind Speed

Configuration Location	ERA-Interim			NCEP-FNL			NCEP-CFS		
	RMSE	Bias	STDE	RMSE	Bias	STDE	RMSE	Bias	STDE
Coron Island	20.06	3.66	19.72	3.47	0.63	3.41	20.34	3.71	20.00
Cuyo Island	20.00	3.65	19.66	5.78	1.06	5.68	18.04	3.29	17.74
Puerto Princesa	5.35	0.98	5.26	0.11	-0.02	0.11	0.51	0.09	0.50

The month of May is a transition between the Easterlies and the Southwest Monsoon. This change has no meaningful effect in terms of wind speed since the range of daily wind speed averages for May are similar to the month of April. Cuyo Island has experienced 16 days of invalid data for May 2012 and a decrease in daily average wind speeds thus, it is not given the same weight for validation. But this low wind speed profile for Cuyo is similar to the other observations in May so, it is still included in the analysis. Simulations for May are yielding very high wind speed values in comparison to the observations at Coron and Cuyo islands. In Figure 44, the mesoscale model generates wind speeds that are seven times higher than the daily wind speed averages of 1 m/s on some days at the weather station. The model output at Cuyo Island even have winds when winds are absent on those days as shown in Figure 44. This shows once again that the mesoscale model is unable to produce zero wind values at this site and one of the reasons why it has a tendency to overestimate wind speeds.

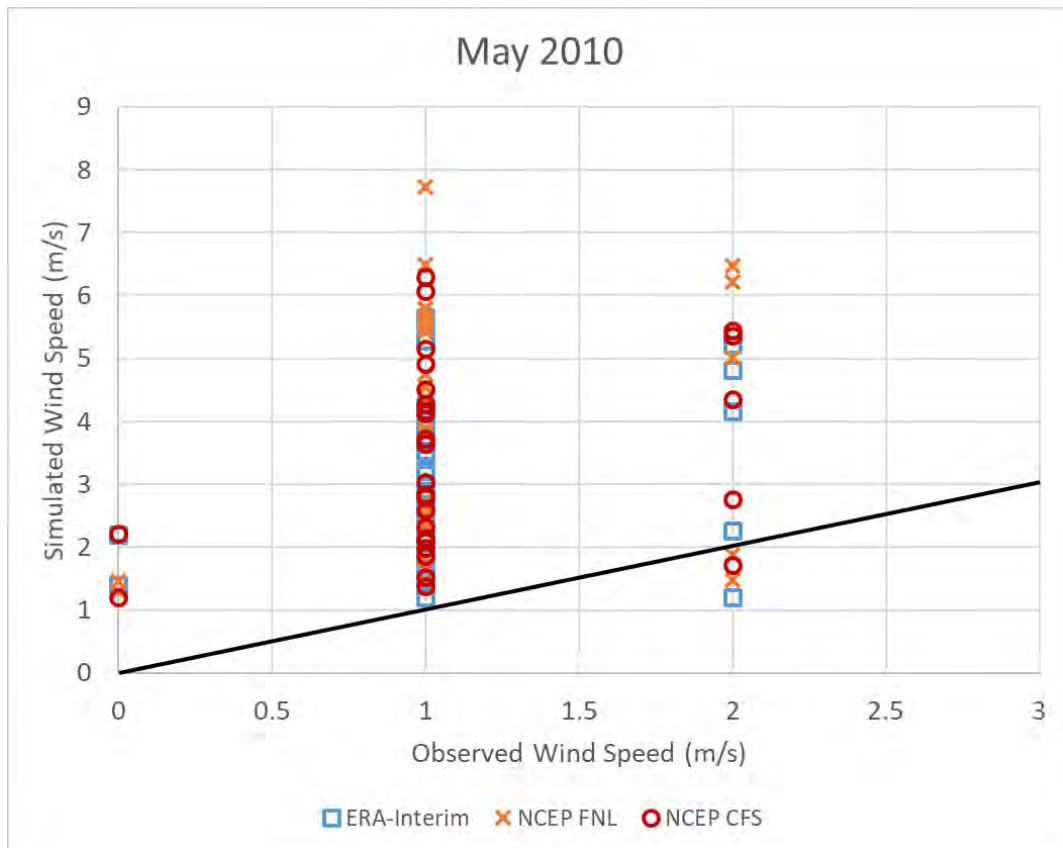


Figure 44. Scatter plot of different WRF model settings with PAGASA station data in Cuyo Island for May 2010.

Table 14. May 2010 Model Errors and Bias Quantification of Wind Speed

Configuration	ERA-Interim			NCEP-FNL			NCEP-CFS		
	RMSE	Bias	STDE	RMSE	Bias	STDE	RMSE	Bias	STDE
Coron Island	14.39	2.59	14.16	20.21	3.63	19.88	17.57	3.15	17.28
Cuyo Island	11.14	2.00	10.95	15.04	2.70	14.79	12.26	2.20	12.06
Puerto Princesa	6.30	1.13	6.20	2.24	0.40	2.21	2.60	0.47	2.56

When looking at Table 14, it can be seen that Coron and Cuyo simulations for May has shown improvement than for January to April since there are lower RMSE, bias, and STDE for May. Focusing on Cuyo Island results, the NCEP-FNL configuration are giving the largest overestimated wind speeds when compared to the ERA-Interim and NCEP-CFS. These high overestimates are attributable to the high bias of NCEP-FNL that can be found in Table 15 and Table 16. For reasons of yielding the smallest overestimates, ERA-Interim is better than NCEP-FNL and NCEP-CFS in modelling winds over Cuyo Island for May. Another reason for this is that the ERA-Interim configuration has the lowest RMSE, bias, and STDE values out of the three model settings.

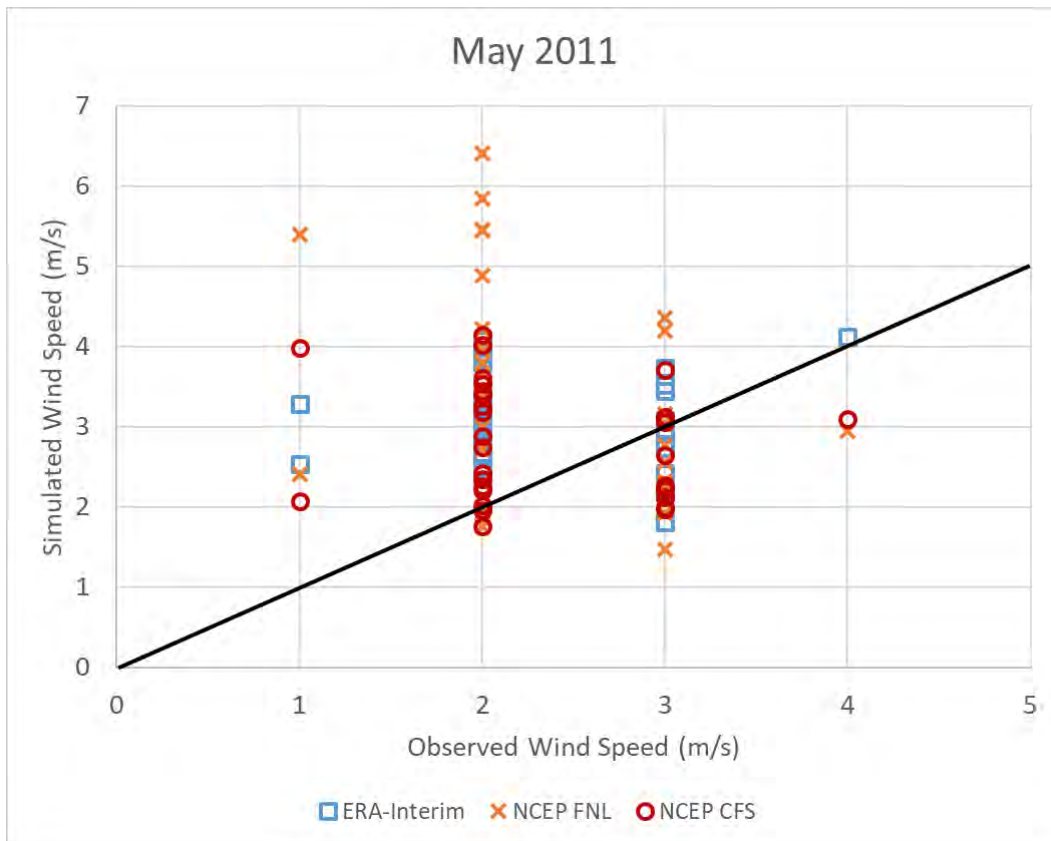


Figure 45. Scatter plot of different WRF model settings with PAGASA station data in Puerto Princesa for May 2011.

Wind speed scatter plot for the May 2011 at Puerto Princesa, found in Figure 45, shows that there is a wider spectrum of wind speed values than for May 2010 which can be found in the Appendix. Average daily wind speeds can now range between 1 m/s to 4 m/s unlike for May 2010 that either has 2 m/s or 3 m/s wind speed. As in the simulations for Cuyo Island for May, NCEP-FNL have the highest difference in value with the observations. ERA-Interim is slightly better than NCEP-FNL when simulating at this location for May because ERA-Interim has lower RMSE, bias, and STDE values which are listed in Table 15 and Table 16. The NCEP-CFS is the best performing configuration at Puerto Princesa for May because it has the lowest RMSE, bias, and STDE values for 2011 and 2012.

Table 15. May 2011 Model Errors and Bias Quantification of Wind Speed

Configuration	ERA-Interim			NCEP-FNL			NCEP-CFS		
	RMSE	Bias	STDE	RMSE	Bias	STDE	RMSE	Bias	STDE
Coron Island	11.26	2.02	11.08	23.71	4.26	23.33	14.07	2.53	13.84
Cuyo Island	22.18	3.98	21.82	32.45	5.83	31.92	23.10	4.15	22.72
Puerto Princesa	4.01	0.72	3.95	5.50	0.99	5.41	2.48	0.45	2.44

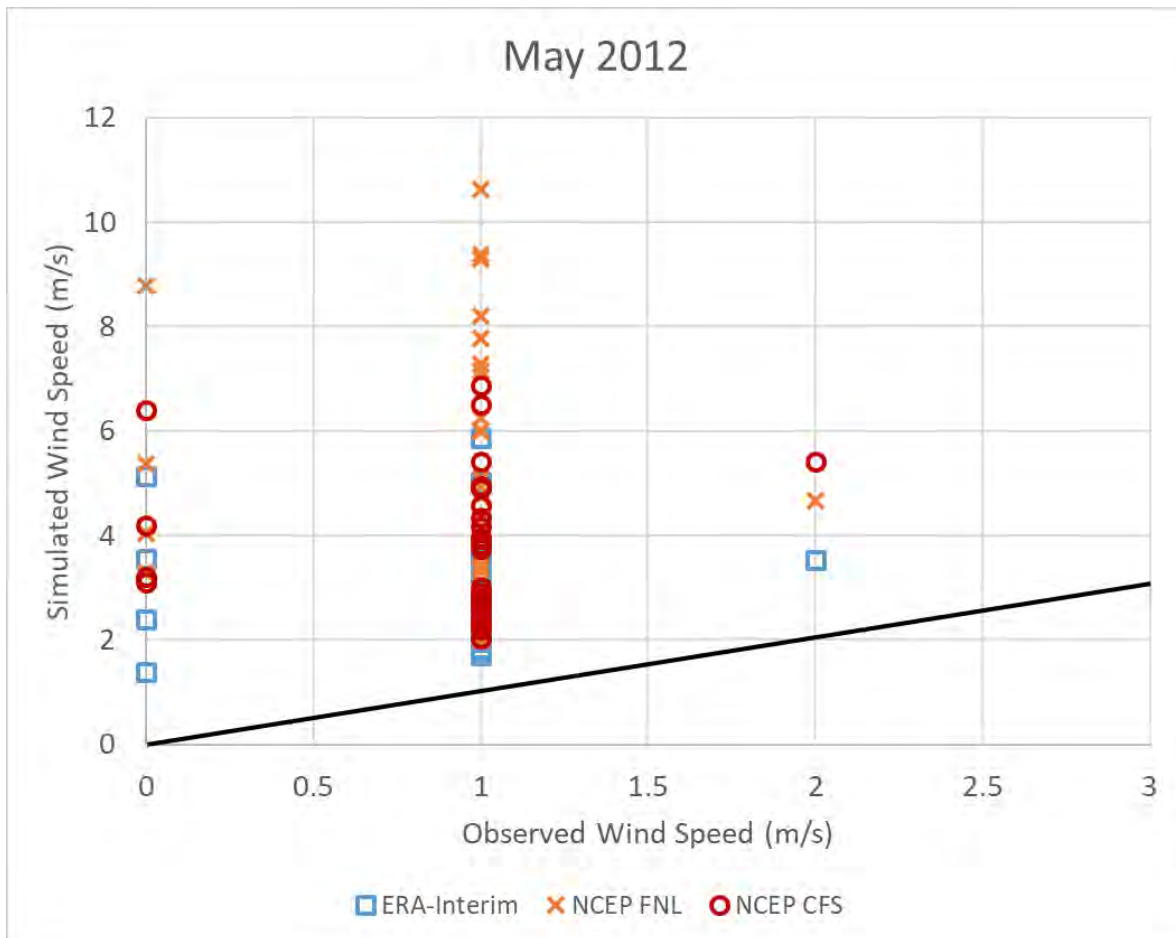


Figure 46. Scatter plot of different WRF model settings with PAGASA station data in Coron Island for May 2012.

Winds have died down for May 2012 upon comparison with May 2010 and 2011 since, as shown in Figure 46, there are several days without wind flow and many are only 1 m/s. This made the mesoscale model to perform poorly since it is unable to generate zero wind conditions and the days with 1 m/s winds from observations are being simulated to range between around 2 – 10 m/s. Despite the lower wind speed regime, Table 16 show that bias and error values are lower or similar to the Table 14 and Table 15 values. This shows that the model is able to maintain its performance even with the change in wind regime at the area. Among the three configurations selected for this study, the ERA-Interim is better than the NCEP-CFS and NCEP-FNL because it gives lower overestimated values for Coron as well as the smallest RMSE, bias and STDE that can be seen in Tables 14 - 16.

Table 16. May 2012 Model Errors and Bias Quantification of Wind Speed

Configuration	ERA-Interim			NCEP-FNL			NCEP-CFS		
	RMSE	Bias	STDE	RMSE	Bias	STDE	RMSE	Bias	STDE
Coron Island	9.54	1.71	9.38	23.27	4.18	22.89	16.29	2.92	16.02
Cuyo Island	9.75	2.52	9.41	23.41	6.04	22.62	18.55	4.79	17.92
Puerto Princesa	6.57	1.18	6.46	7.79	1.40	7.67	2.94	0.53	2.89

The inability of the mesoscale model to produce zero wind is more pronounced with the June simulations for Coron and Cuyo. As shown in Figure 47 and Appendix 1, there are many days with no wind at the stations yet the WRF model would still generate wind values for lull moments of the wind flow at both stations. It must be also noted that there is no data for Cuyo Island for the last five days of June 2010 but it is treated with the same weight as the other June months because it still has data in most of the days. Data observations for 12 days are invalid for the month of June 2012 at Cuyo Island as well so they have been removed.

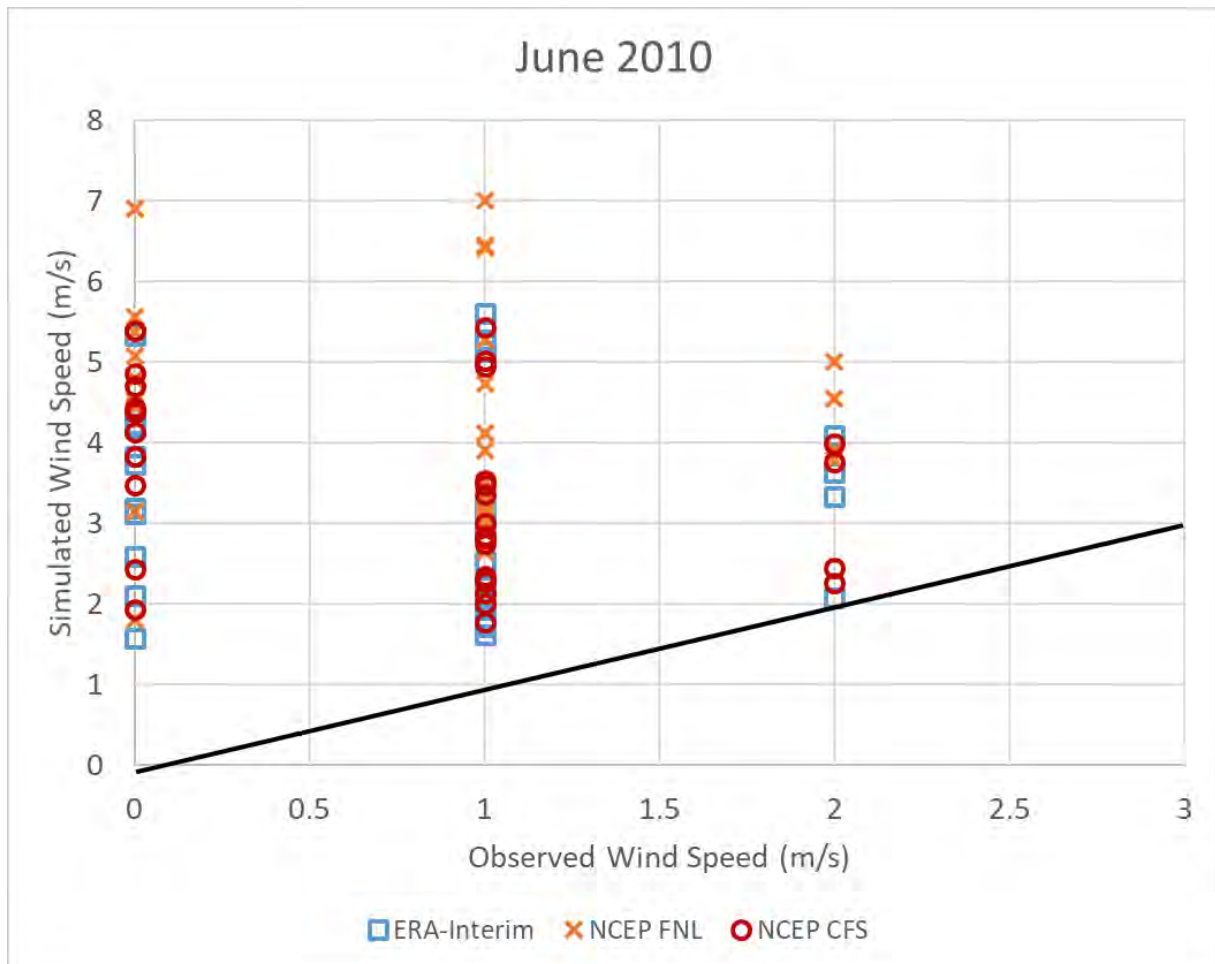


Figure 47. Scatter plot of different WRF model settings with PAGASA station data in Coron Island for June 2010.

Table 17. June 2010 Model Errors and Bias Quantification of Wind Speed

Configuration	ERA-Interim			NCEP-FNL			NCEP-CFS		
	RMSE	Bias	STDE	RMSE	Bias	STDE	RMSE	Bias	STDE
Coron Island	12.68	2.32	12.47	19.24	3.51	18.91	14.26	2.60	14.02
Cuyo Island	12.78	2.56	12.52	20.16	4.03	19.75	15.11	3.02	14.80
Puerto Princesa	5.58	1.02	5.49	4.89	0.89	4.81	6.42	1.17	6.31

The simulation results are overestimates of the wind observations especially with the NCEP-FNL settings which produces values with the highest difference compared to station observations. RMSE,

bias, and STDE values for NCEP-FNL are the highest among the three configurations as seen in Table 17. Some of the daily wind speed averages generated by NCEP-FNL are as high as 14 times in Coron Island and almost ten times overestimation in Cuyo Island. Based on the values in Table 17 and 18, Coron and Cuyo are simulated best by the ERA-Interim model settings. In comparison with the June simulations for Coron and Cuyo, the Puerto Princesa model results are better as shown in Figure 46.

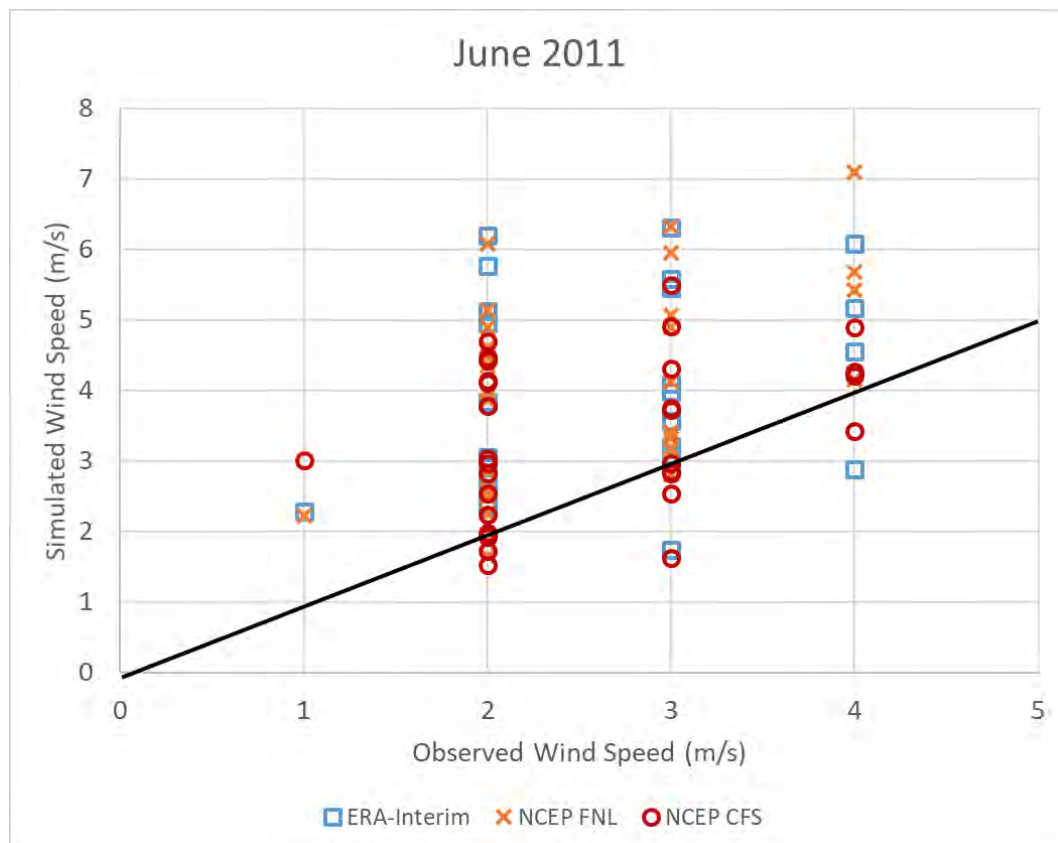


Figure 48. Scatter plot of different WRF model settings with PAGASA station data in Puerto Princesa for June 2011.

For Puerto Princesa, Figure 48 show that the WRF model is performing relatively better than the other sites. There is an overestimation of the daily wind speed averages with the NCEP-FNL performing better than the other two configurations based on the RMSE, bias, and STDE values in Table 12 (Page 102). ERA-Interim and NCEP-FNL are giving similar wind speed values while the NCEP-CFS are generating lower daily average wind speed values that are closer to the PAGASA station records for Puerto Princesa. From Table 18, this is also apparent because ERA-Interim and NCEP-FNL have similar RMSE, bias, and STDE values while NCEP-CFS has the lowest corresponding values. This is also true for the June 2012 values listed in Appendix 3. So, the NCEP-CFS is the best model setting when simulating the month of June for Puerto Princesa.

Table 18. June 2011 Model Errors and Bias Quantification of Wind Speed

Configuration	ERA-Interim			NCEP-FNL			NCEP-CFS		
	RMSE	Bias	STDE	RMSE	Bias	STDE	RMSE	Bias	STDE
Coron Island	15.81	2.89	15.54	27.73	5.06	27.26	16.83	3.07	16.55
Cuyo Island	17.54	3.20	17.25	29.99	5.48	29.49	19.05	3.48	18.73
Puerto Princesa	6.79	1.24	6.67	7.87	1.44	7.73	4.42	0.81	4.35

Typically, the month of June is the beginning of the Southwest Monsoon in the Philippines [151]. This phenomenon causes winds over the Philippines to come from the Southwest direction predominantly but these winds are weaker than the Northwest Monsoon [154]. Thus, the daily average wind speed range are similar to the months of April and May.

July simulation results in Figure 49 are the typical wind speeds for Coron and Cuyo islands which are very similar with the June results. It has been noted that the first 11 days of July 2010 at the Cuyo Island station have no measurements. The missing data have been accounted for the validation to avoid having any influence in the analysis. All the configurations for the model are giving high wind speeds in comparison with the observations and the inability to yield zero wind speeds are again apparent. Based on the daily wind speed average difference, the ERA-Interim settings have the best performance among the three for Coron and Cuyo. ERA-Interim also has the lowest RMSE, bias, and STDE values listed in Table 19.

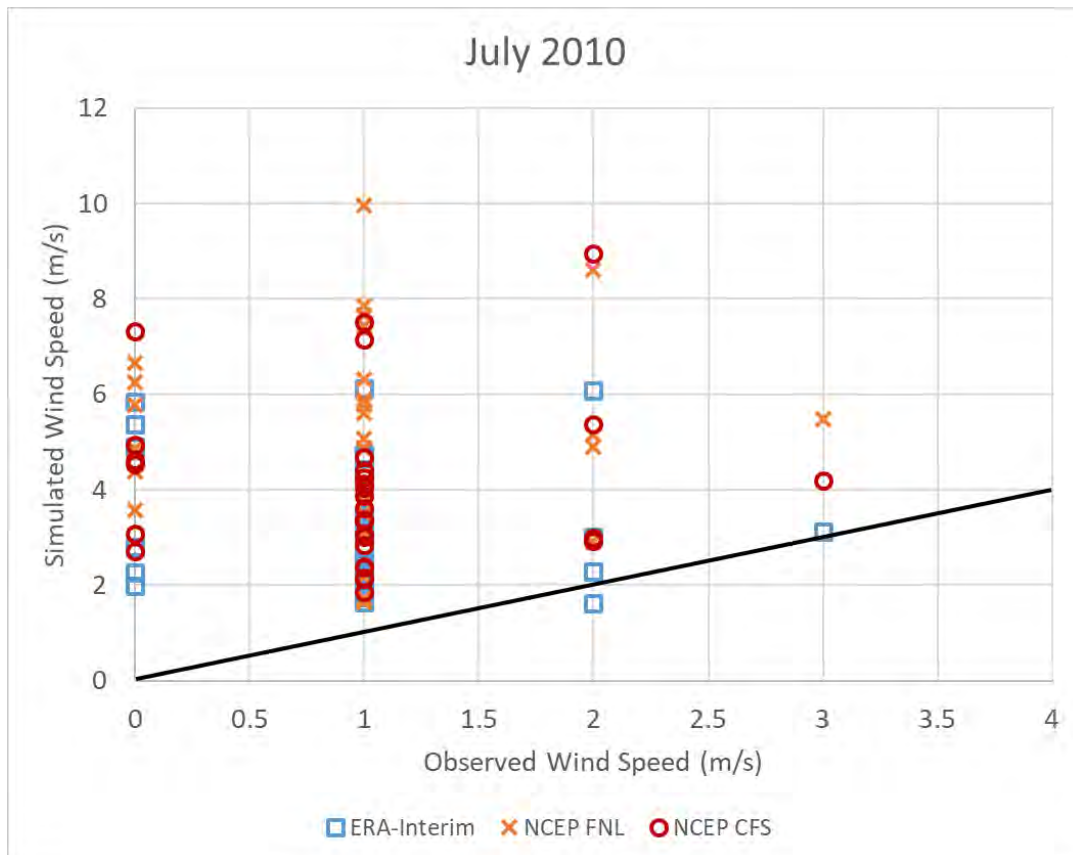


Figure 49. Scatter plot of different WRF model settings with PAGASA station data in Coron Island for July 2010.

Table 19. July 2010 Model Errors and Bias Quantification of Wind Speed

Configuration	ERA-Interim			NCEP-FNL			NCEP-CFS		
	RMSE	Bias	STDE	RMSE	Bias	STDE	RMSE	Bias	STDE
Coron Island	11.62	2.09	11.43	22.95	4.12	22.58	16.94	3.04	16.66
Cuyo Island	12.87	2.88	12.54	23.14	5.18	22.56	19.48	4.36	18.99
Puerto Princesa	7.49	1.35	7.37	7.71	1.38	7.58	5.97	1.07	5.87

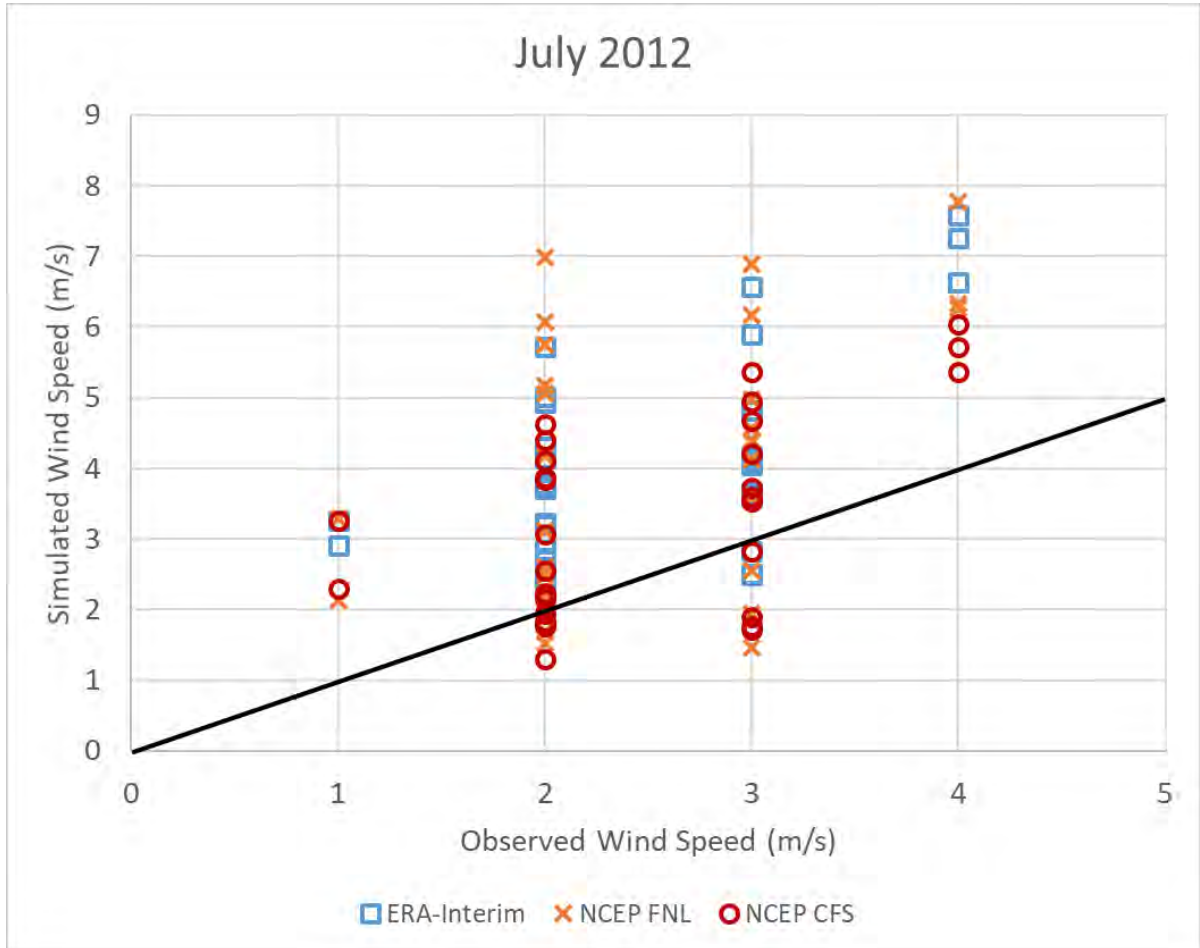


Figure 50. Scatter plot of different WRF model settings with PAGASA station data in Puerto Princesa for July 2012.

At Puerto Princesa, it can be seen in Figure 50 that there is an improvement in mesoscale model performance capabilities for July compared to the Coron and Cuyo islands. Underestimation of daily wind speed average at 2 m/s are occurring which is present in the July 2010 model output shown in Appendix 1. There are also underestimation of daily wind speed averages at 3 m/s. The maximum value of overestimation has decreased to no more than above 8 m/s in this occasion.

Table 20. July 2012 Model Errors and Bias Quantification of Wind Speed

Configuration	ERA-Interim			NCEP-FNL			NCEP-CFS		
	RMSE	Bias	STDE	RMSE	Bias	STDE	RMSE	Bias	STDE
Coron Island	21.19	3.81	20.84	36.20	6.50	35.61	24.90	4.47	24.49
Cuyo Island	23.60	4.24	23.21	39.82	7.15	39.17	31.48	5.65	30.97
Puerto Princesa	8.83	1.59	8.69	8.43	1.51	8.29	4.59	0.83	4.52

NCEP-FNL and ERA-Interim are producing the highest difference between simulation value and measured daily average wind speed which is also true for the July results as listed in Table 19 and Table 20. The NCEP-CFS has lower overestimated value magnitude and clusters nearer to the ideal line. It is also the model configuration that has the lowest RMSE, bias, and STDE values in Table 19 and Table 20. Therefore, it is the best model configuration for modelling Puerto Princesa for the month of July since it performs well in all the three years covered in this study.

Finding that the July months are similar to the June results, it shows that the Southwest Monsoon wind speeds are similar to the Easterlies. The change from dry to wet season and the shift in the prevalent wind direction in the Philippines has no effect to the wind speeds. So, the wind speeds that are coming from the West Pacific Ocean and East Indian Ocean are the same for the Philippines.

The observed wind speeds for the month of August at Coron and Cuyo islands present a broader spectrum once again which are similar with June and July months. There are overestimation of daily average wind speeds from the simulations. This is also characterized by the high RMSE and STDE values that are above 20 m/s and bias that are 3.61 – 5.84 m/s enumerated in Table 21. ERA-Interim and NCEP CFS are yielding similar results and are better in simulating Coron and Cuyo for August than NCEP FNL because their wind speed overestimates are lesser. Between ERA-Interim and NCEP-CFS, it can be seen that ERA-Interim has the lower RMSE, bias, and STDE values than NCEP-CFS so ERA-Interim is better suited in simulating Coron and Cuyo sites for August. This increase in the daily wind speed average made the mesoscale model to perform better but only marginally. It is expected for the mesoscale model to perform in a similar manner as with June and July months because the month of August is still part of the Southwest Monsoon.

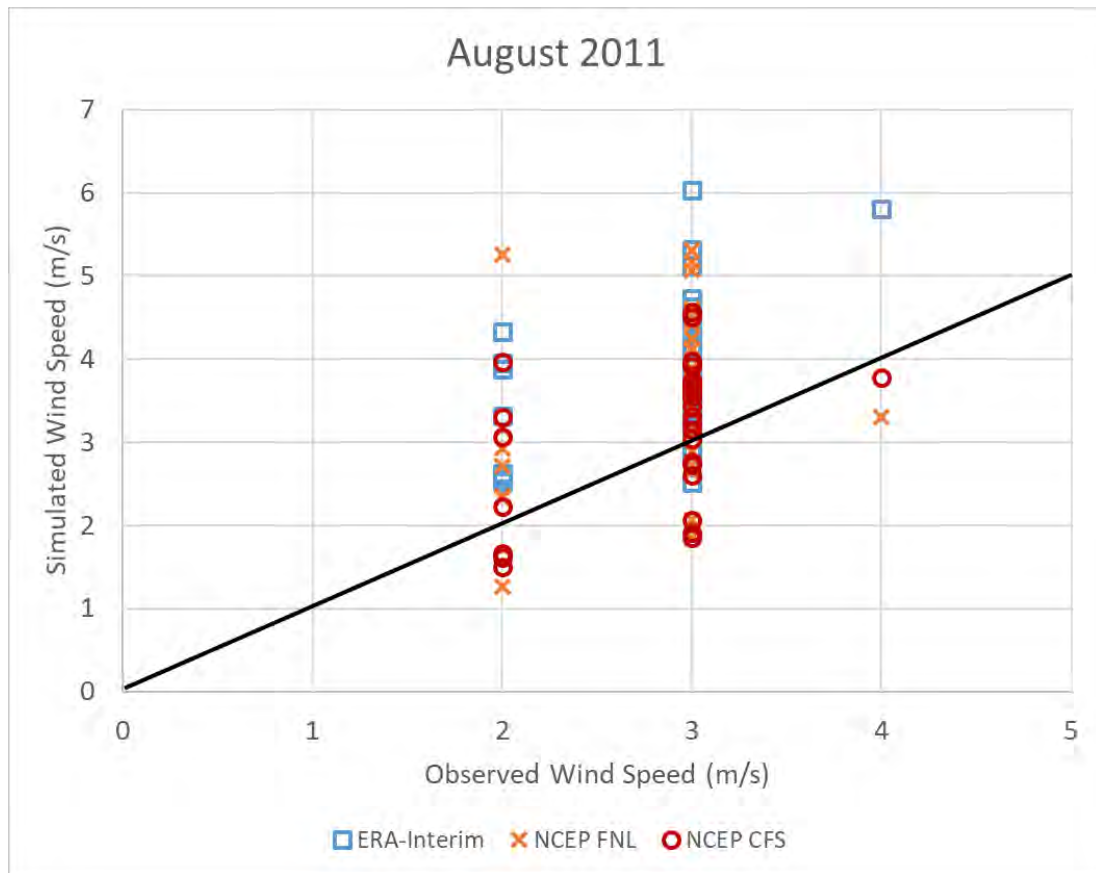


Figure 51. Scatter plot of different WRF model settings with PAGASA station data in Puerto Princesa for August 2011.

The mesoscale model performs better when simulating Puerto Princesa as can be seen in Figure 51 although it overestimates the measured daily average wind speed values which is the same with the June and July model output. The NCEP-CFS is the best configuration for August since the difference of its highest value with the observation is less than for NCEP FNL and ERA-Interim. In addition to that, NCEP-CFS has the smallest RMSE, bias, and STDE values as can be seen in Table 21.

Table 21. August 2011 Model Errors and Bias Quantification of Wind Speed

Configuration	ERA-Interim			NCEP-FNL			NCEP-CFS		
	RMSE	Bias	STDE	RMSE	Bias	STDE	RMSE	Bias	STDE
Coron Island	20.13	3.61	19.79	28.98	5.21	28.51	24.22	4.35	23.82
Cuyo Island	22.45	4.03	22.08	32.53	5.84	32.00	26.43	4.75	26.00
Puerto Princesa	6.10	1.09	6.00	4.28	0.77	4.21	1.86	0.33	1.83

There is still an overall slow wind speeds for August as found in June and July. Low wind speeds are characteristic for the Philippines during the Southwest Monsoon season because the winds coming from the East Indian Ocean must traverse the Indochina Peninsula before reaching the Philippines [154]. So, the winds will be slower because the surface roughness introduced by the Indochina Peninsula will decrease the wind flow that continues towards the Philippines.

With the September model outputs, the simulations are able to perform better than for the results in June – August. The RMSE, bias, and STDE values listed in Table 22 also show lower values compared to the ones calculated for June – August. The month of September is the start when there is a transition from Southwest Monsoon to Northeast Monsoon [152]. As it has been demonstrated from the January and February months, the mesoscale is more capable in simulating the Northeast Monsoon thus, this is the cause of the model performance witnessed for September.

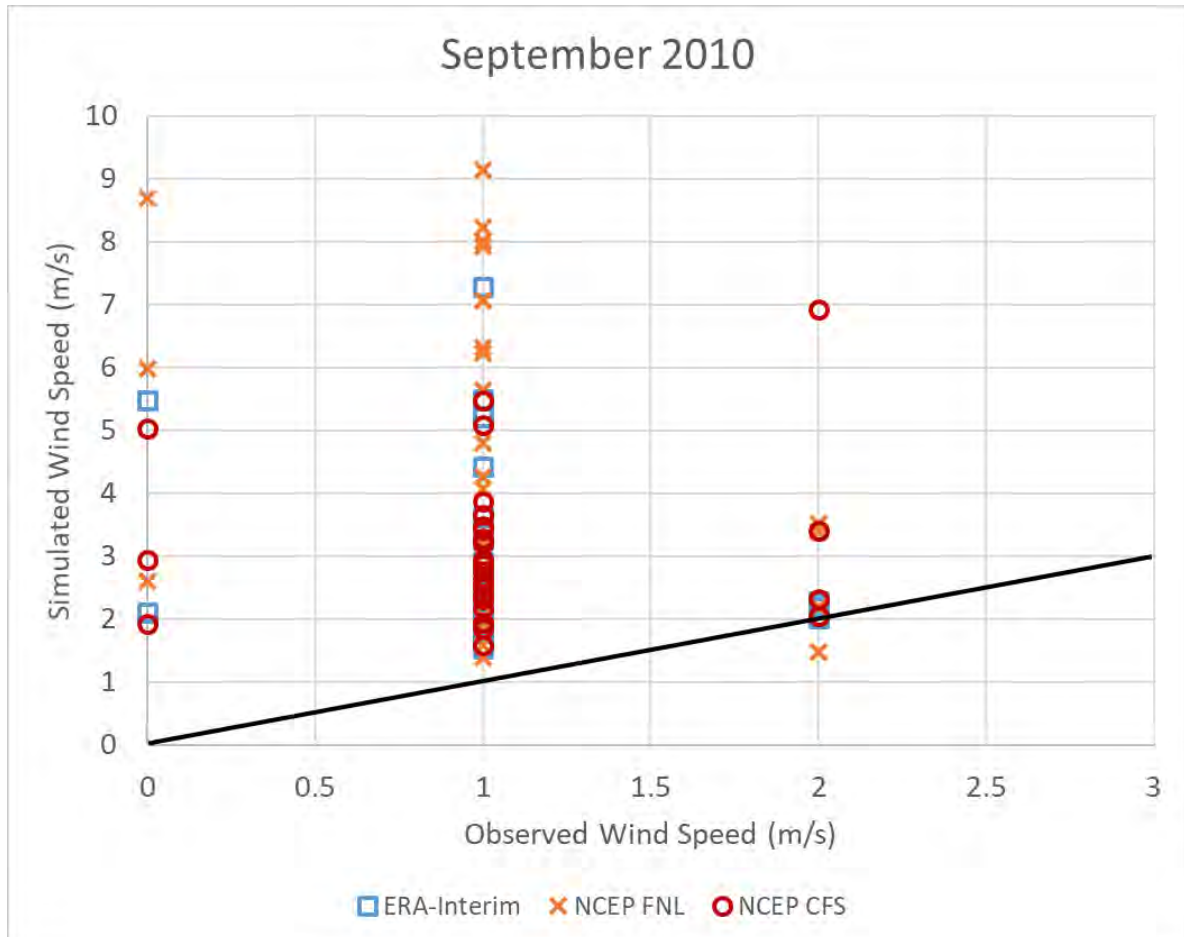


Figure 52. Scatter plot of different WRF model settings with PAGASA station data in Coron Island for September 2010.

Daily average wind speeds over the Coron Island are shown in Figure 52. There are only a few days with no winds so, this contributed to the improved simulation results from the mesoscale model. As the wind speeds are less than 3 m/s, most of the days are overestimated here. Taking into consideration both the scatter plot and calculated values in Table 22, the NCEP-FNL is the worst performing configuration since it gives the highest RMSE, bias, STDE, and overestimation values. The ERA-Interim has the smallest RMSE, bias, and STDE values, found in Table 22 but only by a small margin to the corresponding NCEP-CFS model configuration values for Coron Island.

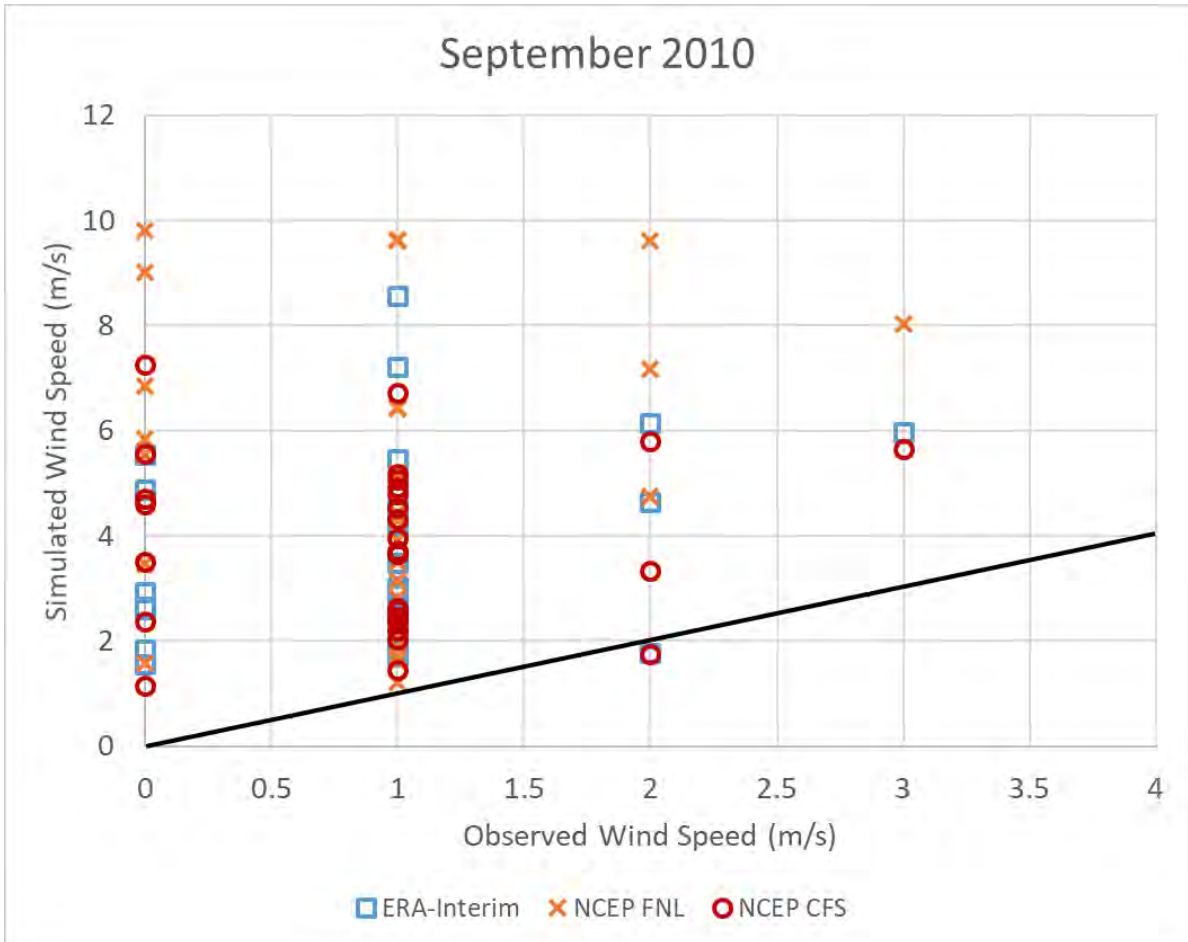


Figure 53. Scatter plot of different WRF model settings with PAGASA station data in Cuyo Island for September 2010.

Simulating Cuyo Island has also improved when compared with the June – August results since the points are now clustered closer to the ideal line as shown in Figure 53. It is also evident with the RMSE, bias, and STDE values for Cuyo Island since they are smaller than June – August. There are many days with no wind for the month but the mesoscale model is still generating winds for those days thus, it shows that it has difficulty in modelling Cuyo for no wind conditions. NCEP-FNL is once again giving the highest difference between the observations and simulation. The NCEP-FNL also has the highest RMSE, bias, and STDE values among the three model settings for the month of September. ERA-Interim and NCEP CFS have similar performance but between the two, ERA-Interim is slightly better based on its calculated RMSE, bias, and STDE values in Table 22 making it the best one among the three for Cuyo Island on September.

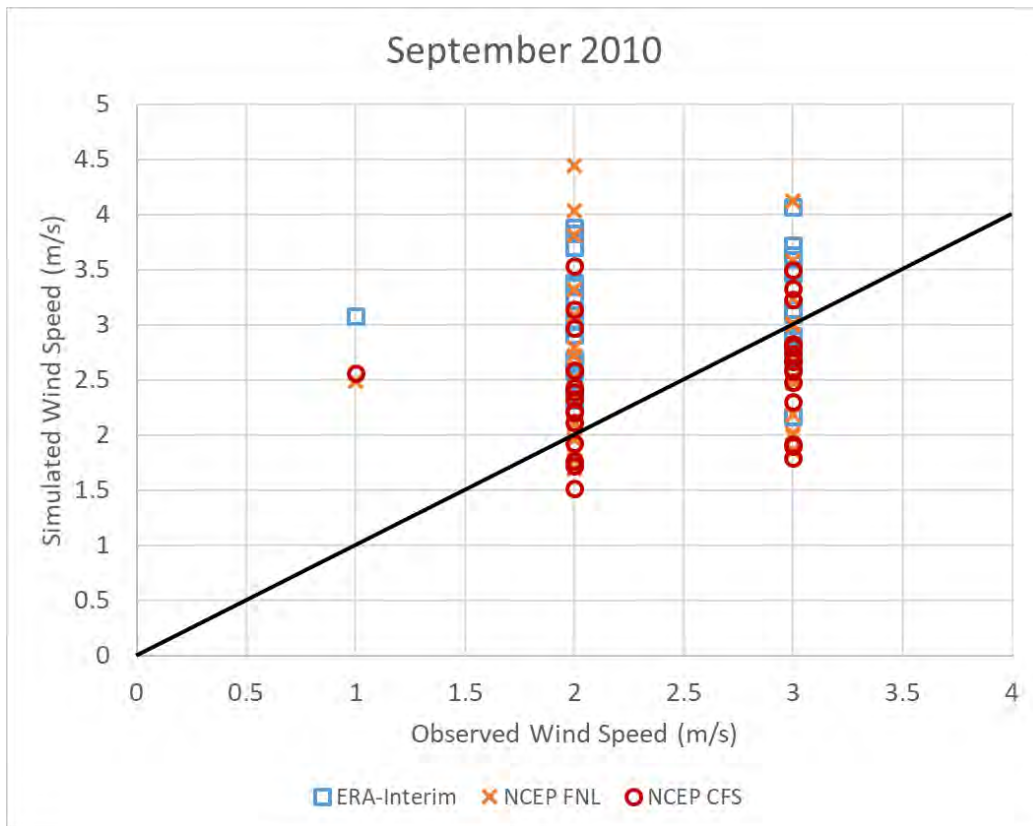


Figure 54. Scatter plot of different WRF model settings with PAGASA station data in Puerto Princesa for September 2010.

Table 22. September 2010 Model Errors and Bias Quantification of Wind Speed

Configuration	ERA-Interim			NCEP-FNL			NCEP-CFS		
	RMSE	Bias	STDE	RMSE	Bias	STDE	RMSE	Bias	STDE
Coron Island	10.53	1.92	10.35	18.46	3.37	18.15	11.04	2.02	10.85
Cuyo Island	14.33	2.62	14.09	23.50	4.29	23.11	15.79	2.88	15.52
Puerto Princesa	3.50	0.64	3.44	1.29	0.24	1.27	0.31	0.06	0.30

It is the Puerto Princesa site that regained better results for September when compared to Coron and Cuyo. Mesoscale model is better when simulating September for Puerto Princesa than with the June – August. As can be seen in Figure 54, ERA-Interim tend to overestimate wind speeds that are 2 m/s and below while equally underestimate and overestimate wind speeds at 3 m/s. NCEP CFS and NCEP FNL can overestimate or underestimate daily average wind speeds for 2 m/s while equally distributed overestimation and underestimation for wind speeds at 3 m/s. The largest overestimation values of daily wind speed averages are now down to 2 – 2.5 times. This better performance is also reflected on the RMSE, bias, and STDE values since there is a significant decrease across all errors and bias for September. NCEP-CFS is the best performing configuration compared to ERA-Interim and NCEP-FNL for Puerto Princesa in the September model output because the RMSE, bias, and STDE values close to zero.

The October simulation results for Coron Island, shown in Figure 55, is similar in performance with the September at the same location. It shows that the transition to Northeast Monsoon is not yet complete but there are some days with higher daily average wind speeds that is the profile of the Northeast Monsoon for the Philippines. There is a general overestimation of the wind speeds and the multiple days with zero wind are still registering 2 – 6 m/s wind speeds for the daily averages on the model output. As such, the bias values can range from 2.90 – 4.31 m/s as found in Table 23.

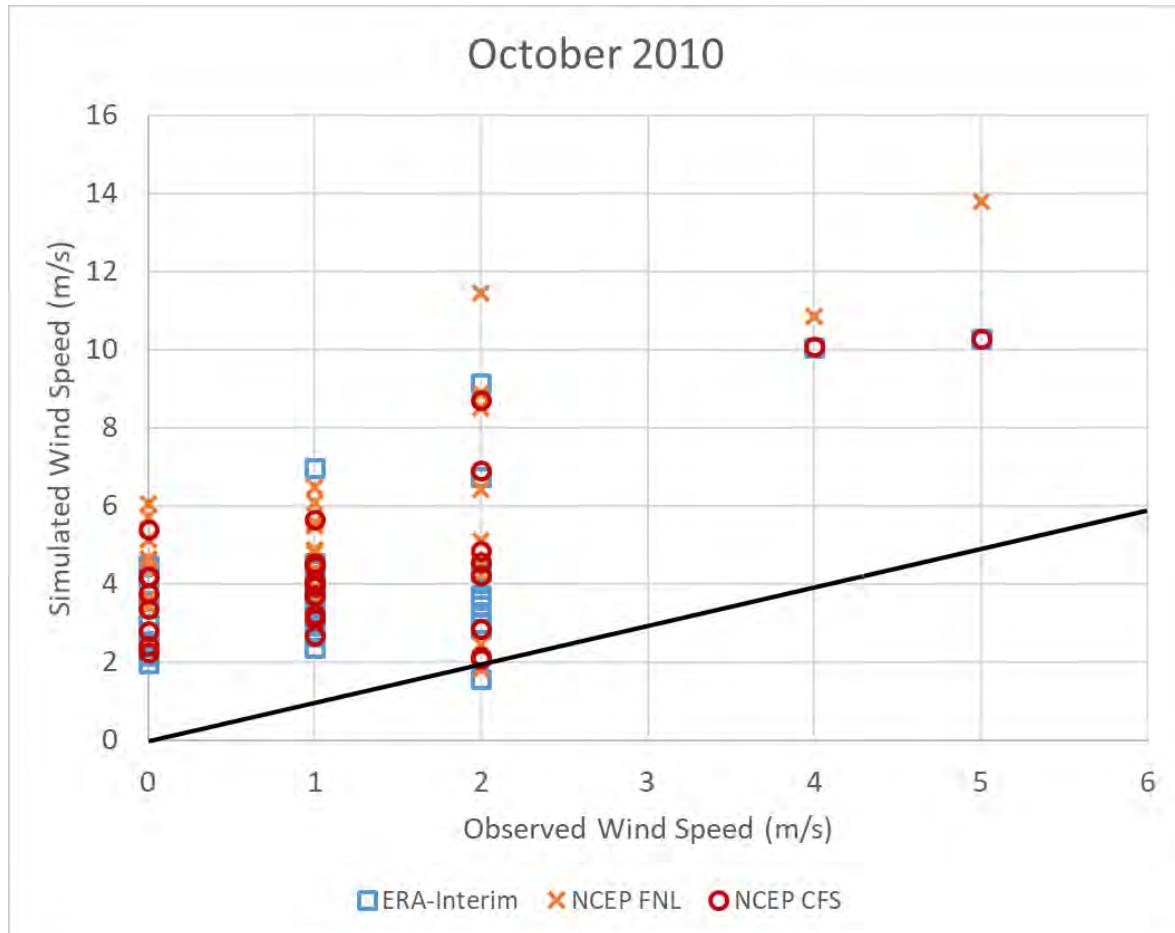


Figure 55. Scatter plot of different WRF model settings with PAGASA station data in Coron Island for October 2010.

ERA-Interim is slightly outperforming the NCEP-CFS and both ERA-Interim and NCEP-CFS are better than the NCEP-FNL model settings. These findings are consistent with the RMSE, bias, and STDE values for Coron Island in Table 23 where it can be seen that values for ERA-Interim and NCEP-CFS are quite close with each other but NCEP-FNL values are larger than the two configurations.

Table 23. October 2010 Model Errors and Bias Quantification of Wind Speed

Configuration	ERA-Interim			NCEP-FNL			NCEP-CFS		
	RMSE	Bias	STDE	RMSE	Bias	STDE	RMSE	Bias	STDE
Coron Island	16.14	2.90	15.88	24.02	4.31	23.63	17.21	3.09	16.93
Cuyo Island	22.87	4.32	22.46	30.81	5.82	30.25	25.97	4.91	25.50
Puerto Princesa	6.90	1.24	6.79	3.90	0.70	3.84	3.33	0.60	3.27

Model output for Cuyo Island that are plotted in Appendix show that it is close to the performance when simulating August for this site. Even the RMSE, bias, and STDE values show this because the error values in Table 23 can range 22 – 30 m/s which is similar to the August values. The difference between the measured daily wind speed average and the WRF results can be as high as 16 times from the NCEP FNL settings which also has the highest bias and error values in Table 20 and Table 21. For this simulated month, the ERA-Interim is the best configuration to model October for Cuyo Island because its highest overestimate is less than those given by the NCEP CFS and NCEP FNL. ERA-Interim also has the smallest RMSE, bias, and STDE values compared to the two model settings.

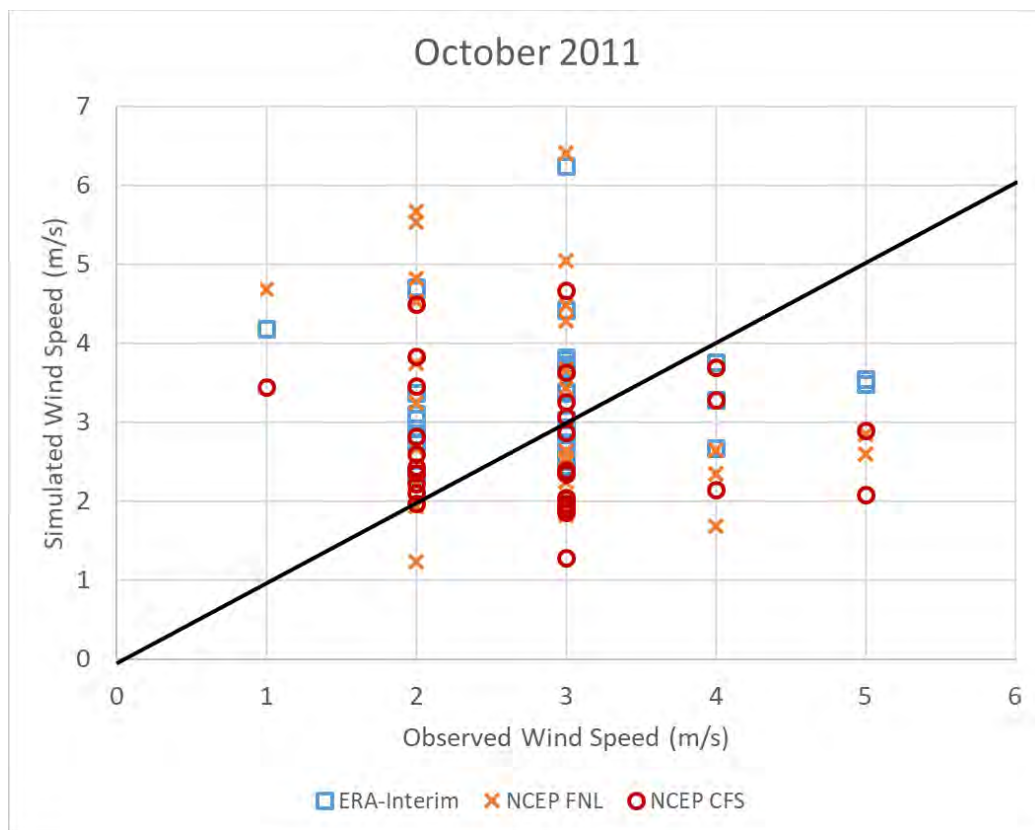


Figure 56. Scatter plot of different WRF model settings with PAGASA station data in Puerto Princesa for October 2011.

Table 24. October 2011 Model Errors and Bias Quantification of Wind Speed

Configuration	ERA-Interim			NCEP-FNL			NCEP-CFS		
	RMSE	Bias	STDE	RMSE	Bias	STDE	RMSE	Bias	STDE
Coron Island	16.54	2.97	16.27	23.15	4.16	22.77	15.83	2.84	15.57
Cuyo Island	23.98	4.31	23.59	23.72	4.26	23.34	19.76	3.55	19.44
Puerto Princesa	2.98	0.53	2.93	2.11	0.38	2.08	0.79	-0.14	0.78

For Puerto Princesa, mesoscale model has a tendency to overestimate daily wind speed values that are 2 m/s or less. It has an equal distribution of overestimated and underestimated values at 3 m/s and underestimates 4 – 5 m/s wind speed values as shown in Figure 56. It is apparent that the Puerto Princesa site is where the model performs relatively well once again. An increase in the

maximum daily average wind speeds for October has enabled the mesoscale model to determine the wind profiles of Puerto Princesa much better than May to September months. The NCEP-CFS model setting has the best performance when comparing the three configurations because it yields the least overestimated values and largest underestimated values. It also has the smallest RMSE, bias, and STDE values for October which are evident from Table 23 and Table 24.

Model performance for November are similar to the October since both months have similar wind profiles at Coron Island. The similarities are on the no wind conditions on several days at Coron Island are not represented by the mesoscale model and the dynamic range of the average wind speeds. ERA-Interim yields the best mesoscale model setting for Coron since NCEP FNL and NCEP CFS gives a few days with higher daily wind speed average value difference with observations than the ERA-Interim. The RMSE, bias, and STDE values of ERA-Interim in Table 25 also give evidence to this also since it has the lowest values.

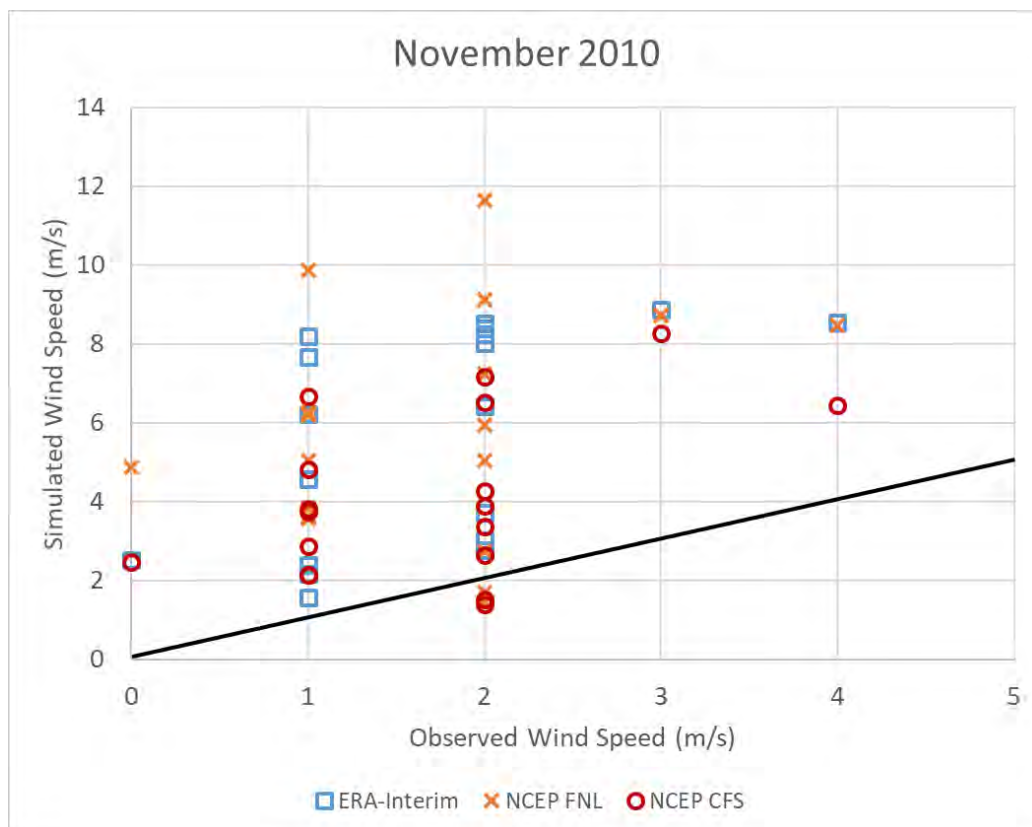


Figure 57. Scatter plot of different WRF model settings with PAGASA station data in Cuyo Island for November 2010.

Looking at Figure 57, it is NCEP-FNL and ERA-Interim that has higher difference with daily wind speed average measured values than NCEP-CFS. It is also shown in Table 25 that NCEP-CFS has the lowest RMSE, bias, and STDE values for Cuyo in November so, it is best represented with wind speed values generated by NCEP-CFS.

Table 25. November 2010 Model Errors and Bias Quantification of Wind Speed

Configuration	ERA-Interim			NCEP-FNL			NCEP-CFS		
	RMSE	Bias	STDE	RMSE	Bias	STDE	RMSE	Bias	STDE
Coron Island	13.37	2.44	13.15	18.64	3.40	18.33	15.23	2.78	14.97
Cuyo Island	16.93	3.99	16.45	17.76	4.19	17.26	10.42	2.46	10.13
Puerto Princesa	3.60	0.66	3.54	4.95	0.90	4.86	1.28	0.23	1.26

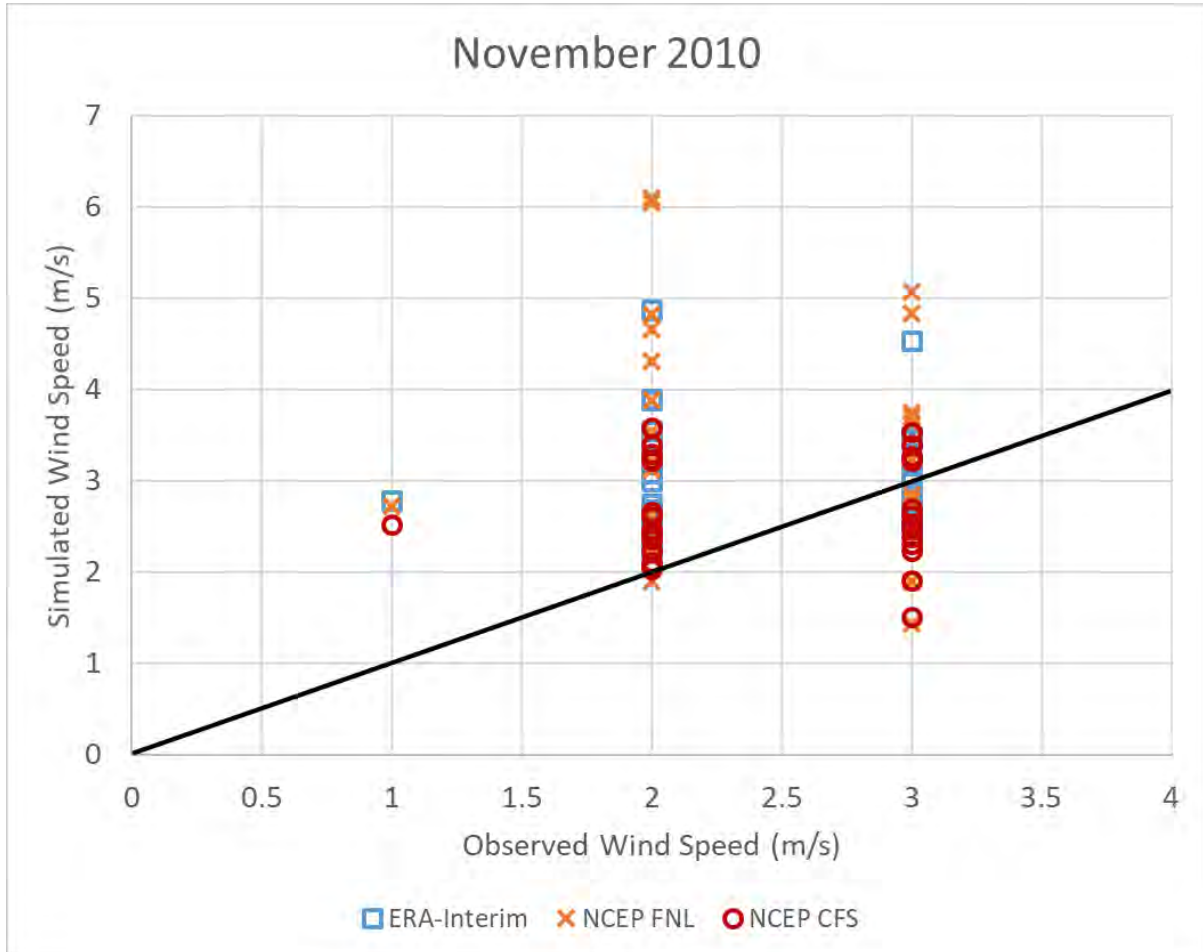


Figure 58. Scatter plot of different WRF model settings with PAGASA station data in Puerto Princesa for November 2010.

The simulation output for Puerto Princesa are plotted in Figure 58 and it shows that daily average wind speeds are mostly overestimated for wind speeds that are 2 m/s or below by the WRF model. For the 3 m/s wind speed, all of the configurations have an evenly distributed data points that underestimate and overestimate the daily average wind speed. Overall, the model has a positive bias for Puerto Princesa that ranges from 0.23 – 0.90 m/s. The NCEP CFS is the best performing model setting for November at Puerto Princesa since the data points from its results are clustered nearer to the ideal line of the scatter plot when compared to the ERA-Interim or NCEP FNL results. Another reason is that NCEP-CFS has the least RMSE, bias, and STDE values for Puerto Princesa in November months.

The December results of all the mesoscale model settings are generally overestimating the wind speeds again. Figure 59 show the Coron Island model output where most of the observed daily

wind speed average are 1 m/s and 2 m/s. With such low wind speeds, it should make the mesoscale model generate higher wind values since these are below the range that the model is capable once again [20]. These values are overestimated by 2 – 8 times by the model outputs. NCEP-CFS is slightly better than the ERA-Interim and NCEP FNL because of its lower overestimated values as well as lesser values for RMSE, bias, and STDE enumerated in Table 26.

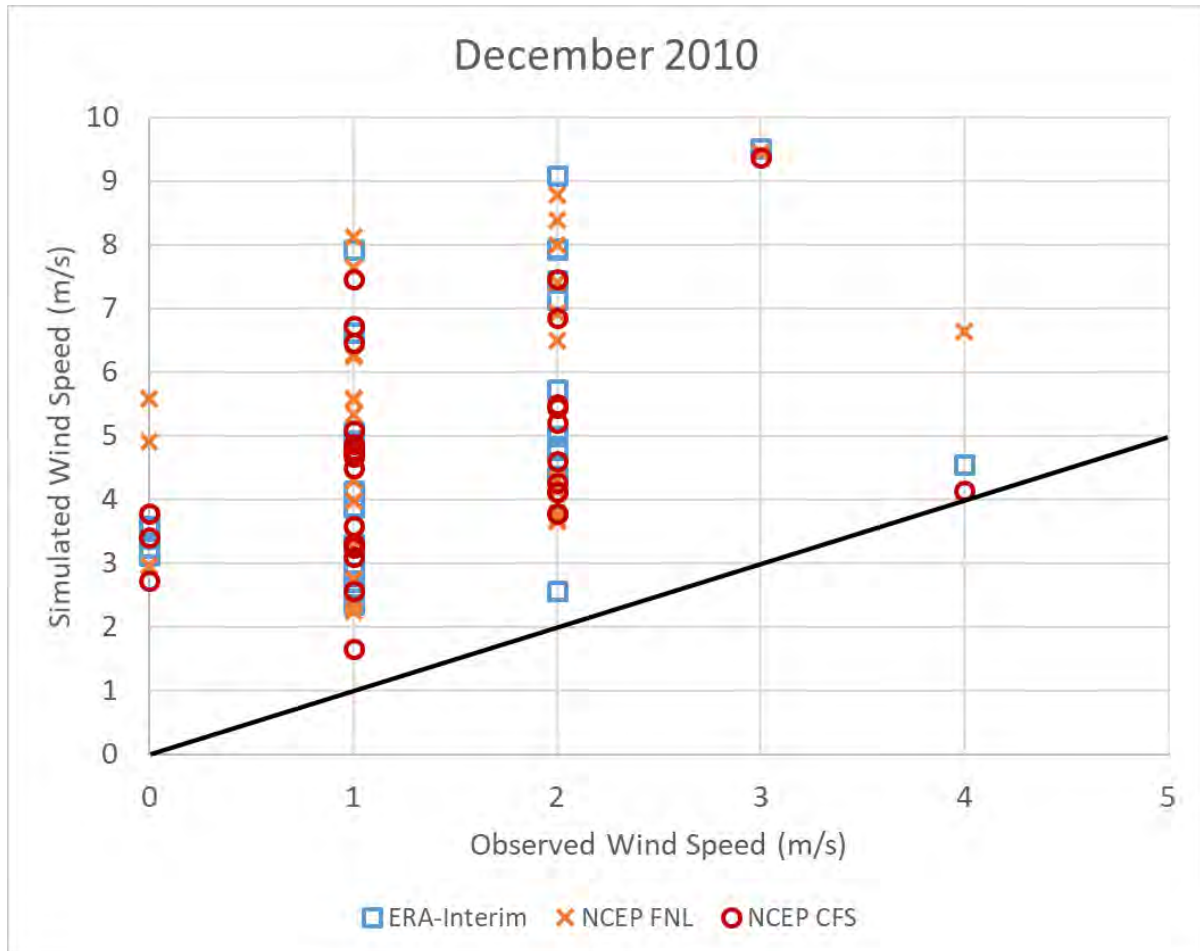


Figure 59. Scatter plot of different WRF model settings with PAGASA station data in Coron Island for December 2010.

All the mesoscale model configurations have trouble simulating the Cuyo Island for December since all have similar daily wind speed average values that are twice to 13 times higher than the observations similar to Figure 59. This difficulty is apparent to the high RMSE, bias, and STDE values for Cuyo Island which is the highest among the three locations as can be seen in Table 26.

Table 26. December 2010 Model Errors and Bias Quantification of Wind Speed

Configuration	ERA-Interim			NCEP-FNL			NCEP-CFS		
	RMSE	Bias	STDE	RMSE	Bias	STDE	RMSE	Bias	STDE
Coron Island	18.86	3.39	18.55	21.65	3.89	21.30	18.19	3.27	17.89
Cuyo Island	39.51	7.10	38.87	33.46	6.01	32.92	36.22	6.51	35.63
Puerto Princesa	10.39	1.87	10.22	7.73	1.39	7.60	8.80	1.58	8.66

The model is once again better in simulating wind speed conditions at Puerto Princesa as presented in Figure 60 and the comparatively low error and bias values in Table 26 and Table 27 in contrast with Coron and Cuyo. There is predominantly overestimation but there are underestimation that occur for this site.

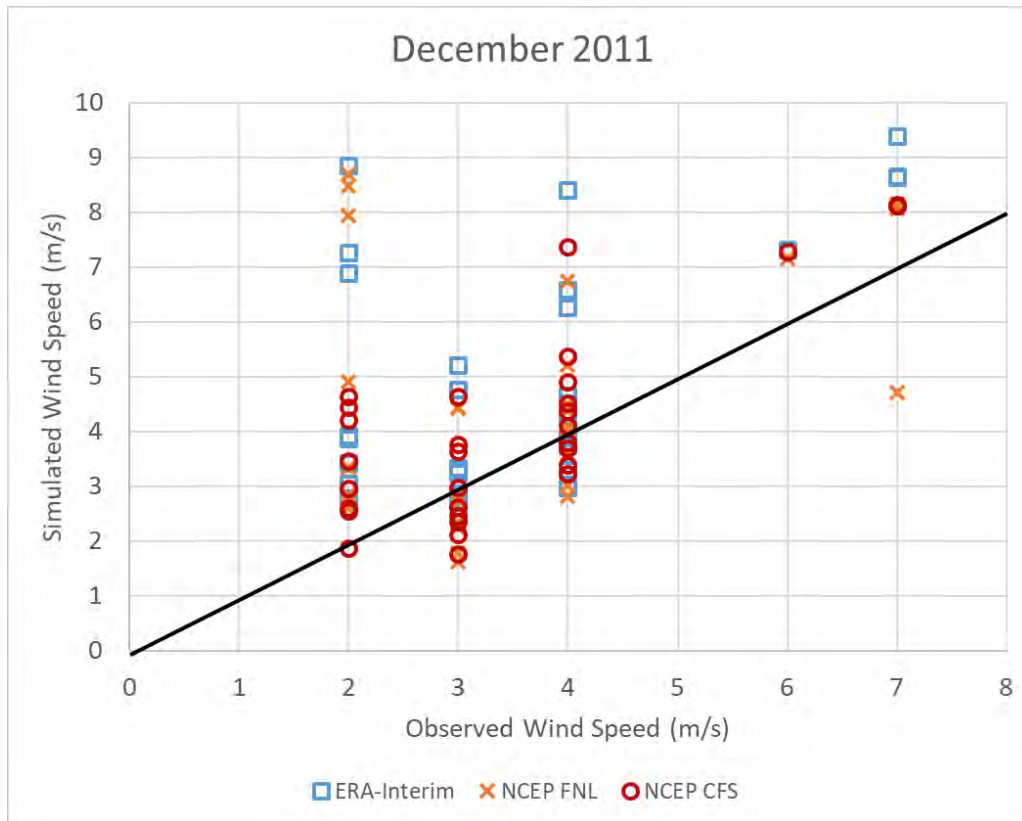


Figure 60. Scatter plot of different WRF model settings with PAGASA station data in Puerto Princesa for December 2011.

ERA-Interim and NCEP-FNL yields higher overestimates in comparison with NCEP-CFS. The clustering of simulated wind speed data from NCEP-CFS are also nearer to the ideal line so, it is the best configuration for modelling Puerto Princesa for December. The RMSE, bias, and STDE values of NCEP-CFS are also the lowest among the three WRF model configurations for the years of 2011 and 2012 as can be found in Table 27 and Table 28, respectively.

Table 27. December 2011 Model Errors and Bias Quantification of Wind Speed

Configuration	ERA-Interim			NCEP-FNL			NCEP-CFS		
	RMSE	Bias	STDE	RMSE	Bias	STDE	RMSE	Bias	STDE
Coron Island	24.47	4.39	24.07	26.36	4.73	25.93	23.33	4.19	22.95
Cuyo Island	29.39	5.28	28.92	29.35	5.27	28.88	27.67	4.97	27.22
Puerto Princesa	7.85	1.41	7.72	4.95	0.89	4.87	3.51	0.63	3.45

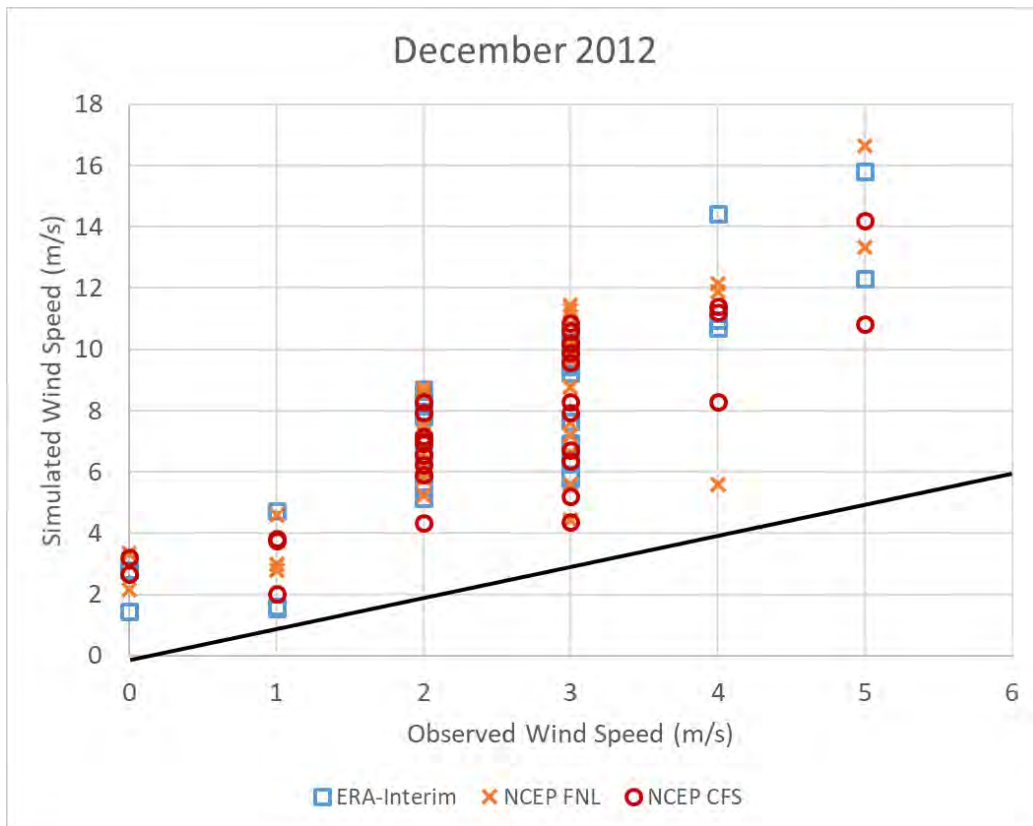


Figure 61. Scatter plot of different WRF model settings with PAGASA station data in Cuyo Island for December 2012.

With Cuyo Island, it can be seen in Figure 61 that there is a constant multiplier to the model output when compared to the daily wind speed average measurements. Here, it can be seen that wind speeds at 1 – 3 m/s are approximately two to four times higher for the WRF model and wind speeds at 4 – 5 m/s are about two to three times. These results suggest that the model has a systematic constant bias for December at Cuyo. Thus, WRF can simulate the wind trends since the values are consistent with the wind speed variation at this location but with a constant multiplicative behaviour that can be known.

Table 28. December 2012 Model Errors and Bias Quantification of Wind Speed

Configuration	ERA-Interim			NCEP-FNL			NCEP-CFS		
	RMSE	Bias	STDE	RMSE	Bias	STDE	RMSE	Bias	STDE
Coron Island	23.00	4.13	22.62	26.92	4.83	26.48	25.71	4.62	25.30
Cuyo Island	29.01	5.21	28.54	29.51	5.30	29.03	27.46	4.93	27.02
Puerto Princesa	5.90	1.06	5.80	5.74	1.03	5.64	6.38	1.15	6.27

All input data have a tendency to overestimate the wind speed in comparison with the observations especially for winds that are less than 4 m/s. This is more pronounced in the low wind speed areas of Coron and Cuyo during the April to August months where most winds are between 0 – 4 m/s. This is also noticeable in months with good wind resource such as January and February where the winds that are 4 m/s and below are overestimated. These are found to be consistent with literature and even with satellite-derived datasets of wind fields [18,127].

The NCEP-CFS and ERA-Interim have similar performance in simulating the winds. Comparing both reanalysis datasets with NCEP-FNL, the average winds of NCEP-FNL gives slightly better performance when accounting for the entire wind speed value range. But it is apparent from the scatter plots that low wind speeds are simulated better using NCEP-CFS, while ERA-Interim yields better results in high wind speed regimes. This is found in line with studies reported in the literature [18,20], while WRF simulates better with wind speeds that are greater than or equal to 4 m/s. This is apparent in the charts as wind speeds that are 2 m/s are overestimated by all input data and the model tends to equally overestimate or underestimate 3 m/s wind occurrences. Then, it begins to give more consistent wind speeds beginning at 4 m/s – 5 m/s. The ability of NCEP-FNL to simulate wind speeds better is also seen with the RMSE values. It ranges from 3.6 m/s to 4 m/s for monthly comparison while ERA-Interim and NCEP-CFSR can range from 5.7 m/s to 6 m/s. The wind analysis for the direction of the wind is the subject for the next section.

A summary of all the results discussed for wind speeds in every location for each month are listed in Table 29. This shows the best mesoscale model settings that is appropriate for a particular time of the year based on the model validation done for each of the selected sites in Palawan Province.

Table 29. Summary of Best Mesoscale Model Configuration for Wind Speeds

Month \ Location	Coron Island	Cuyo Island	Puerto Princesa
January	NCEP-FNL	NCEP-CFS	NCEP-CFS
February	ERA-Interim	NCEP-CFS	NCEP-CFS
March	NCEP-FNL	ERA-Interim	NCEP-CFS
April	NCEP-FNL	NCEP-FNL	NCEP-CFS
May	ERA-Interim	ERA-Interim	NCEP-CFS
June	ERA-Interim	ERA-Interim	NCEP-CFS
July	ERA-Interim	ERA-Interim	NCEP-CFS
August	ERA-Interim	ERA-Interim	NCEP-CFS
September	ERA-Interim	ERA-Interim	NCEP-CFS
October	ERA-Interim	ERA-Interim	NCEP-CFS
November	ERA-Interim	NCEP-CFS	NCEP-CFS
December	NCEP-CFS	NCEP-CFS	NCEP-CFS

Based on the wind speed validation for the mesoscale model, there are certain seasons when a particular model configuration is suitable at a particular location. In Coron Island, the months when Northeast Monsoon occurs are simulated by different settings. The strengthening of the Northeast Monsoon that occurs in December is simulated best by NCEP-CFS while the peak of the monsoon is modelled best with NCEP-FNL. When the Northeast Monsoon start to die down in February, the ERA-Interim becomes the appropriate mesoscale model setting. Transition period in March from Northeast Monsoon to Easterlies and the peak hot-dry season in April are modelled well by the NCEP-FNL. The months of May until November are simulated adequately by the ERA-Interim configuration for Coron

Island. Thus, the Southwest Monsoon is modelled well for Coron by ERA-Interim model settings since the entire season is covered in that duration.

For Cuyo Island, Table 29 shows that January to February and November to December are best simulated using the NCEP-CFS model settings. So, it is the NCEP-CFS that must be utilised during the period when the Northeast Monsoon is strong. In March, ERA-Interim is the best configuration which is the time when the transition from Northeast Monsoon to Easterlies happen. Similar to Coron, Cuyo is also modelled well during the Easterlies of April by the NCEP-FNL configuration. The whole Southwest Monsoon is simulated properly by ERA-Interim since the months of May until October are part of that period. In Puerto Princesa, all the months are suitably simulated using the NCEP-CFS mesoscale model configuration.

It is notable from these results that the majority of good simulation outputs are generated from reanalysis data such as ERA-Interim and NCEP-CFS. Thus, reanalysis data are commonly used as input data for mesoscale models as discussed in Chapter 2. But as Table 29 shows, there are certain locations at particular times of the year when operational datasets such as the NCEP-FNL data used in this study proves to be the appropriate input data for simulation. So, operational datasets should be considered when running mesoscale model for wind profiling. These results will be one of the basis in the dataset selection for generating wind maps for Palawan Province. The other criteria would be the wind direction which will be presented in the following sections.

5.1.2 Mesoscale Model Wind Direction Results

Monthly averages of wind direction are compared and analysed in this section. Each month of the year from 2010 – 2012 are to be discussed and the output of every month for each of the location are placed side by side in the figures. Since these are monthly averages, the error quantification is deemed unnecessary because each month will be analysed based on the predominant wind direction of the season. This is to facilitate the comparison of Coron Island, Cuyo Island, and Puerto Princesa in a similar flow of discussion as the wind speeds in the previous section.

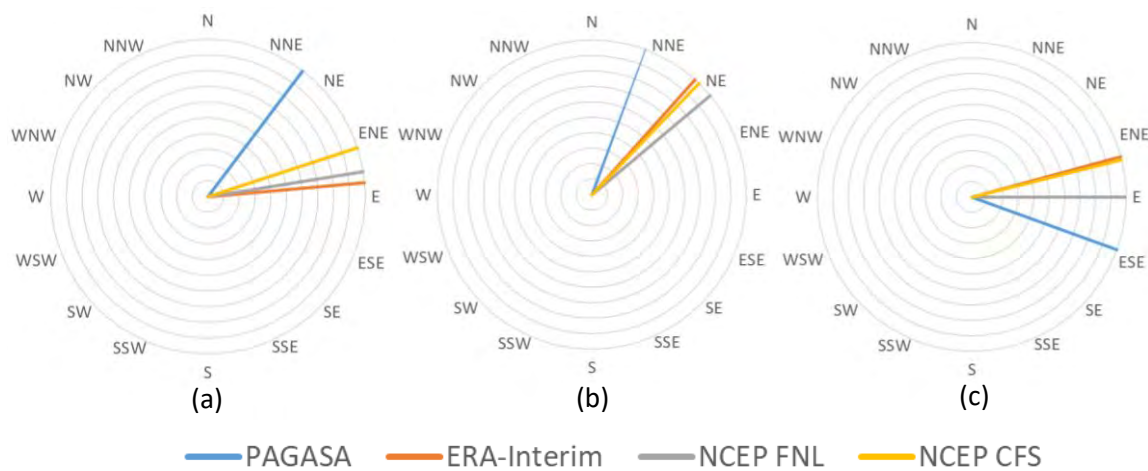


Figure 62. Comparison of average wind direction between WRF output and observation data at (a) Coron Island, (b) Cuyo Island, and (c) Puerto Princesa for the month of January 2012

The wind direction in January is relatively consistent since the monthly average wind direction does not vary much from 2010 – 2012 observations and a representative chart is shown in Figure 62. Wind direction for Coron Island is simulated to be coming from the East in Figure 62 (a) but the measurements have an average of winds coming from the Northeast direction. So, the prevalent wind direction is not reflected well by the simulations for Coron. At the Cuyo Island, all the model configuration runs have the same average wind direction for the month in Figure 62 (b) that indicate the winds are coming from the Northeast. This is a good performance for the model since the observations show that the winds are mostly coming from the North-northeast. Here, ERA-Interim and NCEP CFS are almost equal in wind direction and they are the closest one to the measured wind direction. It is apparent from the measurements that the prevalent Northeast Monsoon wind direction occurs at both Coron and Cuyo Islands. Observations at Puerto Princesa recorded that the average wind direction is maintained to be coming from the general eastern direction for January. The mesoscale model is also performing well in determining the average wind direction at Puerto Princesa as shown in Figure 62 (c) because the results are able to determine that the winds are coming from the East. NCEP FNL is the best performing model settings for January at Puerto Princesa as it gives the Eastern wind direction closest to the observation. This shows that there is a local wind regime for Puerto Princesa because the predominant Northeast Monsoon is not reflected from the measurements.

For February 2010, Figure 63(a) presents that there is an improved wind direction determination for the Coron Island compared to the January 2010 in Figure 62 (a). It shows that the model is able to capture that the wind direction is coming from the East. This shift in direction shows that there is weakened Northeast Monsoon effect over Coron Island.

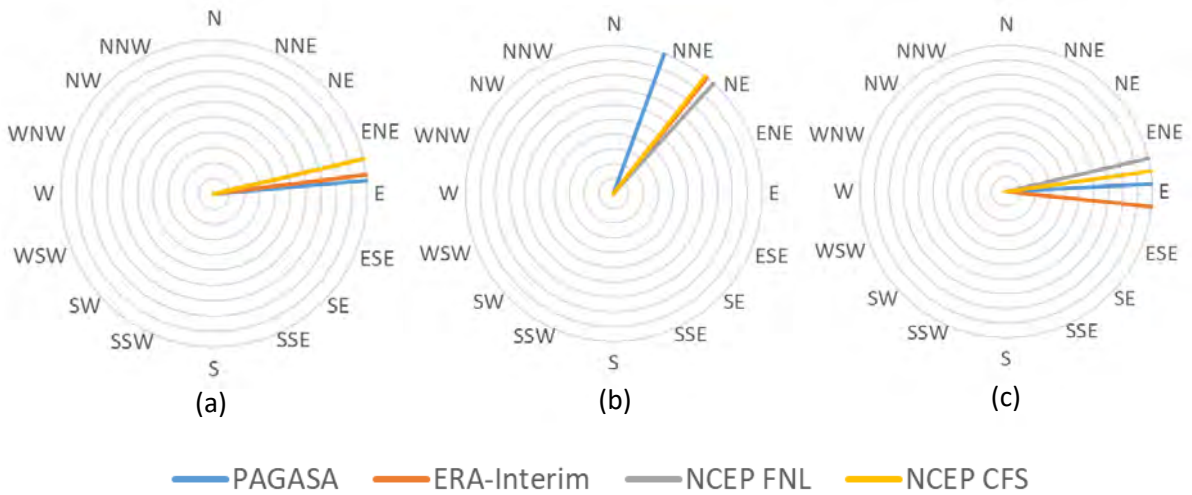


Figure 63. Comparison of average wind direction between WRF output and observation data at (a) Coron Island, (b) Cuyo Island, and (c) Puerto Princesa for the month of February 2010

In Cuyo Island, the wind direction is still generally from the North-northeast as shown in Figure 63 (b) and the model output gives an average direction of Northeast. So, the wind direction is similar to January for Cuyo Island. The Eastern wind direction persists for Puerto Princesa as indicated in Figure 63 (c). This is reflected in the model as all the settings yields the wind to be coming from the East as well. This is a slight improvement over the January simulations for Puerto Princesa.

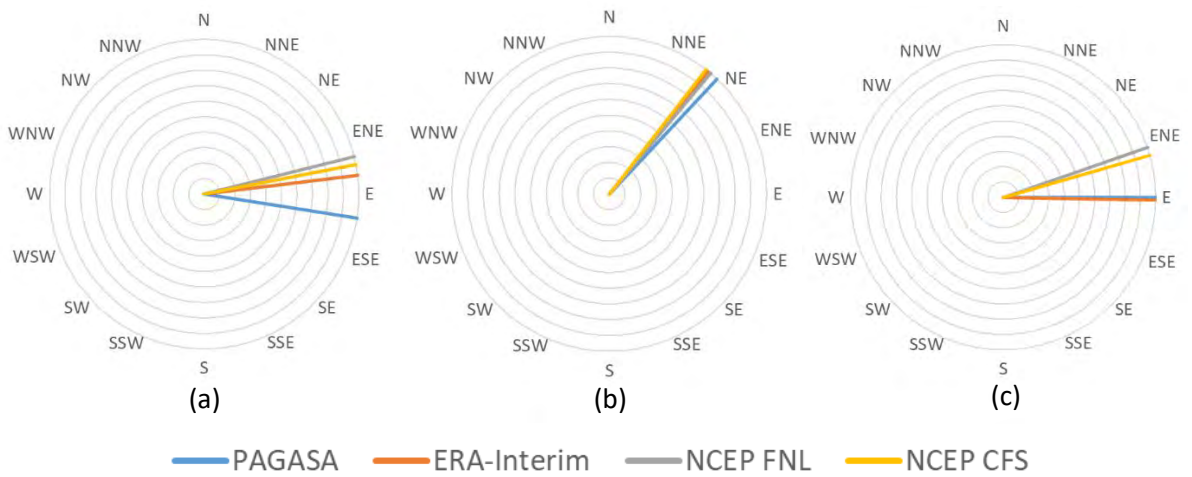


Figure 64. Comparison of average wind direction between WRF output and observation data at (a) Coron Island, (b) Cuyo Island, and (c) Puerto Princesa for the month of March 2010

Looking at Figure 64, the Coron and Cuyo island average wind direction are within the general direction of the measurements. This is especially true for the Puerto Princesa location but the ERA-Interim is almost the same with the observation where the wind is coming from the East. Coron Island measurements found that the prevalent wind direction is coming from the East-northeast and this is reflected from all three model configurations in Figure 64 (a). NCEP FNL output is the closest one to the measured average wind direction so, it is the best performing model setting for Coron on March.

The simulations are able to determine the average wind direction of Northeast for March at Cuyo Island as can be seen in Figure 64 (b). The mesoscale model is able to generate this average wind direction with the ERA-Interim showing the smallest difference with the observation. It shows that during the transition to Easterlies, the Northeast Monsoon highly influences the prevalent wind direction in Cuyo Island. Model performance is also good for the Puerto Princesa simulation results found in Figure 64 (c). Measurements at the site show that the predominant wind direction comes from the East for March. This eastern direction of the wind has been produced by all the configurations and NCEP FNL is yielding the least difference in direction to the observations.

For April, Figure 65(a) show that all three model configurations have slight difficulty in determining the average wind direction at Coron Island. The simulations show that the winds are coming from the East for NCEP-CFS and ERA-Interim while NCEP-CFS yields an East-southeast direction. The winds are coming from the East-northeast thus, the general Eastern direction is common between the simulations and observations. The mesoscale model performs well at Cuyo Island based on Figure 65 (b) because NCEP CFS and ERA-Interim are almost the same with the measured average wind direction. NCEP FNL failed to give a similar result but it is still within the general direction of the prevalent wind. It is interesting to note that despite the onset of the Easterlies, monthly average wind direction for Cuyo Island in April remains to be Northeast which suggest that there is a local effect on the wind direction at this location.

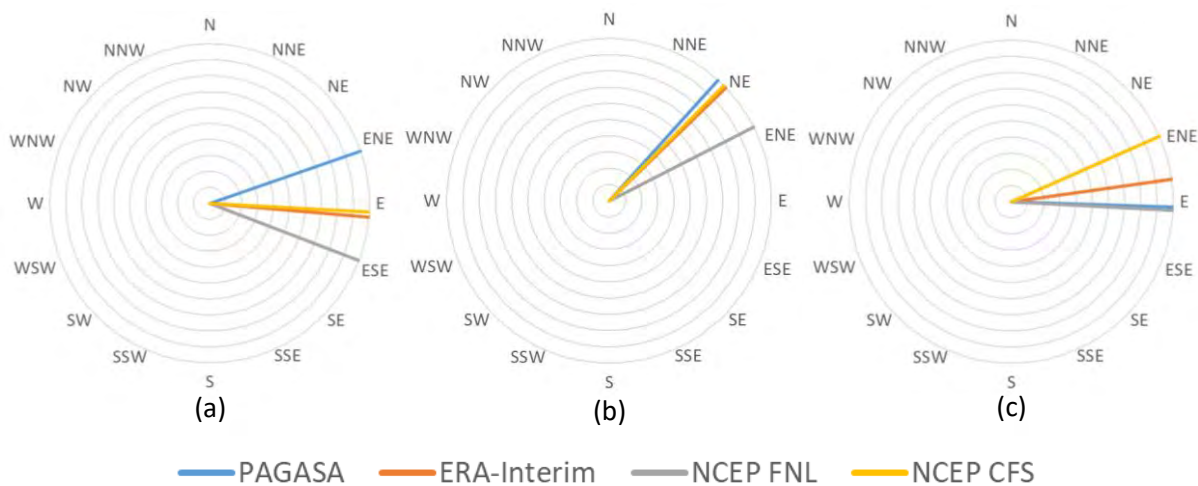


Figure 65. Comparison of average wind direction between WRF output and observation data at (a) Coron Island, (b) Cuyo Island, and (c) Puerto Princesa for the month of April 2011

It is apparent that The Puerto Princesa simulation outputs show that the three configurations are quite capable in producing the average wind direction observed as presented in Figure 65 (c). There is a bigger deviation for ERA-Interim and NCEP CFS from the generally eastern wind flow observed while the NCEP FNL is able to give an average wind direction that is almost equal to the measurements.

There is a slight improvement in performance for the mesoscale model at Coron Island as presented in Figure 66(a). Unlike for the April months, the model is able to reflect the southerly wind direction partially for May. At Cuyo Island, the ERA-Interim is the best performing model configuration since it is able to reproduce the observation that the average wind direction for May comes from South-southeast. Both NCEP CFS and NCEP FNL are still able to get the general direction of the average wind direction since they are within the Southeast direction as shown in Figure 66 (b).

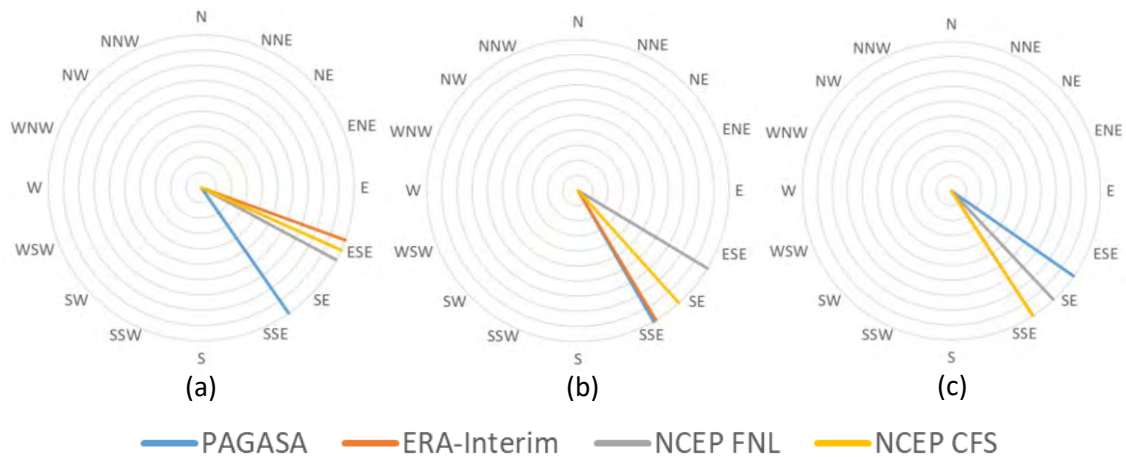


Figure 66. Comparison of average wind direction between WRF output and observation data at (a) Coron Island, (b) Cuyo Island, and (c) Puerto Princesa for the month of May 2010

The three model configurations slightly deviates from the measured average wind direction but all are capable to generate the Southeastern wind direction for May at Puerto Princesa. Both ERA-Interim and NCEP-CFS have the same wind direction value so they overlap in Figure 66 (c) and depicted by the yellow line. Here, the NCEP FNL is closer to the wind direction recorded as can be seen in Figure 66 (c). All the sites also exhibit the transition in May from Easterlies to Southwest Monsoon because the Southern component begins to show in Figure 66.

Simulations give an average wind direction that are coming from the Southwest and South-southwest sector in all the sites being studied in June. In Figure 67(a), the average wind direction is coming from the South-southeast at Coron Island while model results for Coron show that winds are coming from the South-southwest. Although there is a significant difference between the model results and observations, there is an improvement to the model's capacity in determining the wind directions since it is able to give the predominantly southern component of the direction.

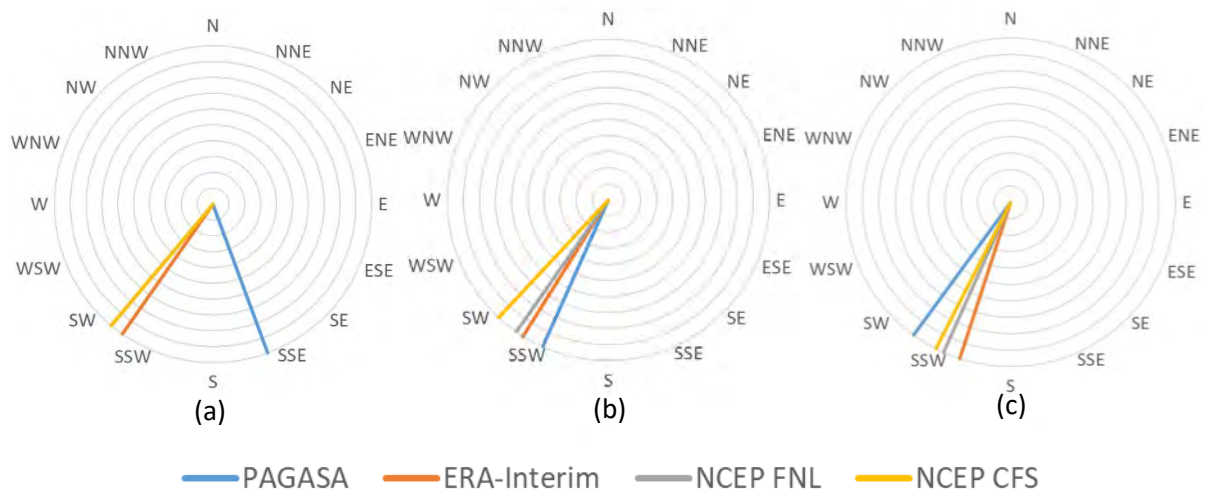


Figure 67. Comparison of average wind direction between WRF output and observation data at (a) Coron Island, (b) Cuyo Island, and (c) Puerto Princesa for the month of June 2012

Cuyo Island and Puerto Princesa are yielding better model output since the observations and simulations are in agreement that the winds are mostly coming from the South-Southwest sector as presented in Figure 67 (b) and Figure 67 (c). The ERA-Interim is the best configuration for Cuyo Island and the NCEP CFS is the best setting for Puerto Princesa since they have the smallest discrepancy with the measurements, respectively. The shift to the general Southwest direction for winds show that the Southwest Monsoon has set in for all the sites. Measurements in Coron Island, shown in Figure 67 (a), do not reflect the Southwest direction and only registers the Southern component of the prevalent wind over the Philippines.

Observed wind directions in July is similar to the wind direction measurements for June as can be seen when Figure 67 and Figure 68 are compared. This shows that there is a predominant wind direction for these times of the year at all the locations. Figure 68 (a) shows that the average wind direction for Coron Island is coming from the South-southeast. Since the different mesoscale model configurations yield outputs for wind direction in the Southwest sector, there is a discrepancy with the measurements that is also seen in June. Thus, the prevalent Southern component is reflected by the simulations again especially by the ERA-Interim configuration.

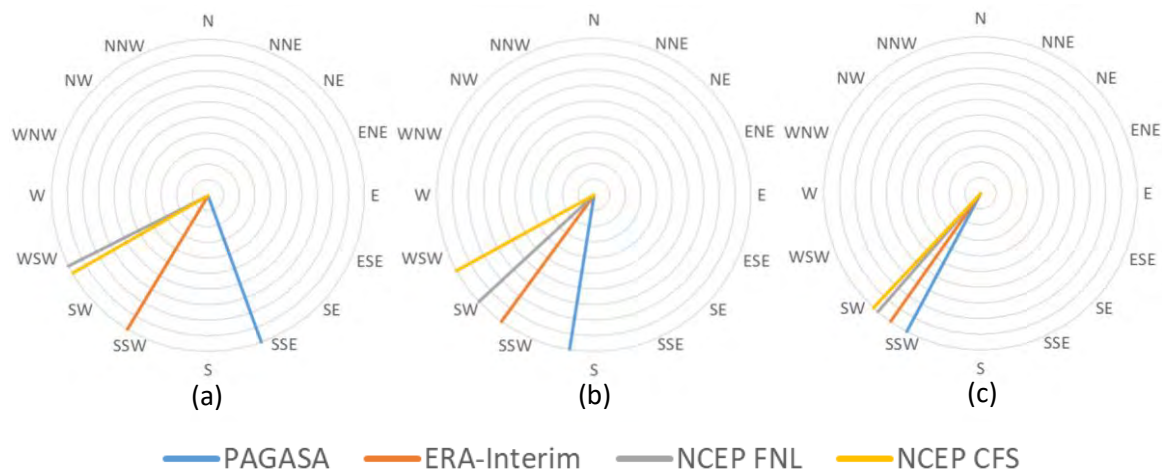


Figure 68. Comparison of average wind direction between WRF output and observation data at (a) Coron Island, (b) Cuyo Island, and (c) Puerto Princesa for the month of July 2011

The predominant wind direction observed for Cuyo Island in July is coming from the South as indicated in Figure 68 (b). Once again, all three configurations are giving average wind direction coming from the Southwest with ERA-Interim being the closest one to the measured monthly average wind direction. It is on the Puerto Princesa simulations where the output from the model is comparable with the observations as shown in Figure 68 (c). Here, the model results agree with the measured wind direction that the prevalent wind is coming from the Southwest or South-southwest. The ERA-Interim gives the closest wind direction to the measurements for Coron, Cuyo, and Puerto Princesa for July. It is apparent in Figure 68 that Cuyo Island and Puerto Princesa reflects the predominant Southwest Monsoon winds while Coron Island continues to be unaffected by the monsoon so, it appears that there is a local wind regime that influences the Coron Island station.

The mesoscale model maintains a general wind direction coming from the Southwest for all August months. In Coron Island, this Southwest direction from the model differs with the measurements as shown in Figure 69(a) where the average wind direction is coming from the South. It is noted that the wind direction has shifted towards Southwest direction because the Eastern component is now absent.

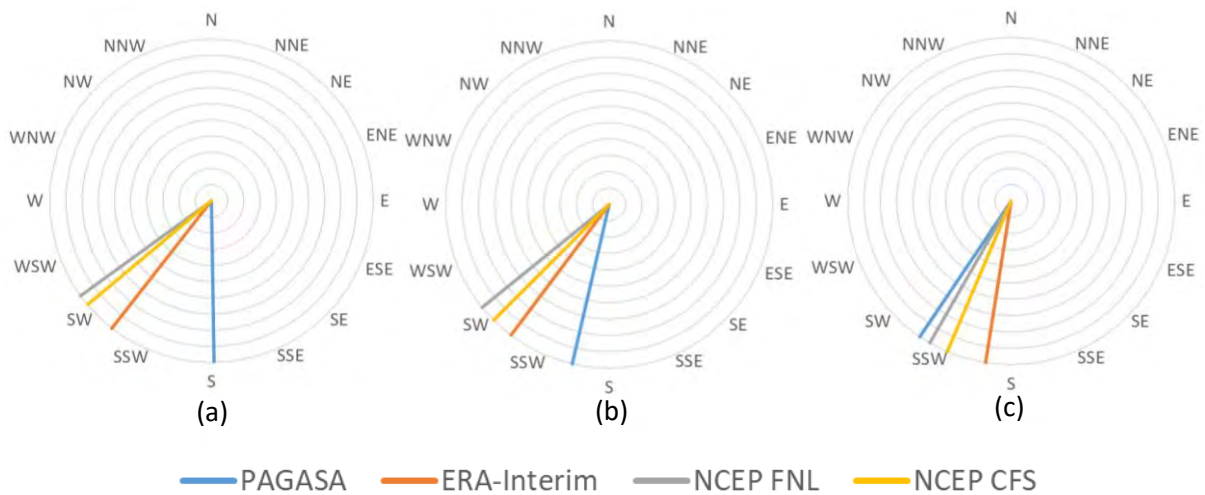


Figure 69. Comparison of average wind direction between WRF output and observation data at (a) Coron Island, (b) Cuyo Island, and (c) Puerto Princesa for the month of August 2012

Model results for Cuyo Island fall between Southwest and South-Southwest for August. As shown in Figure 69 (b), ERA-Interim result is closer to the wind direction observed at Cuyo Island which is between South and South-southwest. The winds are found to be coming from the South-Southwest in Puerto Princesa for August 2012 as can be seen in Figure 69 (c). The NCEP FNL is the best performing model configuration since it is closest to the wind direction observation. The Cuyo Island and Puerto Princesa simulations for August are similar to the June and July model output so, this is an indication of the prevalent wind direction during this part of the year.

There is a significant performance improvement for WRF model for all three sites in September that are plotted in Figure 70 when compared with the other months of a year. Seeing that the measurements have shown that the wind directions has shifted towards the Southwest direction for September, the mesoscale model is able to replicate the general direction for the month.

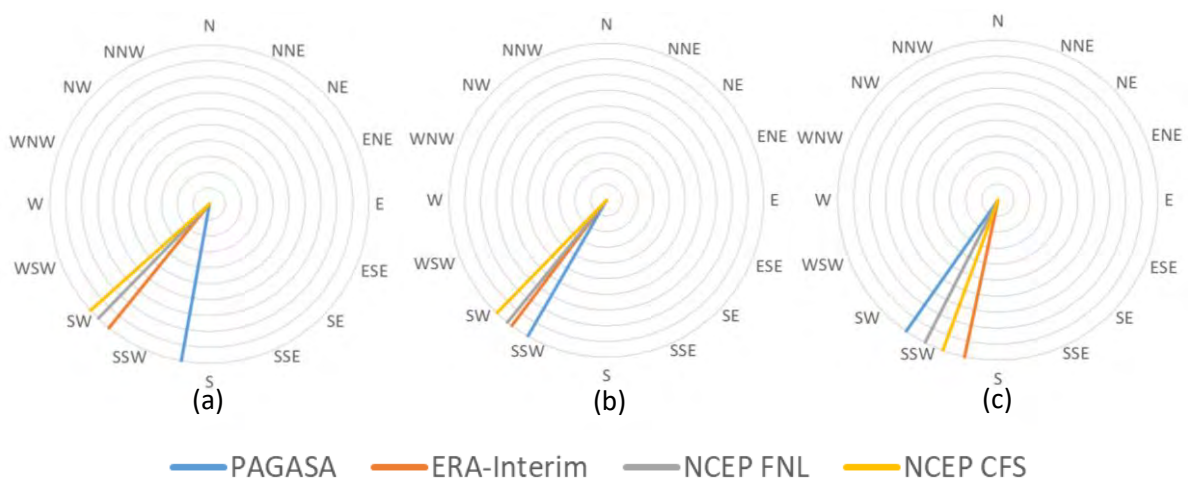


Figure 70. Comparison of average wind direction between WRF output and observation data at (a) Coron Island, (b) Cuyo Island, and (c) Puerto Princesa for the month of September 2011

Observations at Coron Island show a predominantly Southern wind direction but a Western component is apparent in Figure 70 (a). Thus, the Southwestern wind direction produced by the simulations are comparable to this measurement. The sites at Cuyo Island and Puerto Princesa have model outputs for wind direction that are very near the monthly average wind direction observations at their respective locations. ERA-Interim is the best performing configuration for Coron and Cuyo while NCEP FNL is the best model settings for Puerto Princesa for September 2011. With the slight shift in the measured wind direction at Coron Island, all three sites are now being affected by the predominant Southwest Monsoon.

The general wind directions for October, which is found in Figure 71, illustrates a gradual shift towards the Southeast direction compared to the September months. Coron Island’s wind direction becomes East-Southeast as shown in Figure 71 (a). Wind simulation results are still unable to generate that since the outputs are still in the South to South-southwest wind direction sector. But the model still registers that a shift in the prevalent wind has happened and has decreased the Western component in their results.

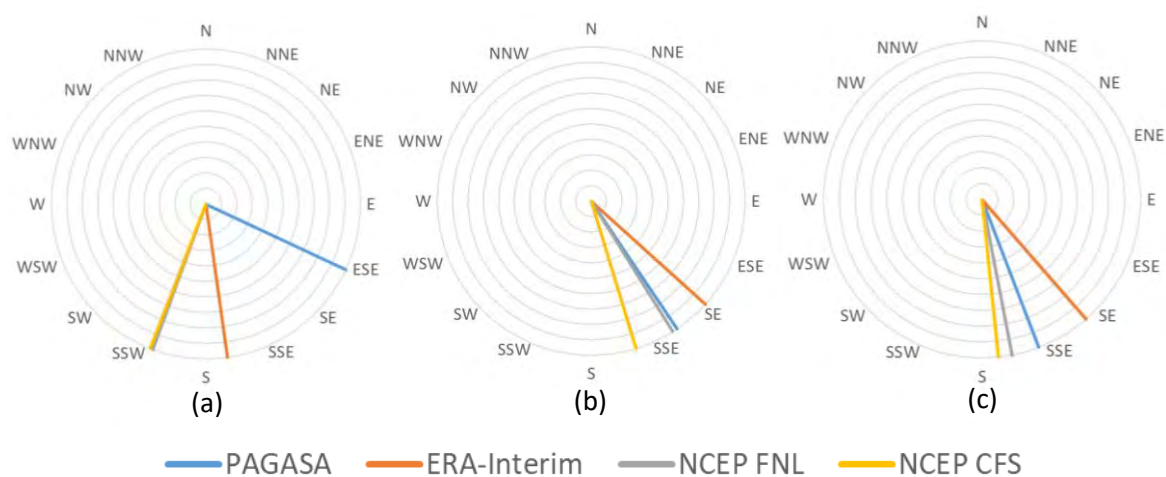


Figure 71. Comparison of average wind direction between WRF output and observation data at (a) Coron Island, (b) Cuyo Island, and (c) Puerto Princesa for the month of October 2011

The mesoscale model fares better in simulating the Cuyo Island and Puerto Princesa locations as shown in Figure 71 (b) and Figure 71 (c), respectively. Measured wind direction for both locations are found to be coming from the South-southeast and the three configurations are producing wind directions within this sector. The NCEP FNL is the best model settings for Cuyo and Puerto Princesa in October since it has the smallest difference to the measurements. All three sites have shown a shift in wind direction which corresponds to the transition from Southwest Monsoon to Northeast Monsoon at this time of the year.

Winds at Coron Island have shifted back to the North-Northeast for November as can be seen in Figure 72(a). Note that NCEP-CFS and NCEP-FNL have the same value so they overlap on the chart.

This shift is only partially reflected in the model since all three configurations are giving average wind directions between East and East-Northeast.

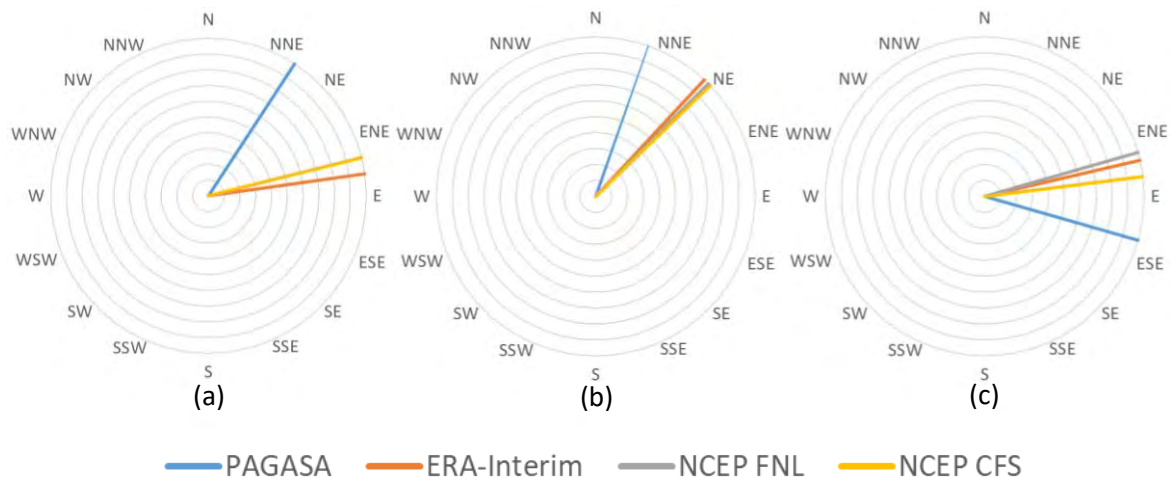


Figure 72. Comparison of average wind direction between WRF output and observation data at (a) Coron Island, (b) Cuyo Island, and (c) Puerto Princesa for the month of November 2012

The mesoscale model is showing better results at Cuyo Island than Coron for November as presented in Figure 72 (b). Measurements show that the winds are coming from the North-Northeast also and the simulations are close to that with a Northeast average wind direction. Although all three configuration have near equal directions, the ERA-Interim yields the closest direction to the observation. There has been only a slight shift in wind direction at Puerto Princesa for November when compared to the other October months. Looking at Figure 72 (c), the wind direction is coming from East-Southeast while it has been coming from the South-southeast for the October months in general. The mesoscale model has been able to determine this change from October to November but the outputs are between East and East-Northeast. Thus, the shift in wind direction is moderately higher for the simulations than the observations. Among the three configurations, the NCEP CFS is giving the nearest average wind direction to the measurements which makes it the best model setting for Puerto Princesa on November 2012. The onset of the Northeast Monsoon is apparent in Coron and Cuyo Islands while the Puerto Princesa station reverts back to the Eastern wind direction that is also present in January to March when the Northeast Monsoon affects the entire country.

The December months are observed to have similar wind directions such as the one in Figure 73 and these are similar with the November monthly average wind directions. Looking at Figure 73 (a), it shows that the mesoscale model is able to generate the average wind direction that is comparable with measurements especially through the use of ERA-Interim and NCEP CFS settings for Coron Island.

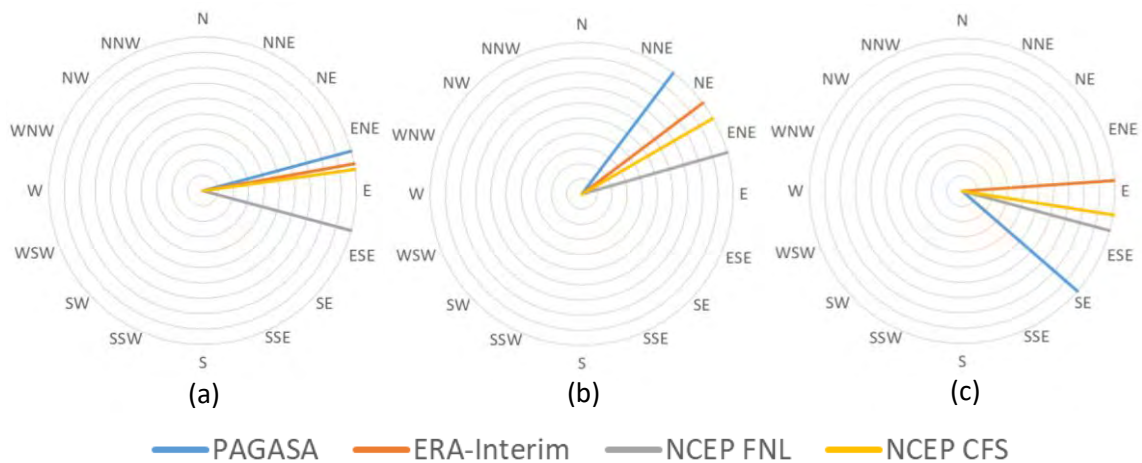


Figure 73. Comparison of average wind direction between WRF output and observation data at (a) Coron Island, (b) Cuyo Island, and (c) Puerto Princesa for the month of December 2011

In Cuyo Island, the model performance is also very much the same as November based on comparison of Figure 72 (b) with Figure 73 (b). For this case, the ERA-Interim is the better configuration since it gives the smallest difference in wind direction among the three settings when compared to the observation. There is also a similar monthly average wind direction in Puerto Princesa for December, shown in Figure 73 (c), as for November in Figure 72 (c). The NCEP FNL is the best model configuration for this case since it has the closest average wind direction to the observations in December 2011 for Puerto Princesa.

A list that summarises the results of the wind direction validation is found in Table 30. These show the best performing model setting on each month of the year at every location that has been included for the model validation. It is apparent that there are differences and similarities between model configurations that are suited for wind speed and wind direction at each month of the year.

Table 30. Summary of Best Mesoscale Model Configuration for Wind Direction

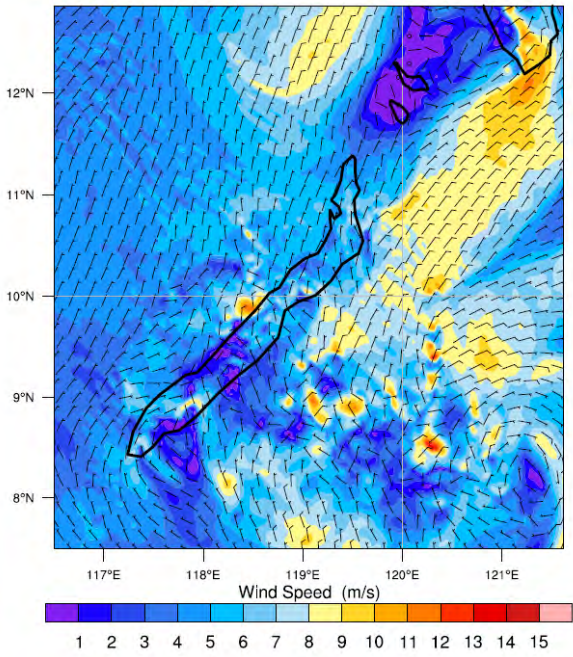
Month \ Location	Coron Island	Cuyo Island	Puerto Princesa
January	NCEP-CFS	ERA-Interim	NCEP-FNL
February	ERA-Interim	NCEP-CFS	NCEP-CFS
March	ERA-Interim	NCEP-FNL	ERA-Interim
April	NCEP-CFS	NCEP-CFS	NCEP-FNL
May	NCEP-FNL	ERA-Interim	NCEP-FNL
June	ERA-Interim	ERA-Interim	NCEP-CFS
July	ERA-Interim	ERA-Interim	ERA-Interim
August	ERA-Interim	ERA-Interim	NCEP-FNL
September	ERA-Interim	ERA-Interim	NCEP-FNL
October	ERA-Interim	NCEP-FNL	NCEP-FNL
November	NCEP-CFS/FNL	ERA-Interim	NCEP-CFS
December	ERA-Interim	ERA-Interim	NCEP-FNL

For Coron and Cuyo islands, it can be seen in Table 30 that ERA-Interim is still the best model configuration for wind direction determination during the Southwest Monsoon since the months that

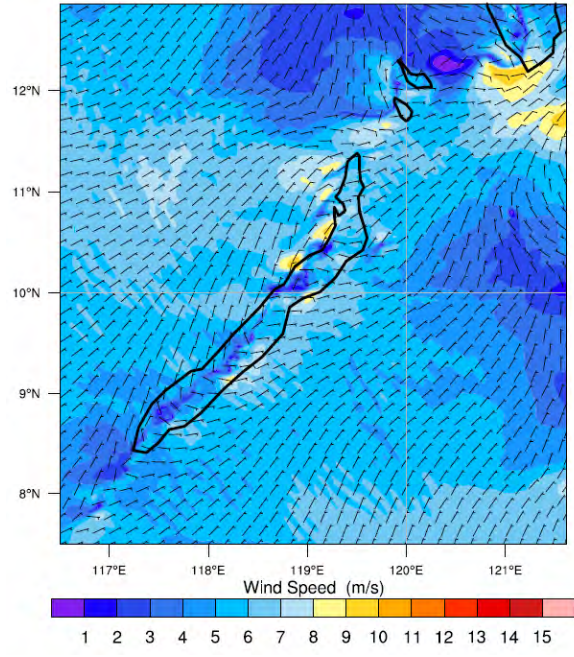
it occurs is covered within that period. The Northeast Monsoon months are capably modelled by a mixture of model settings that employ reanalysis data such as ERA-Interim and NCEP-CFS. The months where there is a transition in the season such as March and May show that the NCEP-FNL is a good model configuration to be used in Coron and Cuyo. In Puerto Princesa, there has been a change in the best model configuration for wind direction because it is a composition of the various model settings considered for the study. Unlike for the wind speed simulations where all months are well modelled by NCEP-CFS, a significant number of months in a year is showing to be simulated with satisfactory results from the NCEP-FNL because there are seven months of the year when this particular model setting performs well. From the results in Table 29 (Page 125) and Table 30, the best performing mesoscale configuration can be selected to produce wind maps for Palawan Province. The results from the comparison of wind speeds are given more consideration in deciding which dataset to be used for the map because the wind speeds have been analysed on a daily basis while wind direction analysis have been done with the purpose of determining the monthly trends that are to be related to the predominant seasonal wind direction. The wind maps generated will be shown and discussed in the next section.

5.2 Wind Maps for Palawan Province

Monthly wind maps have been produced from the simulations using the appropriate dataset based on Table 29 (Page 125) and Table 30 in order to see the offshore wind resource in the vicinity of Palawan Island. Some of these maps are shown in Figure 74 and Figure 75 where January uses the NCEP-CFS output, April map is produced with NCEP-FNL results, and ERA-Interim is used for June and September months. These are maps that show the time when the Northeast Monsoon is strong (January), Easterlies (April), Southwest Monsoon (June), and the transition from Southwest Monsoon to Northeast Monsoon (September).

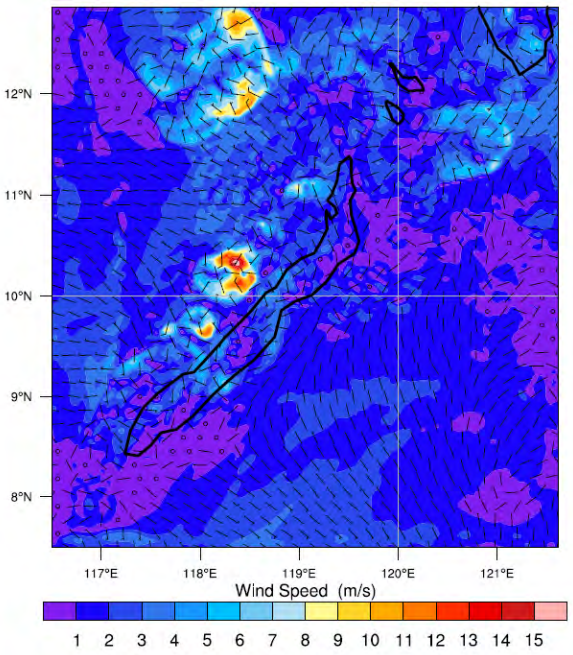


(a)

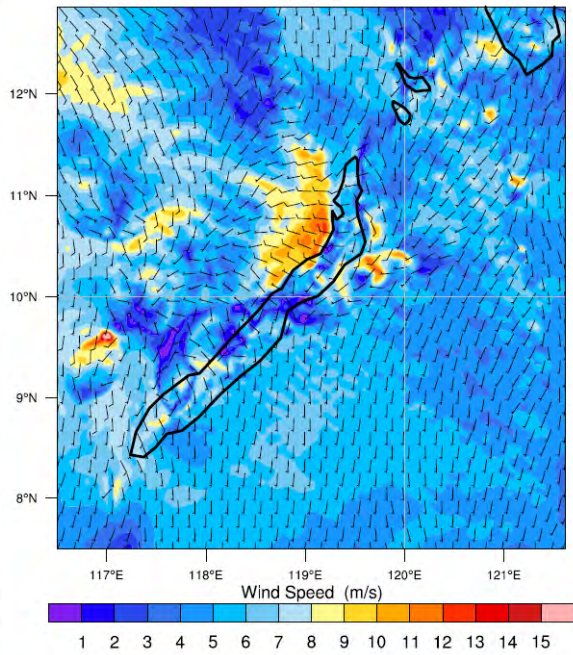


(b)

Figure 74. Wind maps for Palawan Island showing the available offshore wind resource around the island at 80 m: (a) January and (b) April



(a)



(b)

Figure 75. Wind maps for Palawan Island showing the available offshore wind resource around the island at 80 m: (a) June and (b) September

From Figure 74 and Figure 75, it can be seen that the offshore winds at the 80 m level can range from 5 m/s to 12 m/s when considering the vicinity that is 100 km from the shore. This range is

shown to be good wind conditions from Table 6 (Page80) since the range falls under the available to rich area categories. January months of 2010 – 2012 are more productive for wind power generation since majority of the waters have wind speeds greater than 6 m/s as shown in Figure 74 (a). This show that the Northeast Monsoon is indeed strong and the season when wind energy can be a significant power source for the island.

Looking at Figure 74 (b), winds decrease in speed to the range between 5-6 m/s in April when the Easterlies occur. This is indicative that the winds decrease at this time of the year so, wind farms will have lower power production. This is still within the available to subrich area based on Table 6 (Page80) so, there is still potential for power production during that time of the year. Even lower wind speeds happen in June, shown in Figure 75 (a), except for a few pockets in the South China Sea at the Western side of Palawan where wind speeds can be as high as 12 m/s. This show that there is a general decrease in available winds for power production during Southwest Monsoon around the island. Wind speed increases again during September as can be seen in Figure 75 (b).

The area of Palawan that is facing the South China Sea can be a better site for offshore wind projects since the winds there are more consistent. An example of this is the area centred at 10°N, 118°E where it can range from 6 – 12 m/s throughout the year. This makes the location to be a consistent rich area based on the wind classification standard in Table 6 (Page 80). In the Northwestern area, the winds have at least 6 m/s and even in June, there is an area centred at 11°N, 119°E where the winds are still blowing between 5 – 6 m/s range. Thus, this region falls under the subrich to rich area of wind classification. There is only a small patch in the southern end that can have 4-6 m/s speeds but can drop to 1 m/s in June. For parts of the island that is facing Sulu Sea, there is a potential for offshore wind power generation especially during Northeast Monsoon because of the regions there that can have 8 – 10 m/s. Wind variability for the northern part, covered by Sulu Sea, may make wind projects there produce less power.

Based on these wind maps, the areas with potential wind resource have been identified and the locations where the 7SEAS mission had made observations that coincide with those areas have been selected for analysis. Since the Northwestern area are deemed to have good wind resource from the wind maps, Guntao Islands and Notch Island observation locations are chosen for further analysis. It also shows that the Sulu Sea area have potential for offshore wind farm development so, the Balabac Island and Tubbataha Reef are also selected to be investigated. The analysis and investigation of these sites involve comparison and validation with the mesoscale model. These will be done in the following section. These sites will also be the locations to be simulated with microscale model and these results will be discussed in Section 5.3.

5.3 7SEAS Observation Comparison

An intercomparison of the three WRF configuration with the 7SEAS aerosol measurement campaign around Palawan Island has been carried out. Wind observations made while the ship was stationary, facing open seas, and have contiguous data of more than twelve hours were selected for the validation. For simplicity, the WRF configurations listed in Table 5 (Page 74) will be referred by their input data. Local times will be the reference despite the data being given in UTC since daytime and night time atmospheric phenomena affect the winds. Each of the sites are to be discussed in each subsection with a chronological order of the observations made by the 7SEAS campaign.

5.3.1 Balabac Island

The island at the southernmost tip of the main Palawan Island is called Balabac. Figure 76 presents the wind speeds off the coast of Balabac Island when the ship was anchored there on 16 September 2012.

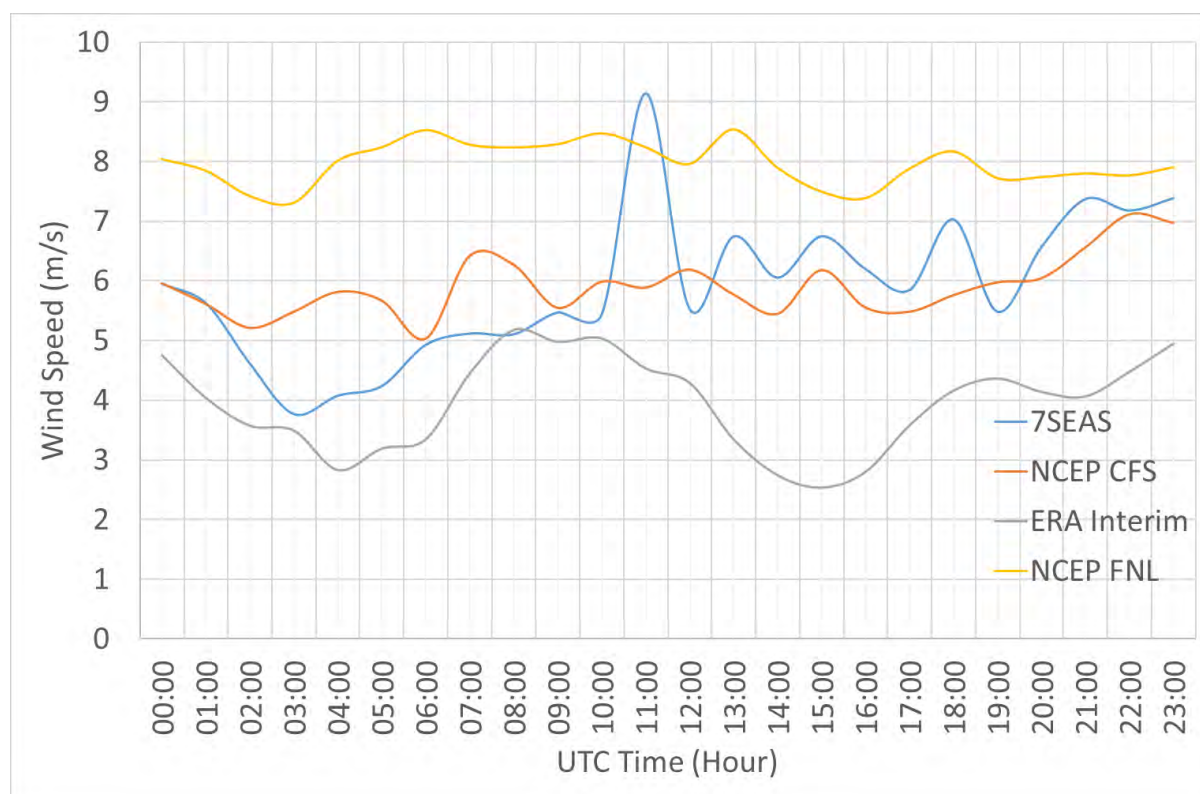


Figure 76. Wind speeds from mesoscale model outputs and actual observations at Balabac Island on 16 September 2012

The ERA-Interim tracks the winds adequately except during the late morning until late afternoon which can be seen in Figure 76. From that point in time, the wind speeds generated by the NCEP-CFS configuration is comparable with the ship observations through the night until early morning of the following day. NCEP-CFS simulates the conditions well but with an underestimated

value most of the time. Late morning until early afternoon is captured slightly better by the ERA-Interim. The sudden spike in wind speed is not reflected in any model settings' output.

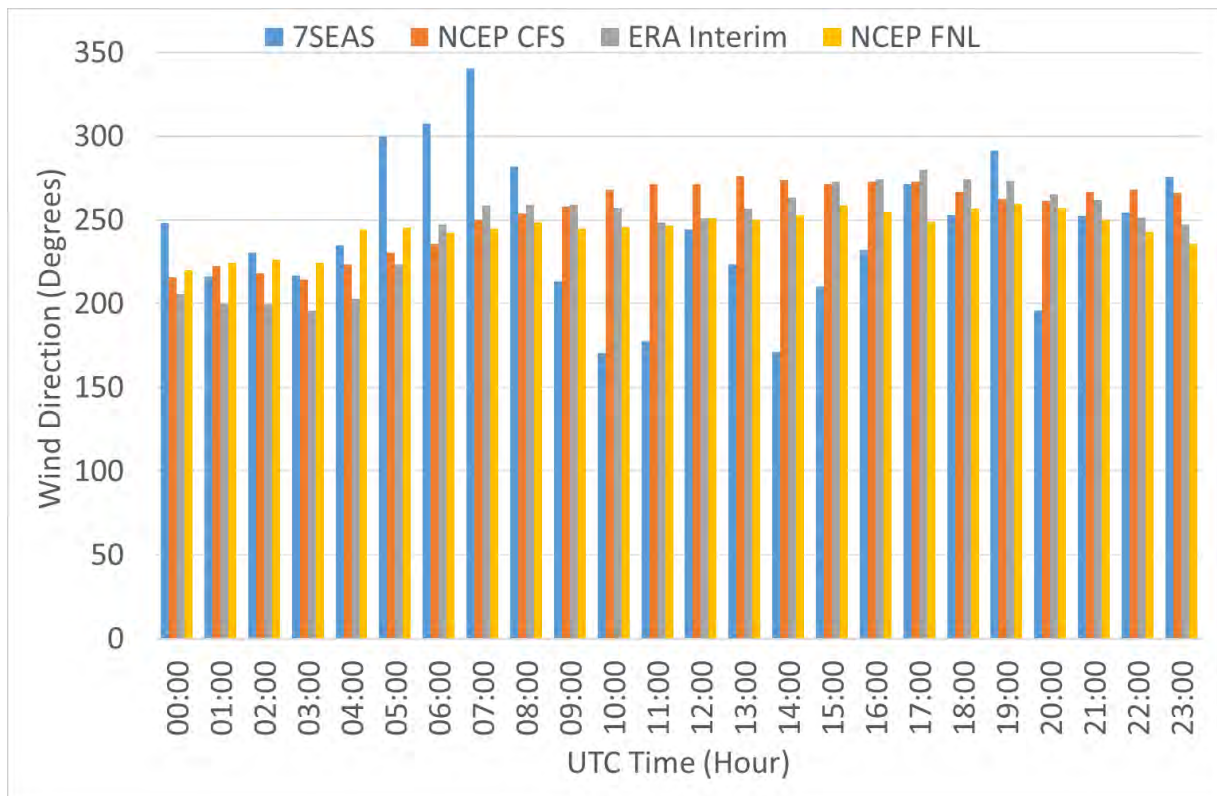


Figure 77. Wind direction values from mesoscale model results and measurements for Balabac Island on 16 September 2012

There is some difficulty for the model in reproducing the wind directions as shown in Figure 77. Winds coming from the Southwest are being generated by the model results. In the morning, the NCEP-FNL are able to determine the wind directions and the varying wind directions throughout the afternoon and evening are not being generated by the WRF.

5.3.2 Guntao Islands

There has been two stationary observations points around Guntao Islands because both North and South Guntao Island has been considered for the measurement campaign. Upon consultation with the crew and science team on board the ship, it was decided that the South Guntao Island is the better location for observation between the two islands. So, the measurements for South Guntao are compared to the mesoscale model results in this section.

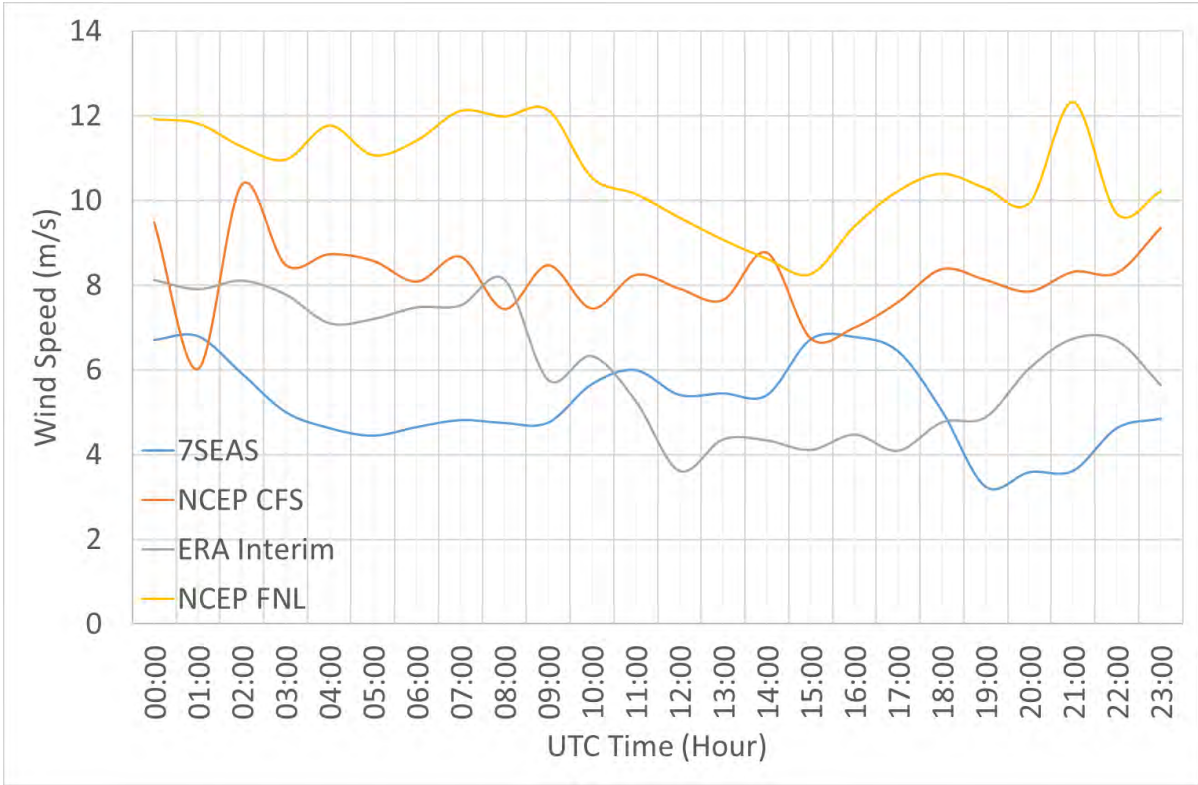


Figure 78. South Guntao Island wind speed measurements and model results for 24 September 2011

Wind speeds are generally overestimated by the NCEP-CFS and NCEP-FNL while the ERA-Interim appears to be the best performing model configuration for this location as shown in Figure 78. There is a smaller difference in the overestimated values from ERA-Interim in the morning until the afternoon since the range is about 2 – 4 m/s. ERA-Interim underestimates the wind speed values in the evening until 2am local time by 2 – 3 m/s. The ERA-Interim output reverts back to overestimating the values beginning at 3 am until dawn.

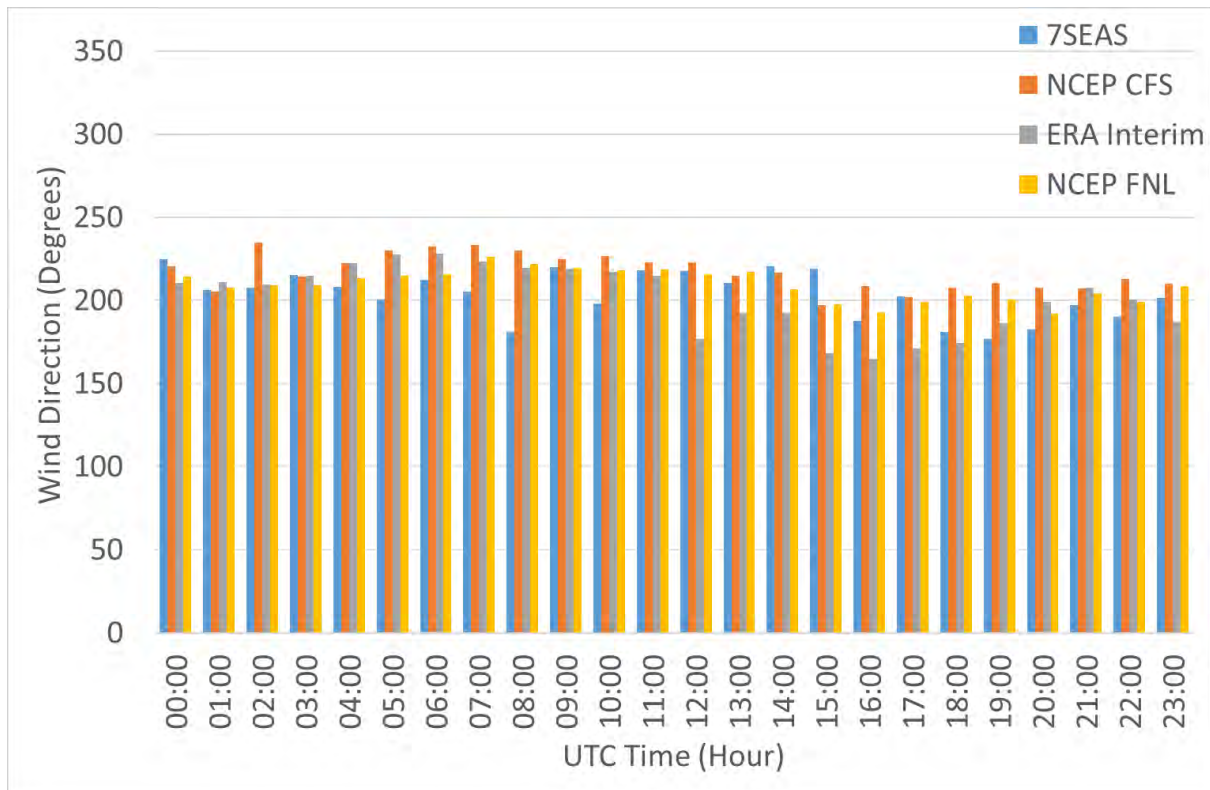


Figure 79. Modelled wind direction alongside measurements for South Guntao Island on 24 September 2011

In terms of the wind direction, the ERA-Interim gives the best performance most of the time for the second day of observation as seen in Figure 79. Generally, the ERA-Interim has difficulty simulating the wind direction late morning until before midnight. Wind directions at midnight until the early morning are sufficiently represented by ERA-Interim.

An example that presents the performance of mesoscale models configured for long-term weather patterns behaves when there is a local disturbance or extreme event is in Figure 80 and Figure 81. It is apparent that both NCEP-CFS and NCEP-FNL are overestimating the wind speeds in Figure 80. The ERA-Interim dataset shows better performance until the sudden drop in wind magnitude observed at night. This has been associated with the approaching typhoon named Nesat at the time [152]. It shows that WRF in ARW mode has limitations when simulating sudden changes in weather conditions due to extreme weather events which may be better suited for the operational mode of WRF [150].

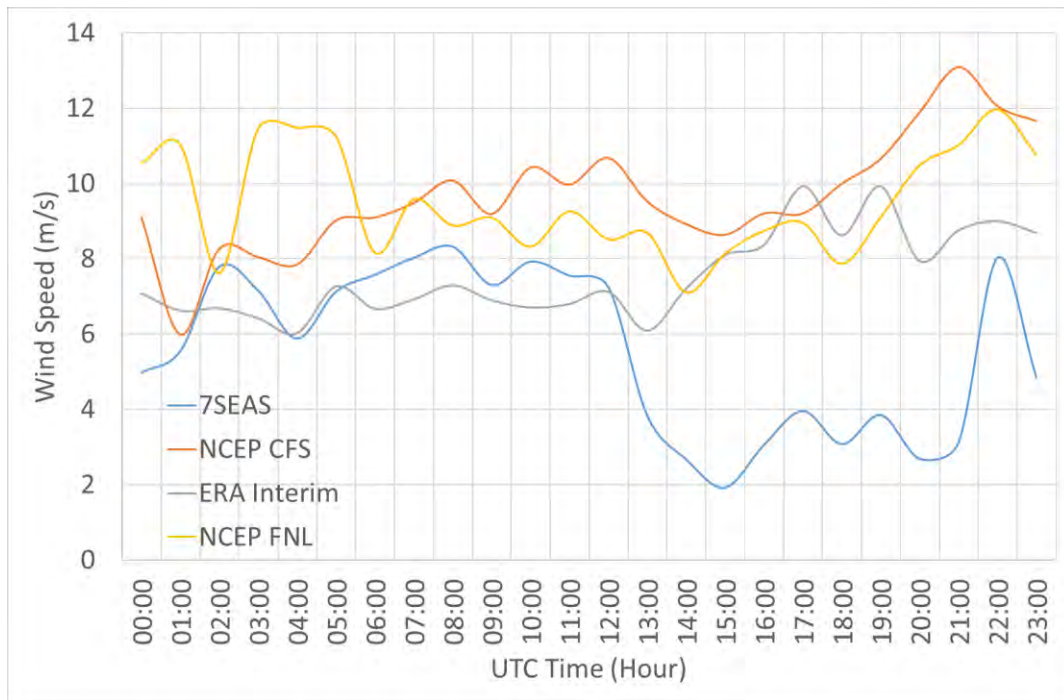


Figure 80. South Guntao Island wind speed measurements and model results for 25 September 2011

This immediate change in the weather because of the approaching typhoon can also be seen in the wind direction data in Figure 81 as the sudden shift from Southwest to Southeast in the evening. WRF was unable to account for this extreme weather event since it was configured to simulate month long weather patterns instead of short-term daily weather conditions. But the wind directions before the typhoon affected the locality have similar West or Southwest winds.

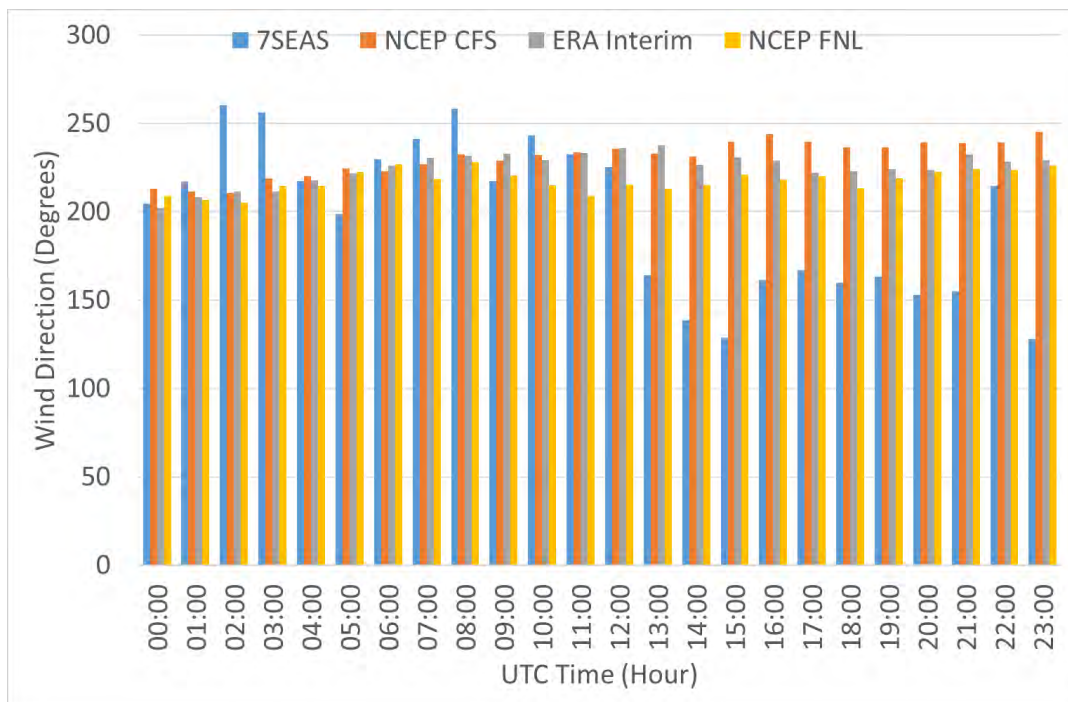


Figure 81. Modelled wind direction alongside measurements for South Guntao Island on 25 September 2011

5.3.3 Notch Island

At the Notch Island, it is shown in Figure 82 that ERA-Interim simulates the wind speeds better than NCEP-CFS and NCEP-FNL. Both NCEP-CFS and NCEP-FNL tend to overestimate the wind speeds while ERA-Interim show similar wind magnitudes as the recorded wind data. But ERA-Interim underestimates wind speed values after midnight while NCEP-CFS is able to track the wind speed trends at those times.

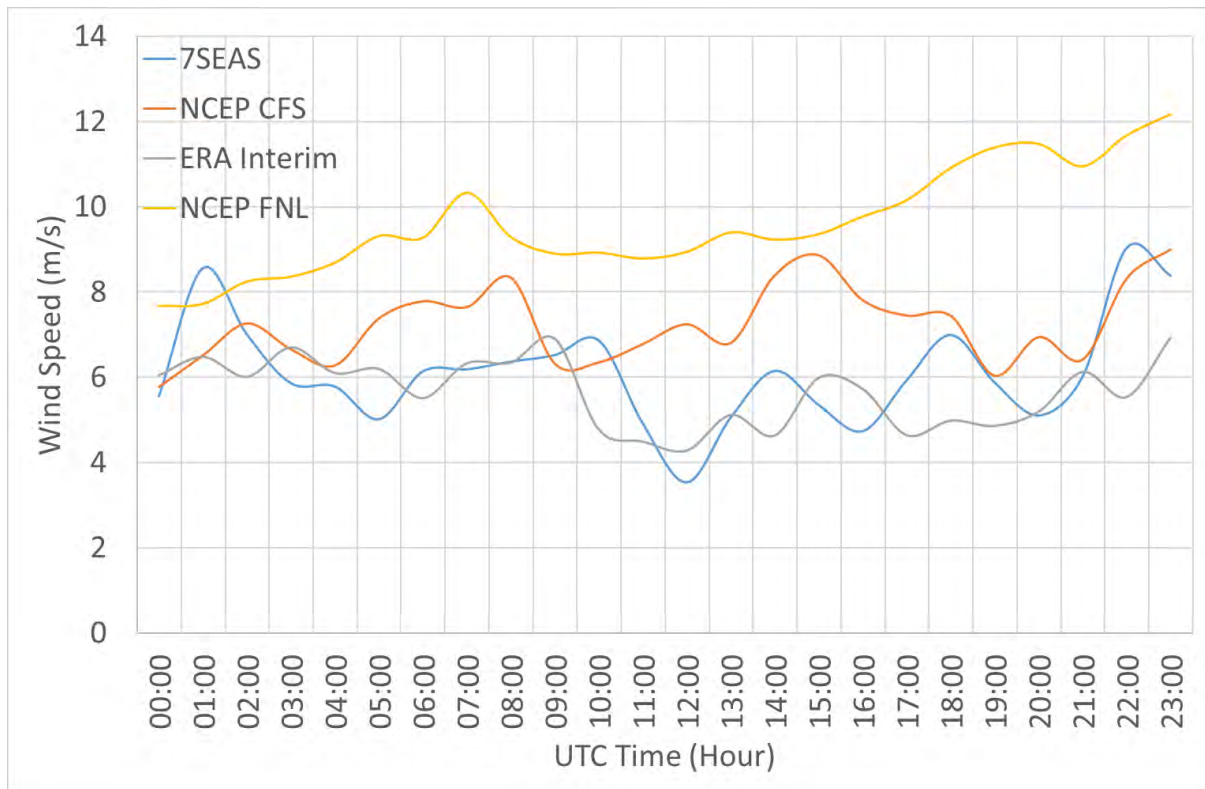


Figure 82. Simulated and observed wind speeds Notch Island on 21 September 2011

The wind directions at Notch Island are presented in Figure 83 where it shows that the three WRF configurations have comparable performance in capturing the wind directions.

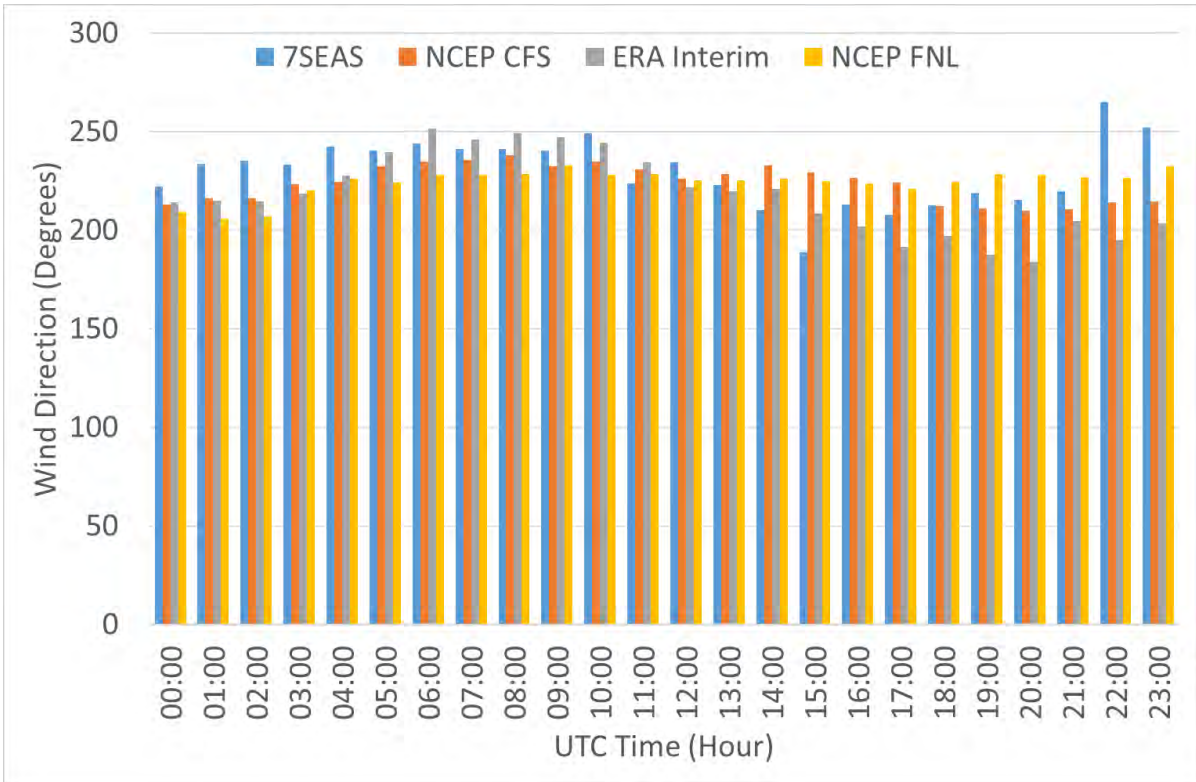


Figure 83. Model outputs and measured wind direction for Notch Island on 21 September 2011

5.3.4 Tubbataha Reef

The last site to be discussed is the Tubbataha Reef which is located far from any coastline. At this location, two observation sites have been selected for analysis. The first site is the Tubbataha North Reef and the other one is the Tubbataha South Reef. Since there is no day where a 24-hour period of observation has been made and the science team found no significant difference between the two locations, the observations at the Tubbataha North Reef has been compared to the mesoscale model outputs in this section.

In Figure 84, it shows that NCEP-CFS and NCEP-FNL are overestimating the magnitudes but NCEP-CFS is the better performing configuration between the two. ERA-Interim is more capable of modelling the wind speeds among the three at this site although there is a slight underestimation between noon time until early evening and a slight overestimation late in the evening until the early morning of the following day.

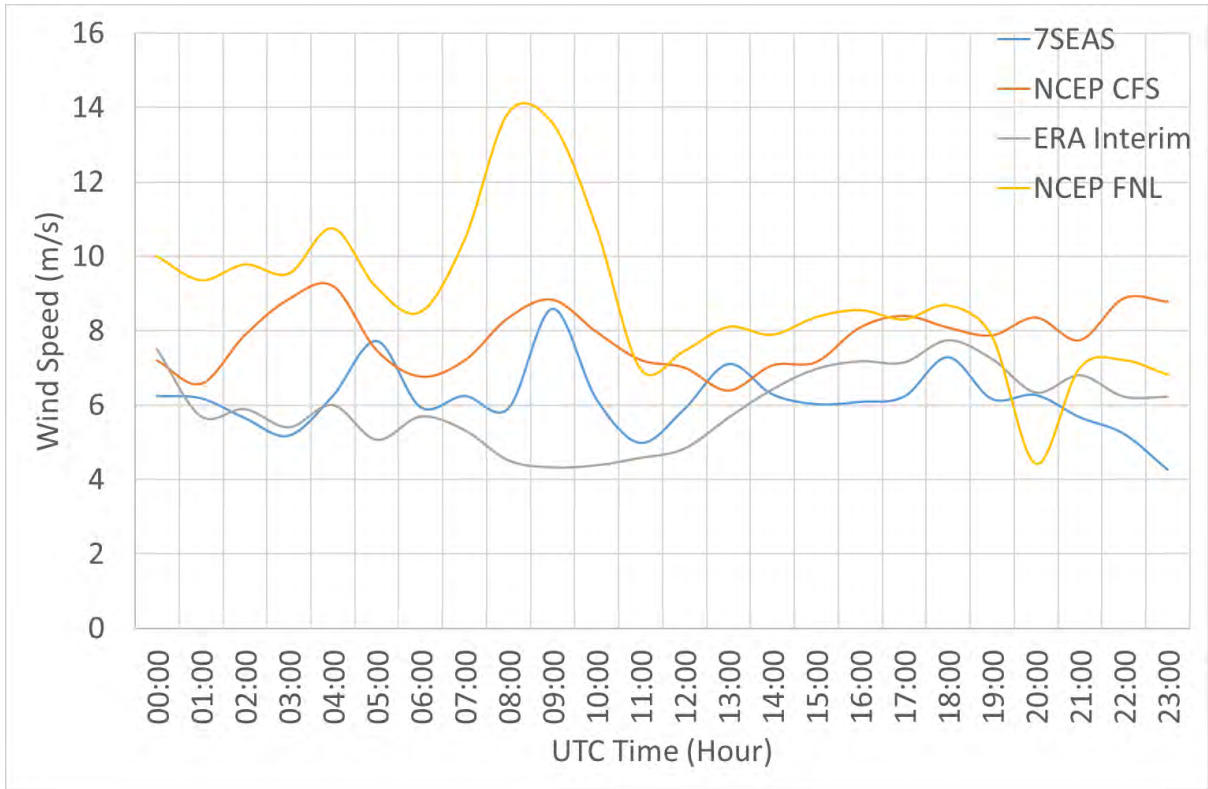


Figure 84. Tubbataha North Reef wind speeds on 22 September 2012

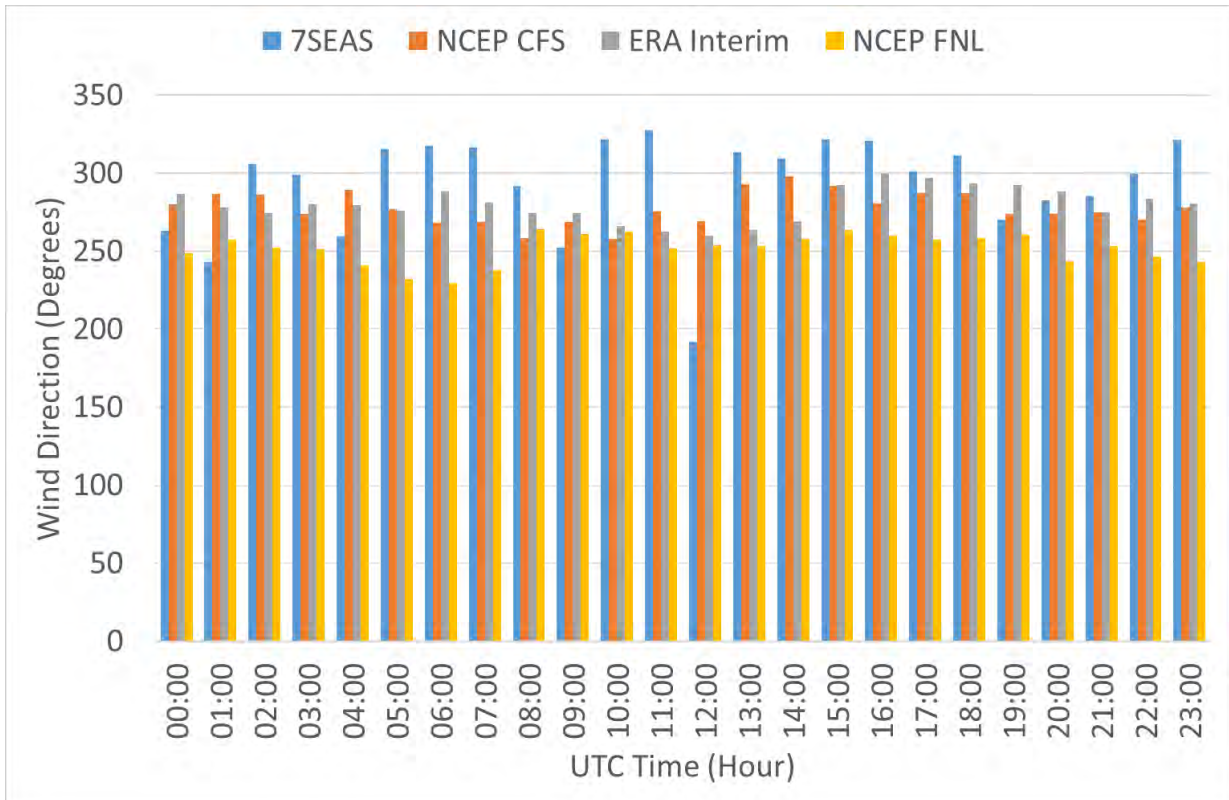


Figure 85. Wind directions for Tubbataha North Reef on 22 September 2012

Figure 85 presents the wind direction for the North Reef where it can be seen that both NCEP-CFS and ERA-Interim are yielding better wind direction values than NCEP-FNL. There are winds coming from

the Northwest based on the wind records on the ship which are absent in the WRF results but the general Western wind directions are still present in the simulations.

To quantify the performance of each WRF configuration, the RMSE has been calculated for wind speed and wind direction. These results are listed in Table 31 for comparison.

Table 31. Error and bias values of wind speed and direction for each mesoscale model configuration settings

Configuration		ERA-Interim			NCEP-FNL			NCEP-CFS		
		RMSE	Bias	STDE	RMSE	Bias	STDE	RMSE	Bias	STDE
Balabac Island	Wind Speed	2.33	-1.95	1.28	2.40	2.06	1.24	1.08	0.01	1.08
	Wind Direction	49.05	4.78	48.82	44.32	2.65	44.24	52.38	11.63	51.08
Guntao Islands	Wind Speed	2.09	0.87	1.90	5.67	5.41	1.69	3.31	2.94	1.50
	Wind Direction	21.71	-1.91	21.63	14.38	5.86	13.14	20.82	13.75	15.64
Notch Island	Wind Speed	1.26	-0.46	1.18	3.81	3.49	1.52	1.75	1.11	1.35
	Wind Direction	22.67	-11.22	19.70	18.05	-5.31	17.26	18.86	-5.65	17.99
Tubbataha Reef	Wind Speed	1.40	-0.18	1.39	3.31	2.74	1.85	2.07	1.66	1.23
	Wind Direction	34.37	-13.56	31.58	54.17	-41.76	34.51	36.10	-15.57	32.57

For Balabac Island, NCEP-CFS has the least RMSE value of 1.08 m/s for wind speed and NCEP-FNL has the smallest value of 44.32° for wind direction. Their corresponding bias and STDE values are also the lowest as found in Table 31. This shows that a combination of both dataset as input data for the mesoscale model is suited for Balabac Island. The RMSE, bias, and STDE values for Guntao Islands present that ERA-Interim is the best performing configuration since they are the lowest among the three configurations for wind speeds. Although NCEP-FNL's RMSE and STDE values for wind direction in Guntao Islands may be better than ERA-Interim, the bias value of -1.91° is the least compared to the other model settings considered in the study for Guntao Islands. Notch Island is where ERA-Interim yields the best wind speed simulations while NCEP-FNL gives the best wind direction. But NCEP-FNL is only marginally better in wind direction compared to NCEP-CFS and ERA-Interim since all three have RMSE, bias, and STDE values that are close to each other as can be seen in Table 31. The Tubbataha Reef area is also the region where ERA-Interim is capable of simulating the wind vectors better than NCEP-CFS and NCEP-FNL configuration settings. This is proven by having the least RMSE, bias, and STDE values compared to the other model settings in Table 31. The best performing model configuration results are used as input data for the microscale model. Since the mesoscale model output wind direction are predominantly Southwest, the model configuration that performs well in generating the wind profile takes precedence in determining the best configuration for each site. A summary is listed in

Table 32.

Table 32. Summary of best model configuration settings at each 7SEAS site

Location	Configuration
Balabac Island	NCEP-CFS
Guntau Islands	ERA-Interim
Notch Island	ERA-Interim
Tubbataha Reef	ERA-Interim

All the best model configuration that are listed in

Table 32 are found to be using reanalysis datasets. This result show that reanalysis data are good input data for mesoscale models in determining daily wind patterns or short-term time scales. The usage of reanalysis data where they demonstrate excellent results are also found in the literature [18,151] as discussed in Chapter 2. The best performing configurations in

Table 32 are the same with the best configuration for September when the mesoscale model is being validated with onshore weather stations in Section 5.1. The next section will deal with the microscale modelling.

5.4 Microscale model

As discussed in Chapter 3, the microscale model chosen for this study is a CFD model developed by WindSim AS. Similar comparison plots have also been done for the CFD outputs but only for locations that have wind measurements for the 7SEAS ship observations. These comparison is made in order to see if there are improvements to the wind profiling for coastal regions and open waters on the selected sites from the 7SEAS campaign. Limited observations in offshore locations have only allowed short term wind simulation comparison for the month of September in 2011 and 2012. Prior to the comparison, the sensitivity of the CFD model has been done and will be discussed in the next subsection.

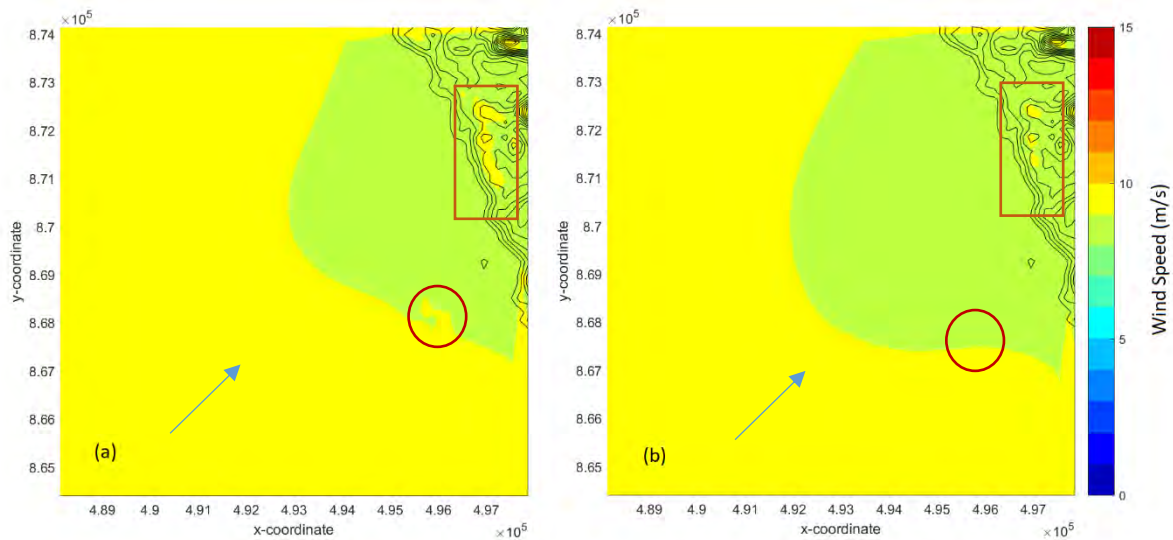
5.4.1 CFD Sensitivity Tests

To determine the configuration suited for the Palawan Island, the sensitivity tests have been carried out for the CFD model. These are whether to consider the mesoscale temperature data in the simulations, varying the grid resolution, and changing the turbulence model. In this section, the results of the tests are to be discussed.

5.4.1.1 *Input Temperature Initialisation*

This involves the usage of the temperature input from the mesoscale model results or not. It is deemed essential to initialise the temperature when improvements from the microscale output is evident [171]. Here, the discussion will be presented for each site selected from the 7SEAS campaign. For these runs, the grid resolution is set to 152m and the turbulence model used is the standard k- ϵ model.

5.4.1.1.1 Balabac Island



Predominant Model Wind Direction: SW

Figure 86. CFD model runs at Balabac Island that compares (a) simulation without WRF temperature and (b) initialisation of temperature with mesoscale model results

In Figure 86(a), it can be seen that there is a small patch, encircled in red, over the water that have higher wind speed where the wind has slowed down in close proximity to it as the coastal effects are felt by the wind flow. This same area is no longer present in Figure 86 (b) within the encircled region. There is also a patch over land, enclosed by a box in Figure 86 (a), where the wind speed appears to increase suddenly then slows down. This patch is dramatically reduced in Figure 86 (b) and a uniform area, enclosed in a box also, can be seen to have slowed down as the winds came nearer to the island. The patches of speed up over land has shrunk for the case where the model is initialised with mesoscale model results temperature. Even though there are no low wind speed occurrence downstream, it is advisable to use temperature initialisation from the WRF results because simulations for slightly stable and unstable atmospheric conditions yield better results [170,171] and the atmospheric conditions in the Philippines are commonly unstable because of the area characterised by many convective systems [153].

5.4.1.1.2 Guntao Islands

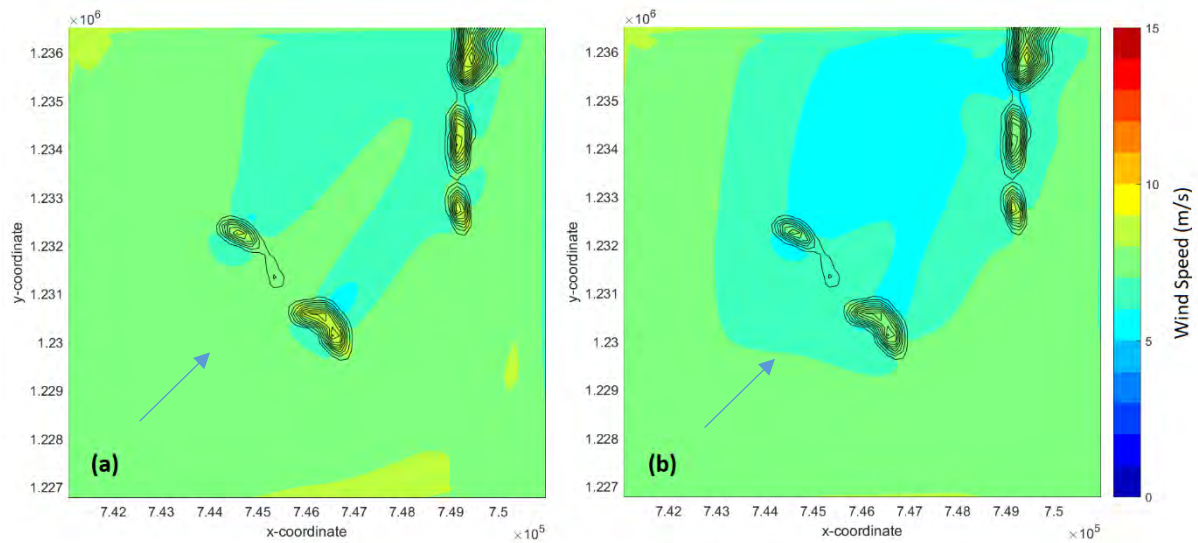


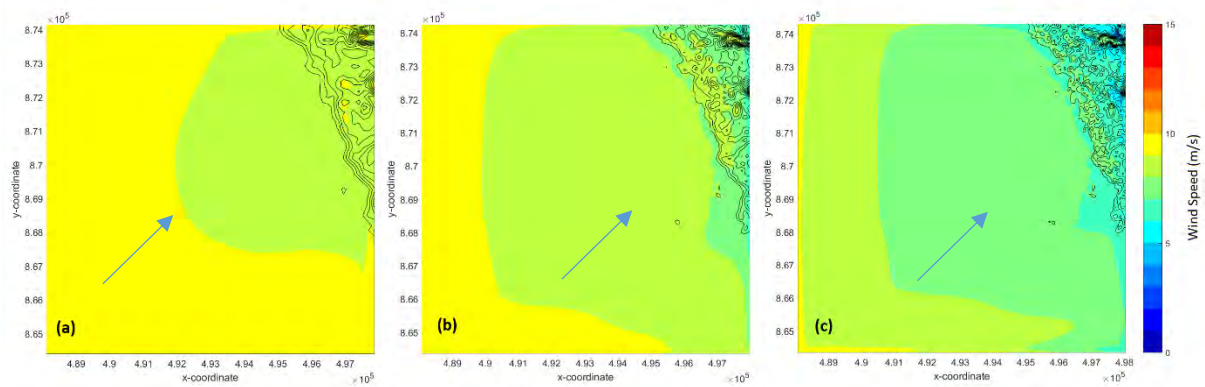
Figure 87. CFD model runs at Guntao Islands that compares (a) simulation without mesoscale model output temperature and (b) initialisation of temperature with mesoscale model results

Wake effects of islands are visible in Figure 87 that appears like a shadow behind the islands. The patches over the water where the wind appear to speed up are present in Figure 87 (a) while it is not there in Figure 87 (b) when the simulation has been initialised with mesoscale model temperature data. There is a larger area where the wind has slowed down further behind the two islands in the middle of the domain. This shows a combined wake effect by the two islands that propagates downstream. The area between the two islands in Figure 87 (a) does not show this and appears the wind is unaffected because the offshore wind speed persists. Thus, the temperature needs to be initialised with the mesoscale model results for Guntao Islands.

5.4.2 Grid resolution sensitivity

The model results are affected by the size of the grid cells used in the simulation. Varying the grid resolution to fine scale will show which grid size will suffice for the analysis. The temperature initialisation test results are already incorporated into the runs and the turbulence model is set to be the standard k- ϵ model. Each study site selected are discussed in the following sections.

5.4.2.1 Balabac Island

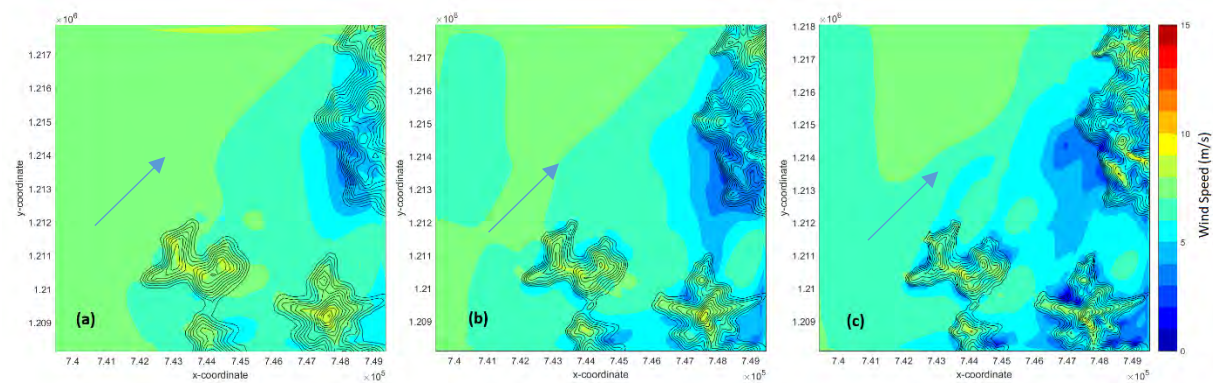


Predominant Model Wind Direction: SW

Figure 88. CFD model runs at Balabac Island that compares different grid resolutions at (a) 152m, (b) 76m, and (c) 38m

Grid resolution at 152m is presented in Figure 88(a) which shows that the coarse topography yields wind speeds that are essentially binary in value. As the grid resolution increases shown in Figure 88 (b) and Figure 88 (c), there is a better wind pattern representation because of the fine scale topography. The wind speed begins to decrease farther from the shore compared to the coarser resolution. Higher points on the land that are close to the coast have higher wind speeds compared to the lower level points behind them which is realistic. Thus, the 38m resolution grid is the suitable cell size for the Balabac Island simulations.

5.4.2.2 Notch Island



Predominant Model Wind Direction: SW

Figure 89. WindSim runs at Notch Island that compares different grid resolutions at (a) 152m, (b) 76m, and (c) 38m

In areas where there are multiple islands, Figure 89 shows that the high grid resolution of 38m gives a better wind flow result because of the shadow effects made by high points on an island to the downwind side behind it. These patches of low wind speeds are the wake effects caused by the islands to the incoming winds. Thus, the 38m grid resolution is deemed to be the best cell size for the WindSim Model.

5.4.3 Turbulence Closure Scheme

With the grid resolution set to 38m, the sensitivity to the turbulence model is now considered. The two turbulence closure scheme are the standard k-ε and RNG k-ε schemes. Both are compared by running simulations at the same site and see the performance of the WindSim.

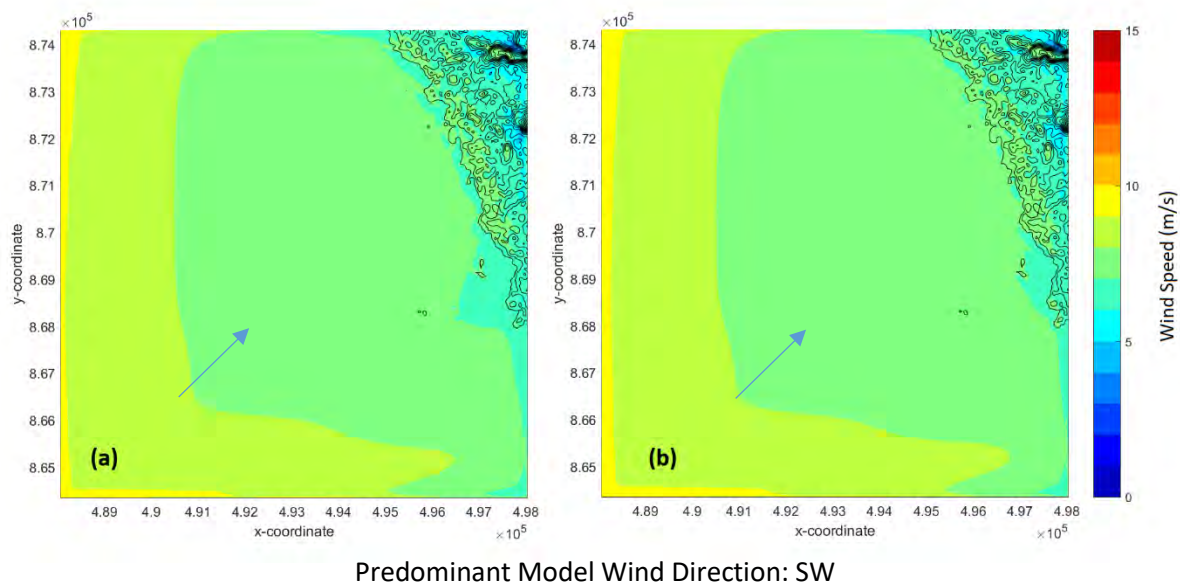


Figure 90. Comparison of different turbulence model using (a) standard k-ε and (b) RNG k-ε over Balabac Island

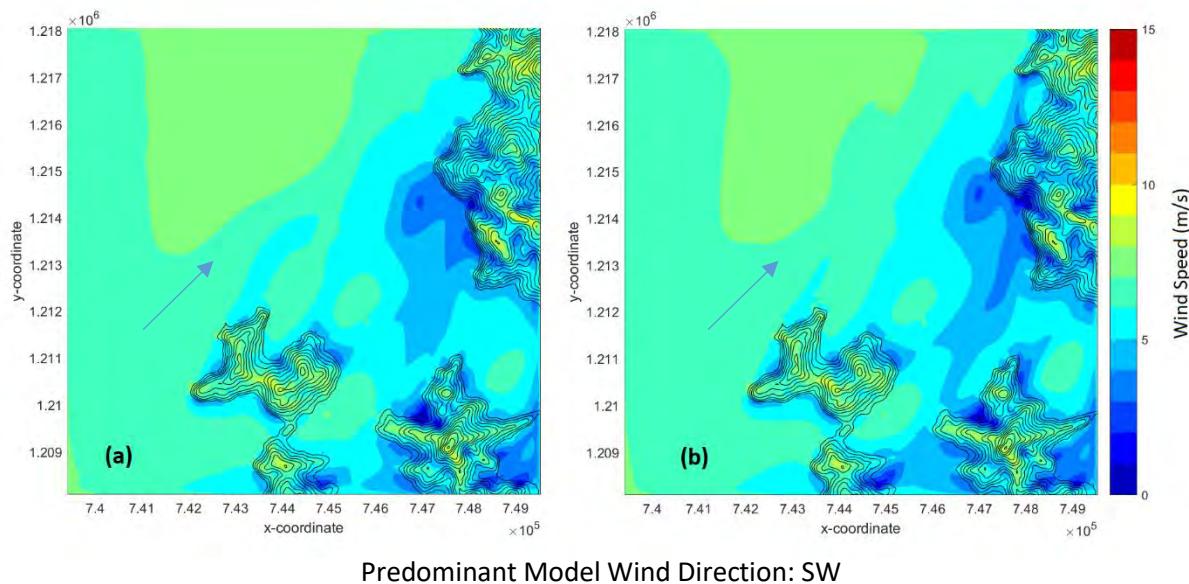


Figure 91. Comparison of different turbulence model using (a) standard k-ε and (b) RNG k-ε over Notch Island

From the figures, it can be seen that there is no significant difference in using either of the two turbulence closure scheme. The terrain is not very complex since the advantage of RNG k-ε over standard k-ε is in solving fluid flow for highly complex geometries [173]. An intensive wind measurement campaign is required that will account for the intricacies of the topography in order to

determine which of the two schemes provides a better representation of the wind flow over the area. In addition, the standard k- ϵ model is widely used because it has been proven to sufficiently model fluid flows in many applications [162] so it is the turbulence model that is used for the study.

The results of the sensitivity tests has determined the appropriate configuration for the microscale model for this study. These settings are listed in Table 33 and includes the other parameters that have been determined from the literature as discussed in Chapter 3.

Table 33. Summary of microscale model configurations

Parameter	Setting
Terrain Elevation	ASTER GDEM v2
Roughness	VCF Tree Cover
Boundary Layer Height	1,500 m
Temperature Input	Initialise from Mesoscale
Grid resolution	38 m
Turbulence Model	Standard k- ϵ

The model settings has been used in simulating the winds over the areas selected for further downscaling. In the next section, the results of microscale model are to be presented.

5.5 Mesoscale and Microscale (CFD) Model Comparison

The results of the CFD simulations are validated with the 7SEAS observations and compared with the mesoscale model in order to see the performance of the microscale model. Comparison for each of the selected sites are discussed in this section. The flow of the discussion is similar with the section on the 7SEAS observation comparison with the mesoscale results where the wind speeds and wind direction at every chosen location are presented. The mesoscale model results used for comparison and input for the CFD model are listed in

Table 32 (Page 149).

The first site to be discussed is the Balabac Island where the NCEP-CFS mesoscale configuration is used as the input data and for performance comparison. It is noticeable that the CFD model and mesoscale model have similar wind speed patterns in Figure 92 but the CFD model produces lower wind speeds. Thus, it is underestimating the wind speed values in Balabac Island.

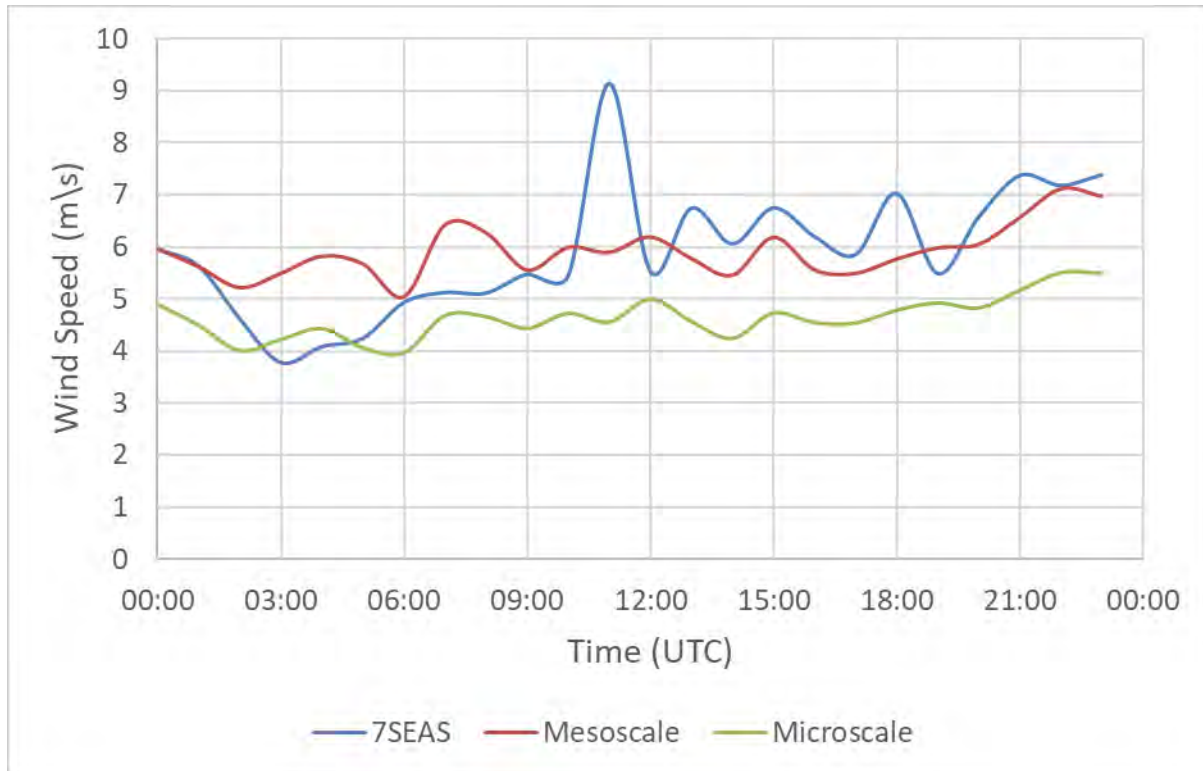


Figure 92. Comparison of mesoscale and microscale model wind speed results off the coast of Balabac Island on 16 September 2012

The sudden dip in wind speed from 5 m/s to about 4 m/s between 2:00 to 5:00 is captured by the CFD model. These times are being overestimated by the mesoscale model. So, the low wind speeds that the mesoscale model cannot simulate are being reproduced by the CFD model. The sudden spike in wind speed between 10:00 to 11:00 are still not reflected by both simulations. This shows that the CFD model is dependent on the quality of input data from the mesoscale model in the same manner that the mesoscale model depends on the input data for its simulations.

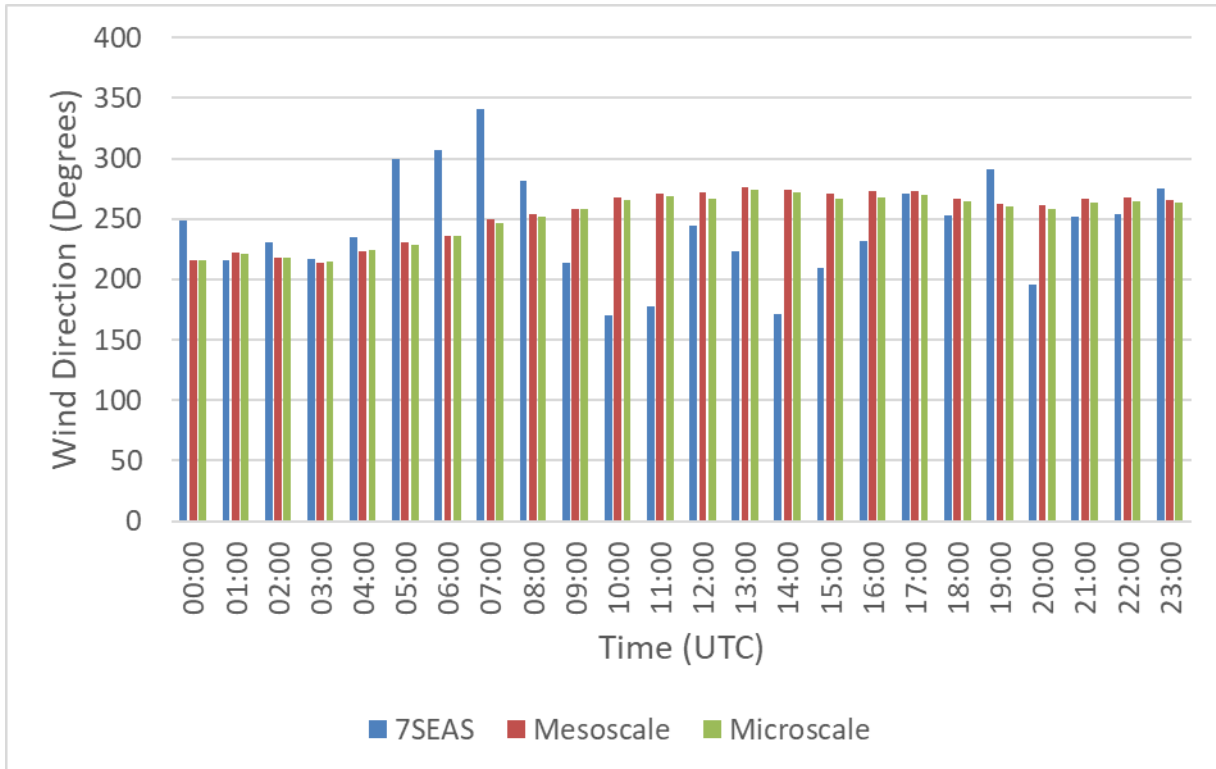


Figure 93. Comparison of mesoscale and microscale model wind direction results off the coast of Balabac Island on 16 September 2012

The wind directions of the CFD model output are shown in Figure 93. Here, it appears that the CFD model is generating the same directions as the mesoscale model. This is expected since the wind speed patterns in Figure 89 for the two models are also similar. Thus, there is no improvement in determining the wind directions using CFD model for this case.

The next site to be discussed is the simulation outputs for the Guntao Islands. Unlike the Balabac Island results, there is a significant difference in the wind patterns generated by the mesoscale model and the CFD model. This difference is the effect of the North and South Guntao Islands on the wind flow which is illustrated in Figure 87. These small islands are not being taken into consideration with the mesoscale model simulations because of the coarser topographical data being used by mesoscale models.

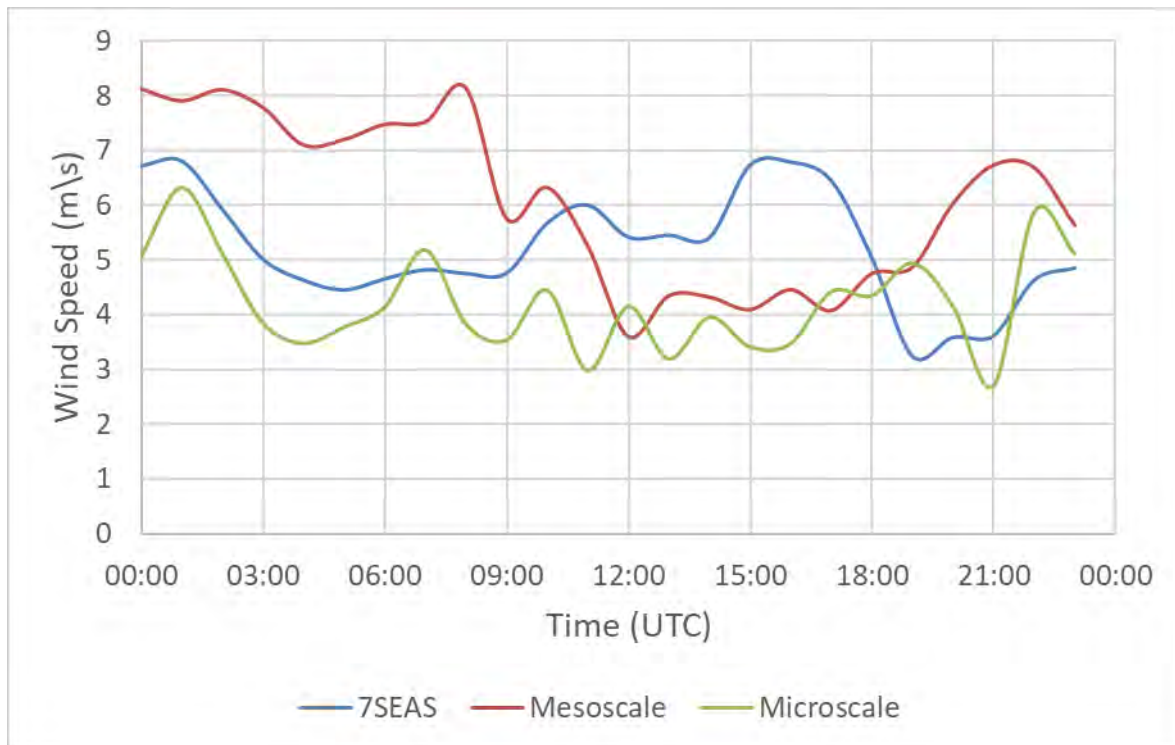


Figure 94. Comparison of mesoscale and microscale model wind speed results off the coast of Guntao Islands on 24 September 2011

It is evident in Figure 94 that the CFD model is more capable in simulating the wind conditions at the Guntao Islands site than the mesoscale model. This shows that the CFD model gives wind speeds that are closer to the observations between 1:00 to 8:00 and also around 20:00 until 23:00. These times corresponds to the daytime period at the site. The mesoscale model and CFD model have similar wind speed value range between 12:00 to 18:00 so, the CFD model cannot adequately simulate the local night time period. The time between 20:00 to 23:00 are periods when the wind speeds slowed down and it is noted that the mesoscale model suddenly increases in wind speeds at those times. In contrast, the CFD model is a better representation of the low wind speed events as can be seen in Figure 94.

For the wind direction shown in Figure 95, the CFD model is producing wind directions that are close to the wind direction generated by the mesoscale model. As with the case in Balabac Island, there is no change in simulation capability in terms of wind direction when microscale model is employed in determining the wind profile at the Guntao Islands site.

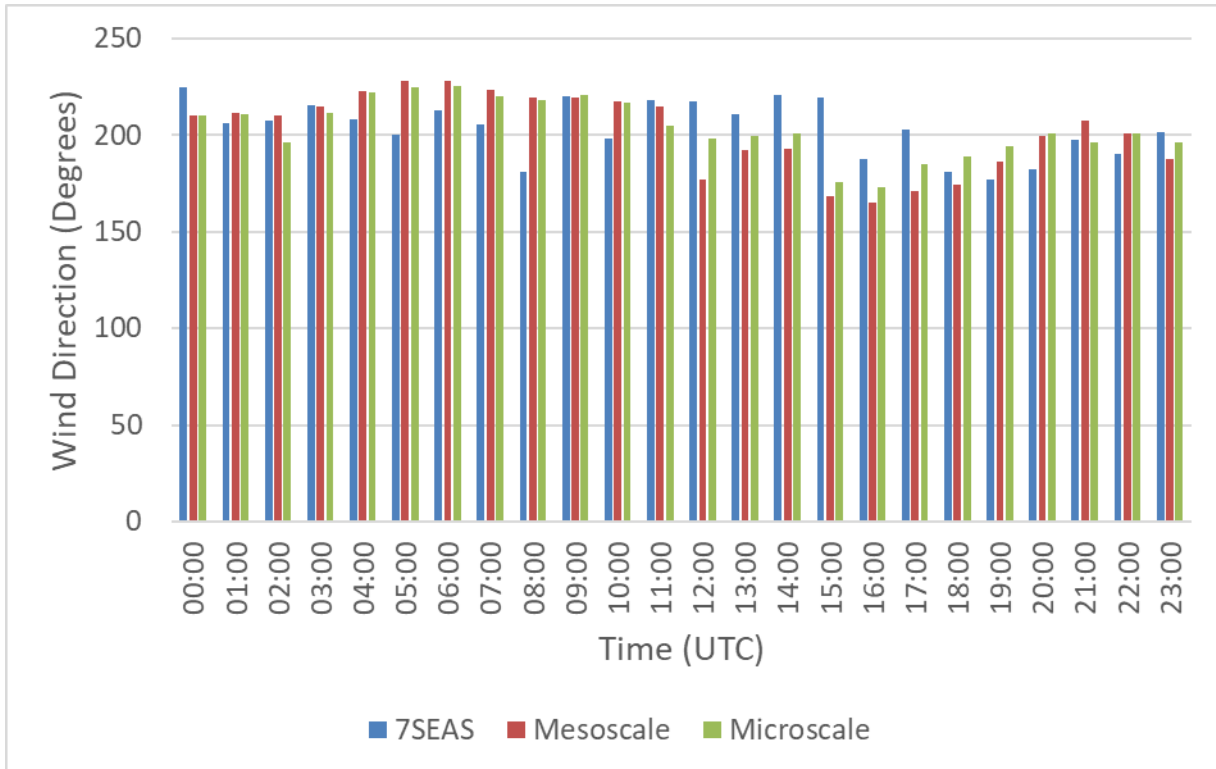


Figure 95. Comparison of mesoscale and microscale model wind direction results off the coast of Guntao Islands on 24 September 2011

The third site is near Notch Island and the wind speed simulation results are shown in Figure 96. Once again, the CFD model is able to simulate early morning local time, which corresponds to 16:00 to 23:00 and midnight to 5:00. The evening local time simulations of the CFD model at Notch Island is performing better than in Guntao Islands because the mesoscale model fares better within that period. This is indicative that the CFD model is still being driven by the mesoscale model results since it is the input data for the simulations. Looking at Figure 97, the wind directions are nearly identical for the mesoscale model and the CFD model. Thus, the CFD model is consistent with the mesoscale model since the point of observation is relatively flat and should follow the predominant wind direction of the mesoscale model.

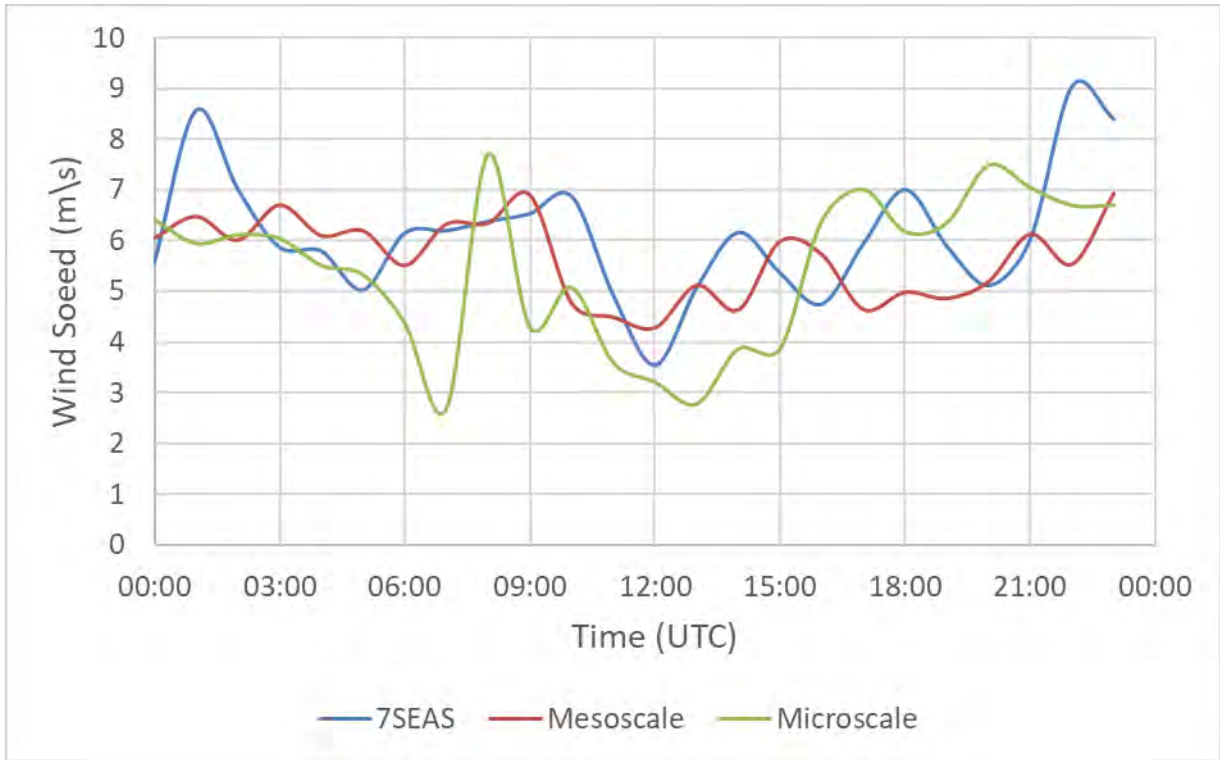


Figure 96. Comparison of mesoscale and microscale model wind speed results off the coast of Notch Island on 21 September 2011

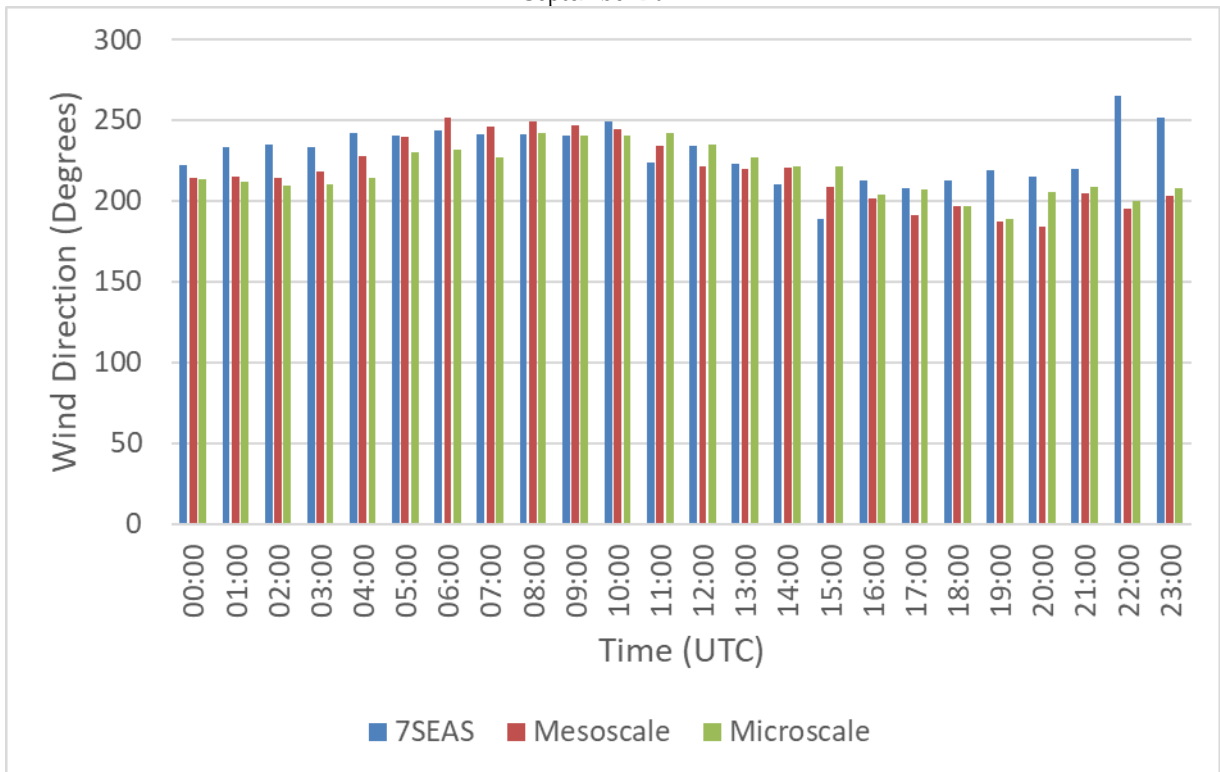


Figure 97. Comparison of mesoscale and microscale model wind direction results off the coast of Notch Island on 21 September 2011

The last site to be compared and validated is the one in Tubbataha Reef. This is an open water location that is approximated to be flat by the CFD model as well as the mesoscale model. The wind speed CFD model results are found in Figure 98 and the wind direction are shown in Figure 99.

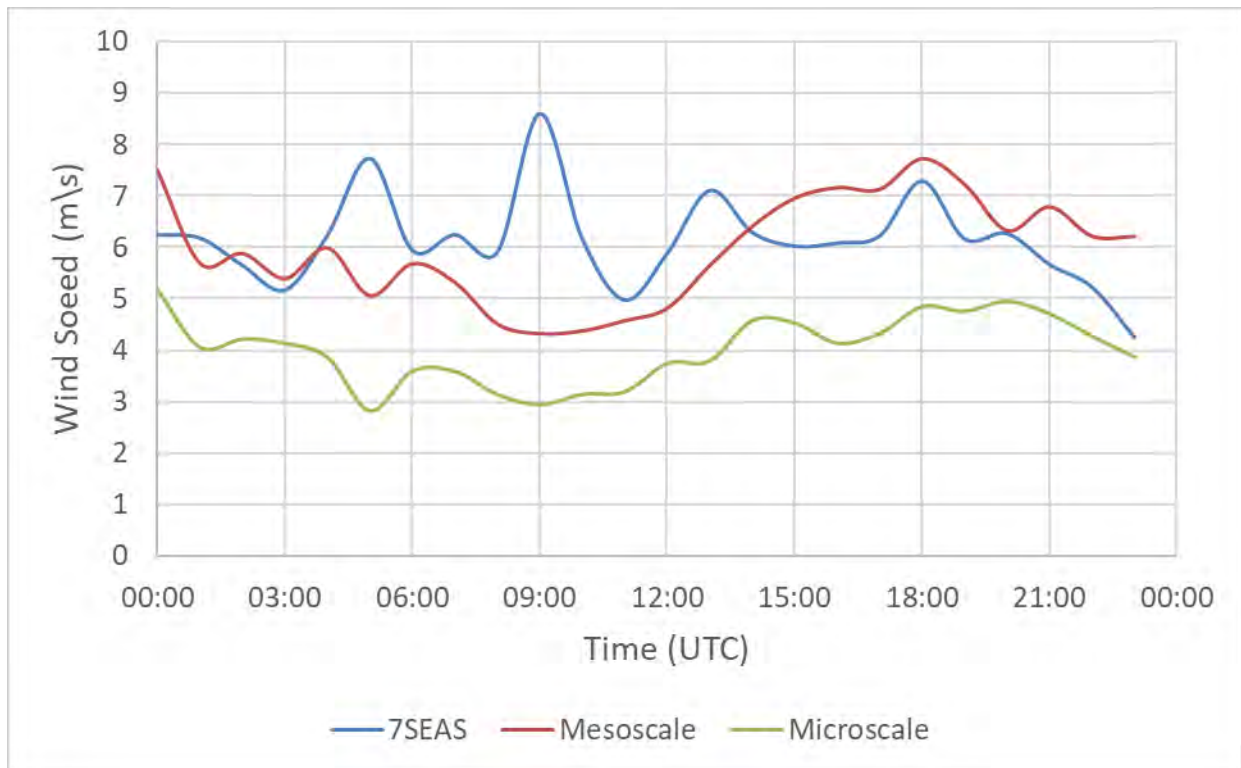


Figure 98. Comparison of mesoscale and microscale model wind speed results off the coast of Tubbataha Reef on 22 September 2012

Both the wind speeds and wind direction are giving the same wind patterns as the mesoscale model. This shows that flat terrains do not benefit from the fine resolution simulation capabilities of microscale model. This suggests that the mesoscale model suffices for flat terrain or open water regions. The wind speed results of the CFD model are lower once again than the mesoscale model output. This is a similar characteristic that has been observed in the CFD model results for Balabac Island. Thus, the mesoscale model has a better simulation results for flat terrain and offshore areas that are far from land. There is also no appreciable change in the wind direction when comparing the mesoscale model to the microscale model in Figure 99. It appears that the CFD model simply follows the wind direction from the mesoscale model input data since there are no topography features that can alter the wind flow in open waters.

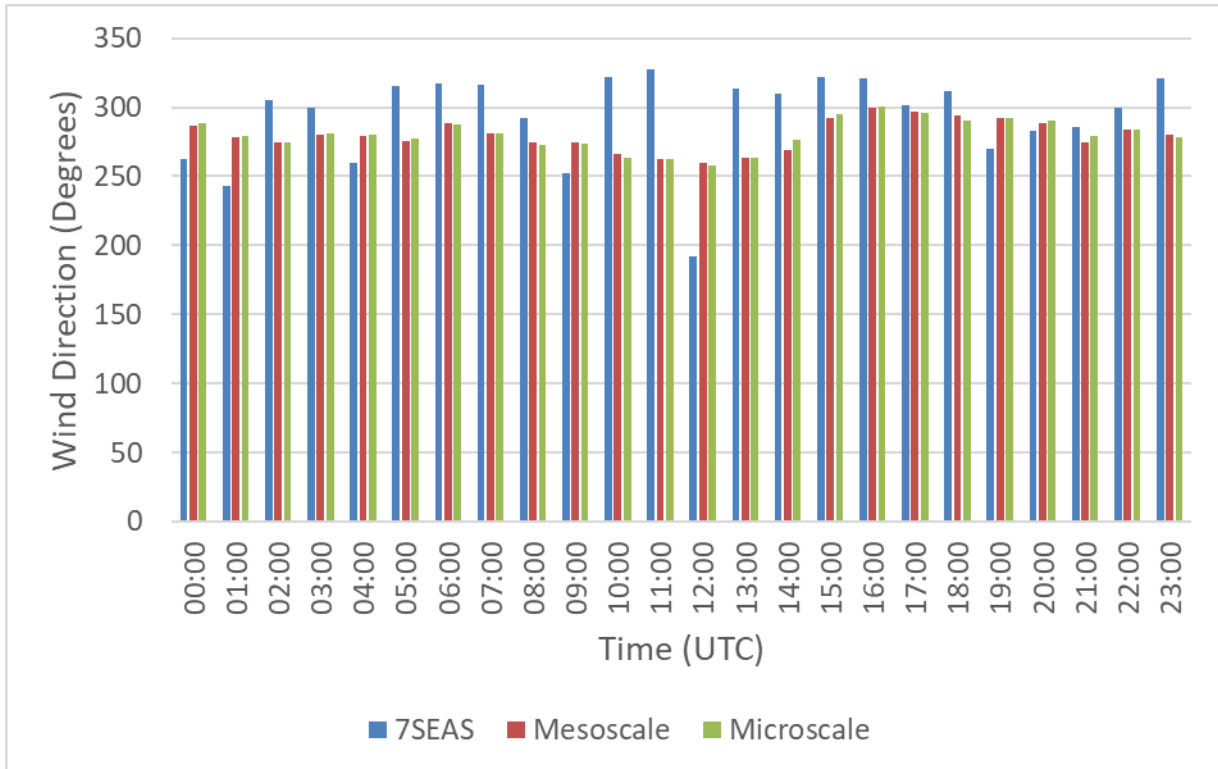


Figure 99. Comparison of mesoscale and microscale model wind direction results off the coast of Tubbataha Reef on 22 September 2012

The errors and bias of the CFD model simulations has also been quantified and compared with the corresponding values from the mesoscale model. The calculated values are listed in Table 34.

Table 34. Microscale Model Errors and Bias Quantification of Wind Speed and Wind Direction

Model		Mesoscale			Microscale		
		RMSE	Bias	STDE	RMSE	Bias	STDE
Balabac Island	Wind Speed	1.08	0.01	1.08	1.63	-1.26	1.03
	Wind Direction	52.38	11.63	51.08	51.62	9.59	50.73
Guntao Islands	Wind Speed	2.09	0.87	1.90	1.59	-1.00	1.24
	Wind Direction	21.71	-1.91	21.63	17.72	0.18	17.72
Notch Island	Wind Speed	1.26	-0.46	1.18	1.69	-0.68	1.54
	Wind Direction	22.67	-11.22	19.70	22.59	-11.14	19.65
Tubbataha Reef	Wind Speed	1.40	-0.18	1.39	2.44	-2.14	1.18
	Wind Direction	34.37	-13.56	31.58	34.14	-13.21	31.48

There are two characteristics that appears when the RMSE, bias, and STDE values of mesoscale model and microscale model are compared. The first one relates to the type of topography at the sites. Based on the results, Tubbataha Reef and Balabac Island are relatively flat terrain locations so the model performance in those areas are similar. It is found that the CFD model yields lower wind speed values in such simple terrains and thus, the error values and bias are also higher compared to the mesoscale model. For sites with small islands such as Guntao Islands and Notch Island, there is not much difference in the RMSE, bias, and STDE values between microscale and mesoscale models. But it must be pointed out that the low wind speed events are simulated better by CFD model while the higher

wind speeds are sufficiently modelled by the mesoscale model. Wind speeds below 4.4 m/s are compared in Table 35 in order to see that the microscale is yielding better wind speed values than the mesoscale for low wind speed conditions.

Table 35. Comparison of low wind speed results between observation, mesoscale, and microscale

Location \ Dataset	7SEAS	Mesoscale	% Error Mesoscale	Microscale	% Error Microscale
Balabac Island	4.08 m/s	5.82 m/s	29.90	4.43 m/s	7.90
	4.24 m/s	5.67 m/s	25.22	4.06 m/s	4.43
Guntao Islands	4.45 m/s	7.20 m/s	38.19	3.77 m/s	18.04
	3.25 m/s	4.88 m/s	33.40	4.94 m/s	34.21
	3.59 m/s	6.03 m/s	40.46	4.15 m/s	13.49
	3.62 m/s	6.73 m/s	46.21	2.71 m/s	33.58
Notch Island	3.54 m/s	4.28 m/s	17.29	3.21 m/s	10.28
Tubbataha Reef	4.25 m/s	6.22 m/s	31.67	3.86 m/s	10.10

The second characteristic is on the wind direction since there is a slight overall improvement in terms of RMSE, bias, and STDE with the CFD model in comparison to the mesoscale model. But these are not visible in the side by side comparison of wind direction of mesoscale and microscale models since the general wind profile in terms of direction almost the same.

5.6 Discussion

The simulation results using the mesoscale model has been analysed for each month from 2010 – 2012 in order to find seasonal patterns in the winds over the Palawan Province. The validation of the mesoscale model has shown that certain model configurations are appropriate for particular months of the year for both wind speed and wind direction. There are also settings that are suited for certain locations around the province. From the results, wind speeds that are 0 – 4 m/s are not being simulated well by the mesoscale model. This is consistent with the results of other studies that uses mesoscale modelling [18,20] and even studies that employs remote sensing methods with satellite data [121,127]. The limitation of the mesoscale model can be addressed by the microscale model which will be discussed in this section. The monthly suitability of the settings also show that a long-term seasonal pattern has been determined for the capability of the mesoscale model to produce wind profiles for the study area.

On seasonal and climate trends; reanalysis data, namely NCEP-CFS and ERA-Interim, are useful for long-term trend analysis for wind farm projects [174]. This has been found to be true in the wind speed validation of the Coron Island, Cuyo Island, and Puerto Princesa locations. The Southwest Monsoon, spanning May – September months, wind speeds are simulated best when the ERA-Interim settings are used in Coron and Cuyo islands. These are consistent with the findings of Dado and Takahashi [151] in their study for the Northwest region of the Philippines. Puerto Princesa wind speeds have been simulated suitably using the NCEP-CFS settings for the entire year as can be seen in Table

29 (Page 125). The Northeast Monsoon has also been adequately modelled using NCEP-CFS configurations for Cuyo Island. These results show that the configuration for the mesoscale model within the Palawan Province is sensitive in certain areas. It demonstrates that regions composed of different islands close to each other requires a particular model configuration that must be determined through validation. This is in contrast with previous studies that have contiguous land masses where a particular model configuration is used for all the months for the entire study domain such as Carvalho et al. [18] and Chancham, Waewsak, and Gagnon [114]. Thus, a unique wind profile for each island in an archipelago may exist and must be considered when studying such types of areas.

Concerning the wind direction, NCEP-FNL can be a good model setting for monthly wind direction averages because its purpose as an operational analysis data are for weather forecasting and diagnostics which are short-term events for the atmosphere [150]. This has proven to be correct by the Puerto Princesa validation since many months, listed in Table 30 (Page 136), at that location are suited to be modelled using NCEP-FNL for wind direction. These findings show that operational datasets must be considered for WRA purposes as there are sites that can be simulated better with operational datasets than reanalysis datasets. This is a significant result determined in this work because many studies [20,127,164] are focused on using reanalysis datasets only. This is another instance where wind simulations for an archipelagic domain may benefit from utilising a different dataset because of complexity in terrain [154] and meteorology [152] than large land masses. In Cuyo and Coron islands, the wind directions are determined best with the ERA-Interim configuration for multiple months of the year. The simulations have shown that the mesoscale model can represent the general wind flow over the Palawan Island. This is demonstrated by the ground based measurements from the PAGASA weather stations so, the outputs from the appropriate mesoscale model configuration can be extracted and generate wind maps.

In terms of location, the mesoscale model had difficulty in simulating the Coron and Cuyo Islands whereas the Puerto Princesa is being simulated adequately. Coron and Cuyo Islands are located within an area where there are many small islands surrounding them. In contrast, Puerto Princesa is located between a bay and the Sulu Sea. This show the difficulty of the mesoscale model in determining winds in groups of islands that are small and close to each other. Since the Puerto Princesa site is facing the open sea, the mesoscale model is able to simulate the wind conditions at that location.

Wind maps for Palawan Province are generated based on the mesoscale model results. This is possible because the coarse resolution domain of the model covers the entire province as presented in Chapter 3. The maps show that wind resource are abundant during the Northeast Monsoon for the Philippines. This is evident from Figure 38(a) and Figure 39(b) where January and September months

have high wind speeds over the region. Recall that January is the time when the Northeast Monsoon winds are strong and September is the transition period from Southwest Monsoon to Northeast Monsoon. Wind resource are moderately good during the Easterlies as shown in Figure 38(b) where April have winds that are adequate for wind power production. It is the Southwest Monsoon when the winds decrease in Palawan but there are certain areas where wind resource are still significantly high such as the area centred at 10°N, 118°E where winds are at least 5 m/s throughout the year. The decrease in wind speed down to 1 – 2 m/s during the Southwest Monsoon is characteristic of the topography of the Southeast Asian region where the winds coming from the Indian Ocean are being affected by the Indochina Peninsula before reaching the Palawan Province [154]. Even though the South China Sea has been determined to possess good offshore wind resource, it is necessary to determine the wind profile of Palawan that faces the South China Sea since there are areas that have poor wind resource during the Southwest Monsoon. The various maps of each month has shown that the Southwest Monsoon is a crucial point of time for the year when determining a good offshore wind farm site because of the overall low wind speed regime experienced in most of the province. These slow winds may cause insufficient wind resource for power production for the months of May to September but there are areas such as within the vicinity of 10°N, 118°E where wind speeds are sustained to be at least 5 m/s even in the Southwest Monsoon season. From the results, the winds are greatly affected by monsoons and must be considered when planning offshore wind projects as they determine the predominant wind flow direction in the region.

CFD model results has shown that there are little difference between the mesoscale model results and the microscale model output in terms of wind direction. This is because the locations near the shore of islands are relatively flat terrain so, topographical features that can influence local wind direction are absent. The Balabac Island wind speeds from the mesoscale model and CFD model have similar pattern. Results from the CFD model are found to be underestimating the wind speeds at the site. This behaviour also occurs in Tubbataha Reef which is the open water site for this study. Thus, Balabac Island is essentially an open water location that is not affected by land masses near it. This finding proves that mesoscale model results are sufficient for wind profiling in open water locations.

For the Notch Island and Guntao Islands, there is a difference between the mesoscale model and CFD model wind speed results. This presents that the site is influenced by nearby islands which affects the wind speeds. In these locations, the daytime period are simulated better by the CFD model compared to the mesoscale model. It has also been determined that low wind speed events are modelled better by the CFD model. It is important that the daytime period can be simulated adequately because it is during the day when energy is needed [25] thus a more accurate potential wind power production for the day period is more important when performing WRA than nighttime.

The ability of the microscale model to simulate the low wind speed regimes in complex terrain is a significant finding because this will be useful in addressing the limitation of mesoscale models where low wind speeds are overestimated. This can allow better wind profiles for areas with no or few wind observations because a better wind characterisation from a wider wind speed range can be represented by combining the mesoscale and microscale model results. The improvement is brought about the determination of low wind speed episodes that may arise in certain areas which will not be determined by the mesoscale model. Such accuracy for low wind speeds offered by the microscale model will enable more accurate wind profiles to be utilised for WRA.

Another area that mesoscale models are having difficulty in simulation are the coasts [20]. In fact, even satellite-based measurements cannot make accurate observations of winds close to the shoreline [121,127]. The approximation made by mesoscale models through smoothening of the terrain are definitely affecting its performance in such land-sea interface. This is especially a problem with Palawan Province where cliffs can be found near the shore. The microscale model is able to compensate this limitation as shown by the results in Notch Island and Guntao Islands. The wind speeds of the microscale model is no longer simply tracking the mesoscale model because of the complex terrain involved but the complex meteorology of land-sea interaction must be taken into account in order to improve the microscale model results.

Overall, the ERA-Interim mesoscale model configuration is the best input data for CFD wind simulations on coastal and open waters surrounding Palawan Island but a more extensive offshore observation is needed to make a better validation study and sensitivity test. The wind maps produced from the mesoscale-microscale model coupling method enables better site selection for intensive wind measurements for offshore wind farm projects. Upon consideration of the wind maps and model validation, these results suggest that the Balabac Island, Guntao Islands, Notch Island, and Tubbataha Reef have potential wind resource where offshore wind measurement campaigns can be deployed to build a better wind profile of the sites that can show the feasibility of offshore wind projects at these locations.

There is a potential onshore wind resource at Palawan Province as it was shown in a prior study for the Philippines [16]. This work extends that WRA by investigating the surrounding waters in the province. With the WRA technique, this study has shown that the waters around Palawan are indeed good sites for wind energy development. This is found to be in agreement with the other research in the South China Sea from various countries [98,101,102,118]. The study has also determined that the Sulu Sea has potential for offshore wind project development but an intensive wind profile study in the area is advised.

The method presented in this study has demonstrated that in the absence of in-situ data, the technique can be used for WRA at offshore locations around Palawan Province. This technique involves using mesoscale models to simulate wind speeds that coincides with long-term onshore observations. It is necessary in order to validate the results and characterise the wind profiles according to monthly and seasonal periods. This will allow the identification of sites because the seasonal variabilities within the domain can be determined [174]. These variabilities will guide the site selection because the locations with consistent winds can be known that will merit further investigation in terms of wind profiles.

A better wind profile for the selected locations deemed to have potential for offshore wind development can be known through the use of microscale models. The microscale model has the capacity to incorporate high resolution digital elevation maps which is important for complex terrain such as the cliffs near the coasts of Palawan. As it has been known that tropical meteorology is complex [152], high spatial resolution of microscale model can offer better wind model results provided that local atmospheric dynamics such as land-sea interaction are incorporated well into the model. Using the mesoscale model results as input data for the microscale model has shown that it is not sufficient for open waters and high wind conditions to improve the wind simulation results. Thus, a long-term offshore wind observation could improve the microscale model output or an improved, new generation, and high resolution input dataset to the mesoscale model can produce a better output. This output can in turn allow the microscale to produce an improved wind profile since a better meteorology of the local vicinity is incorporated in the simulations.

5.7 Summary

The model results found that model configuration for wind speed and wind direction can differ. It is also found that certain locations can vary in the appropriate configuration for simulation depending on the time of the year. Thus, the model settings are to be changed in accordance to the seasons that govern the winds in the Philippines. These seasons are known as the Northeast Monsoon, Easterlies, and Southwest Monsoons. Northeast Monsoon begins in September and ends in March which is characterised by strong winds, cold temperature, and dry spells. Easterlies occurs in April and May which brings hot and dry weather in the Philippines and the winds are coming from the Pacific Ocean. Southwest Monsoon is the time when hot, humid, and wet weather blankets the country and winds are weaker during these times. For brevity, each configuration will be referred by the corresponding input data utilised for the simulation as explained in Chapter 3.

Comparing the mesoscale model results with the PAGASA data, it is found that Coron and Cuyo islands wind speeds are adequately simulated using the ERA-Interim configuration during the

Southwest Monsoon. The Coron Island wind speeds can be modelled by a particular configuration depending on the month during Northeast Monsoon and by NCEP-FNL during the Easterlies as discussed in Chapter 5. Wind speeds over Cuyo Island are simulated well with the NCEP-CFS model settings during the period when the Northeast Monsoon intensifies. Puerto Princesa wind speeds are determined to be capably modelled by the NCEP-CFS for the whole year. Regarding the wind direction, ERA-Interim configuration is still found to be sufficient for simulating Coron and Cuyo islands during the Southwest Monsoon. For other times of the year, a particular configuration is appropriate for a corresponding month in Coron and Cuyo as listed in Table 25. The same is true for Puerto Princesa's wind direction but it is notable that many months are being modelled well with NCEP-FNL settings.

Wind maps with a spatial resolution of 3km x 3km can be generated from the mesoscale model results. These maps show that Palawan Province have good offshore wind resource during the Northeast Monsoon because of the strong winds during that season. Winds speeds decreases when the Easterlies sets in but these are still satisfactory wind conditions for offshore wind farms. During the Southwest Monsoon, the wind speeds decreases drastically but there are areas at the west of Palawan centred at 10°N, 118°E where the winds can reach 12 m/s. The area have a minimum of 5 m/s wind speeds throughout the year so, this is an area that can be further studied by deploying offshore wind observation platforms to further determine the wind profile of the area as a potential development project for offshore wind farms.

From the validations with 7SEAS wind data, it has been found that the output from NCEP-CFS configuration is appropriate for Balabac Island and ERA-Interim are deemed to be suitable for Guntao Islands, Notch Island, and Tubbataha Reef. These has been discussed in Chapter 5 and have been used as input data for the CFD model. The results from the CFD model has demonstrated that Balabac Island and Tubbataha Reef have similar results. The CFD model is tracking the wind speed profile of the mesoscale model but with lower values. There is also no significant difference between the wind direction model outputs between the mesoscale model and microscale model. The similarity between the two sites show that the Balabac Island observation point is similar to open water locations such as the Tubbataha Reef which are essentially flat terrains. Since the output of the mesoscale model are better than the CFD model, the use of microscale model in open waters is not necessary because the wind profiles obtained from mesoscale models are sufficient. The observation points near Guntao Islands and Notch Island show an improvement for the CFD model in wind speed results compared to the mesoscale model during day time period and low wind speed events. This shows that in areas where neighbouring islands can influence the wind profiles near the shore, the CFD model offers better wind simulation results. In terms of the CFD model performance in determining the wind

direction, there is no change that can be seen between the mesoscale model and CFD model but a marginal improvement for the CFD model appears from the calculation of RMSE, bias, and STDE values. This similarity in wind direction suggests that there are no significant terrain features at the observation point that can redirect winds because it is located at coastal waters which is considered flat in the model.

6 CONCLUSION

In this last chapter, the relevant research outcomes will be presented and how these contributes to the body of knowledge on wind characterisation for wind energy development applications. Suggestions in continuing this research will also be discussed in the last section.

6.1 Research Outputs

This work sought to find an appropriate offshore WRA method for areas in the low latitude and small island locations because it would be beneficial for these places to develop offshore wind farm projects for their energy needs. In the low latitude, there are limited data available that can be used to produce wind maps for WRA. In studying the literature, it has been determined that NWP is a viable option when data is scarce which has been discussed in Chapter 2.

High resolution wind maps with long time scales are necessary for WRA so that locating areas with good wind resource can be more accurate and precise as well as find the seasonal wind patterns. The wind maps from the mesoscale model are at 3km x 3km resolution and covers the years of 2010 to 2012 which can be found in Figure 38 and Figure 39. These would be enough to find the areas where good wind resource are available and the three-year period analysed allowed the identification of the seasonal patterns when wind speeds are high.

Coastal regions are found to be troublesome to be simulated by mesoscale model or even observed by satellites. This study incorporated the use of CFD models to remedy this limitation so that a better wind profile for coastal areas can be achieved. Near-shore locations or coastal areas are of interest especially for developing countries because these sites are less expensive in cost and maintenance when compared to offshore wind farms situated far from the shoreline. The utility of CFD models in compensating the overestimated wind speeds from mesoscale models in sites where multiple islands are present have been demonstrated in Chapter 5.

A method for performing WRA for low latitude regions of the planet and small island nations has been developed by studying the Palawan Province in the Philippines. The entire process of data gathering and tidying, model configuration, model validation, and wind map generation have been discussed in Chapter 3 and Chapter 4. These will serve as a guide in performing initial offshore WRA for other locations in the low latitude.

Thus, the relevant findings from these study are as follows:

- WRA can be performed for low latitude regions and small island nations even with limited data availability by using NWP based on the literature.
- Long-term wind maps can be generated from mesoscale model results to locate potential wind development sites and determine the seasonal wind characteristics for further wind profiling studies.
- Microscale model can complement the mesoscale model by addressing the limitation of mesoscale models with regards to low wind speed overestimations and land-sea interaction in coastal areas.
- The method used in this research can be employed for initial WRA in low latitudes and small islands.

6.2 Contribution to Knowledge

This research aimed to find an offshore WRA method that may be adapted to low latitude regions of the world and small islands. It has found that NWP is an available tool for the purpose but there are multiple model settings that must be determined before using it to produce wind profiles that can be used for wind maps. In the course of the simulations and model validations, it has been found that there are seasons or particular months that are modelled better by a corresponding model configuration. These results are summarised in Table 24, 25, and 27. Previous studies [18,144,164] would only focus on a single configuration that the authors deem to be the best one for their study area. It is also common in the literature [20,113,127] to use reanalysis datasets for WRA but operational datasets such as NCEP-FNL that was used in this work should be considered since there are certain months where using it as input data for the mesoscale model yields the best performing simulations. The research has shown that coupling mesoscale model with microscale model will improve wind speed simulations for low wind speed conditions at areas near the coasts. This demonstrates that CFD model are useful and beneficial for characterising wind patterns in coastal areas and not just for onshore and complex terrains [136,143]. The combination of the mesoscale and microscale model can yield better wind profiles for sites close to shorelines and should allow for better accuracy and precision in determining locations that are good for offshore wind development projects. This will allow feasibility studies to be made on offshore locations and enable better decisions regarding proposed offshore wind projects in the low latitudes.

6.3 Recommendations for Future Work

The simulation results can be improved by using the next generation reanalysis data such as ERA-5 because these have higher spatial and temporal resolutions that can allow the mesoscale model to produce fine scale outputs. Since the CFD model is dependent on the data quality coming from the mesoscale model, it will also produce better wind simulation results. The simulation results can also be validated with satellite measurements to enable a wider area of comparison in addition to the point measurements from weather stations or campaigns. Complex meteorology must be incorporated into the microscale model in order to gain a better understanding of wind conditions in the coastlines. The dynamics of land-sea interaction should be included so that an improved wind simulation can be achieved. Wind characterisation of coastal areas are essential as it offers an alternative that has low surface roughness as open seas but at a less expensive cost because it would not be located in deep waters. These type of wind farms are called intertidal and such a project is at the construction phase in Vietnam [65]. A decision support system can also be implemented with the wind simulations in order to develop a platform that can aid in the decision-making of offshore wind energy projects.

References

- [1] Van Kooten GC, Wong L. Economics of wind power when national grids are unreliable. *Energy Policy* 2010;38:1991–8. doi:10.1016/j.enpol.2009.11.080.
- [2] Chang Y, Li Y. Renewable energy and policy options in an integrated ASEAN electricity market: Quantitative assessments and policy implications. *Energy Policy* 2015;85:39–49. doi:10.1016/j.enpol.2015.05.011.
- [3] World Bank. *The World by Income*. World Bank Database 2017:1.
- [4] Pickard M. Global investment in renewable energy projects: How the whole world is jumping on the renewables bandwagon. *Renew Energy Focus* 2016;17:229–30. doi:10.1016/j.ref.2016.10.008.
- [5] Henderson AR, Morgan C, Smith B, Sørensen HC, Barthelmie RJ, Boesmans B. Offshore wind energy in Europe - A review of the state-of-the-art. *Wind Energy* 2003. doi:10.1002/we.82.
- [6] Butterfield S, Musial W, Jonkman J, Sclavounos PD. Engineering challenges for floating offshore wind turbines. *Copenhagen Offshore Wind 2005 Conf Exped Proc* 2005.
- [7] Perveen R, Kishor N, Mohanty SR. Off-shore wind farm development: Present status and challenges. *Renew Sustain Energy Rev* 2014;29:780–92. doi:10.1016/j.rser.2013.08.108.
- [8] Sun X, Huang D, Wu G. The current state of offshore wind energy technology development. *Energy* 2012;41:298–312. doi:10.1016/j.energy.2012.02.054.
- [9] Snyder B, Kaiser MJ. Ecological and economic cost-benefit analysis of offshore wind energy. *Renew Energy* 2009. doi:10.1016/j.renene.2008.11.015.
- [10] Archer CL, Colle BA, Delle Monache L, Dvorak MJ, Lundquist J, Bailey BH, et al. Meteorology for coastal/offshore wind energy in the United States: Recommendations and research needs for the next 10 years. *Bull Am Meteorol Soc* 2014;95:515–9. doi:10.1175/BAMS-D-13-00108.1.
- [11] Jain P, Calcetas PP, An B. *Guidelines for Wind Resource Assessment: Best Practices for Countries Initiating Wind Development*. 2014.
- [12] Warudkar V, Ahmed S. Wind Resource Assessment. *Int J Mining, Metall Mech Eng* 2013;1:204–7.
- [13] Murthy KSR, Rahi OP. A comprehensive review of wind resource assessment. *Renew Sustain Energy Rev* 2016;72:0–1. doi:10.1016/j.rser.2016.10.038.
- [14] Niyomtham L, Lertsathittanakorn C, Waewsak J, Gagnon Y. On the Wind Resource Assessment along the Western Coast of Thailand. *Energy Procedia* 2017;138:1190–5. doi:10.1016/j.egypro.2017.10.387.
- [15] Liu Y, Chen D, Yi Q, Li S. Wind profiles and wave spectra for potential wind farms in South China Sea. Part I: Wind speed profile model. *Energies* 2017;10. doi:10.3390/en10010125.
- [16] Elliott D. *Philippines Wind Energy Resource Atlas Development*. Bus. Invest. Forum Renew. Energy Energy Effic. Asia Pacific Reg., Kuala Lumpur: 2000, p. 1–10.
- [17] Kaldellis JK, Apostolou D, Kapsali M, Kondili E. Environmental and social footprint of offshore wind energy. Comparison with onshore counterpart. *Renew Energy* 2016;92:543–56. doi:10.1016/j.renene.2016.02.018.
- [18] Carvalho D, Rocha A, Gómez-Gesteira M, Silva Santos C. Offshore winds and wind energy

- production estimates derived from ASCAT, OSCAT, numerical weather prediction models and buoys - A comparative study for the Iberian Peninsula Atlantic coast. *Renew Energy* 2017;102:433–44. doi:10.1016/j.renene.2016.10.063.
- [19] Gasset N, Landry M, Gagnon Y. A comparison of wind flow models for wind resource assessment in wind energy applications. *Energies* 2012. doi:10.3390/en5114288.
- [20] Carvalho D, Rocha A, Gómez-Gesteira M. Ocean surface wind simulation forced by different reanalyses: Comparison with observed data along the Iberian Peninsula coast. *Ocean Model* 2012;56:31–42. doi:10.1016/j.ocemod.2012.08.002.
- [21] Rusu E, Onea F. Joint evaluation of the wave and offshore wind energy resources in the developing countries. *Energies* 2017;10. doi:10.3390/en10111866.
- [22] Kahraman C, Kaya I, Cebi S. A comparative analysis for multiattribute selection among renewable energy alternatives using fuzzy axiomatic design and fuzzy analytic hierarchy process. *Energy* 2009;34:1603–16. doi:10.1016/j.energy.2009.07.008.
- [23] Breeze P. *Power Generation Technologies*, 2nd ed. Elsevier Ltd.; 2014.
- [24] Tran TTD, Smith AD. Evaluation of renewable energy technologies and their potential for technical integration and cost-effective use within the U.S. energy sector. *Renew Sustain Energy Rev* 2017;80:1372–88. doi:10.1016/j.rser.2017.05.228.
- [25] Diesendorf M, Elliston B. The feasibility of 100 % renewable electricity systems : A response to critics ☆. *Renew Sustain Energy Rev* 2018;93:318–30. doi:10.1016/j.rser.2018.05.042.
- [26] Olea M. Sustainable technologies to fuel the future. *Renew Energy Focus* 2016;17:221–2. doi:10.1016/j.ref.2016.10.004.
- [27] Jacobson MZ, Delucchi MA. Providing all global energy with wind, water, and solar power, Part I: Technologies, energy resources, quantities and areas of infrastructure, and materials. *Energy Policy* 2011;39:1154–69. doi:10.1016/j.enpol.2010.11.040.
- [28] Jacobson MZ, Delucchi MA, Bauer ZAF, Goodman SC, Chapman WE, Cameron MA, et al. 100% Clean and Renewable Wind, Water, and Sunlight All-Sector Energy Roadmaps for 139 Countries of the World. *Joule* 2017;1:108–21. doi:10.1016/j.joule.2017.07.005.
- [29] Armin Razmjoo A, Sumper A, Davarpanah A. Energy sustainability analysis based on SDGs for developing countries. *Energy Sources, Part A Recover Util Environ Eff* 2019;0:1–16. doi:10.1080/15567036.2019.1602215.
- [30] Lund PD. Effects of energy policies on industry expansion in renewable energy. *Renew Energy* 2009. doi:10.1016/j.renene.2008.03.018.
- [31] Hasan MH, Mahlia TMI, Nur H. A review on energy scenario and sustainable energy in Indonesia. *Renew Sustain Energy Rev* 2012;16:2316–28. doi:10.1016/j.rser.2011.12.007.
- [32] State of Green. *WIND ENERGY How wind energy has changed the Danish energy system* 2017.
- [33] Dent CM. Wind energy development in East Asia and Europe. *Asia Eur J* 2013;11:211–30. doi:10.1007/s10308-013-0360-8.
- [34] Manwell JF, McGowan JG, Rogers AL. *Wind Energy Explained: Theory, Design, and Application* 2nd edition. John Wiley and Sons Ltd.; 2009.
- [35] Ackermann T, Söder L. An overview of wind energy-status 2002. *Renew Sustain Energy Rev* 2002. doi:10.1016/S1364-0321(02)00008-4.

- [36] Hansen AD, Iov F, Blaabjerg F, Hansen LH. Review of Wind Turbine Concepts and their Market Penetration. *Wind Eng* 2004;28:247–63.
- [37] Joselin Herbert GM, Iniyar S, Sreevalsan E, Rajapandian S. A review of wind energy technologies. *Renew Sustain Energy Rev* 2007. doi:10.1016/j.rser.2005.08.004.
- [38] Blanco MI. Economics_Wind_Energy. *Renew Sustain Energy Rev* 2009;13:1372–82.
- [39] Ko DH, Jeong ST, Kim YC. Assessment of wind energy for small-scale wind power in Chuuk State, Micronesia. *Renew Sustain Energy Rev* 2015;52:613–22. doi:10.1016/j.rser.2015.07.160.
- [40] Ritter M, Deckert L. Site assessment, turbine selection, and local feed-in tariffs through the wind energy index. *Appl Energy* 2015;185:1087–99. doi:10.1016/j.apenergy.2015.11.081.
- [41] Ren D. Effects of global warming on wind energy availability. *J Renew Sustain Energy* 2010;2:1–5.
- [42] Zheng C, Li C, Gao C, Liu M. A seasonal grade division of the global offshore wind energy resource. *Acta Oceanol Sin* 2017;36:109–14. doi:10.1007/s13131-017-1043-x.
- [43] Zheng CW, Pan J, Li CY. Global oceanic wind speed trends. *Ocean Coast Manag* 2016;129:15–24. doi:10.1016/j.ocecoaman.2016.05.001.
- [44] Sasaki W. Predictability of global offshore wind and wave power. *Int J Mar Energy* 2017;17:98–109. doi:10.1016/j.ijome.2017.01.003.
- [45] National Aeronautics and Space Agency (NASA). Ocean Wind Power Maps Reveal Possible Wind Energy Sources 2008. https://www.nasa.gov/images/content/258137main_glb-sumwin-press.jpg (accessed March 26, 2018).
- [46] Jiang H, Chen G. A global view on the swell and wind sea climate by the Jason-1 mission: A revisit. *J Atmos Ocean Technol* 2013;30:1833–41. doi:10.1175/JTECH-D-12-00180.1.
- [47] Atlas R, Hoffman RN, Ardizzone J, Leidner SM, Jusem JC, Smith DK, et al. A cross-calibrated, multiplatform ocean surface wind velocity product for meteorological and oceanographic applications. *Bull Am Meteorol Soc* 2011;92:157–74. doi:10.1175/2010BAMS2946.1.
- [48] Zheng CW, Pan J. Assessment of the global ocean wind energy resource. *Renew Sustain Energy Rev* 2014;33:382–91. doi:10.1016/j.rser.2014.01.065.
- [49] Eureka K, Sullivan P, Gleason M, Hettinger D, Heimiller D, Lopez A. An improved global wind resource estimate for integrated assessment models. *Energy Econ* 2017;64:552–67. doi:10.1016/j.eneco.2016.11.015.
- [50] Torralba V, Doblas-Reyes FJ, MacLeod D, Christel I, Davis M. Seasonal climate prediction: A new source of information for the management of wind energy resources. *J Appl Meteorol Climatol* 2017;56:1231–47. doi:10.1175/JAMC-D-16-0204.1.
- [51] Magar V, Gross MS. Offshore wind energy resource assessment under techno-economic and social-ecological constraints. *Ocean Coast Manag* 2018;152. doi:10.1016/j.ocecoaman.2017.10.007.
- [52] Zheng CW, Li CY, Pan J, Liu MY, Xia LL. An overview of global ocean wind energy resource evaluations. *Renew Sustain Energy Rev* 2016;53:1240–51. doi:10.1016/j.rser.2015.09.063.
- [53] Zheng C, Xiao Z, Peng Y, Li C, Du Z. Rezoning global offshore wind energy resources. *Renew Energy* 2018;129:1–11. doi:10.1016/j.renene.2018.05.090.

- [54] Zountouridou EI, Kiokes GC, Chakalis S, Georgilakis PS, Hatziargyriou ND. Offshore floating wind parks in the deep waters of Mediterranean Sea. *Renew Sustain Energy Rev* 2015;51:433–48. doi:10.1016/j.rser.2015.06.027.
- [55] Remy T, Mbistrova A, Pineda I. *Offshore Wind in Europe: Key Trends and Statistics 2017*. Brussels: 2018.
- [56] Schweizer J, Antonini A, Govoni L, Gottardi G, Archetti R, Supino E, et al. Investigating the potential and feasibility of an offshore wind farm in the Northern Adriatic Sea. *Appl Energy* 2016;177:449–63. doi:10.1016/j.apenergy.2016.05.114.
- [57] Soukissian T, Karathanasi F, Axaopoulos P. Satellite-Based Offshore Wind Resource Assessment in the Mediterranean Sea. *IEEE J Ocean Eng* 2016;42:73–86. doi:10.1109/JOE.2016.2565018.
- [58] Castro-Santos L, Diaz-Casas V. Life-cycle cost analysis of floating offshore wind farms. *Renew Energy* 2014;66:41–8. doi:10.1016/j.renene.2013.12.002.
- [59] Castro-Santos L, Diaz-Casas V. Economic influence of location in floating offshore wind farms. *Ocean Eng* 2015;107:13–22. doi:10.1016/j.oceaneng.2015.07.025.
- [60] Castro-Santos L, Diaz-Casas V. Sensitivity analysis of floating offshore wind farms. *Energy Convers Manag* 2015;101:271–7. doi:10.1016/j.enconman.2015.05.032.
- [61] Castro-Santos L. Decision variables for floating offshore wind farms based on life-cycle cost: The case study of Galicia (North-West of Spain). *Ocean Eng* 2016;127:114–23. doi:10.1016/j.oceaneng.2016.10.010.
- [62] Borthwick AGL. Marine Renewable Energy Seascape. *Engineering* 2016;2:69–78. doi:10.1016/J.ENG.2016.01.011.
- [63] Rodrigues S, Restrepo C, Kontos E, Teixeira Pinto R, Bauer P. Trends of offshore wind projects. *Renew Sustain Energy Rev* 2015;49:1114–35. doi:10.1016/j.rser.2015.04.092.
- [64] Onea F, Rusu E. Efficiency assessments for some state of the art wind turbines in the coastal environments of the Black and the Caspian seas. *Energy Explor Exploit* 2016;34:217–24. doi:10.1177/0144598716629872.
- [65] Global Offshore Wind 2016 Report n.d.:58–65. <http://www.gwec.net/wp-content/uploads/2017/05/Global-Offshore-2016-and-Beyond.pdf> (accessed March 12, 2018).
- [66] Geuss M. Massachusetts offshore wind project gets green light at roughly 8.9 cents/kWh. *Ars Tech* 2019. <https://arstechnica.com/tech-policy/2019/04/massachusetts-offshore-wind-project-gets-green-light-at-roughly-8-9-centskwh/> (accessed April 28, 2019).
- [67] Adelaja A, McKeown C, Calnin B, Hailu Y. Assessing offshore wind potential. *Energy Policy* 2012;42:191–200. doi:10.1016/j.enpol.2011.11.072.
- [68] Esteban M, Leary D. Current developments and future prospects of offshore wind and ocean energy. *Appl Energy* 2012;90:128–36. doi:10.1016/j.apenergy.2011.06.011.
- [69] Tsai YC, Huang YF, Yang JT. Strategies for the development of offshore wind technology for far-east countries - A point of view from patent analysis. *Renew Sustain Energy Rev* 2016;60:182–94. doi:10.1016/j.rser.2016.01.102.
- [70] Beiter P, Spitsen P, Nunemaker J, Tian T, Musial W, Lantz E, et al. *2017 Offshore Wind Technologies Market Update*. Alexandria: 2018.

- [71] Kao S, Pearre NS. Administrative arrangement for offshore wind power developments in Taiwan : Challenges and prospects 2017;109:463–72. doi:10.1016/j.enpol.2017.07.027.
- [72] Sawin JL, Rutovitz J, Sverrisson F, Mastny L, Arris L. Renewables 2018 Global status report. Paris: 2018.
- [73] Hou P, Enevoldsen P, Hu W, Chen C, Chen Z. Offshore wind farm repowering optimization. Appl Energy 2017;208:834–44. doi:10.1016/j.apenergy.2017.09.064.
- [74] Gonzalez-Rodriguez AG. Review of offshore wind farm cost components. Energy Sustain Dev 2017;37:10–9. doi:10.1016/j.esd.2016.12.001.
- [75] Tseng Y-C, Lee Y-M, Liao S-J. An Integrated Assessment Framework of Offshore Wind Power Projects Applying Equator Principles and Social Life Cycle Assessment. Sustainability 2017;9:1822. doi:10.3390/su9101822.
- [76] Oh K-Y, Kim J-Y, Lee J-K, Ryu M-S, Lee J-S. An assessment of wind energy potential at the demonstration offshore wind farm in Korea. Energy 2012;46:555–63. doi:10.1016/j.energy.2012.07.056.
- [77] World Bank. The World by Income. World Bank Database 2017:1. <http://databank.worldbank.org/data/download/site-content/wdi/maps/2017/world-by-income-wdi-2017.pdf> (accessed August 10, 2018).
- [78] Arent D, Sullivan P, Heimiller D, Lopez A, Eureka K, Badger J, et al. Improved Offshore Wind Resource Assessment in Global Climate Stabilization Scenarios 2012. doi:10.2172/1055364.
- [79] Zhang H-M, Reynolds RW, Bates JJ. Blended and Gridded High Resolution Global Sea Surface Wind Speed and Climatology from Multiple Satellites: 1987 - Present. Am. Meteorol. Soc. 2006 Annu. Meet., 2006.
- [80] Gaiser PW, St. Germain KM, Twarog EM, Poe GA, Purdy W, Richardson D, et al. The windSat spaceborne polarimetric microwave radiometer: Sensor description and early orbit performance. IEEE Trans Geosci Remote Sens 2004;42:2347–61. doi:10.1109/TGRS.2004.836867.
- [81] Meissner T, Wentz F. Ocean retrievals for WindSat: Radiative transfer model, algorithm, validation. Int Geosci Remote Sens Symp 2005;7:4761–4. doi:10.1109/IGARSS.2005.1526736.
- [82] Hasager CB, Mouche A, Badger M, Bingöl F, Karagali I, Driesenaar T, et al. Offshore wind climatology based on synergetic use of Envisat ASAR , ASCAT and QuikSCAT. Remote Sens Environ 2015;156:247–63. doi:10.1016/j.rse.2014.09.030.
- [83] Pimenta F, Kempton W, Garvine R. Combining meteorological stations and satellite data to evaluate the offshore wind power resource of Southeastern Brazil. Renew Energy 2008;33:2375–87. doi:10.1016/j.renene.2008.01.012.
- [84] Ortiz G, Kampel M. Potencial de energia eólica offshore na margem do Brasil. Inst Nac Pesqui Espac 2011. doi:http://mtc-m16d.sid.inpe.br/col/sid.inpe.br/mtc-m19/2011/07.06.17.10/doc/Ortiz_Potencial.pdf.
- [85] Lima DKS, Leão RPS, dos Santos ACS, de Melo FDC, Couto VM, de Noronha AWT, et al. Estimating the offshore wind resources of the State of Ceará in Brazil. Renew Energy 2015;83:203–21. doi:10.1016/j.renene.2015.04.025.
- [86] Soler-Bientz R, Watson S, Infield D, Ricalde-Cab L. Preliminary study of the offshore wind and temperature profiles at the North of the Yucatán Peninsula. Energy Convers Manag 2011;52:2829–43. doi:10.1016/j.enconman.2011.02.024.

- [87] Elahee MK. Sustainable energy policy for small-island developing state : Mauritius. *Util Policy* 2011;19:71–9. doi:10.1016/j.jup.2010.08.004.
- [88] Khoodaruth A, Oree V, Elahee MK, Clark WW. Exploring options for a 100% renewable energy system in Mauritius by 2050. *Util Policy* 2017;44:38–49. doi:10.1016/j.jup.2016.12.001.
- [89] Offshore Wind Energy - Mauritius Has the Potential to Set Up Offshore Wind Farms. *All Africa* 2016.
- [90] Bundhoo ZMA. Renewable energy exploitation in the small island developing state of Mauritius : Current practice and future potential. *Renew Sustain Energy Rev* 2018;82:2029–38. doi:10.1016/j.rser.2017.07.019.
- [91] Effiom SO, Nwankwojike BN, Abam FI. Economic cost evaluation on the viability of offshore wind turbine farms in Nigeria. *Energy Reports* 2016;2:48–53. doi:10.1016/j.egy.2016.03.001.
- [92] Olaofe ZO. Review of energy systems deployment and development of offshore wind energy resource map at the coastal regions of Africa Electric Supply Company of Malawi. *Energy* 2018;161:1096–114. doi:10.1016/j.energy.2018.07.185.
- [93] Nagababu G, Kachhwaha SS, Naidu NK, Savsani V. Application of reanalysis data to estimate offshore wind potential in EEZ of India based on marine ecosystem considerations. *Energy* 2017;118:622–31. doi:10.1016/j.energy.2016.10.097.
- [94] Kulkarni S, Deo MC, Ghosh S. Performance of the CORDEX regional climate models in simulating offshore wind and wind potential. *Theor Appl Climatol* 2018:1–16. doi:10.1007/s00704-018-2401-0.
- [95] Mani S, Dhingra T. Offshore wind energy policy for India-Key factors to be considered. *Energy Policy* 2013;56:672–83. doi:10.1016/j.enpol.2013.01.031.
- [96] Kota S, Bayne SB, Nimmagadda S. Offshore wind energy: A comparative analysis of UK, USA and India. *Renew Sustain Energy Rev* 2015;41:685–94. doi:10.1016/j.rser.2014.08.080.
- [97] Contestabile P, Di Lauro E, Galli P, Corselli C, Vicinanza D. Offshore wind and wave energy assessment around malè and Magoodhoo Island (Maldives). *Sustain* 2017;9. doi:10.3390/su9040613.
- [98] Chang R, Zhu R, Badger M, Hasager CB, Xing X, Jiang Y. Offshore wind resources assessment from multiple satellite data and WRF modeling over South China Sea. *Remote Sens* 2015;7:467–87. doi:10.3390/rs70100467.
- [99] Nie B, Li J. Technical potential assessment of offshore wind energy over shallow continent shelf along China coast. *Renew Energy* 2018;128:391–9. doi:10.1016/j.renene.2018.05.081.
- [100] Ou L, Xu W, Yue Q, Ma CL, Teng X, Dong YE. Offshore wind zoning in China : Method and experience. *Ocean Coast Manag* 2018;151:99–108. doi:10.1016/j.ocecoaman.2017.10.016.
- [101] Hsieh CH, Dai CF. The analysis of offshore islands wind characteristics in Taiwan by Hilbert-Huang transform. *J Wind Eng Ind Aerodyn* 2012;107–108:160–8. doi:10.1016/j.jweia.2012.04.012.
- [102] Fang HF. Wind energy potential assessment for the offshore areas of Taiwan west coast and Penghu Archipelago. *Renew Energy* 2014;67:237–41. doi:10.1016/j.renene.2013.11.047.
- [103] Chang P-C, Yang R-Y, Lai C-M. Potential of Offshore Wind Energy and Extreme Wind Speed Forecasting on the West Coast of Taiwan. *Energies* 2015;8:1685–700. doi:10.3390/en8031685.

- [104] Chang H, Fan P-S, Kao L-F. Apply Patent Portfolio for Offshore Wind Power Industry Technology. 2014;12:178–89.
- [105] Gao AM-Z. Europe’s Policy Framework for Promoting Offshore Wind Energy: Lessons for Taiwan and Other Countries. *Renew Energy Law Policy RELP* 2015;6:3–16.
- [106] Zhang Y, Zhang C, Chang Y, Liu W, Zhang Y. Offshore wind farm in marine spatial planning and the stakeholders engagement : Opportunities and challenges for Taiwan. *Ocean Coast Manag* 2017;149:69–80. doi:10.1016/j.ocecoaman.2017.09.014.
- [107] Shu ZR, Li QS, Chan PW. Investigation of offshore wind energy potential in Hong Kong based on Weibull distribution function 2015;156:362–73. doi:10.1016/j.apenergy.2015.07.027.
- [108] Shu ZR, Li QS, He YC, Chan PW. Observations of offshore wind characteristics by Doppler-LiDAR for wind energy applications 2016;169:150–63. doi:10.1016/j.apenergy.2016.01.135.
- [109] Gao X, Yang H, Lu L. Study on offshore wind power potential and wind farm optimization in Hong Kong. *Appl Energy* 2014;130:519–31. doi:10.1016/j.apenergy.2014.02.070.
- [110] Gao X, Yang H, Lu L. Investigation into the optimal wind turbine layout patterns for a Hong Kong offshore wind farm. *Energy* 2014;73:430–42. doi:10.1016/j.energy.2014.06.033.
- [111] Gao X, Yang H, Lu L, Koo P. Wind turbine layout optimization using multi-population genetic algorithm and a case study in Hong Kong offshore. *J Wind Eng Ind Aerodyn* 2015;139:89–99. doi:10.1016/j.jweia.2015.01.018.
- [112] CLP Hong Kong Offshore Wind Limited. Hong Kong Offshore Wind Farm in Southeastern Waters 2006:2–13. <http://www.epd.gov.hk/eia/register/profile/latest/esb146.pdf> (accessed August 29, 2018).
- [113] Waewsak J, Landry M, Gagnon Y. Offshore wind power potential of the Gulf of Thailand. *Renew Energy* 2015;81:609–26. doi:10.1016/j.renene.2015.03.069.
- [114] Chancham C, Waewsak J, Gagnon Y. Offshore wind resource assessment and wind power plant optimization in the Gulf of Thailand. *Energy* 2017;139:706–31. doi:10.1016/j.energy.2017.08.026.
- [115] Zheng C, Zhuang H, Li XX, Li XX. Wind energy and wave energy resources assessment in the East China Sea and South China Sea. *Sci China Technol Sci* 2012;55:163–73. doi:10.1007/s11431-011-4646-z.
- [116] Huber M, Roger A, Hamacher T. Optimizing long-term investments for a sustainable development of the ASEAN power system. *Energy* 2015;88:180–93. doi:10.1016/j.energy.2015.04.065.
- [117] Ahmed T, Mekhilef S, Shah R, Mithulananthan N, Seyedmahmoudian M, Horan B. ASEAN power grid: A secure transmission infrastructure for clean and sustainable energy for South-East Asia. *Renew Sustain Energy Rev* 2017;67:1420–35. doi:10.1016/j.rser.2016.09.055.
- [118] Liu Y, Li S, Yi Q, Chen D. Wind profiles and wave spectra for potential wind farms in South China Sea. Part II: Wave spectrum model. *Energies* 2017;10. doi:10.3390/en10010127.
- [119] Guo Q, Xu X, Zhang K, Li Z, Huang W, Mansaray LR, et al. Assessing global ocean wind energy resources using multiple satellite data. *Remote Sens* 2018;10:1–13. doi:10.3390/rs10010100.
- [120] Zhang L, Shi H, Wang Z, Yu H, Yin X, Liao Q. Comparison of wind speeds from spaceborne microwave radiometers with in situ observations and ECMWF data over the global ocean. *Remote Sens* 2018;10. doi:10.3390/rs10030425.

- [121] Carvalho D, Rocha A, Gómez-Gesteira M, Alvarez I, Silva Santos C. Comparison between CCMP, QuikSCAT and buoy winds along the Iberian Peninsula coast. *Remote Sens Environ* 2013;137:173–83. doi:10.1016/j.rse.2013.06.005.
- [122] Nagababu G, Simha RR, Naidu NK, Kachhwaha SS, Savsani V. Application of OSCAT Satellite Data for Offshore Wind Power Potential Assessment of India. *Energy Procedia* 2015;90:89–98. doi:10.1016/j.egypro.2016.11.173.
- [123] Nagababu G, Kachhwaha SS, Savsani V. Estimation of technical and economic potential of offshore wind along the coast of India. *Energy* 2017;138:79–91. doi:10.1016/j.energy.2017.07.032.
- [124] Doubrawa P, Barthelmie RJ, Pryor SC, Hasager CB, Badger M, Karagali I. Satellite winds as a tool for offshore wind resource assessment: The Great Lakes Wind Atlas. *Remote Sens Environ* 2015;168:349–59. doi:10.1016/j.rse.2015.07.008.
- [125] Amirinia G, Mafi S, Mazaheri S. Offshore wind resource assessment of Persian Gulf using uncertainty analysis and GIS. *Renew Energy* 2017;113:915–29. doi:10.1016/j.renene.2017.06.070.
- [126] Gadad S, Deka PC. Offshore wind power resource assessment using Oceansat-2 scatterometer data at a regional scale. *Appl Energy* 2016;176:157–70. doi:10.1016/j.apenergy.2016.05.046.
- [127] Alvarez I, Gomez-Gesteira M, deCastro M, Carvalho D. Comparison of different wind products and buoy wind data with seasonality and interannual climate variability in the southern Bay of Biscay (2000–2009). *Deep Res Part II Top Stud Oceanogr* 2014;106:38–48. doi:10.1016/j.dsr2.2013.09.028.
- [128] National Renewable Energy Laboratory (NREL). QuikSCAT - Annual Wind Power Density at 10 m 2005:2005. https://openei.org/w/images/f/f0/QuikSCAT-_Annual_Wind_Power_Density_at_10m.pdf (accessed August 13, 2018).
- [129] Probst O, Cárdenas D. State of the art and trends in wind resource assessment. *Energies* 2010. doi:10.3390/en3061087.
- [130] Ayotte KW. Computational modelling for wind energy assessment. *J Wind Eng Ind Aerodyn* 2008;96:1571–90.
- [131] Foley AM, Leahy PG, Marvuglia A, McKeogh EJ. Current methods and advances in forecasting of wind power generation. *Renew Energy* 2012;37:1–8. doi:10.1016/j.renene.2011.05.033.
- [132] Wind Power Density Potential. *Glob Wind Atlas 2017:2017*. https://s3-eu-west-1.amazonaws.com/globalwindatlas/posters/World_PD.pdf (accessed March 25, 2018).
- [133] Hersbach H, De Rosnay P, Bell B, Schepers D, Simmons A, Soci C, et al. Operational global reanalysis: progress, future directions and synergies with NWP including updates on the ERA5 production status. *ERA Rep Ser No 27* 2018. doi:10.21957/tkic6g3wm.
- [134] Al-Yahyai S, Charabi Y, Gastli A. Review of the use of numerical weather prediction (NWP) models for wind energy assessment. *Renew Sustain Energy Rev* 2010;14:3192–8. doi:10.1016/j.rser.2010.07.001.
- [135] Ulazia A, Saenz J, Ibarra-Berastegui G. Sensitivity to the use of 3DVAR data assimilation in a mesoscale model for estimating offshore wind energy potential. A case study of the Iberian northern coastline. *Appl Energy* 2016;180:617–27. doi:10.1016/j.apenergy.2016.08.033.
- [136] Bilal M, Birkelund Y, Homola M, Virk MS. Wind over complex terrain - Microscale modelling

- with two types of mesoscale winds at Nygårdsfjell. *Renew Energy* 2016;99:647–53. doi:10.1016/j.renene.2016.07.042.
- [137] Efe B, Unal E, Montes S, Özdemir E, Unal Y, Barutcu B, et al. 72Hr Forecast of Wind Power in Manisa, Turkey By Using the WRF Model Coupled To Windsim. *Renew. Energy Res. Appl. Conf.*, 2012, p. 1–6. doi:10.1109/ICRERA.2012.6477345.
- [138] Castro FA, Santos CS, Costa JC. Development of a meso-microscale coupling procedure for site assessment in complex terrain. *EWEK 2010-European Wind Energy Conf. Exhib.*, EWEA-European Wind Energy Association; 2010.
- [139] Leblebici E, Tuncer IH. Coupled Unsteady OpenFOAM and WRF Solutions for an Accurate Estimation of Wind Energy Potential. *Eur. Congr. Comput. Methods Appl. Sci. Eng.* 2016, 2016, p. 5–10.
- [140] Yan BW, Li QS. Coupled on-site measurement/CFD based Approach for High-resolution Wind Resource Assessment over Complex Terrains. *Energy Convers Manag* 2016;117:351–66.
- [141] Bertram V. *Advanced CFD Analyses for Offshore Wind Power Installations* 2015.
- [142] Castellani F, Gravidahl A, Crasto G, Piccioni E, Vignaroli A. A practical approach in the CFD simulation of off-shore wind farms through the actuator disc technique. *Energy Procedia* 2013;35:274–84. doi:10.1016/j.egypro.2013.07.180.
- [143] Dhunny AZ, Lollchund MR, Rughooputh SDDV. Wind energy evaluation for a highly complex terrain using Computational Fluid Dynamics (CFD). *Renew Energy* 2017;101:1–9. doi:10.1016/j.renene.2016.08.032.
- [144] Bilal M, Solbakken K, Birkelund Y. Wind speed and direction predictions by WRF and WindSim coupling over Nygårdsfjell. *J Phys Conf Ser* 2016;753:082018. doi:10.1088/1742-6596/753/8/082018.
- [145] Churchfield MJ, Lee S, Moriarty PJ, Nrel PJM. Adding Complex Terrain and Stable Atmospheric Condition Capability to the OpenFOAM-based Flow Solver of the Simulator for On/Offshore Wind Farm Applications (SOWFA): Preprint. 1st Symp OpenFOAM Wind Energy 2013;2:02001. doi:10.1051/itmconf/20140202001.
- [146] Xu Y, Bi F, Song J, He H. The temporal and spatial variations in the Pacific wind and wave fields for the period 2002–2011. *Acta Oceanol Sin* 2017;36:26–36. doi:10.1007/s13131-017-1039-6.
- [147] Giannakopoulou E, Nhili R. WRF Model Methodology for Offshore Wind Energy Applications 2016;2014:1–10.
- [148] Santos-Alamillos FJ, Zquez DPV, Ruiz-Arias JA, Lara-Fanego V, Tovar-Pescador J. Analysis of WRF model wind estimate sensitivity to physics parameterization choice and terrain representation in Andalusia (Southern Spain). *J Appl Meteorol Climatol* 2013;52:1592–609. doi:10.1175/JAMC-D-12-0204.1.
- [149] Carvalho D, Rocha A, Gómez-Gesteira M, Silva Santos C. WRF wind simulation and wind energy production estimates forced by different reanalyses: Comparison with observed data for Portugal. *Appl Energy* 2014;117:116–26. doi:10.1016/j.apenergy.2013.12.001.
- [150] Cruz FT, Narisma GT. WRF simulation of the heavy rainfall over Metropolitan Manila, Philippines during tropical cyclone Ketsana: a sensitivity study. *Meteorol Atmos Phys* 2016. doi:10.1007/s00703-015-0425-x.
- [151] Dado JMB, Takahashi HG. Potential impact of sea surface temperature on rainfall over the western Philippines. *Prog Earth Planet Sci* 2017;4:23. doi:10.1186/s40645-017-0137-6.

- [152] Reid JS, Lagrosas ND, Jonsson HH, Reid EA, Sessions WR, Simpas JB, et al. Observations of the temporal variability in aerosol properties and their relationships to meteorology in the summer monsoonal South China Sea/East Sea: The scale-dependent role of monsoonal flows, the Madden-Julian Oscillation, tropical cyclones, squall I. *Atmos Chem Phys* 2015;15:1745–68. doi:10.5194/acp-15-1745-2015.
- [153] Reid JS, Lagrosas ND, Jonsson HH, Reid EA, Atwood SA, Boyd TJ, et al. Aerosol meteorology of Maritime Continent for the 2012 7SEAS southwest monsoon intensive study-Part 2: Philippine receptor observations of fine-scale aerosol behavior. *Atmos Chem Phys* 2016;16:14057–78. doi:10.5194/acp-16-14057-2016.
- [154] Chang CP, Zhuo W, John M, Ching-Hwang L. Annual Cycle of Southeast Asia — Maritime Continent Rainfall and the Asymmetric. *J Clim* 2005;18:287–301.
- [155] Moron V, Lucero A, Hilario F, Lyon B, Robertson AW, DeWitt D. Spatio-temporal variability and predictability of summer monsoon onset over the Philippines. *Clim Dyn* 2009;33:1159–77. doi:10.1007/s00382-008-0520-5.
- [156] Ranada P. Palawan aims for a 100% renewable energy future. *Rappler* 2013.
- [157] Anda RD. Power crisis hits Palawan. *Philipp Dly Inq* 2017.
- [158] Stull R. *Practical Meteorology: An Algebra-based Survey of Atmospheric Science*. Vancouver: University of British Columbia; 2017.
- [159] Dunlop S. *Meteorology Manual: The Practical Guide to the Weather*. Somerset: Haynes Publishing; 2014.
- [160] Cushman-Roisin B, Beckers J. *Introduction to Geophysical Fluid Dynamics: Physical and Numerical Aspects*. 2nd ed. Waltham: Academic Press; 2011.
- [161] Moukalled F, Mangani L, Darwish M. *The Finite Volume Method in Computational Fluid Dynamics: An Advanced Introduction with OpenFOAM and Matlab*. Cham: Springer International Publishing AG; 2016.
- [162] Versteeg HK, Malalasekera W. *An Introduction to Computational Fluid Dynamics: The Finite Volume Method*. 2nd ed. Essex: Pearson Education Limited; 2007.
- [163] Skamarock WC, Klemp JB, Dudhia J, Gill DO, Barker DM, Duda MG, et al. A Description of the Advanced Research WRF Version 3. 2008. doi:10.1080/07377366.2001.10400427.
- [164] Waewsak J, Chancham C, Chiwamongkhonkarn S, Gagnon Y. Wind resource assessment of the southernmost region of Thailand using atmospheric and computational fluid dynamics wind flow modeling. *Energies* 2019;12. doi:10.3390/en12101899.
- [165] Meissner C. *WindSim, Getting started*. WindSim 5. 5th Edition 2010:80. doi:10.1887/0750306920/b833c1.
- [166] Berrisford P, Dee D, Poli P, Brugge R, Fielding K, Fuentes M. *The ERA-Interim Archive* 2011.
- [167] Saha S, Moorthi S, Wu X, Wang J, Nadiga S, Tripp P, et al. The NCEP climate forecast system version 2. *J Clim* 2014;27:2185–208. doi:10.1175/JCLI-D-12-00823.1.
- [168] Peng G. What 's the difference between FNL and GFS ? 2014. doi:10.1118/1.3685581.
- [169] Barstad I. Offshore Validation of a 3 km ERA-Interim Downscaling - WRF Model's Performance on Static Stability. *Wind Energy* 2016;19:515–26. doi:10.1002/we.
- [170] Durán P, Meißner C, Rutledge K, Fonseca R, Martin-Torres J, Adaramola MS. Meso-microscale

- coupling for wind resource assessment using averaged atmospheric stability conditions. *Wind Eur.* 2017, 2017, p. 273–91. doi:10.1127/metz/2019/0937.
- [171] Durán P, Meisner C, Rutledge K, Fonseca R, Martin-Torres J. Meso-microscale coupling for wind resource assessment using average atmospheric conditions. *Wind Eur.* 2018, 2018.
- [172] Philippine Atmospheric, Geophysical, and Astronomical Services Administration (PAGASA). Daily Climatic Data (2010-2011). n.d.
- [173] Hou Q, Zou Z. Comparison between standard and renormalization group k- ϵ models in numerical simulation of swirling flow tundish. *ISIJ Int* 2005;45:325–30. doi:10.2355/isijinternational.45.325.
- [174] Silang A, Uy SN, Dado JM, Cruz FA, Narisma G, Libatique N, et al. Wind energy projection for the Philippines based on climate change modeling. *Energy Procedia*, 2014. doi:10.1016/j.egypro.2014.07.051.

Appendix 1: Mesoscale Model Wind Speed Scatter Plots

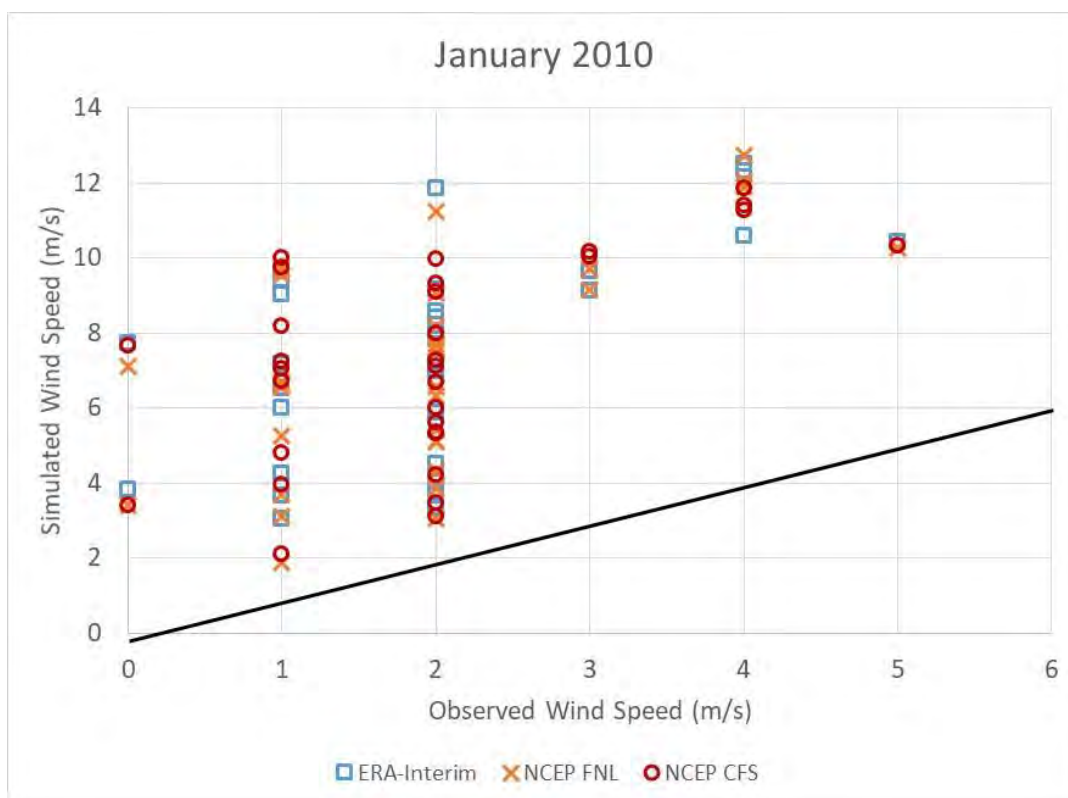


Figure 100. Scatter plot of different WRF model settings with PAGASA station data in Coron Island for January 2010.

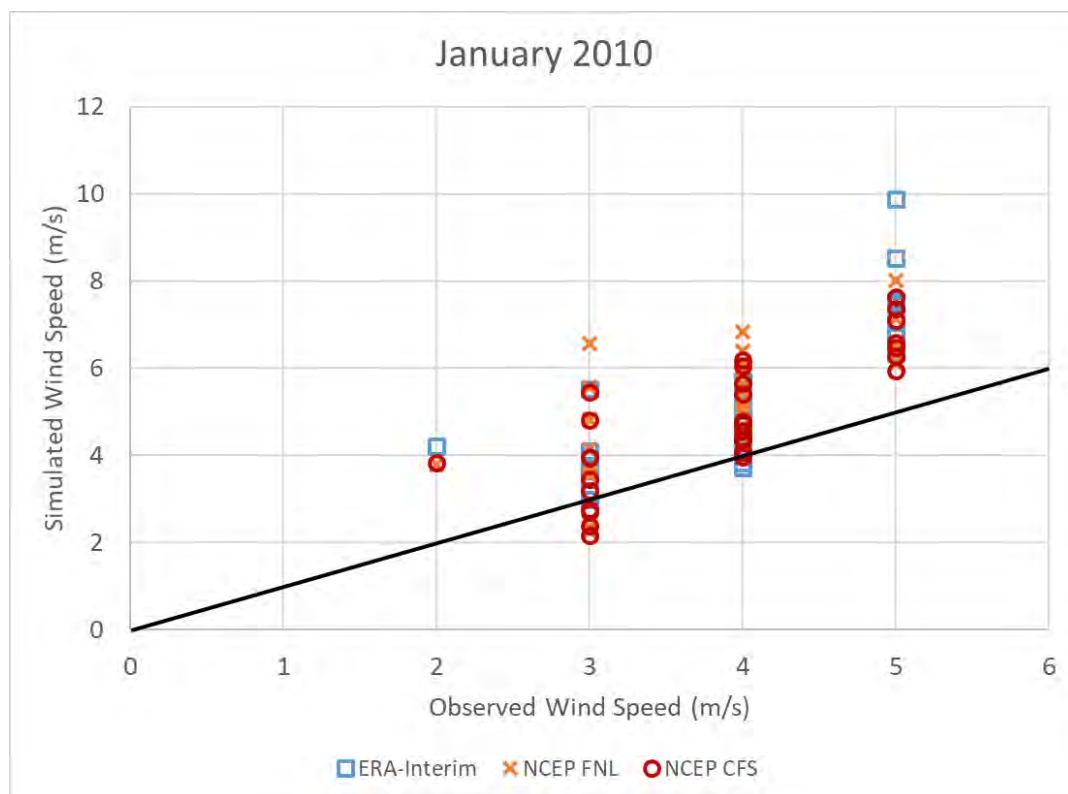


Figure 101. Scatter plot of different WRF model settings with PAGASA station data in Puerto Princesa for January 2010.

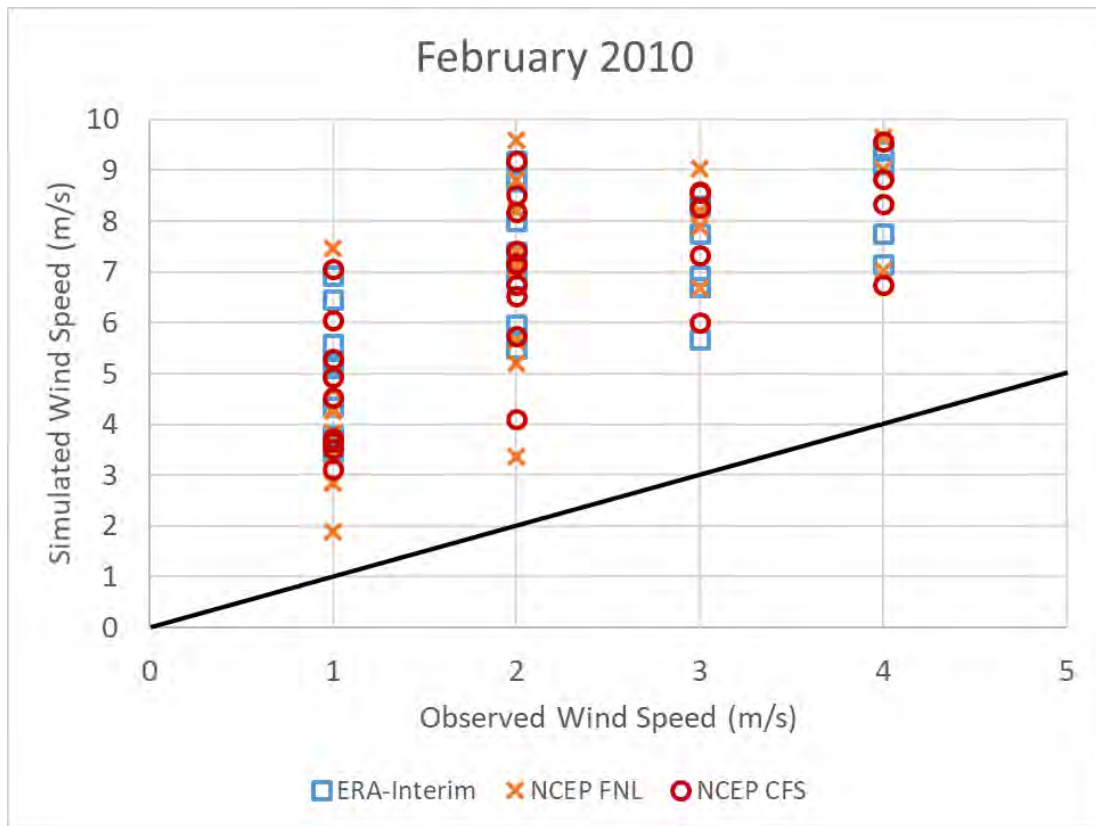


Figure 102. Scatter plot of different WRF model settings with PAGASA station data in Coron Island for February 2010.

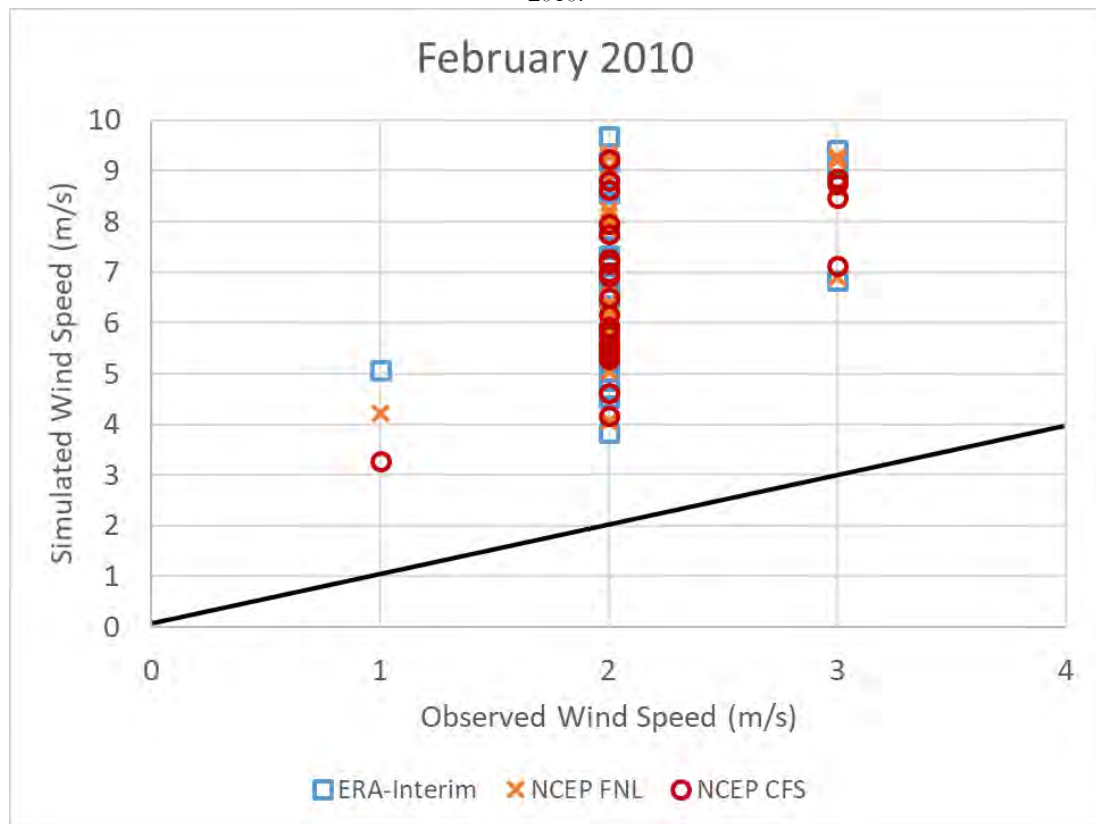


Figure 103. Scatter plot of different WRF model settings with PAGASA station data in Cuyo Island for February 2010.

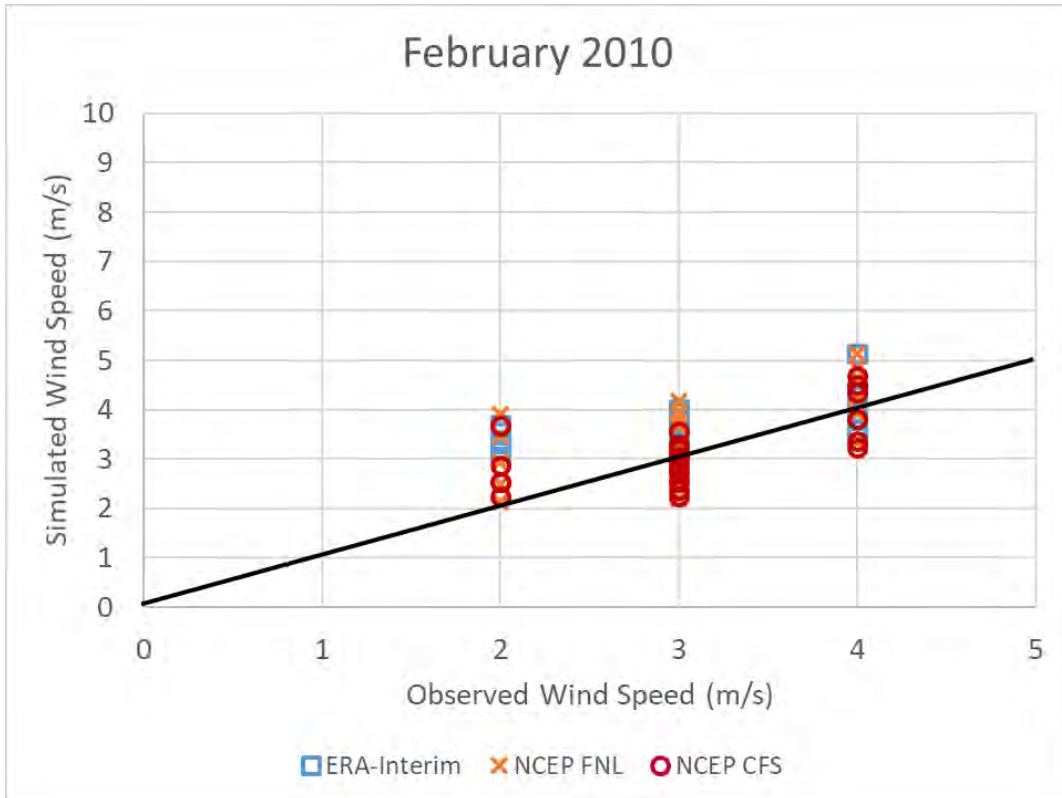


Figure 104. Scatter plot of different WRF model settings with PAGASA station data in Puerto Princesa for February 2010.

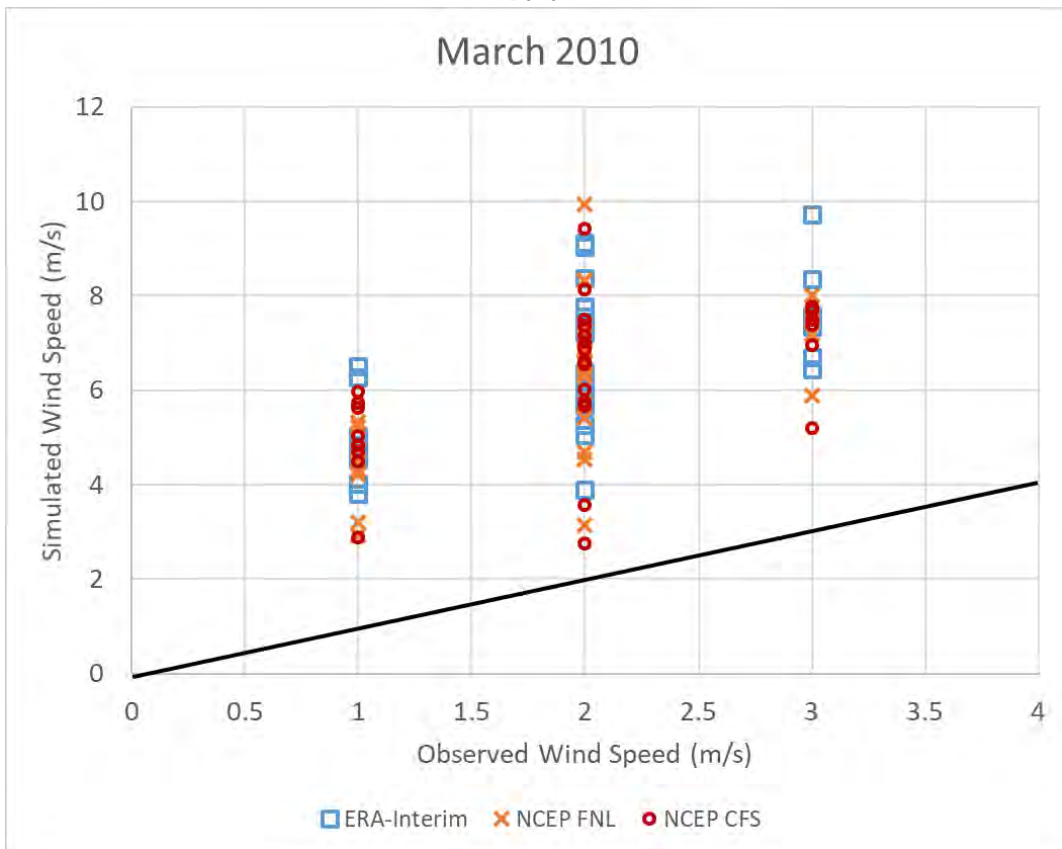


Figure 105. Scatter plot of different WRF model settings with PAGASA station data in Coron Island for March 2010.



Figure 106. Scatter plot of different WRF model settings with PAGASA station data in Cuyo Island for March 2010.

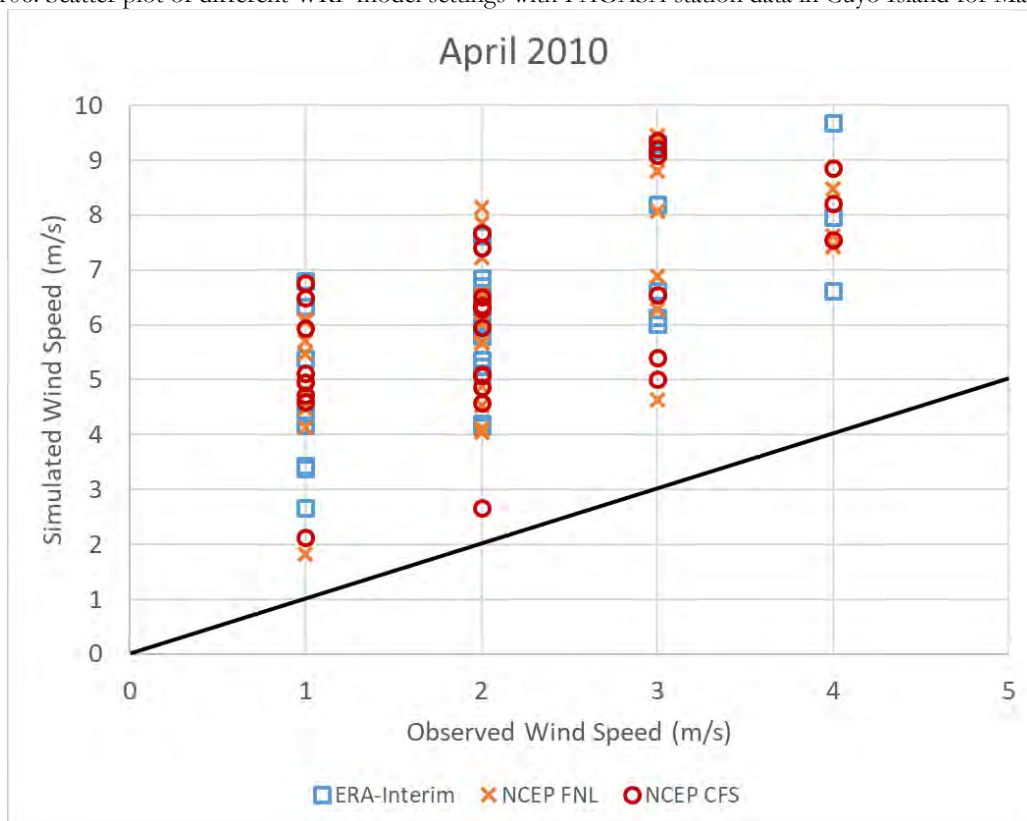


Figure 107. Scatter plot of different WRF model settings with PAGASA station data in Coron Island for April 2010.

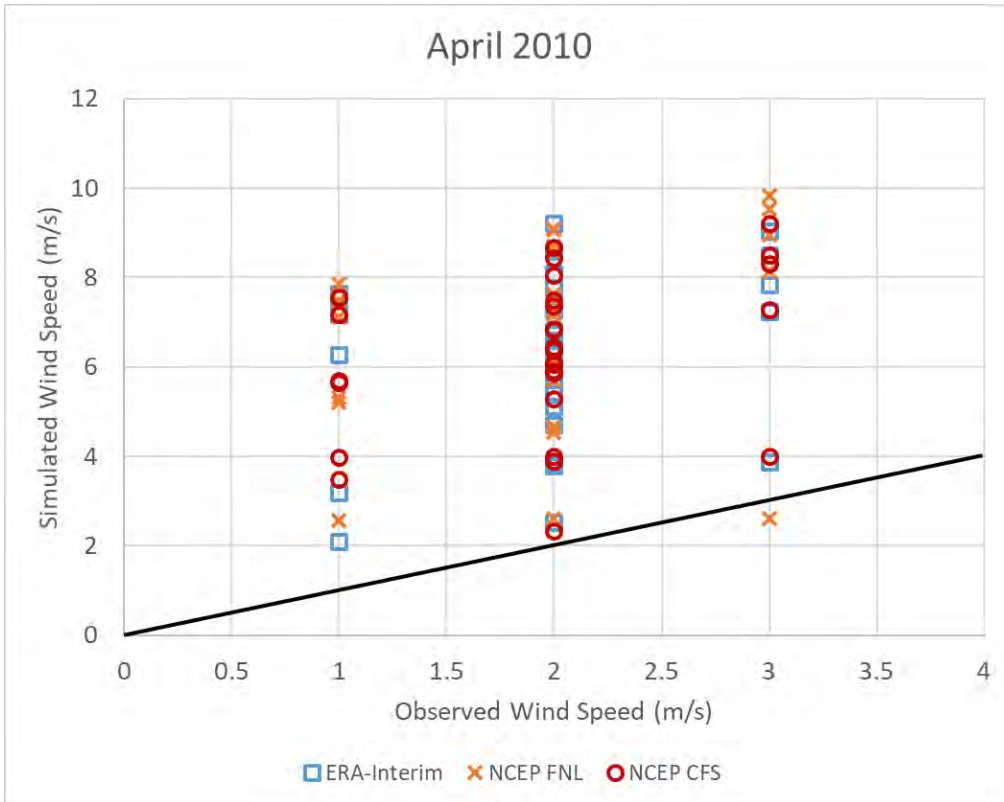


Figure 108. Scatter plot of different WRF model settings with PAGASA station data in Cuyo Island for April 2010.

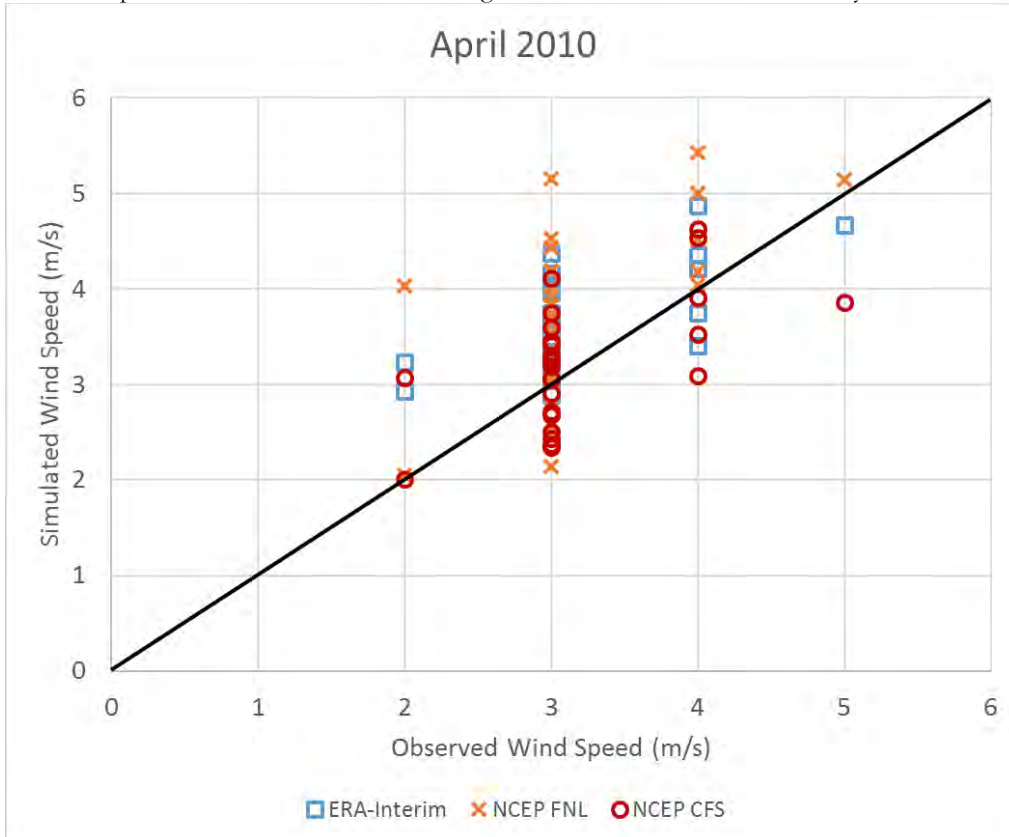


Figure 109. Scatter plot of different WRF model settings with PAGASA station data in Puerto Princesa for April 2010.

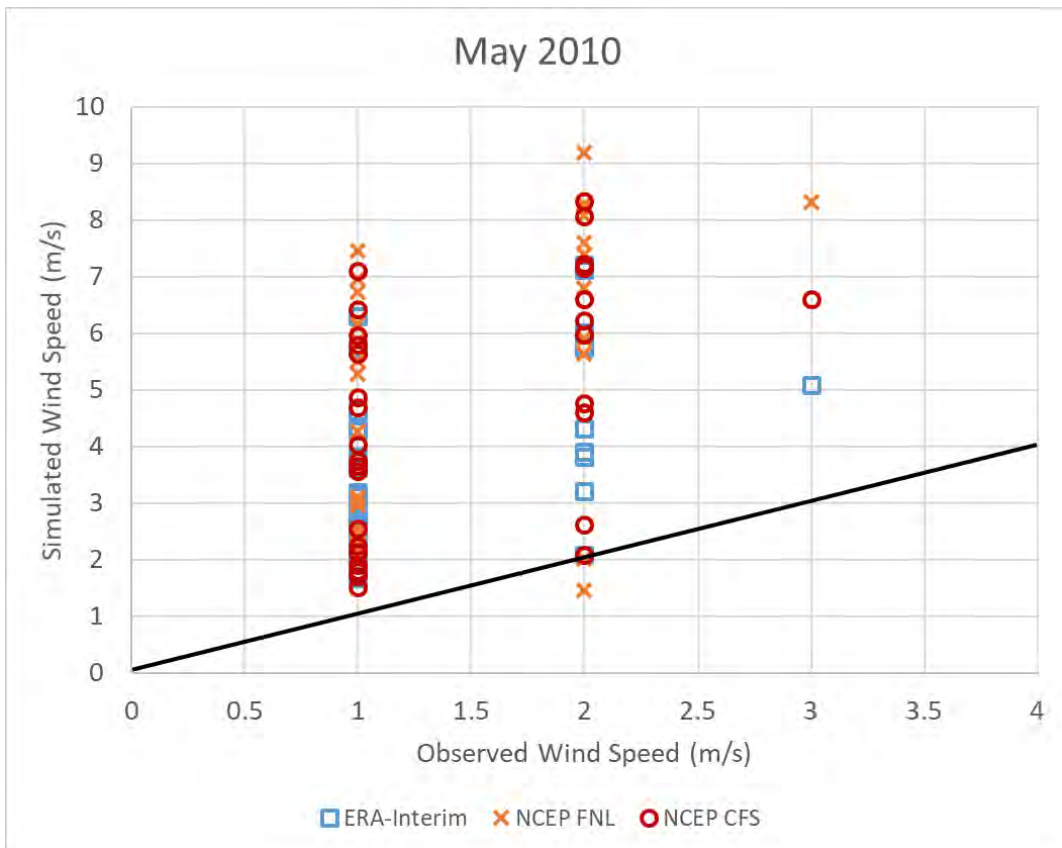


Figure 110. Scatter plot of different WRF model settings with PAGASA station data in Coron Island for May 2010.

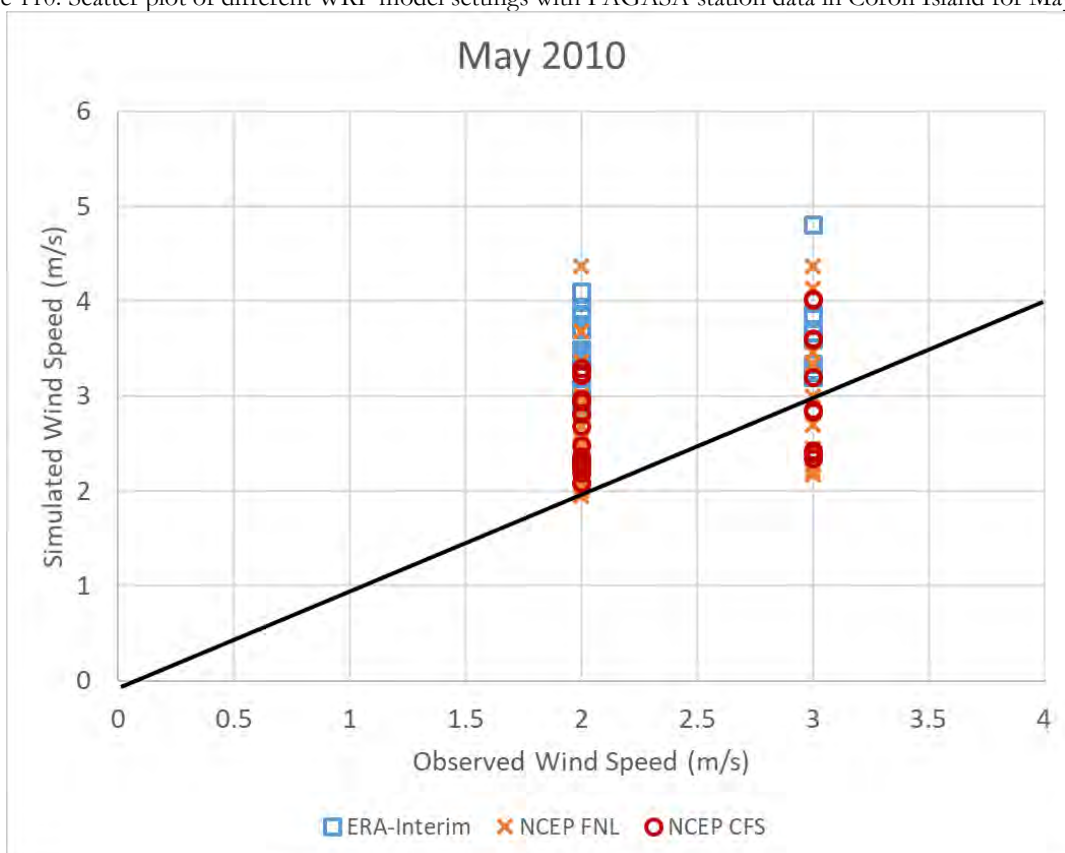


Figure 111. Scatter plot of different WRF model settings with PAGASA station data in Puerto Princesa for May 2010.

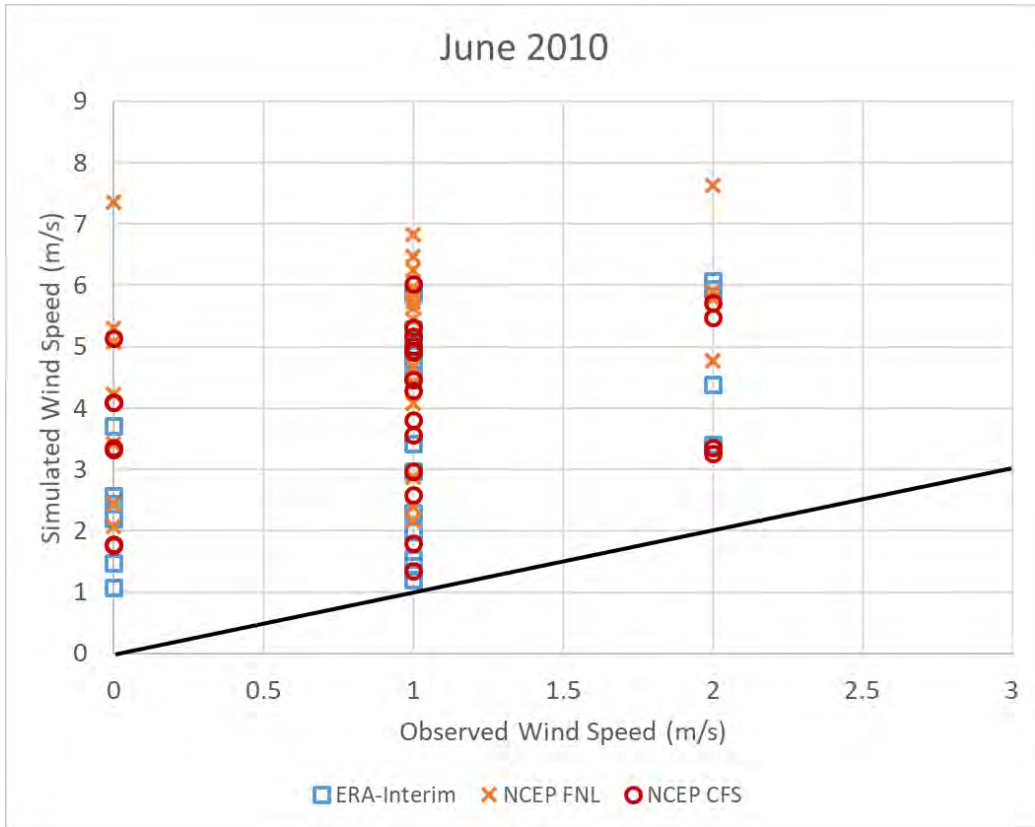


Figure 112. Scatter plot of different WRF model settings with PAGASA station data in Cuyo Island for June 2010.

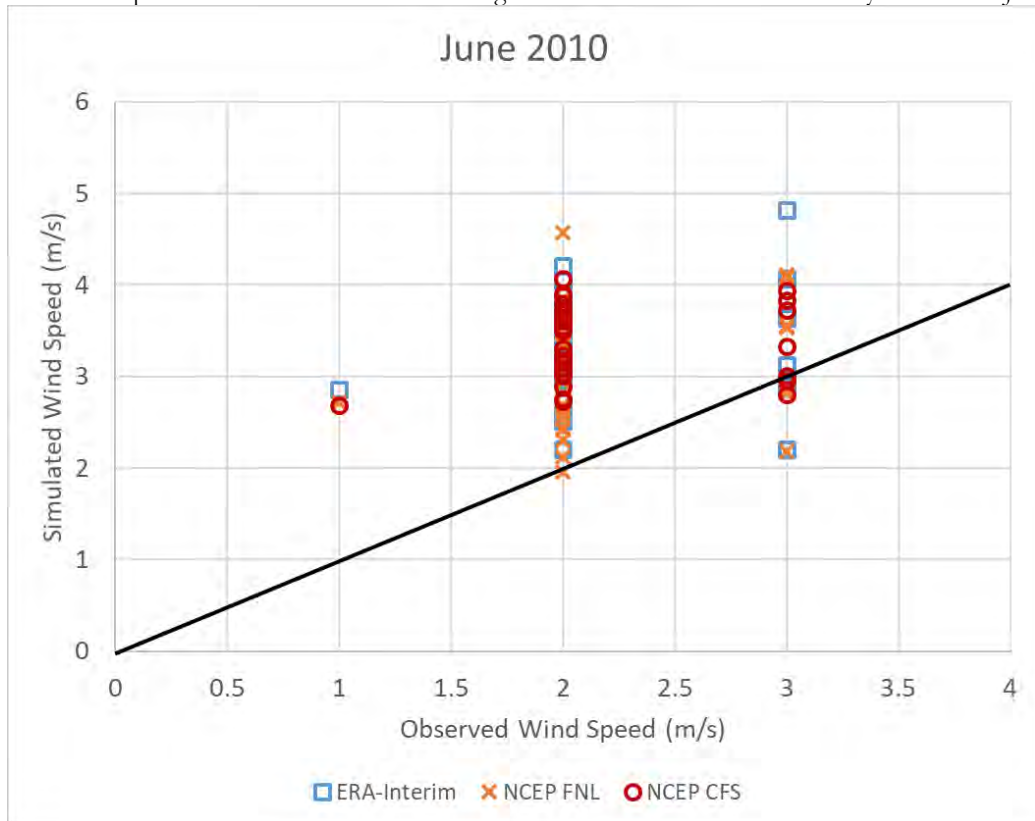


Figure 113. Scatter plot of different WRF model settings with PAGASA station data in Puerto Princesa for June 2010.

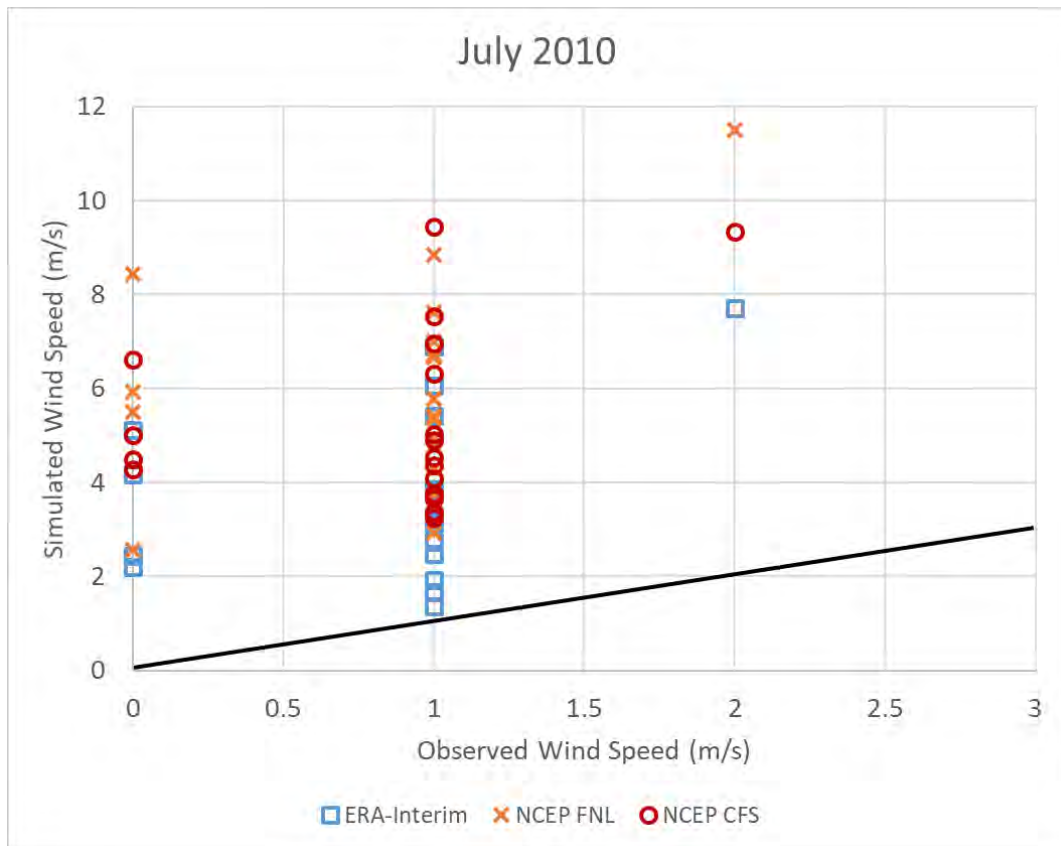


Figure 114. Scatter plot of different WRF model settings with PAGASA station data in Cuyo Island for July 2010.

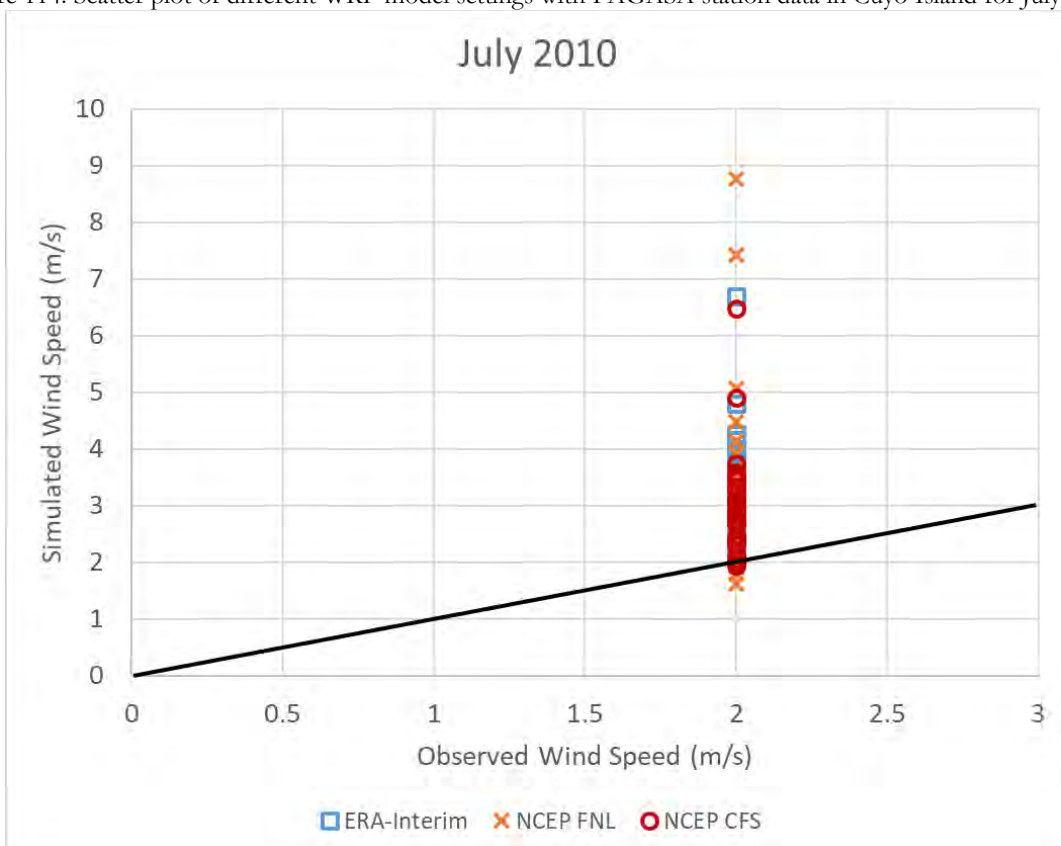


Figure 115. Scatter plot of different WRF model settings with PAGASA station data in Puerto Princesa for July 2010.

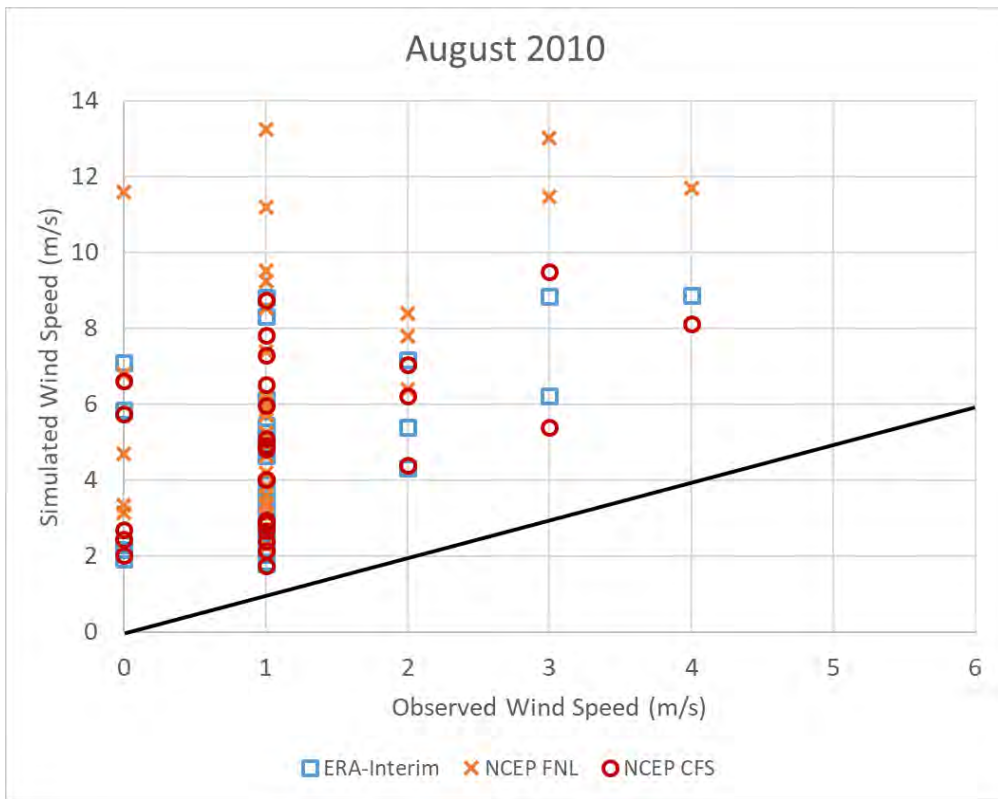


Figure 116. Scatter plot of different WRF model settings with PAGASA station data in Coron Island for August 2010.

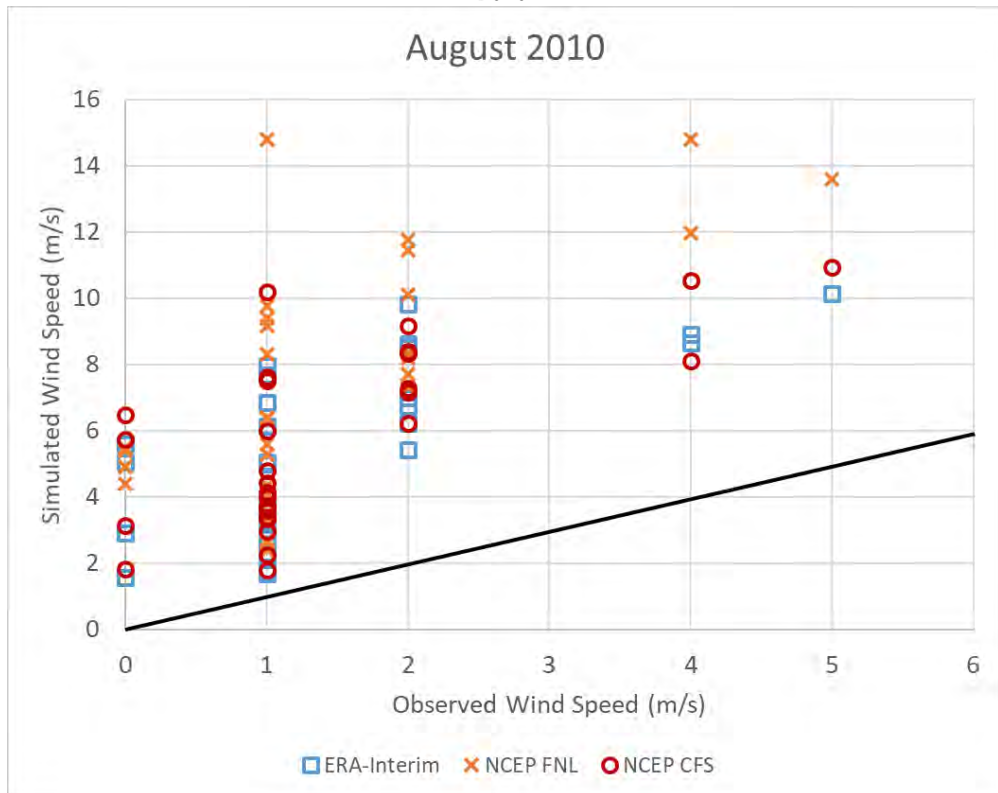


Figure 117. Scatter plot of different WRF model settings with PAGASA station data in Cuyo Island for August 2010.

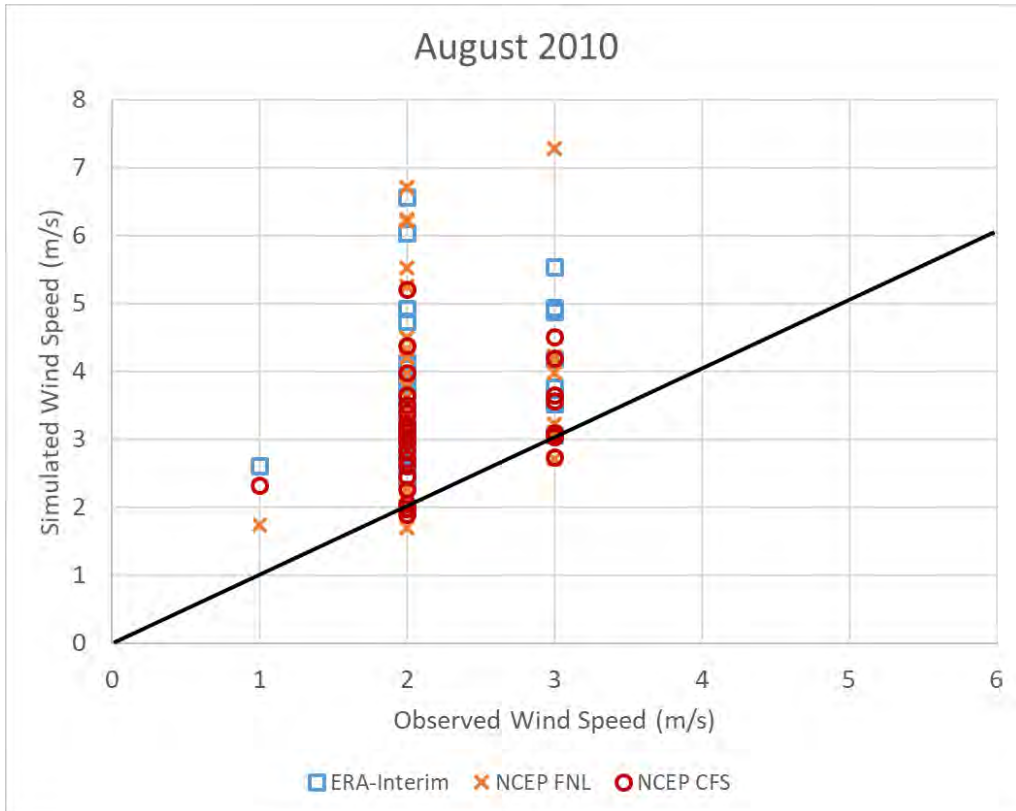


Figure 118. Scatter plot of different WRF model settings with PAGASA station data in Puerto Princesa for August 2010.

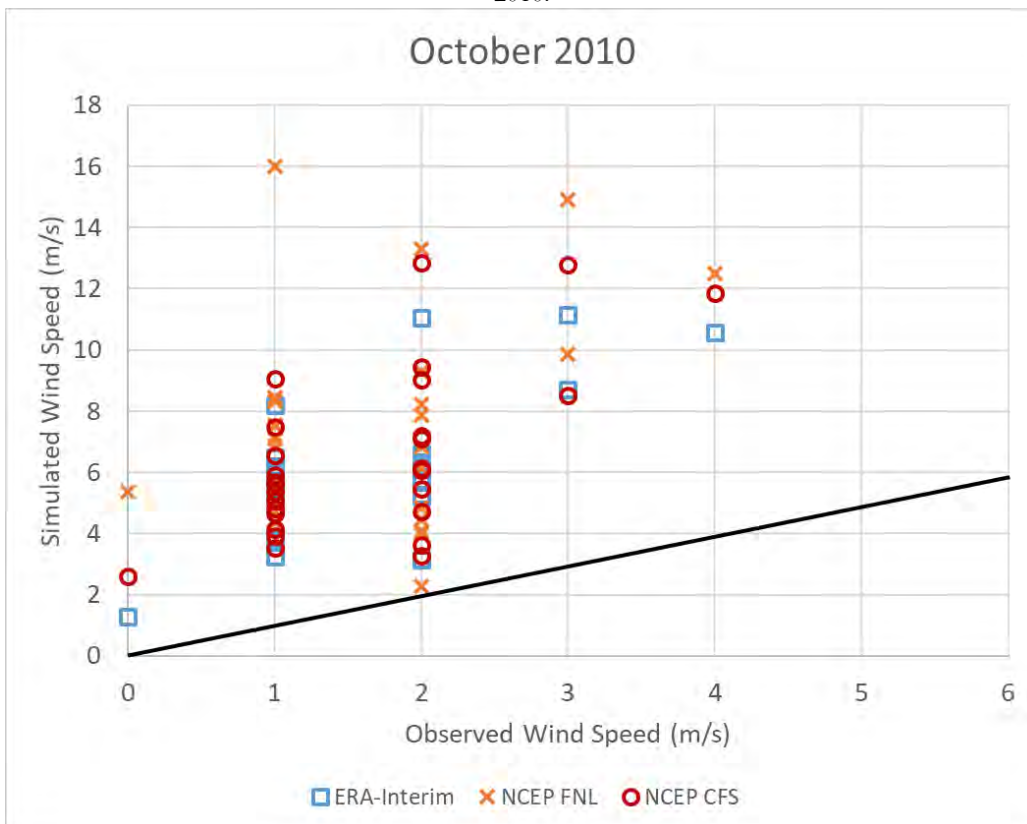


Figure 119. Scatter plot of different WRF model settings with PAGASA station data in Cuyo Island for October 2010.

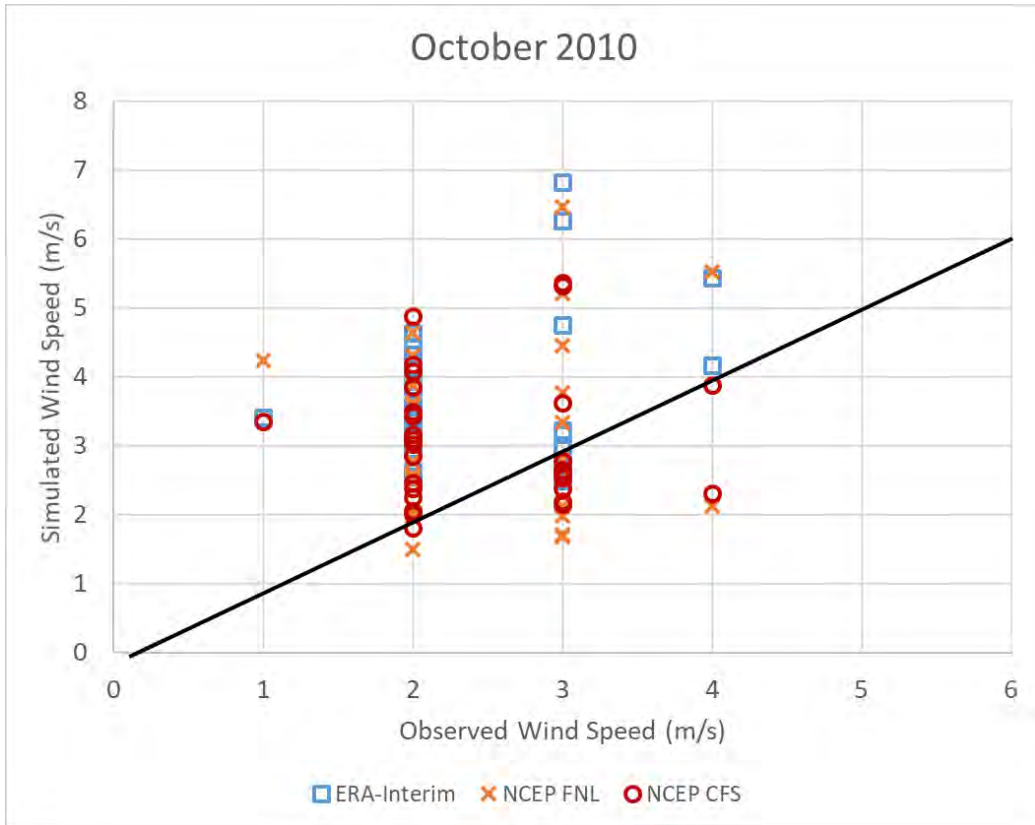


Figure 120. Scatter plot of different WRF model settings with PAGASA station data in Puerto Princesa for October 2010.

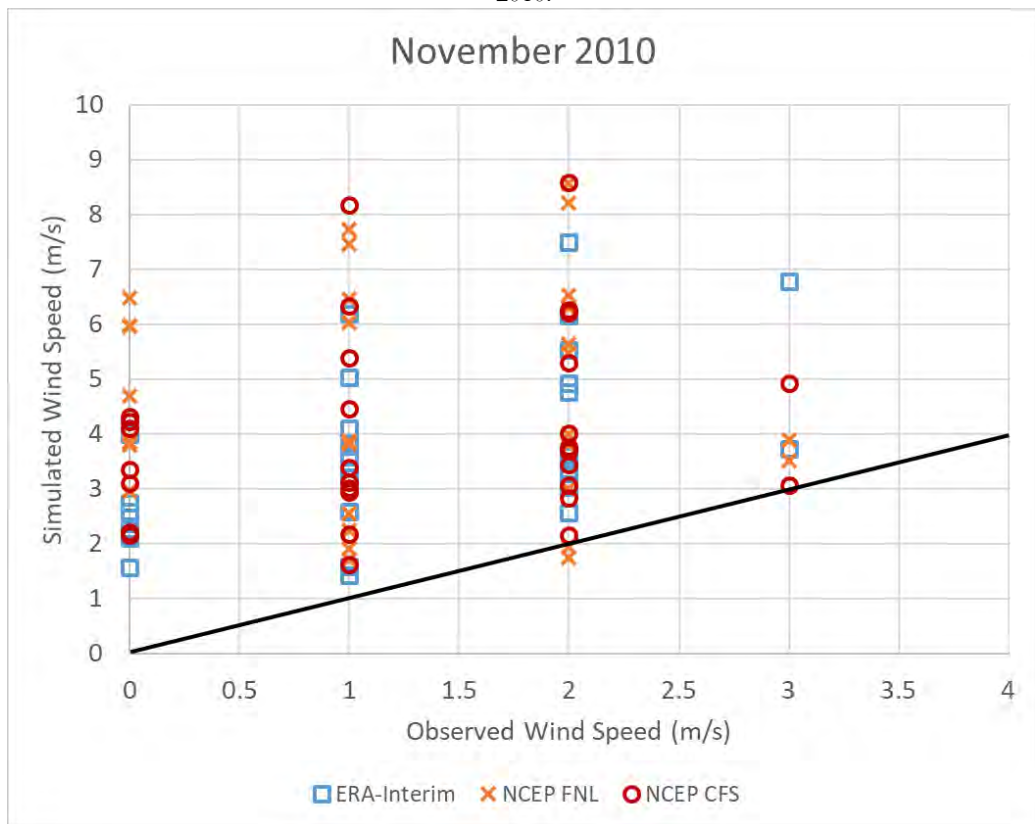


Figure 121 Scatter plot of different WRF model settings with PAGASA station data in Coron Island for November 2010.

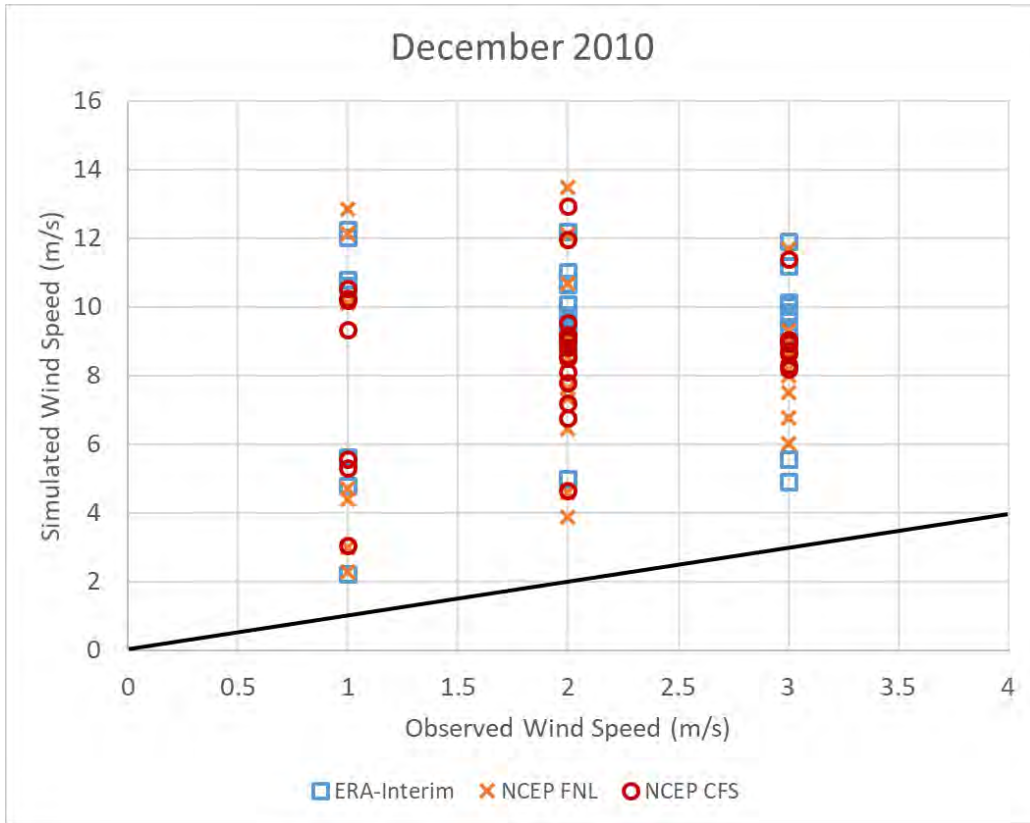


Figure 122. Scatter plot of different WRF model settings with PAGASA station data in Cuyo Island for December 2010.

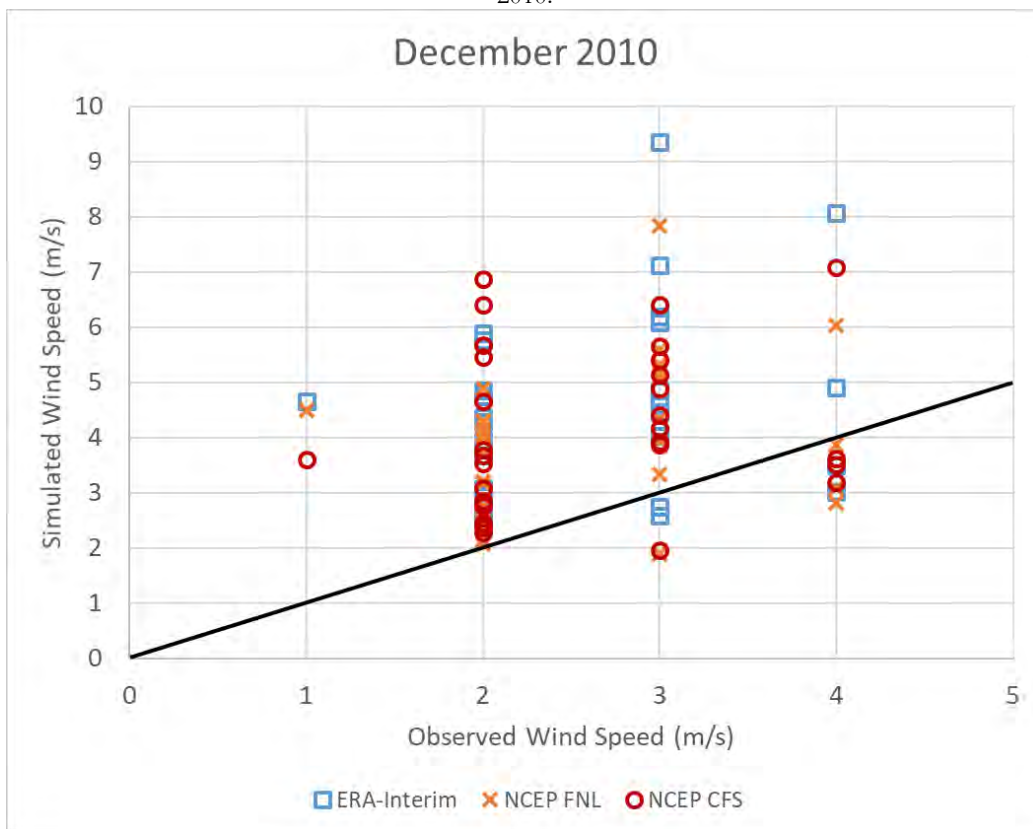


Figure 123. Scatter plot of different WRF model settings with PAGASA station data in Puerto Princesa for December 2010.

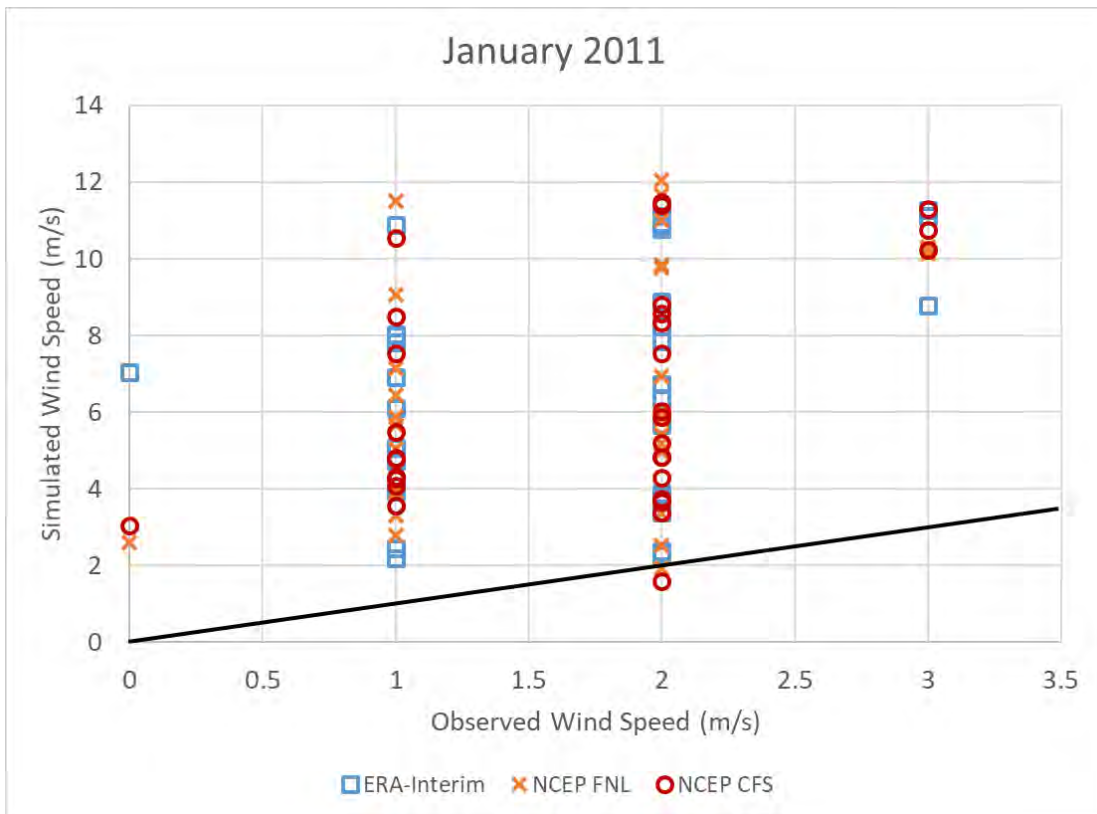


Figure 124. Scatter plot of different WRF model settings with PAGASA station data in Coron Island for January 2011.

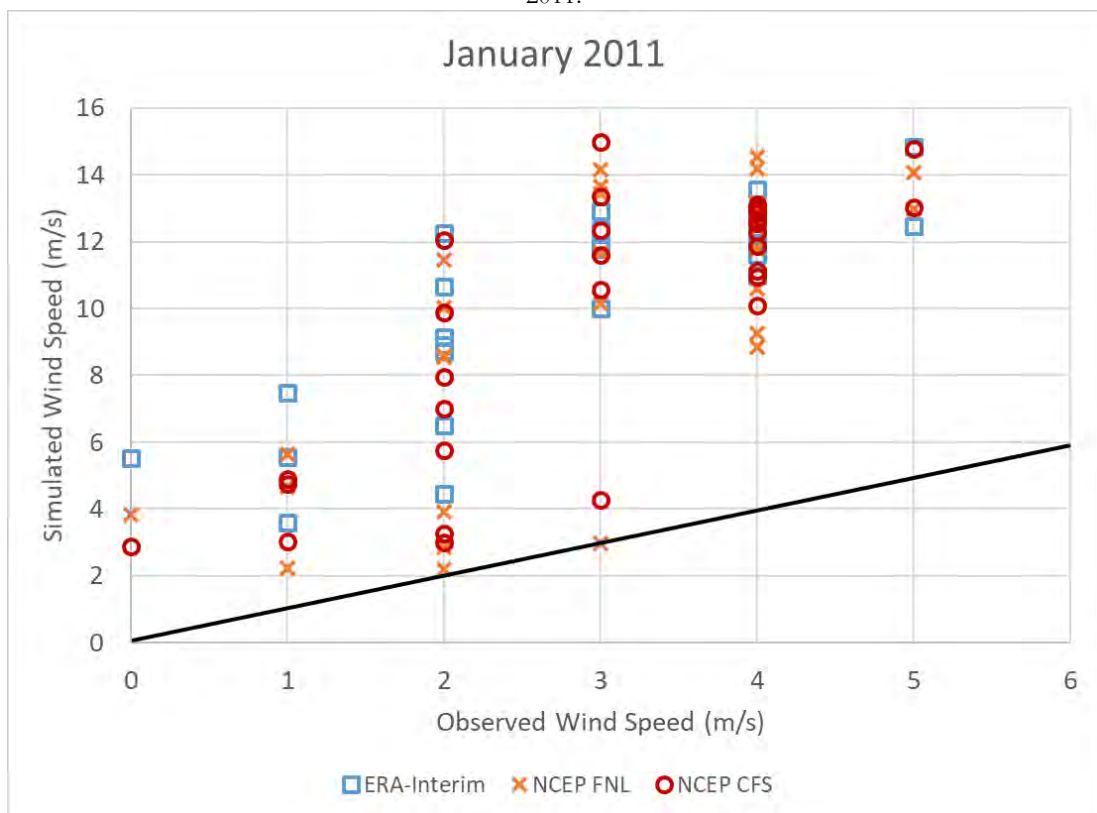


Figure 125. Scatter plot of different WRF model settings with PAGASA station data in Cuyo Island for January 2011.

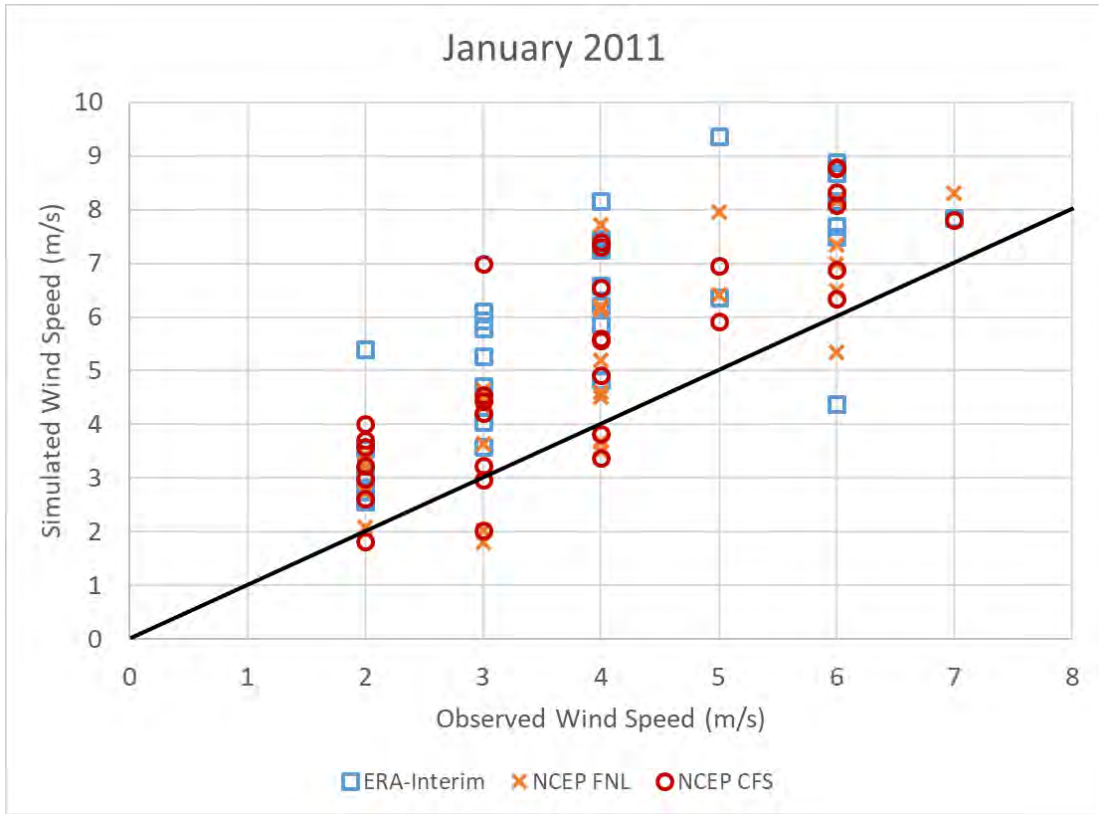


Figure 126. Scatter plot of different WRF model settings with PAGASA station data in Puerto Princesa for January 2011.

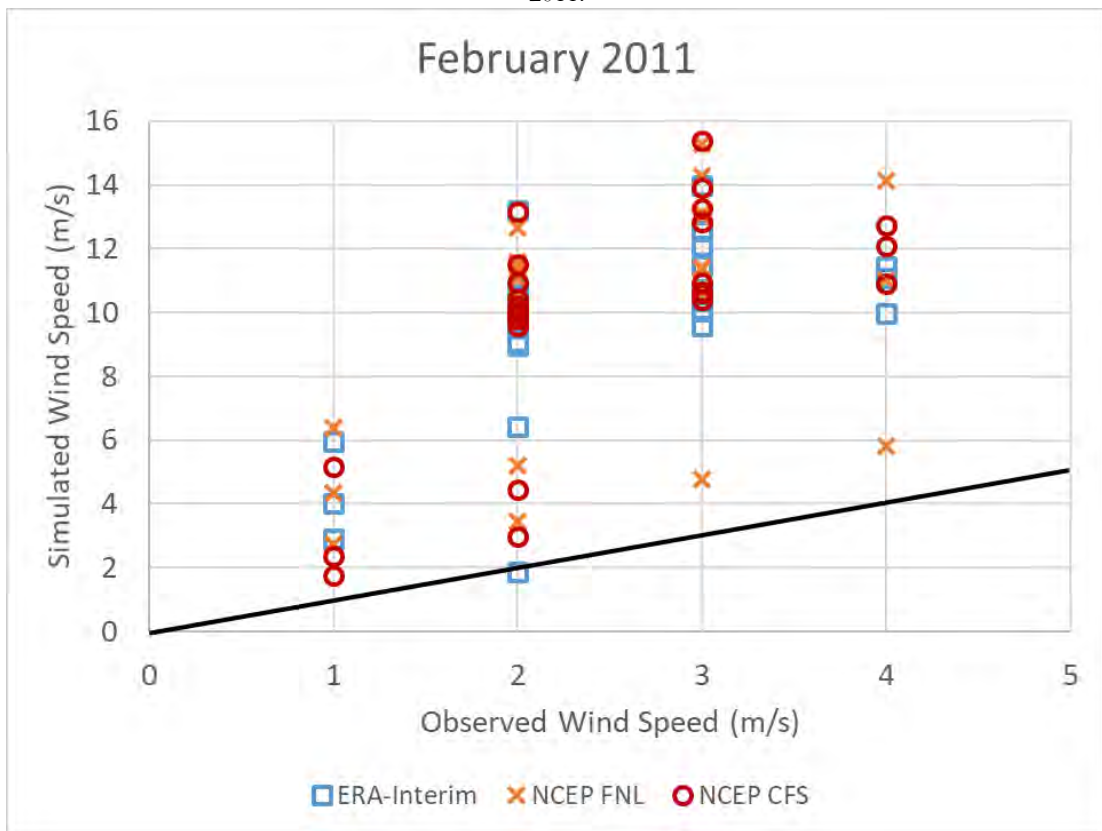


Figure 127. Scatter plot of different WRF model settings with PAGASA station data in Cuyo Island for February 2011.

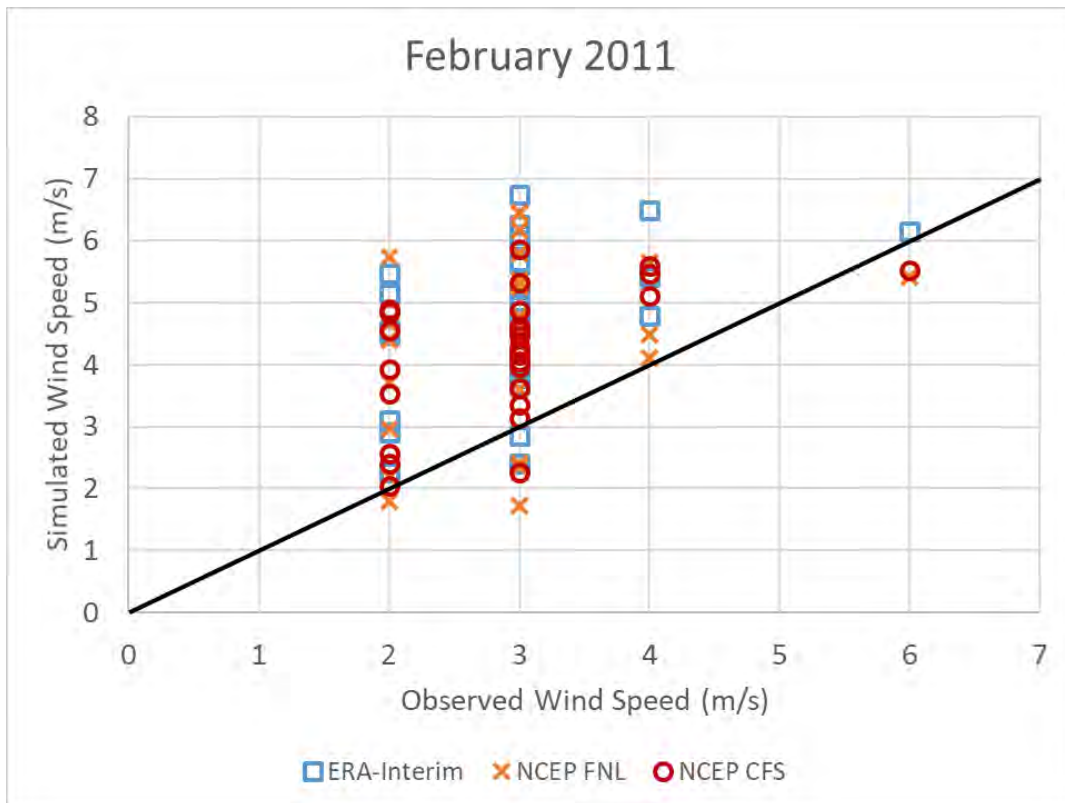


Figure 128. Scatter plot of different WRF model settings with PAGASA station data in Puerto Princesa for February 2011.

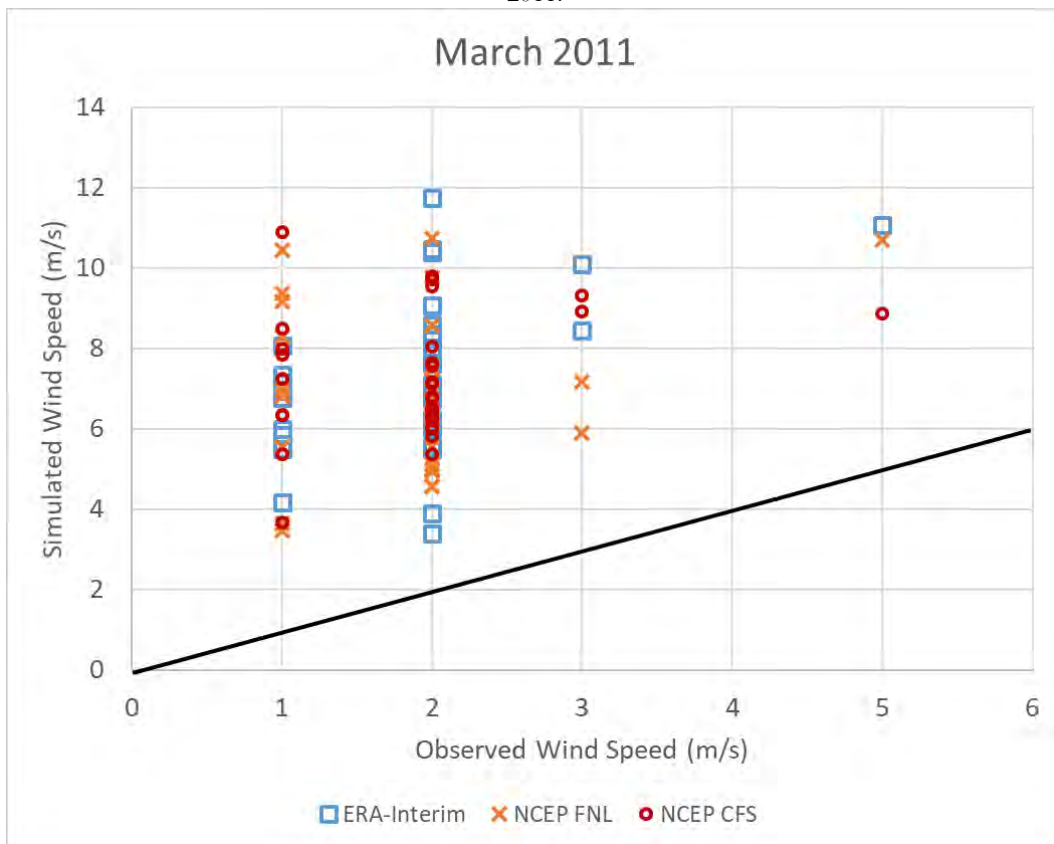


Figure 129. Scatter plot of different WRF model settings with PAGASA station data in Coron Island for March 2011.

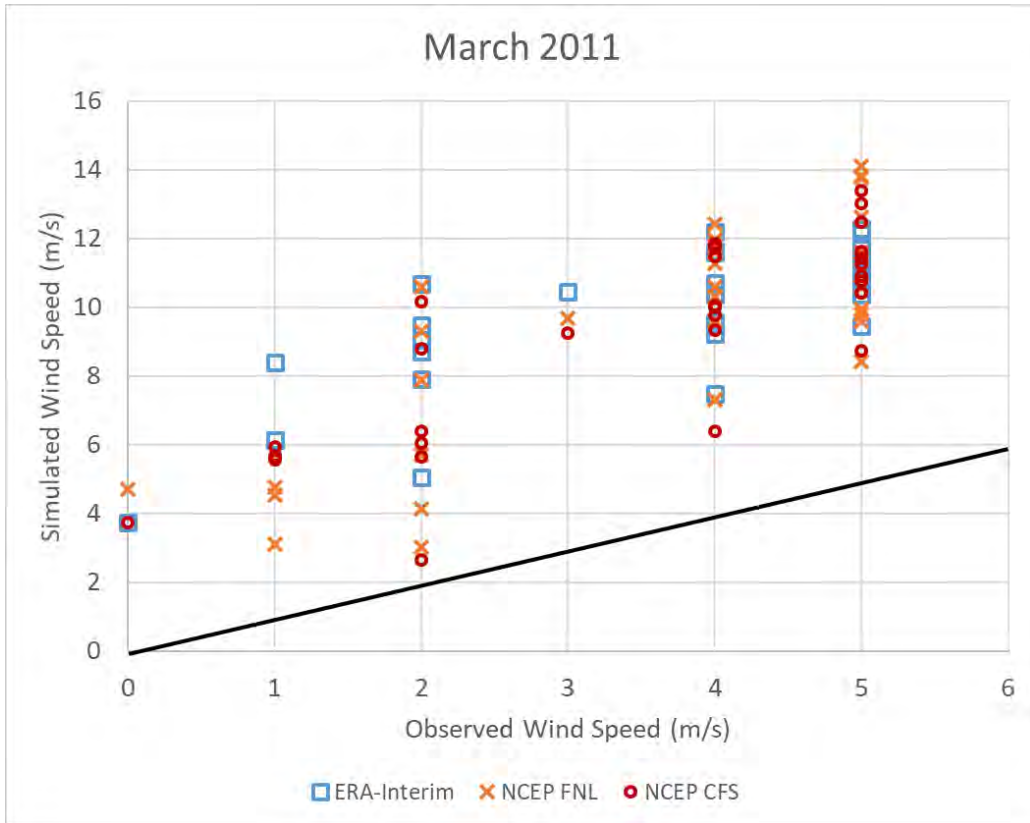


Figure 130. Scatter plot of different WRF model settings with PAGASA station data in Cuyo Island for March 2011.



Figure 131. Scatter plot of different WRF model settings with PAGASA station data in Puerto Princesa for March 2011.

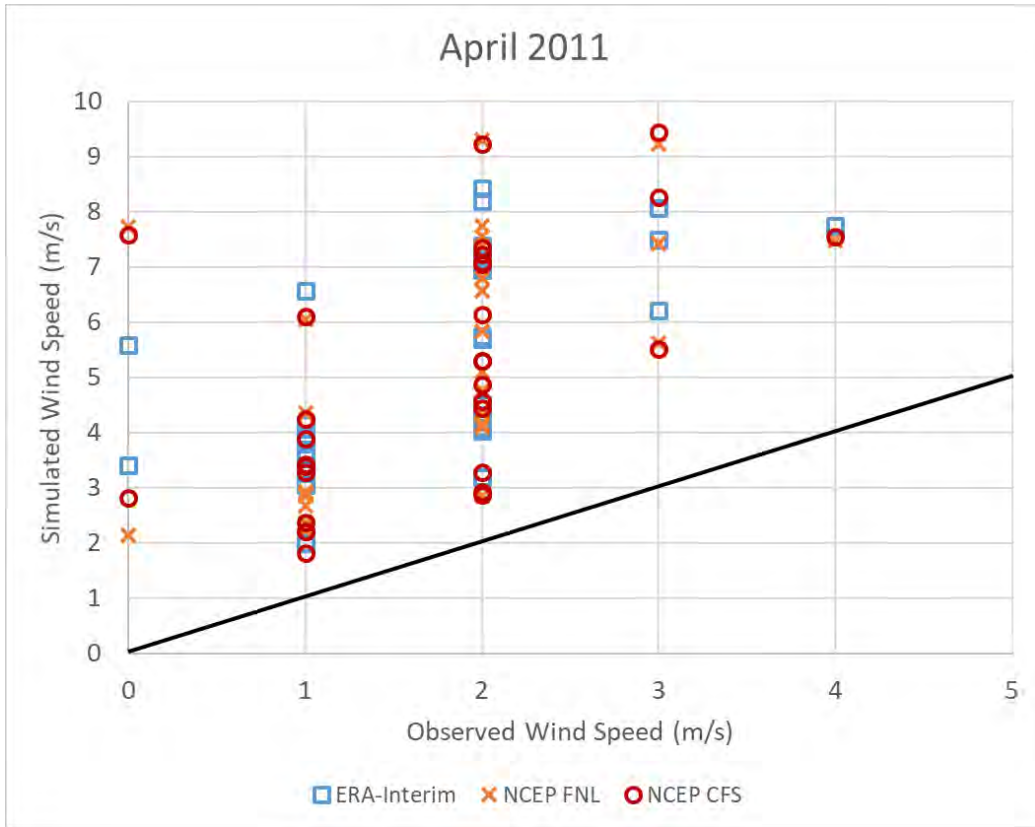


Figure 132. Scatter plot of different WRF model settings with PAGASA station data in Coron Island for April 2011.

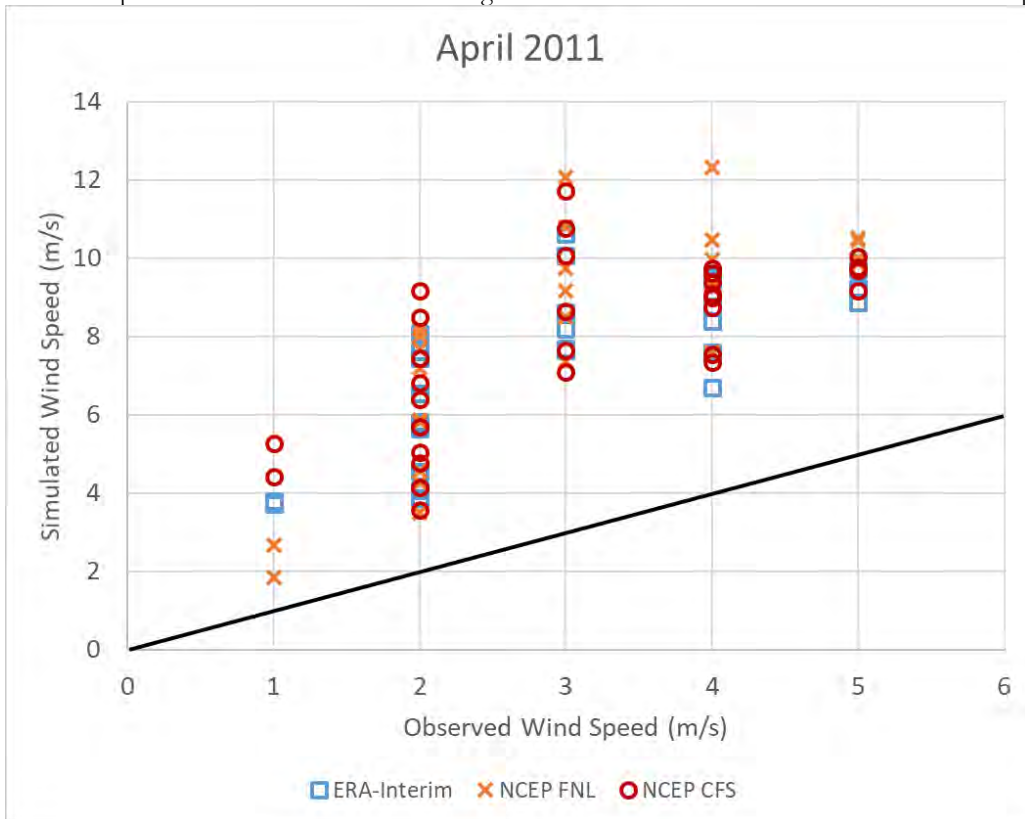


Figure 133. Scatter plot of different WRF model settings with PAGASA station data in Cuyo Island for April 2011.

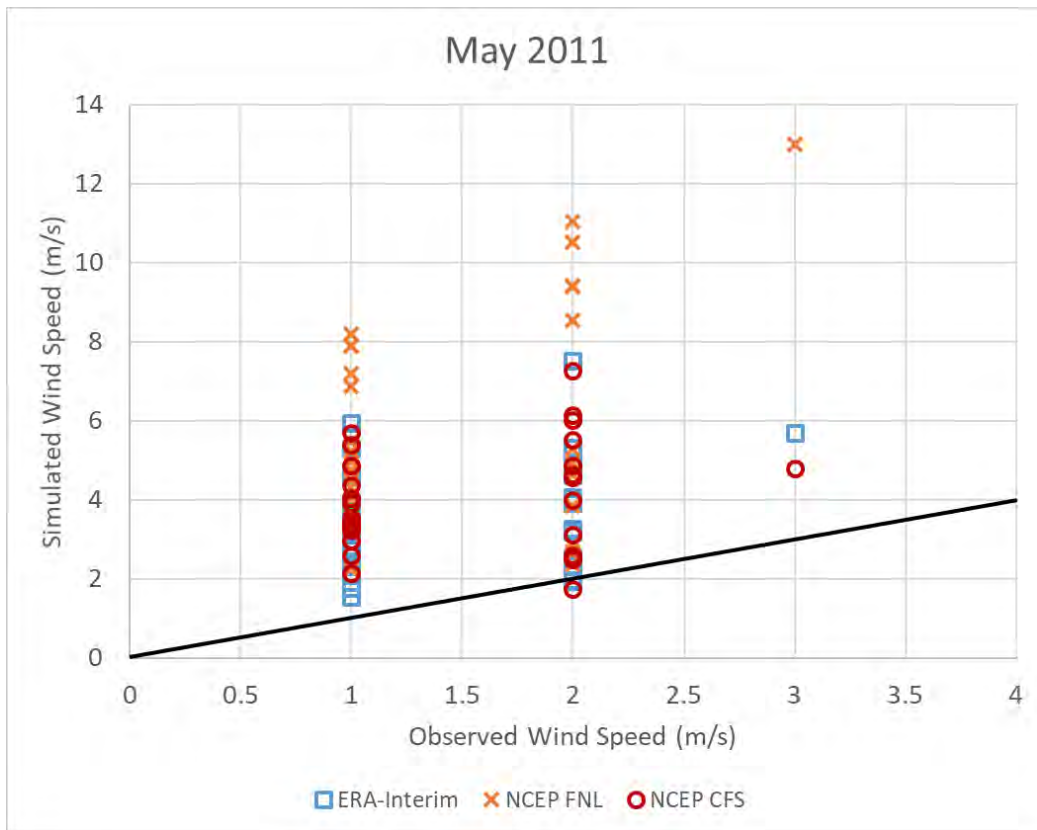


Figure 134. Scatter plot of different WRF model settings with PAGASA station data in Coron Island for May 2011.

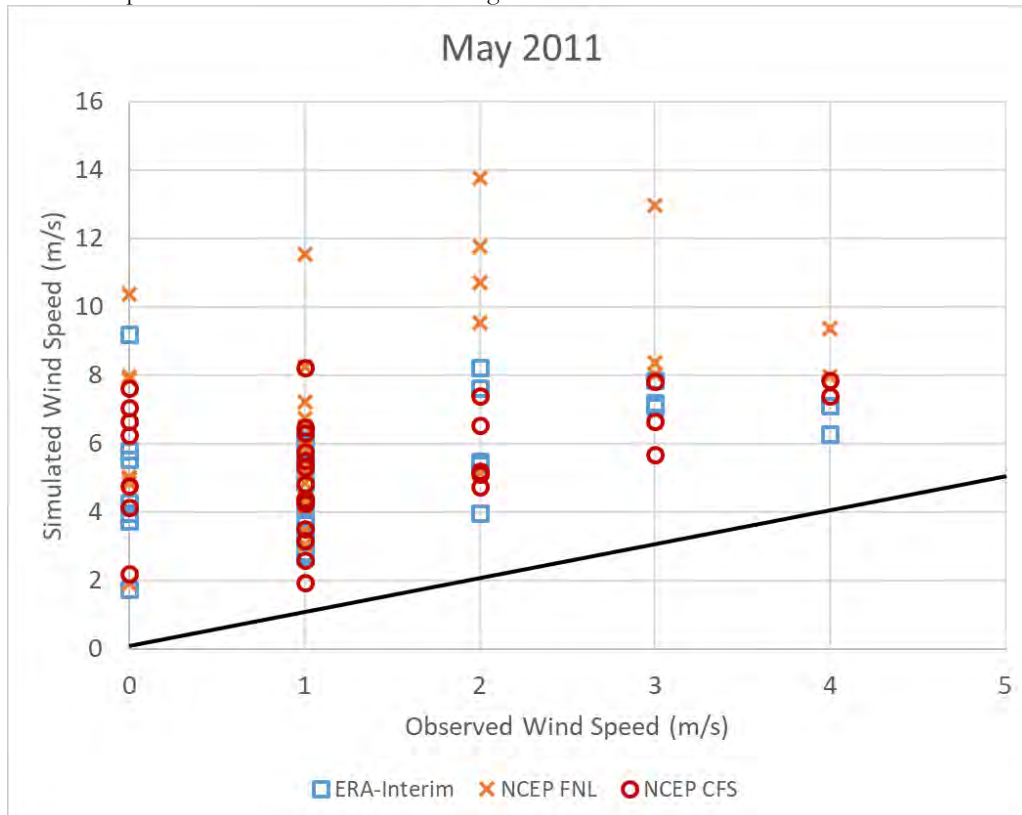


Figure 135. Scatter plot of different WRF model settings with PAGASA station data in Cuyo Island for May 2011.

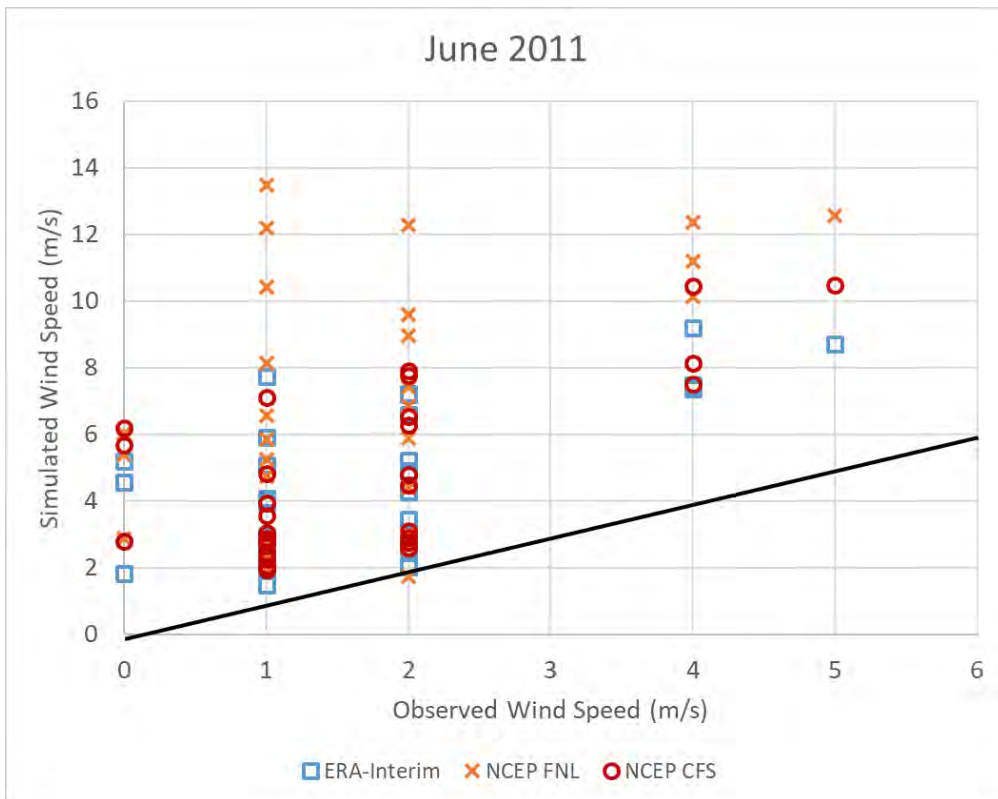


Figure 136. Scatter plot of different WRF model settings with PAGASA station data in Coron Island for June 2011.

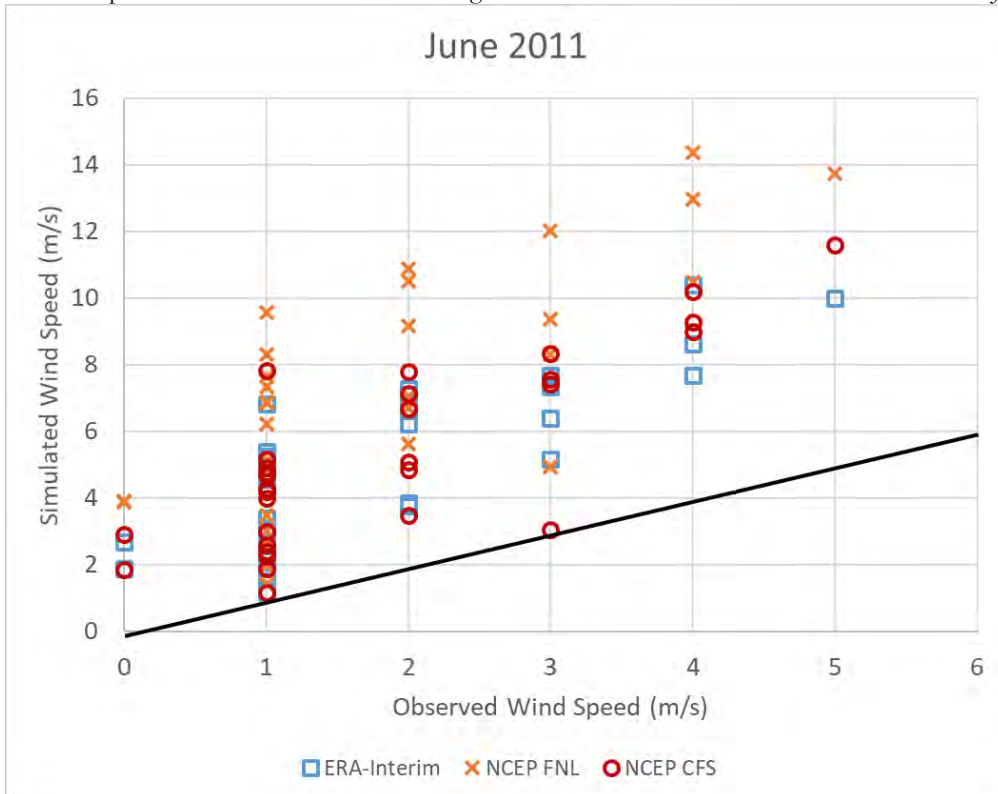


Figure 137. Scatter plot of different WRF model settings with PAGASA station data in Cuyo Island for June 2011.

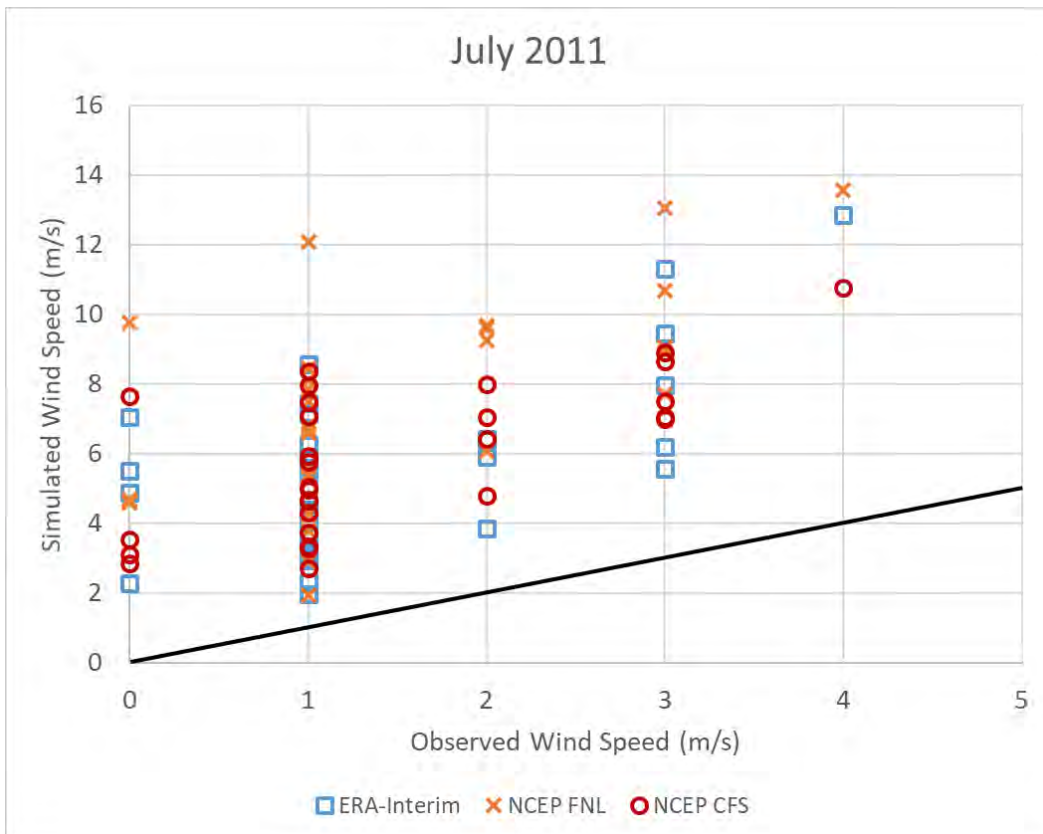


Figure 138. Scatter plot of different WRF model settings with PAGASA station data in Coron Island for July 2011.

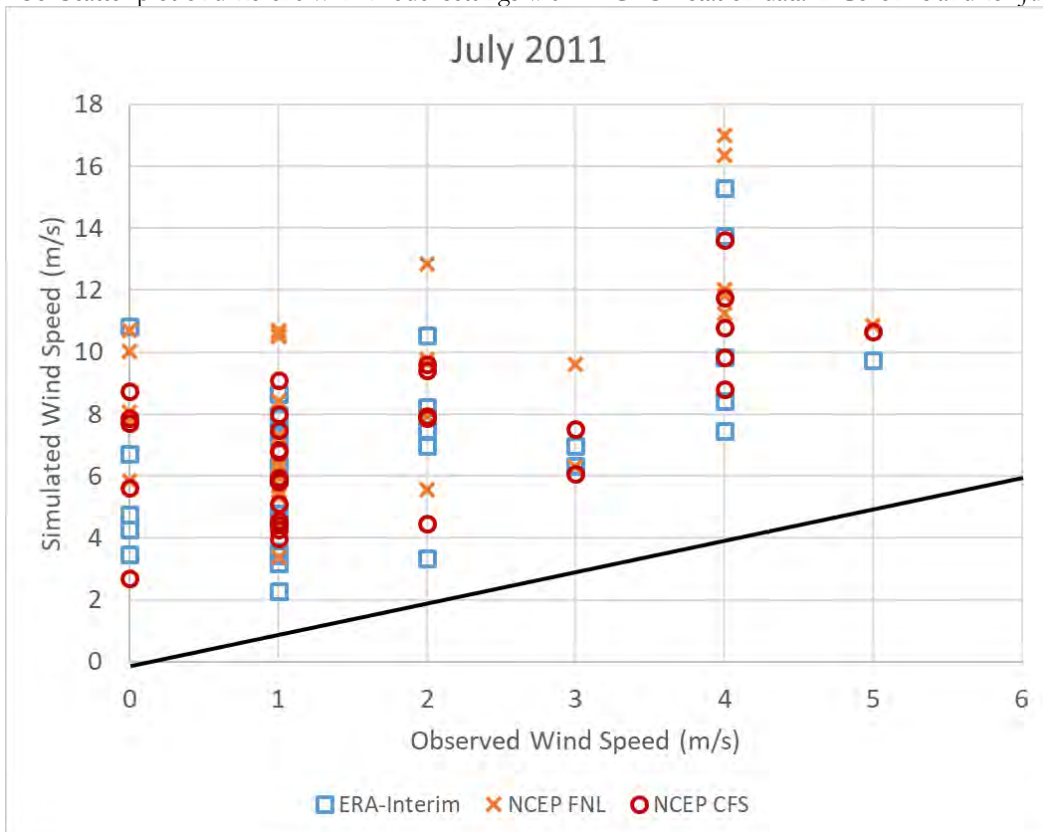


Figure 139. Scatter plot of different WRF model settings with PAGASA station data in Cuyo Island for July 2011.

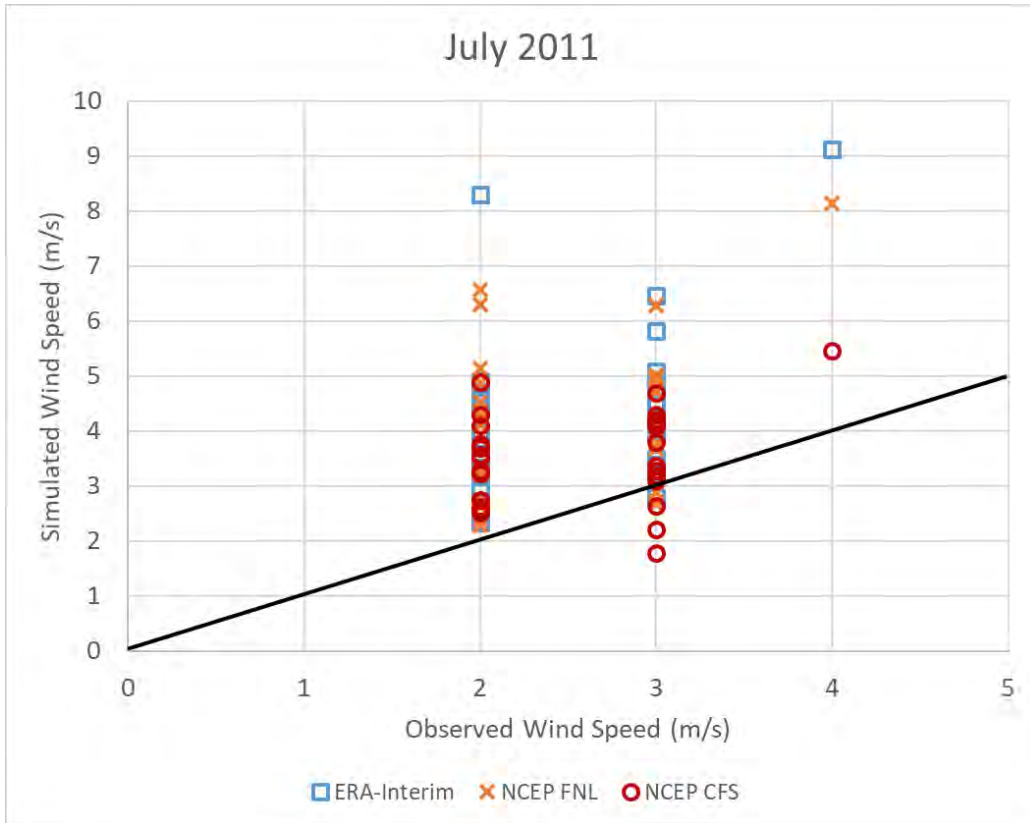


Figure 140. Scatter plot of different WRF model settings with PAGASA station data in Puerto Princesa for July 2011.

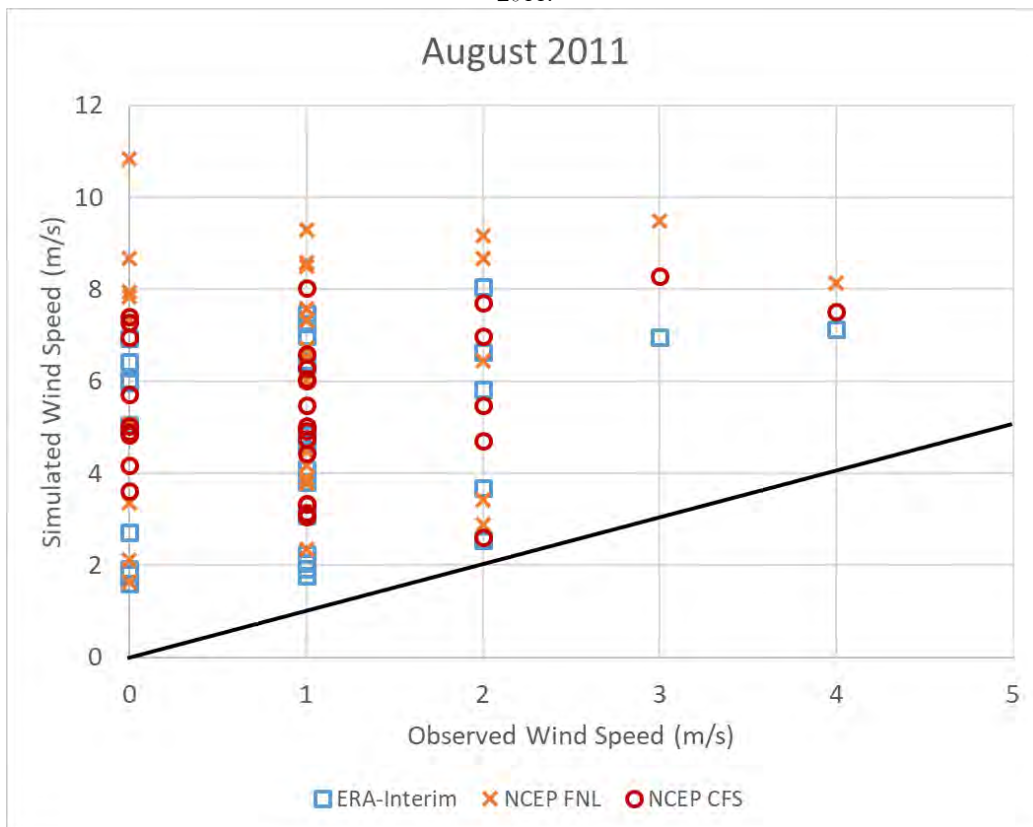


Figure 141. Scatter plot of different WRF model settings with PAGASA station data in Coron Island for August 2011.

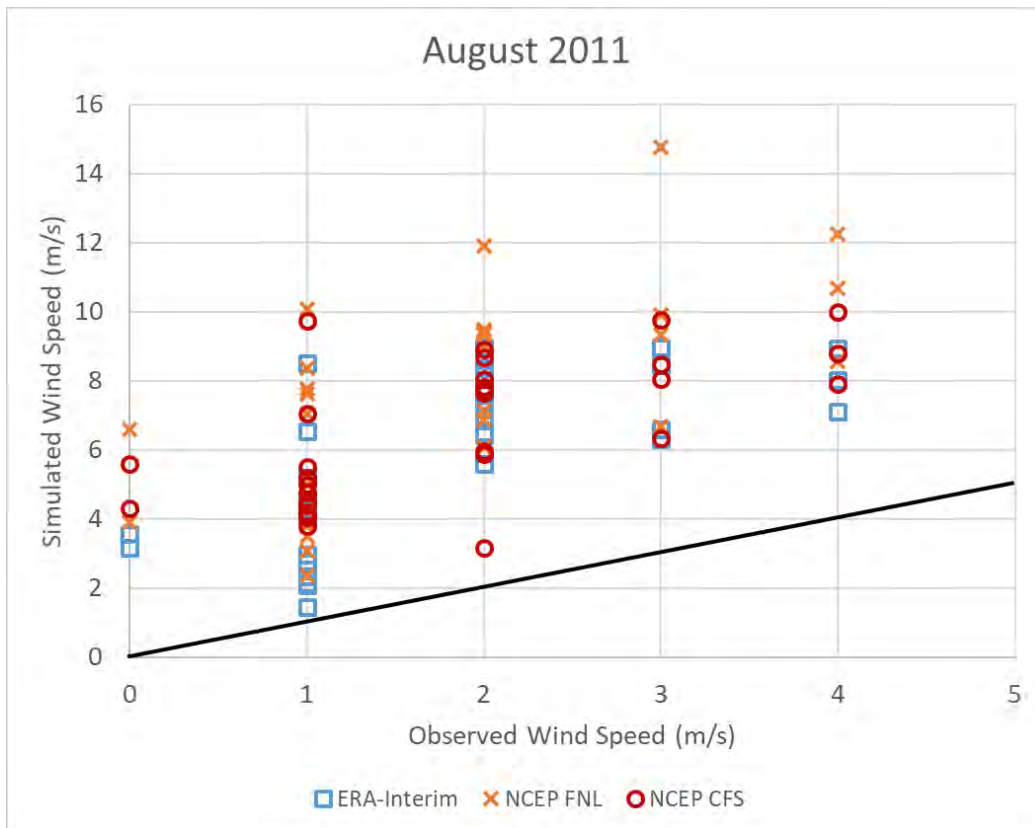


Figure 142. Scatter plot of different WRF model settings with PAGASA station data in Cuyo Island for August 2011.

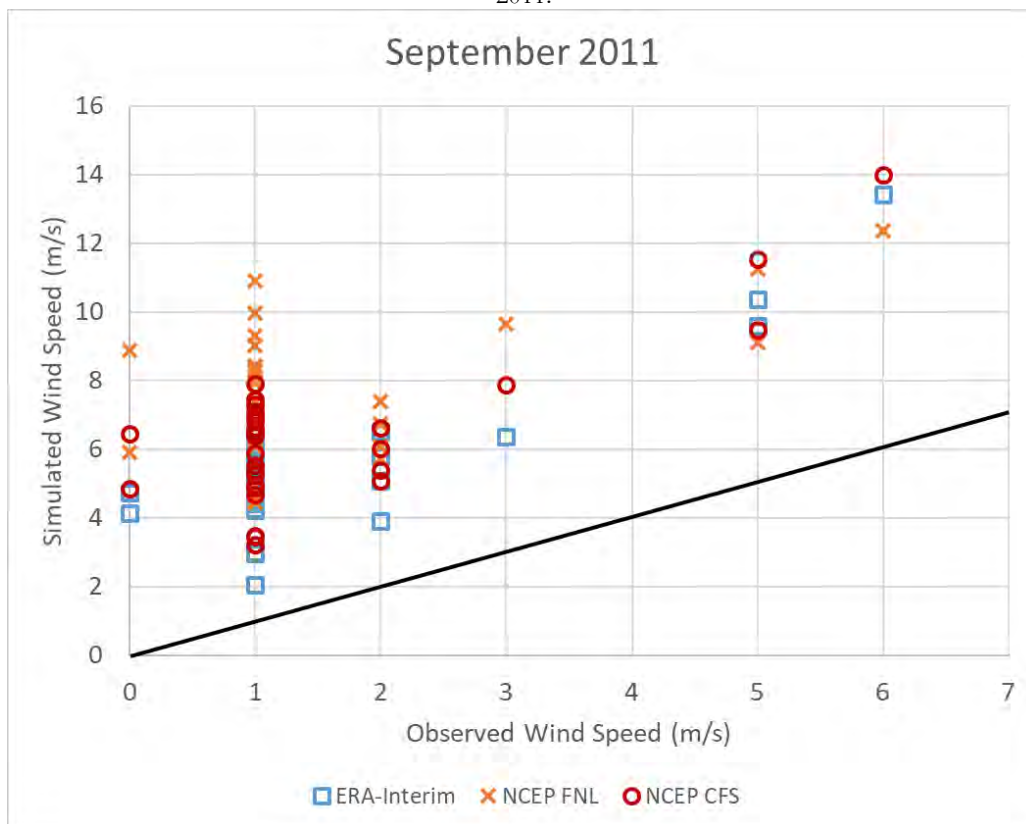


Figure 143. Scatter plot of different WRF model settings with PAGASA station data in Coron Island for September 2011.

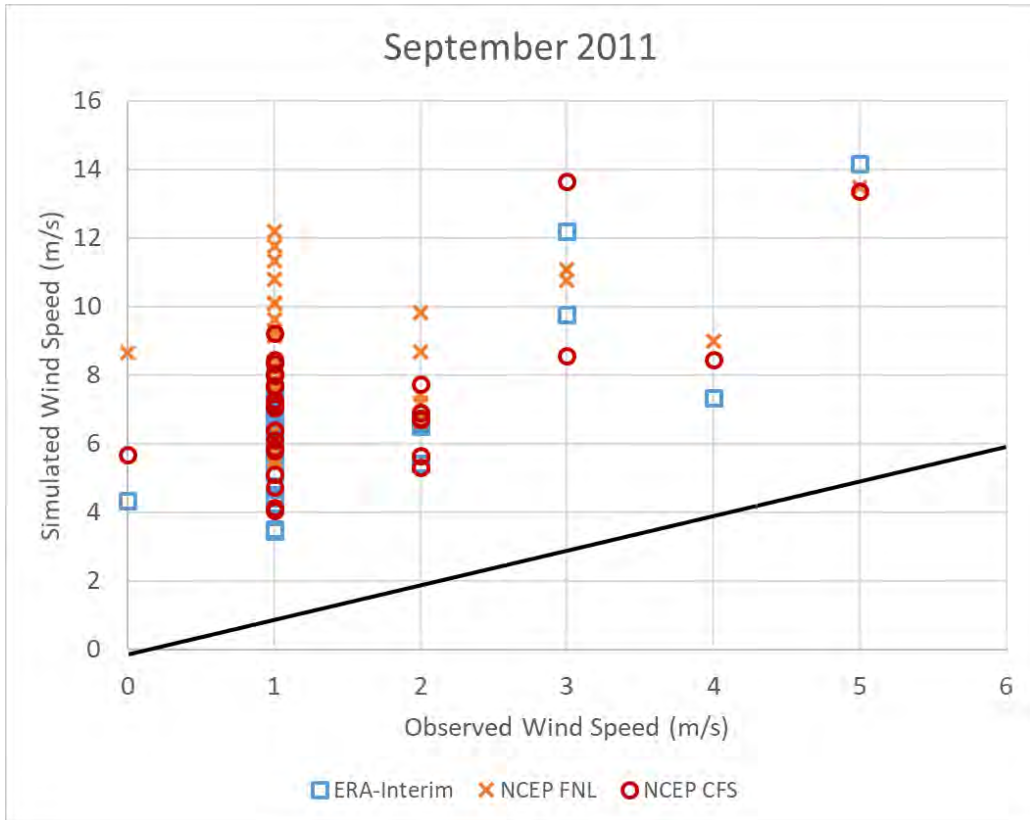


Figure 144. Scatter plot of different WRF model settings with PAGASA station data in Cuyo Island for September 2011.

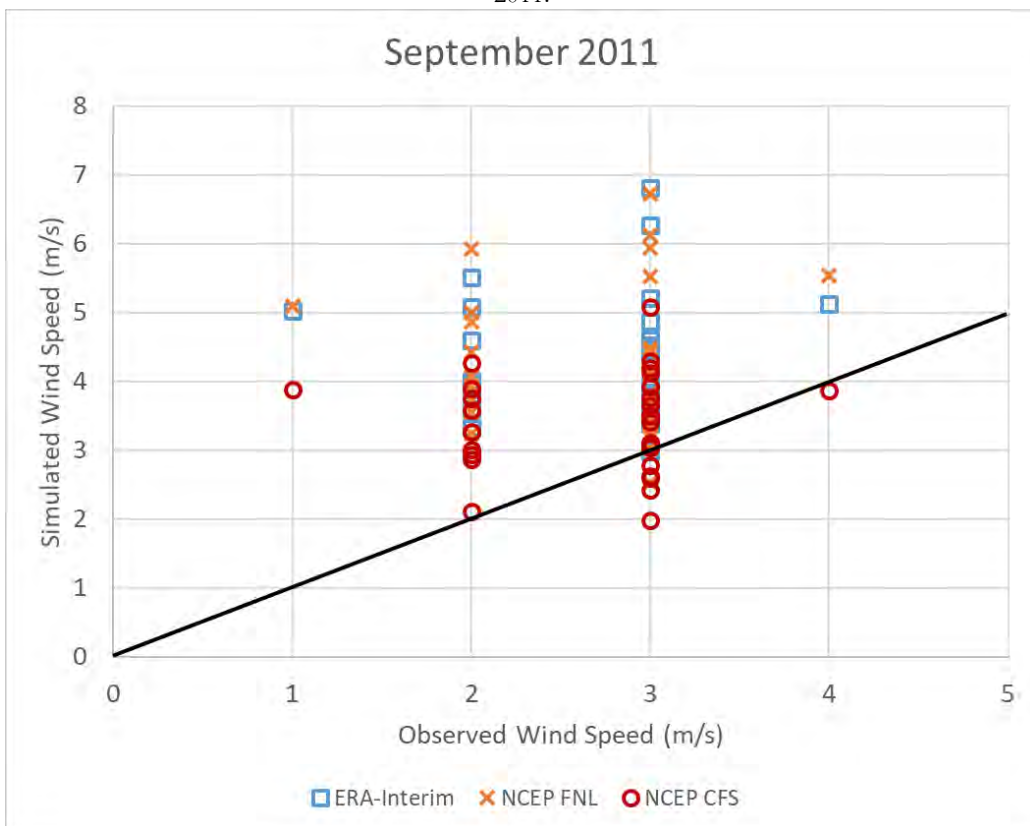


Figure 145. Scatter plot of different WRF model settings with PAGASA station data in Puerto Princesa for September 2011.

Figure 142

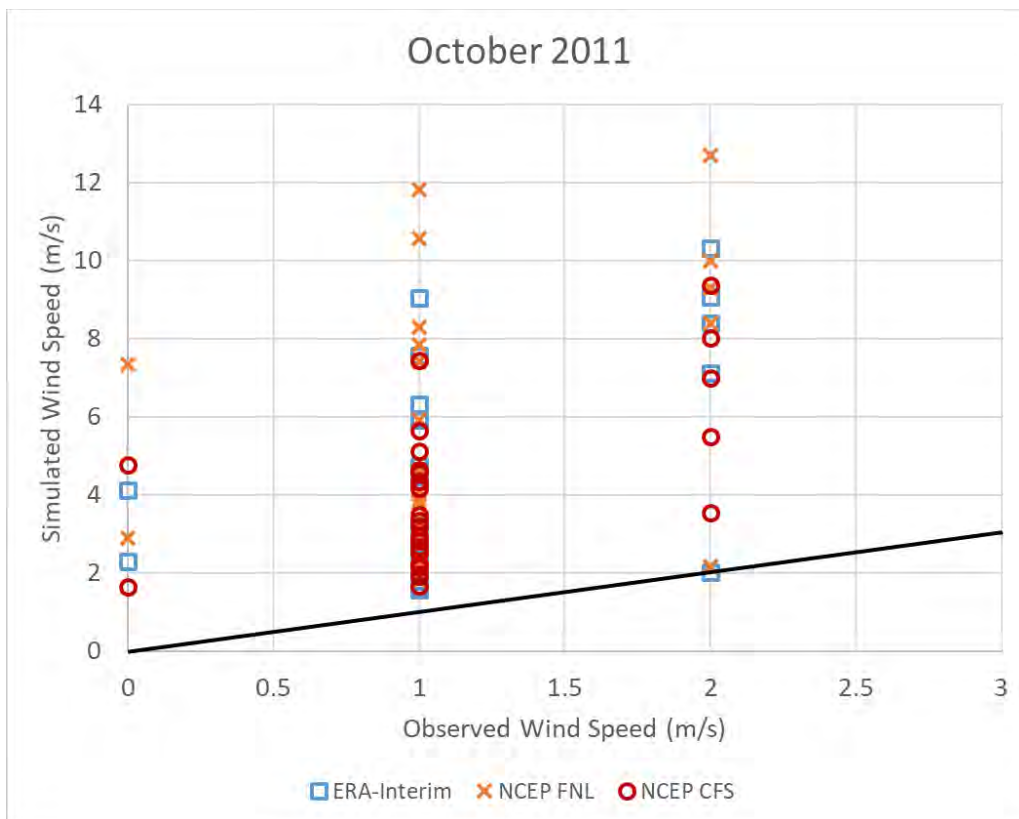


Figure 146. Scatter plot of different WRF model settings with PAGASA station data in Coron Island for October 2011.

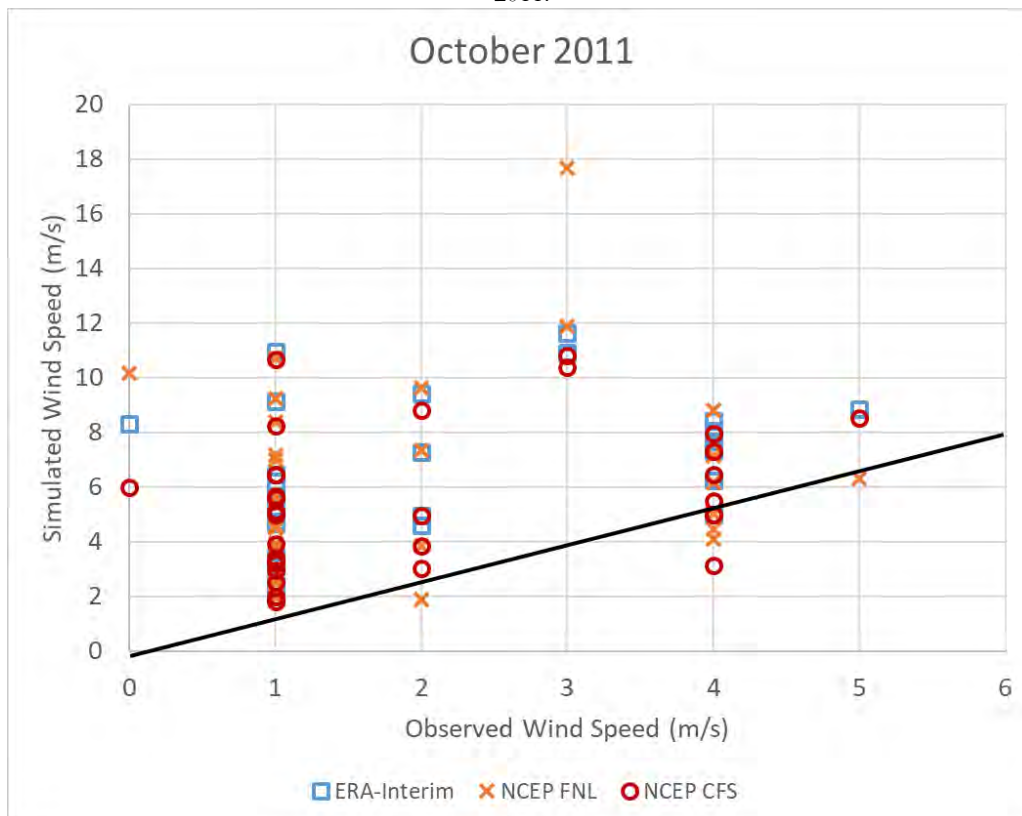


Figure 147. Scatter plot of different WRF model settings with PAGASA station data in Cuyo Island for October 2011.

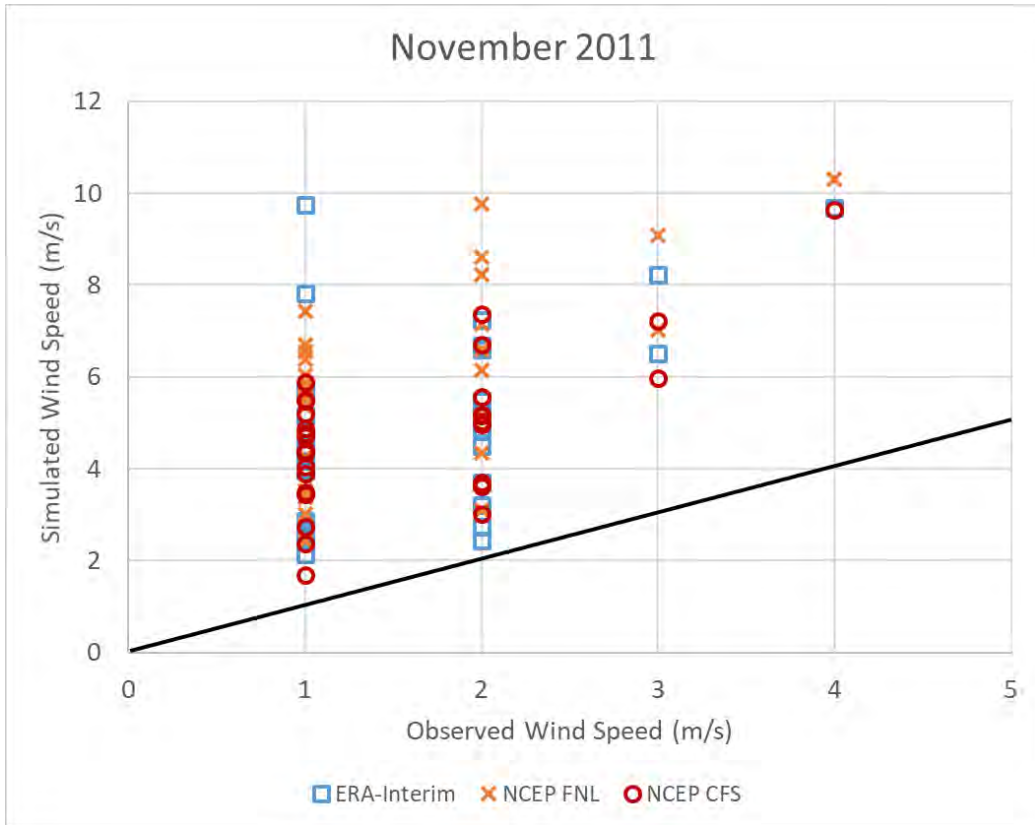


Figure 148. Scatter plot of different WRF model settings with PAGASA station data in Coron Island for November 2011.

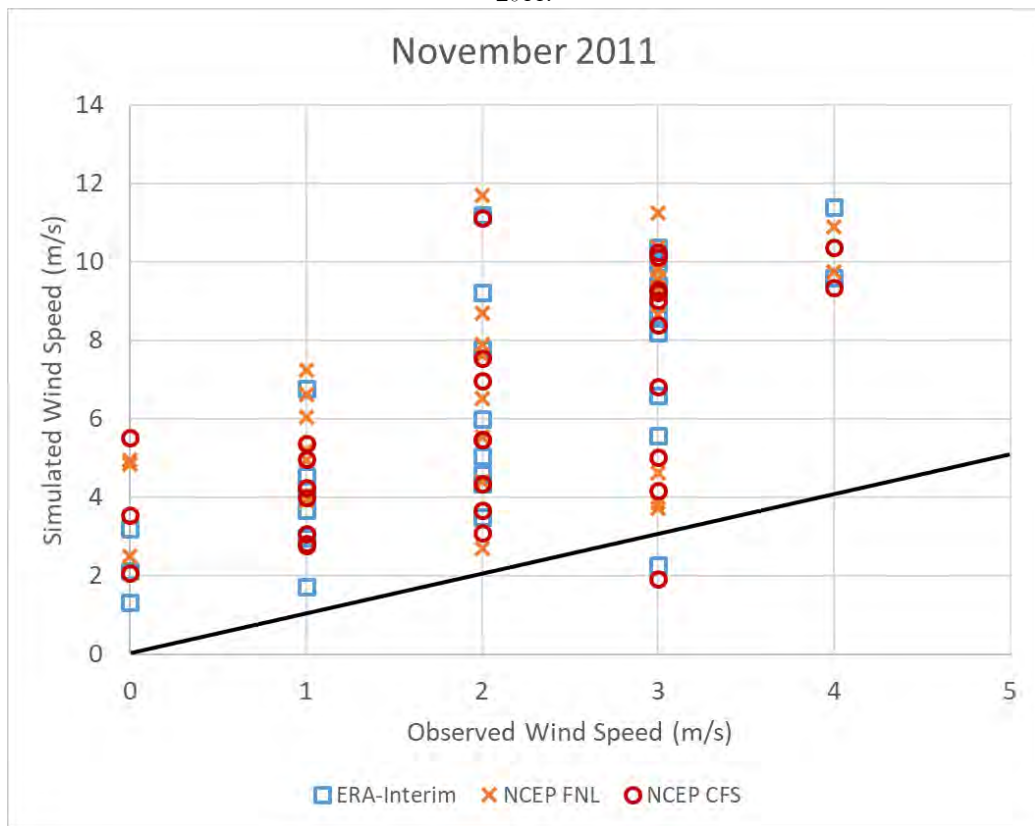


Figure 149. Scatter plot of different WRF model settings with PAGASA station data in Cuyo Island for November 2011.

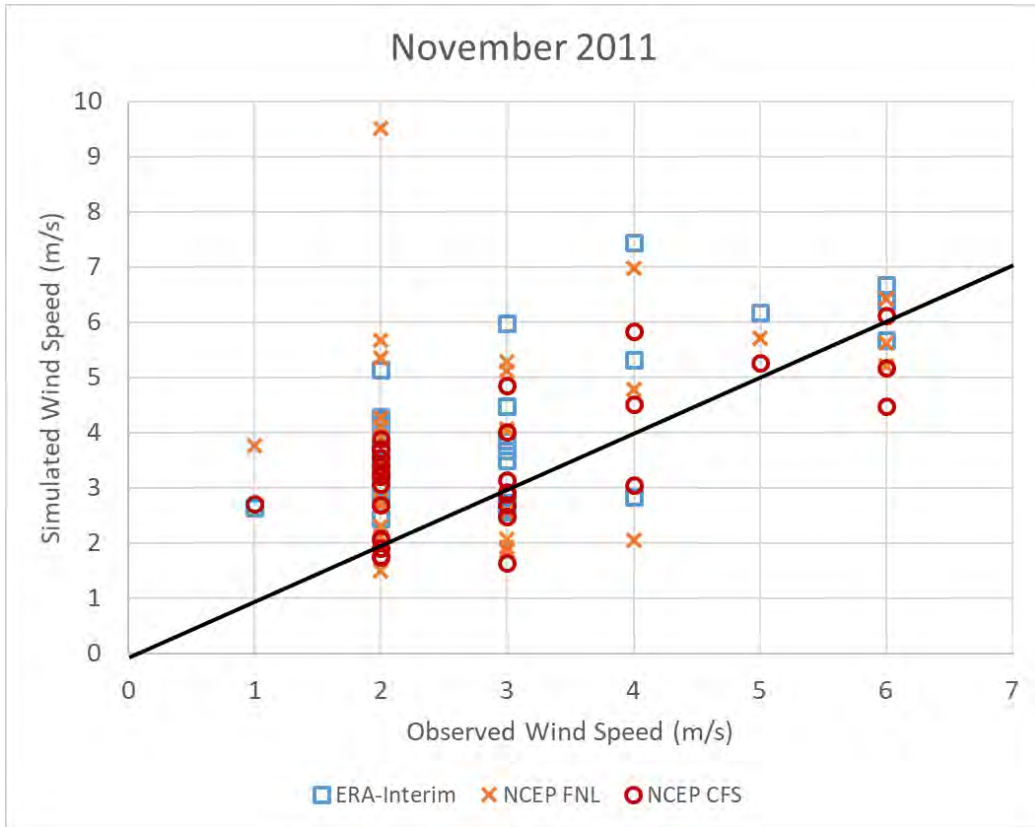


Figure 150. Scatter plot of different WRF model settings with PAGASA station data in Puerto Princesa for November 2011.

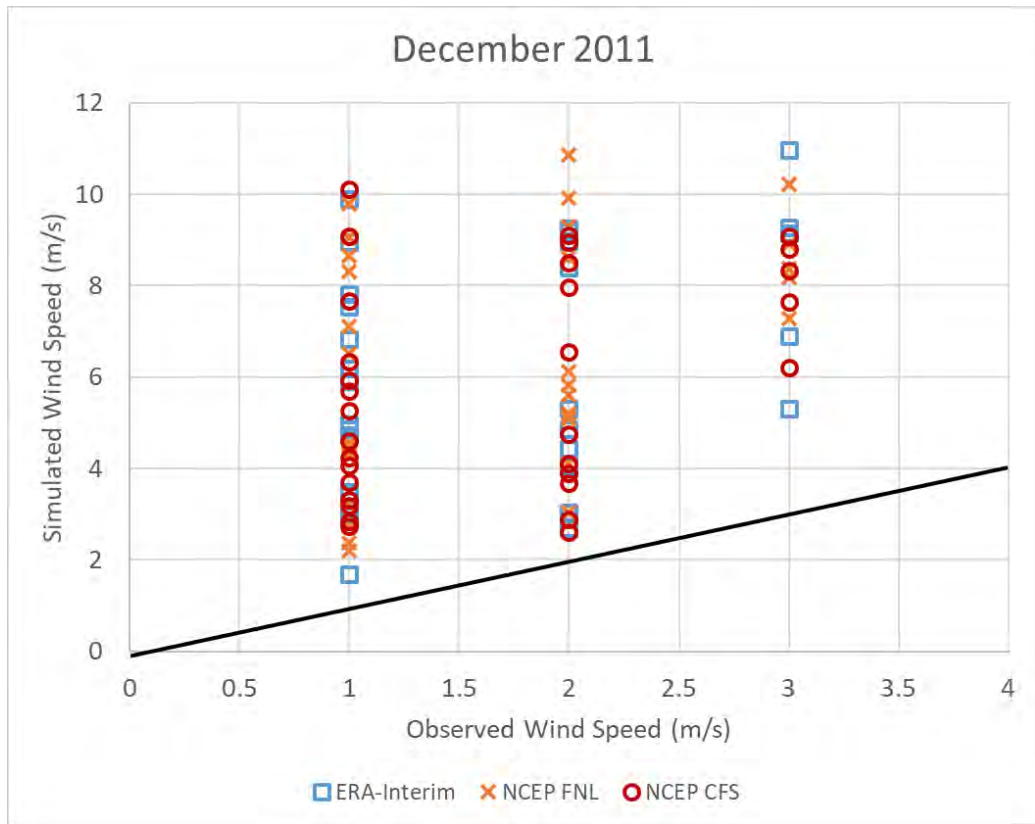


Figure 151. Scatter plot of different WRF model settings with PAGASA station data in Coron Island for December 2011.

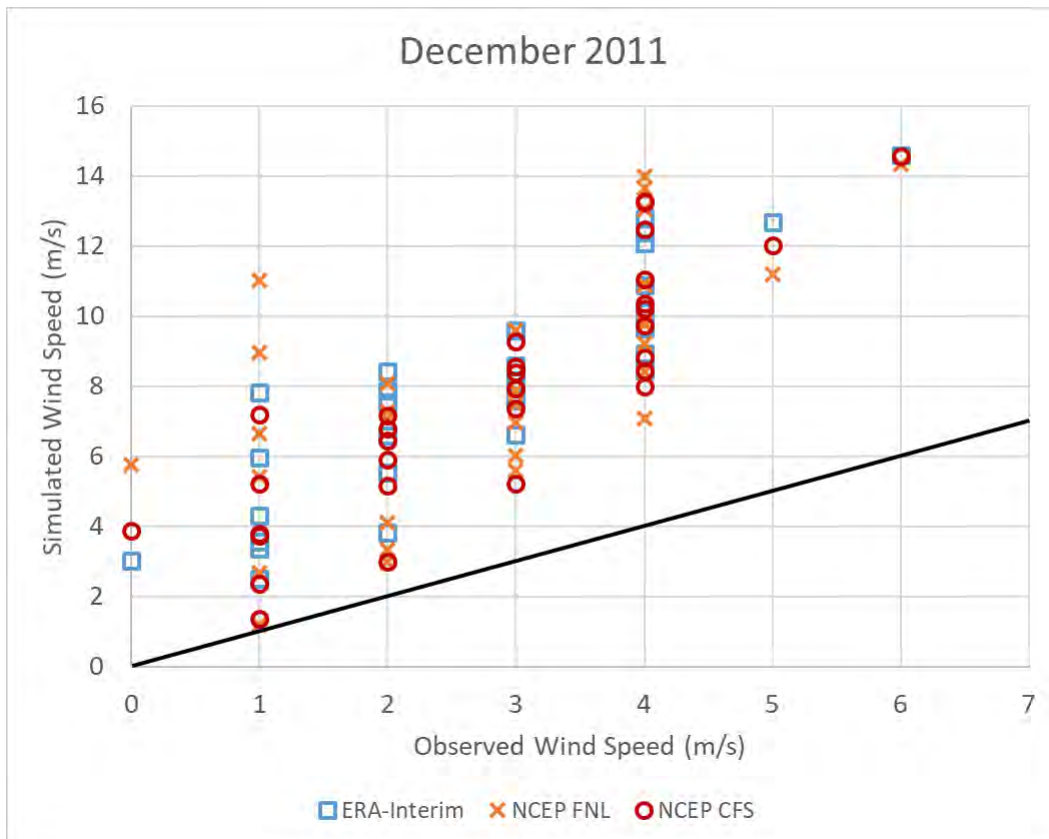


Figure 152. Scatter plot of different WRF model settings with PAGASA station data in Cuyo Island for December 2011.

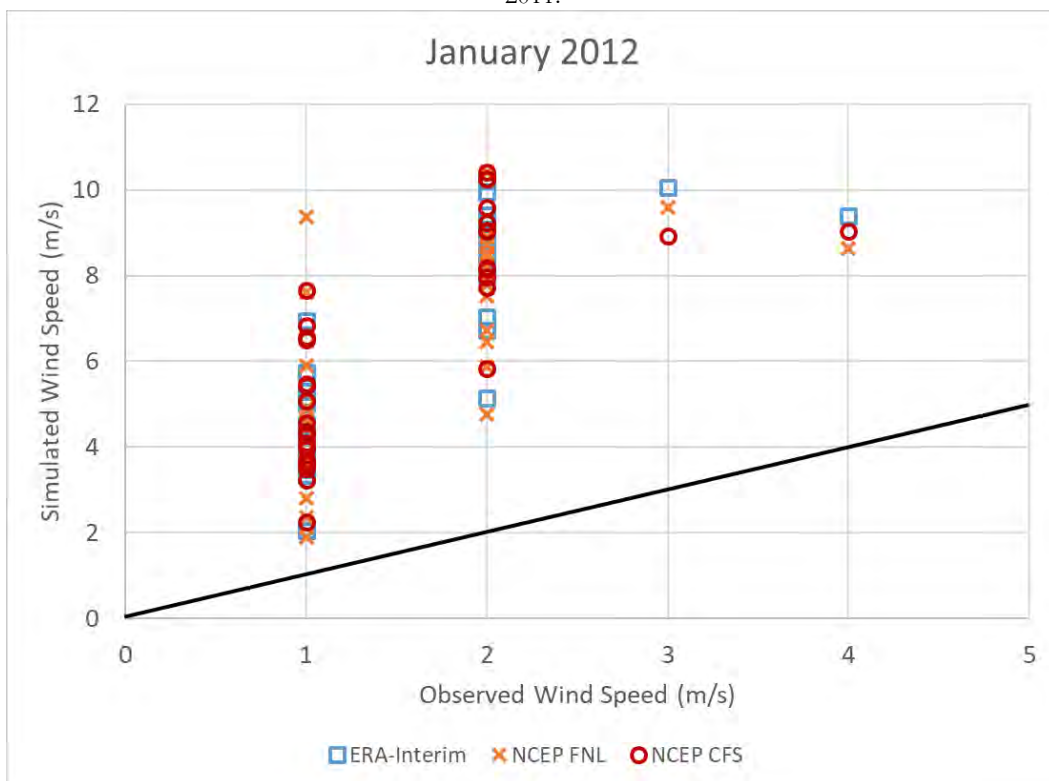


Figure 153. Scatter plot of different WRF model settings with PAGASA station data in Coron Island for January 2012.

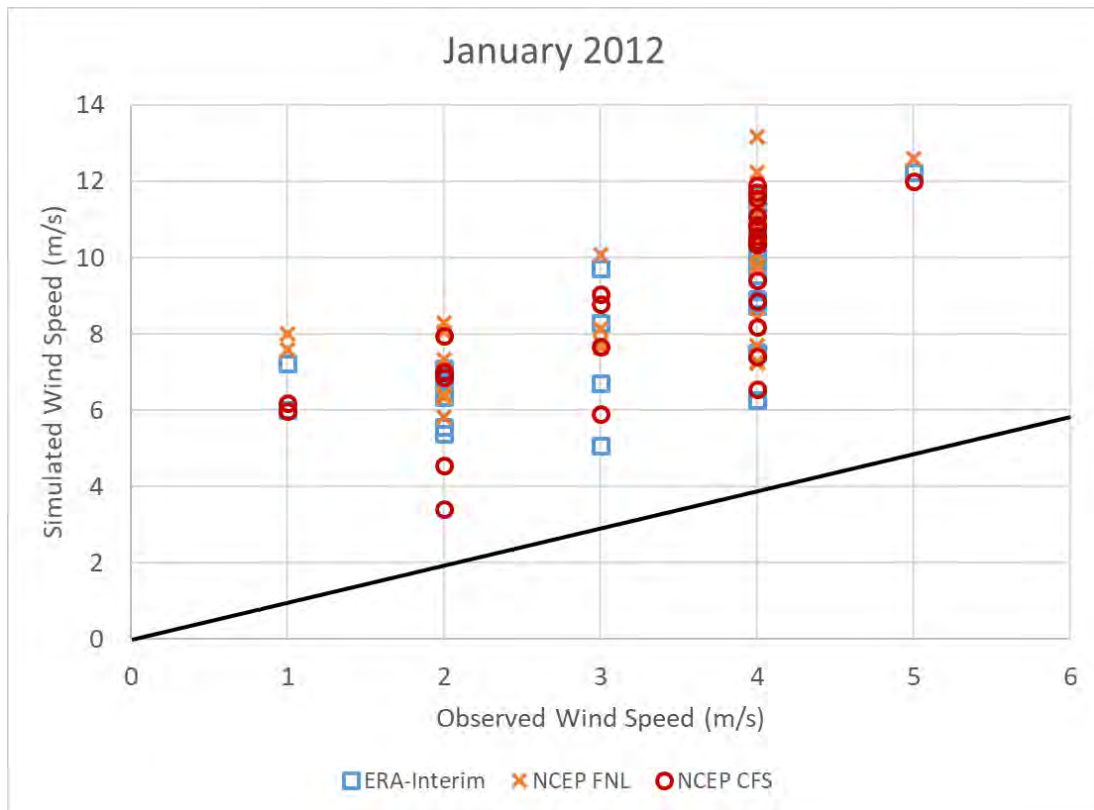


Figure 154. Scatter plot of different WRF model settings with PAGASA station data in Cuyo Island for January 2012.

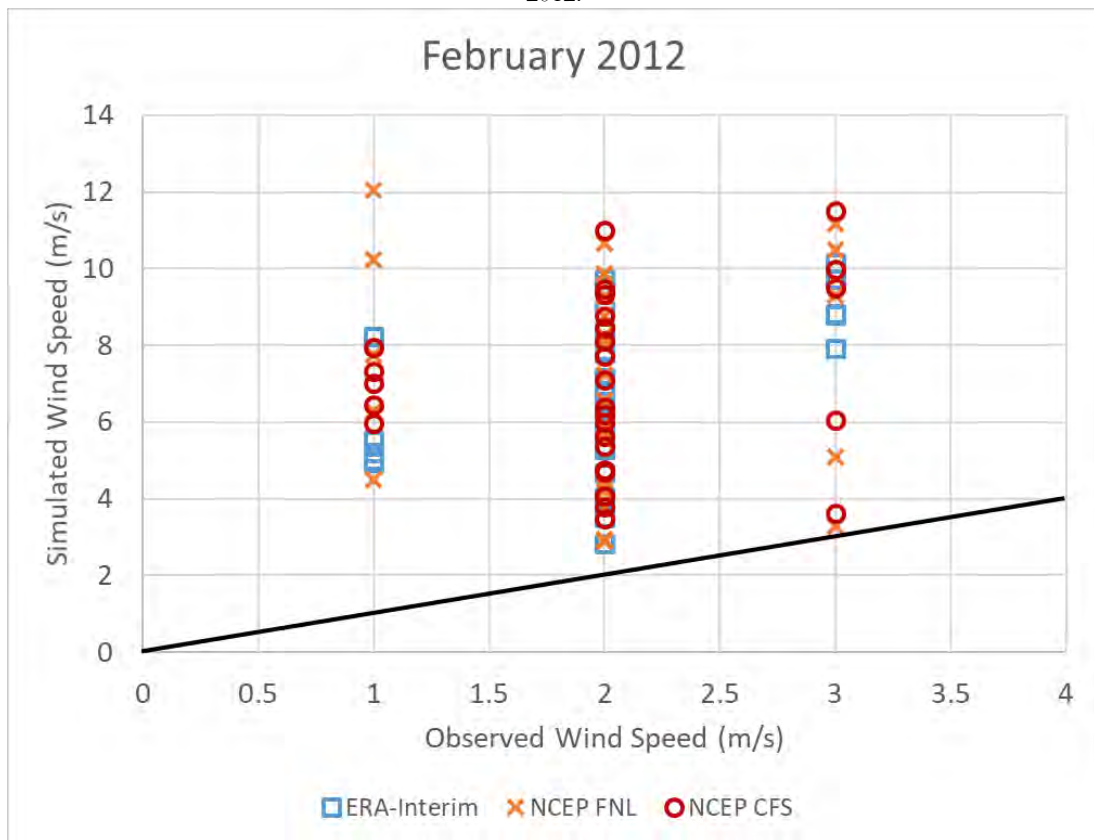


Figure 155. Scatter plot of different WRF model settings with PAGASA station data in Coron Island for February 2012.

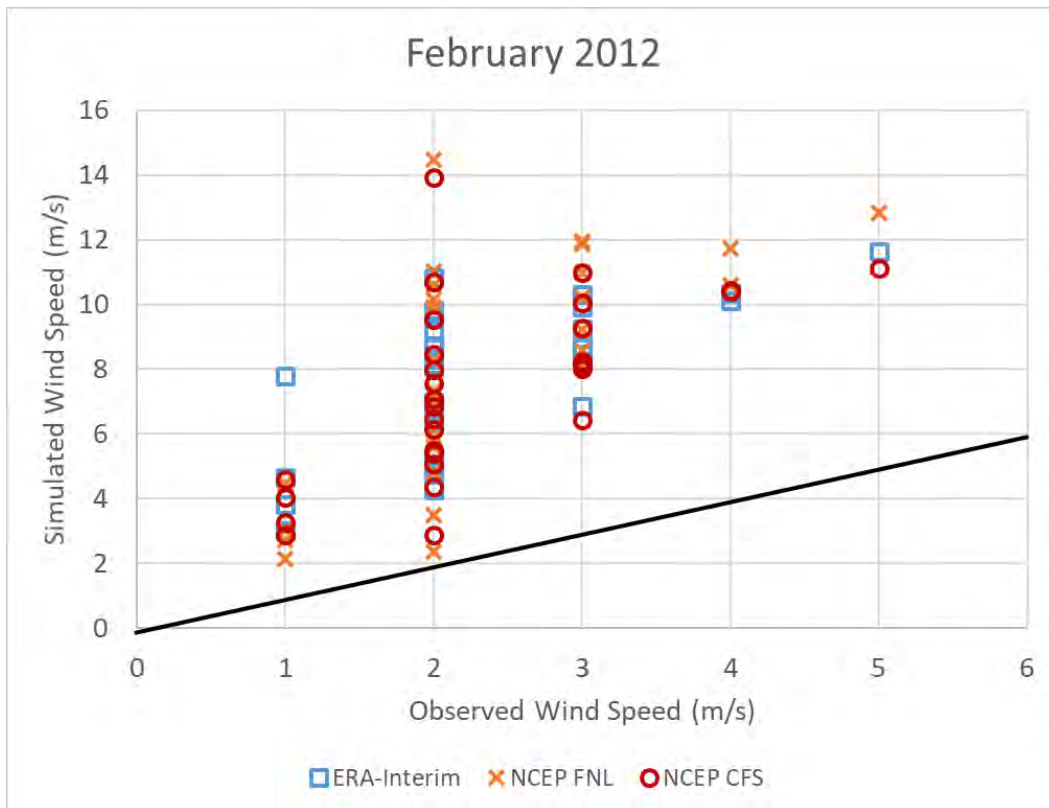


Figure 156. Scatter plot of different WRF model settings with PAGASA station data in Cuyo Island for February 2012.



Figure 157. Scatter plot of different WRF model settings with PAGASA station data in Coron Island for March 2012.

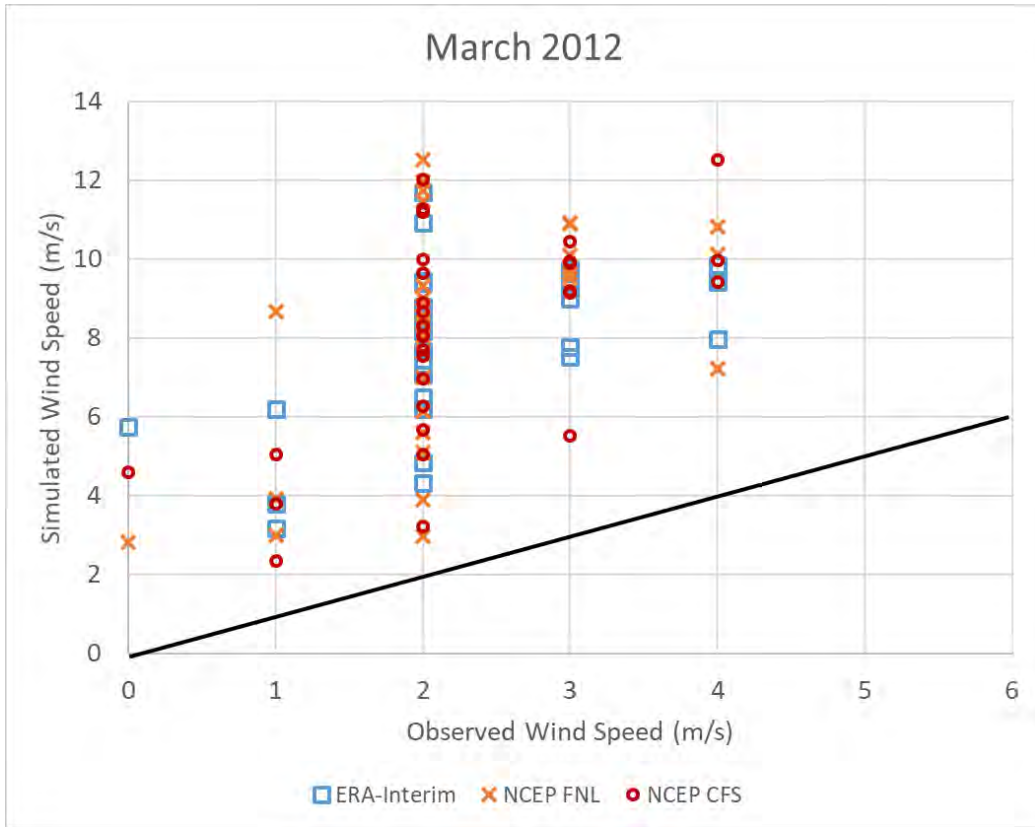


Figure 158. Scatter plot of different WRF model settings with PAGASA station data in Cuyo Island for March 2012.

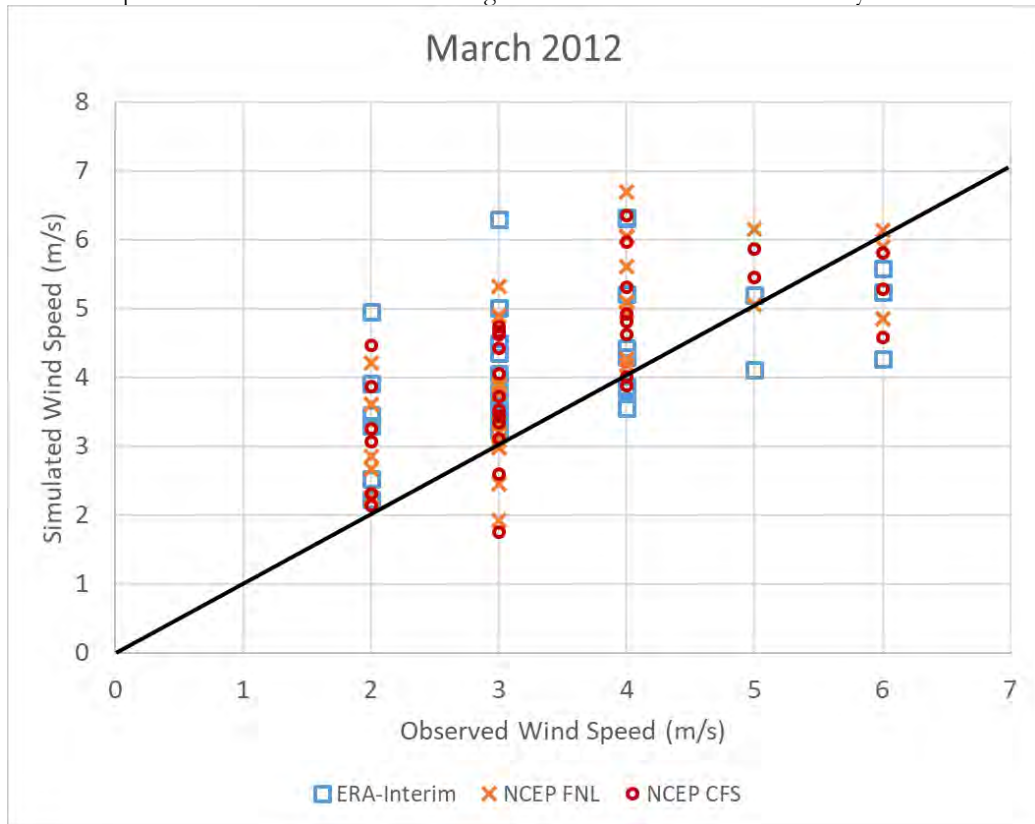


Figure 159. Scatter plot of different WRF model settings with PAGASA station data in Puerto Princesa for March 2012.

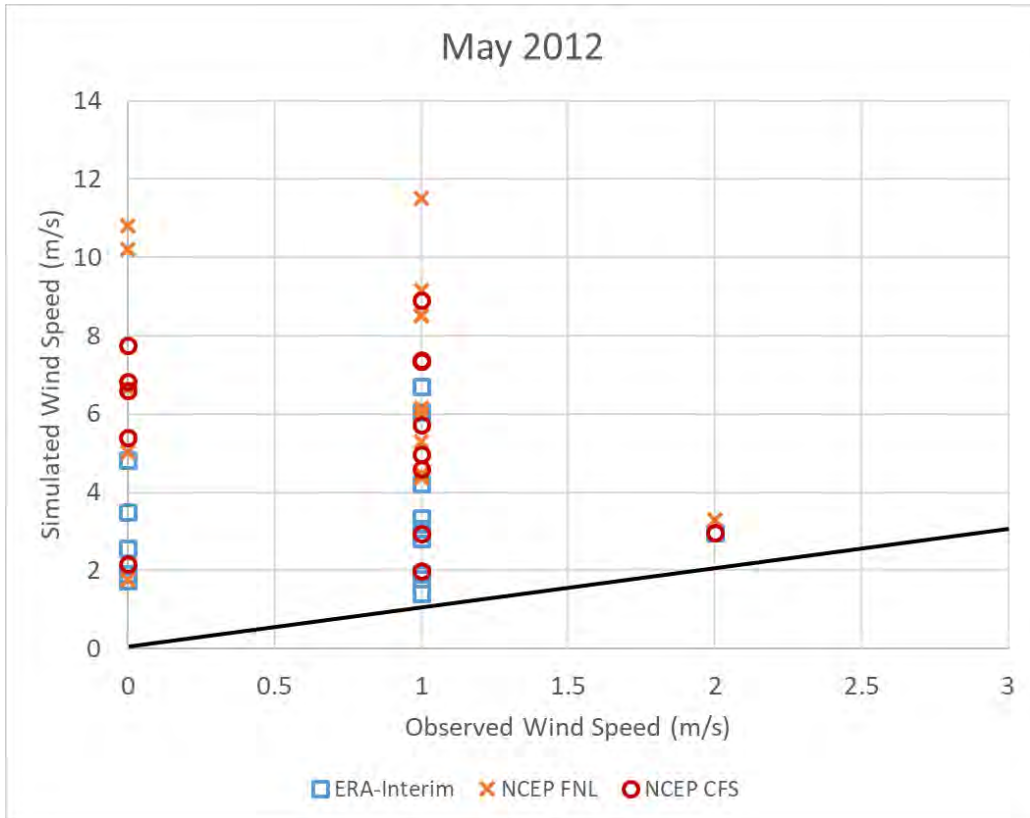


Figure 160. Scatter plot of different WRF model settings with PAGASA station data in Cuyo Island for May 2012.

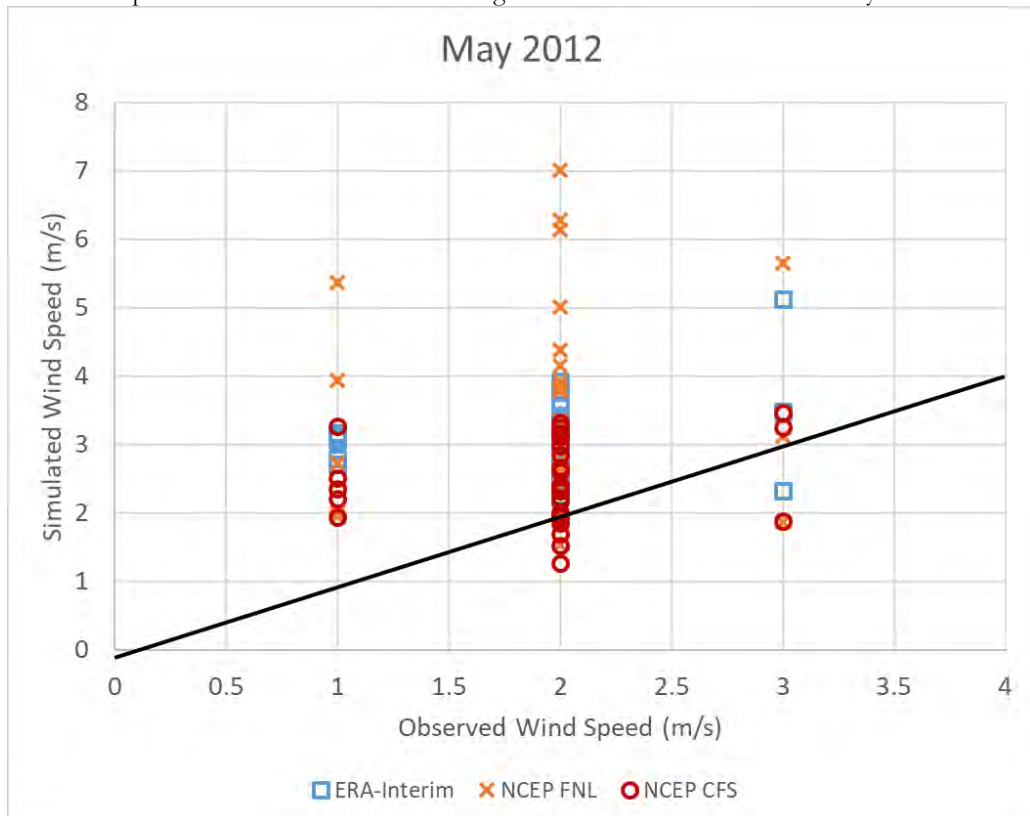


Figure 161. Scatter plot of different WRF model settings with PAGASA station data in Puerto Princesa for May 2012.

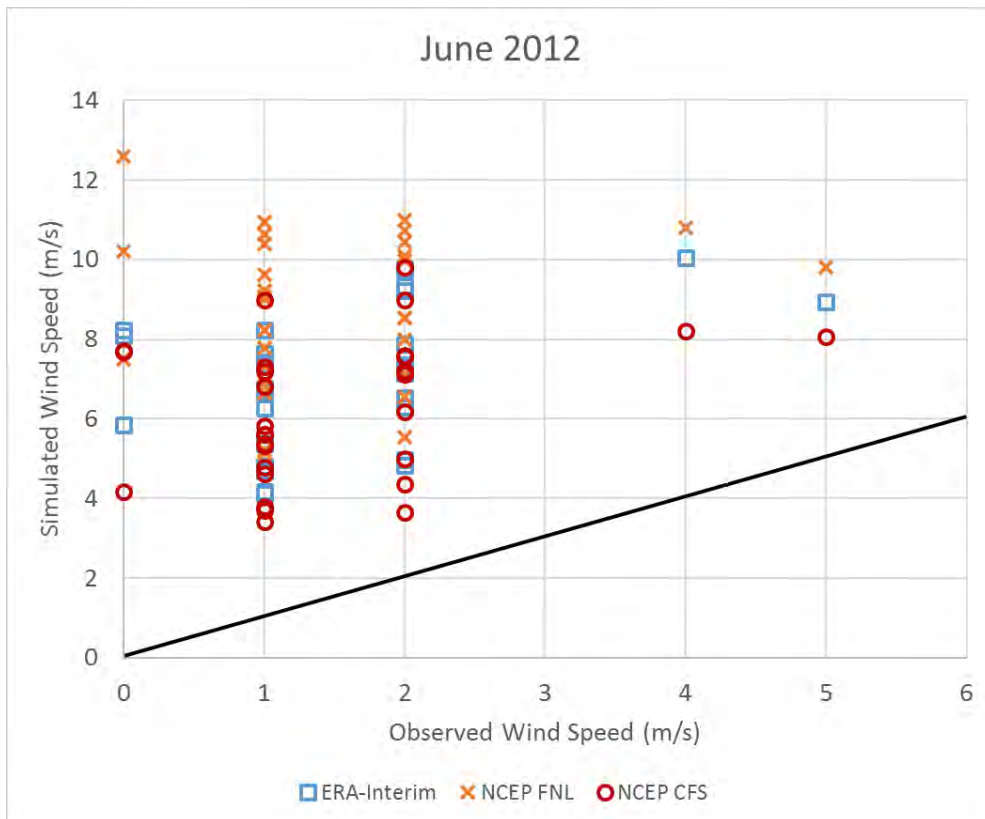


Figure 162. Scatter plot of different WRF model settings with PAGASA station data in Coron Island for June 2012.

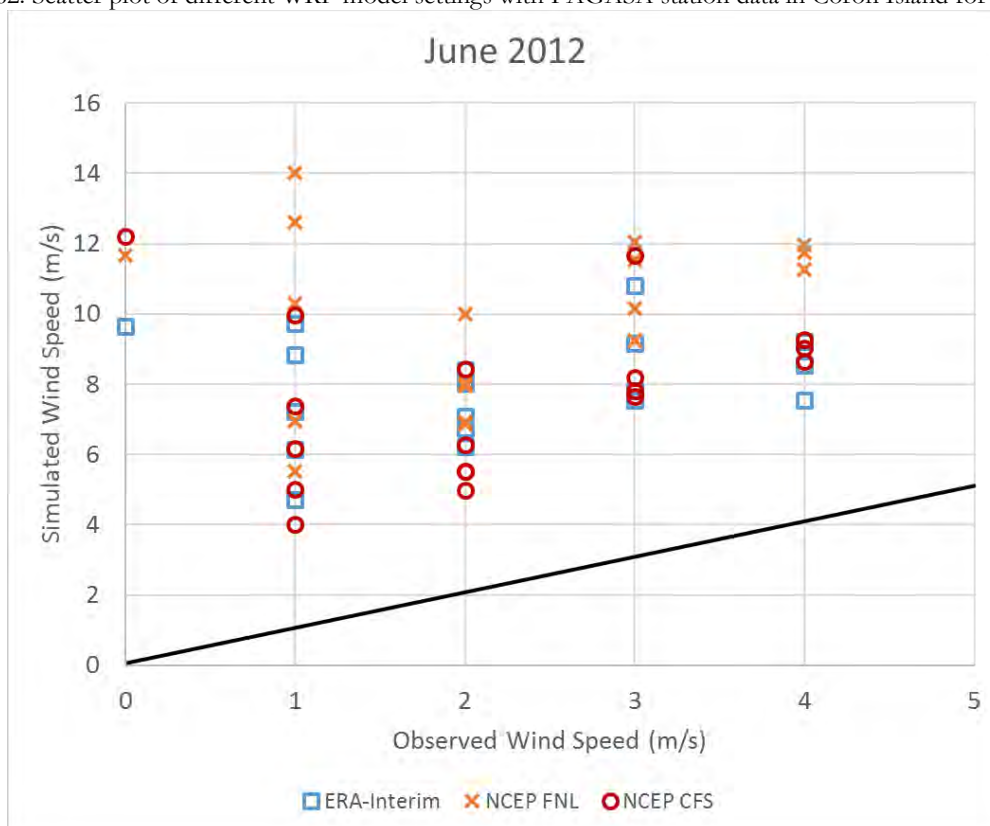


Figure 163. Scatter plot of different WRF model settings with PAGASA station data in Cuyo Island for June 2012.

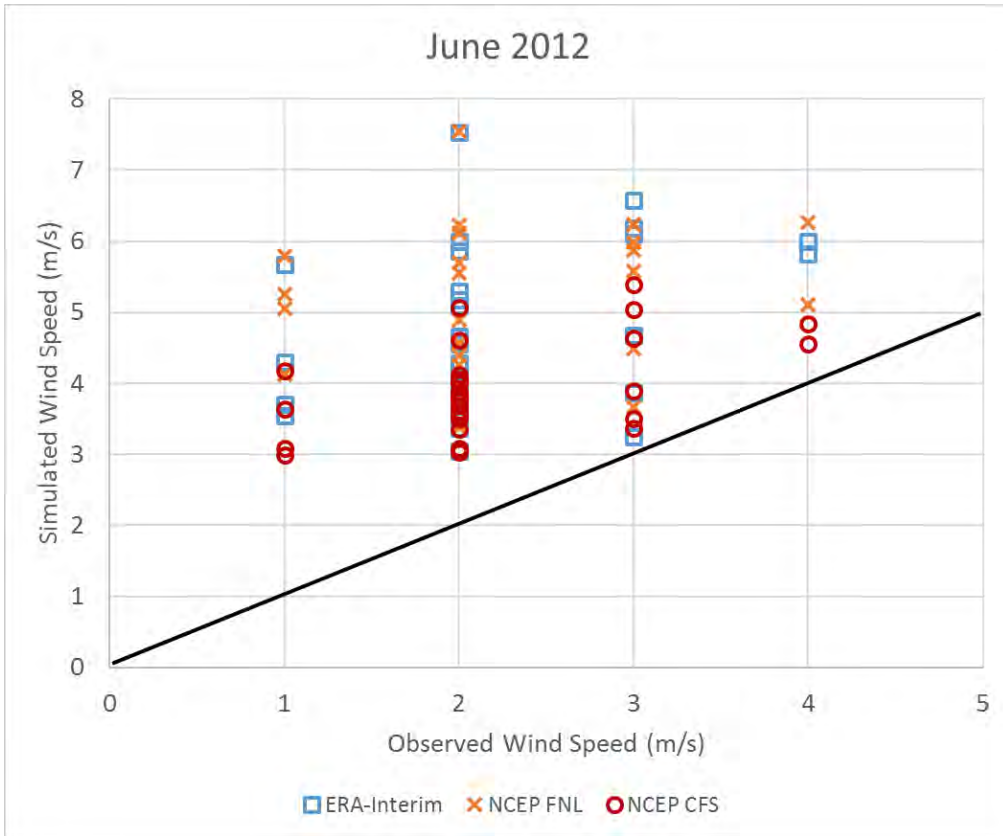


Figure 164. Scatter plot of different WRF model settings with PAGASA station data in Puerto Princesa for June 2012.

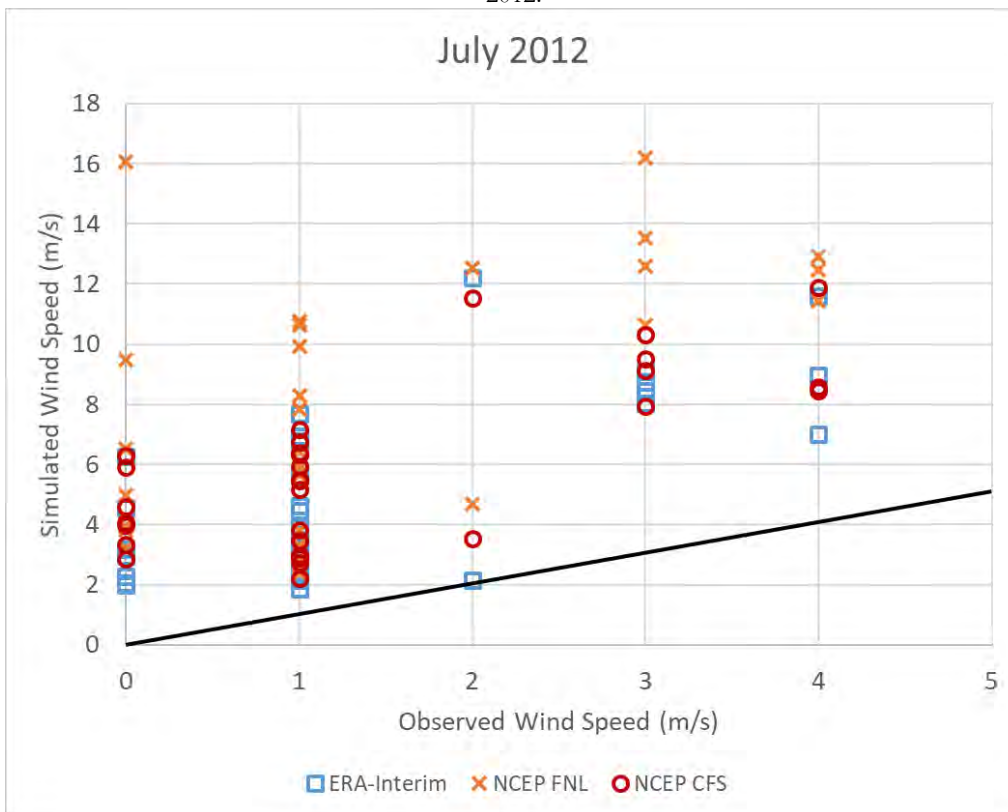


Figure 165. Scatter plot of different WRF model settings with PAGASA station data in Coron Island for July 2012.

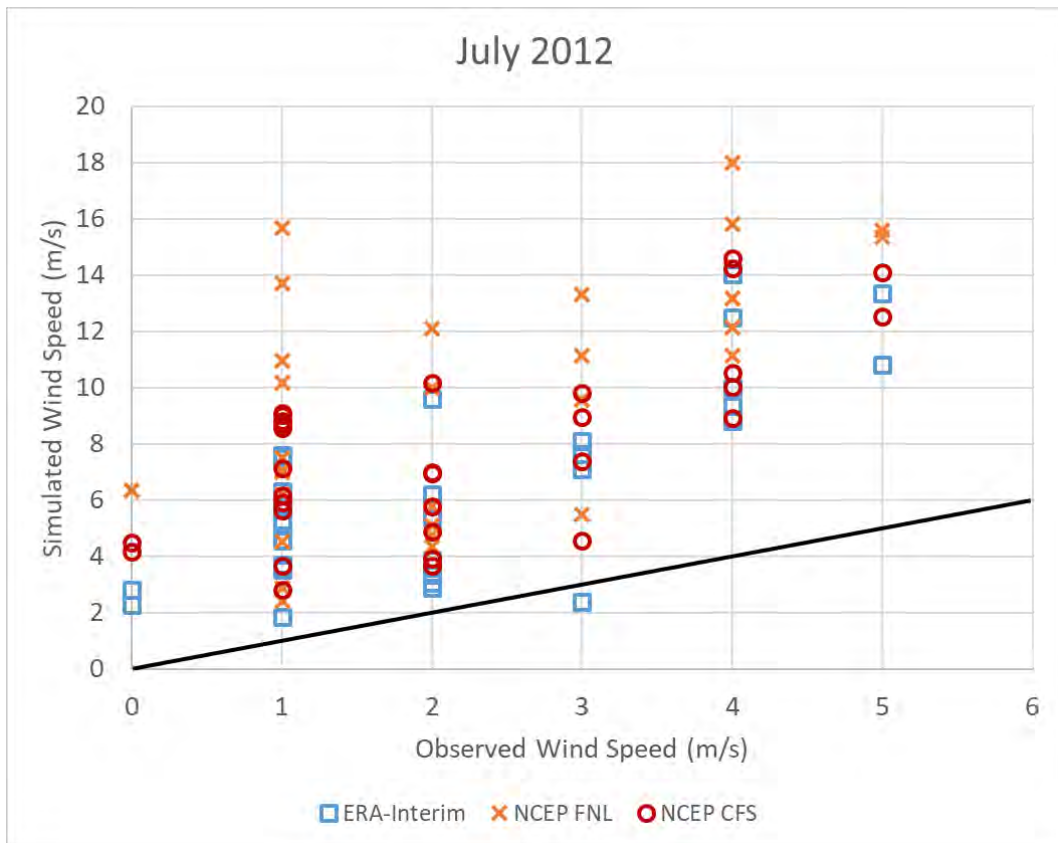


Figure 166. Scatter plot of different WRF model settings with PAGASA station data in Cuyo Island for July 2012.

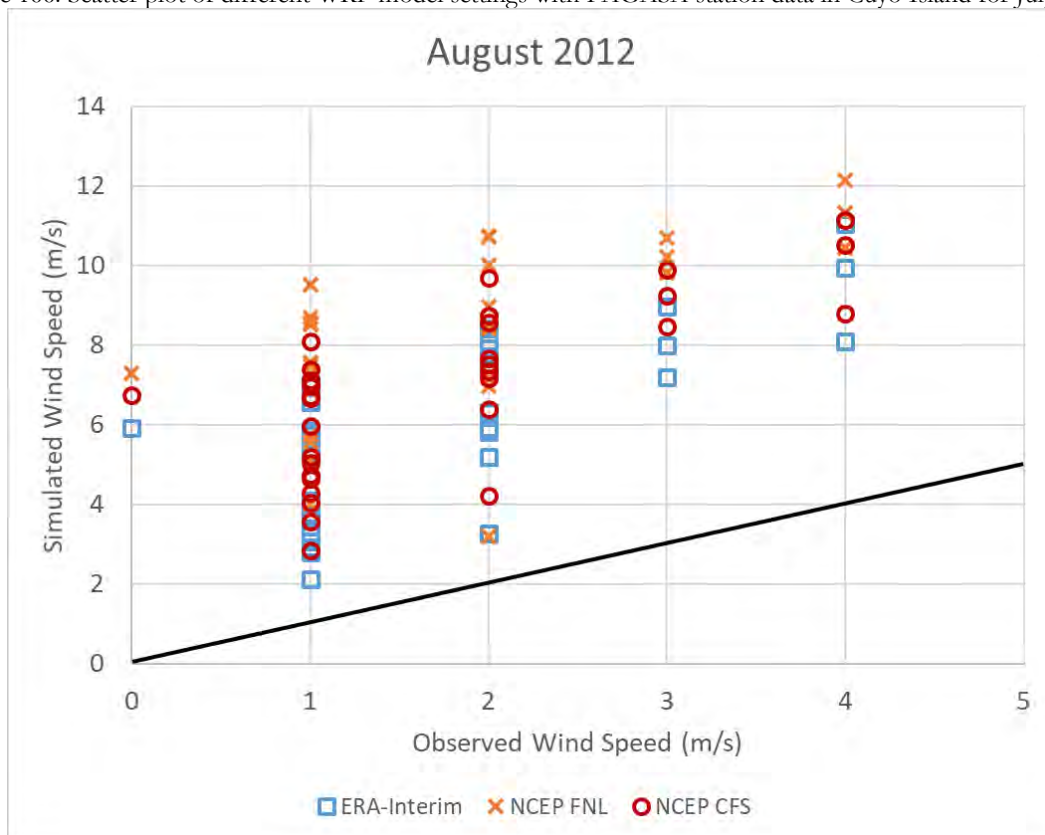


Figure 167. Scatter plot of different WRF model settings with PAGASA station data in Coron Island for August 2012.

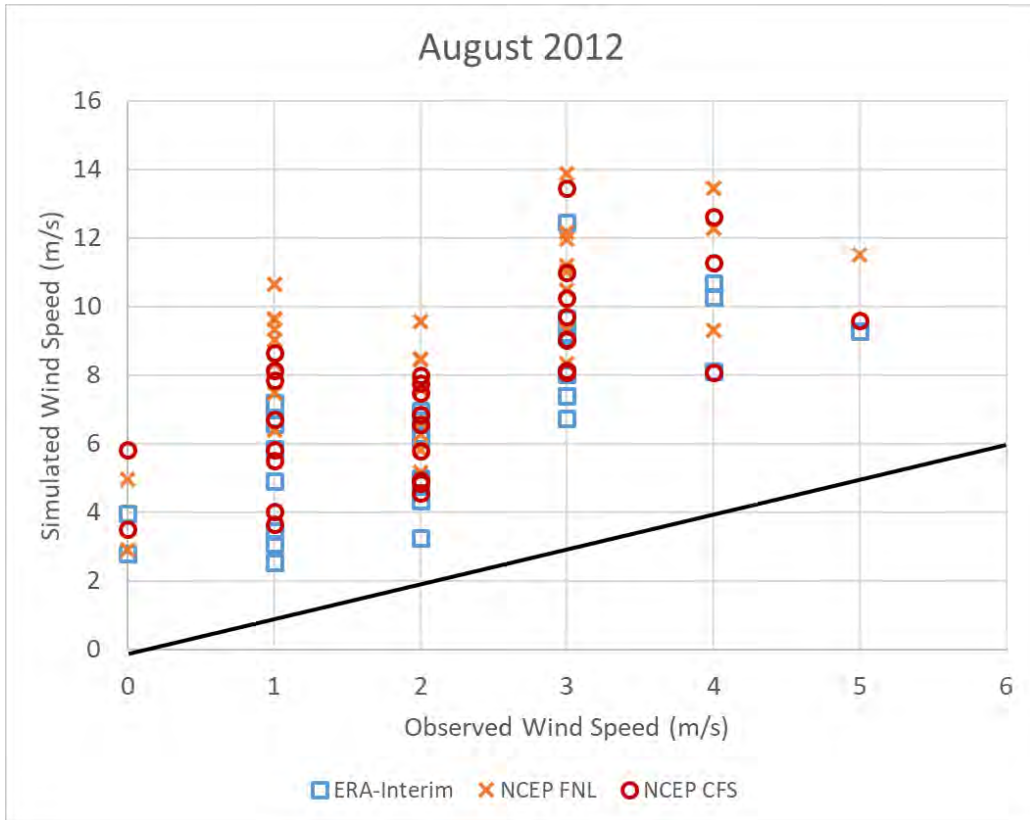


Figure 168. Scatter plot of different WRF model settings with PAGASA station data in Cuyo Island for August 2012.

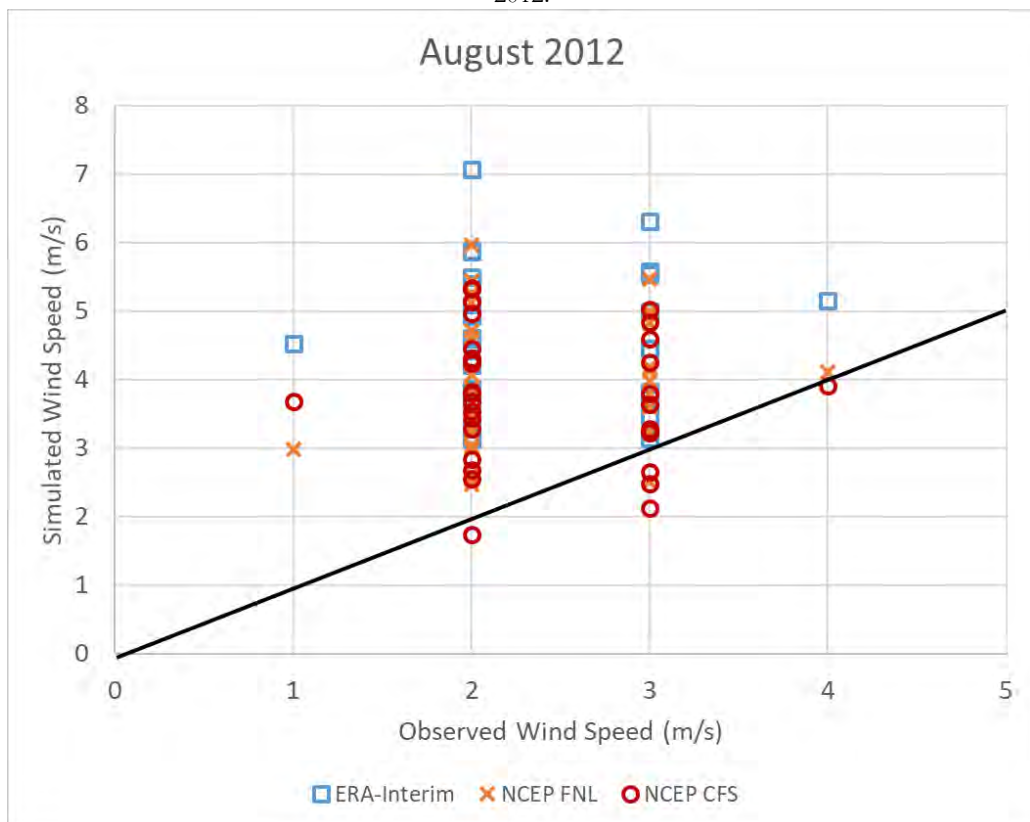


Figure 169. Scatter plot of different WRF model settings with PAGASA station data in Puerto Princesa for August 2012.

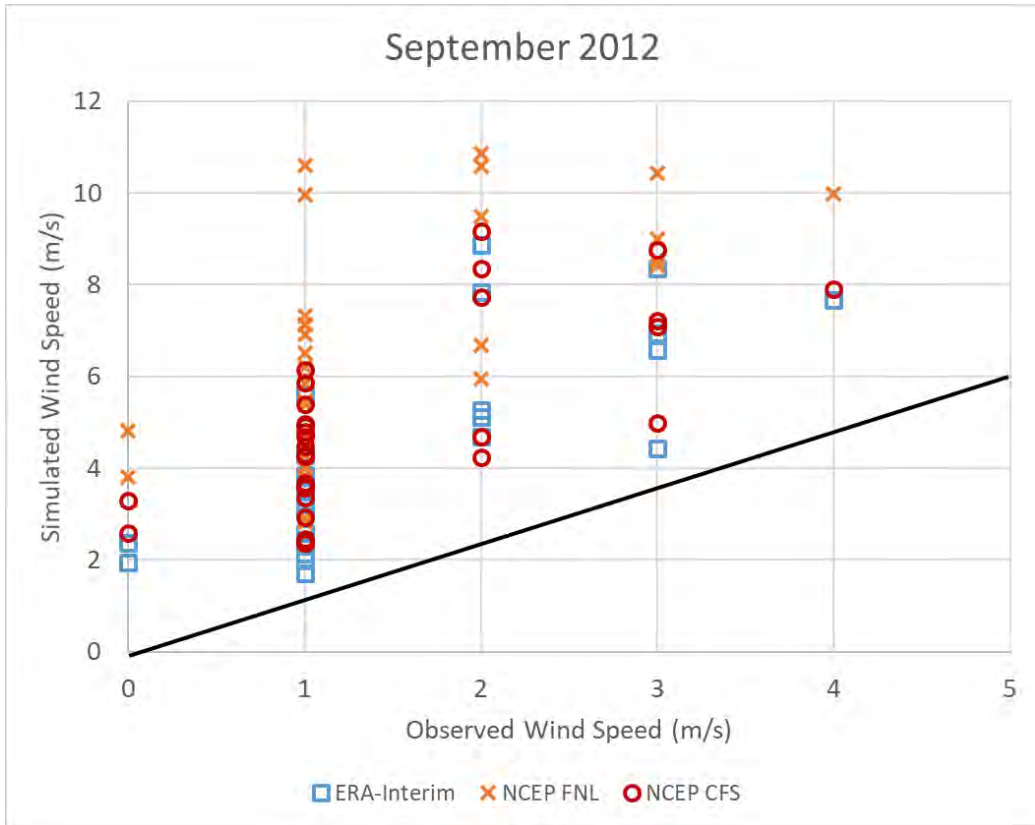


Figure 170. Scatter plot of different WRF model settings with PAGASA station data in Coron Island for September 2012.

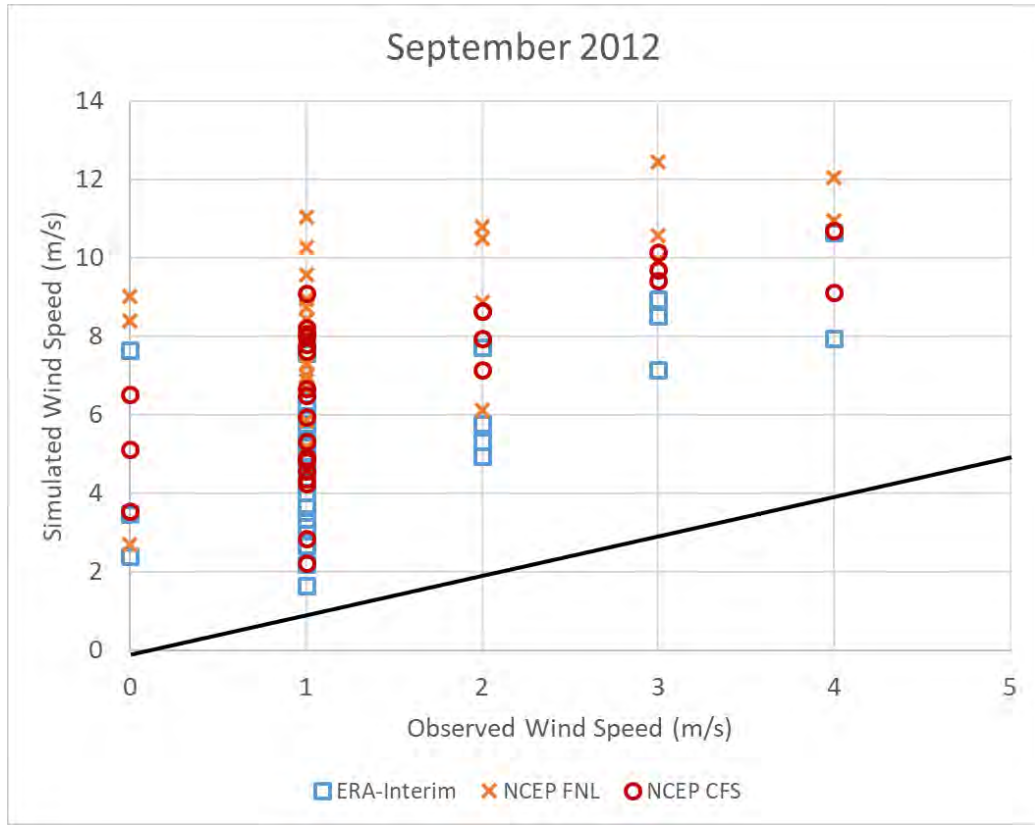


Figure 171. Scatter plot of different WRF model settings with PAGASA station data in Cuyo Island for September 2012.

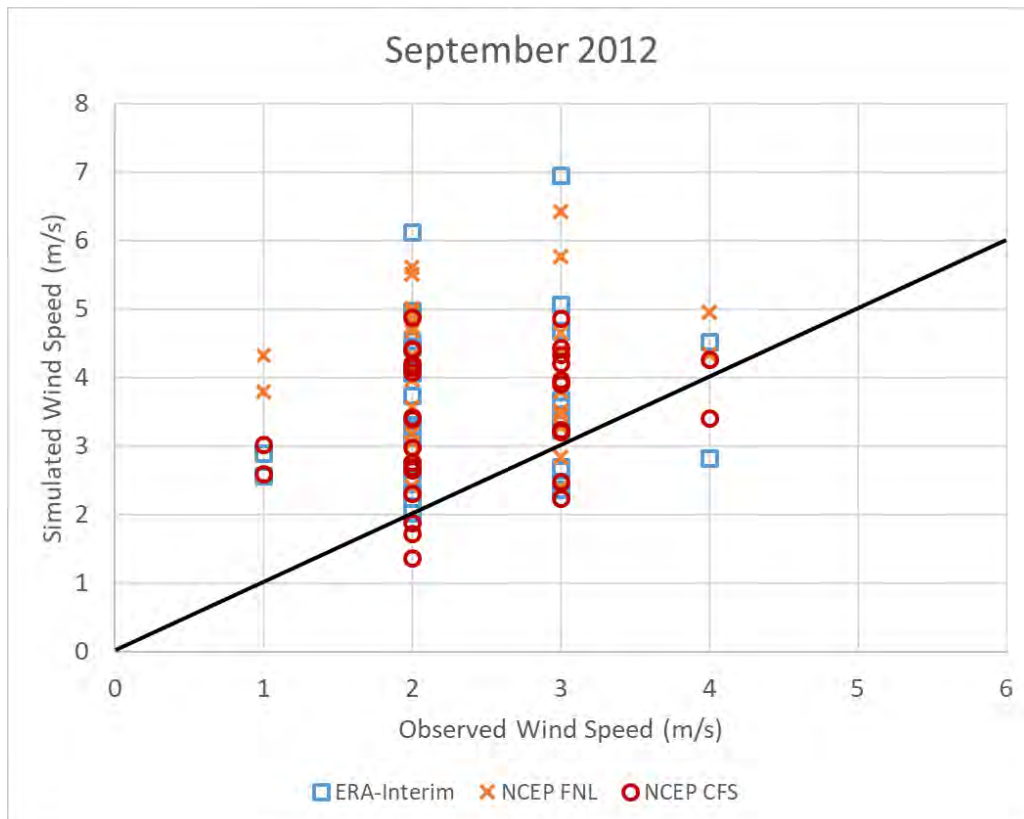


Figure 172. Scatter plot of different WRF model settings with PAGASA station data in Puerto Princesa for September 2012.

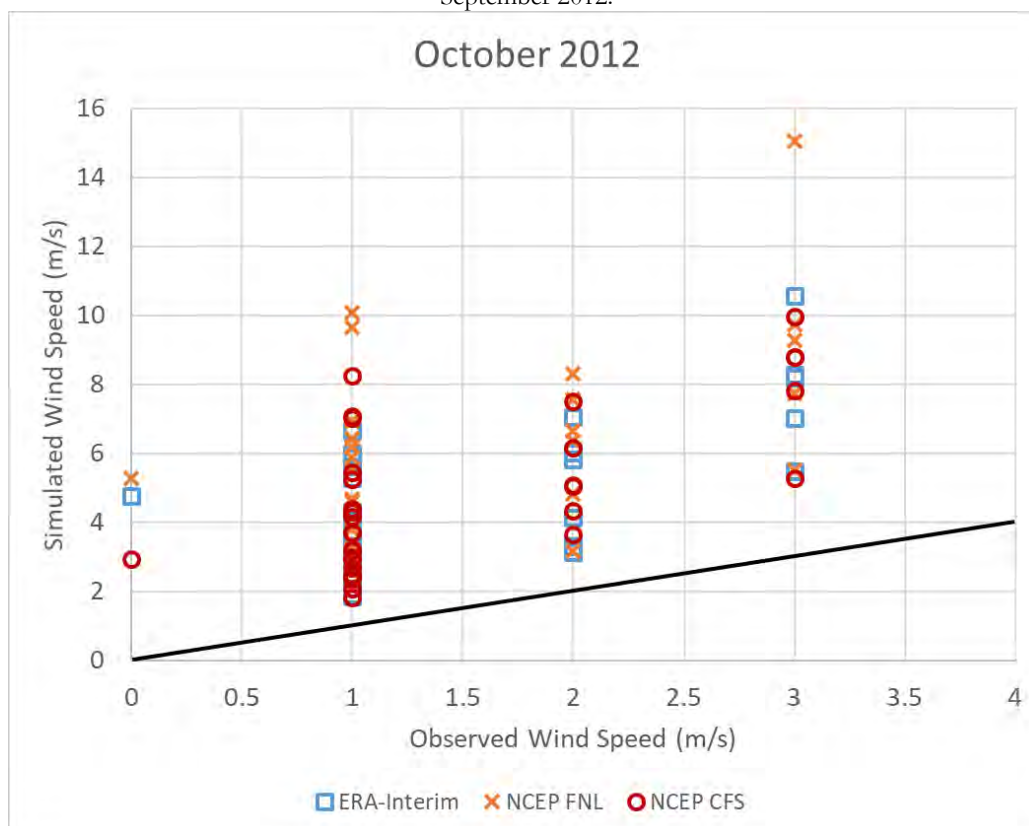


Figure 173. Scatter plot of different WRF model settings with PAGASA station data in Coron Island for October 2012.

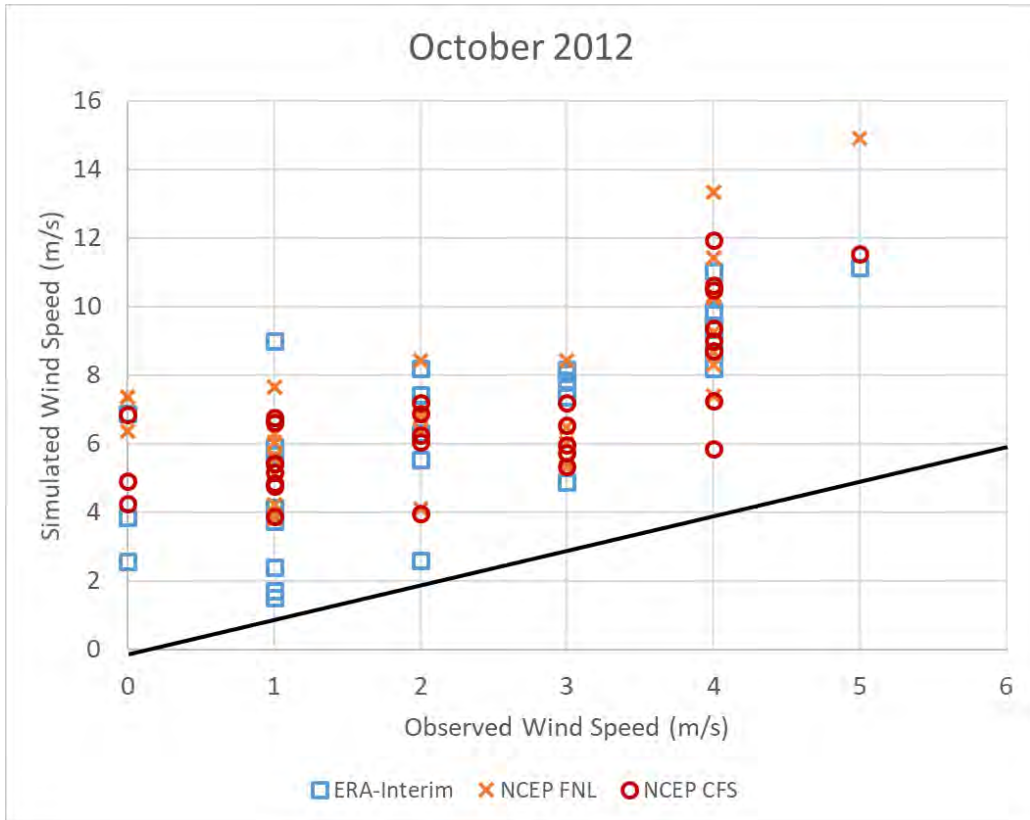


Figure 174. Scatter plot of different WRF model settings with PAGASA station data in Cuyo Island for October 2012.

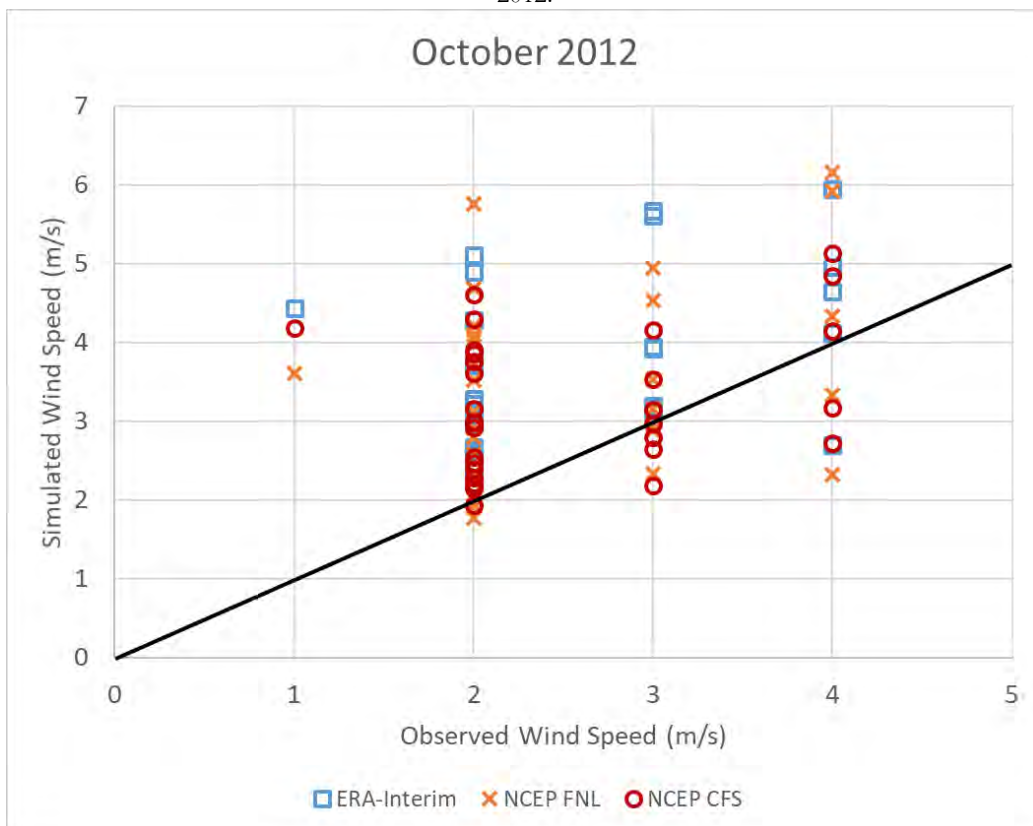


Figure 175. Scatter plot of different WRF model settings with PAGASA station data in Puerto Princesa for October 2012.

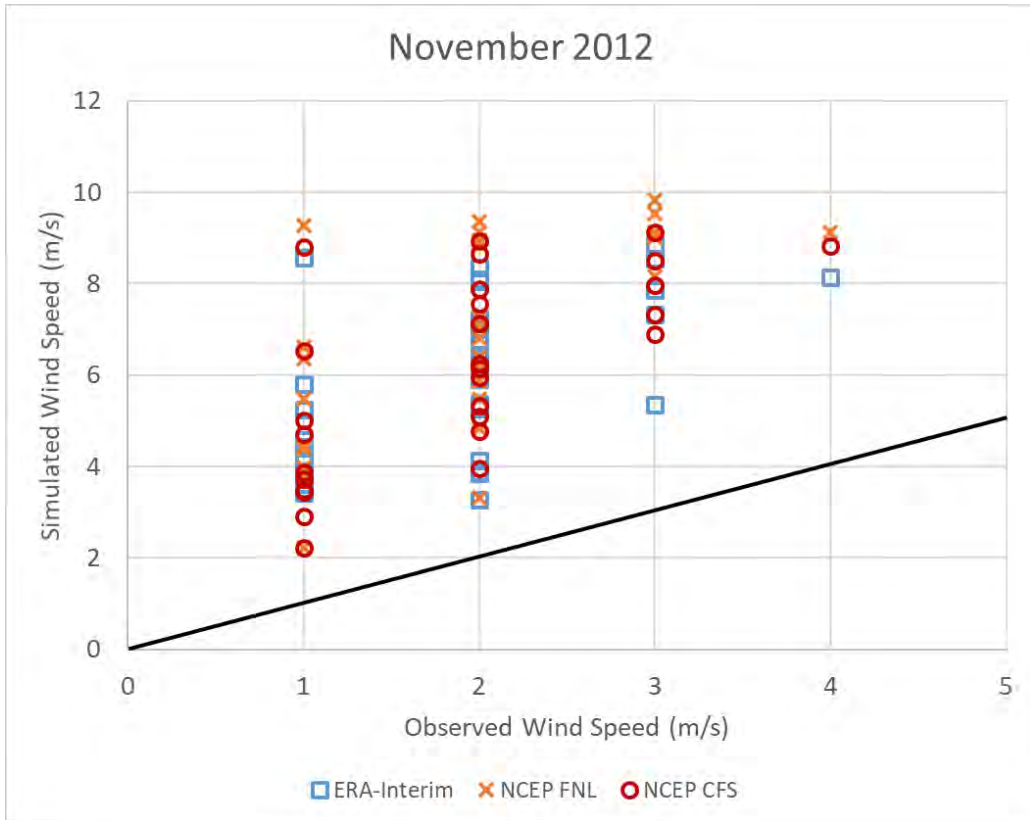


Figure 176. Scatter plot of different WRF model settings with PAGASA station data in Coron Island for November 2012.

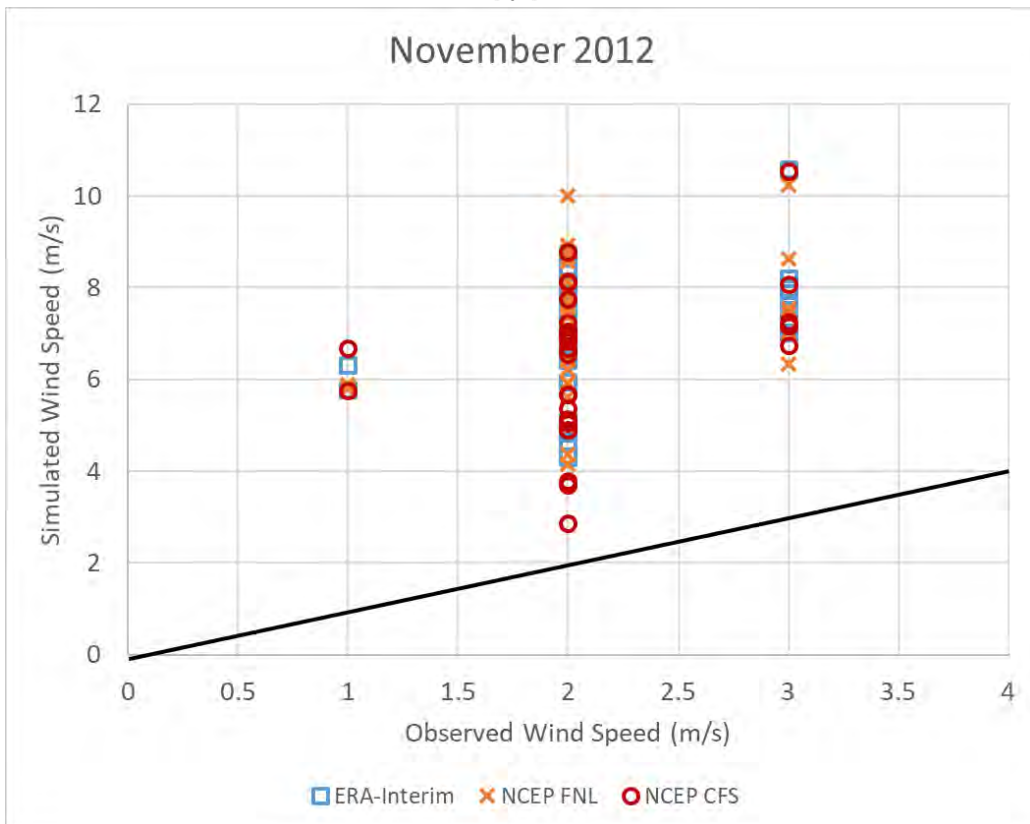


Figure 177. Scatter plot of different WRF model settings with PAGASA station data in Cuyo Island for November 2012.

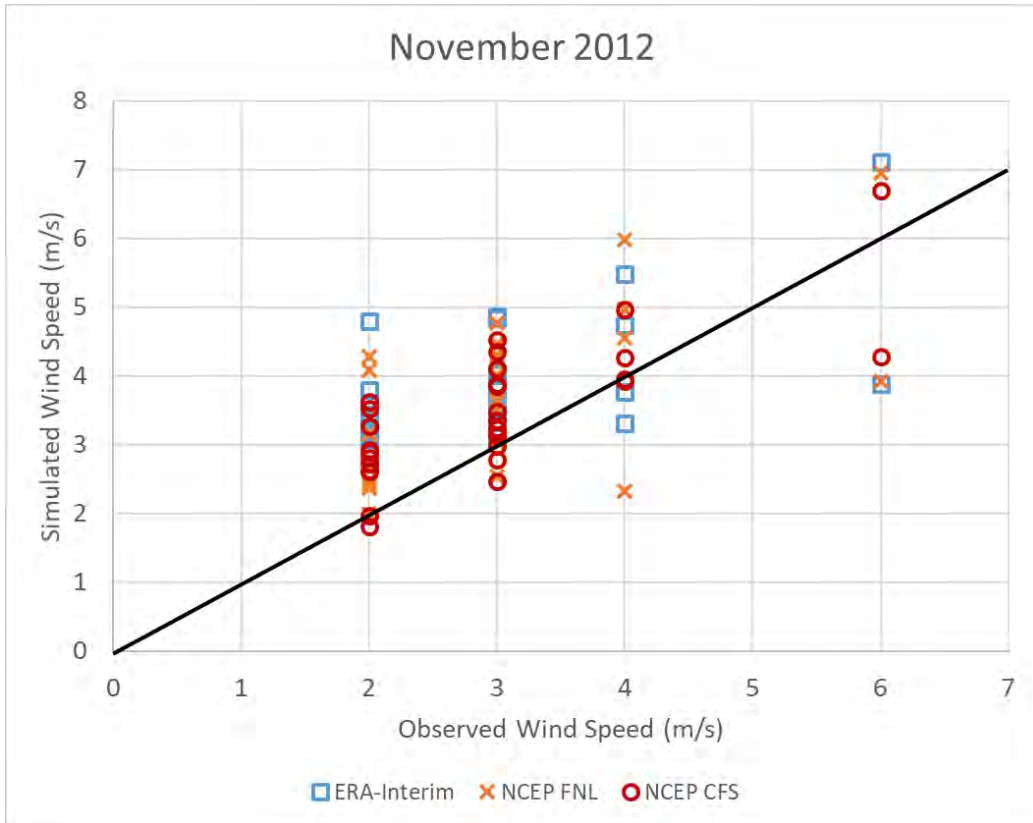


Figure 178. Scatter plot of different WRF model settings with PAGASA station data in Puerto Princesa for November 2012.

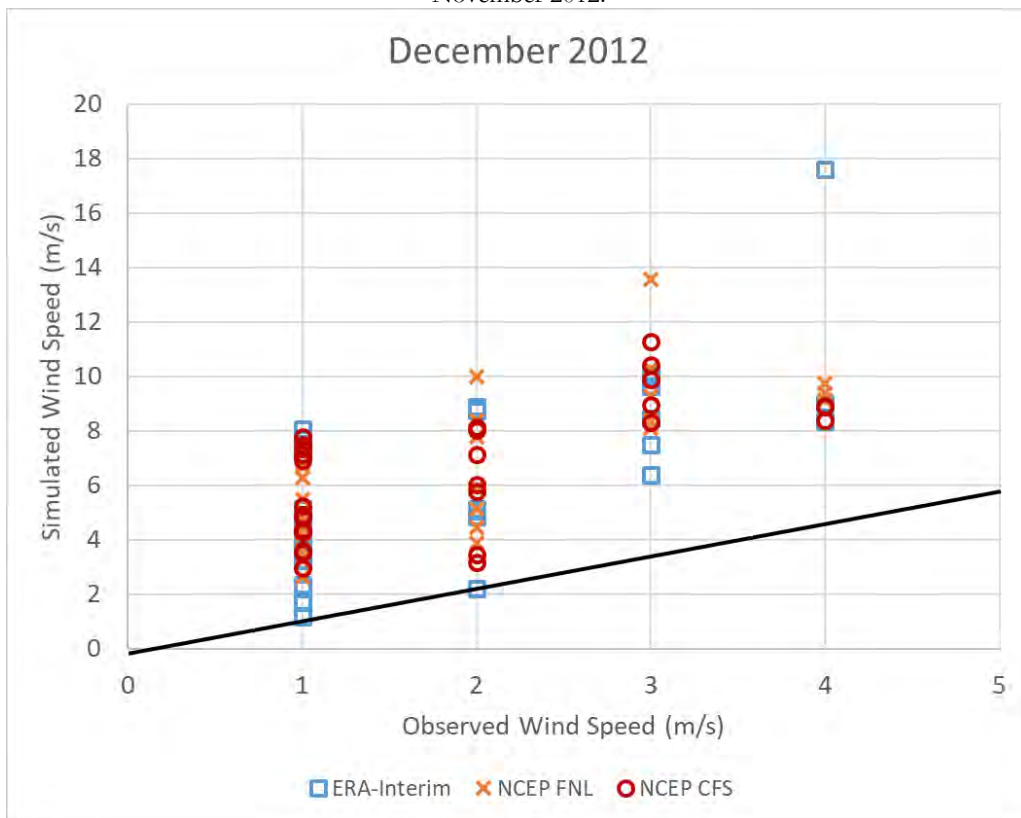


Figure 179. Scatter plot of different WRF model settings with PAGASA station data in Coron Island for December 2012.

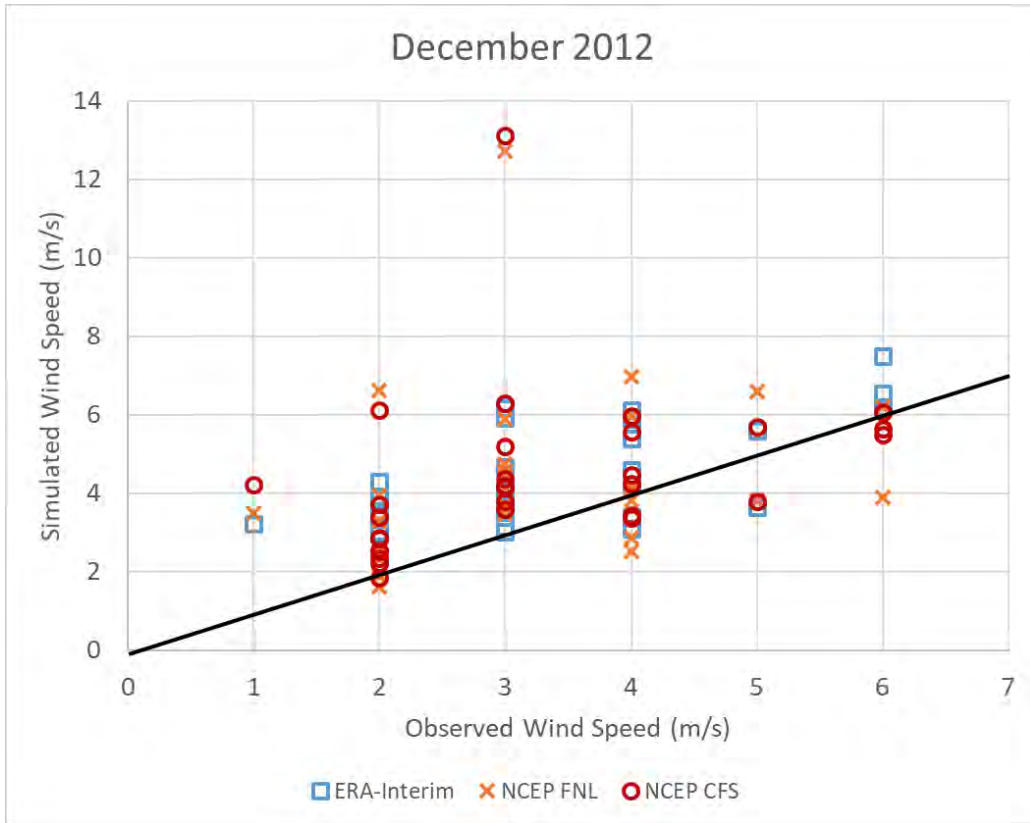


Figure 180. Scatter plot of different WRF model settings with PAGASA station data in Puerto Princesa for December 2012.

Appendix 2: Mesoscale Model Wind Direction Charts

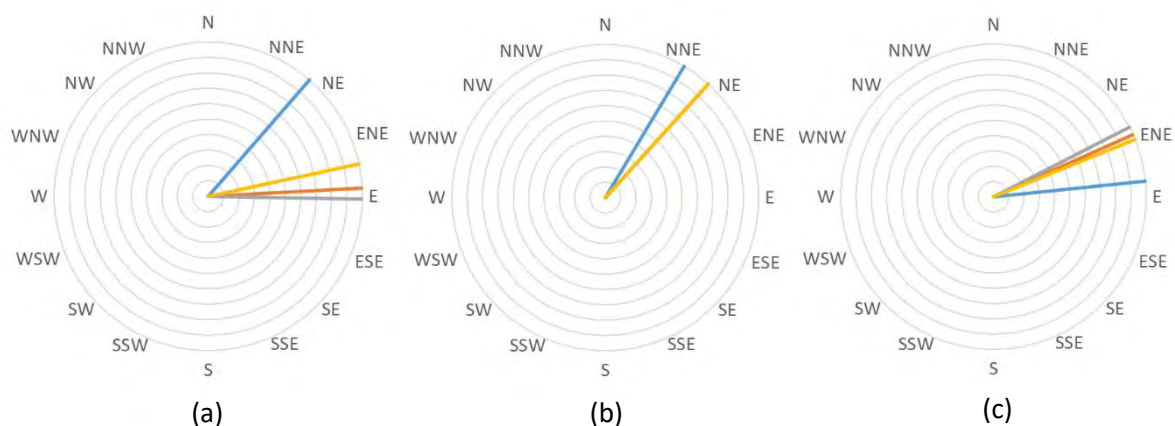


Figure 181. Comparison of average wind direction between WRF output and observation data at (a) Coron Island, (b) Cuyo Island, and (c) Puerto Princesa for the month of January 2010

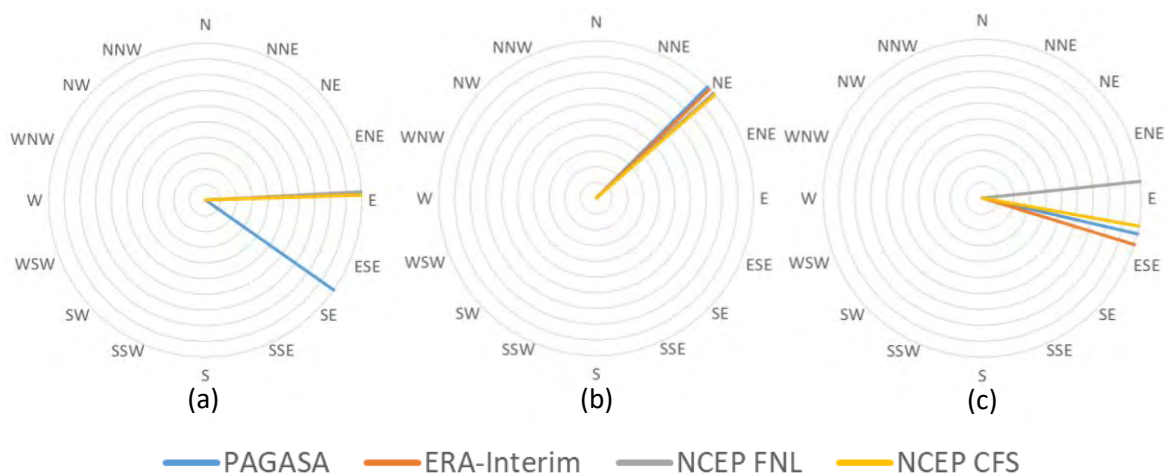


Figure 182. Comparison of average wind direction between WRF output and observation data at (a) Coron Island, (b) Cuyo Island, and (c) Puerto Princesa for the month of April 2010

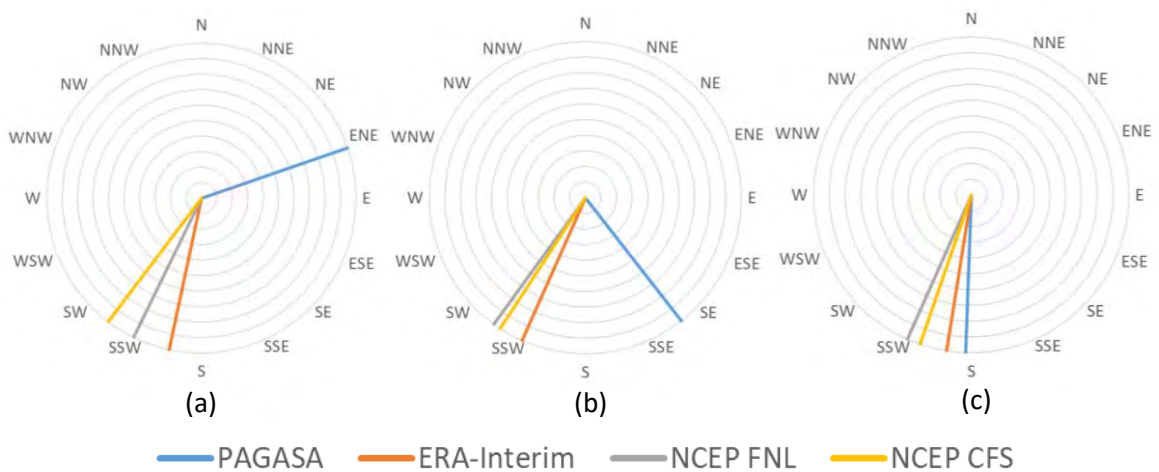


Figure 183. Comparison of average wind direction between WRF output and observation data at (a) Coron Island, (b) Cuyo Island, and (c) Puerto Princesa for the month of June 2010

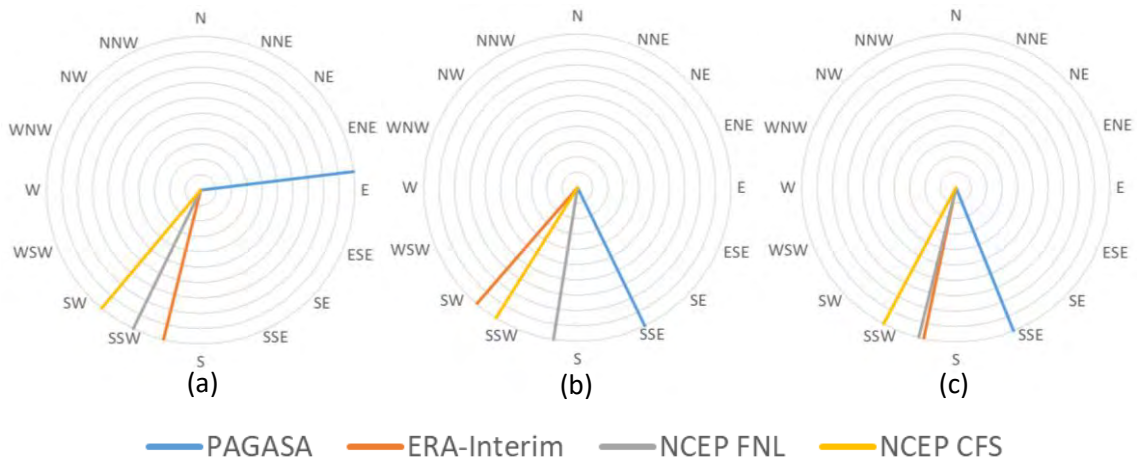


Figure 184. Comparison of average wind direction between WRF output and observation data at (a) Coron Island, (b) Cuyo Island, and (c) Puerto Princesa for the month of July 2010

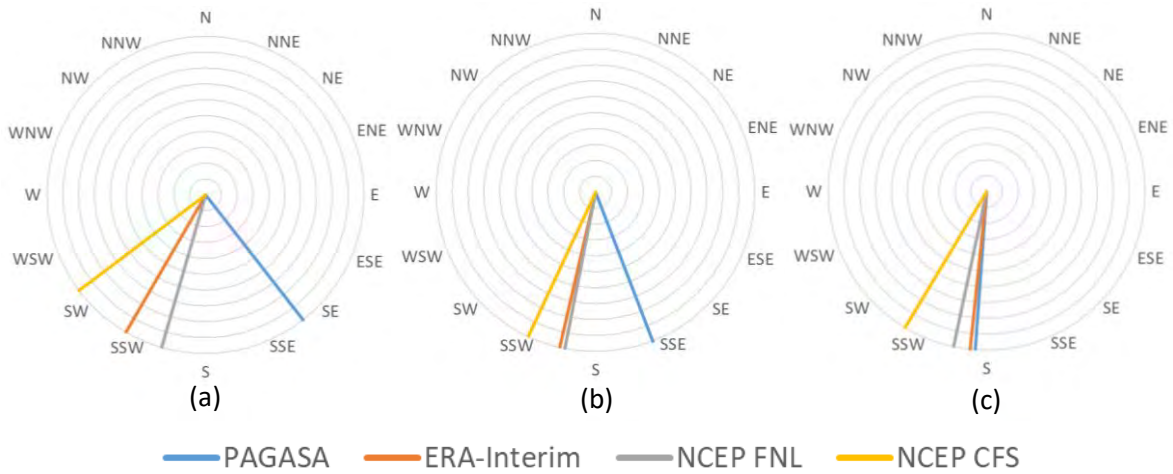


Figure 185. Comparison of average wind direction between WRF output and observation data at (a) Coron Island, (b) Cuyo Island, and (c) Puerto Princesa for the month of August 2010

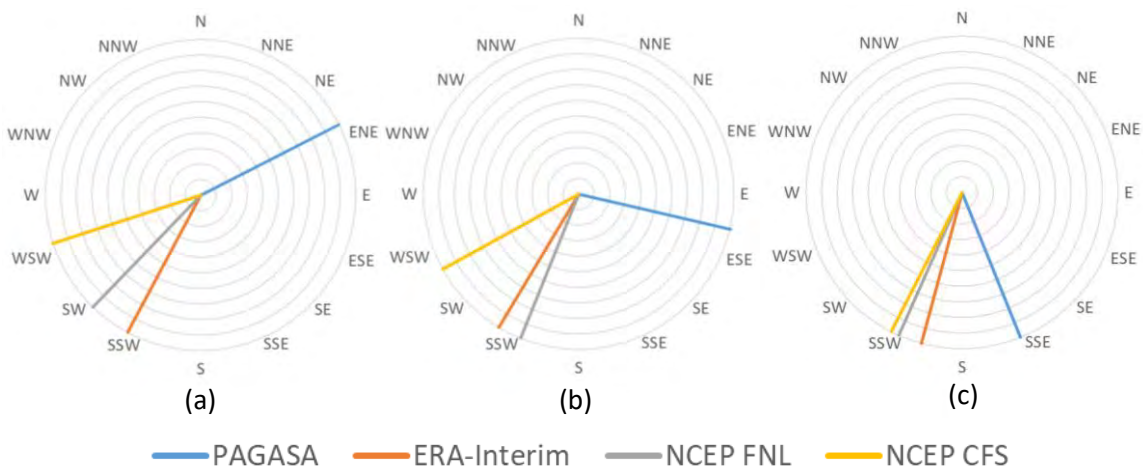


Figure 186. Comparison of average wind direction between WRF output and observation data at (a) Coron Island, (b) Cuyo Island, and (c) Puerto Princesa for the month of September 2010

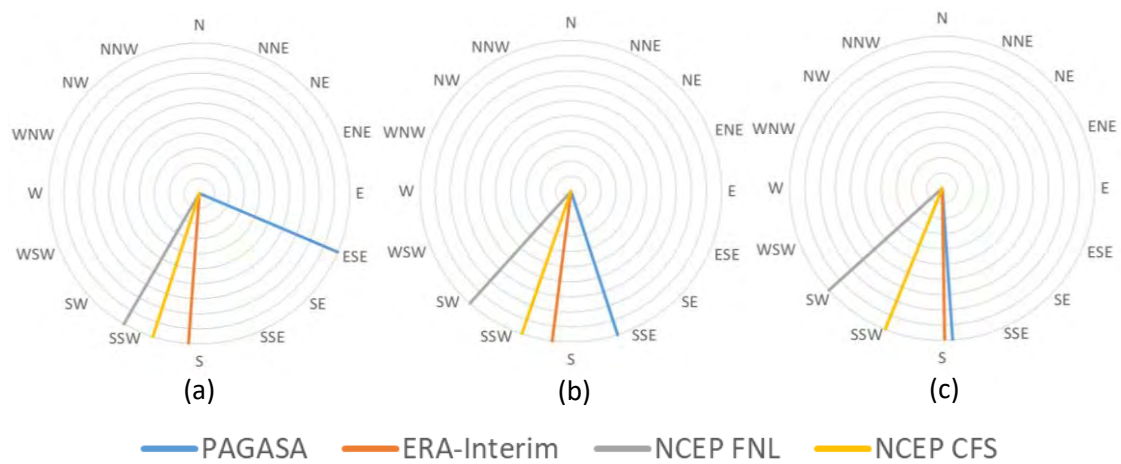


Figure 187. Comparison of average wind direction between WRF output and observation data at (a) Coron Island, (b) Cuyo Island, and (c) Puerto Princesa for the month of October 2010

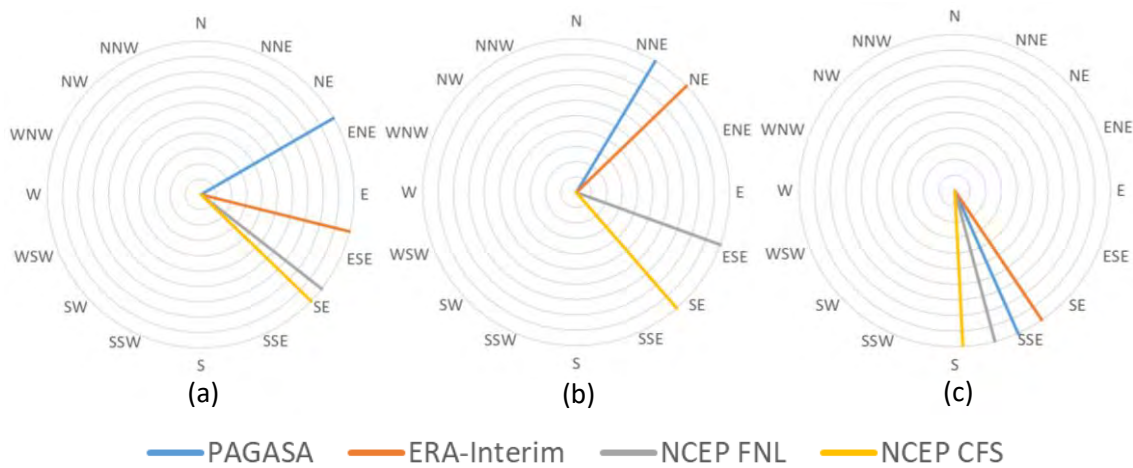


Figure 188. Comparison of average wind direction between WRF output and observation data at (a) Coron Island, (b) Cuyo Island, and (c) Puerto Princesa for the month of November 2010

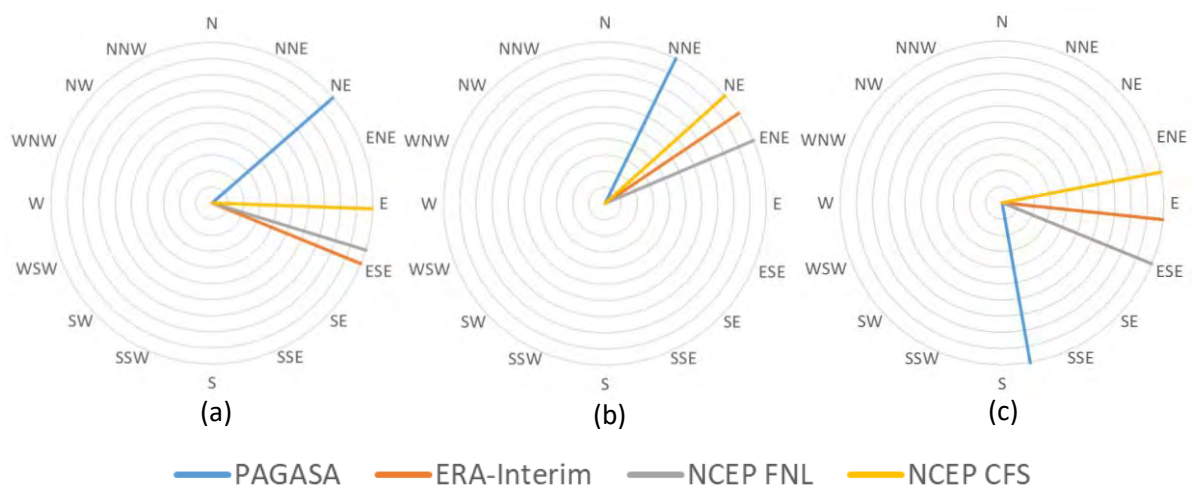


Figure 189. Comparison of average wind direction between WRF output and observation data at (a) Coron Island, (b) Cuyo Island, and (c) Puerto Princesa for the month of December 2010

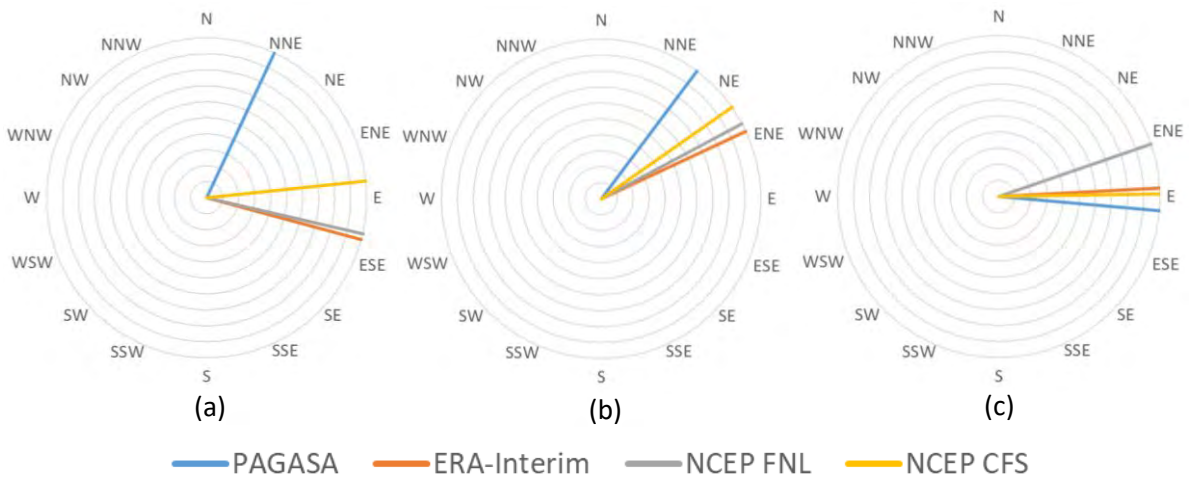


Figure 190. Comparison of average wind direction between WRF output and observation data at (a) Coron Island, (b) Cuyo Island, and (c) Puerto Princesa for the month of January 2011

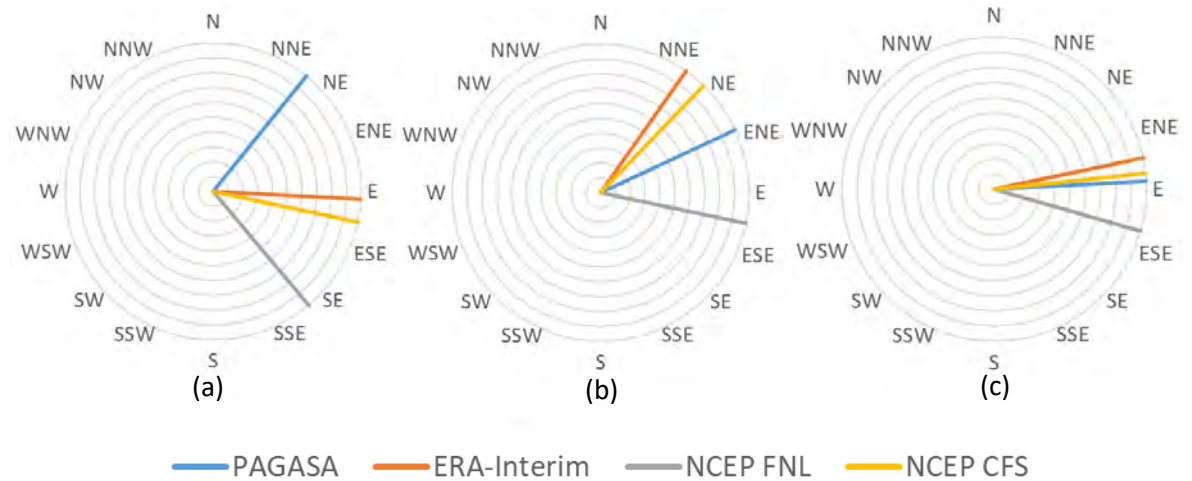


Figure 191. Comparison of average wind direction between WRF output and observation data at (a) Coron Island, (b) Cuyo Island, and (c) Puerto Princesa for the month of February 2011

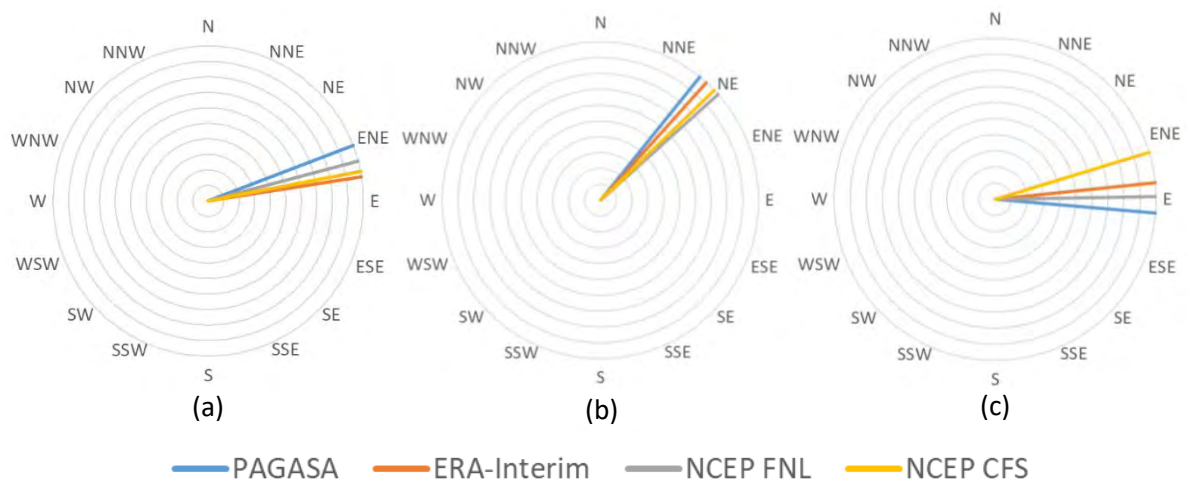


Figure 192. Comparison of average wind direction between WRF output and observation data at (a) Coron Island, (b) Cuyo Island, and (c) Puerto Princesa for the month of March 2011

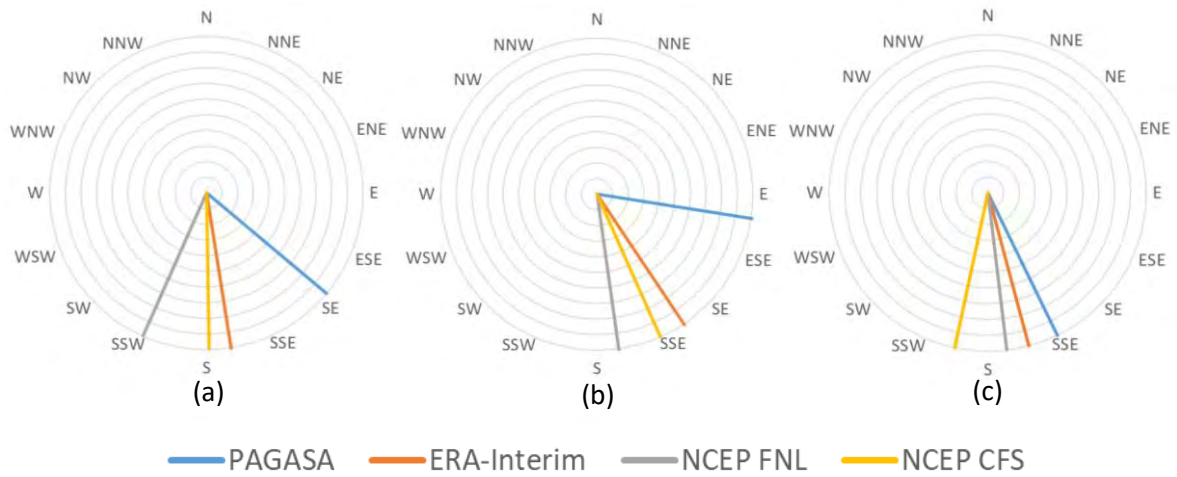


Figure 193. Comparison of average wind direction between WRF output and observation data at (a) Coron Island, (b) Cuyo Island, and (c) Puerto Princesa for the month of May 2011

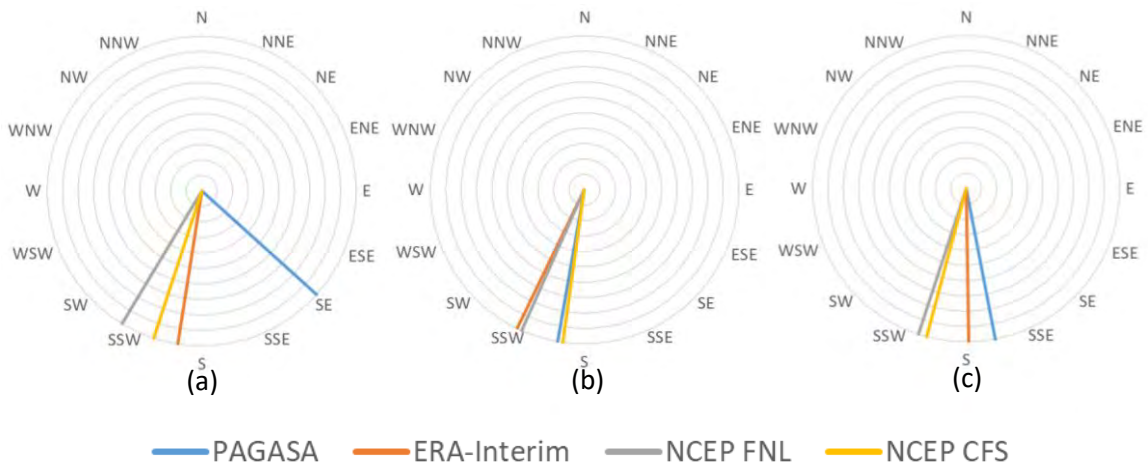


Figure 194. Comparison of average wind direction between WRF output and observation data at (a) Coron Island, (b) Cuyo Island, and (c) Puerto Princesa for the month of June 2011

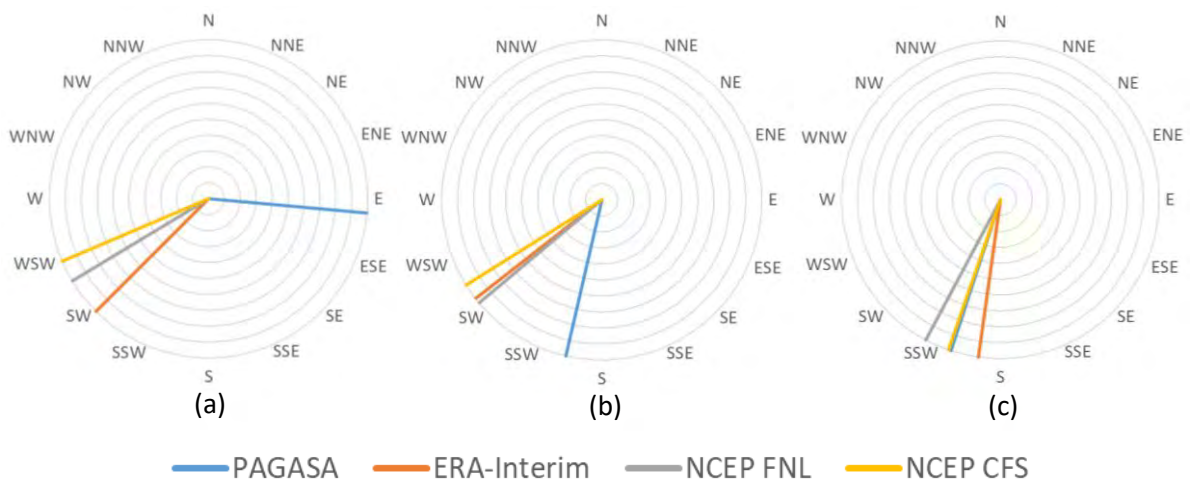


Figure 195. Comparison of average wind direction between WRF output and observation data at (a) Coron Island, (b) Cuyo Island, and (c) Puerto Princesa for the month of August 2011

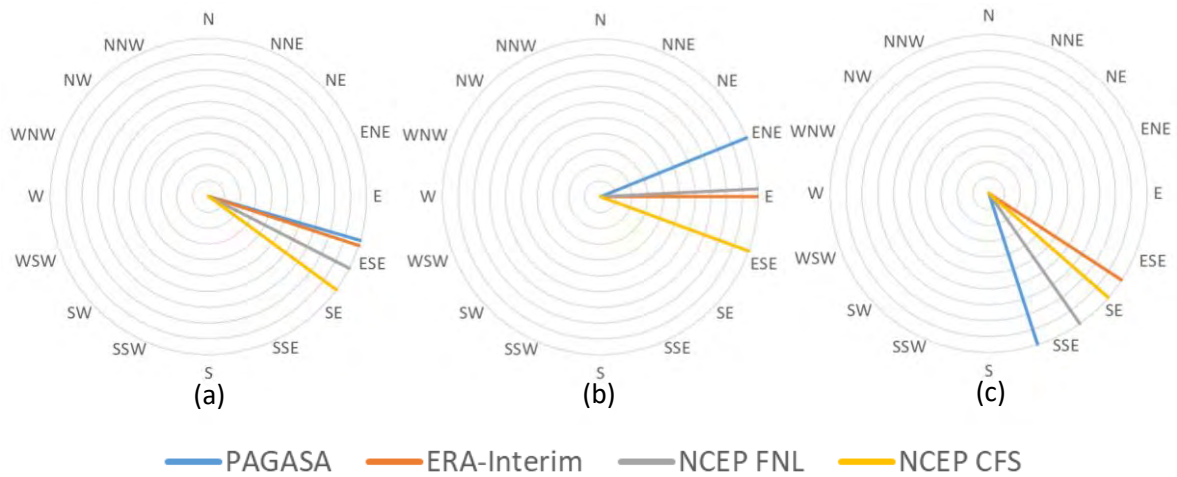


Figure 196. Comparison of average wind direction between WRF output and observation data at (a) Coron Island, (b) Cuyo Island, and (c) Puerto Princesa for the month of November 2011

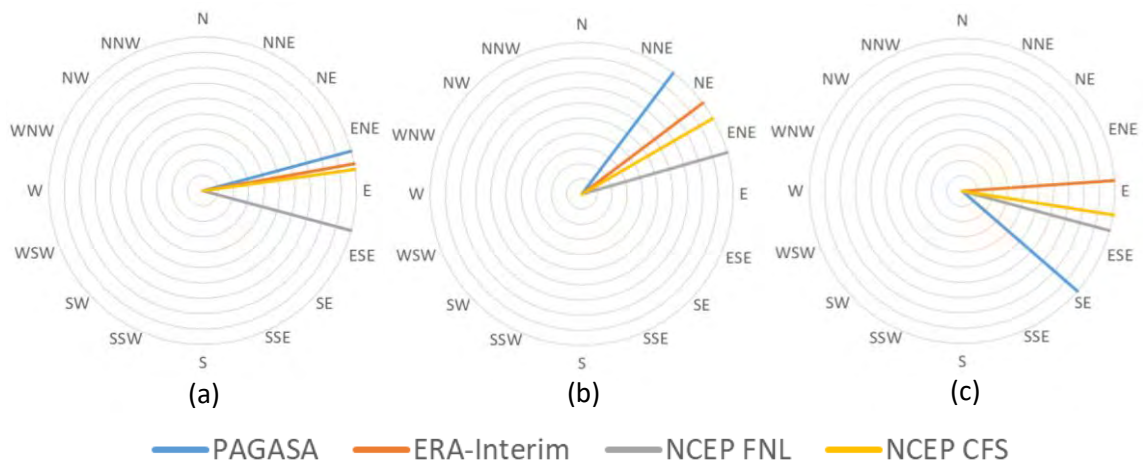


Figure 197. Comparison of average wind direction between WRF output and observation data at (a) Coron Island, (b) Cuyo Island, and (c) Puerto Princesa for the month of December 2011

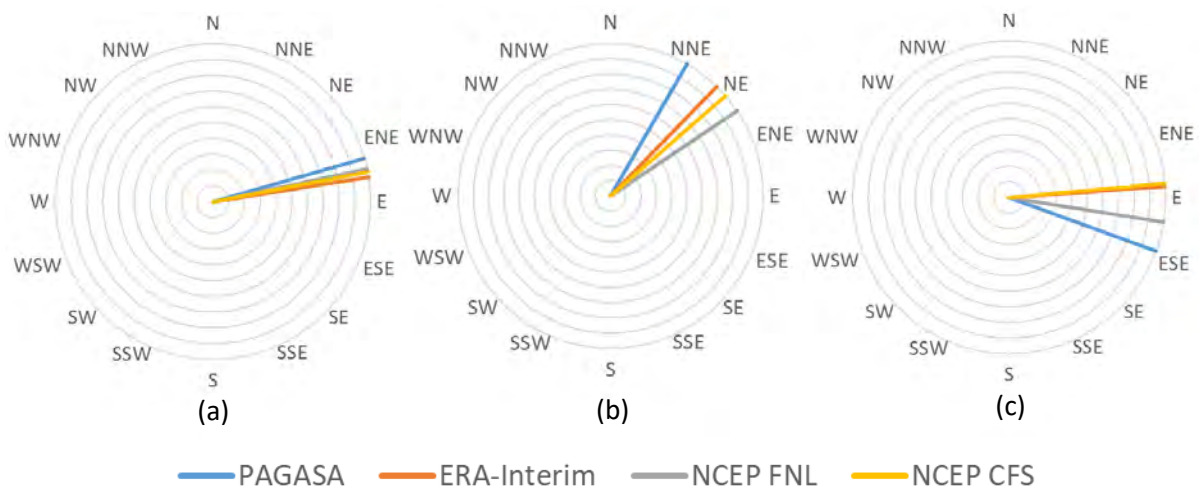


Figure 198. Comparison of average wind direction between WRF output and observation data at (a) Coron Island, (b) Cuyo Island, and (c) Puerto Princesa for the month of February 2012

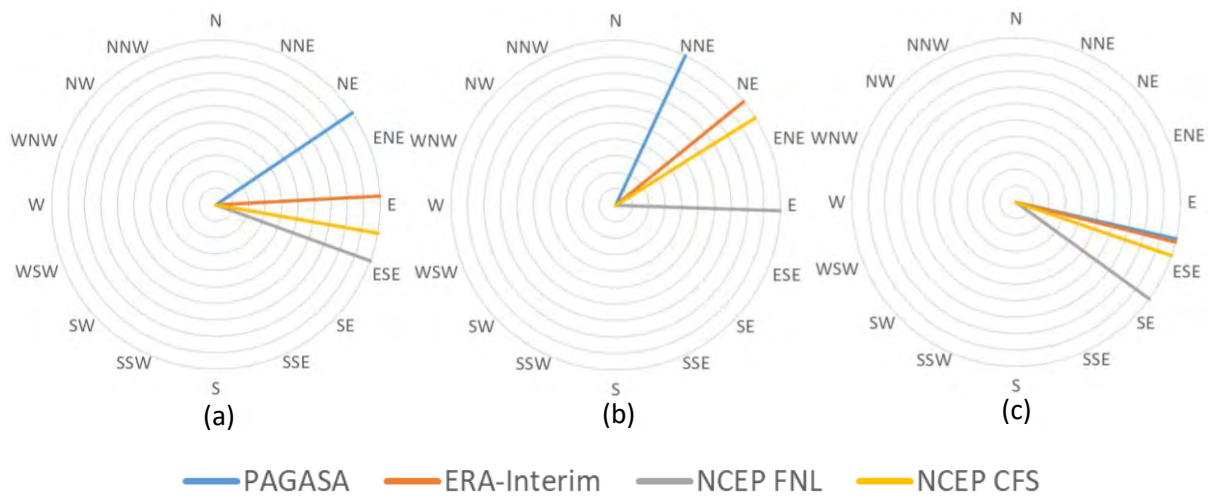


Figure 199. Comparison of average wind direction between WRF output and observation data at (a) Coron Island, (b) Cuyo Island, and (c) Puerto Princesa for the month of March 2012

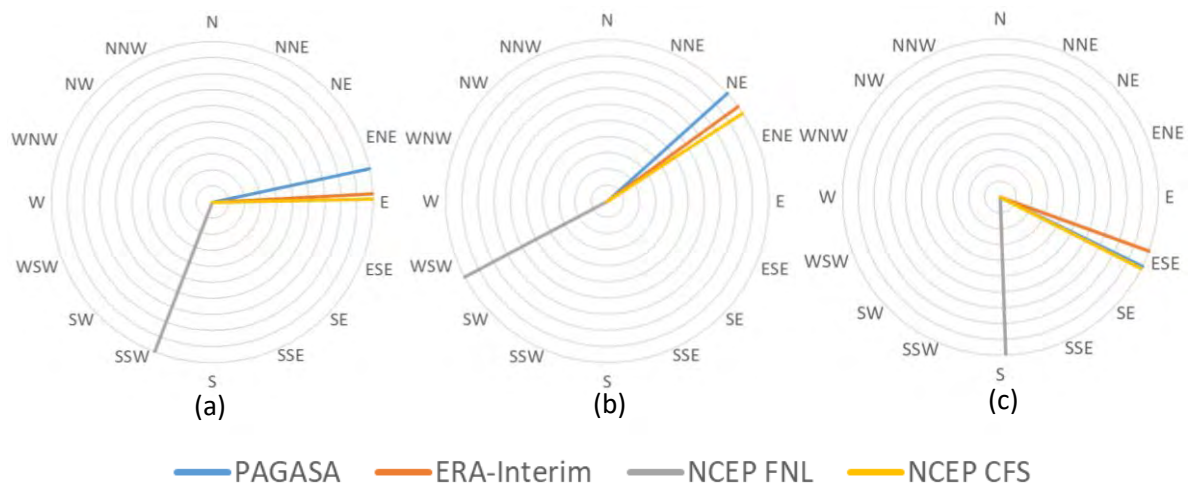


Figure 200. Comparison of average wind direction between WRF output and observation data at (a) Coron Island, (b) Cuyo Island, and (c) Puerto Princesa for the month of April 2012

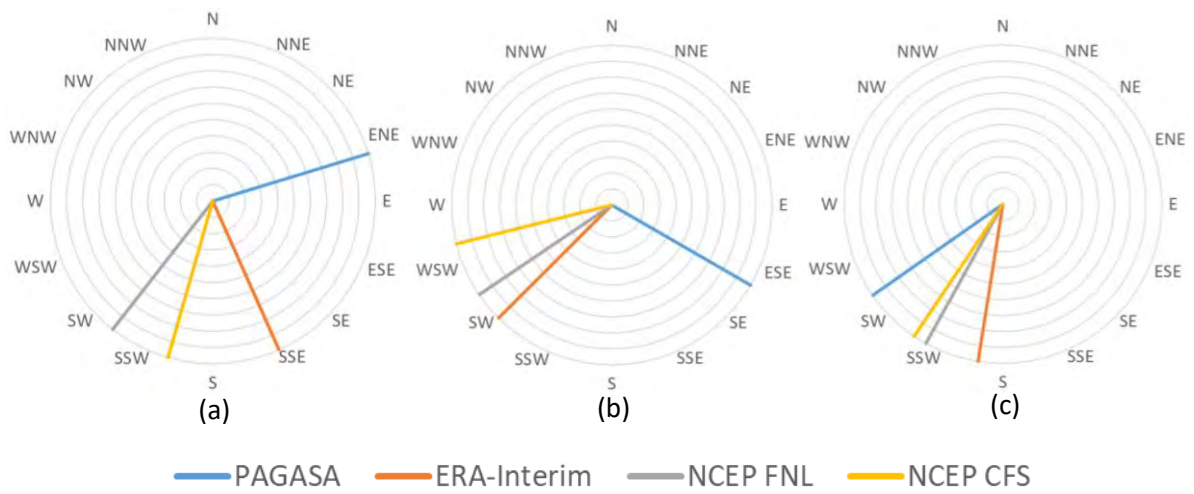


Figure 201. Comparison of average wind direction between WRF output and observation data at (a) Coron Island, (b) Cuyo Island, and (c) Puerto Princesa for the month of May 2012

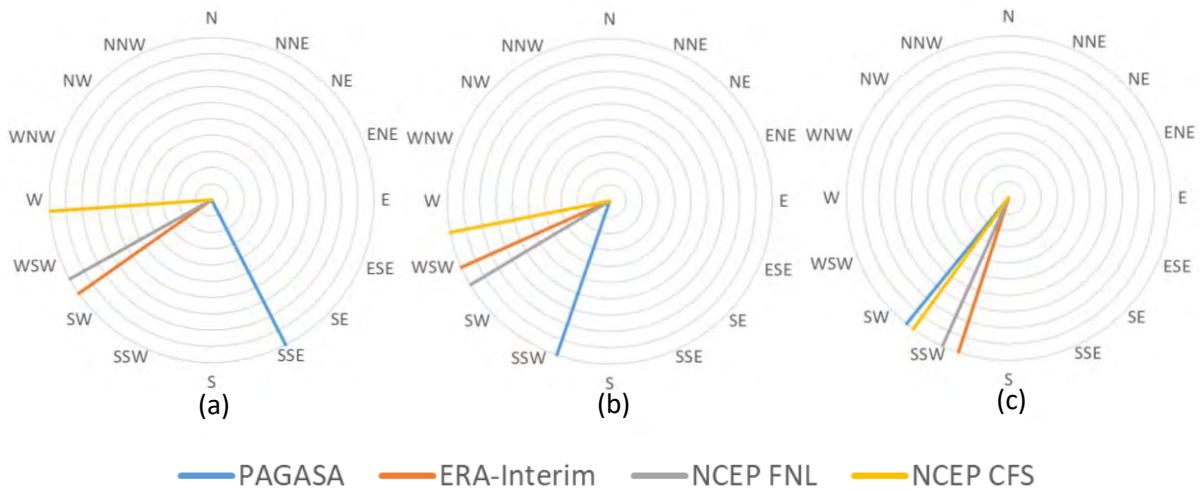


Figure 202. Comparison of average wind direction between WRF output and observation data at (a) Coron Island, (b) Cuyo Island, and (c) Puerto Princesa for the month of July 2012

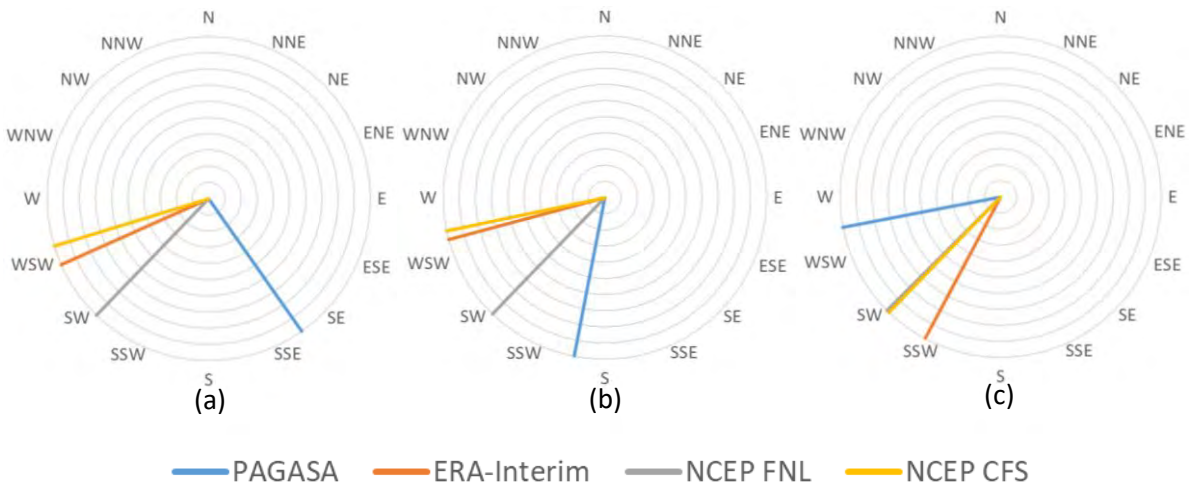


Figure 203. Comparison of average wind direction between WRF output and observation data at (a) Coron Island, (b) Cuyo Island, and (c) Puerto Princesa for the month of September 2012

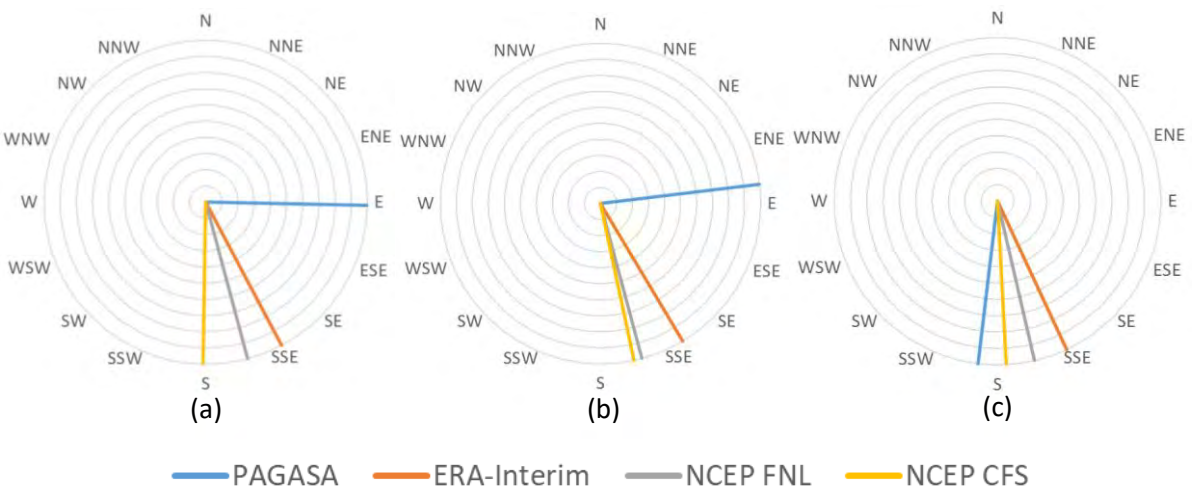


Figure 204. Comparison of average wind direction between WRF output and observation data at (a) Coron Island, (b) Cuyo Island, and (c) Puerto Princesa for the month of October 2012

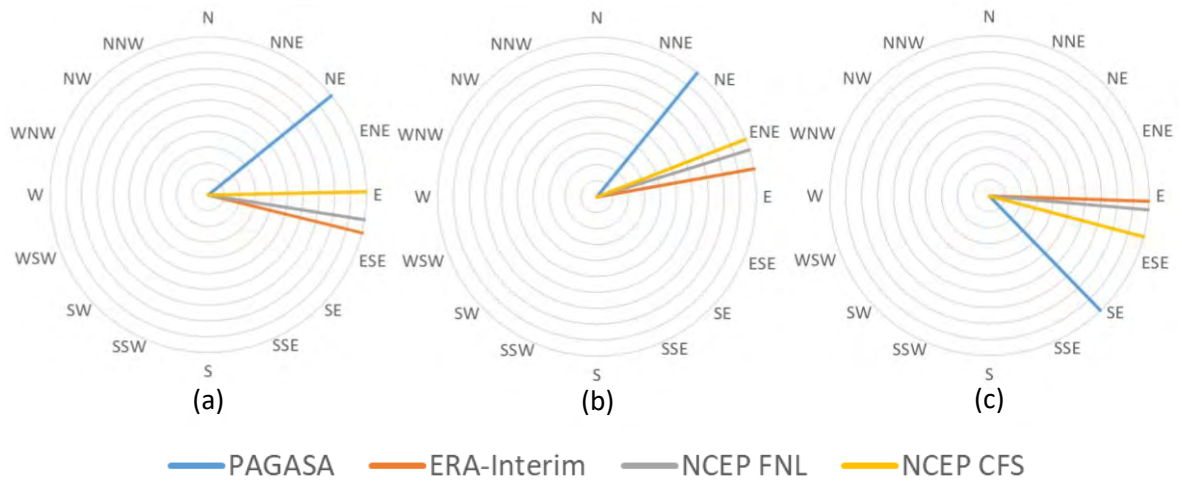


Figure 205. Comparison of average wind direction between WRF output and observation data at (a) Coron Island, (b) Cuyo Island, and (c) Puerto Princesa for the month of December 2012

Appendix 3: PAGASA with Mesoscale Model Wind Speed and Wind Direction Data

Table 35. January 2010 wind data at Coron Island from onshore weather station and meoscale model output

Source Date	PAGASA		ERA-Interim		NCEP FNL		NCEP CFSR	
	Wind Speed (m/s)	Wind Direction (Degrees)	Wind Speed (m/s)	Wind Direction (Degrees)	Wind Speed (m/s)	Wind Direction (Degrees)	Wind Speed (m/s)	Wind Direction (Degrees)
01/01/2010	1	0	9.66	76.91	6.61	71.41	8.18	71.64
02/01/2010	1	0	6.54	72.38	5.25	66.77	7.04	73.05
03/01/2010	1	0	4.27	76.95	3.70	66.58	4.79	90.23
04/01/2010	2	140	5.88	90.10	5.41	98.16	5.33	100.41
05/01/2010	2	0	4.02	82.60	5.08	77.02	6.01	85.46
06/01/2010	2	120	3.33	86.83	3.88	62.86	4.23	63.60
07/01/2010	1	0	3.06	88.18	1.89	57.86	2.10	261.55
08/01/2010	2	0	3.32	83.83	3.05	68.72	3.13	82.25
09/01/2010	2	0	3.79	75.47	4.32	51.86	5.35	68.55
10/01/2010	1	0	3.67	80.73	3.12	72.68	3.96	61.99
11/01/2010	0	0	3.84	60.32	3.40	358.22	3.39	20.79
12/01/2010	2	0	4.52	354.11	5.14	359.35	3.48	1.94
13/01/2010	1	120	7.19	72.07	6.56	66.63	7.25	76.43
14/01/2010	2	90	8.05	70.64	7.61	62.60	9.08	68.78
15/01/2010	2	140	7.20	74.39	6.56	65.56	5.62	61.71
16/01/2010	1	0	6.01	58.95	6.68	61.52	6.73	61.33
17/01/2010	2	40	11.85	65.57	11.23	74.93	9.99	70.37
18/01/2010	4	40	12.31	81.62	11.90	81.41	11.26	81.35
19/01/2010	4	40	12.51	82.40	12.74	83.53	11.87	84.89
20/01/2010	5	40	10.44	79.98	10.26	80.86	10.32	82.67
21/01/2010	2	140	8.58	81.28	9.07	78.05	9.32	78.97
22/01/2010	2	40	9.15	80.50	8.20	72.08	7.11	75.49
23/01/2010	0	0	7.72	73.10	7.11	67.50	7.68	74.21
24/01/2010	1	40	9.02	81.07	9.55	79.70	10.02	79.84
25/01/2010	1	40	9.42	80.20	9.72	79.59	9.75	80.15
26/01/2010	4	40	10.60	77.39	12.07	78.18	11.40	78.42
27/01/2010	3	40	9.65	79.41	9.72	75.74	10.17	79.04
28/01/2010	2	40	8.41	80.13	7.51	73.02	7.26	71.65
29/01/2010	2	40	6.97	75.39	6.33	64.53	6.71	70.13
30/01/2010	2	40	7.81	79.25	7.71	77.06	8.01	76.71
31/01/2010	3	40	9.13	85.82	9.17	83.88	10.05	84.14

Table 36. January 2010 wind data at Cuyo Island from onshore weather station and meoscale model output

Source Date	PAGASA		ERA-Interim		NCEP FNL		NCEP CFSR	
	Wind Speed (m/s)	Wind Direction (Degrees)	Wind Speed (m/s)	Wind Direction (Degrees)	Wind Speed (m/s)	Wind Direction (Degrees)	Wind Speed (m/s)	Wind Direction (Degrees)
01/01/2010	3	20	11.95	43.90	11.87	39.48	11.56	41.68
02/01/2010	3	20	9.83	42.50	8.95	41.10	8.97	40.21
03/01/2010	3	20	6.66	38.74	4.19	39.15	4.62	36.92
04/01/2010	2	20	7.02	38.68	3.54	56.07	3.21	58.19
05/01/2010	2	20	7.68	36.58	7.06	40.02	6.28	35.34
06/01/2010	2	20	8.07	34.22	8.09	37.28	7.96	35.62
07/01/2010	4	20	9.06	39.03	10.24	34.80	9.41	35.18
08/01/2010	3	20	9.07	38.43	9.74	36.31	9.56	37.55
09/01/2010	2	20	8.84	37.21	9.98	37.64	9.79	38.79
10/01/2010	3	20	7.87	37.23	9.80	38.51	8.88	40.64
11/01/2010	3	20	7.12	28.22	9.99	26.94	8.51	27.35
12/01/2010	2	20	9.06	27.65	11.44	28.84	11.16	30.42
13/01/2010	4	20	12.26	38.57	13.13	38.71	13.31	40.45
14/01/2010	5	20	13.45	39.74	14.22	39.44	14.16	39.65
15/01/2010	5	40	13.33	38.22	14.29	40.01	14.22	37.98
16/01/2010	5	40	12.80	39.60	13.60	40.95	13.32	40.63
17/01/2010	5	40	12.94	46.89	11.50	46.63	11.90	46.79
18/01/2010	4	40	10.33	51.75	7.99	51.94	9.18	50.22
19/01/2010	3	40	10.23	51.15	9.04	54.45	8.77	52.00
20/01/2010	3	40	10.60	48.63	10.86	45.31	9.97	45.34
21/01/2010	3	40	9.66	44.99	10.76	43.87	10.25	44.89
22/01/2010	4	40	10.45	44.95	10.99	42.42	10.76	41.19
23/01/2010	4	40	10.35	44.34	11.27	42.34	10.21	42.90
24/01/2010	4	40	10.74	45.43	11.09	45.46	11.01	44.67
25/01/2010	5	40	10.17	45.12	10.44	48.31	10.15	46.93
26/01/2010	4	40	10.86	49.94	11.28	48.89	11.08	47.29
27/01/2010	4	40	10.29	47.20	10.88	45.19	10.83	45.21
28/01/2010	5	40	9.45	44.11	9.66	43.86	9.54	43.27
29/01/2010	5	40	9.60	40.98	9.97	38.25	9.81	38.92
30/01/2010	5	40	8.90	43.45	9.80	43.55	9.48	43.45
31/01/2010	3	40	8.25	46.13	8.90	46.13	8.58	44.16

Table 37. January 2010 wind data at Puerto Princesa from onshore weather station and meoscale model output

Source Date	PAGASA		ERA-Interim		NCEP FNL		NCEP CFSR	
	Wind Speed (m/s)	Wind Direction (Degrees)	Wind Speed (m/s)	Wind Direction (Degrees)	Wind Speed (m/s)	Wind Direction (Degrees)	Wind Speed (m/s)	Wind Direction (Degrees)
01/01/2010	5	90	6.34	65.94	6.49	61.27	6.27	62.57
02/01/2010	4	90	5.50	65.72	4.65	69.08	4.08	67.92
03/01/2010	3	90	2.99	73.64	3.55	90.99	2.77	86.94
04/01/2010	3	90	3.16	101.60	2.37	133.42	2.38	191.36
05/01/2010	3	90	3.31	98.78	2.24	88.81	2.16	93.27
06/01/2010	3	90	3.19	59.08	3.57	66.73	2.70	66.99
07/01/2010	3	20	3.68	40.11	4.13	54.76	3.45	58.04
08/01/2010	2	90	4.21	65.29	3.78	32.53	3.84	51.65
09/01/2010	3	90	3.50	63.97	4.84	61.24	3.97	64.11
10/01/2010	4	90	3.83	78.84	4.42	53.97	4.08	67.66
11/01/2010	3	90	3.52	26.08	3.75	33.11	3.18	45.84
12/01/2010	4	20	4.78	10.72	5.88	2.27	4.34	3.43
13/01/2010	4	90	5.10	51.68	5.11	15.88	6.19	55.70
14/01/2010	5	70	7.46	53.54	6.09	46.82	7.38	52.72
15/01/2010	5	70	6.73	56.26	6.37	45.45	6.48	54.08
16/01/2010	3	90	5.52	45.54	6.58	44.88	5.45	44.47
17/01/2010	5	90	9.88	55.80	8.01	67.70	7.65	56.94
18/01/2010	5	90	8.53	79.81	6.30	110.64	7.11	81.78
19/01/2010	5	90	7.06	88.79	6.50	91.33	5.95	88.17
20/01/2010	4	90	4.18	73.32	5.49	73.43	4.36	73.67
21/01/2010	4	90	3.72	78.04	5.65	66.70	3.96	68.59
22/01/2010	4	90	5.04	68.51	6.13	63.88	5.41	64.44
23/01/2010	4	90	4.79	70.81	5.46	62.72	4.55	67.43
24/01/2010	4	90	5.40	66.55	6.84	66.68	4.80	64.66
25/01/2010	4	90	4.88	67.69	6.39	67.89	6.06	70.11
26/01/2010	5	90	7.55	70.35	7.15	66.19	6.59	67.00
27/01/2010	4	90	5.73	69.22	5.98	61.87	5.64	64.37
28/01/2010	3	90	4.10	73.38	5.57	65.11	4.81	68.84
29/01/2010	4	90	4.52	68.58	4.96	60.83	4.42	65.80
30/01/2010	4	90	4.10	70.94	5.23	62.00	4.71	66.85
31/01/2010	3	90	3.66	82.97	4.80	70.82	3.95	73.52

Table 38. February 2010 wind data at Coron Island from onshore weather station and meoscale model output

Source Date	PAGASA		ERA-Interim		NCEP FNL		NCEP CFSR	
	Wind Speed (m/s)	Wind Direction (Degrees)	Wind Speed (m/s)	Wind Direction (Degrees)	Wind Speed (m/s)	Wind Direction (Degrees)	Wind Speed (m/s)	Wind Direction (Degrees)
01/02/2010	1	40	5.19	78.82	3.84	57.25	5.30	70.04
02/02/2010	1	140	6.46	84.13	4.69	69.48	6.06	70.34
03/02/2010	3	40	6.93	80.24	7.89	84.45	8.27	84.59
04/02/2010	1	120	6.93	83.74	7.47	83.84	7.06	83.07
05/02/2010	2	120	8.00	84.25	8.20	82.12	8.18	83.85
06/02/2010	2	120	8.78	85.28	8.81	81.13	8.52	81.90
07/02/2010	3	40	7.76	87.05	8.21	84.70	8.57	88.73
08/02/2010	4	40	7.15	84.48	9.02	84.55	8.83	84.71
09/02/2010	4	40	9.40	85.48	9.67	84.86	9.57	84.29
10/02/2010	2	40	9.19	84.69	9.58	83.65	9.19	84.02
11/02/2010	3	40	8.30	84.08	9.03	82.08	8.58	82.58
12/02/2010	2	40	7.39	80.50	7.08	75.97	7.17	75.41
13/02/2010	4	140	9.11	80.13	9.64	80.47	8.34	76.83
14/02/2010	4	40	7.74	79.17	7.02	74.06	6.75	73.53
15/02/2010	2	0	5.96	78.13	5.65	72.37	5.73	68.21
16/02/2010	2	120	7.38	84.66	5.20	77.13	6.52	79.95
17/02/2010	2	120	5.50	75.84	3.36	43.60	4.09	47.14
18/02/2010	1	0	5.58	83.06	4.30	74.12	4.53	74.83
19/02/2010	1	140	5.11	84.56	3.35	90.10	3.51	66.24
20/02/2010	1	180	3.61	74.59	1.89	45.13	3.66	42.24
21/02/2010	1	180	4.35	82.52	2.85	64.55	3.71	76.12
22/02/2010	1	40	3.78	77.02	4.26	78.45	4.93	70.29
23/02/2010	1	40	3.45	78.46	2.85	76.14	3.11	79.59
24/02/2010	2	120	7.39	89.45	7.40	86.08	7.41	90.24
25/02/2010	3	40	6.70	86.00	8.15	86.28	7.34	85.41
26/02/2010	2	320	6.85	88.97	7.21	86.93	6.75	88.33
27/02/2010	3	40	5.67	84.43	6.68	83.48	6.02	80.76
28/02/2010	2	40	7.18	85.52	7.23	83.32	7.14	83.36

Table 39. February 2010 wind data at Cuyo Island from onshore weather station and meoscale model output

Source Date	PAGASA		ERA-Interim		NCEP FNL		NCEP CFSR	
	Wind Speed (m/s)	Wind Direction (Degrees)	Wind Speed (m/s)	Wind Direction (Degrees)	Wind Speed (m/s)	Wind Direction (Degrees)	Wind Speed (m/s)	Wind Direction (Degrees)
01/02/2010	2	20	6.51	34.78	6.28	37.62	6.92	36.86
02/02/2010	3	20	6.83	38.41	6.91	36.89	7.12	37.96
03/02/2010	2	20	7.14	42.79	6.09	49.35	6.49	44.54
04/02/2010	2	20	6.85	42.06	6.02	44.52	5.92	40.70
05/02/2010	2	20	7.31	43.58	6.41	44.54	5.92	41.54
06/02/2010	1	20	5.07	41.50	4.20	54.98	3.27	42.88
07/02/2010	2	20	6.67	44.71	5.79	54.24	5.30	51.87
08/02/2010	2	20	5.82	45.04	6.21	52.49	6.17	51.10
09/02/2010	2	20	5.05	47.81	5.68	51.69	5.48	52.86
10/02/2010	2	20	5.43	46.16	6.77	48.71	5.80	44.79
11/02/2010	2	20	7.84	41.51	8.11	43.81	7.97	40.04
12/02/2010	2	20	8.57	41.71	9.05	41.69	8.64	40.59
13/02/2010	2	20	9.69	44.39	9.30	47.28	9.24	42.33
14/02/2010	2	20	8.57	41.48	8.24	38.95	6.99	36.91
15/02/2010	2	20	8.72	40.47	8.83	41.26	7.75	37.24
16/02/2010	3	20	9.41	40.32	9.27	39.64	8.86	39.11
17/02/2010	3	20	9.14	38.25	9.21	33.73	8.73	34.90
18/02/2010	2	20	9.18	37.38	9.34	37.41	8.81	35.39
19/02/2010	3	20	9.05	35.74	8.65	37.40	8.48	33.98
20/02/2010	2	20	7.33	26.90	8.00	29.33	7.17	22.73
21/02/2010	2	20	6.82	30.77	7.85	34.75	7.26	31.42
22/02/2010	2	20	5.37	26.90	6.28	33.12	5.76	29.32
23/02/2010	2	20	4.89	30.27	5.78	32.15	5.40	26.80
24/02/2010	2	20	5.63	44.36	6.35	44.24	5.54	39.96
25/02/2010	2	20	4.54	37.99	5.05	42.24	4.61	36.48
26/02/2010	2	20	3.83	31.98	4.06	43.28	4.16	33.08
27/02/2010	2	20	4.72	37.01	5.51	43.28	5.29	41.04
28/02/2010	2	20	5.52	39.25	5.67	41.37	5.58	41.91

Table 40. February 2010 wind data at Puerto Princesa from onshore weather station and meoscale model output

Source Date	PAGASA		ERA-Interim		NCEP FNL		NCEP CFSR	
	Wind Speed (m/s)	Wind Direction (Degrees)	Wind Speed (m/s)	Wind Direction (Degrees)	Wind Speed (m/s)	Wind Direction (Degrees)	Wind Speed (m/s)	Wind Direction (Degrees)
01/02/2010	3	90	3.38	109.91	2.48	70.99	3.05	74.38
02/02/2010	3	90	3.79	99.78	2.59	71.40	2.80	73.66
03/02/2010	2	90	3.39	89.84	3.47	82.02	2.87	77.71
04/02/2010	3	90	3.56	88.97	3.76	82.53	2.98	90.67
05/02/2010	3	90	2.98	91.86	3.22	77.99	2.78	78.48
06/02/2010	4	90	3.95	102.40	3.33	89.52	3.23	99.68
07/02/2010	3	90	3.43	93.42	4.16	83.87	3.28	82.79
08/02/2010	4	90	3.79	102.35	4.62	88.43	4.35	90.19
09/02/2010	4	90	4.33	91.38	4.23	81.81	4.50	86.47
10/02/2010	4	90	4.28	106.43	3.91	84.40	3.81	92.66
11/02/2010	3	90	3.60	97.17	3.05	71.47	2.80	74.44
12/02/2010	3	90	3.15	82.01	3.95	72.16	2.83	73.95
13/02/2010	4	90	5.14	74.27	5.13	72.51	4.69	71.61
14/02/2010	3	90	3.66	93.63	2.51	81.84	2.74	96.48
15/02/2010	3	90	3.45	78.25	3.68	68.88	2.77	76.54
16/02/2010	4	90	3.59	78.34	4.84	71.58	3.37	70.54
17/02/2010	3	90	3.94	66.89	3.70	58.81	3.56	73.07
18/02/2010	3	90	3.58	55.95	2.98	50.88	2.38	42.96
19/02/2010	2	90	3.70	60.91	3.90	62.34	3.68	53.07
20/02/2010	3	0	3.63	50.92	3.10	34.57	3.03	26.27
21/02/2010	3	90	3.84	66.42	2.19	57.44	2.53	41.46
22/02/2010	2	90	3.32	90.38	2.93	69.01	2.53	113.05
23/02/2010	3	90	3.13	113.14	2.54	60.21	2.24	80.80
24/02/2010	3	90	4.00	100.85	2.70	78.02	2.77	94.63
25/02/2010	3	90	3.29	159.58	2.62	125.83	2.58	118.77
26/02/2010	2	90	3.15	162.61	2.48	139.63	2.53	164.10
27/02/2010	2	90	3.55	135.46	2.12	93.51	2.25	95.95
28/02/2010	3	90	3.67	134.62	2.79	80.46	3.19	76.58

Table 41. March 2010 wind data at Coron Island from onshore weather station and meoscale model output

Source Date	PAGASA		ERA-Interim		NCEP FNL		NCEP CFSR	
	Wind Speed (m/s)	Wind Direction (Degrees)	Wind Speed (m/s)	Wind Direction (Degrees)	Wind Speed (m/s)	Wind Direction (Degrees)	Wind Speed (m/s)	Wind Direction (Degrees)
01/03/2010	2	120	6.33	81.82	7.03	83.91	6.62	84.13
02/03/2010	1	120	5.04	82.97	4.75	77.66	4.70	79.30
03/03/2010	3	140	7.35	86.88	7.59	87.59	7.39	87.42
04/03/2010	3	40	6.70	84.87	7.56	83.83	7.77	85.88
05/03/2010	3	40	7.58	88.48	8.02	85.80	7.69	87.20
06/03/2010	2	0	5.27	85.37	6.29	84.05	5.77	86.81
07/03/2010	2	40	5.68	85.25	6.47	80.92	6.88	84.19
08/03/2010	3	120	6.45	80.44	5.90	73.44	5.20	73.77
09/03/2010	1	120	4.81	55.95	4.47	46.43	4.49	45.17
10/03/2010	1	120	6.51	89.24	5.23	88.26	5.74	86.91
11/03/2010	2	40	7.57	84.95	8.31	80.70	8.13	81.51
12/03/2010	2	0	9.12	84.39	6.35	79.52	7.36	83.47
13/03/2010	2	40	8.38	84.97	8.34	85.05	6.87	83.43
14/03/2010	3	40	9.73	84.69	7.46	82.17	6.97	78.06
15/03/2010	2	40	7.76	80.99	7.38	79.50	7.16	76.52
16/03/2010	2	120	7.21	84.63	7.26	74.54	7.49	76.82
17/03/2010	2	40	5.88	79.76	6.87	70.63	7.01	73.61
18/03/2010	2	140	6.37	78.62	4.68	78.80	5.68	79.92
19/03/2010	2	140	7.35	84.35	5.71	72.20	6.56	78.42
20/03/2010	1	120	4.84	77.76	3.22	52.69	5.62	77.98
21/03/2010	1	120	6.28	77.26	5.33	74.10	5.98	73.12
22/03/2010	2	120	9.05	86.13	9.93	83.91	9.42	86.26
23/03/2010	2	140	7.26	85.55	6.83	80.05	6.87	83.99
24/03/2010	2	140	3.90	80.36	3.15	42.71	2.75	48.31
25/03/2010	1	220	4.03	65.28	2.92	53.64	2.89	66.67
26/03/2010	2	40	5.05	95.88	5.41	82.77	6.01	89.00
27/03/2010	1	120	3.80	95.62	4.31	91.73	4.85	84.79
28/03/2010	1	180	4.55	92.67	4.21	83.95	5.02	84.97
29/03/2010	2	140	7.76	84.23	6.57	81.66	7.38	82.91
30/03/2010	3	140	8.35	80.76	7.20	74.32	7.50	78.25
31/03/2010	2	140	6.04	79.53	4.53	68.47	3.57	68.03

Table 42. March 2010 wind data at Cuyo Island from onshore weather station and meoscale model output

Source Date	PAGASA		ERA-Interim		NCEP FNL		NCEP CFSR	
	Wind Speed (m/s)	Wind Direction (Degrees)	Wind Speed (m/s)	Wind Direction (Degrees)	Wind Speed (m/s)	Wind Direction (Degrees)	Wind Speed (m/s)	Wind Direction (Degrees)
01/03/2010	2	20	5.87	38.52	7.02	43.36	6.72	39.28
02/03/2010	2	20	4.83	38.71	6.00	40.31	5.89	35.99
03/03/2010	2	20	3.60	43.25	5.87	45.45	4.78	44.77
04/03/2010	2	20	5.20	39.80	5.43	42.84	5.04	44.36
05/03/2010	2	20	3.97	43.78	3.70	42.69	4.80	38.76
06/03/2010	2	20	4.10	55.95	4.48	25.20	4.56	31.41
07/03/2010	2	20	4.77	34.62	5.79	39.40	5.40	35.56
08/03/2010	2	20	6.41	37.31	6.41	39.31	6.08	32.90
09/03/2010	2	20	6.40	16.58	6.80	20.28	6.62	16.14
10/03/2010	3	20	9.11	41.54	9.96	38.72	9.87	39.54
11/03/2010	2	40	8.60	42.95	7.86	46.06	8.42	43.77
12/03/2010	2	40	6.97	44.42	6.14	41.89	6.91	41.79
13/03/2010	2	40	6.58	43.78	6.40	45.50	6.33	42.84
14/03/2010	2	40	9.08	47.91	8.34	45.95	8.14	44.09
15/03/2010	2	40	8.14	45.21	8.01	44.41	7.76	43.30
16/03/2010	2	40	8.97	42.72	9.50	44.38	9.23	42.88
17/03/2010	2	40	9.33	40.74	10.02	42.55	9.75	41.51
18/03/2010	3	40	9.64	38.39	10.53	39.23	10.03	38.03
19/03/2010	3	40	9.11	39.86	9.88	38.87	9.72	39.65
20/03/2010	3	40	9.29	37.25	9.85	34.82	9.14	36.86
21/03/2010	3	320	7.88	38.79	9.26	41.66	8.89	37.65
22/03/2010	3	40	7.43	44.44	7.03	52.67	6.43	48.83
23/03/2010	3	40	6.32	41.52	7.56	41.40	6.89	37.13
24/03/2010	2	40	6.36	30.10	7.28	26.14	7.22	26.09
25/03/2010	2	40	6.34	16.80	7.50	30.87	7.23	19.86
26/03/2010	3	40	9.57	39.27	10.20	40.53	9.78	40.29
27/03/2010	3	40	9.87	37.57	11.20	37.98	10.32	37.57
28/03/2010	3	40	10.14	37.02	11.45	39.36	11.13	37.68
29/03/2010	3	40	10.88	41.46	11.41	40.69	11.33	41.45
30/03/2010	3	40	10.16	42.47	10.72	39.62	10.30	40.80
31/03/2010	3	40	9.03	39.66	9.81	38.31	9.34	34.91

Table 43. March 2010 wind data at Puerto Princesa from onshore weather station and meoscale model output

Source Date	PAGASA		ERA-Interim		NCEP FNL		NCEP CFSR	
	Wind Speed (m/s)	Wind Direction (Degrees)	Wind Speed (m/s)	Wind Direction (Degrees)	Wind Speed (m/s)	Wind Direction (Degrees)	Wind Speed (m/s)	Wind Direction (Degrees)
01/03/2010	4	90	4.13	109.39	3.76	81.50	3.50	79.01
02/03/2010	3	90	3.45	125.67	2.98	85.24	2.59	103.28
03/03/2010	3	90	3.81	127.74	2.73	84.26	3.19	84.00
04/03/2010	3	90	3.24	168.52	3.26	93.38	2.96	100.48
05/03/2010	3	90	3.88	139.56	3.37	110.35	2.64	97.78
06/03/2010	3	90	3.37	182.47	2.41	90.51	2.20	112.08
07/03/2010	3	90	3.40	86.43	2.36	87.28	2.36	88.71
08/03/2010	3	90	3.77	122.16	2.99	91.18	2.61	95.46
09/03/2010	3	90	3.90	48.32	3.35	43.19	3.34	37.14
10/03/2010	3	90	4.85	60.85	4.41	49.11	3.78	52.41
11/03/2010	3	90	4.28	79.37	4.55	78.04	4.39	81.09
12/03/2010	4	90	3.29	87.11	4.06	78.54	3.45	80.16
13/03/2010	3	90	3.62	85.65	2.79	84.21	3.10	82.23
14/03/2010	3	90	3.55	87.78	4.36	72.84	3.96	71.90
15/03/2010	4	90	4.25	85.62	4.34	67.62	3.82	67.20
16/03/2010	4	90	4.16	73.14	5.64	62.81	4.71	66.79
17/03/2010	5	90	4.29	76.40	5.27	67.22	4.38	66.72
18/03/2010	4	90	4.38	71.31	5.04	59.83	4.63	64.12
19/03/2010	4	90	3.82	79.55	5.31	68.85	4.72	73.56
20/03/2010	4	90	4.01	83.34	3.91	57.65	2.94	75.45
21/03/2010	4	90	3.62	68.13	4.06	55.59	3.84	56.94
22/03/2010	4	90	4.06	85.83	5.30	82.77	4.81	81.06
23/03/2010	3	90	4.22	129.02	3.14	95.31	3.14	98.20
24/03/2010	3	90	3.46	76.88	2.91	53.57	2.67	50.14
25/03/2010	3	90	3.24	26.43	2.40	16.24	2.87	5.58
26/03/2010	4	90	4.44	68.35	5.88	72.14	4.52	63.55
27/03/2010	5	90	4.59	77.88	5.62	70.04	4.35	70.72
28/03/2010	4	90	4.62	71.38	5.74	64.04	4.66	63.14
29/03/2010	5	90	5.74	74.75	6.01	70.26	5.02	69.04
30/03/2010	5	90	3.97	76.97	5.48	68.96	4.31	73.00
31/03/2010	4	90	3.04	87.69	5.13	68.29	3.16	82.12

Table 44. April 2010 wind data at Coron Island from onshore weather station and meoscale model output

Source Date	PAGASA		ERA-Interim		NCEP FNL		NCEP CFSR	
	Wind Speed (m/s)	Wind Direction (Degrees)	Wind Speed (m/s)	Wind Direction (Degrees)	Wind Speed (m/s)	Wind Direction (Degrees)	Wind Speed (m/s)	Wind Direction (Degrees)
01/04/2010	1	120	6.79	82.56	6.10	75.53	6.50	80.29
02/04/2010	2	120	6.31	85.34	6.02	74.68	6.30	79.62
03/04/2010	1	120	6.32	81.52	5.70	80.73	5.95	75.45
04/04/2010	2	140	5.37	80.82	4.11	69.58	5.08	72.63
05/04/2010	2	90	5.99	84.45	5.68	77.81	6.35	78.21
06/04/2010	4	140	6.62	82.29	7.43	79.62	8.20	82.36
07/04/2010	1	120	5.38	83.38	6.06	65.08	6.75	76.86
08/04/2010	2	120	5.79	81.65	7.23	81.35	6.35	73.92
09/04/2010	1	120	4.17	81.66	4.47	74.69	5.11	77.94
10/04/2010	2	140	7.62	85.47	7.85	81.91	7.67	80.41
11/04/2010	3	140	8.19	88.33	9.45	86.46	9.22	85.89
12/04/2010	2	40	5.24	80.28	4.87	57.94	4.87	70.44
13/04/2010	2	120	6.85	84.81	8.14	82.38	7.41	84.30
14/04/2010	3	40	9.30	84.25	8.79	82.79	9.35	83.64
15/04/2010	3	120	6.62	82.29	4.63	76.69	5.40	71.78
16/04/2010	4	140	9.68	90.30	8.48	84.27	7.55	84.46
17/04/2010	3	140	9.18	83.36	8.06	77.67	9.09	82.77
18/04/2010	4	140	7.97	83.82	7.62	80.95	8.86	83.59
19/04/2010	2	120	5.94	86.68	6.57	84.45	6.31	83.61
20/04/2010	2	120	6.31	86.93	5.68	84.22	5.95	87.33
21/04/2010	2	120	6.71	89.54	6.53	87.68	6.51	90.29
22/04/2010	3	180	6.13	84.00	6.89	84.75	6.55	85.30
23/04/2010	2	140	4.20	81.18	4.52	76.03	4.58	64.08
24/04/2010	2	140	5.11	89.89	5.68	85.61	5.09	82.81
25/04/2010	3	120	6.02	86.62	6.28	81.36	5.01	64.02
26/04/2010	1	120	3.43	67.98	1.81	244.81	2.12	124.49
27/04/2010	2	120	4.14	74.00	4.03	98.24	2.66	228.00
28/04/2010	1	140	4.38	137.63	4.14	119.31	4.72	126.99
29/04/2010	1	180	2.66	149.66	4.80	98.59	4.59	99.42
30/04/2010	1	140	3.37	85.04	5.47	86.74	4.96	90.21

Table 45. April 2010 wind data at Cuyo Island from onshore weather station and meoscale model output

Source Date	PAGASA		ERA-Interim		NCEP FNL		NCEP CFSR	
	Wind Speed (m/s)	Wind Direction (Degrees)	Wind Speed (m/s)	Wind Direction (Degrees)	Wind Speed (m/s)	Wind Direction (Degrees)	Wind Speed (m/s)	Wind Direction (Degrees)
01/04/2010	3	40	7.25	41.78	8.15	41.99	7.28	43.72
02/04/2010	2	40	6.82	36.68	7.63	38.15	6.45	38.48
03/04/2010	3	40	8.49	39.30	9.54	39.62	8.51	36.43
04/04/2010	2	40	8.10	37.56	8.70	37.50	8.06	36.70
05/04/2010	2	40	6.32	39.01	7.18	40.49	6.42	36.89
06/04/2010	2	40	6.79	37.08	7.29	40.44	6.07	38.61
07/04/2010	2	40	7.28	38.76	9.05	40.35	7.37	37.79
08/04/2010	2	40	6.75	37.34	7.28	42.00	6.82	37.65
09/04/2010	2	40	5.77	31.64	7.53	34.69	6.38	33.99
10/04/2010	2	40	6.59	38.02	7.51	45.90	6.84	38.52
11/04/2010	2	40	5.94	40.55	6.65	45.77	6.10	42.63
12/04/2010	2	40	5.39	31.30	6.12	28.62	5.86	26.79
13/04/2010	1	40	6.27	37.73	5.20	56.87	5.66	46.25
14/04/2010	1	20	7.55	42.28	7.11	44.78	5.71	45.89
15/04/2010	2	20	7.77	41.40	8.59	40.33	7.49	37.18
16/04/2010	2	20	9.20	42.92	9.08	43.81	8.44	41.43
17/04/2010	3	20	9.03	45.70	9.84	42.79	9.20	44.55
18/04/2010	2	20	8.59	43.16	9.09	44.69	8.67	43.05
19/04/2010	2	20	5.11	37.33	6.62	42.32	5.91	36.48
20/04/2010	1	20	3.18	25.62	5.31	38.31	3.98	38.64
21/04/2010	2	20	3.83	30.69	4.53	33.85	3.89	34.18
22/04/2010	2	20	3.79	23.40	4.66	41.17	4.00	27.06
23/04/2010	2	20	4.71	26.87	5.69	29.32	6.09	23.02
24/04/2010	1	20	7.18	35.52	7.86	38.37	7.17	36.14
25/04/2010	1	20	7.64	41.80	7.47	40.33	7.56	35.51
26/04/2010	3	20	7.83	30.72	8.96	24.40	8.31	29.17
27/04/2010	2	20	5.41	17.53	6.03	106.43	5.28	5.55
28/04/2010	3	140	3.88	168.51	2.60	144.66	3.99	157.60
29/04/2010	2	140	2.52	179.79	2.61	117.54	2.34	319.85
30/04/2010	1	270	2.09	66.79	2.56	26.48	3.49	32.08

Table 46. April 2010 wind data at Puerto Princesa from onshore weather station and meoscale model output

Source Date	PAGASA		ERA-Interim		NCEP FNL		NCEP CFSR	
	Wind Speed (m/s)	Wind Direction (Degrees)	Wind Speed (m/s)	Wind Direction (Degrees)	Wind Speed (m/s)	Wind Direction (Degrees)	Wind Speed (m/s)	Wind Direction (Degrees)
01/04/2010	4	90	3.40	79.30	5.43	69.87	4.63	73.11
02/04/2010	3	90	3.69	83.95	4.53	72.93	3.30	95.95
03/04/2010	5	90	4.66	77.02	5.14	68.38	3.86	65.24
04/04/2010	4	90	4.35	102.74	4.18	67.80	3.53	75.27
05/04/2010	4	90	3.74	99.21	4.04	72.01	3.09	76.75
06/04/2010	3	90	3.59	79.43	3.73	62.74	3.24	73.46
07/04/2010	3	90	4.01	86.07	4.43	64.34	3.45	67.97
08/04/2010	3	90	3.61	119.53	3.68	67.90	3.25	75.33
09/04/2010	3	90	3.60	72.25	3.05	61.52	3.27	76.42
10/04/2010	3	90	3.29	100.49	3.93	67.71	3.06	73.70
11/04/2010	3	90	4.16	126.77	4.02	87.56	3.60	89.86
12/04/2010	3	90	3.06	137.62	2.49	98.96	2.36	95.18
13/04/2010	3	90	3.42	93.63	3.09	70.04	2.43	70.92
14/04/2010	3	90	4.37	100.05	4.18	77.47	3.75	96.28
15/04/2010	3	90	3.68	96.86	3.64	74.95	2.68	81.65
16/04/2010	4	90	4.87	79.41	4.52	72.96	3.91	73.90
17/04/2010	4	90	4.21	80.35	5.00	69.97	4.54	76.80
18/04/2010	3	90	3.96	103.81	5.15	68.04	4.11	74.19
19/04/2010	3	90	4.04	107.37	3.54	84.23	2.91	92.25
20/04/2010	3	90	3.33	143.11	2.77	107.90	2.38	143.85
21/04/2010	3	110	3.63	166.41	2.56	121.93	2.71	157.48
22/04/2010	3	90	2.89	153.12	2.14	83.29	2.34	119.37
23/04/2010	3	90	3.29	92.04	2.47	74.27	2.50	57.08
24/04/2010	3	90	3.34	76.99	3.84	74.13	3.06	75.98
25/04/2010	3	90	3.75	84.75	4.19	73.78	3.42	76.97
26/04/2010	3	90	3.24	74.96	3.03	55.76	3.19	47.95
27/04/2010	3	270	3.61	1.30	3.36	98.72	2.69	349.63
28/04/2010	2	90	2.93	236.60	4.03	156.70	3.07	157.68
29/04/2010	3	180	3.61	185.64	3.14	182.59	3.44	178.53
30/04/2010	2	180	3.23	165.25	2.05	111.81	2.01	130.44

Table 47. May 2010 wind data at Coron Island from onshore weather station and meoscale model output

Source Date	PAGASA		ERA-Interim		NCEP FNL		NCEP CFSR	
	Wind Speed (m/s)	Wind Direction (Degrees)	Wind Speed (m/s)	Wind Direction (Degrees)	Wind Speed (m/s)	Wind Direction (Degrees)	Wind Speed (m/s)	Wind Direction (Degrees)
01/05/2010	1	120	3.20	86.83	4.27	93.60	3.66	89.54
02/05/2010	1	120	2.82	94.49	2.09	101.17	2.55	81.93
03/05/2010	2	120	3.20	76.32	1.46	106.90	2.63	75.96
04/05/2010	1	180	3.62	89.27	2.96	54.97	4.04	83.50
05/05/2010	2	140	3.82	90.43	5.63	88.26	4.61	99.88
06/05/2010	1	180	4.27	80.58	5.88	86.23	5.96	80.85
07/05/2010	2	120	5.75	85.72	7.38	84.26	6.22	83.64
08/05/2010	1	40	5.72	86.87	6.95	86.51	6.42	86.88
09/05/2010	1	120	4.28	87.67	6.16	87.52	4.87	85.25
10/05/2010	2	180	3.90	83.61	5.90	76.03	4.77	72.86
11/05/2010	2	140	5.76	84.17	8.27	84.41	8.34	85.15
12/05/2010	2	140	7.17	86.94	9.20	85.15	8.07	88.83
13/05/2010	2	120	7.22	87.85	8.24	82.55	7.22	85.48
14/05/2010	2	120	6.01	85.93	8.09	82.63	6.60	83.39
15/05/2010	2	120	7.12	86.21	7.61	83.41	7.16	85.22
16/05/2010	1	140	6.29	86.86	7.46	80.08	7.11	80.14
17/05/2010	3	40	5.09	88.77	8.33	85.05	6.61	81.90
18/05/2010	2	140	4.31	83.77	6.81	92.09	5.97	83.19
19/05/2010	1	120	3.82	86.64	5.52	89.74	5.65	81.69
20/05/2010	1	120	4.62	91.73	6.72	79.64	5.81	90.84
21/05/2010	1	120	3.12	86.90	5.29	94.13	4.70	92.51
22/05/2010	1	210	1.68	138.68	2.56	132.58	2.14	103.94
23/05/2010	1	40	2.89	199.74	3.59	196.96	3.56	195.31
24/05/2010	1	320	2.75	191.95	3.11	175.77	3.75	186.30
25/05/2010	1	180	2.32	219.31	2.22	190.24	2.25	201.31
26/05/2010	1	140	2.33	90.52	2.46	155.95	1.80	183.83
27/05/2010	1	180	2.08	104.73	2.46	162.55	1.51	187.71
28/05/2010	2	180	2.09	102.28	2.01	204.14	2.09	87.66
29/05/2010	1	220	1.68	136.24	3.05	211.69	1.72	123.51
30/05/2010	1	180	2.67	218.39	2.48	239.07	2.12	233.76
31/05/2010	1	210	2.53	186.02	2.37	192.93	1.91	275.46

Table 48. May 2010 wind data at Cuyo Island from onshore weather station and meoscale model output

Source Date	PAGASA		ERA-Interim		NCEP FNL		NCEP CFSR	
	Wind Speed (m/s)	Wind Direction (Degrees)	Wind Speed (m/s)	Wind Direction (Degrees)	Wind Speed (m/s)	Wind Direction (Degrees)	Wind Speed (m/s)	Wind Direction (Degrees)
01/05/2010	1	320	2.49	169.39	1.48	168.82	2.80	234.66
02/05/2010	0	0	2.21	323.51	1.30	337.70	2.21	306.84
03/05/2010	1	0	3.21	9.22	2.62	6.17	2.85	9.44
04/05/2010	1	320	2.20	138.57	4.55	21.32	2.09	17.70
05/05/2010	1	270	2.54	93.95	2.35	95.62	3.03	123.65
06/05/2010	1	20	4.04	23.84	5.57	37.72	5.16	37.47
07/05/2010	1	320	5.28	38.94	5.80	45.70	4.91	48.38
08/05/2010	1	320	2.62	25.75	3.87	49.11	3.65	56.48
09/05/2010	1	320	2.88	264.80	3.81	26.62	3.73	31.39
10/05/2010	1	320	3.71	16.84	6.49	36.41	6.07	32.64
11/05/2010	1	20	5.55	39.24	5.79	56.14	4.18	90.51
12/05/2010	1	0	3.54	43.64	4.75	61.25	4.26	68.98
13/05/2010	2	40	4.82	34.60	5.01	42.16	4.35	45.96
14/05/2010	1	40	4.26	30.66	5.52	43.26	4.13	42.58
15/05/2010	2	40	5.23	39.46	6.48	44.91	5.44	44.81
16/05/2010	1	40	5.66	38.18	7.73	42.76	6.30	38.65
17/05/2010	2	40	4.16	30.59	6.22	42.88	5.37	37.12
18/05/2010	1	40	3.94	22.17	5.65	65.75	4.51	36.23
19/05/2010	1	220	2.81	22.83	4.35	47.59	2.10	85.88
20/05/2010	1	270	1.66	359.93	5.43	43.47	1.99	332.86
21/05/2010	2	0	2.26	338.90	1.87	322.21	2.76	39.88
22/05/2010	1	0	1.83	300.95	1.79	228.62	1.86	251.01
23/05/2010	1	150	3.41	203.63	2.72	192.77	2.81	208.32
24/05/2010	1	220	2.60	196.67	2.24	187.46	2.79	201.31
25/05/2010	1	220	1.88	238.21	1.68	216.25	2.15	211.76
26/05/2010	1	220	1.49	286.17	2.28	179.59	1.52	234.42
27/05/2010	0	0	1.40	347.98	1.46	186.36	1.20	304.15
28/05/2010	2	220	1.20	284.60	1.47	220.03	1.72	346.02
29/05/2010	1	220	1.20	213.05	2.64	224.80	1.39	282.20
30/05/2010	1	220	2.69	223.15	2.27	231.84	2.33	228.91
31/05/2010	1	220	3.24	223.12	2.52	233.65	2.61	235.31

Table 49. May 2010 wind data at Puerto Princesa from onshore weather station and meoscale model output

Source Date	PAGASA		ERA-Interim		NCEP FNL		NCEP CFSR	
	Wind Speed (m/s)	Wind Direction (Degrees)	Wind Speed (m/s)	Wind Direction (Degrees)	Wind Speed (m/s)	Wind Direction (Degrees)	Wind Speed (m/s)	Wind Direction (Degrees)
01/05/2010	2	90	2.91	165.71	2.24	183.93	2.31	168.83
02/05/2010	2	90	3.03	163.29	2.13	183.31	2.37	169.29
03/05/2010	3	110	3.20	158.35	2.18	180.92	2.35	167.14
04/05/2010	2	90	3.03	168.60	2.00	160.30	2.24	170.53
05/05/2010	2	90	3.03	160.37	2.03	183.84	2.33	178.62
06/05/2010	2	90	2.89	134.05	1.94	129.70	2.20	115.17
07/05/2010	3	90	3.82	87.38	4.13	76.28	4.02	82.68
08/05/2010	2	90	3.86	123.03	2.11	112.46	2.69	153.78
09/05/2010	2	110	2.93	162.67	2.22	107.84	2.25	169.88
10/05/2010	2	180	2.90	157.04	2.11	67.03	2.09	102.57
11/05/2010	3	90	3.34	82.52	3.34	100.58	4.02	92.40
12/05/2010	3	90	4.80	107.33	4.37	82.93	3.60	128.27
13/05/2010	3	90	3.67	123.72	3.00	85.45	2.84	99.64
14/05/2010	3	90	3.60	116.37	2.45	82.57	2.40	82.30
15/05/2010	2	90	3.92	112.11	3.36	75.29	2.95	82.79
16/05/2010	2	90	3.83	106.13	3.68	73.98	3.23	80.27
17/05/2010	3	90	3.87	105.46	3.45	78.69	3.61	93.11
18/05/2010	2	140	3.46	114.67	4.37	94.06	2.30	112.01
19/05/2010	2	140	3.44	146.61	2.50	95.94	2.08	142.08
20/05/2010	3	140	3.20	150.81	2.27	98.07	2.43	120.55
21/05/2010	2	140	3.08	182.50	2.33	165.44	2.28	168.04
22/05/2010	2	140	3.49	182.12	2.17	192.52	2.49	174.57
23/05/2010	2	180	3.41	169.43	2.48	159.52	3.24	190.92
24/05/2010	2	160	4.11	178.98	3.01	188.24	3.22	188.93
25/05/2010	2	160	3.38	173.70	2.52	178.62	3.30	190.04
26/05/2010	3	160	3.25	170.11	2.70	183.99	3.20	190.16
27/05/2010	2	140	3.44	181.50	2.68	177.08	2.97	188.95
28/05/2010	3	180	3.28	162.61	2.21	181.87	2.86	193.44
29/05/2010	2	180	3.70	175.69	2.97	190.07	2.82	183.98
30/05/2010	2	180	3.72	174.76	2.68	187.52	2.95	189.08
31/05/2010	2	160	3.49	166.95	2.84	183.18	2.81	184.46

Table 50. June 2010 wind data at Coron Island from onshore weather station and meoscale model output

Source Date	PAGASA		ERA-Interim		NCEP FNL		NCEP CFSR	
	Wind Speed (m/s)	Wind Direction (Degrees)	Wind Speed (m/s)	Wind Direction (Degrees)	Wind Speed (m/s)	Wind Direction (Degrees)	Wind Speed (m/s)	Wind Direction (Degrees)
01/06/2010	0	0	3.12	245.69	5.38	214.40	4.14	217.17
02/06/2010	1	0	5.27	204.59	6.43	209.64	5.03	200.08
03/06/2010	0	0	5.33	203.01	6.90	213.17	5.40	210.46
04/06/2010	1	0	5.13	210.02	6.45	214.93	5.43	207.37
05/06/2010	1	220	5.60	204.86	7.00	229.66	4.94	212.07
06/06/2010	0	0	3.83	233.99	4.44	254.16	3.83	248.23
07/06/2010	1	0	1.93	44.69	3.29	285.64	2.31	311.07
08/06/2010	0	0	1.58	29.81	1.81	234.68	1.94	277.93
09/06/2010	1	220	2.04	269.48	2.65	287.62	3.36	213.11
10/06/2010	1	0	1.76	348.70	5.27	229.31	2.28	243.53
11/06/2010	1	220	2.22	303.72	3.52	280.18	2.75	285.83
12/06/2010	1	0	2.14	44.50	2.89	191.49	2.13	280.81
13/06/2010	1	180	1.73	82.29	3.00	290.91	1.77	300.58
14/06/2010	1	0	2.09	20.65	3.17	94.03	2.01	21.32
15/06/2010	1	180	3.04	70.24	4.12	92.89	2.85	85.93
16/06/2010	2	220	4.09	96.29	4.55	101.74	3.76	109.05
17/06/2010	2	140	3.63	91.67	3.90	155.63	2.45	158.76
18/06/2010	1	120	3.18	21.53	4.73	212.52	3.01	222.08
19/06/2010	0	0	2.59	285.25	5.56	190.53	4.38	194.73
20/06/2010	0	0	3.73	206.00	4.52	190.09	4.43	199.59
21/06/2010	2	180	3.34	202.88	5.00	198.20	3.99	179.60
22/06/2010	1	140	3.17	198.21	3.91	176.99	3.54	181.50
23/06/2010	2	90	2.07	290.37	3.79	216.28	2.26	243.54
24/06/2010	1	0	2.53	267.59	3.10	252.88	2.35	240.59
25/06/2010	0	0	3.20	205.86	4.79	214.80	2.43	257.90
26/06/2010	0	0	2.11	280.81	4.79	208.46	3.47	218.58
27/06/2010	1	220	1.63	311.90	3.06	146.46	2.82	274.68
28/06/2010	1	0	2.97	292.02	3.12	206.18	3.48	267.71
29/06/2010	0	0	4.19	261.04	3.15	221.19	4.70	241.97
30/06/2010	0	0	4.24	234.39	5.07	193.71	4.86	222.79

Table 51. June 2010 wind data at Cuyo Island from onshore weather station and meoscale model output

Source Date	PAGASA		ERA-Interim		NCEP FNL		NCEP CFSR	
	Wind Speed (m/s)	Wind Direction (Degrees)	Wind Speed (m/s)	Wind Direction (Degrees)	Wind Speed (m/s)	Wind Direction (Degrees)	Wind Speed (m/s)	Wind Direction (Degrees)
01/06/2010	2	220	5.95	218.19	5.90	215.85	5.48	217.38
02/06/2010	2	220	6.08	207.96	7.63	199.54	5.72	198.34
03/06/2010	1	220	5.84	211.79	6.83	205.56	6.02	200.00
04/06/2010	1	220	5.10	211.93	6.25	210.16	5.31	206.69
05/06/2010	1	220	5.28	215.81	6.48	220.18	5.17	217.75
06/06/2010	1	220	4.54	219.21	5.96	227.50	5.02	218.80
07/06/2010	1	220	2.97	240.69	5.45	244.78	4.30	239.69
08/06/2010	0	0	2.44	237.63	3.43	222.66	3.35	220.98
09/06/2010	0	0	2.56	205.20	5.08	212.97	4.09	216.53
10/06/2010	0	0	2.20	236.55	7.36	199.68	3.32	222.21
11/06/2010	0	0	2.20	249.81	4.22	223.47	4.10	229.37
12/06/2010	1	120	1.21	161.38	2.88	218.14	2.97	220.19
13/06/2010	0	0	1.48	192.26	2.44	279.29	1.76	244.29
14/06/2010	0	0	1.07	37.50	2.07	202.12	1.79	325.89
15/06/2010	1	220	1.42	113.97	2.17	345.57	1.34	166.21
16/06/2010	1	220	1.99	131.94	2.38	122.70	1.80	139.09
17/06/2010	1	220	2.30	173.12	5.65	237.86	3.56	221.91
18/06/2010	1	220	4.74	252.56	5.86	210.96	4.47	219.54
19/06/2010	0	0	3.71	257.63	5.30	193.35	5.14	183.88
20/06/2010	1	220	4.94	228.35	4.68	207.21	4.93	189.85
21/06/2010	1	120	5.13	199.59	5.73	193.81	4.92	185.56
22/06/2010	1	120	3.42	180.46	4.41	175.87	3.80	181.27
23/06/2010	1	220	1.54	245.68	4.08	204.93	2.58	209.86
24/06/2010	2	220	3.41	237.91	4.77	217.45	3.26	229.14
25/06/2010	2	120	4.39	225.67	5.79	198.39	3.36	227.16
26/06/2010	No Data	No Data	3.84	213.70	3.96	186.31	3.98	208.54
27/06/2010	No Data	No Data	2.24	246.25	3.34	187.69	4.04	250.54
28/06/2010	No Data	No Data	4.69	286.28	4.41	234.73	4.67	247.14
29/06/2010	No Data	No Data	5.55	232.92	4.47	237.49	6.01	215.62
30/06/2010	No Data	No Data	4.68	227.83	6.14	190.97	5.60	210.11

Table 52. June 2010 wind data at Puerto Princesa from onshore weather station and meoscale model output

Source Date	PAGASA		ERA-Interim		NCEP FNL		NCEP CFSR	
	Wind Speed (m/s)	Wind Direction (Degrees)	Wind Speed (m/s)	Wind Direction (Degrees)	Wind Speed (m/s)	Wind Direction (Degrees)	Wind Speed (m/s)	Wind Direction (Degrees)
01/06/2010	3	160	4.82	191.50	3.53	205.25	3.94	201.32
02/06/2010	3	160	4.07	188.95	4.08	201.52	3.73	196.10
03/06/2010	3	160	3.65	196.13	4.11	200.70	3.84	204.50
04/06/2010	2	270	3.37	184.61	3.59	193.01	3.73	196.25
05/06/2010	2	180	3.25	201.11	2.94	196.55	3.18	205.24
06/06/2010	2	180	3.08	191.17	2.54	179.71	2.76	206.79
07/06/2010	3	160	2.89	166.13	2.18	173.68	2.95	198.23
08/06/2010	2	160	2.51	189.56	2.44	192.93	3.01	197.99
09/06/2010	2	160	3.66	179.37	3.51	196.34	3.53	198.94
10/06/2010	2	160	3.41	183.81	3.48	203.12	3.30	194.50
11/06/2010	2	270	3.24	191.95	3.19	203.18	3.50	195.96
12/06/2010	2	180	3.35	181.36	3.35	201.13	3.23	195.27
13/06/2010	2	180	3.48	179.24	2.12	267.78	3.03	191.80
14/06/2010	2	180	3.07	157.61	1.96	226.47	2.73	190.80
15/06/2010	1	160	2.85	168.13	2.72	207.74	2.69	191.04
16/06/2010	3	160	3.12	170.45	2.82	186.25	2.80	193.27
17/06/2010	3	180	2.92	163.65	2.86	209.10	3.33	210.10
18/06/2010	2	160	2.97	188.24	3.17	197.93	3.89	201.93
19/06/2010	2	290	2.21	212.50	3.84	199.79	3.70	194.32
20/06/2010	2	180	3.16	196.25	2.42	215.60	4.07	196.38
21/06/2010	2	220	3.78	221.46	3.02	205.33	3.09	191.65
22/06/2010	2	160	4.05	182.61	2.56	202.77	3.62	202.63
23/06/2010	2	180	3.04	177.80	3.38	207.25	3.61	197.35
24/06/2010	2	180	3.30	180.52	3.47	202.99	3.54	196.90
25/06/2010	2	180	4.21	187.36	4.58	196.41	3.80	199.02
26/06/2010	2	180	3.27	183.00	2.30	225.23	3.91	199.64
27/06/2010	2	160	2.53	190.15	2.62	197.79	3.15	195.16
28/06/2010	3	160	2.20	187.83	3.55	197.02	3.00	204.27
29/06/2010	2	180	2.59	214.89	2.69	214.47	2.89	218.61
30/06/2010	2	180	2.52	256.22	3.76	206.38	3.62	205.50

Table 53. July 2010 wind data at Coron Island from onshore weather station and meoscale model output

Source Date	PAGASA		ERA-Interim		NCEP FNL		NCEP CFSR	
	Wind Speed (m/s)	Wind Direction (Degrees)	Wind Speed (m/s)	Wind Direction (Degrees)	Wind Speed (m/s)	Wind Direction (Degrees)	Wind Speed (m/s)	Wind Direction (Degrees)
01/07/2010	1	180	2.20	207.88	3.01	195.93	3.36	217.48
02/07/2010	1	0	2.00	118.99	2.18	286.03	2.17	306.47
03/07/2010	1	0	2.07	55.90	1.64	283.60	1.85	268.90
04/07/2010	1	0	2.03	59.57	1.73	302.60	2.37	301.92
05/07/2010	1	0	1.66	354.38	3.06	304.92	2.13	311.40
06/07/2010	1	180	1.98	339.72	3.51	265.31	2.84	6.15
07/07/2010	1	0	2.79	88.77	4.06	217.25	3.87	88.45
08/07/2010	2	0	3.03	140.17	4.89	184.88	5.38	186.34
09/07/2010	0	0	5.38	221.32	6.25	197.80	4.53	214.97
10/07/2010	1	0	4.75	194.20	4.88	202.77	4.14	229.94
11/07/2010	0	0	2.79	184.08	4.40	173.54	3.07	246.26
12/07/2010	1	0	2.49	304.10	3.90	156.01	3.01	244.24
13/07/2010	0	0	2.00	225.97	3.56	136.87	2.71	210.98
14/07/2010	0	0	2.27	180.22	4.87	151.09	4.95	188.87
15/07/2010	3	320	3.12	165.19	5.47	183.47	4.20	186.31
16/07/2010	1	0	2.20	167.48	5.61	216.40	3.35	226.36
17/07/2010	1	0	1.80	9.44	7.68	223.70	3.09	296.61
18/07/2010	1	0	2.22	154.97	7.86	178.47	7.51	230.98
19/07/2010	0	0	4.91	185.16	6.67	188.20	7.32	234.99
20/07/2010	1	180	3.23	206.25	5.90	185.69	4.04	202.84
21/07/2010	1	220	2.29	249.58	5.06	218.80	2.39	223.75
22/07/2010	2	180	2.29	240.00	5.17	232.59	2.99	250.36
23/07/2010	1	220	3.47	216.55	7.42	199.83	4.40	241.53
24/07/2010	1	120	6.11	207.10	9.96	173.29	7.15	205.72
25/07/2010	2	180	6.09	171.02	8.62	163.38	8.96	179.62
26/07/2010	1	180	4.35	155.02	5.78	141.34	4.69	173.25
27/07/2010	1	0	1.76	136.90	6.33	170.88	3.39	187.08
28/07/2010	2	220	1.62	320.60	2.91	264.11	2.93	246.48
29/07/2010	1	180	2.28	287.44	4.86	194.28	4.25	270.49
30/07/2010	1	210	4.68	246.57	5.79	218.52	3.62	265.47
31/07/2010	0	0	5.84	225.17	5.78	197.04	4.63	204.19

Table 54. July 2010 wind data at Cuyo Island from onshore weather station and meoscale model output

Source Date	PAGASA		ERA-Interim		NCEP FNL		NCEP CFSR	
	Wind Speed (m/s)	Wind Direction (Degrees)	Wind Speed (m/s)	Wind Direction (Degrees)	Wind Speed (m/s)	Wind Direction (Degrees)	Wind Speed (m/s)	Wind Direction (Degrees)
01/07/2010	No Data	No Data	2.65	196.96	1.93	178.53	2.38	199.47
02/07/2010	No Data	No Data	1.60	189.42	1.94	340.39	1.76	282.04
03/07/2010	No Data	No Data	1.68	22.23	1.81	299.35	1.27	277.99
04/07/2010	No Data	No Data	1.49	331.92	2.18	294.47	1.69	300.18
05/07/2010	No Data	No Data	1.63	306.70	5.54	296.19	3.77	340.95
06/07/2010	No Data	No Data	2.84	348.34	5.43	295.47	3.00	39.34
07/07/2010	No Data	No Data	4.50	8.18	5.31	226.15	4.07	135.34
08/07/2010	No Data	No Data	4.61	268.48	3.89	189.68	5.70	188.33
09/07/2010	No Data	No Data	6.66	213.20	6.64	186.98	5.89	204.22
10/07/2010	No Data	No Data	4.52	196.34	4.66	206.63	5.71	219.08
11/07/2010	No Data	No Data	2.09	201.67	4.33	167.48	4.17	210.05
12/07/2010	1	20	1.91	279.11	2.93	185.73	3.66	214.11
13/07/2010	1	220	2.74	230.18	3.74	176.03	3.39	203.73
14/07/2010	1	120	3.24	193.12	4.30	143.11	5.03	182.18
15/07/2010	1	180	3.15	173.00	5.79	182.77	4.54	184.74
16/07/2010	0	0	2.21	181.07	5.94	209.28	4.50	210.43
17/07/2010	1	120	1.36	270.13	7.00	216.36	4.38	262.43
18/07/2010	1	220	2.73	221.52	7.63	182.93	6.97	224.70
19/07/2010	1	220	3.80	187.78	6.66	192.53	7.53	211.97
20/07/2010	1	220	2.48	212.20	5.79	181.29	4.10	201.36
21/07/2010	1	220	3.81	226.46	5.34	217.22	3.35	213.68
22/07/2010	0	0	4.18	222.60	5.50	220.70	5.01	239.77
23/07/2010	0	0	5.11	234.70	8.43	213.18	6.61	228.26
24/07/2010	2	220	7.70	202.70	11.50	175.80	9.34	205.93
25/07/2010	1	220	6.90	172.42	8.84	159.57	9.44	176.91
26/07/2010	1	220	3.79	163.93	4.77	142.35	3.77	177.81
27/07/2010	1	220	1.67	241.19	5.43	178.98	3.25	194.91
28/07/2010	0	0	2.44	263.26	2.57	203.62	4.29	225.51
29/07/2010	1	220	3.85	273.58	4.94	205.85	3.74	256.60
30/07/2010	1	220	6.05	254.24	6.73	212.93	4.91	225.61
31/07/2010	1	220	5.42	216.35	6.68	187.48	6.33	202.08

Table 55. July 2010 wind data at Puerto Princesa from onshore weather station and meoscale model output

Source Date	PAGASA		ERA-Interim		NCEP FNL		NCEP CFSR	
	Wind Speed (m/s)	Wind Direction (Degrees)	Wind Speed (m/s)	Wind Direction (Degrees)	Wind Speed (m/s)	Wind Direction (Degrees)	Wind Speed (m/s)	Wind Direction (Degrees)
01/07/2010	2	180	3.93	181.42	3.02	192.52	3.24	202.78
02/07/2010	2	180	3.47	174.93	2.23	182.44	2.31	207.31
03/07/2010	2	180	3.18	169.43	1.81	156.56	2.39	197.79
04/07/2010	2	90	2.63	154.36	1.93	172.10	2.72	208.10
05/07/2010	2	90	2.42	169.42	1.62	131.34	2.06	179.67
06/07/2010	2	140	2.19	330.18	2.49	203.34	1.98	317.43
07/07/2010	2	20	2.88	53.80	2.04	212.28	2.39	296.66
08/07/2010	2	270	2.67	295.49	2.51	190.64	3.32	199.99
09/07/2010	2	140	3.03	209.34	3.55	201.12	3.75	201.79
10/07/2010	2	180	3.46	213.81	3.23	214.93	2.48	194.67
11/07/2010	2	140	3.76	183.27	2.83	197.88	3.31	206.28
12/07/2010	2	320	2.76	155.34	2.82	199.12	3.12	205.59
13/07/2010	2	140	2.85	173.74	3.15	210.10	3.08	202.48
14/07/2010	2	180	4.26	188.29	3.34	202.53	3.31	197.10
15/07/2010	2	160	4.15	182.88	3.53	203.32	3.49	198.83
16/07/2010	2	140	3.98	181.78	3.92	204.08	3.53	199.70
17/07/2010	2	140	3.02	168.99	3.53	191.54	2.13	174.20
18/07/2010	2	140	2.88	185.20	5.07	194.08	2.76	199.56
19/07/2010	2	160	3.44	201.11	4.13	200.28	2.86	187.31
20/07/2010	2	160	3.58	188.83	3.52	201.61	2.86	202.29
21/07/2010	2	160	3.03	196.56	3.65	201.00	2.89	200.04
22/07/2010	2	140	3.10	195.05	2.93	199.96	2.86	209.24
23/07/2010	2	160	3.79	200.54	4.48	196.98	2.92	217.30
24/07/2010	2	180	3.55	204.36	8.77	185.51	4.90	203.52
25/07/2010	2	180	6.69	179.18	7.43	184.70	6.47	191.90
26/07/2010	2	160	4.80	190.20	2.93	192.47	3.59	209.25
27/07/2010	2	180	3.77	185.60	3.49	182.25	3.46	195.87
28/07/2010	2	140	2.78	187.73	2.51	196.05	3.04	193.17
29/07/2010	2	180	2.76	247.23	2.36	191.80	1.95	219.56
30/07/2010	2	140	2.33	197.40	2.91	216.79	2.67	234.78
31/07/2010	2	140	2.57	216.35	3.19	211.77	3.34	216.42

Table 56. August 2010 wind data at Coron Island from onshore weather station and meoscale model output

Source Date	PAGASA		ERA-Interim		NCEP FNL		NCEP CFSR	
	Wind Speed (m/s)	Wind Direction (Degrees)	Wind Speed (m/s)	Wind Direction (Degrees)	Wind Speed (m/s)	Wind Direction (Degrees)	Wind Speed (m/s)	Wind Direction (Degrees)
01/08/2010	1	0	2.63	240.21	2.24	194.70	2.67	206.92
02/08/2010	0	0	2.31	281.77	3.15	295.65	2.69	285.89
03/08/2010	1	320	3.91	280.39	3.84	282.42	4.88	274.26
04/08/2010	1	270	5.44	268.46	5.87	196.37	6.51	271.19
05/08/2010	1	0	3.54	253.89	13.24	194.37	5.09	267.75
06/08/2010	3	180	6.21	224.50	13.01	216.52	5.39	240.64
07/08/2010	4	180	8.87	210.26	11.70	205.44	8.11	218.94
08/08/2010	3	220	8.85	199.47	11.46	200.68	9.51	206.23
09/08/2010	1	180	6.15	191.49	9.24	196.70	7.30	197.95
10/08/2010	1	180	3.29	202.84	6.17	187.57	4.89	201.08
11/08/2010	0	0	2.16	231.59	4.70	177.75	2.44	263.98
12/08/2010	1	0	1.80	274.56	3.38	126.50	2.14	307.97
13/08/2010	1	120	2.99	192.89	5.72	167.18	1.75	198.60
14/08/2010	1	140	3.46	104.64	4.64	125.22	2.40	149.30
15/08/2010	1	180	3.41	75.92	3.60	78.52	2.95	68.75
16/08/2010	1	270	2.44	82.69	3.32	0.87	2.93	351.50
17/08/2010	0	0	1.91	316.49	3.34	195.83	2.01	331.70
18/08/2010	1	120	2.03	133.48	4.93	174.18	2.85	197.67
19/08/2010	1	180	1.85	88.16	3.16	204.73	4.03	196.53
20/08/2010	1	270	2.05	297.62	4.19	216.29	4.03	237.39
21/08/2010	1	320	4.64	230.56	5.25	192.32	4.81	239.59
22/08/2010	1	320	4.89	200.98	6.01	193.42	4.93	201.25
23/08/2010	2	180	4.31	201.22	6.40	226.31	4.40	223.30
24/08/2010	1	180	2.94	211.38	8.53	242.87	2.85	268.31
25/08/2010	0	0	7.10	259.50	11.59	252.98	6.61	261.50
26/08/2010	1	40	8.81	236.80	11.18	230.53	8.73	244.89
27/08/2010	1	180	8.32	193.91	9.52	203.21	7.83	224.38
28/08/2010	2	180	7.17	189.65	8.40	197.23	6.21	204.03
29/08/2010	0	0	5.85	201.52	6.79	206.96	5.74	216.44
30/08/2010	1	0	5.27	216.14	7.39	237.71	5.98	225.82
31/08/2010	2	180	5.40	227.41	7.81	239.45	7.05	230.02

Table 57. August 2010 wind data at Cuyo Island from onshore weather station and meoscale model output

Source Date	PAGASA		ERA-Interim		NCEP FNL		NCEP CFSR	
	Wind Speed (m/s)	Wind Direction (Degrees)	Wind Speed (m/s)	Wind Direction (Degrees)	Wind Speed (m/s)	Wind Direction (Degrees)	Wind Speed (m/s)	Wind Direction (Degrees)
01/08/2010	1	220	3.18	214.15	2.69	193.80	3.60	191.56
02/08/2010	1	220	4.03	258.41	3.80	255.43	3.70	256.62
03/08/2010	1	220	6.84	285.29	6.36	283.45	7.63	282.23
04/08/2010	1	220	7.69	265.15	9.18	224.87	10.20	272.38
05/08/2010	1	220	7.98	234.33	14.80	202.83	7.54	248.61
06/08/2010	4	220	8.65	239.89	14.79	214.35	8.11	238.42
07/08/2010	5	220	10.14	203.81	13.58	199.68	10.95	216.90
08/08/2010	4	220	8.90	199.55	11.97	192.98	10.55	205.64
09/08/2010	1	220	6.15	192.98	9.39	196.19	7.51	202.26
10/08/2010	1	220	3.60	201.35	6.39	191.83	4.78	203.50
11/08/2010	0	0	2.92	207.71	5.48	171.12	3.14	230.97
12/08/2010	1	220	2.30	228.67	3.26	88.16	2.98	229.25
13/08/2010	1	220	2.31	168.13	5.61	166.13	1.78	173.20
14/08/2010	1	0	3.00	119.28	4.01	116.52	2.26	39.10
15/08/2010	1	20	3.53	33.84	4.33	32.48	3.40	22.88
16/08/2010	1	20	3.26	5.94	2.40	61.11	3.73	7.19
17/08/2010	0	0	1.56	17.25	4.39	208.16	1.81	253.38
18/08/2010	1	120	1.67	146.07	5.28	181.15	4.13	202.13
19/08/2010	1	120	1.80	107.04	2.62	164.55	3.33	202.07
20/08/2010	1	20	2.80	277.87	3.35	217.25	4.42	230.61
21/08/2010	0	0	5.05	243.88	4.90	178.33	5.74	238.38
22/08/2010	0	0	5.60	213.74	5.39	203.70	6.47	210.95
23/08/2010	1	220	5.06	206.75	8.31	222.49	5.99	212.93
24/08/2010	1	220	4.99	229.32	9.77	221.39	4.01	240.23
25/08/2010	2	220	8.51	233.37	11.44	230.56	8.33	242.45
26/08/2010	2	220	9.83	214.37	11.76	208.18	9.16	227.79
27/08/2010	2	220	8.63	195.92	10.11	200.62	8.36	213.57
28/08/2010	2	220	7.01	192.76	8.20	196.65	7.28	205.11
29/08/2010	2	220	5.42	203.92	7.31	210.70	6.21	217.20
30/08/2010	2	220	6.21	225.30	7.71	235.84	7.18	226.74
31/08/2010	2	220	6.75	228.68	8.33	237.00	8.40	223.35

Table 58. August 2010 wind data at Puerto Princesa from onshore weather station and meoscale model output

Source Date	PAGASA		ERA-Interim		NCEP FNL		NCEP CFSR	
	Wind Speed (m/s)	Wind Direction (Degrees)	Wind Speed (m/s)	Wind Direction (Degrees)	Wind Speed (m/s)	Wind Direction (Degrees)	Wind Speed (m/s)	Wind Direction (Degrees)
01/08/2010	2	90	4.11	182.65	3.01	197.25	3.16	204.20
02/08/2010	2	160	2.87	193.22	1.92	169.22	2.27	200.00
03/08/2010	2	320	2.76	201.98	2.26	235.06	1.99	239.28
04/08/2010	2	320	4.07	238.94	5.52	214.16	3.24	241.23
05/08/2010	2	140	3.46	198.65	6.71	214.20	3.11	246.76
06/08/2010	2	180	6.56	208.15	6.21	220.95	3.51	225.22
07/08/2010	3	180	5.55	207.03	7.29	197.20	4.51	202.57
08/08/2010	2	180	6.04	199.96	6.24	195.60	5.21	205.52
09/08/2010	2	180	4.92	193.02	5.25	192.29	4.38	207.62
10/08/2010	3	180	3.53	201.80	3.98	191.13	3.09	223.03
11/08/2010	2	160	3.86	186.35	3.43	183.22	2.84	207.22
12/08/2010	2	140	3.46	189.61	3.13	192.32	2.60	221.63
13/08/2010	2	140	3.45	177.09	4.22	176.30	2.45	195.79
14/08/2010	2	180	3.80	170.99	3.62	182.15	3.23	155.68
15/08/2010	1	180	2.61	123.39	1.74	160.97	2.33	189.52
16/08/2010	2	160	3.06	76.56	1.90	142.63	1.90	323.80
17/08/2010	2	320	2.67	63.12	1.70	38.12	2.06	181.84
18/08/2010	2	140	2.92	157.54	3.76	176.89	2.71	197.66
19/08/2010	3	140	3.77	181.88	3.11	190.53	3.58	201.15
20/08/2010	2	140	3.00	215.41	2.28	195.03	3.21	189.77
21/08/2010	2	290	2.43	219.36	2.84	210.63	3.04	218.62
22/08/2010	2	270	4.06	204.24	2.15	201.54	2.99	200.61
23/08/2010	2	160	4.74	197.13	3.96	203.42	3.99	207.78
24/08/2010	3	160	4.18	187.55	3.22	231.90	3.04	201.91
25/08/2010	3	160	3.07	184.53	2.72	209.72	2.73	199.59
26/08/2010	2	160	3.59	213.51	4.32	205.35	3.14	209.14
27/08/2010	3	180	4.89	209.77	4.19	202.81	3.65	206.76
28/08/2010	3	180	4.94	196.93	4.22	196.43	4.19	207.30
29/08/2010	2	180	3.41	200.05	3.78	198.93	2.97	213.14
30/08/2010	2	160	3.90	196.22	4.49	215.20	3.39	201.82
31/08/2010	2	180	4.14	190.54	3.15	206.94	3.66	201.36

Table 59. September 2010 wind data at Coron Island from onshore weather station and meoscale model output

Source Date	PAGASA		ERA-Interim		NCEP FNL		NCEP CFSR	
	Wind Speed (m/s)	Wind Direction (Degrees)	Wind Speed (m/s)	Wind Direction (Degrees)	Wind Speed (m/s)	Wind Direction (Degrees)	Wind Speed (m/s)	Wind Direction (Degrees)
01/09/2010	1	180	5.21	198.87	7.06	212.61	5.47	211.75
02/09/2010	0	0	5.47	200.59	8.70	231.66	5.03	213.13
03/09/2010	1	220	5.50	200.89	9.13	225.36	5.09	210.54
04/09/2010	1	180	3.63	194.83	6.22	210.46	3.28	201.44
05/09/2010	1	0	2.01	201.32	2.81	227.07	2.17	235.69
06/09/2010	0	0	2.11	18.25	2.60	293.88	1.93	318.32
07/09/2010	1	0	2.23	305.46	5.64	234.94	1.94	309.73
08/09/2010	1	0	2.43	179.47	7.07	223.83	2.35	214.65
09/09/2010	1	0	1.90	241.95	4.27	206.16	2.37	243.57
10/09/2010	1	0	2.18	244.50	2.03	334.23	2.32	308.43
11/09/2010	0	0	5.47	338.33	5.97	334.18	2.94	304.45
12/09/2010	1	0	4.42	288.28	7.93	248.64	2.55	294.60
13/09/2010	1	220	7.29	193.78	8.23	190.67	3.21	229.18
14/09/2010	1	140	3.27	160.45	6.31	182.47	3.47	198.10
15/09/2010	1	0	2.88	207.36	3.08	218.22	2.77	187.71
16/09/2010	2	120	2.23	221.19	3.51	201.38	2.33	232.54
17/09/2010	1	0	2.22	202.48	3.21	151.71	2.57	270.79
18/09/2010	1	180	1.88	282.32	4.81	207.78	2.86	254.44
19/09/2010	1	0	2.04	238.69	8.02	240.04	2.50	232.19
20/09/2010	2	0	2.28	168.98	3.39	185.46	3.40	180.10
21/09/2010	2	0	2.18	77.28	2.20	191.94	2.04	21.40
22/09/2010	1	120	2.91	79.22	1.97	300.03	1.59	352.51
23/09/2010	1	120	2.17	274.66	3.19	289.63	2.95	299.67
24/09/2010	1	0	1.78	314.48	1.39	345.42	3.43	286.54
25/09/2010	1	220	2.18	250.85	1.58	332.82	3.65	310.17
26/09/2010	2	0	2.02	63.45	1.48	124.64	6.92	270.62
27/09/2010	1	140	2.88	75.48	1.85	256.39	3.88	227.19
28/09/2010	1	0	2.06	230.53	2.48	61.67	1.84	309.48
29/09/2010	1	0	1.54	350.89	1.90	38.54	1.95	320.64
30/09/2010	1	40	2.32	245.20	4.07	230.05	2.66	312.21

Table 60. September 2010 wind data at Cuyo Island from onshore weather station and meoscale model output

Source Date	PAGASA		ERA-Interim		NCEP FNL		NCEP CFSR	
	Wind Speed (m/s)	Wind Direction (Degrees)	Wind Speed (m/s)	Wind Direction (Degrees)	Wind Speed (m/s)	Wind Direction (Degrees)	Wind Speed (m/s)	Wind Direction (Degrees)
01/09/2010	3	220	5.98	204.73	8.03	213.25	5.66	208.74
02/09/2010	2	220	6.14	202.90	9.61	223.42	5.81	208.82
03/09/2010	0	0	5.55	205.35	9.80	215.20	5.57	214.94
04/09/2010	1	220	2.98	207.81	6.43	212.35	2.59	209.71
05/09/2010	0	0	1.85	342.87	3.46	227.59	1.16	233.65
06/09/2010	1	220	3.49	339.13	3.50	271.92	1.45	274.33
07/09/2010	0	0	2.94	317.70	6.86	233.23	2.38	241.79
08/09/2010	2	220	1.77	227.47	7.16	226.51	3.33	210.70
09/09/2010	1	220	2.88	232.22	4.31	208.53	2.21	249.92
10/09/2010	1	0	4.20	335.83	3.14	327.37	2.38	330.58
11/09/2010	1	20	7.23	339.25	9.61	310.31	4.32	324.98
12/09/2010	1	20	8.57	271.92	9.64	254.51	3.67	240.09
13/09/2010	1	220	4.52	192.68	9.61	196.88	5.06	207.00
14/09/2010	0	0	4.89	183.38	5.55	196.33	4.60	201.13
15/09/2010	1	220	3.04	198.45	5.07	208.98	4.54	201.99
16/09/2010	1	220	1.76	198.02	2.83	151.55	4.79	220.55
17/09/2010	1	220	1.72	216.98	3.91	199.66	3.66	224.89
18/09/2010	1	220	1.85	245.63	5.20	224.41	4.93	232.68
19/09/2010	0	0	1.57	209.45	9.02	215.97	4.71	202.68
20/09/2010	1	220	1.88	173.64	4.42	223.85	2.64	187.73
21/09/2010	1	20	4.47	32.08	2.13	143.21	3.73	23.38
22/09/2010	1	20	2.53	29.70	1.89	29.13	2.03	358.73
23/09/2010	1	270	2.07	268.53	6.44	250.90	3.97	239.23
24/09/2010	1	20	2.32	283.82	1.63	322.78	5.17	267.83
25/09/2010	1	20	2.44	222.08	1.21	80.72	6.73	277.60
26/09/2010	0	0	2.66	22.31	1.58	5.38	7.26	264.67
27/09/2010	1	20	5.45	26.99	2.36	340.99	2.46	219.90
28/09/2010	2	20	4.64	19.64	4.75	26.20	1.76	356.84
29/09/2010	1	20	2.52	331.21	1.71	80.99	2.37	307.48
30/09/2010	0	0	2.61	247.05	5.84	227.45	3.52	276.26

Table 61. September 2010 wind data at Puerto Princesa from onshore weather station and meoscale model output

Source Date	PAGASA		ERA-Interim		NCEP FNL		NCEP CFSR	
	Wind Speed (m/s)	Wind Direction (Degrees)	Wind Speed (m/s)	Wind Direction (Degrees)	Wind Speed (m/s)	Wind Direction (Degrees)	Wind Speed (m/s)	Wind Direction (Degrees)
01/09/2010	2	160	3.35	228.52	4.03	195.93	3.14	237.33
02/09/2010	2	180	3.70	201.38	4.44	202.90	3.53	212.31
03/09/2010	3	180	3.47	199.02	4.12	200.51	2.74	212.95
04/09/2010	2	160	3.88	176.32	3.32	198.38	2.59	197.49
05/09/2010	1	180	3.08	171.47	2.49	192.60	2.56	197.18
06/09/2010	2	270	2.64	122.83	1.70	169.95	2.44	195.95
07/09/2010	3	270	2.17	235.30	1.86	195.15	2.82	188.32
08/09/2010	3	180	2.86	194.60	2.02	230.12	3.23	205.48
09/09/2010	3	180	2.86	173.76	3.24	191.01	2.60	184.79
10/09/2010	2	50	2.32	318.58	1.97	171.56	2.33	210.24
11/09/2010	2	0	3.38	329.26	2.72	323.59	1.72	340.21
12/09/2010	2	160	3.22	316.60	2.52	212.78	1.92	234.29
13/09/2010	3	270	3.72	258.12	3.58	211.98	2.66	233.15
14/09/2010	2	270	3.83	202.07	3.81	197.71	2.59	199.17
15/09/2010	3	160	4.07	195.20	2.67	199.28	2.48	229.82
16/09/2010	3	160	3.63	177.90	3.00	198.56	3.50	204.54
17/09/2010	3	160	3.14	181.87	3.01	210.13	2.58	186.03
18/09/2010	2	160	2.66	190.64	3.09	205.40	2.21	205.72
19/09/2010	2	180	3.04	208.91	2.36	193.80	2.97	221.77
20/09/2010	3	160	3.47	189.10	2.48	237.03	3.33	199.43
21/09/2010	3	140	2.72	111.00	2.52	190.91	2.30	199.04
22/09/2010	3	110	2.90	110.03	2.19	175.53	1.92	41.14
23/09/2010	3	180	3.10	173.54	2.48	177.82	2.80	209.75
24/09/2010	3	140	2.71	199.11	1.86	217.19	1.79	189.18
25/09/2010	2	160	2.91	224.02	1.78	164.32	1.77	226.62
26/09/2010	2	290	2.97	168.21	1.82	145.29	1.51	216.92
27/09/2010	3	90	2.73	75.23	1.99	125.37	1.90	193.68
28/09/2010	2	40	2.70	11.21	2.10	352.32	2.39	194.55
29/09/2010	2	0	2.36	283.61	2.13	218.24	2.11	221.25
30/09/2010	2	90	2.57	210.53	2.79	207.98	2.22	211.71

Table 62. October 2010 wind data at Coron Island from onshore weather station and meoscale model output

Source Date	PAGASA		ERA-Interim		NCEP FNL		NCEP CFSR	
	Wind Speed (m/s)	Wind Direction (Degrees)	Wind Speed (m/s)	Wind Direction (Degrees)	Wind Speed (m/s)	Wind Direction (Degrees)	Wind Speed (m/s)	Wind Direction (Degrees)
01/10/2010	2	180	3.46	197.39	5.10	192.60	4.86	208.00
02/10/2010	0	0	4.16	149.02	5.71	141.26	5.40	182.66
03/10/2010	0	0	4.48	92.73	3.44	80.46	3.38	132.24
04/10/2010	0	0	1.96	73.31	4.63	196.52	2.43	78.29
05/10/2010	1	180	3.75	100.62	5.48	130.83	4.52	94.80
06/10/2010	1	120	3.30	80.17	3.79	83.84	3.70	67.24
07/10/2010	2	140	1.55	154.27	1.84	290.59	2.07	121.28
08/10/2010	2	40	3.01	101.36	2.46	264.18	2.84	89.62
09/10/2010	0	0	3.58	189.77	4.39	212.49	2.25	266.18
10/10/2010	1	180	4.35	179.53	6.08	183.87	4.04	196.39
11/10/2010	1	180	2.36	189.81	3.79	240.75	3.23	206.53
12/10/2010	0	0	2.17	278.29	4.65	268.15	2.79	287.06
13/10/2010	1	180	3.95	255.61	3.71	279.84	4.04	284.09
14/10/2010	1	180	6.96	206.97	5.57	278.77	4.55	295.75
15/10/2010	1	220	2.93	313.40	6.48	305.66	3.93	291.46
16/10/2010	1	180	3.37	321.11	4.79	321.12	4.46	305.94
17/10/2010	0	0	4.45	320.89	5.13	309.83	4.19	310.05
18/10/2010	2	220	9.13	253.50	11.44	254.54	8.70	258.83
19/10/2010	5	220	10.27	224.37	13.79	227.86	10.27	232.70
20/10/2010	4	210	10.05	202.99	10.84	222.67	10.09	214.98
21/10/2010	2	210	6.75	230.62	8.52	235.78	6.90	238.54
22/10/2010	2	210	3.71	220.62	6.42	247.11	4.56	239.11
23/10/2010	1	220	4.53	203.18	4.23	287.42	3.10	274.30
24/10/2010	1	180	2.70	230.67	4.38	313.65	2.69	311.59
25/10/2010	1	0	2.66	269.90	4.87	301.51	3.72	317.40
26/10/2010	0	0	2.51	299.93	3.63	278.18	3.76	293.22
27/10/2010	0	0	2.95	89.18	6.06	106.90	4.20	115.98
28/10/2010	2	40	3.61	88.57	8.88	88.30	4.23	84.71
29/10/2010	2	140	2.85	66.91	4.24	80.58	2.15	11.13
30/10/2010	1	40	3.05	40.49	3.91	26.63	5.65	61.33
31/10/2010	2	40	4.31	75.56	4.48	67.18	2.14	55.15

Table 63. October 2010 wind data at Cuyo Island from onshore weather station and meoscale model output

Source Date	PAGASA		ERA-Interim		NCEP FNL		NCEP CFSR	
	Wind Speed (m/s)	Wind Direction (Degrees)	Wind Speed (m/s)	Wind Direction (Degrees)	Wind Speed (m/s)	Wind Direction (Degrees)	Wind Speed (m/s)	Wind Direction (Degrees)
01/10/2010	2	180	5.27	186.43	6.12	185.76	6.07	210.05
02/10/2010	1	150	3.25	142.51	5.03	145.60	5.90	178.89
03/10/2010	2	20	5.20	38.85	3.99	36.57	3.62	64.15
04/10/2010	2	20	6.57	36.33	4.85	324.37	4.71	40.77
05/10/2010	2	20	3.15	58.42	2.28	126.18	3.27	48.10
06/10/2010	2	20	5.75	30.58	4.06	24.73	5.46	29.29
07/10/2010	2	20	6.56	28.62	4.45	38.42	6.14	39.27
08/10/2010	1	120	3.78	220.97	4.72	262.86	3.91	204.83
09/10/2010	2	220	6.33	194.94	6.83	203.63	7.09	212.32
10/10/2010	1	220	5.42	184.83	7.10	184.76	5.61	197.77
11/10/2010	1	220	3.89	253.21	6.87	234.13	4.82	196.30
12/10/2010	1	20	3.79	304.94	7.56	269.72	3.54	274.74
13/10/2010	1	220	6.49	261.85	5.44	269.30	5.68	272.57
14/10/2010	1	220	8.20	228.27	8.31	258.78	9.05	275.04
15/10/2010	1	220	5.20	326.14	15.99	302.60	6.55	289.38
16/10/2010	2	20	6.61	322.64	8.23	321.07	9.46	307.82
17/10/2010	2	320	6.25	311.30	9.29	306.25	9.04	309.02
18/10/2010	2	220	11.06	252.04	13.31	249.46	12.84	254.45
19/10/2010	3	220	11.16	221.78	14.90	223.59	12.78	228.76
20/10/2010	4	320	10.56	200.55	12.49	216.85	11.86	214.40
21/10/2010	3	220	8.71	210.30	9.88	228.71	8.50	226.78
22/10/2010	2	220	5.22	227.68	7.86	244.92	7.18	245.87
23/10/2010	1	220	5.55	212.65	7.52	257.04	7.50	248.10
24/10/2010	1	220	5.23	226.72	7.11	306.75	4.15	284.53
25/10/2010	1	220	5.45	245.44	8.45	298.05	5.06	321.43
26/10/2010	1	220	3.88	267.53	4.36	274.97	4.66	308.69
27/10/2010	0	0	1.29	5.02	5.37	275.17	2.59	33.76
28/10/2010	1	220	6.20	46.32	5.66	151.85	5.36	48.71
29/10/2010	No Data	No Data	9.43	35.62	3.34	13.86	7.70	40.76
30/10/2010	No Data	No Data	9.49	37.38	7.81	12.81	4.82	50.35
31/10/2010	No Data	No Data	8.02	38.29	9.24	38.63	5.62	38.94

Table 64. October 2010 wind data at Puerto Princesa from onshore weather station and meoscale model output

Source Date	PAGASA		ERA-Interim		NCEP FNL		NCEP CFSR	
	Wind Speed (m/s)	Wind Direction (Degrees)	Wind Speed (m/s)	Wind Direction (Degrees)	Wind Speed (m/s)	Wind Direction (Degrees)	Wind Speed (m/s)	Wind Direction (Degrees)
01/10/2010	2	180	3.94	189.66	3.04	204.59	3.09	244.17
02/10/2010	2	180	4.65	189.55	3.89	184.76	4.19	199.51
03/10/2010	2	90	3.41	180.44	2.58	178.01	3.17	194.66
04/10/2010	2	50	3.12	18.25	1.50	167.79	2.06	91.36
05/10/2010	3	90	2.70	328.62	2.13	178.82	2.15	100.68
06/10/2010	2	320	2.95	121.09	2.05	163.94	1.82	298.10
07/10/2010	3	270	3.16	48.90	1.99	341.47	2.20	8.04
08/10/2010	2	90	3.48	224.93	2.03	210.83	2.05	241.27
09/10/2010	1	160	3.41	220.27	4.24	197.54	3.35	208.28
10/10/2010	2	180	4.45	198.84	4.31	208.74	4.88	201.82
11/10/2010	2	220	3.36	224.50	2.54	208.50	3.50	209.25
12/10/2010	2	180	2.55	193.28	2.49	181.20	2.86	229.50
13/10/2010	3	160	2.50	209.73	1.71	217.88	2.66	225.82
14/10/2010	2	270	3.87	187.71	2.55	205.11	3.03	211.95
15/10/2010	2	0	2.63	157.39	4.63	302.84	2.26	178.90
16/10/2010	2	160	3.59	27.46	1.99	344.49	2.02	354.74
17/10/2010	3	320	4.76	330.65	2.80	319.66	2.79	320.95
18/10/2010	4	270	5.43	243.89	5.52	246.36	3.89	228.23
19/10/2010	3	220	6.83	237.68	6.47	232.17	5.37	232.90
20/10/2010	3	320	6.26	197.04	5.21	220.47	5.33	200.45
21/10/2010	2	270	4.12	209.28	3.58	219.35	3.86	221.65
22/10/2010	2	160	4.32	194.03	2.53	216.76	4.08	198.10
23/10/2010	2	180	3.84	194.31	3.62	247.40	3.44	207.65
24/10/2010	2	180	3.15	193.04	2.76	353.50	2.46	210.97
25/10/2010	3	180	3.01	201.66	4.45	325.87	3.63	342.85
26/10/2010	3	180	2.61	314.99	3.76	301.97	2.38	312.15
27/10/2010	3	270	2.74	198.32	1.68	198.98	2.15	201.29
28/10/2010	3	90	3.02	109.61	3.33	193.08	2.62	196.68
29/10/2010	2	90	3.15	84.76	3.58	165.33	2.38	117.39
30/10/2010	4	40	4.17	40.42	2.13	5.76	2.32	8.79
31/10/2010	3	90	3.22	65.71	2.65	336.08	2.54	70.05

Table 65. November 2010 wind data at Coron Island from onshore weather station and meoscale model output

Source Date	PAGASA		ERA-Interim		NCEP FNL		NCEP CFSR	
	Wind Speed (m/s)	Wind Direction (Degrees)	Wind Speed (m/s)	Wind Direction (Degrees)	Wind Speed (m/s)	Wind Direction (Degrees)	Wind Speed (m/s)	Wind Direction (Degrees)
01/11/2010	1	40	3.77	71.21	2.55	18.81	2.95	30.05
02/11/2010	1	40	5.04	106.58	7.73	104.41	6.33	98.41
03/11/2010	2	270	4.76	101.08	8.21	122.69	5.29	106.43
04/11/2010	1	0	3.62	92.93	1.71	111.46	3.12	69.24
05/11/2010	2	0	3.50	14.09	4.00	315.95	2.84	41.40
06/11/2010	1	180	1.43	4.18	7.47	176.30	4.47	116.59
07/11/2010	0	0	2.74	176.04	5.98	146.05	4.23	181.82
08/11/2010	1	0	3.21	127.11	1.90	145.39	3.02	148.86
09/11/2010	1	0	2.59	83.27	2.24	105.74	1.62	61.52
10/11/2010	0	0	2.10	116.27	4.69	196.89	2.20	62.25
11/11/2010	0	0	2.27	163.82	6.47	164.11	3.11	244.17
12/11/2010	2	120	3.60	151.98	5.47	173.96	4.02	175.91
13/11/2010	2	120	3.28	81.58	2.99	111.29	3.43	105.50
14/11/2010	2	140	3.35	82.20	3.81	65.69	3.06	58.98
15/11/2010	3	0	3.74	77.34	3.89	69.06	3.07	66.52
16/11/2010	2	140	5.53	79.04	6.54	117.92	6.20	90.09
17/11/2010	3	40	6.78	93.54	3.51	141.23	4.93	105.04
18/11/2010	2	140	4.93	97.72	1.94	292.29	3.76	97.30
19/11/2010	2	140	3.03	77.53	1.75	72.89	3.69	97.35
20/11/2010	0	0	2.58	103.17	3.85	100.76	3.36	92.45
21/11/2010	1	210	3.58	102.54	3.82	85.86	3.39	93.84
22/11/2010	0	0	1.57	346.37	2.97	255.30	2.17	316.32
23/11/2010	1	90	1.58	49.71	3.87	250.16	2.17	268.12
24/11/2010	2	0	2.57	84.78	5.63	103.75	2.15	288.21
25/11/2010	0	0	2.17	223.81	3.80	59.48	4.10	334.78
26/11/2010	0	0	3.99	106.80	5.96	69.08	4.33	346.14
27/11/2010	1	0	6.20	84.20	6.47	64.27	8.18	82.68
28/11/2010	2	40	6.15	74.90	6.30	51.23	6.27	79.49
29/11/2010	2	90	7.49	86.05	8.57	80.69	8.58	82.88
30/11/2010	1	0	4.11	69.82	6.03	77.80	5.39	68.58

Table 66. November 2010 wind data at Cuyo Island from onshore weather station and meoscale model output

Source Date	PAGASA		ERA-Interim		NCEP FNL		NCEP CFSR	
	Wind Speed (m/s)	Wind Direction (Degrees)	Wind Speed (m/s)	Wind Direction (Degrees)	Wind Speed (m/s)	Wind Direction (Degrees)	Wind Speed (m/s)	Wind Direction (Degrees)
01/11/2010	No Data	No Data	7.42	40.74	8.62	35.49	6.47	36.94
02/11/2010	No Data	No Data	3.01	143.05	6.76	146.33	3.69	169.33
03/11/2010	No Data	No Data	3.60	105.23	5.49	141.09	3.04	103.93
04/11/2010	No Data	No Data	6.85	25.61	4.85	14.96	6.31	23.83
05/11/2010	No Data	No Data	5.00	9.50	7.79	326.38	6.20	29.68
06/11/2010	No Data	No Data	3.44	207.38	8.91	194.50	5.73	154.32
07/11/2010	No Data	No Data	3.65	164.72	5.67	152.49	5.30	190.37
08/11/2010	No Data	No Data	2.85	146.76	3.36	15.59	2.01	146.71
09/11/2010	No Data	No Data	4.55	36.54	2.44	322.34	3.48	15.23
10/11/2010	No Data	No Data	2.47	41.31	5.97	207.29	3.83	243.04
11/11/2010	No Data	No Data	2.69	178.88	7.25	173.91	3.49	220.75
12/11/2010	No Data	No Data	3.30	153.69	5.90	165.62	3.96	176.70
13/11/2010	1	20	6.23	34.49	3.56	46.18	3.74	63.49
14/11/2010	2	20	8.38	36.81	5.95	34.11	7.17	33.63
15/11/2010	2	40	8.51	37.69	7.25	60.46	6.51	40.42
16/11/2010	2	20	6.41	50.31	5.03	144.51	3.36	94.38
17/11/2010	1	20	2.39	118.72	3.84	137.69	2.87	142.14
18/11/2010	1	20	2.16	45.68	3.61	268.66	2.15	297.29
19/11/2010	2	20	3.72	31.60	1.70	239.08	1.40	59.46
20/11/2010	2	20	3.03	34.73	2.75	115.21	2.65	91.27
21/11/2010	2	20	2.77	28.32	1.45	166.17	1.53	111.99
22/11/2010	0	0	2.51	43.20	4.87	224.70	2.48	229.86
23/11/2010	1	220	1.57	102.41	6.20	222.67	3.81	240.78
24/11/2010	1	20	4.58	30.65	5.05	60.89	2.16	284.81
25/11/2010	1	20	7.68	34.14	9.86	40.37	4.82	287.03
26/11/2010	2	20	8.03	33.88	11.64	40.01	3.89	248.28
27/11/2010	2	20	8.24	40.88	9.12	45.36	4.27	137.14
28/11/2010	4	20	8.55	41.48	8.48	39.62	6.45	38.94
29/11/2010	1	20	8.19	47.59	6.26	55.36	6.68	52.08
30/11/2010	3	20	8.87	37.99	8.73	44.59	8.27	43.98

Table 67. November 2010 wind data at Puerto Princesa from onshore weather station and meoscale model output

Source Date	PAGASA		ERA-Interim		NCEP FNL		NCEP CFSR	
	Wind Speed (m/s)	Wind Direction (Degrees)	Wind Speed (m/s)	Wind Direction (Degrees)	Wind Speed (m/s)	Wind Direction (Degrees)	Wind Speed (m/s)	Wind Direction (Degrees)
01/11/2010	3	270	2.56	256.42	2.85	74.95	3.40	76.97
02/11/2010	3	160	2.71	198.44	3.23	240.65	1.51	179.94
03/11/2010	3	70	3.03	185.76	4.84	171.08	2.23	178.73
04/11/2010	3	70	2.52	41.27	1.43	215.50	2.48	25.52
05/11/2010	2	70	3.00	352.76	3.22	308.93	3.30	342.14
06/11/2010	2	160	2.26	176.70	4.66	208.37	2.04	299.65
07/11/2010	2	160	2.55	170.82	4.82	183.21	3.22	202.50
08/11/2010	2	270	3.41	183.33	2.17	221.13	3.59	197.78
09/11/2010	3	90	2.56	147.85	2.45	187.33	2.53	195.51
10/11/2010	2	160	2.29	173.51	3.14	202.38	2.06	194.94
11/11/2010	2	90	3.44	190.39	6.05	200.47	2.61	221.47
12/11/2010	2	140	3.90	187.94	4.31	193.96	3.39	201.44
13/11/2010	2	270	2.34	139.92	2.36	165.26	2.39	184.64
14/11/2010	2	90	3.54	68.68	1.89	55.95	2.45	26.78
15/11/2010	2	270	3.89	80.58	3.12	346.41	2.36	44.30
16/11/2010	3	90	3.46	93.57	1.90	206.14	2.31	217.06
17/11/2010	2	90	2.75	131.91	3.89	182.29	2.67	196.83
18/11/2010	3	270	3.45	202.90	1.89	177.18	2.70	190.59
19/11/2010	2	90	3.08	184.05	2.20	202.85	2.11	208.91
20/11/2010	2	270	2.68	155.88	2.65	129.87	2.24	200.35
21/11/2010	3	270	2.52	172.17	2.79	202.38	2.38	202.42
22/11/2010	1	270	2.79	132.78	2.73	184.64	2.52	205.85
23/11/2010	3	180	2.86	183.65	3.70	154.95	3.23	207.31
24/11/2010	3	90	2.76	147.19	5.07	156.59	3.27	206.19
25/11/2010	3	90	3.08	84.14	2.52	89.49	2.63	174.46
26/11/2010	3	90	2.99	40.83	3.22	7.27	1.92	319.43
27/11/2010	2	90	3.39	78.48	6.09	65.74	3.23	176.01
28/11/2010	2	270	4.88	68.11	3.54	78.08	2.47	107.17
29/11/2010	3	90	4.53	81.07	3.63	76.02	3.53	76.16
30/11/2010	3	90	3.49	61.51	3.75	60.06	3.25	61.56

Table 68. December 2010 wind data at Coron Island from onshore weather station and meoscale model output

Source Date	PAGASA		ERA-Interim		NCEP FNL		NCEP CFSR	
	Wind Speed (m/s)	Wind Direction (Degrees)	Wind Speed (m/s)	Wind Direction (Degrees)	Wind Speed (m/s)	Wind Direction (Degrees)	Wind Speed (m/s)	Wind Direction (Degrees)
01/12/2010	2	40	7.92	80.43	6.92	73.75	5.43	69.10
02/12/2010	2	40	4.78	68.25	4.13	55.38	5.21	57.28
03/12/2010	2	40	7.45	72.48	8.79	81.46	7.45	74.45
04/12/2010	3	40	9.52	82.56	9.45	80.59	9.37	83.46
05/12/2010	1	40	5.07	72.37	8.12	80.92	6.73	72.34
06/12/2010	2	0	2.56	57.19	3.69	36.17	4.12	37.92
07/12/2010	1	320	2.36	0.70	3.41	49.69	1.66	287.47
08/12/2010	0	0	3.25	348.09	4.90	16.85	2.73	339.57
09/12/2010	1	0	2.86	349.63	5.59	348.35	3.58	49.99
10/12/2010	1	120	2.54	38.26	5.57	350.49	2.57	0.79
11/12/2010	1	90	4.13	334.56	6.25	330.13	3.10	5.90
12/12/2010	1	0	3.88	215.77	6.28	244.35	6.46	157.51
13/12/2010	1	40	2.57	133.34	2.35	193.76	4.87	161.37
14/12/2010	1	0	3.00	78.33	2.37	63.86	4.71	85.25
15/12/2010	1	120	3.32	74.43	3.25	61.86	5.08	79.40
16/12/2010	0	0	3.12	66.81	2.95	6.35	3.78	59.29
17/12/2010	1	270	6.62	83.33	3.98	44.91	4.49	72.49
18/12/2010	2	140	7.94	81.83	8.00	85.89	6.85	78.49
19/12/2010	2	40	5.72	81.62	6.50	76.49	3.78	71.46
20/12/2010	2	40	4.99	76.45	7.41	79.69	4.60	75.09
21/12/2010	1	0	3.89	89.77	5.34	72.14	7.46	81.46
22/12/2010	1	0	2.63	69.61	2.24	4.33	4.79	72.68
23/12/2010	1	0	2.44	353.10	2.75	348.27	3.32	55.38
24/12/2010	1	0	4.92	77.22	7.64	67.21	3.25	25.95
25/12/2010	2	0	7.14	69.76	3.79	57.69	4.12	56.10
26/12/2010	1	0	7.93	71.14	4.30	68.67	4.68	50.24
27/12/2010	2	0	4.38	58.66	3.65	82.61	4.26	53.50
28/12/2010	2	0	9.09	78.58	8.39	82.82	5.49	81.53
29/12/2010	4	140	4.54	64.93	6.65	72.45	4.15	67.61
30/12/2010	2	0	4.84	69.64	4.31	39.99	3.78	349.57
31/12/2010	0	0	3.59	76.08	5.59	62.83	3.40	26.90

Table 69. December 2010 wind data at Cuyo Island from onshore weather station and meoscale model output

Source Date	PAGASA		ERA-Interim		NCEP FNL		NCEP CFSR	
	Wind Speed (m/s)	Wind Direction (Degrees)	Wind Speed (m/s)	Wind Direction (Degrees)	Wind Speed (m/s)	Wind Direction (Degrees)	Wind Speed (m/s)	Wind Direction (Degrees)
01/12/2010	2	20	9.60	48.32	8.93	43.26	9.54	43.89
02/12/2010	3	20	9.59	39.15	8.47	37.95	8.99	37.65
03/12/2010	3	20	9.86	46.47	8.65	44.55	8.92	47.83
04/12/2010	2	20	9.41	47.82	7.64	51.49	7.78	49.93
05/12/2010	2	20	9.25	40.49	7.62	42.80	9.02	43.69
06/12/2010	3	20	9.75	36.28	9.32	32.00	9.04	37.20
07/12/2010	3	20	11.21	32.36	8.97	40.22	8.73	38.59
08/12/2010	1	20	12.26	30.67	12.85	28.89	10.20	35.66
09/12/2010	1	20	12.03	23.83	12.14	10.50	10.53	37.98
10/12/2010	1	20	10.64	26.39	4.70	343.17	10.24	35.02
11/12/2010	3	20	5.56	327.67	7.99	312.25	8.32	57.62
12/12/2010	3	20	4.90	194.63	6.03	228.44	8.64	174.18
13/12/2010	1	220	2.22	114.28	2.29	197.12	3.06	141.38
14/12/2010	1	20	4.80	35.66	3.00	23.42	5.32	39.66
15/12/2010	1	20	5.61	34.68	4.38	38.90	5.57	44.86
16/12/2010	2	20	5.00	40.55	3.89	16.05	4.65	25.42
17/12/2010	2	20	8.94	42.54	8.49	35.08	9.19	38.85
18/12/2010	3	20	9.20	46.25	6.76	50.54	8.96	46.50
19/12/2010	2	20	8.87	43.04	6.45	41.23	6.77	35.74
20/12/2010	2	20	9.52	43.69	8.94	41.95	8.10	42.02
21/12/2010	2	20	9.50	41.86	9.11	46.74	8.60	48.35
22/12/2010	2	20	9.75	38.03	7.33	41.40	9.11	45.84
23/12/2010	3	20	10.02	25.23	7.51	12.37	9.05	31.14
24/12/2010	2	20	10.09	40.55	4.58	58.78	8.50	34.87
25/12/2010	2	20	11.02	41.07	9.03	37.15	7.20	45.71
26/12/2010	2	20	12.20	46.30	12.12	38.85	11.96	39.70
27/12/2010	3	20	11.91	43.67	11.67	36.60	11.41	42.32
28/12/2010	3	20	10.14	43.95	8.18	44.49	8.21	42.35
29/12/2010	2	20	10.67	42.17	10.67	40.66	8.82	37.13
30/12/2010	1	20	10.80	42.52	10.11	35.83	9.33	27.62
31/12/2010	2	20	10.66	40.56	13.47	30.61	12.94	34.83

Table 70. December 2010 wind data at Puerto Princesa from onshore weather station and mesoscale model output

Source Date	PAGASA		ERA-Interim		NCEP FNL		NCEP CFSR	
	Wind Speed (m/s)	Wind Direction (Degrees)	Wind Speed (m/s)	Wind Direction (Degrees)	Wind Speed (m/s)	Wind Direction (Degrees)	Wind Speed (m/s)	Wind Direction (Degrees)
01/12/2010	3	90	6.08	69.59	5.18	64.54	5.41	59.70
02/12/2010	3	90	4.46	65.50	4.34	64.79	3.93	60.87
03/12/2010	3	40	7.13	66.21	5.33	72.59	6.41	74.74
04/12/2010	2	90	5.88	78.87	3.70	79.28	4.65	82.20
05/12/2010	3	90	4.04	73.06	3.33	66.77	4.17	58.26
06/12/2010	3	90	4.58	54.39	3.94	37.78	3.88	47.55
07/12/2010	2	270	4.38	35.86	3.22	326.37	2.86	22.64
08/12/2010	2	270	3.68	7.56	4.89	351.22	3.68	54.95
09/12/2010	3	270	2.75	326.58	5.58	343.62	5.13	67.86
10/12/2010	2	290	2.94	35.41	4.06	346.71	6.40	70.51
11/12/2010	2	270	2.78	349.96	4.30	339.32	5.68	76.37
12/12/2010	2	270	3.02	184.23	2.06	235.65	6.87	193.72
13/12/2010	2	270	2.55	234.72	2.13	167.23	3.79	209.57
14/12/2010	3	90	2.58	56.99	1.88	58.89	1.97	75.78
15/12/2010	2	90	3.07	75.04	2.46	63.43	3.54	76.72
16/12/2010	2	270	2.71	62.27	2.49	22.91	2.29	51.90
17/12/2010	4	90	4.92	78.90	3.87	65.39	3.51	55.03
18/12/2010	3	90	6.19	78.29	5.07	78.16	5.65	72.72
19/12/2010	4	90	3.50	87.27	2.82	83.96	3.19	71.93
20/12/2010	2	270	3.95	63.66	4.28	68.79	2.80	62.64
21/12/2010	1	270	4.66	57.46	4.49	66.18	3.61	72.93
22/12/2010	2	270	4.27	63.83	4.02	66.16	5.46	74.39
23/12/2010	4	90	3.02	23.68	3.09	7.46	3.62	64.13
24/12/2010	2	270	3.06	352.94	2.76	5.50	2.76	344.47
25/12/2010	2	270	3.01	1.33	2.16	13.06	2.43	60.70
26/12/2010	3	90	9.36	59.70	7.84	65.59	4.90	50.53
27/12/2010	4	90	8.06	63.52	6.04	60.09	7.09	61.21
28/12/2010	3	90	4.85	78.71	5.08	76.02	4.41	72.68
29/12/2010	2	90	4.86	68.07	4.16	60.54	2.46	77.91
30/12/2010	2	270	4.74	60.80	4.29	76.84	2.37	13.32
31/12/2010	2	90	5.77	61.67	3.18	32.82	3.09	23.74

Table 71. January 2011 wind data at Coron Island from onshore weather station and meoscale model output

Source Date	PAGASA		ERA-Interim		NCEP FNL		NCEP CFSR	
	Wind Speed (m/s)	Wind Direction (Degrees)	Wind Speed (m/s)	Wind Direction (Degrees)	Wind Speed (m/s)	Wind Direction (Degrees)	Wind Speed (m/s)	Wind Direction (Degrees)
01/01/2011	2	40	11.11	75.88	5.87	77.08	7.54	73.59
02/01/2011	3	40	11.26	77.30	10.31	74.17	11.30	72.83
03/01/2011	1	40	10.87	77.78	11.50	78.29	10.53	75.42
04/01/2011	2	40	10.86	76.86	11.02	74.43	8.58	78.77
05/01/2011	1	0	8.00	78.52	9.07	76.33	5.48	68.21
06/01/2011	1	0	2.19	35.22	3.31	28.73	3.55	33.96
07/01/2011	0	0	7.04	80.55	2.61	4.94	3.05	8.44
08/01/2011	2	0	3.86	53.92	5.41	354.50	4.29	29.62
09/01/2011	1	0	8.01	79.53	5.05	119.93	7.53	84.64
10/01/2011	2	40	6.36	66.44	5.81	72.06	3.74	50.30
11/01/2011	2	40	5.67	61.91	6.03	46.63	3.66	59.11
12/01/2011	2	0	3.83	74.98	4.95	91.46	4.83	94.02
13/01/2011	1	0	2.46	101.30	2.77	326.53	4.32	116.81
14/01/2011	2	0	2.26	289.52	2.53	318.46	1.58	317.60
15/01/2011	2	40	3.38	345.64	3.36	44.34	3.38	79.79
16/01/2011	2	40	2.37	342.56	9.77	78.57	8.34	81.10
17/01/2011	1	0	4.74	59.78	5.86	62.88	8.48	70.51
18/01/2011	2	40	7.86	64.36	5.17	68.49	6.02	76.51
19/01/2011	2	140	8.25	100.32	1.92	168.84	5.20	112.45
20/01/2011	1	0	6.92	156.53	3.93	178.85	4.27	151.32
21/01/2011	1	0	7.82	198.35	6.45	95.17	4.28	116.75
22/01/2011	2	40	6.72	101.39	5.86	75.41	4.84	84.33
23/01/2011	1	0	3.92	75.36	3.83	77.01	4.09	68.13
24/01/2011	2	40	6.73	73.42	6.94	77.39	5.88	76.86
25/01/2011	2	40	10.79	77.40	12.05	76.61	11.39	74.69
26/01/2011	2	40	10.92	76.35	11.67	75.54	11.47	76.66
27/01/2011	3	40	11.11	76.73	10.25	73.49	10.24	75.67
28/01/2011	2	0	8.87	74.85	9.85	73.49	8.81	77.23
29/01/2011	3	40	8.77	71.41	10.12	73.04	10.75	74.68
30/01/2011	1	40	5.08	63.77	5.66	71.10	4.82	67.07
31/01/2011	1	0	6.12	65.30	7.15	69.47	4.77	79.64

Table 72. January 2011 wind data at Cuyo Island from onshore weather station and meoscale model output

Source Date	PAGASA		ERA-Interim		NCEP FNL		NCEP CFSR	
	Wind Speed (m/s)	Wind Direction (Degrees)	Wind Speed (m/s)	Wind Direction (Degrees)	Wind Speed (m/s)	Wind Direction (Degrees)	Wind Speed (m/s)	Wind Direction (Degrees)
01/01/2011	2	20	12.27	44.76	11.47	39.38	12.04	41.69
02/01/2011	4	20	11.96	48.77	11.81	45.53	12.99	45.11
03/01/2011	4	40	12.74	46.83	12.78	50.59	12.86	44.25
04/01/2011	4	40	12.13	45.94	11.77	48.78	12.54	43.91
05/01/2011	3	40	11.78	42.09	11.67	45.50	12.35	40.80
06/01/2011	3	40	12.34	30.27	13.64	25.12	11.61	38.32
07/01/2011	3	40	12.92	36.52	13.44	27.05	13.34	29.66
08/01/2011	4	40	12.59	39.24	9.26	26.36	11.14	34.65
09/01/2011	2	40	9.13	44.41	2.84	129.28	5.76	52.78
10/01/2011	3	40	11.86	38.30	10.15	37.21	10.55	31.17
11/01/2011	4	40	11.61	39.81	10.59	36.34	10.10	41.93
12/01/2011	3	40	10.01	38.79	2.96	55.52	4.29	101.22
13/01/2011	2	40	8.91	31.86	2.21	87.93	3.27	88.24
14/01/2011	1	40	3.60	29.91	2.22	236.30	3.03	31.17
15/01/2011	0	0	5.51	352.23	3.84	0.97	2.90	30.25
16/01/2011	4	40	13.57	35.61	12.93	47.07	13.11	41.30
17/01/2011	5	40	14.85	36.93	14.06	38.48	14.77	39.63
18/01/2011	4	40	10.99	51.50	8.84	42.46	10.94	44.99
19/01/2011	1	40	5.54	133.87	5.63	203.86	4.90	165.23
20/01/2011	1	40	7.47	170.66	4.65	190.21	4.74	171.14
21/01/2011	2	40	6.51	194.98	3.91	86.77	3.01	119.40
22/01/2011	2	40	4.45	107.37	8.55	41.01	6.99	41.26
23/01/2011	2	40	8.74	39.40	8.59	40.01	7.95	39.55
24/01/2011	2	40	10.65	39.98	10.03	39.58	9.87	40.18
25/01/2011	4	40	12.10	45.33	12.82	43.64	11.86	45.60
26/01/2011	4	40	12.86	42.24	14.19	42.42	12.99	48.31
27/01/2011	4	40	12.81	44.00	14.55	41.86	12.87	47.80
28/01/2011	4	40	12.24	45.54	13.16	43.32	12.28	43.95
29/01/2011	4	40	11.97	43.37	12.40	43.09	12.66	44.88
30/01/2011	5	40	12.47	38.82	12.97	38.11	13.04	38.85
31/01/2011	3	40	12.90	37.83	14.17	36.83	14.99	35.54

Table 73. January 2011 wind data at Puerto Princesa from onshore weather station and meoscale model output

Source Date	PAGASA		ERA-Interim		NCEP FNL		NCEP CFSR	
	Wind Speed (m/s)	Wind Direction (Degrees)	Wind Speed (m/s)	Wind Direction (Degrees)	Wind Speed (m/s)	Wind Direction (Degrees)	Wind Speed (m/s)	Wind Direction (Degrees)
01/01/2011	4	90	7.47	67.08	6.13	65.01	6.55	61.05
02/01/2011	6	90	8.69	61.29	6.98	54.57	8.78	61.25
03/01/2011	7	90	7.85	63.27	8.31	64.60	7.80	59.91
04/01/2011	6	90	7.69	70.51	7.35	65.83	6.89	61.37
05/01/2011	5	90	6.37	65.78	6.42	65.48	5.93	54.15
06/01/2011	3	90	4.72	26.78	4.44	16.56	7.00	51.34
07/01/2011	4	90	4.83	30.13	4.60	8.70	4.92	49.57
08/01/2011	3	90	5.27	42.22	4.32	35.32	2.96	2.88
09/01/2011	2	90	5.40	65.21	3.26	5.35	3.58	83.19
10/01/2011	4	90	6.22	64.12	3.51	77.05	3.38	67.82
11/01/2011	4	90	7.26	61.96	3.67	55.22	3.82	47.80
12/01/2011	3	90	5.94	65.64	1.81	42.78	2.03	234.87
13/01/2011	3	90	4.04	78.13	2.03	145.44	3.23	204.55
14/01/2011	2	70	2.56	116.39	2.08	136.42	2.98	207.53
15/01/2011	2	90	2.75	352.82	2.76	28.39	1.82	135.88
16/01/2011	4	90	8.17	62.04	7.72	76.95	7.31	70.41
17/01/2011	6	70	4.37	25.08	5.34	39.73	8.09	58.03
18/01/2011	4	90	6.59	47.17	4.50	73.36	5.60	57.52
19/01/2011	2	90	2.97	172.34	2.72	193.02	3.72	180.56
20/01/2011	2	90	3.09	229.69	2.76	190.23	4.01	202.30
21/01/2011	2	270	2.96	253.38	3.44	159.67	2.62	206.26
22/01/2011	2	90	3.55	147.57	3.23	87.80	3.23	81.42
23/01/2011	3	90	3.57	56.25	3.63	57.41	4.21	67.46
24/01/2011	3	90	5.78	60.29	4.65	57.95	4.55	54.93
25/01/2011	5	90	9.36	61.14	7.96	58.74	6.96	64.22
26/01/2011	6	90	8.16	57.97	8.18	59.26	8.33	59.21
27/01/2011	6	90	8.88	56.84	8.17	57.99	8.79	57.53
28/01/2011	6	90	7.50	55.67	6.50	53.70	6.34	52.01
29/01/2011	4	90	7.37	59.78	6.20	54.27	7.40	59.13
30/01/2011	4	90	5.86	59.07	5.20	55.18	5.57	52.78
31/01/2011	3	90	6.10	54.62	4.45	48.89	4.43	42.50

Table 74. February 2011 wind data at Coron Island from onshore weather station and meoscale model output

Source Date	PAGASA		ERA-Interim		NCEP FNL		NCEP CFSR	
	Wind Speed (m/s)	Wind Direction (Degrees)	Wind Speed (m/s)	Wind Direction (Degrees)	Wind Speed (m/s)	Wind Direction (Degrees)	Wind Speed (m/s)	Wind Direction (Degrees)
01/02/2011	1	40	6.81	80.30	4.32	74.60	6.40	78.62
02/02/2011	2	0	3.91	87.78	2.46	300.90	3.19	65.46
03/02/2011	0	0	2.79	66.46	4.63	349.98	2.77	348.75
04/02/2011	1	0	3.85	30.66	5.57	7.20	5.16	356.84
05/02/2011	1	40	3.79	352.77	3.88	344.90	3.79	350.17
06/02/2011	1	40	2.40	255.77	2.96	351.35	3.17	17.45
07/02/2011	0	0	2.60	55.85	2.01	303.89	3.64	15.18
08/02/2011	3	140	1.77	50.41	3.28	331.50	3.32	276.17
09/02/2011	2	0	2.36	104.50	2.20	9.23	2.39	135.90
10/02/2011	1	0	2.32	64.60	2.86	8.62	2.03	42.26
11/02/2011	0	0	2.23	76.67	4.63	355.30	2.91	7.81
12/02/2011	1	40	6.65	82.03	4.48	81.61	4.61	75.99
13/02/2011	2	140	6.74	84.89	3.35	93.16	4.71	54.56
14/02/2011	2	140	3.86	81.63	4.35	63.07	4.42	68.04
15/02/2011	2	140	7.09	83.02	8.87	72.49	7.17	75.35
16/02/2011	2	40	6.78	84.77	7.25	73.60	7.06	78.90
17/02/2011	2	0	4.44	82.27	6.30	75.99	5.57	69.33
18/02/2011	1	120	4.01	96.63	3.62	77.97	5.43	70.11
19/02/2011	2	40	5.07	78.78	7.07	83.47	6.28	71.89
20/02/2011	2	40	5.32	89.28	4.99	66.14	5.36	65.63
21/02/2011	2	0	4.54	87.63	4.94	87.24	4.55	80.89
22/02/2011	1	40	6.97	88.23	7.19	83.36	6.38	85.15
23/02/2011	2	40	7.66	85.99	6.04	81.51	7.66	84.77
24/02/2011	2	40	6.76	84.60	4.29	60.94	6.57	76.21
25/02/2011	2	0	7.49	86.81	7.15	75.68	7.21	78.07
26/02/2011	2	0	5.99	71.36	5.95	60.09	5.83	57.10
27/02/2011	2	0	2.46	74.52	2.13	302.78	4.23	44.49
28/02/2011	1	0	5.36	35.74	6.14	39.03	4.25	24.01

Table 75. February 2011 wind data at Cuyo Island from onshore weather station and meoscale model output

Source Date	PAGASA		ERA-Interim		NCEP FNL		NCEP CFSR	
	Wind Speed (m/s)	Wind Direction (Degrees)	Wind Speed (m/s)	Wind Direction (Degrees)	Wind Speed (m/s)	Wind Direction (Degrees)	Wind Speed (m/s)	Wind Direction (Degrees)
01/02/2011	3	40	14.00	38.67	15.28	34.67	15.37	35.16
02/02/2011	3	40	12.08	35.45	14.27	27.92	13.93	33.27
03/02/2011	3	40	12.54	21.67	13.02	357.08	13.28	22.15
04/02/2011	4	40	11.45	18.53	14.12	332.14	12.07	21.02
05/02/2011	4	40	11.09	23.43	5.81	359.83	12.75	29.20
06/02/2011	3	40	10.37	25.75	4.76	354.77	10.64	22.05
07/02/2011	2	40	6.41	27.79	5.18	356.77	4.43	22.79
08/02/2011	2	40	1.88	37.28	3.44	324.61	2.99	264.12
09/02/2011	1	220	2.90	29.29	2.72	16.90	1.75	63.53
10/02/2011	1	270	4.00	31.63	4.34	16.34	2.37	22.29
11/02/2011	1	320	5.96	24.43	6.39	16.14	5.17	21.93
12/02/2011	2	40	10.53	40.26	11.43	38.22	11.52	36.86
13/02/2011	2	40	10.24	43.42	11.58	38.33	10.95	38.41
14/02/2011	2	40	9.54	35.88	11.31	34.90	9.57	38.11
15/02/2011	2	40	10.78	44.08	11.53	43.95	9.93	41.67
16/02/2011	2	40	9.87	41.00	10.29	42.56	9.77	41.85
17/02/2011	2	40	9.07	38.06	10.23	38.98	9.86	38.70
18/02/2011	2	40	9.75	35.37	11.03	36.83	10.44	38.69
19/02/2011	2	40	10.21	39.65	10.51	40.88	10.21	39.03
20/02/2011	2	40	10.05	39.64	10.41	38.87	9.92	42.23
21/02/2011	3	40	10.12	39.36	11.36	39.13	10.38	39.78
22/02/2011	4	40	9.95	44.26	11.00	42.92	10.91	41.28
23/02/2011	3	40	9.59	43.58	10.77	41.50	10.60	42.32
24/02/2011	2	40	8.98	41.93	9.83	37.69	10.03	41.36
25/02/2011	3	40	10.04	43.81	10.60	43.24	10.60	43.51
26/02/2011	3	40	10.72	40.56	11.41	38.10	10.93	39.72
27/02/2011	3	40	11.49	30.44	13.11	31.33	12.83	32.77
28/02/2011	2	40	13.19	32.54	12.67	35.72	13.16	31.89

Table 76. February 2011 wind data at Puerto Princesa from onshore weather station and meoscale model output

Source Date	PAGASA		ERA-Interim		NCEP FNL		NCEP CFSR	
	Wind Speed (m/s)	Wind Direction (Degrees)	Wind Speed (m/s)	Wind Direction (Degrees)	Wind Speed (m/s)	Wind Direction (Degrees)	Wind Speed (m/s)	Wind Direction (Degrees)
01/02/2011	3	90	6.26	56.80	4.49	34.90	4.28	44.80
02/02/2011	3	90	6.09	55.27	3.61	10.55	3.62	32.35
03/02/2011	3	0	5.66	48.37	5.78	346.36	4.16	10.18
04/02/2011	3	0	5.21	7.44	6.46	339.40	5.32	352.67
05/02/2011	3	90	4.69	352.05	4.78	337.16	4.22	354.69
06/02/2011	3	90	4.00	27.99	2.39	13.63	3.14	2.19
07/02/2011	3	90	2.86	28.83	2.35	23.27	3.35	343.01
08/02/2011	3	270	2.41	11.18	1.73	342.80	2.25	22.73
09/02/2011	2	90	3.11	79.05	2.19	190.46	2.04	182.27
10/02/2011	2	90	2.26	107.43	1.80	72.24	2.57	10.13
11/02/2011	2	90	2.90	51.64	2.95	38.16	2.40	47.65
12/02/2011	2	90	4.48	66.79	4.68	68.70	3.53	61.26
13/02/2011	2	90	5.14	72.45	4.66	61.65	4.84	63.89
14/02/2011	2	90	4.56	62.05	3.71	18.76	4.55	65.02
15/02/2011	3	90	6.74	67.05	6.43	63.38	4.56	69.38
16/02/2011	3	90	5.02	71.77	5.36	68.56	4.05	67.10
17/02/2011	3	90	3.68	75.91	4.52	59.92	3.97	58.74
18/02/2011	3	90	4.65	54.17	4.54	49.74	4.47	56.91
19/02/2011	3	90	4.86	62.36	5.25	61.93	4.63	62.73
20/02/2011	3	90	3.79	41.79	5.27	49.70	4.17	59.25
21/02/2011	3	90	5.62	71.73	6.17	68.66	4.88	65.55
22/02/2011	4	90	6.49	74.85	4.10	59.60	5.11	61.90
23/02/2011	4	90	4.80	75.36	5.65	64.22	5.60	65.05
24/02/2011	4	90	5.42	69.01	4.48	52.66	5.47	61.65
25/02/2011	3	90	6.00	70.75	4.71	58.63	5.86	64.65
26/02/2011	6	90	6.15	64.55	5.41	59.43	5.53	55.93
27/02/2011	2	90	4.53	22.13	4.40	15.16	3.92	14.07
28/02/2011	2	0	5.47	333.57	5.74	351.38	4.89	4.67

Table 77. March 2011 wind data at Coron Island from onshore weather station and meoscale model output

Source Date	PAGASA		ERA-Interim		NCEP FNL		NCEP CFSR	
	Wind Speed (m/s)	Wind Direction (Degrees)	Wind Speed (m/s)	Wind Direction (Degrees)	Wind Speed (m/s)	Wind Direction (Degrees)	Wind Speed (m/s)	Wind Direction (Degrees)
01/03/2011	2	270	8.36	83.47	4.98	50.61	5.99	80.58
02/03/2011	1	140	7.35	94.10	3.47	118.02	5.36	108.49
03/03/2011	2	140	9.07	87.60	6.41	107.75	6.74	98.02
04/03/2011	3	140	10.10	86.75	5.90	101.51	9.32	89.11
05/03/2011	2	0	10.38	85.14	8.58	88.63	9.72	88.08
06/03/2011	2	0	8.01	88.41	6.96	86.96	5.36	82.40
07/03/2011	1	0	4.17	77.13	3.64	84.64	3.67	68.14
08/03/2011	2	140	6.75	88.62	4.58	74.24	7.12	82.79
09/03/2011	2	40	7.95	80.17	6.27	74.42	7.17	78.54
10/03/2011	2	0	7.63	78.43	4.56	63.07	6.78	76.70
11/03/2011	1	120	6.93	85.30	5.55	54.20	7.25	76.21
12/03/2011	2	0	7.06	78.72	7.21	64.49	6.30	69.72
13/03/2011	1	0	7.14	76.90	6.81	69.14	6.35	77.91
14/03/2011	2	40	3.90	82.04	4.94	74.47	6.35	69.48
15/03/2011	2	40	3.38	88.32	5.55	27.86	8.06	86.41
16/03/2011	2	40	10.48	79.17	9.76	76.37	9.54	78.75
17/03/2011	2	40	11.74	74.89	10.74	76.59	9.79	78.52
18/03/2011	5	40	11.07	82.74	10.70	80.99	8.86	77.80
19/03/2011	3	40	8.46	85.45	7.16	66.14	8.93	80.14
20/03/2011	2	140	5.56	65.55	6.71	76.71	6.47	82.46
21/03/2011	2	40	7.11	84.19	6.33	77.99	6.22	81.76
22/03/2011	2	40	5.49	85.06	5.11	65.34	6.02	73.28
23/03/2011	2	180	6.02	77.36	7.50	74.99	7.56	73.89
24/03/2011	2	140	6.24	75.49	7.53	76.61	6.51	72.42
25/03/2011	1	0	5.99	76.06	8.29	69.54	7.99	69.79
26/03/2011	1	40	6.77	73.44	10.45	66.94	8.49	73.21
27/03/2011	1	210	5.49	63.48	9.16	69.70	7.85	74.53
28/03/2011	2	0	7.87	75.85	7.02	75.31	7.63	77.74
29/03/2011	2	40	8.60	79.88	6.17	75.07	5.82	70.00
30/03/2011	1	40	8.07	79.82	9.36	79.53	10.89	84.73
31/03/2011	1	40	5.84	86.41	6.97	73.11	6.34	73.82

Table 78. March 2011 wind data at Cuyo Island from onshore weather station and meoscale model output

Source Date	PAGASA		ERA-Interim		NCEP FNL		NCEP CFSR	
	Wind Speed (m/s)	Wind Direction (Degrees)	Wind Speed (m/s)	Wind Direction (Degrees)	Wind Speed (m/s)	Wind Direction (Degrees)	Wind Speed (m/s)	Wind Direction (Degrees)
01/03/2011	2	40	5.06	51.77	5.69	55.03	6.39	51.26
02/03/2011	0	0	3.72	87.49	4.70	107.32	3.75	132.81
03/03/2011	2	40	7.91	48.58	4.14	133.90	2.65	105.35
04/03/2011	2	40	9.47	46.80	3.01	111.27	5.65	43.26
05/03/2011	1	40	8.38	48.32	3.10	95.00	5.67	48.69
06/03/2011	1	40	6.14	40.92	4.53	32.11	5.94	37.64
07/03/2011	1	40	6.15	30.28	4.75	16.24	5.58	25.21
08/03/2011	2	40	8.71	40.89	9.30	36.73	8.80	39.57
09/03/2011	2	40	10.67	39.42	10.59	40.65	10.16	41.10
10/03/2011	4	40	11.62	39.79	12.43	37.95	11.48	39.03
11/03/2011	5	40	12.29	38.86	13.76	37.90	13.03	40.15
12/03/2011	5	40	11.82	37.49	12.62	32.30	11.42	39.66
13/03/2011	5	40	9.45	40.44	9.61	39.93	8.74	40.69
14/03/2011	4	40	9.23	35.33	11.80	35.33	10.01	36.60
15/03/2011	3	40	10.45	37.06	9.68	28.72	9.26	44.91
16/03/2011	4	40	11.60	44.25	10.31	43.39	11.75	42.04
17/03/2011	4	40	12.19	46.29	11.60	44.44	11.85	45.00
18/03/2011	5	40	11.29	46.82	10.60	49.21	10.91	43.97
19/03/2011	4	40	9.50	44.78	11.28	39.08	10.06	43.85
20/03/2011	2	40	9.04	36.50	7.88	44.08	6.05	47.70
21/03/2011	4	40	7.49	44.27	7.30	37.45	6.40	37.44
22/03/2011	4	40	9.58	35.23	10.60	38.46	9.34	38.81
23/03/2011	5	40	10.36	38.48	11.42	38.76	10.76	41.78
24/03/2011	4	40	10.72	38.83	11.96	38.61	11.75	41.05
25/03/2011	5	40	11.44	36.86	13.83	39.26	12.48	38.57
26/03/2011	5	40	12.13	39.32	14.11	43.35	13.39	40.21
27/03/2011	5	40	11.29	37.18	11.60	43.91	11.25	42.57
28/03/2011	4	40	10.36	41.38	9.64	38.40	9.76	38.91
29/03/2011	5	40	10.76	41.64	9.95	38.16	10.42	37.84
30/03/2011	5	40	11.13	41.76	8.43	40.93	10.41	43.92
31/03/2011	5	40	11.29	39.67	9.81	33.43	11.61	36.97

Table 79. March 2011 wind data at Puerto Princesa from onshore weather station and meoscale model output

Source Date	PAGASA		ERA-Interim		NCEP FNL		NCEP CFSR	
	Wind Speed (m/s)	Wind Direction (Degrees)	Wind Speed (m/s)	Wind Direction (Degrees)	Wind Speed (m/s)	Wind Direction (Degrees)	Wind Speed (m/s)	Wind Direction (Degrees)
01/03/2011	3	90	7.39	84.17	5.33	57.13	7.05	69.48
02/03/2011	3	180	6.22	142.60	5.07	180.13	6.81	154.13
03/03/2011	3	180	4.77	116.92	6.22	165.71	4.49	180.50
04/03/2011	3	90	3.59	78.21	4.98	161.68	2.56	85.04
05/03/2011	3	90	5.14	86.37	3.83	121.37	4.14	92.64
06/03/2011	2	90	3.73	101.38	2.01	174.60	2.78	89.32
07/03/2011	2	90	2.94	69.86	2.36	70.41	2.53	19.92
08/03/2011	2	90	3.44	78.25	3.16	68.91	4.11	67.66
09/03/2011	3	90	6.10	71.27	5.43	62.91	5.82	64.55
10/03/2011	6	90	6.94	62.33	5.63	59.09	5.21	60.71
11/03/2011	5	90	7.56	62.79	5.88	51.61	6.57	59.13
12/03/2011	4	90	4.39	60.79	4.54	47.95	6.29	57.50
13/03/2011	3	90	4.83	72.63	5.06	66.98	4.66	68.79
14/03/2011	4	90	3.12	76.28	3.96	62.43	3.12	50.60
15/03/2011	4	90	3.86	354.05	4.10	343.65	6.65	70.72
16/03/2011	5	90	7.28	69.33	5.40	77.39	5.67	73.53
17/03/2011	6	90	6.79	69.76	6.08	74.01	7.37	63.41
18/03/2011	5	90	6.55	71.99	5.61	77.93	5.87	67.79
19/03/2011	4	90	5.17	71.01	3.80	46.58	6.20	64.57
20/03/2011	3	90	4.20	62.13	3.73	73.18	4.00	75.01
21/03/2011	2	90	4.24	73.00	2.64	86.53	2.07	108.57
22/03/2011	3	90	4.49	72.39	5.08	54.21	3.68	59.17
23/03/2011	5	90	6.17	66.14	6.97	61.63	6.45	59.14
24/03/2011	5	90	5.94	67.43	6.61	63.50	5.92	62.13
25/03/2011	5	70	6.35	64.57	5.14	48.84	6.48	60.06
26/03/2011	5	90	6.02	60.58	7.16	45.29	5.58	55.24
27/03/2011	5	90	5.31	46.27	8.78	53.50	6.61	59.63
28/03/2011	4	90	6.85	61.71	6.00	67.11	5.41	63.16
29/03/2011	5	90	6.88	70.66	5.64	73.77	4.98	66.94
30/03/2011	5	90	6.44	76.08	4.93	77.34	6.42	69.97
31/03/2011	5	90	5.32	72.61	4.27	76.61	3.87	71.58

Table 80. April 2011 wind data at Coron Island from onshore weather station and meoscale model output

Source Date	PAGASA		ERA-Interim		NCEP FNL		NCEP CFSR	
	Wind Speed (m/s)	Wind Direction (Degrees)	Wind Speed (m/s)	Wind Direction (Degrees)	Wind Speed (m/s)	Wind Direction (Degrees)	Wind Speed (m/s)	Wind Direction (Degrees)
01/04/2011	2	320	4.20	100.99	4.39	79.21	2.92	77.34
02/04/2011	1	40	3.27	72.88	2.68	309.36	2.20	230.09
03/04/2011	1	0	1.99	95.42	2.25	196.04	1.83	249.18
04/04/2011	1	40	3.59	81.88	2.88	108.41	2.21	58.32
05/04/2011	2	140	8.19	90.52	7.75	88.24	7.04	90.66
06/04/2011	3	0	8.07	88.17	9.23	81.69	9.44	85.90
07/04/2011	3	40	7.49	88.06	7.43	79.09	8.27	85.05
08/04/2011	2	40	7.39	85.04	6.57	80.34	7.36	82.29
09/04/2011	2	40	7.10	80.42	7.55	77.54	7.24	75.76
10/04/2011	2	40	4.51	84.97	5.84	80.39	5.31	81.42
11/04/2011	0	0	3.41	76.99	2.14	32.47	2.82	190.29
12/04/2011	2	320	6.94	87.69	4.76	68.46	7.08	79.52
13/04/2011	2	140	8.42	86.33	9.30	82.87	9.23	85.06
14/04/2011	1	120	6.56	87.47	6.06	82.50	6.10	79.65
15/04/2011	2	120	5.69	89.39	7.36	84.59	6.13	81.44
16/04/2011	1	120	4.17	84.72	4.35	82.13	4.25	80.08
17/04/2011	2	40	3.20	82.42	2.86	74.86	2.87	69.11
18/04/2011	1	40	3.06	75.81	2.36	316.05	2.38	19.72
19/04/2011	1	0	3.80	358.51	2.92	351.26	3.39	78.70
20/04/2011	2	0	7.14	86.92	6.80	85.63	4.87	74.03
21/04/2011	2	0	5.75	89.78	5.11	88.12	4.57	88.91
22/04/2011	1	0	3.26	86.39	2.85	81.34	3.28	90.92
23/04/2011	1	40	3.97	84.31	2.23	5.52	3.43	72.26
24/04/2011	2	0	4.32	83.20	4.15	76.50	3.28	102.95
25/04/2011	0	0	5.59	90.04	7.73	81.37	7.59	91.01
26/04/2011	2	180	4.03	87.27	4.10	157.36	4.44	82.31
27/04/2011	1	120	3.66	81.92	2.37	141.00	3.88	69.39
28/04/2011	2	0	4.09	86.25	4.33	83.35	5.30	81.48
29/04/2011	3	140	6.21	83.31	5.61	76.90	5.51	75.87
30/04/2011	4	40	7.75	86.42	7.48	85.31	7.54	85.41

Table 81. April 2011 wind data at Cuyo Island from onshore weather station and meoscale model output

Source Date	PAGASA		ERA-Interim		NCEP FNL		NCEP CFSR	
	Wind Speed (m/s)	Wind Direction (Degrees)	Wind Speed (m/s)	Wind Direction (Degrees)	Wind Speed (m/s)	Wind Direction (Degrees)	Wind Speed (m/s)	Wind Direction (Degrees)
01/04/2011	3	40	10.62	36.45	10.81	37.90	11.72	33.30
02/04/2011	4	40	8.39	29.56	9.35	30.63	9.09	27.96
03/04/2011	2	40	6.55	30.62	7.66	29.33	7.46	29.44
04/04/2011	3	40	7.65	36.49	8.49	37.44	7.66	35.85
05/04/2011	4	40	9.57	43.47	10.47	45.41	9.75	42.25
06/04/2011	5	40	9.18	44.23	9.88	45.57	9.17	44.66
07/04/2011	4	40	8.77	42.64	9.38	43.16	9.00	42.44
08/04/2011	4	40	9.53	41.90	9.98	41.85	9.62	41.61
09/04/2011	4	40	9.44	41.82	9.23	38.22	9.38	37.78
10/04/2011	5	40	8.86	36.65	10.00	40.02	9.77	39.40
11/04/2011	5	40	9.24	33.48	10.43	30.46	9.68	27.86
12/04/2011	3	40	10.06	38.55	12.06	36.80	10.78	40.44
13/04/2011	5	40	9.73	42.56	10.52	42.32	10.04	43.54
14/04/2011	3	40	8.19	42.73	9.74	40.18	8.64	39.13
15/04/2011	4	40	6.70	35.59	7.61	41.18	7.54	38.95
16/04/2011	2	40	5.64	29.05	5.87	31.80	5.68	29.72
17/04/2011	2	40	3.86	22.10	4.26	22.49	4.78	23.35
18/04/2011	2	40	4.08	357.40	3.49	351.32	3.56	347.64
19/04/2011	2	140	5.80	13.98	5.82	14.85	5.05	16.47
20/04/2011	2	40	8.08	42.05	8.03	42.80	9.17	36.13
21/04/2011	3	40	8.63	37.48	9.16	38.95	10.07	34.61
22/04/2011	2	40	7.62	29.99	8.19	28.86	8.48	35.63
23/04/2011	2	40	7.46	25.90	8.20	19.28	6.83	31.05
24/04/2011	4	40	8.73	35.15	12.33	22.22	8.75	30.48
25/04/2011	2	40	5.81	43.39	7.19	130.42	4.15	47.78
26/04/2011	1	40	3.71	23.05	2.66	169.09	4.42	21.66
27/04/2011	1	20	3.81	18.52	1.85	336.73	5.26	24.88
28/04/2011	2	40	4.55	33.14	4.57	25.41	6.39	35.34
29/04/2011	4	40	7.59	41.12	7.56	37.61	7.35	37.34
30/04/2011	3	20	7.70	41.77	7.37	42.13	7.09	41.66

Table 82. April 2011 wind data at Puerto Princesa from onshore weather station and meoscale model output

Source Date	PAGASA		ERA-Interim		NCEP FNL		NCEP CFSR	
	Wind Speed (m/s)	Wind Direction (Degrees)	Wind Speed (m/s)	Wind Direction (Degrees)	Wind Speed (m/s)	Wind Direction (Degrees)	Wind Speed (m/s)	Wind Direction (Degrees)
01/04/2011	4	90	3.34	97.02	4.21	81.48	2.64	81.22
02/04/2011	2	90	4.00	70.06	2.69	73.06	2.47	59.84
03/04/2011	2	90	3.60	82.49	2.40	80.87	2.03	74.34
04/04/2011	4	90	3.14	74.36	3.20	78.46	2.35	78.83
05/04/2011	5	90	5.74	75.04	6.18	73.35	4.07	71.88
06/04/2011	4	90	3.88	81.09	4.63	73.83	4.07	71.50
07/04/2011	4	90	3.70	78.97	4.35	75.01	3.73	70.79
08/04/2011	4	90	5.08	72.11	5.71	70.72	4.99	68.36
09/04/2011	3	90	4.84	71.73	4.61	70.71	4.22	64.26
10/04/2011	3	90	3.73	73.59	4.69	68.36	4.41	65.92
11/04/2011	4	90	3.88	63.76	3.33	46.90	3.33	39.12
12/04/2011	4	90	4.98	67.27	5.12	56.57	5.08	59.01
13/04/2011	5	90	3.77	81.71	4.77	66.44	4.64	72.65
14/04/2011	4	90	3.30	83.74	4.35	74.41	2.75	75.19
15/04/2011	3	90	3.47	106.38	2.80	89.09	2.23	83.69
16/04/2011	2	90	3.36	81.56	2.66	91.29	2.83	75.90
17/04/2011	2	90	3.01	91.91	2.19	74.07	2.13	78.29
18/04/2011	3	140	2.95	111.65	2.15	21.24	2.26	45.83
19/04/2011	3	90	3.35	44.74	2.84	348.31	2.92	1.92
20/04/2011	3	90	3.78	76.22	3.04	75.62	3.38	73.68
21/04/2011	3	90	3.80	80.21	2.92	77.65	2.87	52.68
22/04/2011	3	90	3.58	73.71	2.62	70.64	3.44	48.00
23/04/2011	2	90	4.04	45.78	2.92	9.97	3.35	54.59
24/04/2011	2	90	3.74	54.25	4.13	2.95	2.70	44.05
25/04/2011	3	90	5.27	84.77	2.77	330.54	3.77	86.72
26/04/2011	3	90	2.91	151.16	2.58	169.59	1.86	129.61
27/04/2011	3	90	2.84	132.56	2.12	155.47	2.16	49.87
28/04/2011	3	90	3.06	116.44	2.06	115.00	2.31	70.90
29/04/2011	3	90	3.62	74.75	3.67	77.37	2.72	76.49
30/04/2011	2	90	4.11	71.41	3.14	83.15	3.45	69.05

Table 83. May 2011 wind data at Coron Island from onshore weather station and meoscale model output

Source Date	PAGASA		ERA-Interim		NCEP FNL		NCEP CFSR	
	Wind Speed (m/s)	Wind Direction (Degrees)	Wind Speed (m/s)	Wind Direction (Degrees)	Wind Speed (m/s)	Wind Direction (Degrees)	Wind Speed (m/s)	Wind Direction (Degrees)
01/05/2011	2	40	4.94	89.72	4.64	65.54	4.66	73.53
02/05/2011	2	120	5.31	92.50	5.29	78.99	6.02	85.89
03/05/2011	1	120	3.93	54.83	4.74	52.45	3.55	72.89
04/05/2011	2	120	3.28	86.51	9.40	81.29	7.28	86.75
05/05/2011	1	140	3.69	307.77	5.47	93.54	4.87	91.78
06/05/2011	1	140	4.57	336.14	3.32	302.49	2.59	254.73
07/05/2011	1	320	5.95	317.73	6.87	320.49	2.14	289.36
08/05/2011	2	210	7.53	252.81	11.03	259.72	3.12	244.28
09/05/2011	3	210	5.69	205.81	13.00	226.42	4.78	215.32
10/05/2011	2	180	3.19	231.98	8.54	234.54	4.56	201.04
11/05/2011	1	0	2.34	184.87	4.97	199.30	4.37	191.16
12/05/2011	2	220	1.94	120.85	2.63	214.35	2.56	179.23
13/05/2011	1	220	3.26	84.18	2.23	72.39	3.23	100.27
14/05/2011	2	140	4.63	91.56	3.85	93.39	5.51	94.03
15/05/2011	2	140	4.07	88.46	4.94	85.19	4.00	68.57
16/05/2011	2	40	2.54	89.34	2.88	60.71	2.59	77.01
17/05/2011	2	0	2.53	81.45	2.69	352.77	2.51	72.20
18/05/2011	1	0	2.78	83.52	3.20	17.63	3.36	45.69
19/05/2011	2	140	1.96	81.05	2.37	320.24	1.75	322.88
20/05/2011	1	0	3.14	88.40	3.66	330.51	2.97	90.30
21/05/2011	1	0	2.09	112.15	4.51	327.58	3.48	77.35
22/05/2011	1	0	1.54	175.60	3.16	329.46	2.96	335.61
23/05/2011	1	0	1.78	233.38	4.02	307.54	3.31	321.66
24/05/2011	1	0	2.43	276.34	4.31	302.69	4.04	331.93
25/05/2011	1	320	2.31	268.31	5.23	282.67	3.24	290.86
26/05/2011	2	220	2.34	299.55	10.53	247.23	4.87	283.06
27/05/2011	2	220	3.93	205.52	9.42	249.46	6.14	257.25
28/05/2011	1	220	5.28	194.50	7.20	220.40	5.40	226.03
29/05/2011	1	180	3.66	199.23	7.88	229.07	5.71	196.76
30/05/2011	1	180	3.33	186.01	7.89	198.68	4.86	189.97
31/05/2011	1	180	2.76	172.42	8.18	195.91	3.92	193.78

Table 84. May 2011 wind data at Cuyo Island from onshore weather station and meoscale model output

Source Date	PAGASA		ERA-Interim		NCEP FNL		NCEP CFSR	
	Wind Speed (m/s)	Wind Direction (Degrees)	Wind Speed (m/s)	Wind Direction (Degrees)	Wind Speed (m/s)	Wind Direction (Degrees)	Wind Speed (m/s)	Wind Direction (Degrees)
01/05/2011	3	20	7.86	39.84	8.36	37.62	7.83	38.62
02/05/2011	4	40	7.10	40.05	7.97	38.46	7.40	40.25
03/05/2011	3	20	7.20	17.83	8.03	28.21	6.65	30.01
04/05/2011	2	40	7.62	30.53	5.13	92.06	4.74	112.36
05/05/2011	1	20	5.63	348.26	4.17	63.65	4.24	48.14
06/05/2011	1	40	6.02	313.84	4.35	334.23	4.36	347.00
07/05/2011	0	0	9.19	296.19	10.38	300.84	4.13	289.78
08/05/2011	2	20	8.21	256.64	13.78	249.59	5.20	251.03
09/05/2011	3	320	7.09	191.21	12.95	213.40	5.67	215.49
10/05/2011	2	220	5.49	206.60	9.53	219.80	5.10	198.21
11/05/2011	1	220	2.82	175.84	4.85	200.99	3.50	201.98
12/05/2011	0	0	1.75	67.50	1.90	194.20	2.20	195.43
13/05/2011	1	20	3.81	28.11	3.47	19.99	1.93	4.69
14/05/2011	1	20	3.71	34.93	3.06	45.97	2.59	63.41
15/05/2011	1	40	6.12	35.88	4.44	28.80	5.52	27.49
16/05/2011	1	40	6.12	33.75	5.25	27.15	5.77	28.44
17/05/2011	0	0	3.95	32.93	4.97	17.02	4.77	21.98
18/05/2011	1	220	3.67	18.00	5.39	2.03	4.82	10.16
19/05/2011	0	0	5.53	31.35	5.01	0.17	7.04	9.67
20/05/2011	1	20	5.36	31.52	5.88	353.86	5.30	33.94
21/05/2011	1	20	5.92	19.75	6.51	336.06	6.31	19.98
22/05/2011	0	0	5.79	15.16	4.86	337.94	6.24	345.08
23/05/2011	1	320	4.86	349.45	7.21	314.37	6.47	338.40
24/05/2011	0	0	4.27	344.94	7.88	310.70	7.61	338.88
25/05/2011	0	0	3.73	316.38	7.96	283.66	6.66	306.79
26/05/2011	1	320	4.08	276.58	11.55	242.98	8.22	276.61
27/05/2011	2	220	5.40	204.05	11.76	228.03	7.41	245.87
28/05/2011	4	220	6.28	197.78	9.38	209.50	7.85	216.82
29/05/2011	2	220	3.96	196.97	10.70	202.42	6.53	196.54
30/05/2011	1	220	3.23	182.61	8.25	196.23	4.39	190.95
31/05/2011	1	220	2.71	178.73	6.74	196.38	3.17	198.67

Table 85. May 2011 wind data at Puerto Princesa from onshore weather station and mesoscale model output

Source Date	PAGASA		ERA-Interim		NCEP FNL		NCEP CFSR	
	Wind Speed (m/s)	Wind Direction (Degrees)	Wind Speed (m/s)	Wind Direction (Degrees)	Wind Speed (m/s)	Wind Direction (Degrees)	Wind Speed (m/s)	Wind Direction (Degrees)
01/05/2011	2	90	3.79	79.83	3.00	68.66	3.44	72.50
02/05/2011	4	90	4.12	80.29	2.94	73.50	3.10	67.35
03/05/2011	3	90	2.97	358.42	3.03	25.74	2.64	36.66
04/05/2011	2	270	2.46	349.44	1.86	214.06	2.21	310.90
05/05/2011	3	270	3.52	33.47	2.24	27.14	2.12	338.57
06/05/2011	3	140	3.45	347.82	2.33	142.49	1.97	77.61
07/05/2011	2	180	3.91	305.23	4.22	324.66	1.96	147.06
08/05/2011	2	90	4.09	258.63	5.46	259.39	2.26	205.10
09/05/2011	3	220	2.95	177.14	4.19	223.64	3.06	221.34
10/05/2011	2	180	2.98	202.50	3.65	221.10	2.88	214.09
11/05/2011	2	270	3.28	179.27	3.38	191.08	3.26	204.45
12/05/2011	3	140	2.91	163.35	2.78	179.72	3.12	192.33
13/05/2011	3	90	2.43	127.10	1.92	146.50	2.22	184.93
14/05/2011	1	90	2.53	154.27	2.41	82.12	2.07	137.99
15/05/2011	2	90	2.48	123.59	2.32	132.47	1.75	112.38
16/05/2011	2	90	3.10	60.51	1.93	70.69	2.35	43.63
17/05/2011	2	90	3.09	63.61	2.72	30.91	2.02	51.21
18/05/2011	3	140	2.74	96.31	3.16	22.28	2.23	52.18
19/05/2011	3	90	3.09	58.59	2.29	25.81	3.70	352.35
20/05/2011	2	90	3.14	45.14	3.96	344.96	3.61	343.26
21/05/2011	2	90	2.81	86.42	3.80	336.04	2.42	10.62
22/05/2011	2	90	3.08	30.59	1.93	318.22	4.03	339.60
23/05/2011	3	220	1.80	24.90	1.47	30.61	2.00	308.21
24/05/2011	2	0	2.65	338.18	1.77	314.61	3.53	333.10
25/05/2011	3	270	2.18	215.60	2.56	250.19	2.27	323.54
26/05/2011	2	270	3.10	169.38	6.41	250.95	2.75	245.13
27/05/2011	2	140	3.84	197.83	5.45	236.02	3.40	238.09
28/05/2011	1	270	3.28	194.99	5.39	202.80	3.98	194.54
29/05/2011	2	270	3.05	215.86	5.84	213.39	4.15	192.72
30/05/2011	2	180	2.78	187.58	4.89	199.81	3.19	203.82
31/05/2011	3	180	3.74	182.34	4.36	198.39	3.12	194.54

Table 86. June 2011 wind data at Coron Island from onshore weather station and meoscale model output

Source Date	PAGASA		ERA-Interim		NCEP FNL		NCEP CFSR	
	Wind Speed (m/s)	Wind Direction (Degrees)	Wind Speed (m/s)	Wind Direction (Degrees)	Wind Speed (m/s)	Wind Direction (Degrees)	Wind Speed (m/s)	Wind Direction (Degrees)
01/06/2011	1	180	2.54	204.41	2.65	191.97	2.25	191.96
02/06/2011	1	220	1.93	82.33	1.96	140.28	1.93	40.43
03/06/2011	2	0	2.02	80.35	1.74	332.55	2.58	77.73
04/06/2011	2	180	2.78	78.38	3.02	164.61	2.90	103.80
05/06/2011	2	120	3.44	85.06	2.58	101.89	2.76	105.12
06/06/2011	1	120	2.92	74.28	2.88	74.29	2.67	28.26
07/06/2011	1	0	2.01	269.29	4.74	289.89	2.76	287.44
08/06/2011	1	180	5.91	274.12	12.19	239.65	3.05	275.40
09/06/2011	1	0	5.07	216.94	10.44	193.05	3.57	240.12
10/06/2011	1	0	3.97	186.89	8.12	173.84	4.83	198.12
11/06/2011	1	120	2.83	177.91	6.55	183.31	3.95	207.38
12/06/2011	2	40	2.51	266.89	4.39	224.81	3.11	226.54
13/06/2011	1	140	4.08	239.25	5.24	197.70	2.89	253.00
14/06/2011	2	220	4.29	193.65	6.86	193.99	4.48	223.35
15/06/2011	2	140	5.22	191.37	7.41	195.69	6.28	196.42
16/06/2011	0	0	5.20	218.54	6.01	201.05	6.19	209.34
17/06/2011	0	0	4.56	211.89	5.41	248.34	5.67	217.96
18/06/2011	1	210	7.74	223.46	13.47	226.78	7.10	229.28
19/06/2011	2	120	7.21	198.34	12.28	209.03	7.90	226.00
20/06/2011	4	180	7.48	192.51	11.21	197.29	7.50	206.79
21/06/2011	2	180	7.18	198.69	8.98	205.00	6.53	223.86
22/06/2011	2	180	6.59	222.02	9.60	228.24	7.77	230.98
23/06/2011	5	220	8.72	224.43	12.57	228.09	10.49	224.71
24/06/2011	4	210	9.19	209.79	12.36	211.67	10.44	200.23
25/06/2011	4	180	7.36	199.33	10.13	199.41	8.15	193.25
26/06/2011	2	180	4.91	196.23	5.89	205.56	4.79	184.32
27/06/2011	1	220	2.82	204.81	2.17	234.85	2.43	235.06
28/06/2011	1	220	1.49	173.58	2.27	263.46	2.41	49.16
29/06/2011	0	0	1.82	59.38	2.88	310.53	2.80	339.01
30/06/2011	1	210	2.77	334.91	5.86	249.48	2.04	308.97

Table 87. June 2011 wind data at Cuyo Island from onshore weather station and meoscale model output

Source Date	PAGASA		ERA-Interim		NCEP FNL		NCEP CFSR	
	Wind Speed (m/s)	Wind Direction (Degrees)	Wind Speed (m/s)	Wind Direction (Degrees)	Wind Speed (m/s)	Wind Direction (Degrees)	Wind Speed (m/s)	Wind Direction (Degrees)
01/06/2011	1	220	2.15	207.35	1.98	193.87	1.15	244.68
02/06/2011	1	220	1.66	309.61	1.44	276.07	2.24	3.09
03/06/2011	0	0	1.89	29.09	3.87	277.44	1.84	58.67
04/06/2011	1	120	1.95	40.01	3.48	175.60	2.39	174.09
05/06/2011	0	0	2.69	1.02	3.91	30.52	2.90	51.57
06/06/2011	1	270	4.57	25.68	5.15	23.58	5.18	19.58
07/06/2011	1	270	5.24	329.80	7.66	267.66	4.29	333.78
08/06/2011	2	220	6.23	251.48	10.88	218.47	5.08	251.70
09/06/2011	1	220	3.41	198.42	8.31	188.85	4.68	212.08
10/06/2011	1	220	3.07	192.45	6.84	170.17	4.92	206.59
11/06/2011	1	220	2.93	242.37	6.89	185.90	4.19	223.18
12/06/2011	3	20	5.17	264.63	4.93	249.83	3.06	260.34
13/06/2011	1	20	5.21	246.15	6.21	207.97	4.77	265.27
14/06/2011	2	220	3.78	211.42	7.05	189.53	4.85	240.70
15/06/2011	3	220	6.40	200.13	8.31	204.78	7.57	205.28
16/06/2011	2	220	6.62	209.50	6.70	207.14	6.67	205.36
17/06/2011	1	220	6.83	228.34	9.56	240.38	7.84	218.92
18/06/2011	4	250	8.61	214.44	14.36	225.61	9.00	224.33
19/06/2011	3	220	7.68	197.87	12.02	198.27	8.34	217.96
20/06/2011	2	220	7.29	195.93	10.50	189.90	7.78	206.80
21/06/2011	2	220	7.10	207.53	9.16	210.27	7.14	226.45
22/06/2011	4	220	7.68	225.02	10.47	223.74	9.28	226.41
23/06/2011	5	220	9.98	214.06	13.74	218.06	11.59	216.38
24/06/2011	4	220	10.39	199.10	12.96	198.78	10.21	196.13
25/06/2011	3	220	7.34	197.72	9.36	199.88	7.43	193.34
26/06/2011	2	220	3.85	196.25	5.63	205.13	3.49	194.51
27/06/2011	1	220	2.14	203.18	3.03	207.62	1.89	194.94
28/06/2011	1	320	1.16	270.04	2.75	231.27	2.99	18.78
29/06/2011	1	220	2.68	323.66	4.78	269.26	4.01	22.66
30/06/2011	1	20	5.39	341.78	7.35	235.18	2.59	325.35

Table 88. June 2011 wind data at Puerto Princesa from onshore weather station and meoscale model output

Source Date	PAGASA		ERA-Interim		NCEP FNL		NCEP CFSR	
	Wind Speed (m/s)	Wind Direction (Degrees)	Wind Speed (m/s)	Wind Direction (Degrees)	Wind Speed (m/s)	Wind Direction (Degrees)	Wind Speed (m/s)	Wind Direction (Degrees)
01/06/2011	3	140	3.21	194.00	3.33	198.33	2.97	228.08
02/06/2011	3	90	3.04	158.90	2.81	189.96	2.54	201.41
03/06/2011	2	70	3.05	166.27	1.86	148.67	2.23	198.80
04/06/2011	2	140	3.04	167.40	2.10	210.84	2.82	202.15
05/06/2011	2	140	2.76	137.76	2.49	182.44	2.55	183.35
06/06/2011	2	270	2.43	92.56	1.65	112.55	1.53	123.01
07/06/2011	2	140	2.37	77.08	2.26	236.99	1.98	223.56
08/06/2011	2	180	2.90	216.89	4.48	245.64	2.97	234.95
09/06/2011	3	270	3.08	171.49	4.13	230.42	2.85	243.52
10/06/2011	3	140	3.99	193.66	4.90	186.59	3.73	200.88
11/06/2011	2	180	2.59	183.66	3.87	199.83	3.78	199.13
12/06/2011	1	110	2.28	190.16	2.22	207.99	3.02	197.12
13/06/2011	2	70	2.36	217.84	3.99	188.15	3.04	198.89
14/06/2011	4	220	2.88	200.69	4.15	204.43	3.43	194.34
15/06/2011	2	270	4.96	195.50	4.89	201.33	4.47	205.40
16/06/2011	2	270	6.19	195.87	5.14	199.10	4.70	200.98
17/06/2011	2	180	3.84	198.72	4.35	201.70	4.42	200.65
18/06/2011	2	180	5.77	196.29	4.62	217.09	4.13	196.11
19/06/2011	2	180	5.12	199.68	6.08	204.76	4.11	200.96
20/06/2011	3	220	5.59	196.66	6.32	197.40	4.92	197.58
21/06/2011	4	180	5.16	198.68	5.42	197.59	4.21	198.82
22/06/2011	4	180	4.56	194.46	5.68	202.37	4.27	198.87
23/06/2011	3	180	6.31	198.76	5.95	206.16	5.50	202.94
24/06/2011	4	180	6.08	196.70	7.10	197.43	4.89	194.60
25/06/2011	3	180	5.46	199.11	5.07	195.63	4.31	202.42
26/06/2011	3	180	4.10	185.96	3.41	197.67	3.75	189.38
27/06/2011	3	180	3.57	181.25	3.17	186.20	2.82	184.82
28/06/2011	2	90	3.03	185.03	2.85	185.37	1.92	180.23
29/06/2011	2	90	2.71	179.91	2.60	187.64	1.72	55.87
30/06/2011	3	180	1.73	94.64	3.18	205.71	1.63	202.16

Table 89. July 2011 wind data at Coron Island from onshore weather station and meoscale model output

Source Date	PAGASA		ERA-Interim		NCEP FNL		NCEP CFSR	
	Wind Speed (m/s)	Wind Direction (Degrees)	Wind Speed (m/s)	Wind Direction (Degrees)	Wind Speed (m/s)	Wind Direction (Degrees)	Wind Speed (m/s)	Wind Direction (Degrees)
01/07/2011	0	0	4.88	328.50	4.68	326.07	2.84	302.00
02/07/2011	0	0	5.52	332.74	4.58	321.67	3.53	305.28
03/07/2011	1	140	2.31	59.81	1.93	311.32	2.72	313.98
04/07/2011	1	140	2.32	20.28	2.92	296.32	3.74	102.33
05/07/2011	2	220	3.86	226.24	6.07	259.89	4.80	222.69
06/07/2011	3	210	5.57	235.52	8.92	256.75	7.06	221.08
07/07/2011	2	210	6.43	221.41	9.61	229.15	8.00	224.88
08/07/2011	1	210	7.16	201.44	8.45	221.48	7.47	207.17
09/07/2011	3	220	6.20	200.34	7.72	227.51	6.99	211.30
10/07/2011	3	180	7.96	204.96	9.05	246.43	7.50	229.55
11/07/2011	2	220	6.39	209.56	9.68	234.18	7.05	228.39
12/07/2011	2	180	5.90	198.97	9.25	219.87	6.43	206.62
13/07/2011	1	210	4.40	199.04	7.52	212.69	5.04	224.23
14/07/2011	1	180	3.20	209.87	5.61	200.71	3.34	239.65
15/07/2011	1	0	1.98	56.23	2.99	239.27	3.27	272.39
16/07/2011	1	220	3.06	245.92	4.25	247.45	4.66	271.16
17/07/2011	1	220	5.92	235.47	6.70	235.71	5.93	245.51
18/07/2011	1	210	6.24	225.53	6.59	222.32	7.07	228.16
19/07/2011	1	180	5.59	198.42	5.40	226.02	5.78	219.90
20/07/2011	1	210	3.62	197.35	3.78	238.98	3.32	233.63
21/07/2011	0	0	2.28	207.31	4.63	235.40	3.10	280.17
22/07/2011	1	0	2.94	244.06	4.27	259.01	4.95	265.65
23/07/2011	1	320	3.08	226.59	5.40	240.42	4.67	245.80
24/07/2011	1	210	4.10	245.39	7.86	244.99	4.30	246.39
25/07/2011	1	0	5.43	283.89	6.82	241.83	4.65	274.29
26/07/2011	3	210	11.30	261.82	13.05	228.04	8.91	251.41
27/07/2011	4	220	12.87	218.47	13.57	223.30	10.77	236.62
28/07/2011	3	220	9.45	195.39	10.68	200.52	8.64	213.56
29/07/2011	1	220	7.45	203.68	8.12	208.74	7.96	220.22
30/07/2011	0	0	7.04	224.35	9.77	225.91	7.65	241.73
31/07/2011	1	210	8.56	237.60	12.07	243.62	8.37	238.82

Table 90. July 2011 wind data at Cuyo Island from onshore weather station and meoscale model output

Source Date	PAGASA		ERA-Interim		NCEP FNL		NCEP CFSR	
	Wind Speed (m/s)	Wind Direction (Degrees)	Wind Speed (m/s)	Wind Direction (Degrees)	Wind Speed (m/s)	Wind Direction (Degrees)	Wind Speed (m/s)	Wind Direction (Degrees)
01/07/2011	1	320	7.33	330.58	5.32	315.85	4.55	333.81
02/07/2011	1	220	7.95	334.42	7.30	300.94	6.77	319.18
03/07/2011	1	270	3.17	10.62	5.51	15.07	5.85	334.18
04/07/2011	0	0	3.46	11.33	5.86	332.66	2.69	142.44
05/07/2011	4	220	7.45	230.51	11.23	243.86	8.78	231.79
06/07/2011	5	220	9.73	218.34	10.86	240.62	10.66	215.50
07/07/2011	4	220	8.42	215.71	12.01	215.50	9.82	216.55
08/07/2011	2	220	7.47	205.28	9.63	211.94	7.86	210.69
09/07/2011	3	220	6.95	204.72	9.61	218.26	7.52	212.36
10/07/2011	1	220	7.87	206.11	10.50	234.45	7.98	227.19
11/07/2011	1	220	7.26	203.83	10.52	225.53	7.49	219.18
12/07/2011	1	220	6.33	197.75	10.63	211.29	6.83	209.75
13/07/2011	1	220	4.60	201.98	8.40	205.51	5.11	218.44
14/07/2011	2	220	3.33	214.21	5.56	208.42	4.48	236.64
15/07/2011	1	220	2.26	252.68	3.38	235.29	3.99	266.03
16/07/2011	1	220	3.44	260.81	4.49	256.81	5.80	268.89
17/07/2011	1	220	5.98	226.67	6.41	230.85	5.93	240.73
18/07/2011	2	220	6.97	213.57	7.92	214.84	7.92	221.53
19/07/2011	3	220	6.31	202.14	6.30	213.65	6.07	213.88
20/07/2011	1	220	4.77	212.40	5.94	229.73	4.28	242.72
21/07/2011	1	220	3.57	231.55	6.26	235.11	4.44	288.42
22/07/2011	0	0	4.27	242.88	8.06	233.15	7.70	264.32
23/07/2011	0	0	4.77	242.57	7.69	246.24	5.61	252.96
24/07/2011	0	0	6.70	262.32	10.02	245.52	7.87	250.50
25/07/2011	0	0	10.84	276.21	10.70	233.00	8.73	268.23
26/07/2011	4	220	15.28	247.30	16.35	215.86	11.75	250.04
27/07/2011	4	220	13.76	204.72	16.99	209.66	13.63	224.04
28/07/2011	4	220	9.82	188.94	11.83	193.61	10.79	210.08
29/07/2011	2	220	8.23	209.51	9.75	204.62	9.42	219.30
30/07/2011	1	220	8.65	218.50	10.71	215.13	9.10	235.10
31/07/2011	2	220	10.55	222.73	12.87	229.08	9.60	230.41

Table 91. July 2011 wind data at Puerto Princesa from onshore weather station and meoscale model output

Source Date	PAGASA		ERA-Interim		NCEP FNL		NCEP CFSR	
	Wind Speed (m/s)	Wind Direction (Degrees)	Wind Speed (m/s)	Wind Direction (Degrees)	Wind Speed (m/s)	Wind Direction (Degrees)	Wind Speed (m/s)	Wind Direction (Degrees)
01/07/2011	3	320	3.50	334.01	2.68	320.39	1.79	338.04
02/07/2011	3	340	5.82	327.50	3.67	325.52	2.65	334.23
03/07/2011	2	340	2.96	317.52	2.28	325.01	2.75	321.11
04/07/2011	3	90	2.80	175.39	2.70	246.04	2.22	227.30
05/07/2011	2	270	3.21	196.76	4.13	208.80	2.59	220.56
06/07/2011	2	220	4.72	198.43	4.37	241.95	3.69	199.39
07/07/2011	3	180	4.50	206.11	4.72	207.20	4.69	207.65
08/07/2011	3	180	4.14	211.30	4.93	200.44	4.15	207.88
09/07/2011	2	180	3.29	205.47	4.53	195.38	3.23	210.83
10/07/2011	2	180	4.58	196.80	3.94	238.60	4.30	200.31
11/07/2011	2	180	4.53	201.42	4.27	210.78	3.77	208.55
12/07/2011	3	180	5.09	195.65	4.97	201.25	4.30	209.05
13/07/2011	3	180	3.98	187.55	4.21	198.95	3.28	204.07
14/07/2011	3	160	3.95	179.43	4.02	197.05	3.11	208.77
15/07/2011	3	140	3.22	172.35	2.90	182.45	3.20	198.47
16/07/2011	2	180	2.34	189.95	2.75	192.87	3.26	200.55
17/07/2011	2	160	4.00	189.85	3.37	196.96	2.62	220.91
18/07/2011	3	180	4.82	195.13	4.12	201.62	4.08	206.88
19/07/2011	3	180	4.51	194.35	3.78	199.17	3.38	212.54
20/07/2011	2	180	3.95	185.81	2.63	197.59	2.75	211.79
21/07/2011	2	140	3.59	186.02	3.21	202.26	2.57	207.15
22/07/2011	2	270	2.91	212.73	2.39	210.66	2.51	203.83
23/07/2011	2	270	2.92	208.94	3.32	195.44	3.57	221.94
24/07/2011	2	250	3.34	257.37	4.87	234.92	3.28	225.36
25/07/2011	2	270	4.38	266.34	6.30	238.42	4.10	245.56
26/07/2011	4	270	9.12	252.38	8.13	234.20	5.46	232.83
27/07/2011	2	250	8.31	208.24	6.56	216.49	4.89	216.41
28/07/2011	3	180	6.47	194.77	6.29	200.36	4.18	209.50
29/07/2011	3	180	3.40	210.78	5.02	200.04	4.22	205.34
30/07/2011	2	160	4.91	197.96	5.14	201.05	3.51	204.87
31/07/2011	3	180	4.04	202.09	4.73	230.15	3.80	205.47

Table 92. August 2011 wind data at Coron Island from onshore weather station and meoscale model output

Source Date	PAGASA		ERA-Interim		NCEP FNL		NCEP CFSR	
	Wind Speed (m/s)	Wind Direction (Degrees)	Wind Speed (m/s)	Wind Direction (Degrees)	Wind Speed (m/s)	Wind Direction (Degrees)	Wind Speed (m/s)	Wind Direction (Degrees)
01/08/2011	2	210	8.06	232.71	9.17	232.13	7.71	233.50
02/08/2011	2	220	6.64	246.92	8.67	239.70	6.97	239.09
03/08/2011	0	0	6.05	249.14	7.83	250.50	6.96	250.23
04/08/2011	0	0	5.97	257.44	7.95	253.52	7.41	251.06
05/08/2011	1	210	7.48	221.18	8.59	239.25	8.03	238.77
06/08/2011	0	0	6.94	206.58	8.68	229.20	7.27	231.43
07/08/2011	1	180	6.38	198.40	6.52	222.80	6.01	223.93
08/08/2011	1	0	4.65	195.46	7.59	225.04	5.04	232.14
09/08/2011	1	0	4.09	200.22	6.49	211.85	4.92	239.10
10/08/2011	0	0	2.71	159.37	5.08	208.80	4.84	256.58
11/08/2011	0	0	1.81	84.10	1.65	290.98	4.90	267.50
12/08/2011	1	40	1.77	221.28	2.36	264.50	3.33	285.03
13/08/2011	2	40	3.68	100.35	2.90	261.34	4.71	305.83
14/08/2011	1	40	2.25	121.19	3.80	170.54	3.13	191.97
15/08/2011	1	120	2.05	330.15	4.17	171.79	3.07	288.66
16/08/2011	0	0	1.93	255.27	2.12	340.26	3.62	276.06
17/08/2011	0	0	1.60	331.18	3.36	294.98	4.18	266.13
18/08/2011	1	180	1.92	324.78	3.90	278.13	3.15	243.26
19/08/2011	1	140	1.77	318.21	4.48	233.91	4.42	235.55
20/08/2011	2	0	2.53	231.56	3.42	234.61	2.61	253.39
21/08/2011	1	0	3.09	209.86	4.50	247.40	3.34	263.30
22/08/2011	1	180	3.80	200.64	6.01	230.41	4.76	247.96
23/08/2011	0	0	5.05	215.00	7.33	234.93	5.04	257.29
24/08/2011	0	0	6.42	253.27	10.85	225.95	5.71	252.84
25/08/2011	1	210	4.83	273.20	9.29	265.29	5.49	251.63
26/08/2011	1	210	6.98	236.73	8.51	241.12	6.29	236.88
27/08/2011	3	210	6.95	222.52	9.48	221.98	8.29	229.90
28/08/2011	1	180	7.26	213.13	7.33	213.15	6.60	222.53
29/08/2011	2	180	5.83	208.24	6.45	228.01	5.47	225.28
30/08/2011	1	180	6.46	224.52	6.72	231.02	6.05	230.61
31/08/2011	4	210	7.13	218.69	8.15	230.78	7.51	230.32

Table 93. August 2011 wind data at Cuyo Island from onshore weather station and meoscale model output

Source Date	PAGASA		ERA-Interim		NCEP FNL		NCEP CFSR	
	Wind Speed (m/s)	Wind Direction (Degrees)	Wind Speed (m/s)	Wind Direction (Degrees)	Wind Speed (m/s)	Wind Direction (Degrees)	Wind Speed (m/s)	Wind Direction (Degrees)
01/08/2011	3	220	8.97	215.78	9.91	220.29	8.49	221.53
02/08/2011	2	220	7.70	228.01	9.37	228.72	7.82	226.11
03/08/2011	2	220	7.15	230.45	9.43	239.56	7.70	242.52
04/08/2011	2	220	7.28	236.21	9.32	245.81	8.68	243.36
05/08/2011	2	220	8.36	215.00	9.37	229.69	8.90	231.48
06/08/2011	1	220	8.50	207.22	10.08	220.89	9.73	222.28
07/08/2011	1	220	6.53	202.14	7.77	216.60	7.04	217.56
08/08/2011	1	220	5.19	203.46	8.36	214.43	5.19	232.30
09/08/2011	1	220	4.53	213.68	7.62	208.96	4.99	247.35
10/08/2011	0	0	3.57	223.56	6.58	204.97	5.59	256.29
11/08/2011	1	320	2.13	267.64	3.91	281.20	5.49	263.16
12/08/2011	1	20	2.08	325.36	3.81	270.28	4.09	296.29
13/08/2011	0	0	3.16	243.65	3.90	266.11	4.29	313.79
14/08/2011	1	220	2.73	168.76	3.90	179.86	4.19	207.31
15/08/2011	1	320	1.45	253.99	3.08	140.24	4.52	237.13
16/08/2011	1	20	2.34	286.83	2.37	233.63	3.80	262.08
17/08/2011	1	20	2.95	308.15	3.51	288.40	4.39	254.23
18/08/2011	1	220	4.07	267.14	7.04	253.33	4.77	223.95
19/08/2011	1	220	4.27	252.98	5.00	230.99	4.05	220.23
20/08/2011	2	220	5.59	229.46	6.07	244.13	3.16	242.22
21/08/2011	2	220	6.43	216.50	7.14	237.13	5.97	253.09
22/08/2011	3	220	6.30	214.71	9.33	234.10	8.04	234.27
23/08/2011	2	220	6.96	218.04	9.47	226.86	7.81	237.09
24/08/2011	2	220	8.98	242.16	11.91	227.37	7.65	248.07
25/08/2011	3	220	8.45	238.00	14.76	246.33	9.78	230.13
26/08/2011	4	220	8.94	230.87	12.25	228.76	10.01	216.26
27/08/2011	4	220	8.01	211.92	10.69	210.32	8.81	216.67
28/08/2011	4	220	7.12	202.12	8.57	210.98	7.90	209.64
29/08/2011	3	220	6.58	208.44	6.68	220.37	6.34	214.72
30/08/2011	2	220	6.51	215.48	6.89	227.10	5.89	224.80
31/08/2011	2	220	8.16	217.27	9.03	228.33	8.06	225.11

Table 94. August 2011 wind data at Puerto Princesa from onshore weather station and meoscale model output

Source Date	PAGASA		ERA-Interim		NCEP FNL		NCEP CFSR	
	Wind Speed (m/s)	Wind Direction (Degrees)	Wind Speed (m/s)	Wind Direction (Degrees)	Wind Speed (m/s)	Wind Direction (Degrees)	Wind Speed (m/s)	Wind Direction (Degrees)
01/08/2011	3	180	5.31	190.61	4.57	199.82	3.71	205.38
02/08/2011	2	180	4.32	188.43	3.17	200.85	3.97	197.89
03/08/2011	3	270	4.09	184.45	3.42	234.24	3.23	211.71
04/08/2011	3	270	3.70	234.78	4.61	246.11	3.32	221.89
05/08/2011	3	180	6.03	189.61	4.11	234.97	3.61	204.09
06/08/2011	3	180	5.11	191.94	5.07	198.62	4.50	199.77
07/08/2011	3	160	4.73	189.85	3.90	194.74	3.92	197.81
08/08/2011	3	160	4.41	182.59	4.61	193.77	3.44	197.09
09/08/2011	3	140	3.83	173.78	4.24	199.89	3.66	198.25
10/08/2011	3	180	3.73	181.19	3.66	197.05	2.77	210.17
11/08/2011	3	350	3.18	167.73	2.64	180.87	1.85	210.06
12/08/2011	3	340	3.21	169.31	2.06	127.07	2.06	191.57
13/08/2011	2	140	3.32	179.06	1.26	266.83	1.66	188.40
14/08/2011	2	140	3.88	175.06	2.72	184.09	3.07	203.86
15/08/2011	3	160	3.38	165.10	3.12	203.87	3.04	196.67
16/08/2011	2	180	2.52	182.14	2.35	205.34	1.49	202.58
17/08/2011	2	270	2.58	161.24	2.33	267.38	1.61	60.87
18/08/2011	3	180	2.51	166.83	1.85	244.85	1.92	203.19
19/08/2011	3	140	2.85	159.75	2.72	194.32	2.60	212.48
20/08/2011	2	180	2.63	186.07	2.92	192.26	2.22	209.75
21/08/2011	3	180	3.33	198.96	2.89	201.10	2.73	217.30
22/08/2011	3	180	3.04	209.90	3.85	204.71	3.16	217.70
23/08/2011	3	180	3.92	193.65	4.47	202.71	3.56	199.62
24/08/2011	2	140	3.96	226.59	5.25	237.19	3.30	202.25
25/08/2011	3	270	3.59	218.78	5.16	246.51	3.60	206.99
26/08/2011	3	220	4.26	188.46	5.31	211.45	4.57	200.48
27/08/2011	3	180	4.63	199.00	4.13	202.85	3.73	211.36
28/08/2011	3	180	4.48	191.45	4.41	198.18	3.98	200.16
29/08/2011	3	180	4.42	190.16	3.18	195.06	3.74	199.48
30/08/2011	3	270	4.15	188.52	3.57	190.22	3.55	190.91
31/08/2011	4	180	5.81	193.04	3.31	202.71	3.78	202.38

Table 95. September 2011 wind data at Coron Island from onshore weather station and meoscale model output

Source Date	PAGASA		ERA-Interim		NCEP FNL		NCEP CFSR	
	Wind Speed (m/s)	Wind Direction (Degrees)	Wind Speed (m/s)	Wind Direction (Degrees)	Wind Speed (m/s)	Wind Direction (Degrees)	Wind Speed (m/s)	Wind Direction (Degrees)
01/09/2011	2	210	6.50	219.22	7.39	227.00	6.62	234.32
02/09/2011	2	210	5.80	225.01	6.73	234.13	6.03	231.87
03/09/2011	2	220	5.08	223.85	6.08	244.61	5.38	235.03
04/09/2011	1	320	5.84	243.15	8.30	251.48	6.44	240.61
05/09/2011	1	320	5.27	253.16	8.43	250.88	7.44	241.12
06/09/2011	1	210	5.61	229.56	8.01	245.90	6.82	236.98
07/09/2011	1	0	5.43	222.67	9.31	245.11	7.11	226.03
08/09/2011	1	180	4.99	206.50	10.90	224.36	6.50	213.52
09/09/2011	1	220	4.50	197.81	8.26	184.22	5.89	200.81
10/09/2011	0	0	4.15	185.79	5.90	163.75	4.85	208.57
11/09/2011	1	220	2.98	207.06	4.92	188.63	3.23	242.90
12/09/2011	1	0	2.04	296.35	4.46	247.03	3.49	256.05
13/09/2011	1	320	5.01	255.65	7.94	248.16	6.62	252.89
14/09/2011	1	210	5.73	235.77	8.43	242.04	6.39	253.43
15/09/2011	1	210	4.70	211.34	6.11	234.34	5.24	219.04
16/09/2011	1	220	4.21	203.64	6.08	210.82	4.97	208.22
17/09/2011	2	220	3.90	204.39	5.72	222.60	5.07	224.73
18/09/2011	1	220	5.51	200.34	6.26	217.34	5.54	228.67
19/09/2011	1	0	4.54	203.80	7.07	208.07	4.88	210.63
20/09/2011	1	220	4.24	217.18	7.39	224.30	5.36	230.00
21/09/2011	0	0	4.74	198.19	8.89	222.67	6.45	230.78
22/09/2011	1	220	6.15	209.76	9.98	223.70	7.32	227.17
23/09/2011	3	220	6.36	202.71	9.65	224.07	7.89	229.04
24/09/2011	1	220	5.48	197.31	9.03	211.36	6.96	228.27
25/09/2011	1	210	4.99	226.26	6.24	213.54	7.90	241.15
26/09/2011	5	210	10.37	243.90	9.10	232.73	11.54	240.84
27/09/2011	6	210	13.43	223.61	12.38	228.27	13.98	214.24
28/09/2011	5	180	9.59	193.11	11.25	211.59	9.47	204.88
29/09/2011	1	180	4.41	187.53	6.35	201.03	4.69	190.16
30/09/2011	1	320	2.97	262.08	4.64	249.28	3.46	255.43

Table 96. September 2011 wind data at Cuyo Island from onshore weather station and meoscale model output

Source Date	PAGASA		ERA-Interim		NCEP FNL		NCEP CFSR	
	Wind Speed (m/s)	Wind Direction (Degrees)	Wind Speed (m/s)	Wind Direction (Degrees)	Wind Speed (m/s)	Wind Direction (Degrees)	Wind Speed (m/s)	Wind Direction (Degrees)
01/09/2011	1	220	7.04	214.03	8.11	225.54	7.16	232.12
02/09/2011	2	220	6.65	211.01	6.64	229.86	5.32	227.80
03/09/2011	2	220	6.59	225.27	6.85	235.57	5.67	235.45
04/09/2011	1	220	7.57	235.57	9.14	245.98	7.04	240.41
05/09/2011	1	220	6.90	236.82	10.10	249.96	7.98	233.98
06/09/2011	2	220	6.75	223.73	9.82	233.68	7.74	227.20
07/09/2011	1	220	7.04	215.20	11.33	237.20	8.34	220.76
08/09/2011	1	220	6.92	207.08	10.80	222.30	7.70	211.01
09/09/2011	1	220	4.43	201.67	9.31	176.63	6.39	201.79
10/09/2011	1	220	4.50	186.16	6.37	172.97	6.10	213.66
11/09/2011	1	220	3.50	210.36	5.55	192.57	4.74	230.32
12/09/2011	1	20	3.45	268.93	5.39	235.57	4.12	255.88
13/09/2011	1	320	6.19	238.40	8.34	237.62	7.68	236.41
14/09/2011	4	220	7.34	223.04	8.98	228.08	8.45	225.08
15/09/2011	2	220	6.52	209.25	7.42	219.08	6.75	212.59
16/09/2011	1	220	5.59	204.06	7.55	207.07	5.88	208.45
17/09/2011	2	220	5.43	213.92	7.19	214.94	6.70	218.08
18/09/2011	2	220	6.74	204.03	8.68	213.81	6.89	223.87
19/09/2011	1	220	5.87	213.19	8.32	201.13	5.79	219.72
20/09/2011	0	0	4.34	212.84	8.66	209.77	5.69	227.30
21/09/2011	1	220	5.19	216.25	10.08	217.51	6.40	226.03
22/09/2011	1	220	6.43	211.36	12.19	221.85	8.06	230.14
23/09/2011	1	220	6.99	208.21	11.78	220.18	8.44	225.38
24/09/2011	1	220	6.14	204.52	9.63	208.25	7.29	227.65
25/09/2011	1	220	6.69	225.94	7.68	220.15	9.21	238.50
26/09/2011	3	220	12.21	229.37	11.09	227.56	13.66	229.77
27/09/2011	5	220	14.16	210.18	13.47	216.74	13.37	203.41
28/09/2011	3	220	9.77	183.96	10.76	202.55	8.56	194.62
29/09/2011	1	250	5.14	197.78	5.99	196.69	4.04	198.77
30/09/2011	1	220	4.25	257.45	5.81	240.82	5.11	246.76

Table 97. September 2011 wind data at Puerto Princesa from onshore weather station and meoscale model output

Source Date	PAGASA		ERA-Interim		NCEP FNL		NCEP CFSR	
	Wind Speed (m/s)	Wind Direction (Degrees)	Wind Speed (m/s)	Wind Direction (Degrees)	Wind Speed (m/s)	Wind Direction (Degrees)	Wind Speed (m/s)	Wind Direction (Degrees)
01/09/2011	3	180	4.46	189.29	4.48	201.49	3.41	210.52
02/09/2011	3	180	4.48	184.26	3.19	226.67	2.60	213.55
03/09/2011	3	160	4.61	183.16	3.02	209.91	3.66	194.54
04/09/2011	2	270	4.02	197.71	3.73	251.67	3.26	202.06
05/09/2011	3	270	3.82	203.54	3.41	242.07	3.05	206.61
06/09/2011	3	270	3.69	203.70	3.48	234.13	3.03	201.47
07/09/2011	3	270	5.22	192.02	3.67	235.48	4.20	199.76
08/09/2011	2	270	5.51	186.79	4.07	214.23	4.26	200.24
09/09/2011	2	270	3.32	211.83	5.92	185.49	3.58	206.53
10/09/2011	2	180	4.60	186.22	4.86	187.71	3.75	209.81
11/09/2011	2	180	3.96	186.95	3.55	202.98	2.86	197.20
12/09/2011	3	90	2.99	166.19	2.53	179.80	1.98	176.24
13/09/2011	2	270	3.59	181.78	3.24	191.36	2.11	177.67
14/09/2011	3	270	4.52	194.94	3.48	200.91	3.10	201.94
15/09/2011	3	180	3.83	183.07	3.23	192.72	3.52	193.75
16/09/2011	3	180	3.95	195.73	3.58	203.50	2.79	206.34
17/09/2011	3	180	3.82	215.04	4.42	201.85	2.42	199.77
18/09/2011	3	180	3.84	198.96	4.11	203.15	2.62	219.32
19/09/2011	3	270	3.38	194.53	3.83	203.11	3.49	198.87
20/09/2011	2	160	3.95	183.26	3.94	200.43	2.94	198.51
21/09/2011	2	270	3.88	190.74	4.43	195.49	3.02	196.13
22/09/2011	4	270	5.12	194.57	5.54	226.10	3.87	212.32
23/09/2011	1	250	5.03	193.41	5.09	204.14	3.88	205.65
24/09/2011	3	180	3.67	190.23	6.13	201.16	3.93	192.65
25/09/2011	2	180	5.08	192.00	5.00	198.70	3.89	194.15
26/09/2011	3	270	4.87	195.18	5.52	199.79	4.29	203.19
27/09/2011	3	220	6.81	200.43	6.72	209.91	5.09	200.89
28/09/2011	3	220	6.27	200.92	5.94	212.62	3.76	206.03
29/09/2011	3	180	4.45	192.51	4.07	196.42	4.12	199.89
30/09/2011	3	140	3.41	174.70	3.35	191.20	3.11	180.44

Table 98. October 2011 wind data at Coron Island from onshore weather station and meoscale model output

Source Date	PAGASA		ERA-Interim		NCEP FNL		NCEP CFSR	
	Wind Speed (m/s)	Wind Direction (Degrees)	Wind Speed (m/s)	Wind Direction (Degrees)	Wind Speed (m/s)	Wind Direction (Degrees)	Wind Speed (m/s)	Wind Direction (Degrees)
01/10/2011	2	220	8.40	253.23	9.28	235.26	8.01	252.45
02/10/2011	2	220	9.07	223.06	9.99	218.27	9.37	224.50
03/10/2011	2	180	7.12	192.68	8.39	201.18	7.00	209.48
04/10/2011	0	0	4.11	187.57	7.35	194.44	4.76	202.63
05/10/2011	1	210	2.62	219.33	5.92	199.76	4.17	244.37
06/10/2011	1	320	2.32	328.60	3.21	273.97	4.35	297.01
07/10/2011	1	220	6.31	267.94	8.29	239.47	5.12	291.05
08/10/2011	1	270	9.04	208.30	10.57	194.54	4.34	270.38
09/10/2011	1	0	5.92	186.81	7.42	170.20	4.17	240.72
10/10/2011	1	220	2.88	172.63	4.47	167.29	4.57	260.33
11/10/2011	1	210	2.14	309.27	3.80	303.45	3.21	301.94
12/10/2011	1	320	7.56	319.17	11.83	309.49	7.43	271.05
13/10/2011	2	210	10.32	258.77	12.69	220.69	5.48	242.77
14/10/2011	1	210	4.47	203.28	7.83	198.59	3.48	227.73
15/10/2011	1	0	2.75	187.36	4.64	208.93	2.22	278.02
16/10/2011	1	0	2.58	76.69	3.32	137.88	1.67	95.33
17/10/2011	1	0	2.72	75.59	2.77	66.43	2.83	60.55
18/10/2011	1	120	3.06	70.83	3.72	98.80	3.35	82.19
19/10/2011	1	120	3.22	71.42	2.87	119.99	5.64	92.09
20/10/2011	1	0	3.15	69.60	2.04	243.56	2.67	32.58
21/10/2011	1	0	1.58	66.76	4.46	213.87	1.93	333.10
22/10/2011	0	0	2.30	48.09	2.90	142.69	1.64	41.49
23/10/2011	1	40	2.92	75.13	3.09	85.22	1.91	357.34
24/10/2011	2	120	2.02	65.72	2.16	86.49	3.54	91.18
25/10/2011	1	0	2.70	76.28	2.17	273.10	2.96	95.76
26/10/2011	1	0	2.12	66.57	1.78	348.90	2.22	61.15
27/10/2011	1	0	1.78	342.83	2.37	285.26	2.53	66.28
28/10/2011	1	0	2.35	320.75	3.87	353.40	2.81	353.09
29/10/2011	1	180	2.12	15.36	2.21	259.43	2.14	253.00
30/10/2011	1	180	4.74	86.73	4.10	93.69	4.65	83.55
31/10/2011	1	0	1.67	293.78	3.37	54.33	1.97	311.96

Table 99. October 2011 wind data at Cuyo Island from onshore weather station and meoscale model output

Source Date	PAGASA		ERA-Interim		NCEP FNL		NCEP CFSR	
	Wind Speed (m/s)	Wind Direction (Degrees)	Wind Speed (m/s)	Wind Direction (Degrees)	Wind Speed (m/s)	Wind Direction (Degrees)	Wind Speed (m/s)	Wind Direction (Degrees)
01/10/2011	2	320	9.42	243.58	9.65	228.04	8.82	244.11
02/10/2011	3	220	10.93	211.03	11.87	213.73	10.80	215.89
03/10/2011	4	220	7.32	190.18	8.80	197.89	7.95	202.59
04/10/2011	2	250	4.60	193.54	7.34	189.81	4.97	198.99
05/10/2011	1	320	3.11	259.68	5.63	204.83	5.15	253.21
06/10/2011	1	320	5.26	322.56	5.34	306.13	8.23	306.00
07/10/2011	1	320	9.14	268.29	9.23	250.47	10.67	285.61
08/10/2011	0	0	8.31	216.19	10.18	197.60	6.01	261.83
09/10/2011	1	220	6.22	181.77	7.00	170.58	6.46	236.00
10/10/2011	1	220	2.29	200.26	3.91	162.43	5.00	250.45
11/10/2011	1	220	5.06	342.47	7.18	323.03	6.44	315.05
12/10/2011	3	320	11.63	279.57	17.66	296.28	10.38	280.21
13/10/2011	1	220	10.94	241.20	10.70	214.21	5.61	246.75
14/10/2011	1	220	5.02	208.93	8.39	197.32	5.67	232.52
15/10/2011	1	220	1.98	168.68	4.60	202.35	2.52	235.16
16/10/2011	1	220	2.43	68.44	2.62	113.55	1.82	141.45
17/10/2011	1	20	4.75	35.24	4.48	27.27	3.29	13.39
18/10/2011	2	20	7.26	39.26	3.85	37.42	3.84	38.37
19/10/2011	1	20	5.94	43.03	1.96	0.71	3.42	47.96
20/10/2011	2	20	4.95	34.03	1.89	266.69	3.01	9.34
21/10/2011	1	320	3.22	18.42	3.73	211.61	2.96	326.53
22/10/2011	1	20	3.40	13.81	2.47	135.72	3.93	359.71
23/10/2011	1	20	4.66	33.46	2.05	140.13	3.22	38.29
24/10/2011	1	120	6.45	38.18	3.72	36.96	1.99	46.09
25/10/2011	4	20	7.66	39.61	6.18	34.39	5.00	23.13
26/10/2011	4	20	8.08	38.16	7.13	39.23	6.44	44.71
27/10/2011	4	20	8.04	33.95	5.03	33.14	5.48	37.48
28/10/2011	5	20	8.83	25.60	6.32	25.31	8.54	32.24
29/10/2011	4	20	6.25	37.29	4.46	45.93	3.13	66.70
30/10/2011	4	20	4.98	45.85	4.09	40.82	4.99	45.33
31/10/2011	4	20	8.41	28.95	7.62	29.46	7.31	26.84

Table 100. October 2011 wind data at Puerto Princesa from onshore weather station and meoscale model output

Source Date	PAGASA		ERA-Interim		NCEP FNL		NCEP CFSR	
	Wind Speed (m/s)	Wind Direction (Degrees)	Wind Speed (m/s)	Wind Direction (Degrees)	Wind Speed (m/s)	Wind Direction (Degrees)	Wind Speed (m/s)	Wind Direction (Degrees)
01/10/2011	3	270	4.42	244.59	4.29	236.30	3.26	234.65
02/10/2011	3	180	6.25	196.25	6.41	204.30	4.67	201.78
03/10/2011	2	270	4.69	194.07	5.67	196.95	4.50	200.56
04/10/2011	2	180	2.92	202.88	4.53	196.34	3.83	204.06
05/10/2011	3	180	2.94	178.76	3.67	197.00	2.87	187.70
06/10/2011	3	180	2.44	142.26	1.91	159.63	1.29	7.24
07/10/2011	2	270	3.38	189.98	3.24	241.12	1.97	248.94
08/10/2011	2	270	4.71	236.60	4.82	212.51	2.60	202.48
09/10/2011	1	270	4.18	198.29	4.68	195.66	3.45	202.34
10/10/2011	2	270	3.11	194.01	2.67	204.53	2.36	236.44
11/10/2011	2	90	2.33	4.42	2.20	151.62	2.22	358.06
12/10/2011	3	0	3.74	331.55	5.05	276.28	2.39	323.99
13/10/2011	2	290	2.84	242.29	5.54	234.36	3.46	230.75
14/10/2011	3	90	3.68	189.95	4.48	200.56	3.64	196.05
15/10/2011	2	270	3.04	199.21	3.75	197.11	2.82	206.74
16/10/2011	3	110	3.04	192.25	2.49	187.80	2.05	190.65
17/10/2011	3	110	2.71	136.15	1.85	133.81	1.98	157.15
18/10/2011	4	90	2.68	83.83	2.65	96.38	2.15	60.58
19/10/2011	3	90	3.37	84.55	2.63	194.79	2.39	167.21
20/10/2011	3	90	2.51	131.90	2.25	183.32	2.35	200.94
21/10/2011	3	90	2.85	64.99	2.54	206.92	1.94	176.38
22/10/2011	3	90	2.56	73.05	3.43	195.89	1.86	210.21
23/10/2011	2	90	2.34	110.66	1.93	150.75	2.11	182.89
24/10/2011	2	270	2.74	84.62	1.23	237.34	2.44	189.64
25/10/2011	3	90	3.80	76.40	1.83	162.05	2.03	144.80
26/10/2011	5	90	3.48	82.10	2.60	67.21	2.89	66.12
27/10/2011	5	90	3.55	67.16	2.85	81.43	2.09	91.89
28/10/2011	4	90	3.76	51.87	1.69	5.04	3.70	47.01
29/10/2011	4	90	3.28	3.64	2.34	103.50	3.29	130.93
30/10/2011	3	270	3.82	75.24	1.99	86.38	1.91	90.11
31/10/2011	3	90	3.40	53.22	2.52	56.75	3.08	40.18

Table 101. November 2011 wind data at Coron Island from onshore weather station and meoscale model output

Source Date	PAGASA		ERA-Interim		NCEP FNL		NCEP CFSR	
	Wind Speed (m/s)	Wind Direction (Degrees)	Wind Speed (m/s)	Wind Direction (Degrees)	Wind Speed (m/s)	Wind Direction (Degrees)	Wind Speed (m/s)	Wind Direction (Degrees)
01/11/2011	1	0	2.55	49.35	3.38	356.81	2.75	333.27
02/11/2011	1	140	5.66	92.37	6.37	65.29	4.41	92.92
03/11/2011	2	40	4.89	117.29	9.76	90.62	5.18	108.57
04/11/2011	2	40	2.73	137.99	5.15	80.29	3.70	117.78
05/11/2011	2	210	2.44	177.23	3.11	308.71	3.67	235.11
06/11/2011	2	210	4.50	192.75	8.22	202.14	5.57	208.64
07/11/2011	1	210	4.49	177.46	5.88	185.64	5.49	197.90
08/11/2011	1	0	2.64	165.74	5.52	176.36	4.35	203.15
09/11/2011	1	210	2.80	174.88	5.79	205.60	4.72	209.37
10/11/2011	1	210	3.95	193.50	5.54	211.15	4.78	203.02
11/11/2011	1	180	2.13	158.21	3.53	171.46	3.48	178.62
12/11/2011	1	40	5.15	79.76	6.70	82.70	5.50	83.60
13/11/2011	1	0	4.05	61.68	4.25	40.72	4.05	41.24
14/11/2011	1	0	2.86	49.45	5.80	56.91	3.44	54.44
15/11/2011	1	0	9.74	200.92	7.44	111.66	3.90	27.00
16/11/2011	2	140	5.49	139.73	6.59	149.32	4.98	146.91
17/11/2011	1	140	5.69	92.38	5.36	92.62	4.89	119.11
18/11/2011	1	0	7.83	83.06	6.55	80.28	5.89	83.44
19/11/2011	1	180	4.51	74.54	6.03	74.17	5.20	64.68
20/11/2011	2	120	7.24	75.87	8.61	77.49	7.37	74.97
21/11/2011	3	40	6.50	63.69	7.03	58.09	5.98	52.85
22/11/2011	3	40	8.22	66.50	9.08	72.58	7.23	66.56
23/11/2011	2	40	6.68	73.12	7.16	70.92	6.70	76.09
24/11/2011	2	40	6.59	72.54	5.14	60.39	5.16	65.25
25/11/2011	4	40	9.68	78.66	10.31	77.80	9.63	80.48
26/11/2011	2	40	5.20	65.04	5.14	37.55	5.03	37.95
27/11/2011	2	320	3.22	74.79	4.35	82.55	3.61	95.30
28/11/2011	2	120	3.70	87.31	6.15	89.85	3.02	117.81
29/11/2011	1	120	4.17	88.03	3.01	90.80	2.37	103.04
30/11/2011	1	320	2.59	73.61	2.43	49.06	1.69	291.75

Table 102. November 2011 wind data at Cuyo Island from onshore weather station and meoscale model output

Source Date	PAGASA		ERA-Interim		NCEP FNL		NCEP CFSR	
	Wind Speed (m/s)	Wind Direction (Degrees)	Wind Speed (m/s)	Wind Direction (Degrees)	Wind Speed (m/s)	Wind Direction (Degrees)	Wind Speed (m/s)	Wind Direction (Degrees)
01/11/2011	3	20	8.19	24.49	9.57	19.85	6.82	13.91
02/11/2011	2	20	3.50	110.41	7.89	50.69	3.66	91.66
03/11/2011	1	20	4.23	168.85	7.24	117.73	3.06	162.60
04/11/2011	1	220	2.97	150.40	3.91	42.43	2.76	176.35
05/11/2011	0	0	3.21	223.74	4.84	235.41	5.53	225.54
06/11/2011	2	220	5.99	200.33	8.69	201.89	7.55	212.94
07/11/2011	1	220	3.67	172.94	6.63	179.48	4.97	212.69
08/11/2011	0	0	2.12	173.54	4.93	173.51	3.53	206.79
09/11/2011	1	220	1.72	203.77	5.20	196.09	4.00	222.66
10/11/2011	1	220	2.97	206.09	4.94	227.60	4.26	213.79
11/11/2011	0	0	1.32	3.82	2.50	178.08	2.06	206.32
12/11/2011	2	220	5.05	36.32	5.55	41.48	5.47	36.27
13/11/2011	3	220	8.94	34.62	10.36	34.26	9.02	38.25
14/11/2011	3	20	8.64	29.85	9.34	39.74	8.41	34.91
15/11/2011	2	20	9.23	233.56	7.63	138.69	5.48	337.37
16/11/2011	2	50	4.59	149.00	6.51	151.92	4.34	158.68
17/11/2011	1	0	4.55	64.07	4.08	42.85	2.82	142.99
18/11/2011	1	20	6.78	46.26	6.04	41.34	5.36	36.34
19/11/2011	2	20	7.77	41.89	4.40	38.00	6.96	36.86
20/11/2011	3	20	10.09	40.74	9.78	43.64	9.22	42.89
21/11/2011	2	20	11.21	43.06	11.68	39.46	11.13	39.90
22/11/2011	3	20	10.38	41.39	11.25	46.19	10.26	43.49
23/11/2011	3	20	9.43	43.69	9.85	44.22	9.29	44.49
24/11/2011	4	20	9.60	43.04	9.74	40.21	9.35	40.72
25/11/2011	4	20	11.41	47.75	10.90	45.54	10.38	46.67
26/11/2011	3	20	9.96	40.97	8.65	38.50	10.12	37.78
27/11/2011	3	20	6.60	39.54	3.71	35.96	5.03	40.66
28/11/2011	3	20	2.28	38.02	4.62	54.73	1.92	179.68
29/11/2011	2	20	4.34	37.61	2.69	44.91	3.08	14.59
30/11/2011	3	120	5.57	24.87	3.86	21.08	4.18	15.47

Table 103. November 2011 wind data at Puerto Princesa from onshore weather station and meoscale model output

Source Date	PAGASA		ERA-Interim		NCEP FNL		NCEP CFSR	
	Wind Speed (m/s)	Wind Direction (Degrees)	Wind Speed (m/s)	Wind Direction (Degrees)	Wind Speed (m/s)	Wind Direction (Degrees)	Wind Speed (m/s)	Wind Direction (Degrees)
01/11/2011	3	270	3.68	16.67	5.12	347.82	2.89	5.75
02/11/2011	2	90	2.44	20.24	3.93	351.28	2.06	312.16
03/11/2011	2	90	4.14	182.95	9.51	180.51	3.38	194.17
04/11/2011	2	270	4.22	179.73	5.36	155.67	3.26	203.41
05/11/2011	3	180	3.50	191.10	2.58	190.49	2.69	199.95
06/11/2011	3	180	3.84	199.96	4.07	206.53	3.15	210.93
07/11/2011	2	270	4.28	188.83	4.26	197.57	3.55	203.60
08/11/2011	2	270	3.74	186.39	3.30	203.25	3.69	202.91
09/11/2011	2	110	3.22	185.94	3.45	201.31	3.07	197.29
10/11/2011	2	270	3.35	182.51	3.15	201.71	3.21	197.56
11/11/2011	2	270	3.39	179.70	2.30	201.49	2.09	211.40
12/11/2011	2	270	2.80	112.78	2.12	84.04	1.75	94.09
13/11/2011	2	70	4.10	67.18	4.11	46.22	3.89	54.15
14/11/2011	3	90	4.48	59.42	4.04	47.06	4.01	56.40
15/11/2011	1	270	2.65	336.63	3.76	121.04	2.70	138.43
16/11/2011	2	270	5.14	175.58	5.67	183.96	3.71	174.51
17/11/2011	2	270	3.69	178.99	2.67	194.19	1.90	192.19
18/11/2011	2	270	3.01	77.41	1.49	34.47	1.77	52.97
19/11/2011	2	90	3.52	65.61	2.77	78.27	2.70	65.10
20/11/2011	3	90	5.98	63.96	5.28	71.92	4.86	62.03
21/11/2011	6	90	6.37	60.53	5.62	55.00	5.18	53.00
22/11/2011	4	90	7.44	60.21	6.98	60.90	5.83	61.64
23/11/2011	5	90	6.17	66.84	5.71	62.14	5.27	63.53
24/11/2011	6	90	5.68	67.58	5.21	65.36	4.47	62.52
25/11/2011	6	90	6.68	70.34	6.42	66.90	6.12	65.82
26/11/2011	4	90	5.32	66.22	4.78	57.91	4.51	60.41
27/11/2011	4	90	2.84	69.80	2.05	223.89	3.05	84.18
28/11/2011	3	90	2.64	141.16	2.06	200.18	2.93	216.21
29/11/2011	3	90	2.74	111.97	1.93	98.80	2.48	192.53
30/11/2011	3	90	2.56	119.69	1.86	161.35	1.64	48.11

Table 104. December 2011 wind data at Coron Island from onshore weather station and meoscale model output

Source Date	PAGASA		ERA-Interim		NCEP FNL		NCEP CFSR	
	Wind Speed (m/s)	Wind Direction (Degrees)	Wind Speed (m/s)	Wind Direction (Degrees)	Wind Speed (m/s)	Wind Direction (Degrees)	Wind Speed (m/s)	Wind Direction (Degrees)
01/12/2011	1	0	2.98	86.12	2.73	87.52	3.33	92.62
02/12/2011	1	40	1.68	53.12	2.37	356.62	2.74	128.00
03/12/2011	1	120	3.15	88.70	2.21	240.18	3.70	96.98
04/12/2011	1	180	4.73	103.64	4.28	208.40	2.84	239.84
05/12/2011	2	40	4.03	86.47	5.62	93.67	4.10	72.20
06/12/2011	2	0	4.86	67.94	5.82	70.73	6.56	70.08
07/12/2011	3	0	6.90	67.49	8.91	74.83	8.34	73.43
08/12/2011	1	40	8.95	77.14	8.32	91.65	9.07	80.36
09/12/2011	1	40	7.82	97.28	9.79	139.62	6.34	112.26
10/12/2011	1	40	7.55	122.83	9.06	154.82	5.93	171.29
11/12/2011	1	120	6.19	101.98	6.50	125.47	4.24	157.01
12/12/2011	2	320	5.32	89.35	6.12	89.97	3.68	86.44
13/12/2011	2	40	4.04	83.32	5.10	70.38	4.76	65.08
14/12/2011	1	0	4.85	76.70	4.52	70.46	5.26	74.90
15/12/2011	3	0	5.32	71.71	7.28	69.73	6.21	67.99
16/12/2011	1	40	3.47	31.32	4.35	36.41	4.07	29.59
17/12/2011	2	40	8.98	57.80	9.91	64.69	8.51	66.37
18/12/2011	2	40	9.19	80.30	10.86	81.41	9.10	83.40
19/12/2011	2	40	8.39	86.15	9.30	84.79	8.95	85.62
20/12/2011	1	40	4.96	76.06	4.56	72.69	5.69	65.18
21/12/2011	1	0	6.83	79.51	7.11	83.90	7.67	83.25
22/12/2011	2	40	4.43	88.15	5.20	73.23	3.90	75.78
23/12/2011	2	0	2.68	111.48	3.04	350.00	2.62	5.78
24/12/2011	2	320	3.03	46.31	4.10	14.58	2.88	21.67
25/12/2011	1	180	9.89	69.11	8.65	70.41	10.11	73.54
26/12/2011	3	90	10.96	72.91	10.21	70.19	7.64	64.75
27/12/2011	3	40	9.14	69.61	8.19	72.09	8.81	75.85
28/12/2011	3	320	9.27	80.65	8.37	81.27	9.08	82.73
29/12/2011	2	40	9.25	83.26	8.61	82.36	7.96	83.06
30/12/2011	1	0	5.90	76.91	4.49	44.62	4.60	48.03
31/12/2011	1	120	3.49	81.28	3.21	35.75	3.19	34.63

Table 105. December 2011 wind data at Cuyo Island from onshore weather station and meoscale model output

Source Date	PAGASA		ERA-Interim		NCEP FNL		NCEP CFSR	
	Wind Speed (m/s)	Wind Direction (Degrees)	Wind Speed (m/s)	Wind Direction (Degrees)	Wind Speed (m/s)	Wind Direction (Degrees)	Wind Speed (m/s)	Wind Direction (Degrees)
01/12/2011	1	180	3.37	41.21	2.69	43.45	2.37	40.56
02/12/2011	1	20	2.51	56.38	1.20	330.80	1.38	165.62
03/12/2011	0	0	3.02	59.60	5.77	28.23	3.88	44.45
04/12/2011	1	20	4.32	67.88	6.64	325.44	3.73	56.02
05/12/2011	2	20	5.53	25.14	3.34	49.04	5.16	24.20
06/12/2011	4	20	8.94	41.05	7.07	40.80	7.99	40.49
07/12/2011	4	20	9.70	41.74	8.41	47.45	8.84	43.42
08/12/2011	2	20	7.54	57.09	7.27	96.43	6.46	88.64
09/12/2011	1	120	5.97	134.77	11.03	173.88	5.21	198.55
10/12/2011	1	220	7.81	146.93	8.98	158.20	7.20	187.25
11/12/2011	1	120	3.57	134.12	5.42	140.87	3.81	147.08
12/12/2011	2	20	3.83	36.15	3.00	82.58	2.99	30.27
13/12/2011	3	20	6.64	31.99	5.60	30.85	5.22	28.93
14/12/2011	2	20	8.41	39.10	8.07	38.62	7.16	41.15
15/12/2011	3	20	9.61	39.85	9.60	42.93	9.27	42.92
16/12/2011	4	20	12.08	33.41	13.65	32.96	13.27	34.73
17/12/2011	4	20	12.79	41.01	14.01	45.35	12.47	44.61
18/12/2011	4	20	8.46	50.79	9.21	49.03	8.45	48.38
19/12/2011	2	20	7.89	45.28	7.05	54.43	6.79	51.55
20/12/2011	3	20	8.59	40.60	7.89	39.56	8.57	40.31
21/12/2011	2	20	6.60	42.63	4.10	43.38	5.92	45.56
22/12/2011	3	20	7.60	37.04	6.03	37.70	7.37	33.85
23/12/2011	4	20	9.69	35.32	9.78	32.10	10.23	34.08
24/12/2011	4	20	10.89	38.15	9.83	34.61	9.73	36.40
25/12/2011	4	20	12.40	43.58	13.06	42.61	13.24	43.16
26/12/2011	6	20	14.60	43.64	14.35	41.61	14.57	44.35
27/12/2011	5	20	12.68	48.33	11.18	44.17	12.01	48.56
28/12/2011	3	20	8.14	49.87	7.47	47.60	7.94	47.28
29/12/2011	3	20	7.74	48.79	6.96	45.11	8.40	46.24
30/12/2011	4	20	9.65	42.64	10.90	37.12	10.38	39.34
31/12/2011	4	20	10.10	37.99	10.88	38.08	11.07	37.86

Table 106. December 2011 wind data at Puerto Princesa from onshore weather station and meoscale model output

Source Date	PAGASA		ERA-Interim		NCEP FNL		NCEP CFSR	
	Wind Speed (m/s)	Wind Direction (Degrees)	Wind Speed (m/s)	Wind Direction (Degrees)	Wind Speed (m/s)	Wind Direction (Degrees)	Wind Speed (m/s)	Wind Direction (Degrees)
01/12/2011	3	270	2.71	88.07	1.63	105.17	2.12	197.29
02/12/2011	3	140	2.79	159.82	1.78	269.41	2.63	189.10
03/12/2011	2	180	3.93	103.50	2.84	148.50	2.61	142.99
04/12/2011	2	180	3.42	127.64	2.73	210.26	2.56	185.38
05/12/2011	3	90	2.82	169.16	2.33	204.46	1.77	99.01
06/12/2011	3	90	2.88	5.16	2.77	356.67	2.47	334.03
07/12/2011	3	270	4.76	52.21	4.44	59.09	3.64	37.78
08/12/2011	2	270	3.87	47.54	4.91	113.74	4.21	12.74
09/12/2011	2	90	7.27	168.75	8.49	205.65	2.96	201.02
10/12/2011	2	180	8.85	181.58	8.70	186.08	4.65	203.22
11/12/2011	2	180	6.89	149.53	7.94	161.92	4.45	169.01
12/12/2011	2	270	3.06	129.98	3.34	138.04	3.47	170.90
13/12/2011	2	90	2.75	101.03	2.60	83.03	1.86	69.94
14/12/2011	3	270	3.28	57.40	2.24	35.61	2.36	42.97
15/12/2011	4	90	3.74	60.23	4.38	53.73	3.81	54.06
16/12/2011	4	20	3.90	26.43	5.22	45.34	4.51	44.41
17/12/2011	4	40	8.40	60.23	6.75	12.62	7.37	27.51
18/12/2011	6	90	7.32	84.57	7.15	94.48	7.28	82.99
19/12/2011	4	90	4.66	85.37	4.49	86.63	4.90	85.64
20/12/2011	4	90	2.97	83.69	2.82	82.25	3.69	65.50
21/12/2011	3	90	3.34	73.41	2.73	72.25	3.76	72.10
22/12/2011	3	90	3.24	60.90	2.80	73.94	2.98	68.37
23/12/2011	4	290	4.27	41.26	3.59	23.57	3.39	33.31
24/12/2011	4	0	6.59	64.16	4.03	37.02	4.37	52.85
25/12/2011	7	70	8.66	61.11	8.07	59.61	8.12	57.46
26/12/2011	7	90	8.63	55.02	8.16	55.93	8.15	55.15
27/12/2011	7	70	9.39	60.55	4.72	41.82	8.12	58.94
28/12/2011	4	90	6.27	75.33	4.39	73.57	5.37	80.80
29/12/2011	4	90	3.30	91.18	3.02	85.14	3.23	80.52
30/12/2011	4	90	4.52	71.49	4.08	53.47	4.11	50.27
31/12/2011	3	90	5.21	61.80	4.42	40.54	4.65	48.19

Table 107. January 2012 wind data at Coron Island from onshore weather station and meoscale model output

Date	PAGASA		ERA-Interim		NCEP FNL		NCEP CFSR	
	Wind Speed (m/s)	Wind Direction (Degrees)	Wind Speed (m/s)	Wind Direction (Degrees)	Wind Speed (m/s)	Wind Direction (Degrees)	Wind Speed (m/s)	Wind Direction (Degrees)
01/01/2012	1	0	3.48	87.35	2.81	6.60	3.70	38.23
02/01/2012	1	0	4.55	89.80	1.89	237.68	2.25	28.74
03/01/2012	1	0	5.02	78.61	3.70	83.92	3.62	81.62
04/01/2012	2	0	6.73	80.49	8.45	77.06	7.72	77.92
05/01/2012	2	40	9.42	77.49	6.72	69.93	9.06	73.95
06/01/2012	1	90	6.96	71.53	4.45	59.89	5.47	61.89
07/01/2012	2	40	5.14	65.35	4.77	41.34	5.83	55.90
08/01/2012	2	40	8.51	67.83	6.46	63.04	7.97	68.05
09/01/2012	2	40	8.45	73.15	7.52	66.59	8.16	68.31
10/01/2012	2	40	8.99	68.67	8.72	73.64	9.24	73.88
11/01/2012	2	40	9.94	79.25	8.53	70.73	10.41	77.54
12/01/2012	2	40	10.23	76.55	10.43	75.71	9.60	76.15
13/01/2012	2	40	9.04	81.91	8.91	78.86	10.26	80.39
14/01/2012	4	40	9.40	84.41	8.63	83.24	9.04	82.92
15/01/2012	1	90	4.23	84.21	4.56	37.90	3.50	51.07
16/01/2012	1	0	4.04	87.61	5.26	25.20	4.28	63.04
17/01/2012	1	90	5.75	87.90	9.37	68.96	4.56	88.99
18/01/2012	1	120	4.03	84.55	7.60	95.38	7.66	86.48
19/01/2012	1	40	3.34	84.67	4.89	55.56	5.42	89.85
20/01/2012	1	0	2.05	197.65	3.57	354.38	4.09	51.22
21/01/2012	1	0	3.90	88.83	4.17	77.31	3.96	48.73
22/01/2012	1	0	5.07	90.92	4.15	77.39	6.50	83.43
23/01/2012	1	0	5.11	80.59	5.90	72.21	6.83	76.39
24/01/2012	1	0	3.54	78.24	2.36	52.48	3.24	65.89
25/01/2012	1	120	4.45	82.31	3.72	40.03	5.08	76.53
26/01/2012	2	120	8.88	79.75	8.20	74.95	10.26	77.94
27/01/2012	3	0	10.05	77.80	9.58	77.31	8.93	76.75
28/01/2012	2	90	7.03	85.28	7.80	87.12	8.19	86.02
29/01/2012	1	0	5.15	81.52	4.69	73.50	6.56	85.24
30/01/2012	2	40	8.02	86.78	5.88	79.20	9.05	88.19
31/01/2012	1	0	5.29	87.64	3.83	88.47	4.37	77.90

Table 108. January 2012 wind data at Cuyo Island from onshore weather station and meoscale model output

Source Date	PAGASA		ERA-Interim		NCEP FNL		NCEP CFSR	
	Wind Speed (m/s)	Wind Direction (Degrees)	Wind Speed (m/s)	Wind Direction (Degrees)	Wind Speed (m/s)	Wind Direction (Degrees)	Wind Speed (m/s)	Wind Direction (Degrees)
01/01/2012	4	20	9.83	37.02	10.75	31.67	10.56	33.64
02/01/2012	4	20	9.53	40.68	10.64	36.28	10.45	38.78
03/01/2012	4	20	8.82	40.37	7.21	39.96	7.41	38.81
04/01/2012	3	20	9.72	42.33	10.07	43.22	9.03	42.85
05/01/2012	4	20	11.46	44.37	13.16	40.70	11.90	44.99
06/01/2012	4	20	10.39	43.63	11.18	39.92	10.81	41.57
07/01/2012	4	20	10.60	37.52	10.71	36.65	10.43	39.86
08/01/2012	4	20	11.26	47.33	10.48	40.60	10.36	43.76
09/01/2012	4	20	11.46	45.90	11.46	42.91	11.56	46.85
10/01/2012	4	20	11.67	46.85	11.26	45.86	10.85	49.77
11/01/2012	4	20	11.31	45.97	12.24	41.38	11.08	45.67
12/01/2012	4	20	11.18	46.98	11.60	44.42	11.71	47.93
13/01/2012	4	20	10.22	45.98	10.07	44.50	10.86	48.37
14/01/2012	3	20	8.28	47.32	7.77	49.05	8.78	43.88
15/01/2012	2	20	6.33	40.28	8.05	39.45	7.96	34.35
16/01/2012	3	20	5.06	36.39	7.63	139.17	5.89	36.10
17/01/2012	1	20	7.23	41.95	7.99	159.23	5.98	43.45
18/01/2012	2	20	7.10	40.13	5.81	133.44	3.41	89.41
19/01/2012	2	20	5.37	32.39	6.34	35.43	4.55	44.02
20/01/2012	2	20	5.55	27.31	8.29	26.81	6.87	33.69
21/01/2012	4	20	6.27	37.99	7.28	36.32	8.85	37.65
22/01/2012	4	20	7.51	39.46	7.68	42.06	6.55	42.17
23/01/2012	4	20	8.90	38.20	8.42	43.85	8.19	42.31
24/01/2012	4	20	8.73	37.07	9.79	37.61	9.40	38.15
25/01/2012	4	20	10.12	38.23	11.17	37.00	10.33	38.22
26/01/2012	5	20	12.22	47.03	12.60	43.69	11.99	47.56
27/01/2012	4	20	10.66	50.32	9.68	47.12	10.43	47.97
28/01/2012	2	20	6.90	44.21	7.31	42.40	7.00	44.05
29/01/2012	1	20	6.01	38.98	7.58	37.08	6.19	37.39
30/01/2012	3	20	6.71	48.75	8.12	44.54	7.67	50.31
31/01/2012	2	20	6.79	40.15	6.42	35.31	7.01	36.36

Table 109. January 2012 wind data at Puerto Princesa from onshore weather station and meoscale model output

Source Date	PAGASA		ERA-Interim		NCEP FNL		NCEP CFSR	
	Wind Speed (m/s)	Wind Direction (Degrees)	Wind Speed (m/s)	Wind Direction (Degrees)	Wind Speed (m/s)	Wind Direction (Degrees)	Wind Speed (m/s)	Wind Direction (Degrees)
01/01/2012	3	290	4.75	44.15	3.89	20.56	3.87	29.17
02/01/2012	3	270	4.58	67.05	3.79	29.39	4.49	56.95
03/01/2012	3	90	3.63	63.77	4.31	62.31	3.64	69.96
04/01/2012	3	270	6.02	69.07	5.55	68.48	4.02	66.16
05/01/2012	6	90	6.90	65.50	7.15	57.03	5.20	57.86
06/01/2012	6	40	6.71	56.73	5.99	52.85	6.44	56.95
07/01/2012	3	90	5.08	59.30	4.74	51.14	4.63	54.09
08/01/2012	5	90	8.23	59.96	6.97	60.20	5.85	54.21
09/01/2012	5	90	5.89	59.11	5.76	54.72	4.71	48.88
10/01/2012	4	90	7.77	58.09	7.35	62.12	6.53	63.53
11/01/2012	7	70	7.77	69.28	7.40	65.58	7.18	68.37
12/01/2012	7	90	7.33	70.89	6.57	63.82	6.93	63.63
13/01/2012	5	90	6.16	76.68	5.57	68.06	6.52	69.12
14/01/2012	3	90	3.90	86.92	3.44	84.70	3.67	77.16
15/01/2012	2	90	2.67	174.44	3.15	331.75	2.39	17.40
16/01/2012	3	90	3.20	80.40	3.53	330.34	3.49	341.74
17/01/2012	2	90	2.94	83.46	2.34	307.85	2.30	33.72
18/01/2012	2	90	3.06	83.63	3.23	171.39	4.06	60.00
19/01/2012	3	270	2.99	87.57	2.58	103.45	3.12	142.52
20/01/2012	3	90	2.87	70.60	2.89	31.36	2.54	64.73
21/01/2012	4	90	2.64	80.37	3.52	45.68	3.40	47.66
22/01/2012	5	90	3.78	92.22	3.79	72.28	2.76	67.49
23/01/2012	5	90	4.32	73.80	4.75	69.94	3.98	68.18
24/01/2012	5	90	4.40	69.07	4.79	53.59	4.28	56.75
25/01/2012	4	70	5.02	57.03	5.24	48.14	4.70	54.22
26/01/2012	8	70	9.38	65.03	8.03	58.96	7.74	64.99
27/01/2012	6	90	6.84	71.46	5.89	64.94	6.06	67.34
28/01/2012	3	90	4.20	90.70	4.18	78.52	4.02	79.67
29/01/2012	3	90	2.39	93.04	2.43	85.81	2.06	216.33
30/01/2012	4	90	4.13	79.72	5.35	70.06	4.30	77.79
31/01/2012	3	90	3.93	80.75	3.67	76.96	3.70	84.41

Table 110. February 2012 wind data at Coron Island from onshore weather station and meoscale model output

Source Date	PAGASA		ERA-Interim		NCEP FNL		NCEP CFSR	
	Wind Speed (m/s)	Wind Direction (Degrees)	Wind Speed (m/s)	Wind Direction (Degrees)	Wind Speed (m/s)	Wind Direction (Degrees)	Wind Speed (m/s)	Wind Direction (Degrees)
01/02/2012	1	40	5.01	83.13	4.49	72.82	5.97	82.63
02/02/2012	1	40	5.21	80.51	7.76	60.51	7.94	79.65
03/02/2012	3	40	10.14	85.26	11.18	79.19	11.51	79.99
04/02/2012	3	40	9.73	80.78	10.48	76.96	9.97	75.39
05/02/2012	2	40	7.15	81.21	5.83	67.24	5.99	62.40
06/02/2012	2	0	4.06	82.77	5.73	57.20	7.10	77.81
07/02/2012	2	0	2.83	80.54	3.75	54.19	3.47	66.05
08/02/2012	1	180	4.95	90.20	6.26	74.19	6.45	76.14
09/02/2012	2	40	6.52	82.82	9.87	77.56	8.76	81.91
10/02/2012	2	40	5.30	72.55	6.57	68.07	6.40	72.65
11/02/2012	2	220	3.50	86.59	4.19	66.60	3.79	40.88
12/02/2012	1	0	8.24	39.13	12.04	63.02	7.02	65.07
13/02/2012	2	40	9.56	102.47	10.65	98.40	10.99	87.19
14/02/2012	2	140	7.87	92.09	8.76	85.83	7.73	92.27
15/02/2012	2	40	3.97	72.12	7.25	65.70	4.08	63.00
16/02/2012	1	40	5.52	54.97	10.24	56.83	7.33	79.24
17/02/2012	2	40	9.72	83.10	8.12	105.26	9.49	88.21
18/02/2012	3	40	8.83	90.31	3.29	58.27	3.63	83.50
19/02/2012	3	320	7.92	81.12	5.09	99.34	6.06	94.10
20/02/2012	2	120	8.90	88.56	2.95	164.32	5.64	102.12
21/02/2012	2	40	5.30	85.75	2.88	93.45	4.75	88.21
22/02/2012	2	140	5.74	85.00	4.32	76.50	5.38	87.53
23/02/2012	2	140	6.81	83.34	7.99	83.51	8.12	84.78
24/02/2012	2	120	8.35	87.34	8.27	82.37	8.45	87.23
25/02/2012	2	40	5.31	80.31	5.95	72.35	4.69	63.12
26/02/2012	2	0	4.68	79.64	4.18	70.30	4.08	74.56
27/02/2012	2	40	7.80	83.32	9.29	83.53	9.33	88.12
28/02/2012	2	120	6.31	81.24	5.55	76.58	6.20	75.25
29/02/2012	3	40	8.80	81.16	9.29	80.11	9.50	84.63

Table 111. February 2012 wind data at Cuyo Island from onshore weather station and meoscale model output

Date	PAGASA		ERA-Interim		NCEP FNL		NCEP CFSR	
	Wind Speed (m/s)	Wind Direction (Degrees)	Wind Speed (m/s)	Wind Direction (Degrees)	Wind Speed (m/s)	Wind Direction (Degrees)	Wind Speed (m/s)	Wind Direction (Degrees)
01/02/2012	2	20	6.41	36.09	4.82	28.75	6.15	36.35
02/02/2012	3	20	6.86	36.59	8.07	40.81	8.16	45.85
03/02/2012	3	20	9.93	48.10	11.96	48.95	10.97	51.05
04/02/2012	4	20	10.34	49.02	10.59	49.38	10.40	47.99
05/02/2012	2	20	9.83	41.52	10.59	40.15	10.69	39.61
06/02/2012	3	20	8.73	36.74	10.22	35.68	9.27	46.96
07/02/2012	2	20	8.09	30.92	9.91	33.69	7.98	37.45
08/02/2012	3	20	10.31	39.65	11.87	41.81	10.05	43.09
09/02/2012	2	20	9.64	43.56	11.01	45.75	9.53	45.89
10/02/2012	4	20	10.12	38.90	11.74	41.54	10.45	40.44
11/02/2012	2	20	10.82	33.92	14.48	29.03	13.93	34.47
12/02/2012	5	20	11.63	36.37	12.84	61.83	11.12	42.85
13/02/2012	2	20	5.03	129.63	5.79	114.69	5.06	87.10
14/02/2012	2	20	6.72	38.53	7.19	46.51	6.46	40.82
15/02/2012	2	20	8.16	29.82	10.14	39.66	8.45	31.00
16/02/2012	3	20	9.25	38.89	11.00	69.35	6.44	50.36
17/02/2012	2	20	4.75	67.00	6.12	124.86	5.39	122.52
18/02/2012	1	20	7.78	44.03	4.47	23.34	4.59	17.40
19/02/2012	2	20	8.65	41.59	2.35	175.99	2.89	61.72
20/02/2012	1	20	3.02	66.47	3.04	152.96	2.86	115.25
21/02/2012	1	320	3.81	34.17	2.12	23.15	3.27	29.54
22/02/2012	1	20	4.66	40.85	2.71	27.67	4.04	48.16
23/02/2012	2	20	4.27	32.22	3.50	64.32	4.35	51.35
24/02/2012	2	20	4.87	40.62	5.60	42.30	5.50	42.95
25/02/2012	2	20	6.98	36.03	7.34	38.78	7.08	36.08
26/02/2012	3	20	8.67	34.74	9.20	32.88	8.00	34.06
27/02/2012	2	20	9.20	42.41	8.29	47.95	6.84	49.23
28/02/2012	2	20	8.30	41.33	6.98	43.23	7.58	42.47
29/02/2012	3	20	8.47	45.98	8.57	49.80	8.25	48.83

Table 112. February 2012 wind data at Puerto Princesa from onshore weather station and meoscale model output

Source Date	PAGASA		ERA-Interim		NCEP FNL		NCEP CFSR	
	Wind Speed (m/s)	Wind Direction (Degrees)	Wind Speed (m/s)	Wind Direction (Degrees)	Wind Speed (m/s)	Wind Direction (Degrees)	Wind Speed (m/s)	Wind Direction (Degrees)
01/02/2012	3	90	3.65	85.06	2.07	160.30	2.04	104.74
02/02/2012	3	90	3.32	68.57	3.85	54.01	3.01	55.28
03/02/2012	4	90	4.72	72.43	7.37	68.27	6.39	69.11
04/02/2012	4	90	6.18	74.40	6.23	66.43	5.76	68.19
05/02/2012	3	90	4.47	75.12	5.06	59.73	4.64	52.29
06/02/2012	4	90	3.23	75.70	4.40	50.68	5.68	62.05
07/02/2012	3	270	4.51	27.56	4.42	39.83	4.03	78.98
08/02/2012	3	90	4.46	55.74	7.40	59.07	4.78	57.10
09/02/2012	6	90	5.63	70.40	6.78	63.08	6.21	69.57
10/02/2012	5	90	3.52	73.84	5.24	62.54	4.71	64.68
11/02/2012	5	90	5.84	63.83	5.05	40.16	5.40	46.66
12/02/2012	5	90	5.10	4.52	6.69	312.66	4.26	34.67
13/02/2012	4	90	5.68	168.69	6.93	156.36	8.11	115.14
14/02/2012	2	90	2.74	185.51	3.30	135.93	3.49	111.02
15/02/2012	2	90	2.93	54.80	3.71	53.63	2.40	48.64
16/02/2012	4	290	5.05	23.80	5.41	95.44	2.90	13.08
17/02/2012	4	90	6.91	119.86	8.90	142.90	3.12	230.63
18/02/2012	2	140	4.17	106.15	3.05	75.67	3.02	187.20
19/02/2012	3	90	3.58	86.94	2.71	190.28	2.52	89.05
20/02/2012	3	90	3.32	118.21	3.45	155.62	2.53	134.29
21/02/2012	2	90	2.74	172.68	1.69	200.71	2.29	133.26
22/02/2012	2	90	2.26	115.78	1.68	81.00	2.43	93.59
23/02/2012	3	90	2.77	110.06	3.30	95.81	3.79	96.70
24/02/2012	4	90	4.11	95.50	3.73	80.29	3.84	82.77
25/02/2012	3	90	2.80	91.11	2.77	74.18	2.93	82.54
26/02/2012	4	90	3.35	60.31	3.03	62.08	2.77	59.51
27/02/2012	5	90	6.16	68.02	5.48	74.76	4.28	90.04
28/02/2012	2	270	2.94	87.14	3.71	79.34	3.36	72.92
29/02/2012	3	70	4.30	75.76	4.99	65.92	4.77	68.44

Table 113. March 2012 wind data at Coron Island from onshore weather station and meoscale model output

Source Date	PAGASA		ERA-Interim		NCEP FNL		NCEP CFSR	
	Wind Speed (m/s)	Wind Direction (Degrees)	Wind Speed (m/s)	Wind Direction (Degrees)	Wind Speed (m/s)	Wind Direction (Degrees)	Wind Speed (m/s)	Wind Direction (Degrees)
01/03/2012	3	40	8.09	81.83	8.30	76.61	8.27	78.49
02/03/2012	2	40	9.70	83.26	10.77	81.69	10.14	84.44
03/03/2012	3	40	9.80	81.08	10.97	77.73	10.44	78.71
04/03/2012	3	40	9.44	81.19	10.07	76.85	10.11	77.09
05/03/2012	3	40	7.81	84.30	9.72	80.65	9.84	83.14
06/03/2012	2	40	6.72	85.55	8.05	82.63	8.34	86.38
07/03/2012	2	40	7.80	86.88	8.12	84.49	8.12	85.45
08/03/2012	2	40	7.02	85.88	8.61	83.74	8.29	83.54
09/03/2012	3	40	4.70	75.51	7.35	78.10	5.75	69.81
10/03/2012	2	40	6.42	81.99	6.13	68.39	7.39	78.33
11/03/2012	1	40	6.31	83.62	7.90	78.97	6.60	79.91
12/03/2012	2	40	6.79	81.16	9.86	81.87	7.42	78.77
13/03/2012	2	40	7.35	82.77	7.98	78.98	7.03	78.07
14/03/2012	3	40	7.80	85.21	9.29	83.44	9.17	86.71
15/03/2012	4	40	7.65	87.08	9.33	83.62	8.12	86.55
16/03/2012	2	40	8.52	84.13	8.81	82.11	8.58	84.53
17/03/2012	1	40	8.29	83.97	8.67	79.08	9.14	84.70
18/03/2012	1	40	5.21	82.73	3.39	47.86	5.49	72.98
19/03/2012	2	40	3.21	109.23	4.08	350.90	2.01	7.41
20/03/2012	1	40	3.25	57.00	10.62	318.47	2.62	250.39
21/03/2012	1	0	4.49	38.98	5.77	231.48	4.02	358.93
22/03/2012	2	140	6.80	84.87	5.64	170.50	10.04	89.46
23/03/2012	1	40	4.32	160.12	3.57	155.33	5.52	209.21
24/03/2012	1	180	3.32	159.06	2.26	147.52	4.93	159.80
25/03/2012	1	140	5.67	89.09	3.42	79.55	7.43	88.10
26/03/2012	2	40	7.67	85.11	6.90	85.96	9.98	87.26
27/03/2012	2	40	9.50	77.98	6.80	72.54	4.50	60.30
28/03/2012	1	220	7.05	74.59	6.75	72.74	3.80	65.27
29/03/2012	2	0	7.38	85.51	7.04	70.73	7.23	91.77
30/03/2012	2	140	6.98	86.91	9.68	114.29	5.12	99.11
31/03/2012	1	0	5.44	85.42	3.75	129.00	2.21	85.71

Table 114. March 2012 wind data at Cuyo Island from onshore weather station and mesoscale model output

Source Date	PAGASA		ERA-Interim		NCEP FNL		NCEP CFSR	
	Wind Speed (m/s)	Wind Direction (Degrees)	Wind Speed (m/s)	Wind Direction (Degrees)	Wind Speed (m/s)	Wind Direction (Degrees)	Wind Speed (m/s)	Wind Direction (Degrees)
01/03/2012	3	20	9.27	47.01	9.53	47.34	9.13	46.49
02/03/2012	2	20	9.39	48.93	9.00	50.12	8.32	49.75
03/03/2012	4	20	9.85	45.21	10.81	47.67	9.98	47.72
04/03/2012	3	20	9.75	44.53	10.93	47.43	10.44	48.49
05/03/2012	4	20	7.96	45.28	10.11	45.78	9.42	51.05
06/03/2012	2	20	7.07	44.15	6.99	47.16	5.04	54.29
07/03/2012	1	0	3.78	41.45	3.92	49.64	5.04	50.40
08/03/2012	2	20	6.21	41.50	6.14	44.14	6.27	46.65
09/03/2012	2	20	7.32	36.98	7.65	42.11	7.54	39.27
10/03/2012	3	20	8.99	43.19	10.09	42.49	9.90	45.11
11/03/2012	3	20	9.69	41.99	10.88	43.40	9.95	46.04
12/03/2012	2	20	8.80	45.00	9.32	51.25	8.88	48.19
13/03/2012	2	20	8.41	44.67	8.81	46.98	8.67	45.67
14/03/2012	2	20	8.18	45.30	8.05	48.73	7.70	49.72
15/03/2012	2	20	8.17	44.02	8.38	47.48	8.03	43.97
16/03/2012	2	20	7.67	47.98	8.58	48.22	8.07	47.06
17/03/2012	2	20	8.21	43.94	9.00	44.82	8.28	46.96
18/03/2012	3	20	7.52	43.16	9.64	36.60	9.20	36.06
19/03/2012	2	20	8.49	26.56	12.51	343.07	9.99	26.82
20/03/2012	2	20	9.45	6.03	11.48	292.31	9.64	10.17
21/03/2012	4	20	9.43	25.33	7.23	232.87	12.52	5.09
22/03/2012	2	20	6.49	91.65	5.09	181.38	11.26	183.66
23/03/2012	2	20	4.84	168.41	3.88	186.24	5.66	225.32
24/03/2012	1	220	3.16	173.40	2.99	193.44	3.78	175.35
25/03/2012	0	0	5.73	43.17	2.83	92.08	4.58	96.82
26/03/2012	2	20	8.53	42.82	5.59	49.34	6.96	50.11
27/03/2012	2	20	11.69	40.92	11.75	40.85	12.03	37.92
28/03/2012	2	20	10.92	41.64	11.97	37.91	11.18	42.03
29/03/2012	3	20	7.78	42.36	9.64	63.14	5.52	42.63
30/03/2012	1	20	6.20	35.37	8.67	157.91	2.36	29.41
31/03/2012	2	20	4.33	47.43	2.96	139.64	3.22	25.23

Table 115. March 2012 wind data at Puerto Princesa from onshore weather station and meoscale model output

Source Date	PAGASA		ERA-Interim		NCEP FNL		NCEP CFSR	
	Wind Speed (m/s)	Wind Direction (Degrees)	Wind Speed (m/s)	Wind Direction (Degrees)	Wind Speed (m/s)	Wind Direction (Degrees)	Wind Speed (m/s)	Wind Direction (Degrees)
01/03/2012	6	90	4.27	77.21	4.86	63.53	4.59	65.78
02/03/2012	4	90	5.21	75.69	5.62	72.75	5.31	77.51
03/03/2012	6	90	5.24	69.64	6.14	65.74	5.81	67.69
04/03/2012	5	70	4.11	72.04	6.15	62.32	5.87	64.34
05/03/2012	4	90	3.87	70.26	6.04	65.45	5.97	72.61
06/03/2012	2	90	3.30	101.17	4.21	76.58	4.47	89.02
07/03/2012	3	90	3.77	100.71	3.33	81.86	3.72	83.16
08/03/2012	3	90	3.80	89.44	2.98	79.95	3.52	78.59
09/03/2012	3	90	3.48	76.74	3.08	80.85	3.44	71.96
10/03/2012	4	90	3.55	73.09	5.10	69.76	4.81	63.84
11/03/2012	4	90	6.31	66.54	6.69	63.29	6.36	62.74
12/03/2012	6	90	5.59	74.19	5.89	71.87	5.29	64.44
13/03/2012	3	90	4.49	65.26	4.90	66.84	4.74	60.37
14/03/2012	5	90	5.19	75.88	5.06	68.59	5.45	73.31
15/03/2012	4	70	4.30	72.23	4.18	76.84	4.02	70.95
16/03/2012	4	90	4.42	78.96	4.96	66.55	4.63	67.06
17/03/2012	4	90	3.80	81.21	4.27	73.25	3.88	69.61
18/03/2012	3	90	3.64	69.18	3.91	45.08	4.05	64.64
19/03/2012	3	270	3.22	72.06	3.20	340.92	3.33	18.39
20/03/2012	3	0	4.36	341.80	3.77	309.81	4.63	346.39
21/03/2012	2	270	4.95	344.45	3.61	271.56	3.87	339.06
22/03/2012	2	270	2.23	10.43	2.67	191.56	3.07	274.90
23/03/2012	2	90	2.53	203.71	2.26	182.54	2.30	240.64
24/03/2012	2	90	3.91	192.17	2.25	188.01	3.25	224.05
25/03/2012	3	90	3.52	149.56	2.98	173.69	3.11	177.15
26/03/2012	3	90	5.01	86.51	1.93	101.62	4.43	113.09
27/03/2012	3	90	6.30	75.80	5.33	76.45	4.67	67.35
28/03/2012	4	90	6.33	73.23	6.06	63.25	4.93	61.58
29/03/2012	3	90	4.05	88.40	2.46	342.06	2.60	41.55
30/03/2012	2	90	3.45	129.77	2.85	204.79	2.14	189.53
31/03/2012	3	90	3.38	60.69	3.86	197.94	1.75	19.17

Table 116. April 2012 wind data at Coron Island from onshore weather station and meoscale model output

Source Date	PAGASA		ERA-Interim		NCEP FNL		NCEP CFSR	
	Wind Speed (m/s)	Wind Direction (Degrees)	Wind Speed (m/s)	Wind Direction (Degrees)	Wind Speed (m/s)	Wind Direction (Degrees)	Wind Speed (m/s)	Wind Direction (Degrees)
01/04/2012	2	40	6.92	89.23	4.97	96.89	6.56	89.74
02/04/2012	2	140	5.68	82.15	3.16	91.14	5.54	83.72
03/04/2012	1	140	4.41	84.68	2.32	43.35	3.26	86.08
04/04/2012	1	0	5.48	87.46	2.22	354.95	5.77	93.09
05/04/2012	1	120	4.20	83.56	2.56	322.68	4.93	81.71
06/04/2012	1	20	3.82	88.59	2.65	268.06	4.37	80.73
07/04/2012	2	40	5.56	84.89	2.92	78.58	6.60	81.78
08/04/2012	1	40	8.83	86.94	2.17	118.76	9.06	87.79
09/04/2012	3	40	7.48	85.73	1.89	121.76	6.20	79.82
10/04/2012	2	40	6.30	82.57	2.26	333.08	5.24	80.17
11/04/2012	2	40	5.47	84.67	2.57	291.04	6.89	88.21
12/04/2012	2	120	6.39	88.51	1.97	255.60	6.72	92.28
13/04/2012	2	220	6.22	86.92	2.14	258.61	7.22	88.74
14/04/2012	2	140	6.91	87.37	2.01	0.01	7.03	83.59
15/04/2012	2	40	4.70	81.61	1.82	147.22	4.74	71.16
16/04/2012	2	0	3.96	88.16	1.65	158.71	5.18	84.03
17/04/2012	1	320	4.59	84.33	1.94	41.25	5.90	84.83
18/04/2012	3	0	5.41	89.90	1.68	1.49	6.58	83.11
19/04/2012	2	40	4.58	85.81	2.16	339.93	5.14	76.20
20/04/2012	2	40	3.90	84.07	2.41	307.36	4.60	75.27
21/04/2012	1	140	3.69	67.99	2.75	293.70	3.33	62.51
22/04/2012	1	40	4.65	89.58	2.38	328.86	3.68	83.33
23/04/2012	1	0	7.93	91.00	2.02	345.37	6.24	101.25
24/04/2012	1	90	7.28	94.86	1.57	308.03	5.24	107.26
25/04/2012	1	90	3.19	105.80	1.97	271.03	3.14	145.94
26/04/2012	1	0	2.75	87.48	1.69	355.54	1.48	147.27
27/04/2012	1	0	3.69	88.98	2.25	30.55	4.01	95.86
28/04/2012	2	140	5.00	91.04	1.64	11.56	5.18	94.39
29/04/2012	2	140	5.02	85.20	1.61	259.51	5.58	89.51
30/04/2012	1	120	3.83	86.98	1.68	182.20	4.03	72.39

Table 117. April 2012 wind data at Cuyo Island from onshore weather station and meoscale model output

Source Date	PAGASA		ERA-Interim		NCEP FNL		NCEP CFSR	
	Wind Speed (m/s)	Wind Direction (Degrees)	Wind Speed (m/s)	Wind Direction (Degrees)	Wind Speed (m/s)	Wind Direction (Degrees)	Wind Speed (m/s)	Wind Direction (Degrees)
01/04/2012	1	20	2.71	86.72	1.97	131.41	2.48	60.14
02/04/2012	2	20	4.84	34.18	2.03	314.01	3.10	48.76
03/04/2012	1	20	6.28	38.00	4.18	19.53	5.61	40.04
04/04/2012	1	0	6.01	39.24	3.50	7.55	3.54	39.03
05/04/2012	1	20	5.19	33.93	3.16	332.10	3.31	40.08
06/04/2012	1	20	6.06	38.80	2.78	276.04	4.02	39.87
07/04/2012	1	0	7.60	42.27	1.73	277.25	4.82	53.75
08/04/2012	1	20	8.52	47.23	1.72	237.59	6.40	50.25
09/04/2012	2	20	8.71	40.96	1.86	299.19	7.70	38.63
10/04/2012	3	20	9.02	39.77	2.21	309.14	8.66	43.84
11/04/2012	2	20	7.08	41.97	2.59	290.25	4.74	61.95
12/04/2012	1	0	2.65	34.07	1.85	222.45	2.19	100.91
13/04/2012	1	0	3.50	32.62	1.92	214.46	4.27	49.17
14/04/2012	1	20	6.78	36.92	1.86	305.14	5.85	44.22
15/04/2012	2	20	5.86	29.90	2.94	240.62	5.93	33.64
16/04/2012	1	20	3.05	23.13	1.69	255.89	4.16	39.63
17/04/2012	1	20	4.05	27.40	2.36	246.94	5.60	39.34
18/04/2012	2	20	3.85	34.51	2.45	276.57	5.33	39.54
19/04/2012	2	20	4.04	35.41	2.71	290.57	4.75	36.92
20/04/2012	2	20	5.08	29.28	3.51	292.27	5.62	33.65
21/04/2012	1	20	5.47	21.47	2.23	272.23	5.93	28.77
22/04/2012	1	20	6.20	38.08	1.63	305.95	4.56	38.54
23/04/2012	0	0	2.81	66.94	1.65	302.57	4.18	153.63
24/04/2012	0	0	2.06	89.73	2.07	269.72	2.55	153.43
25/04/2012	1	320	2.36	173.47	1.47	272.58	2.61	207.49
26/04/2012	1	320	1.74	15.24	1.65	270.00	1.63	12.17
27/04/2012	1	220	1.82	357.33	1.91	254.47	1.62	39.47
28/04/2012	0	0	2.55	25.27	2.02	259.63	2.81	63.36
29/04/2012	1	220	3.58	20.71	1.82	209.68	4.13	41.78
30/04/2012	0	0	5.07	30.88	1.18	3.51	5.73	33.63

Table 118. April 2012 wind data at Puerto Princesa from onshore weather station and meoscale model output

Source Date	PAGASA		ERA-Interim		NCEP FNL		NCEP CFSR	
	Wind Speed (m/s)	Wind Direction (Degrees)	Wind Speed (m/s)	Wind Direction (Degrees)	Wind Speed (m/s)	Wind Direction (Degrees)	Wind Speed (m/s)	Wind Direction (Degrees)
01/04/2012	3	90	2.85	142.86	2.30	175.29	2.13	206.83
02/04/2012	3	90	3.23	123.27	2.14	154.72	2.10	110.33
03/04/2012	3	90	3.38	82.90	2.01	166.24	2.14	72.96
04/04/2012	2	90	3.83	93.97	2.16	204.22	2.05	105.13
05/04/2012	3	90	3.42	86.61	2.11	188.34	2.17	168.38
06/04/2012	3	90	3.32	76.22	2.00	177.51	1.93	136.47
07/04/2012	3	90	3.54	80.39	2.79	189.24	3.22	93.36
08/04/2012	3	90	6.02	81.75	3.13	179.41	2.32	144.92
09/04/2012	3	90	3.62	88.76	2.42	192.58	2.56	79.48
10/04/2012	3	90	3.78	76.95	2.57	200.46	3.49	66.38
11/04/2012	2	270	3.25	80.19	2.16	184.76	4.42	82.46
12/04/2012	2	270	4.26	94.88	2.19	199.85	3.18	158.21
13/04/2012	2	160	2.94	124.74	2.34	193.75	2.66	106.93
14/04/2012	2	90	3.48	105.03	2.53	184.82	3.17	91.04
15/04/2012	2	90	3.45	105.36	2.71	198.10	2.35	85.89
16/04/2012	2	90	3.14	107.80	2.80	191.26	2.68	78.85
17/04/2012	2	90	3.22	136.06	2.60	176.99	2.11	101.99
18/04/2012	3	90	3.40	124.42	2.74	186.03	2.58	77.19
19/04/2012	3	90	3.56	108.03	2.45	172.13	2.56	77.52
20/04/2012	2	90	3.16	98.62	2.28	173.16	2.41	87.06
21/04/2012	3	90	3.02	73.87	2.53	178.55	2.22	53.40
22/04/2012	3	90	3.36	48.87	2.29	168.54	2.62	20.80
23/04/2012	2	160	3.03	85.55	2.07	160.16	2.48	106.64
24/04/2012	2	90	3.19	113.50	2.03	134.23	2.30	162.05
25/04/2012	2	140	3.26	190.80	2.19	160.99	2.21	199.27
26/04/2012	1	160	3.15	139.07	2.85	182.33	2.13	188.96
27/04/2012	2	140	3.23	172.88	2.44	174.30	2.44	184.48
28/04/2012	2	160	3.05	172.68	2.16	167.44	2.22	175.76
29/04/2012	2	140	2.57	151.00	2.22	159.79	2.09	157.24
30/04/2012	2	90	2.59	118.31	2.18	164.24	1.87	129.15

Table 119. May 2012 wind data at Coron Island from onshore weather station and meoscale model output

Source Date	PAGASA		ERA-Interim		NCEP FNL		NCEP CFSR	
	Wind Speed (m/s)	Wind Direction (Degrees)	Wind Speed (m/s)	Wind Direction (Degrees)	Wind Speed (m/s)	Wind Direction (Degrees)	Wind Speed (m/s)	Wind Direction (Degrees)
01/05/2012	1	120	3.28	103.02	2.00	159.41	4.94	99.48
02/05/2012	1	220	2.01	254.82	2.20	283.53	2.19	65.42
03/05/2012	1	0	1.77	6.01	2.45	297.59	2.03	3.64
04/05/2012	1	210	1.70	72.01	3.41	303.09	2.66	0.03
05/05/2012	0	0	1.39	19.16	3.30	158.58	3.20	19.56
06/05/2012	1	40	2.08	113.51	5.99	136.42	4.95	115.63
07/05/2012	1	140	2.42	94.10	5.10	104.18	6.52	116.82
08/05/2012	0	0	2.39	51.85	4.05	64.16	3.11	160.58
09/05/2012	1	120	2.61	31.83	2.58	271.96	2.91	214.13
10/05/2012	1	0	3.56	336.75	4.30	98.05	2.43	336.55
11/05/2012	1	0	2.09	299.01	6.02	96.70	2.56	349.20
12/05/2012	1	210	2.13	314.07	8.21	172.74	2.78	292.43
13/05/2012	1	220	1.97	324.79	9.31	183.26	3.74	257.25
14/05/2012	1	0	2.12	225.70	7.29	177.19	4.90	220.14
15/05/2012	2	220	3.53	205.14	4.67	192.29	5.41	217.78
16/05/2012	1	220	2.77	224.30	3.31	181.28	3.84	209.82
17/05/2012	1	0	2.05	45.80	2.98	189.35	2.24	226.78
18/05/2012	1	0	1.84	82.43	2.59	257.57	2.28	13.06
19/05/2012	1	0	2.54	47.59	2.07	319.90	3.02	25.25
20/05/2012	1	0	2.71	65.94	2.80	269.52	2.36	92.12
21/05/2012	1	0	1.82	34.45	4.95	266.99	2.82	314.67
22/05/2012	1	0	2.51	235.00	7.78	256.71	3.95	276.43
23/05/2012	1	0	5.03	209.43	9.39	256.76	5.42	251.75
24/05/2012	1	220	5.87	203.68	10.62	217.77	6.88	241.40
25/05/2012	0	0	5.15	208.41	8.79	201.16	6.40	244.25
26/05/2012	0	0	3.55	217.12	5.38	208.89	4.20	259.59
27/05/2012	1	0	2.29	211.70	3.59	260.29	3.96	284.65
28/05/2012	1	0	1.96	320.20	4.27	297.05	4.58	281.35
29/05/2012	1	320	1.79	0.24	6.25	291.25	4.34	290.97
30/05/2012	1	0	1.77	278.54	4.75	300.21	3.93	311.32
31/05/2012	1	0	2.37	14.30	7.15	277.52	4.16	297.07

Table 120. May 2012 wind data at Cuyo Island from onshore weather station and meoscale model output

Source Date	PAGASA		ERA-Interim		NCEP FNL		NCEP CFSR	
	Wind Speed (m/s)	Wind Direction (Degrees)	Wind Speed (m/s)	Wind Direction (Degrees)	Wind Speed (m/s)	Wind Direction (Degrees)	Wind Speed (m/s)	Wind Direction (Degrees)
01/05/2012	0	0	2.57	164.36	1.77	198.16	2.17	155.08
02/05/2012	2	120	2.97	201.20	3.28	203.92	2.96	200.83
03/05/2012	1	220	1.92	254.10	4.37	296.35	1.99	280.50
04/05/2012	1	220	1.41	68.50	6.00	275.70	2.93	315.02
05/05/2012	1	320	1.78	341.41	5.29	227.68	4.59	315.47
06/05/2012	0	0	1.72	113.71	5.01	144.49	5.38	124.99
07/05/2012	No Data	No Data	1.95	35.24	2.60	56.02	5.45	147.52
08/05/2012	No Data	No Data	3.48	354.30	4.49	37.03	4.07	194.16
09/05/2012	No Data	No Data	4.43	343.02	4.88	268.89	3.07	215.55
10/05/2012	No Data	No Data	5.97	342.93	4.13	195.71	3.07	315.20
11/05/2012	No Data	No Data	5.44	334.10	4.25	149.74	3.12	334.42
12/05/2012	No Data	No Data	4.36	333.76	10.36	193.11	4.81	303.13
13/05/2012	No Data	No Data	2.83	277.70	10.58	177.21	5.11	268.68
14/05/2012	No Data	No Data	3.25	232.17	6.86	169.68	5.63	231.69
15/05/2012	No Data	No Data	4.32	219.22	4.54	181.56	5.59	215.12
16/05/2012	No Data	No Data	2.60	182.66	3.64	186.17	2.94	220.13
17/05/2012	No Data	No Data	1.98	210.46	2.26	183.49	1.38	204.96
18/05/2012	No Data	No Data	1.30	84.25	2.02	299.09	2.20	5.19
19/05/2012	No Data	No Data	1.60	43.60	2.90	326.23	2.16	41.03
20/05/2012	No Data	No Data	3.80	209.25	3.77	294.27	3.11	181.74
21/05/2012	No Data	No Data	3.09	269.01	5.20	267.98	4.06	280.67
22/05/2012	No Data	No Data	4.05	244.57	8.57	253.01	5.86	296.83
23/05/2012	0	0	4.82	225.30	10.22	248.14	6.82	259.68
24/05/2012	1	20	6.05	216.87	11.50	211.39	7.38	241.95
25/05/2012	1	220	6.70	210.54	9.16	196.33	7.34	237.45
26/05/2012	1	220	4.20	215.09	6.15	206.88	4.96	255.32
27/05/2012	1	220	3.07	257.05	4.47	250.53	5.71	281.48
28/05/2012	0	0	1.90	290.22	6.64	281.59	6.59	284.16
29/05/2012	1	20	2.80	306.55	8.49	262.73	8.91	282.37
30/05/2012	1	220	3.33	268.95	8.54	292.42	7.35	311.92
31/05/2012	0	0	3.49	243.92	10.80	247.90	7.76	294.90

Table 121. May 2012 wind data at Puerto Princesa from onshore weather station and meoscale model output

Source Date	PAGASA		ERA-Interim		NCEP FNL		NCEP CFSR	
	Wind Speed (m/s)	Wind Direction (Degrees)	Wind Speed (m/s)	Wind Direction (Degrees)	Wind Speed (m/s)	Wind Direction (Degrees)	Wind Speed (m/s)	Wind Direction (Degrees)
01/05/2012	2	90	3.29	174.27	2.58	212.81	2.36	315.37
02/05/2012	2	270	2.98	169.61	2.48	202.60	2.01	173.15
03/05/2012	2	320	2.25	147.04	1.96	171.94	1.97	282.13
04/05/2012	1	270	2.80	270.74	2.01	61.22	2.52	294.73
05/05/2012	2	130	2.58	24.49	3.35	253.90	1.69	225.37
06/05/2012	2	90	3.03	133.21	2.67	197.16	2.20	226.54
07/05/2012	2	160	3.05	162.77	3.84	167.90	2.41	211.52
08/05/2012	2	320	3.01	147.22	1.99	220.39	2.67	222.27
09/05/2012	3	290	2.32	153.93	1.86	343.39	1.88	195.61
10/05/2012	1	290	2.71	330.52	1.96	199.40	1.93	218.92
11/05/2012	2	290	3.01	330.58	3.79	212.83	1.93	222.84
12/05/2012	2	270	2.69	258.64	7.01	208.87	2.85	242.01
13/05/2012	1	180	3.07	166.08	5.37	208.39	3.27	222.89
14/05/2012	2	180	3.29	187.51	6.28	185.70	3.17	198.56
15/05/2012	2	270	3.56	219.43	4.15	191.01	2.99	227.34
16/05/2012	3	160	3.49	194.56	3.12	210.29	3.25	209.50
17/05/2012	2	270	3.59	196.56	2.75	195.89	2.99	198.95
18/05/2012	2	90	3.17	171.69	2.56	186.76	2.23	198.71
19/05/2012	2	290	3.16	171.90	1.93	157.48	2.61	14.83
20/05/2012	2	140	2.93	171.64	2.01	173.86	2.32	139.85
21/05/2012	2	270	2.47	217.01	2.42	230.83	2.34	355.98
22/05/2012	1	290	3.12	176.22	3.94	247.47	2.35	236.49
23/05/2012	2	320	3.92	186.54	6.15	249.21	3.26	231.29
24/05/2012	3	270	5.13	193.35	5.65	228.85	3.46	240.72
25/05/2012	2	220	3.38	200.54	5.01	201.58	3.32	208.16
26/05/2012	2	270	3.80	189.41	3.93	198.49	3.11	197.90
27/05/2012	1	270	3.17	200.08	2.73	204.10	2.22	184.15
28/05/2012	2	270	2.78	171.89	1.54	173.44	1.85	170.57
29/05/2012	2	270	2.24	180.33	1.97	269.93	1.52	189.85
30/05/2012	2	250	3.21	182.11	1.99	278.74	1.27	171.61
31/05/2012	2	220	3.43	184.00	4.38	243.55	2.40	213.36

Table 122. June 2012 wind data at Coron Island from onshore weather station and meoscale model output

Source Date	PAGASA		ERA-Interim		NCEP FNL		NCEP CFSR	
	Wind Speed (m/s)	Wind Direction (Degrees)	Wind Speed (m/s)	Wind Direction (Degrees)	Wind Speed (m/s)	Wind Direction (Degrees)	Wind Speed (m/s)	Wind Direction (Degrees)
01/06/2012	1	210	4.69	225.96	6.64	250.79	5.32	243.10
02/06/2012	1	0	6.75	230.01	9.06	244.39	5.60	221.75
03/06/2012	1	320	5.37	238.85	7.78	244.90	3.41	261.06
04/06/2012	1	320	6.28	223.43	8.22	223.31	5.82	219.74
05/06/2012	2	210	7.31	208.05	9.97	220.84	7.56	203.73
06/06/2012	2	210	7.35	198.91	10.08	216.31	7.20	199.48
07/06/2012	1	140	6.70	190.85	10.63	203.39	5.36	191.23
08/06/2012	1	0	4.16	197.65	6.84	194.88	4.61	199.92
09/06/2012	1	210	4.11	205.99	5.14	215.11	3.80	211.23
10/06/2012	1	210	4.70	229.57	7.32	239.23	4.77	242.15
11/06/2012	2	270	6.28	239.19	8.54	237.96	6.17	240.09
12/06/2012	1	270	7.43	232.24	9.63	234.62	7.18	236.49
13/06/2012	2	270	7.15	229.29	7.99	247.82	7.12	231.89
14/06/2012	1	270	7.64	232.11	9.21	221.57	7.31	227.74
15/06/2012	1	220	7.64	226.34	9.00	219.08	6.81	225.06
16/06/2012	0	0	8.21	223.13	10.21	213.66	7.70	217.51
17/06/2012	2	210	9.33	209.23	10.98	214.42	8.99	202.39
18/06/2012	4	180	10.04	198.43	10.80	203.62	8.21	197.14
19/06/2012	5	180	8.94	196.09	9.80	198.17	8.06	196.14
20/06/2012	2	180	7.86	194.96	8.52	198.03	7.19	189.48
21/06/2012	2	210	6.53	200.05	7.11	199.99	4.98	199.71
22/06/2012	1	0	4.80	203.86	5.20	215.17	3.69	207.55
23/06/2012	2	0	4.83	205.14	5.55	217.76	3.65	214.80
24/06/2012	0	0	5.84	232.47	7.49	237.30	4.17	250.15
25/06/2012	1	320	8.22	236.00	10.95	245.57	5.60	250.76
26/06/2012	0	0	8.09	223.54	12.59	226.21	7.67	254.61
27/06/2012	1	0	7.33	210.03	10.39	208.74	8.98	250.67
28/06/2012	2	210	9.75	213.28	10.72	219.14	9.80	226.01
29/06/2012	2	180	9.22	194.39	10.45	197.76	7.58	196.72
30/06/2012	2	0	4.96	191.70	6.54	190.04	4.36	193.92

Table 123. June 2012 wind data at Cuyo Island from onshore weather station and meoscale model output

Source Date	PAGASA		ERA-Interim		NCEP FNL		NCEP CFSR	
	Wind Speed (m/s)	Wind Direction (Degrees)	Wind Speed (m/s)	Wind Direction (Degrees)	Wind Speed (m/s)	Wind Direction (Degrees)	Wind Speed (m/s)	Wind Direction (Degrees)
01/06/2012	3	220	7.54	231.62	9.23	232.35	7.64	229.56
02/06/2012	4	220	7.55	213.34	11.74	237.66	9.03	218.48
03/06/2012	4	220	8.54	227.50	11.27	230.05	8.65	229.83
04/06/2012	2	220	8.39	220.41	10.00	213.41	8.42	214.37
05/06/2012	4	220	9.20	214.10	11.95	211.03	9.27	206.22
06/06/2012	3	220	7.81	205.14	11.53	205.96	7.80	203.79
07/06/2012	1	220	7.21	193.98	10.30	195.77	6.16	196.77
08/06/2012	1	220	4.71	198.92	6.94	197.37	5.01	208.96
09/06/2012	No Data	No Data	4.77	210.13	5.87	209.84	5.01	220.21
10/06/2012	No Data	No Data	5.22	234.62	7.05	238.38	5.58	236.79
11/06/2012	No Data	No Data	6.09	237.25	9.01	238.64	6.42	243.63
12/06/2012	No Data	No Data	8.35	227.22	10.95	229.69	9.01	230.13
13/06/2012	No Data	No Data	9.14	225.83	10.80	241.50	9.52	234.67
14/06/2012	No Data	No Data	9.04	226.69	9.63	221.04	9.13	231.32
15/06/2012	No Data	No Data	9.67	221.12	10.26	223.18	9.16	230.17
16/06/2012	No Data	No Data	10.17	215.60	10.85	210.01	10.32	219.02
17/06/2012	No Data	No Data	10.89	205.80	12.61	209.21	9.97	206.12
18/06/2012	No Data	No Data	10.62	198.45	11.48	201.31	8.60	200.18
19/06/2012	No Data	No Data	9.05	197.92	9.59	199.24	7.69	200.01
20/06/2012	No Data	No Data	8.03	196.33	8.37	200.14	6.73	195.63
21/06/2012	2	220	7.09	203.44	7.95	199.47	5.52	206.87
22/06/2012	2	220	6.23	214.77	6.87	207.99	4.98	228.70
23/06/2012	2	220	6.72	217.39	6.91	220.73	5.53	231.14
24/06/2012	2	220	8.04	228.16	8.03	242.50	6.28	254.01
25/06/2012	1	220	9.73	226.60	12.61	235.19	7.38	254.21
26/06/2012	1	220	8.83	219.55	14.01	217.94	9.97	250.56
27/06/2012	0	0	9.65	218.14	11.67	209.74	12.21	238.47
28/06/2012	3	150	10.80	206.33	12.03	213.36	11.66	218.80
29/06/2012	3	220	9.15	193.75	10.15	193.81	8.18	203.01
30/06/2012	1	220	6.15	191.57	5.52	197.38	4.02	219.46

Table 124. June 2012 wind data at Puerto Princesa from onshore weather station and meoscale model output

Source Date	PAGASA		ERA-Interim		NCEP FNL		NCEP CFSR	
	Wind Speed (m/s)	Wind Direction (Degrees)	Wind Speed (m/s)	Wind Direction (Degrees)	Wind Speed (m/s)	Wind Direction (Degrees)	Wind Speed (m/s)	Wind Direction (Degrees)
01/06/2012	2	270	3.47	187.52	3.75	206.38	3.87	197.58
02/06/2012	1	290	3.54	209.52	5.05	237.17	2.99	213.50
03/06/2012	2	290	3.86	190.65	3.95	199.71	3.79	207.05
04/06/2012	2	290	4.11	200.42	5.54	202.45	3.87	200.34
05/06/2012	2	180	4.55	205.35	6.22	201.61	4.01	198.72
06/06/2012	1	240	4.29	198.48	5.26	196.74	3.63	216.98
07/06/2012	3	180	4.67	188.72	5.87	192.52	3.89	199.08
08/06/2012	2	160	3.95	190.91	4.25	193.52	3.69	196.65
09/06/2012	2	180	3.04	175.74	3.69	196.10	3.03	202.27
10/06/2012	2	270	3.37	183.72	3.66	196.21	3.36	194.61
11/06/2012	3	270	3.25	211.94	3.66	205.09	3.51	241.28
12/06/2012	2	270	5.10	195.14	4.89	206.51	4.13	198.96
13/06/2012	2	180	3.60	210.12	3.44	219.12	3.55	222.35
14/06/2012	2	180	5.30	197.26	4.57	204.74	4.06	205.69
15/06/2012	2	270	5.86	199.03	4.57	205.01	3.99	201.28
16/06/2012	3	180	6.58	199.66	5.98	201.12	5.38	199.45
17/06/2012	3	180	6.10	198.22	6.24	199.78	5.04	203.29
18/06/2012	4	180	5.99	197.30	6.26	196.82	4.84	202.22
19/06/2012	3	180	6.18	196.92	5.57	201.13	4.63	206.93
20/06/2012	4	180	5.81	200.71	5.11	198.50	4.55	205.65
21/06/2012	3	180	3.87	211.35	4.49	193.81	3.36	210.51
22/06/2012	2	270	4.09	199.83	3.88	205.05	3.08	220.29
23/06/2012	2	180	3.84	209.71	3.68	205.60	3.50	201.93
24/06/2012	2	180	4.66	196.01	3.38	199.83	3.75	195.11
25/06/2012	2	160	4.28	201.01	4.40	236.36	3.61	201.22
26/06/2012	1	270	5.67	200.20	5.80	230.80	4.17	231.33
27/06/2012	2	180	5.18	203.57	7.55	202.44	3.78	221.46
28/06/2012	2	270	7.53	200.76	5.69	205.62	5.06	203.83
29/06/2012	2	180	5.99	196.69	6.12	196.75	4.60	205.74
30/06/2012	1	180	3.70	198.39	4.12	194.70	3.08	208.79

Table 125. July 2012 wind data at Coron Island from onshore weather station and meoscale model output

Source Date	PAGASA		ERA-Interim		NCEP FNL		NCEP CFSR	
	Wind Speed (m/s)	Wind Direction (Degrees)	Wind Speed (m/s)	Wind Direction (Degrees)	Wind Speed (m/s)	Wind Direction (Degrees)	Wind Speed (m/s)	Wind Direction (Degrees)
01/07/2012	1	0	2.27	157.36	2.58	270.71	2.72	347.19
02/07/2012	0	0	3.16	281.22	6.53	296.72	4.09	307.98
03/07/2012	0	0	4.57	235.64	16.07	235.05	5.91	267.65
04/07/2012	1	320	6.95	191.92	10.75	194.38	6.76	202.87
05/07/2012	1	0	3.92	177.44	5.64	177.93	5.46	194.06
06/07/2012	0	0	1.98	248.30	3.21	266.00	3.33	299.36
07/07/2012	0	0	2.96	259.33	3.82	311.95	4.57	322.44
08/07/2012	1	180	3.49	305.75	3.78	278.28	2.21	348.13
09/07/2012	1	0	2.41	234.52	6.00	185.44	3.46	276.03
10/07/2012	1	210	3.66	244.52	6.41	199.64	5.17	241.44
11/07/2012	1	210	4.46	206.65	5.91	186.35	5.94	216.71
12/07/2012	1	320	3.19	193.98	2.36	235.06	2.95	261.31
13/07/2012	1	320	2.15	288.72	3.26	306.65	2.88	340.61
14/07/2012	1	320	1.85	311.03	2.81	271.50	3.00	313.92
15/07/2012	0	0	2.06	278.26	3.94	284.17	2.85	298.72
16/07/2012	2	180	2.14	299.24	4.69	232.84	3.52	288.04
17/07/2012	1	0	2.44	333.30	3.31	255.74	3.82	281.54
18/07/2012	0	0	2.27	2.12	4.98	269.39	3.98	291.98
19/07/2012	1	210	4.63	247.87	7.85	261.41	5.50	272.35
20/07/2012	4	220	7.01	228.20	12.47	242.68	8.44	253.25
21/07/2012	3	220	8.44	216.70	12.60	224.22	9.11	230.49
22/07/2012	4	210	8.96	204.00	11.43	214.52	8.58	218.68
23/07/2012	3	210	8.73	198.54	10.65	204.58	7.93	205.99
24/07/2012	1	210	6.76	199.63	8.29	215.24	6.33	208.69
25/07/2012	1	210	5.61	227.32	9.94	236.29	6.39	246.07
26/07/2012	0	0	6.26	256.03	9.48	245.28	6.29	262.64
27/07/2012	1	320	7.68	261.95	10.62	232.41	7.16	261.45
28/07/2012	3	220	8.02	253.57	13.54	226.44	9.49	252.61
29/07/2012	3	220	9.09	249.49	16.20	235.90	10.33	253.47
30/07/2012	2	220	12.20	241.29	12.53	247.13	11.54	245.80
31/07/2012	4	220	11.61	236.64	12.91	241.46	11.87	241.47

Table 126. July 2012 wind data at Cuyo Island from onshore weather station and meoscale model output

Source Date	PAGASA		ERA-Interim		NCEP FNL		NCEP CFSR	
	Wind Speed (m/s)	Wind Direction (Degrees)	Wind Speed (m/s)	Wind Direction (Degrees)	Wind Speed (m/s)	Wind Direction (Degrees)	Wind Speed (m/s)	Wind Direction (Degrees)
01/07/2012	1	0	1.85	267.58	2.89	290.45	3.68	322.13
02/07/2012	1	320	5.13	294.01	13.70	269.69	8.69	304.62
03/07/2012	1	320	7.50	240.09	15.67	223.24	8.57	267.78
04/07/2012	3	220	8.10	191.41	11.14	188.50	8.95	205.55
05/07/2012	2	220	3.36	171.25	5.11	177.16	4.87	198.20
06/07/2012	3	220	2.37	306.26	5.51	258.52	4.55	306.52
07/07/2012	1	20	5.29	330.28	6.21	318.99	8.82	320.73
08/07/2012	1	20	6.33	318.25	4.54	273.87	5.92	289.17
09/07/2012	1	220	4.56	277.22	7.49	198.06	6.18	247.28
10/07/2012	1	220	3.69	229.97	6.99	190.77	5.64	226.85
11/07/2012	2	220	5.39	207.08	5.78	176.92	6.97	211.88
12/07/2012	1	220	3.67	217.22	2.40	251.39	2.80	240.10
13/07/2012	2	320	2.89	250.08	5.12	313.43	3.67	338.27
14/07/2012	0	0	2.81	268.89	6.33	305.51	4.50	319.52
15/07/2012	0	0	2.28	329.71	6.34	258.65	4.17	299.55
16/07/2012	2	220	3.05	280.18	4.34	231.23	3.92	282.14
17/07/2012	2	220	3.88	258.52	4.75	259.60	5.76	273.72
18/07/2012	1	220	3.53	254.74	7.06	270.02	7.13	289.44
19/07/2012	1	220	5.65	246.58	10.16	262.02	9.09	271.11
20/07/2012	3	220	7.64	221.53	13.30	238.87	9.80	245.97
21/07/2012	4	220	9.37	204.64	13.16	217.17	10.54	222.07
22/07/2012	4	220	10.00	204.63	12.14	208.24	10.05	218.36
23/07/2012	4	220	8.83	197.06	11.15	202.28	8.93	208.35
24/07/2012	3	220	7.10	198.27	9.58	211.39	7.39	206.94
25/07/2012	2	220	6.20	224.37	9.99	229.95	6.99	246.46
26/07/2012	1	220	7.60	248.61	10.94	242.06	9.04	263.28
27/07/2012	2	220	9.58	256.21	12.12	231.74	10.16	259.71
28/07/2012	5	220	10.83	234.84	15.59	222.02	12.52	240.23
29/07/2012	4	320	12.51	238.60	18.00	226.84	14.59	243.08
30/07/2012	4	220	14.03	228.46	15.80	232.73	14.24	235.59
31/07/2012	5	220	13.35	225.09	15.37	233.08	14.10	228.93

Table 127. July 2012 wind data at Puerto Princesa from onshore weather station and meoscale model output

Source Date	PAGASA		ERA-Interim		NCEP FNL		NCEP CFSR	
	Wind Speed (m/s)	Wind Direction (Degrees)	Wind Speed (m/s)	Wind Direction (Degrees)	Wind Speed (m/s)	Wind Direction (Degrees)	Wind Speed (m/s)	Wind Direction (Degrees)
01/07/2012	2	270	3.22	175.41	2.22	196.24	2.21	183.05
02/07/2012	2	180	2.73	161.73	2.02	267.40	1.29	63.83
03/07/2012	2	290	4.31	187.90	5.17	232.26	3.06	221.55
04/07/2012	2	320	4.94	192.76	6.99	190.58	3.86	202.31
05/07/2012	3	180	4.82	183.95	4.12	193.16	3.73	204.51
06/07/2012	3	290	2.83	184.40	2.56	193.74	1.72	187.33
07/07/2012	2	0	2.45	153.84	1.53	101.07	2.14	340.40
08/07/2012	3	90	2.50	143.31	1.94	143.05	1.90	257.91
09/07/2012	1	270	3.26	263.02	2.14	216.83	2.30	216.19
10/07/2012	1	270	2.90	189.72	3.29	204.36	3.26	227.64
11/07/2012	3	140	3.59	228.37	3.57	204.52	2.83	211.83
12/07/2012	2	160	3.78	196.37	2.10	209.75	2.55	225.46
13/07/2012	2	270	3.19	170.62	2.13	141.53	1.76	183.98
14/07/2012	2	70	2.72	189.66	3.11	192.68	1.83	218.12
15/07/2012	2	290	2.42	174.68	1.68	155.74	1.93	264.80
16/07/2012	3	180	2.49	212.00	1.45	162.41	1.77	230.62
17/07/2012	2	270	2.83	199.00	2.48	196.40	1.80	182.11
18/07/2012	2	180	2.70	172.34	2.61	231.14	2.23	205.70
19/07/2012	3	270	3.66	203.19	4.56	245.65	3.53	239.16
20/07/2012	3	270	4.09	198.52	4.98	235.44	4.68	232.53
21/07/2012	2	180	5.01	193.92	5.76	208.29	4.40	203.55
22/07/2012	3	180	6.58	193.60	6.89	202.65	5.36	199.92
23/07/2012	3	180	5.90	195.01	6.17	197.61	4.94	199.74
24/07/2012	2	180	4.15	188.00	5.05	198.67	4.11	197.92
25/07/2012	3	180	4.16	182.19	4.38	206.34	3.59	206.29
26/07/2012	2	270	3.71	249.45	4.18	235.18	3.85	240.69
27/07/2012	3	270	4.05	241.50	4.40	226.85	4.21	237.18
28/07/2012	2	270	5.72	239.01	6.08	223.31	4.63	234.79
29/07/2012	4	280	7.58	239.87	7.78	238.60	5.36	234.38
30/07/2012	4	270	7.26	232.13	6.27	231.46	5.72	227.09
31/07/2012	4	270	6.63	214.96	6.34	230.20	6.03	228.86

Table 128. August 2012 wind data at Coron Island from onshore weather station and meoscale model output

Source Date	PAGASA		ERA-Interim		NCEP FNL		NCEP CFSR	
	Wind Speed (m/s)	Wind Direction (Degrees)	Wind Speed (m/s)	Wind Direction (Degrees)	Wind Speed (m/s)	Wind Direction (Degrees)	Wind Speed (m/s)	Wind Direction (Degrees)
01/08/2012	4	220	11.05	229.28	12.15	230.94	11.15	229.48
02/08/2012	4	220	9.95	225.47	11.33	226.40	10.53	223.40
03/08/2012	3	220	8.97	228.25	10.70	230.55	9.89	226.61
04/08/2012	2	220	8.10	225.82	10.72	228.65	9.70	218.16
05/08/2012	3	220	7.99	213.18	10.21	227.70	9.25	219.95
06/08/2012	2	220	7.92	206.96	10.02	230.08	8.75	210.20
07/08/2012	3	220	7.20	216.03	9.83	228.26	8.47	229.97
08/08/2012	2	220	7.39	221.40	8.97	227.06	7.52	226.32
09/08/2012	2	220	5.20	199.65	7.18	222.32	6.40	218.36
10/08/2012	1	0	3.77	202.30	5.75	238.55	5.20	214.00
11/08/2012	1	180	3.30	205.06	6.86	240.36	4.30	226.65
12/08/2012	1	210	3.08	220.75	8.54	238.22	5.06	241.19
13/08/2012	1	220	5.85	237.75	9.53	235.57	6.72	238.85
14/08/2012	4	220	8.10	232.35	10.46	225.00	8.81	231.56
15/08/2012	2	220	8.42	204.54	10.74	216.38	8.58	213.89
16/08/2012	1	220	7.03	186.81	8.69	196.60	8.09	193.06
17/08/2012	2	220	3.27	190.67	3.19	222.94	4.22	192.22
18/08/2012	1	40	2.11	277.58	4.02	265.45	2.84	300.84
19/08/2012	1	220	2.80	242.01	7.58	266.89	4.66	271.04
20/08/2012	1	320	5.31	210.96	8.57	256.66	6.66	252.66
21/08/2012	2	0	5.91	211.06	8.49	245.29	7.66	236.41
22/08/2012	1	220	5.62	219.51	7.50	241.88	6.97	229.27
23/08/2012	2	210	5.83	224.04	6.98	243.56	7.35	227.36
24/08/2012	1	210	5.62	227.43	7.24	244.86	7.13	234.75
25/08/2012	0	0	5.91	226.43	7.30	239.02	6.73	238.98
26/08/2012	2	220	6.32	220.54	8.41	231.48	7.17	230.11
27/08/2012	1	210	6.56	197.76	7.28	228.12	7.41	220.82
28/08/2012	1	210	4.10	196.47	5.09	222.42	4.74	206.99
29/08/2012	1	0	2.93	209.07	5.56	246.51	3.57	228.22
30/08/2012	1	0	3.63	226.78	8.53	254.87	4.05	242.02
31/08/2012	1	210	5.75	214.18	3.80	199.50	5.97	244.65

Table 129. August 2012 wind data at Cuyo Island from onshore weather station and meoscale model output

Source Date	PAGASA		ERA-Interim		NCEP FNL		NCEP CFSR	
	Wind Speed (m/s)	Wind Direction (Degrees)	Wind Speed (m/s)	Wind Direction (Degrees)	Wind Speed (m/s)	Wind Direction (Degrees)	Wind Speed (m/s)	Wind Direction (Degrees)
01/08/2012	3	220	12.45	219.00	13.89	226.83	13.46	221.99
02/08/2012	4	220	10.69	213.70	13.46	222.29	12.61	215.79
03/08/2012	4	220	10.27	217.29	12.28	224.26	11.29	222.42
04/08/2012	3	220	9.64	212.94	12.15	222.52	10.99	211.89
05/08/2012	3	220	9.13	209.45	11.98	220.39	10.24	210.27
06/08/2012	3	220	9.23	210.74	11.18	224.64	9.71	213.89
07/08/2012	3	220	8.03	211.52	10.47	220.75	9.05	221.61
08/08/2012	4	220	8.11	210.44	9.32	218.64	8.09	217.38
09/08/2012	2	220	6.13	207.40	7.58	215.06	6.86	212.24
10/08/2012	2	220	4.98	209.44	6.28	229.00	5.79	216.12
11/08/2012	2	220	4.86	222.17	6.63	240.94	4.93	226.80
12/08/2012	1	220	4.92	226.81	8.33	241.54	5.50	243.48
13/08/2012	2	220	6.97	233.29	9.56	231.40	6.56	244.26
14/08/2012	3	220	9.24	220.64	11.03	222.45	9.01	223.06
15/08/2012	5	220	9.27	203.67	11.51	205.82	9.60	203.47
16/08/2012	3	220	6.74	188.87	8.35	198.93	8.08	195.92
17/08/2012	2	220	3.25	200.09	5.16	224.99	4.57	202.36
18/08/2012	1	220	2.54	249.08	6.38	257.64	4.01	255.96
19/08/2012	1	220	3.45	243.91	9.63	261.50	5.83	268.88
20/08/2012	1	0	5.84	214.44	10.65	251.72	6.70	241.93
21/08/2012	1	220	6.74	214.38	9.64	234.61	8.65	228.53
22/08/2012	1	270	7.20	216.16	9.02	233.79	8.14	219.50
23/08/2012	3	220	7.39	218.33	9.32	232.08	8.14	224.86
24/08/2012	2	220	6.68	217.76	8.46	236.63	8.01	229.88
25/08/2012	2	220	6.29	218.92	7.60	237.37	7.47	230.20
26/08/2012	2	220	6.82	212.87	8.47	228.12	7.76	219.81
27/08/2012	1	220	6.57	202.07	7.49	223.49	7.85	211.86
28/08/2012	2	220	4.32	203.71	5.82	220.07	4.85	209.15
29/08/2012	0	0	2.79	234.62	4.98	245.69	3.51	225.38
30/08/2012	1	0	3.09	247.76	9.34	246.38	3.65	249.70
31/08/2012	0	0	3.97	221.75	2.90	251.69	5.81	251.02

Table 130. August 2012 wind data at Puerto Princesa from onshore weather station and meoscale model output

Source Date	PAGASA		ERA-Interim		NCEP FNL		NCEP CFSR	
	Wind Speed (m/s)	Wind Direction (Degrees)	Wind Speed (m/s)	Wind Direction (Degrees)	Wind Speed (m/s)	Wind Direction (Degrees)	Wind Speed (m/s)	Wind Direction (Degrees)
01/08/2012	3	270	6.32	199.41	4.95	210.41	5.03	208.14
02/08/2012	2	200	7.07	192.65	5.97	203.00	5.34	203.49
03/08/2012	2	180	5.88	192.31	5.44	211.93	4.97	200.97
04/08/2012	2	180	5.87	191.40	5.13	200.01	5.33	199.54
05/08/2012	2	220	5.39	195.16	5.25	203.99	5.14	198.07
06/08/2012	3	220	5.58	196.48	4.99	204.02	4.83	197.73
07/08/2012	2	240	5.49	194.74	4.60	206.72	4.23	203.45
08/08/2012	3	180	5.54	192.76	4.82	198.39	4.26	204.82
09/08/2012	2	240	5.10	196.03	4.07	198.73	4.29	206.32
10/08/2012	2	240	3.72	190.01	3.24	189.33	2.84	211.24
11/08/2012	3	180	3.83	177.86	3.22	200.70	3.28	194.20
12/08/2012	3	140	3.79	178.27	3.99	213.38	3.80	196.14
13/08/2012	3	270	4.45	184.85	4.18	230.03	3.22	203.06
14/08/2012	4	270	5.15	193.10	4.11	209.84	3.91	200.59
15/08/2012	3	180	5.00	190.33	5.48	198.51	4.60	205.70
16/08/2012	2	180	5.10	188.99	4.71	196.40	4.46	206.89
17/08/2012	2	180	4.61	187.58	3.46	197.78	3.83	208.93
18/08/2012	3	270	3.46	165.62	2.52	212.35	2.48	199.00
19/08/2012	2	320	3.15	187.55	3.29	252.00	1.74	182.12
20/08/2012	3	180	3.73	174.76	4.13	244.03	2.66	211.98
21/08/2012	3	290	4.46	185.69	3.60	233.14	3.63	199.79
22/08/2012	2	180	4.59	197.00	3.04	210.62	3.68	204.82
23/08/2012	1	270	4.52	192.15	2.98	212.80	3.68	204.00
24/08/2012	2	160	4.53	191.64	2.98	199.53	3.79	200.03
25/08/2012	2	140	3.87	191.65	3.00	228.30	3.28	211.51
26/08/2012	2	160	4.93	188.91	3.42	197.61	3.54	201.05
27/08/2012	2	180	4.21	201.03	3.86	201.33	4.31	207.18
28/08/2012	2	160	3.14	210.25	2.47	221.04	3.44	206.98
29/08/2012	2	220	3.28	172.77	2.54	206.63	2.68	203.94
30/08/2012	3	270	3.14	167.48	3.80	241.28	2.13	198.47
31/08/2012	2	270	3.71	191.58	2.62	191.43	2.55	213.96

Table 131. September 2012 wind data at Coron Island from onshore weather station and meoscale model output

Source Date	PAGASA		ERA-Interim		NCEP FNL		NCEP CFSR	
	Wind Speed (m/s)	Wind Direction (Degrees)	Wind Speed (m/s)	Wind Direction (Degrees)	Wind Speed (m/s)	Wind Direction (Degrees)	Wind Speed (m/s)	Wind Direction (Degrees)
01/09/2012	2	210	5.12	201.93	5.95	225.65	4.24	227.20
02/09/2012	2	0	5.28	209.51	6.67	218.98	4.69	244.09
03/09/2012	1	0	3.58	200.33	7.31	218.35	4.97	234.23
04/09/2012	1	210	2.58	189.41	5.46	208.36	3.60	242.39
05/09/2012	1	210	1.71	330.96	4.65	154.03	2.37	180.59
06/09/2012	1	0	2.60	294.61	2.90	356.19	2.45	305.16
07/09/2012	1	320	3.55	301.07	5.40	322.62	3.37	301.17
08/09/2012	1	180	2.40	278.07	2.82	9.48	2.37	289.62
09/09/2012	1	180	1.99	293.47	7.13	167.54	3.67	239.90
10/09/2012	1	220	3.48	220.08	9.97	201.33	5.40	228.46
11/09/2012	1	0	4.32	243.67	10.60	196.13	6.15	240.63
12/09/2012	2	210	4.68	237.19	10.85	210.06	7.72	239.99
13/09/2012	4	210	7.68	237.39	9.99	221.76	7.90	237.80
14/09/2012	3	220	8.36	224.46	10.43	219.67	8.75	223.81
15/09/2012	2	270	8.86	221.92	10.58	210.78	9.17	217.09
16/09/2012	2	210	7.84	233.22	9.48	201.49	8.36	231.32
17/09/2012	1	210	5.61	249.70	6.91	213.69	4.69	266.28
18/09/2012	1	0	3.85	226.84	6.20	220.28	4.92	264.78
19/09/2012	1	0	3.05	212.29	5.84	207.63	4.27	251.55
20/09/2012	0	0	1.94	146.03	3.82	217.52	2.60	264.18
21/09/2012	0	0	2.38	306.54	4.81	230.11	3.30	282.26
22/09/2012	1	0	3.48	288.47	4.27	283.30	4.48	287.30
23/09/2012	1	0	3.20	293.07	4.00	254.39	4.30	286.11
24/09/2012	1	210	2.14	283.42	4.00	262.00	3.58	284.52
25/09/2012	1	210	3.27	265.32	3.83	267.92	2.92	294.38
26/09/2012	3	220	4.42	261.24	8.43	260.90	4.99	269.80
27/09/2012	3	220	6.93	250.31	9.00	246.11	7.22	251.28
28/09/2012	3	210	6.57	239.65	8.55	238.18	7.08	233.33
29/09/2012	1	210	4.27	236.88	7.13	242.83	5.86	241.82
30/09/2012	1	210	3.66	204.07	6.51	235.88	4.80	229.05

Table 132. September 2012 wind data at Cuyo Island from onshore weather station and meoscale model output

Source Date	PAGASA		ERA-Interim		NCEP FNL		NCEP CFSR	
	Wind Speed (m/s)	Wind Direction (Degrees)	Wind Speed (m/s)	Wind Direction (Degrees)	Wind Speed (m/s)	Wind Direction (Degrees)	Wind Speed (m/s)	Wind Direction (Degrees)
01/09/2012	1	220	6.14	229.28	8.41	229.29	4.57	240.16
02/09/2012	0	0	7.64	216.77	8.39	208.84	6.51	249.32
03/09/2012	1	220	4.83	210.27	8.43	219.27	4.82	229.72
04/09/2012	1	220	3.35	225.83	7.00	198.17	4.84	247.55
05/09/2012	1	220	2.20	229.88	5.17	160.38	2.84	224.34
06/09/2012	0	0	2.40	310.25	2.70	308.55	3.55	304.69
07/09/2012	2	0	5.33	334.43	8.87	327.91	7.94	314.97
08/09/2012	1	0	5.21	332.83	8.04	16.06	5.33	348.26
09/09/2012	0	0	3.47	282.85	9.03	214.89	5.13	238.71
10/09/2012	1	220	4.01	248.38	11.04	201.54	7.79	242.23
11/09/2012	2	320	4.94	258.85	10.50	197.23	7.14	252.18
12/09/2012	1	320	5.19	249.97	10.27	212.98	8.06	246.63
13/09/2012	2	220	7.72	239.29	10.79	227.50	8.64	240.58
14/09/2012	3	220	8.94	219.10	10.57	223.26	9.41	224.63
15/09/2012	4	220	10.65	209.92	12.06	210.53	10.70	214.24
16/09/2012	3	220	8.53	227.27	9.96	205.99	9.71	221.14
17/09/2012	1	220	5.77	261.20	8.75	227.64	6.48	266.81
18/09/2012	1	320	3.16	224.66	6.68	232.17	4.92	276.53
19/09/2012	1	180	1.65	214.63	6.86	236.07	4.37	263.02
20/09/2012	1	220	2.66	222.98	5.84	214.27	2.22	278.79
21/09/2012	1	0	4.68	319.14	7.83	232.60	4.25	298.12
22/09/2012	1	320	7.57	302.21	7.27	269.52	8.21	292.86
23/09/2012	2	320	5.76	302.20	6.12	254.64	8.65	288.22
24/09/2012	1	220	3.64	287.80	7.87	253.06	7.61	268.47
25/09/2012	1	220	5.19	274.08	9.56	241.64	9.10	252.95
26/09/2012	3	220	7.14	266.26	12.44	253.87	10.15	258.82
27/09/2012	4	220	7.95	250.73	10.95	244.21	9.11	251.78
28/09/2012	1	220	6.35	237.68	8.95	232.40	7.99	229.14
29/09/2012	1	220	5.89	229.88	7.32	241.60	5.96	237.96
30/09/2012	1	220	5.32	226.88	7.92	232.46	6.66	229.27

Table 133. September 2012 wind data at Puerto Princesa from onshore weather station and meoscale model output

Source Date	PAGASA		ERA-Interim		NCEP FNL		NCEP CFSR	
	Wind Speed (m/s)	Wind Direction (Degrees)	Wind Speed (m/s)	Wind Direction (Degrees)	Wind Speed (m/s)	Wind Direction (Degrees)	Wind Speed (m/s)	Wind Direction (Degrees)
01/09/2012	2	290	4.11	189.80	4.75	204.92	2.70	204.29
02/09/2012	2	180	4.46	195.24	5.01	202.15	2.99	202.11
03/09/2012	2	290	4.07	190.07	4.68	204.60	3.40	197.85
04/09/2012	2	160	3.74	192.40	3.56	200.00	3.43	212.00
05/09/2012	3	180	3.59	176.43	3.50	198.34	3.22	212.29
06/09/2012	2	270	2.70	159.64	2.41	170.93	2.65	87.92
07/09/2012	4	340	2.82	324.46	4.34	329.40	3.42	342.73
08/09/2012	2	320	2.24	347.98	3.97	290.65	2.30	300.90
09/09/2012	1	270	2.57	174.25	3.79	214.02	2.60	208.62
10/09/2012	2	290	3.12	183.17	4.83	215.81	4.43	233.52
11/09/2012	3	270	2.66	242.82	6.42	205.81	3.96	241.27
12/09/2012	2	270	3.26	209.62	4.12	208.12	4.21	237.33
13/09/2012	4	270	4.53	232.33	4.95	221.00	4.27	226.93
14/09/2012	3	270	6.95	192.35	4.65	212.91	3.91	219.75
15/09/2012	2	270	6.12	193.30	5.62	202.95	4.42	199.62
16/09/2012	2	270	4.99	208.19	4.96	200.10	4.08	204.69
17/09/2012	3	270	4.69	252.50	3.80	199.26	3.24	259.26
18/09/2012	3	320	2.70	212.77	3.28	249.52	2.24	256.13
19/09/2012	2	250	3.32	180.31	2.86	211.37	1.89	226.78
20/09/2012	3	320	3.44	176.29	2.84	194.37	2.48	210.57
21/09/2012	2	180	2.34	169.98	3.06	237.42	1.36	143.37
22/09/2012	2	320	2.02	196.18	3.19	245.46	1.73	249.33
23/09/2012	1	250	2.90	180.65	4.32	236.35	3.03	238.20
24/09/2012	3	270	2.36	191.83	2.40	320.06	4.86	233.05
25/09/2012	2	280	2.51	178.83	5.51	235.27	4.88	233.58
26/09/2012	3	250	3.68	256.17	5.77	249.73	4.44	253.43
27/09/2012	3	250	5.07	249.28	4.38	243.09	4.22	248.07
28/09/2012	3	270	3.23	199.09	3.46	201.21	4.35	200.55
29/09/2012	2	140	4.53	191.56	3.18	245.53	2.76	240.60
30/09/2012	2	180	4.07	188.39	4.33	196.41	4.16	198.14

Table 134. October 2012 wind data at Coron Island from onshore weather station and meoscale model output

Source Date	PAGASA		ERA-Interim		NCEP FNL		NCEP CFSR	
	Wind Speed (m/s)	Wind Direction (Degrees)	Wind Speed (m/s)	Wind Direction (Degrees)	Wind Speed (m/s)	Wind Direction (Degrees)	Wind Speed (m/s)	Wind Direction (Degrees)
01/10/2012	1	180	5.29	198.55	6.92	222.19	5.45	209.88
02/10/2012	2	210	7.06	220.06	8.32	231.70	7.50	233.42
03/10/2012	3	210	8.27	223.41	9.73	227.45	9.96	229.77
04/10/2012	1	210	5.99	210.34	9.64	207.93	8.27	231.41
05/10/2012	0	0	4.78	202.68	5.28	228.92	2.92	262.19
06/10/2012	1	0	4.07	110.03	2.62	19.87	2.08	296.20
07/10/2012	1	210	2.39	97.99	2.20	293.90	1.84	358.22
08/10/2012	1	0	1.85	89.29	3.07	300.90	2.67	313.66
09/10/2012	1	0	2.44	273.44	3.23	302.79	2.99	281.67
10/10/2012	1	180	2.85	258.12	2.10	232.64	2.94	260.59
11/10/2012	1	210	3.30	231.31	3.78	173.75	2.48	296.09
12/10/2012	1	0	2.74	219.79	3.23	205.72	2.37	9.55
13/10/2012	1	0	3.66	249.10	4.60	203.03	3.22	217.76
14/10/2012	1	0	2.36	240.48	6.42	201.99	3.71	202.84
15/10/2012	1	320	2.33	272.08	5.88	220.22	4.17	170.81
16/10/2012	1	0	1.90	52.67	3.00	215.79	3.70	138.69
17/10/2012	1	0	2.32	57.08	3.17	169.86	4.30	109.80
18/10/2012	1	120	5.62	86.49	4.67	98.26	5.26	123.02
19/10/2012	2	0	3.14	72.61	3.16	68.58	3.65	73.90
20/10/2012	1	0	4.31	76.17	5.55	72.09	4.40	50.72
21/10/2012	3	40	7.02	73.46	7.73	80.38	7.81	82.62
22/10/2012	2	0	3.30	73.59	6.65	74.23	5.09	69.64
23/10/2012	1	320	2.30	54.34	3.03	4.22	3.18	355.89
24/10/2012	1	0	6.65	352.92	10.09	343.93	7.04	349.10
25/10/2012	3	180	10.57	213.17	15.04	199.21	8.80	190.37
26/10/2012	2	140	5.81	114.01	6.36	117.35	6.15	123.67
27/10/2012	3	40	5.47	84.37	5.51	79.39	5.28	74.94
28/10/2012	1	40	5.89	77.43	6.21	79.20	7.07	75.36
29/10/2012	3	120	8.19	81.42	9.27	83.43	8.78	83.46
30/10/2012	2	40	6.02	79.65	7.56	81.64	5.06	70.85
31/10/2012	2	40	4.15	73.90	4.81	59.47	4.33	58.91

Table 135. October 2012 wind data at Cuyo Island from onshore weather station and meoscale model output

Source Date	PAGASA		ERA-Interim		NCEP FNL		NCEP CFSR	
	Wind Speed (m/s)	Wind Direction (Degrees)	Wind Speed (m/s)	Wind Direction (Degrees)	Wind Speed (m/s)	Wind Direction (Degrees)	Wind Speed (m/s)	Wind Direction (Degrees)
01/10/2012	1	220	5.68	204.26	7.66	224.82	6.63	226.54
02/10/2012	4	220	8.66	220.23	8.69	238.00	8.70	236.03
03/10/2012	4	220	9.35	221.06	10.24	229.57	10.48	230.90
04/10/2012	4	220	8.20	210.68	10.35	208.13	9.36	230.35
05/10/2012	2	220	6.31	213.09	6.91	215.23	6.25	256.62
06/10/2012	1	20	4.13	302.13	5.66	301.59	5.41	309.34
07/10/2012	2	20	2.59	22.49	4.12	321.79	3.96	295.69
08/10/2012	0	0	2.57	278.68	6.37	284.07	4.27	294.78
09/10/2012	1	0	3.75	279.95	5.11	292.34	4.77	292.20
10/10/2012	1	320	3.90	258.69	4.23	258.07	4.84	270.57
11/10/2012	2	220	5.53	223.76	6.77	208.83	6.04	231.29
12/10/2012	0	0	6.89	192.34	7.35	217.25	6.86	221.16
13/10/2012	2	220	7.42	219.22	8.41	214.18	7.20	223.59
14/10/2012	0	0	3.86	223.46	7.35	212.07	4.91	218.27
15/10/2012	1	0	1.70	240.28	6.06	216.30	5.15	206.84
16/10/2012	1	0	1.50	105.32	5.56	213.56	5.43	185.47
17/10/2012	1	0	2.40	129.86	3.91	180.69	6.62	166.10
18/10/2012	1	0	5.90	39.77	3.82	51.43	3.88	90.07
19/10/2012	1	20	8.99	37.16	6.29	37.41	6.76	34.56
20/10/2012	4	20	9.84	38.00	8.32	42.92	9.00	37.92
21/10/2012	4	20	9.89	42.90	7.40	48.28	5.85	57.76
22/10/2012	4	20	9.34	36.56	9.26	40.98	7.26	35.97
23/10/2012	4	20	9.80	21.89	11.43	24.87	10.62	20.89
24/10/2012	5	320	11.15	343.56	14.92	318.56	11.54	337.19
25/10/2012	4	120	11.03	192.96	13.33	187.71	11.94	186.09
26/10/2012	3	20	4.89	100.76	5.31	100.65	5.33	105.28
27/10/2012	3	20	8.04	42.46	8.41	44.02	7.18	39.63
28/10/2012	3	20	7.85	43.53	6.49	48.56	5.97	53.60
29/10/2012	3	20	8.16	47.98	6.03	53.91	6.55	51.85
30/10/2012	2	20	8.20	42.53	6.35	45.01	6.87	44.93
31/10/2012	3	20	7.37	41.10	5.45	36.41	5.73	30.40

Table 136. October 2012 wind data at Puerto Princesa from onshore weather station and meoscale model output

Source Date	PAGASA		ERA-Interim		NCEP FNL		NCEP CFSR	
	Wind Speed (m/s)	Wind Direction (Degrees)	Wind Speed (m/s)	Wind Direction (Degrees)	Wind Speed (m/s)	Wind Direction (Degrees)	Wind Speed (m/s)	Wind Direction (Degrees)
01/10/2012	2	180	4.89	186.69	4.10	193.67	4.30	192.17
02/10/2012	3	180	5.67	187.31	4.95	241.24	3.53	197.39
03/10/2012	4	280	4.96	199.52	5.92	242.37	5.14	235.14
04/10/2012	3	270	5.61	194.51	4.54	204.51	4.17	233.08
05/10/2012	2	250	5.11	191.15	4.68	197.01	3.91	224.33
06/10/2012	2	280	4.28	185.22	3.13	192.74	2.39	249.63
07/10/2012	2	270	2.38	163.15	2.58	194.45	2.20	231.07
08/10/2012	4	270	2.70	298.98	2.32	251.41	2.72	235.77
09/10/2012	2	320	2.45	167.43	1.90	277.12	2.28	257.54
10/10/2012	2	280	2.67	181.82	2.04	190.44	2.98	246.82
11/10/2012	3	320	3.20	181.49	3.53	198.93	2.80	318.62
12/10/2012	2	280	3.29	136.82	2.30	211.80	1.94	240.20
13/10/2012	2	160	2.47	201.16	4.02	196.95	2.99	209.33
14/10/2012	2	270	2.66	198.51	3.52	201.57	3.17	204.06
15/10/2012	2	320	3.15	183.29	2.91	184.57	2.55	197.48
16/10/2012	2	160	3.23	179.98	1.77	178.86	2.48	183.06
17/10/2012	3	90	3.13	175.20	2.33	173.66	2.65	212.09
18/10/2012	2	90	2.62	148.58	2.80	166.89	3.60	209.25
19/10/2012	2	70	2.97	69.03	1.94	96.23	2.14	33.89
20/10/2012	4	90	4.12	61.18	4.34	77.58	3.17	49.60
21/10/2012	4	70	5.95	66.53	3.33	87.34	4.15	79.21
22/10/2012	3	80	3.92	64.42	2.96	76.83	2.18	114.42
23/10/2012	3	320	3.95	33.95	3.16	6.52	3.15	5.58
24/10/2012	4	0	4.65	329.72	6.17	324.26	4.85	322.35
25/10/2012	2	240	3.71	235.48	5.76	209.28	3.75	226.81
26/10/2012	1	220	4.44	162.86	3.62	163.12	4.19	177.15
27/10/2012	2	90	2.57	100.50	2.07	97.17	2.21	106.79
28/10/2012	2	90	3.08	76.39	4.21	82.26	2.93	60.11
29/10/2012	2	90	5.11	80.12	4.21	89.38	4.61	96.11
30/10/2012	2	90	3.03	87.05	3.71	73.63	3.86	67.27
31/10/2012	3	90	3.15	87.94	2.89	80.43	2.97	70.54

Table 137. November 2012 wind data at Coron Island from onshore weather station and meoscale model output

Source Date	PAGASA		ERA-Interim		NCEP FNL		NCEP CFSR	
	Wind Speed (m/s)	Wind Direction (Degrees)	Wind Speed (m/s)	Wind Direction (Degrees)	Wind Speed (m/s)	Wind Direction (Degrees)	Wind Speed (m/s)	Wind Direction (Degrees)
01/11/2012	1	0	4.09	84.97	3.98	66.72	3.44	58.20
02/11/2012	1	0	3.62	80.32	2.22	65.42	2.91	76.19
03/11/2012	2	0	3.27	80.77	3.32	61.11	3.95	68.90
04/11/2012	2	40	3.86	77.53	4.84	81.80	5.11	83.33
05/11/2012	1	0	3.43	70.51	3.80	72.41	3.48	64.80
06/11/2012	1	0	3.51	90.95	3.66	63.46	2.22	63.32
07/11/2012	1	0	3.89	82.63	4.39	74.49	3.88	80.22
08/11/2012	1	0	4.43	86.15	4.46	72.79	3.71	64.87
09/11/2012	2	40	7.03	88.53	7.25	81.60	7.13	85.42
10/11/2012	2	40	3.87	83.86	5.48	69.42	4.78	66.22
11/11/2012	1	40	5.25	51.24	5.47	49.59	5.01	45.17
12/11/2012	3	40	8.54	78.73	9.53	79.63	7.97	79.77
13/11/2012	2	120	6.45	80.08	9.12	76.90	7.55	93.76
14/11/2012	3	40	5.36	89.75	9.02	89.61	6.91	90.45
15/11/2012	1	0	4.59	85.23	6.61	85.67	4.72	67.50
16/11/2012	1	40	8.56	84.82	9.28	83.84	8.81	83.81
17/11/2012	1	0	5.80	80.59	6.36	74.73	6.54	72.99
18/11/2012	2	0	5.90	82.95	6.23	82.31	6.25	81.66
19/11/2012	2	140	4.13	84.35	5.87	78.94	5.34	72.51
20/11/2012	3	40	7.31	85.52	8.16	83.39	7.33	84.59
21/11/2012	2	40	8.09	85.71	8.89	82.85	7.89	87.19
22/11/2012	2	40	8.04	86.20	9.36	83.83	7.12	86.03
23/11/2012	2	40	5.28	83.11	6.82	78.19	6.15	80.72
24/11/2012	2	40	6.68	84.64	7.07	79.14	6.26	77.95
25/11/2012	4	40	8.15	83.21	9.13	80.68	8.82	82.34
26/11/2012	2	40	5.36	81.74	6.39	67.89	5.94	69.23
27/11/2012	2	40	8.36	84.11	8.96	82.04	8.93	82.12
28/11/2012	3	40	7.87	83.16	9.83	82.13	8.49	82.42
29/11/2012	3	40	8.84	85.47	9.13	77.22	9.11	80.21
30/11/2012	2	40	7.23	81.86	8.96	77.43	8.65	76.32

Table 138. November 2012 wind data at Cuyo Island from onshore weather station and meoscale model output

Source Date	PAGASA		ERA-Interim		NCEP FNL		NCEP CFSR	
	Wind Speed (m/s)	Wind Direction (Degrees)	Wind Speed (m/s)	Wind Direction (Degrees)	Wind Speed (m/s)	Wind Direction (Degrees)	Wind Speed (m/s)	Wind Direction (Degrees)
01/11/2012	3	20	7.02	42.13	7.43	40.32	7.16	40.83
02/11/2012	2	20	7.77	40.22	6.81	40.54	6.96	38.29
03/11/2012	1	20	6.31	33.94	5.80	33.83	6.68	36.51
04/11/2012	2	20	4.31	27.04	4.37	41.87	5.13	42.46
05/11/2012	1	20	5.78	26.93	5.88	26.92	5.75	23.06
06/11/2012	2	0	8.14	32.39	7.37	37.35	7.04	34.72
07/11/2012	2	20	8.71	36.34	8.56	39.77	6.93	41.56
08/11/2012	2	20	7.64	38.87	7.94	41.75	5.68	50.57
09/11/2012	2	20	5.95	44.92	6.22	48.01	5.36	50.05
10/11/2012	3	20	7.53	32.48	7.54	37.75	7.17	33.63
11/11/2012	3	20	10.59	35.28	10.25	35.16	10.54	34.31
12/11/2012	3	20	8.20	54.03	8.62	50.37	7.27	51.90
13/11/2012	2	20	4.65	61.49	7.55	46.11	2.86	85.85
14/11/2012	2	20	4.84	52.98	4.16	74.86	5.04	51.73
15/11/2012	3	20	7.99	37.80	6.34	41.38	8.08	36.65
16/11/2012	2	20	6.60	48.06	6.43	54.45	6.83	49.16
17/11/2012	3	20	7.63	41.78	7.04	44.37	6.74	45.02
18/11/2012	2	20	7.29	43.38	7.10	43.13	7.05	41.88
19/11/2012	2	20	7.81	36.56	7.69	39.80	6.55	37.79
20/11/2012	2	20	7.79	46.81	7.69	47.39	4.90	52.64
21/11/2012	2	20	6.43	48.50	5.94	60.85	3.78	69.54
22/11/2012	2	20	5.11	53.44	5.60	55.29	3.69	54.28
23/11/2012	2	20	6.50	38.79	5.92	39.13	4.91	40.37
24/11/2012	2	20	8.35	45.66	8.93	45.55	8.13	45.90
25/11/2012	2	20	8.66	48.26	10.01	45.75	8.79	46.97
26/11/2012	2	20	7.88	40.43	8.80	43.66	8.12	42.91
27/11/2012	2	20	7.67	49.29	7.86	54.20	6.67	51.34
28/11/2012	2	20	7.17	46.00	7.43	49.75	5.67	49.87
29/11/2012	2	20	7.60	48.68	8.67	49.47	7.24	49.86
30/11/2012	2	20	7.68	46.14	8.15	50.04	7.75	45.91

Table 139. November 2012 wind data at Puerto Princesa from onshore weather station and meoscale model output

Source Date	PAGASA		ERA-Interim		NCEP FNL		NCEP CFSR	
	Wind Speed (m/s)	Wind Direction (Degrees)	Wind Speed (m/s)	Wind Direction (Degrees)	Wind Speed (m/s)	Wind Direction (Degrees)	Wind Speed (m/s)	Wind Direction (Degrees)
01/11/2012	2	90	3.37	74.62	3.15	75.60	2.93	73.08
02/11/2012	2	270	3.21	81.31	3.39	78.39	2.90	69.75
03/11/2012	2	90	3.37	64.27	2.47	62.89	2.62	52.82
04/11/2012	4	90	3.31	71.65	2.33	62.58	3.92	66.40
05/11/2012	2	90	3.21	62.66	2.37	71.20	1.82	71.84
06/11/2012	2	290	3.44	34.02	2.64	50.34	2.73	11.96
07/11/2012	3	90	3.80	64.10	3.63	64.55	3.48	65.60
08/11/2012	2	90	3.60	44.89	4.09	56.95	3.28	75.03
09/11/2012	3	90	3.23	82.63	4.22	80.71	3.13	87.22
10/11/2012	3	70	3.49	70.17	3.50	65.98	3.25	71.68
11/11/2012	3	0	4.84	29.22	4.30	21.04	3.35	13.91
12/11/2012	6	80	7.11	85.44	6.96	73.89	6.70	84.56
13/11/2012	6	110	3.88	106.38	3.93	88.46	4.28	119.95
14/11/2012	3	90	3.13	167.48	2.54	163.04	2.47	152.64
15/11/2012	2	110	3.09	66.39	1.99	78.16	2.61	57.06
16/11/2012	2	90	3.37	71.30	3.17	60.88	3.63	61.39
17/11/2012	3	90	4.04	70.61	4.25	75.65	4.53	84.76
18/11/2012	3	90	3.53	82.39	4.01	75.94	4.11	72.75
19/11/2012	3	90	3.89	74.16	3.06	76.29	2.79	80.59
20/11/2012	2	270	3.80	65.55	2.43	75.62	1.97	273.74
21/11/2012	2	90	4.80	78.93	2.69	95.21	2.81	176.99
22/11/2012	3	90	4.87	95.33	4.01	94.66	3.14	99.87
23/11/2012	3	90	3.24	90.54	3.66	80.26	2.98	87.04
24/11/2012	4	90	3.77	72.48	4.56	66.21	3.95	63.73
25/11/2012	4	90	5.49	76.78	4.97	68.01	4.27	70.92
26/11/2012	3	90	3.32	82.53	4.45	63.87	3.86	58.36
27/11/2012	4	90	4.74	75.88	5.98	72.70	4.97	74.91
28/11/2012	3	90	3.55	85.99	4.46	74.29	3.88	77.91
29/11/2012	3	90	3.59	89.93	4.77	72.51	4.35	69.94
30/11/2012	2	90	3.17	86.97	4.29	67.69	3.53	67.74

Table 140. December 2012 wind data at Coron Island from onshore weather station and meoscale model output

Source Date	PAGASA		ERA-Interim		NCEP FNL		NCEP CFSR	
	Wind Speed (m/s)	Wind Direction (Degrees)	Wind Speed (m/s)	Wind Direction (Degrees)	Wind Speed (m/s)	Wind Direction (Degrees)	Wind Speed (m/s)	Wind Direction (Degrees)
01/12/2012	1	40	7.18	82.77	6.81	73.15	7.34	76.48
02/12/2012	1	40	3.91	71.70	4.66	81.64	4.94	78.80
03/12/2012	1	40	3.25	78.50	3.24	63.11	4.33	63.31
04/12/2012	1	0	3.52	343.93	6.29	61.83	6.92	51.02
05/12/2012	4	140	17.61	188.03	9.37	93.38	8.93	104.10
06/12/2012	2	120	5.06	191.18	5.87	107.43	3.46	120.76
07/12/2012	2	120	2.20	177.04	3.88	130.49	3.15	132.24
08/12/2012	1	0	2.33	208.61	3.63	246.91	3.60	217.98
09/12/2012	1	0	2.20	203.26	4.23	231.56	4.34	210.00
10/12/2012	1	210	1.75	20.85	2.64	149.30	4.36	139.12
11/12/2012	1	0	1.19	84.69	3.35	351.83	2.96	100.31
12/12/2012	1	40	3.72	99.78	7.25	82.42	3.51	56.98
13/12/2012	3	0	7.51	90.73	8.10	89.85	8.32	85.08
14/12/2012	1	0	5.13	88.99	7.50	83.56	7.48	85.51
15/12/2012	1	0	4.92	78.82	6.66	80.11	5.24	69.67
16/12/2012	2	40	5.15	79.96	5.13	66.46	5.77	81.33
17/12/2012	2	40	5.13	81.23	4.47	70.47	6.04	75.49
18/12/2012	1	40	3.65	67.79	5.01	62.45	4.26	54.44
19/12/2012	2	40	4.85	75.92	7.77	73.01	7.14	76.50
20/12/2012	2	90	8.89	79.79	9.99	81.52	8.01	74.42
21/12/2012	4	90	9.03	79.35	9.74	77.64	8.87	77.54
22/12/2012	3	40	6.39	77.81	9.27	76.76	8.95	76.36
23/12/2012	1	0	7.72	79.88	7.52	66.34	7.76	77.92
24/12/2012	3	40	8.45	74.54	10.29	77.82	9.89	75.98
25/12/2012	1	0	4.62	47.49	4.89	39.29	4.83	39.34
26/12/2012	3	40	9.62	55.00	8.40	38.87	11.29	69.97
27/12/2012	3	140	10.03	81.96	13.57	104.68	10.41	86.00
28/12/2012	2	40	8.75	85.75	8.39	96.95	8.14	86.12
29/12/2012	4	40	8.36	83.21	9.15	83.39	8.37	83.56
30/12/2012	1	40	4.85	76.60	4.29	51.19	4.40	50.71
31/12/2012	1	120	8.06	81.75	5.50	79.01	7.15	80.61

Table 141. December 2012 wind data at Cuyo Island from onshore weather station and meoscale model output

Source Date	PAGASA		ERA-Interim		NCEP FNL		NCEP CFSR	
	Wind Speed (m/s)	Wind Direction (Degrees)	Wind Speed (m/s)	Wind Direction (Degrees)	Wind Speed (m/s)	Wind Direction (Degrees)	Wind Speed (m/s)	Wind Direction (Degrees)
01/12/2012	2	20	7.95	47.51	8.54	44.97	7.95	43.01
02/12/2012	2	20	5.66	37.88	5.24	43.21	6.22	37.74
03/12/2012	2	20	8.16	31.71	8.57	36.14	8.28	32.64
04/12/2012	5	20	12.30	7.56	13.34	40.45	14.19	38.98
05/12/2012	4	120	14.43	207.85	5.59	120.33	8.30	148.41
06/12/2012	1	180	4.73	187.27	2.78	69.41	3.74	97.99
07/12/2012	1	180	1.59	169.89	2.97	151.47	2.03	134.49
08/12/2012	0	0	1.44	242.09	3.34	232.67	3.21	228.47
09/12/2012	1	220	1.53	289.31	4.58	224.70	3.82	212.93
10/12/2012	0	0	2.78	353.95	2.14	266.94	2.65	151.90
11/12/2012	2	20	5.13	22.54	7.26	14.31	4.33	43.41
12/12/2012	3	20	6.95	37.13	7.62	46.87	5.20	74.16
13/12/2012	3	20	6.33	47.01	6.61	47.89	6.36	51.99
14/12/2012	3	20	5.91	45.59	5.60	51.13	6.70	49.76
15/12/2012	2	20	5.50	41.34	7.48	42.99	7.16	42.40
16/12/2012	2	20	7.04	41.01	6.61	39.38	6.95	43.27
17/12/2012	3	20	7.63	41.97	8.76	43.02	8.30	42.41
18/12/2012	3	20	9.50	36.48	9.63	39.33	9.56	37.04
19/12/2012	3	20	10.08	44.51	10.81	45.51	9.90	46.12
20/12/2012	3	20	10.07	46.58	10.33	47.13	10.18	46.32
21/12/2012	3	20	9.21	47.24	9.79	47.39	10.22	45.44
22/12/2012	3	20	10.24	45.35	11.45	46.51	10.60	45.25
23/12/2012	4	20	10.71	45.38	11.89	42.87	11.22	46.47
24/12/2012	3	20	10.60	48.01	11.28	46.36	10.87	47.32
25/12/2012	4	20	10.97	34.07	12.15	33.04	11.41	31.89
26/12/2012	5	20	15.82	41.30	16.65	41.03	10.81	55.54
27/12/2012	2	20	8.72	51.14	8.74	132.88	5.90	62.18
28/12/2012	3	20	5.78	49.69	4.42	99.10	4.35	64.77
29/12/2012	2	20	6.49	44.10	6.15	50.82	6.55	48.45
30/12/2012	2	20	7.82	38.37	5.78	29.11	7.01	32.18
31/12/2012	3	20	9.44	45.14	7.21	39.80	7.93	42.73

Table 142. December 2012 wind data at Puerto Princesa from onshore weather station and meoscale model output

Source Date	PAGASA		ERA-Interim		NCEP FNL		NCEP CFSR	
	Wind Speed (m/s)	Wind Direction (Degrees)	Wind Speed (m/s)	Wind Direction (Degrees)	Wind Speed (m/s)	Wind Direction (Degrees)	Wind Speed (m/s)	Wind Direction (Degrees)
01/12/2012	3	90	4.08	74.71	4.58	69.95	4.14	68.22
02/12/2012	2	90	3.35	72.17	3.29	56.38	3.40	67.19
03/12/2012	2	90	3.46	33.98	2.33	53.99	2.52	39.20
04/12/2012	2	320	4.30	35.66	6.62	10.25	6.13	352.32
05/12/2012	3	260	3.55	267.13	12.71	158.28	13.12	170.56
06/12/2012	2	220	3.40	188.32	3.94	171.48	3.73	187.65
07/12/2012	2	160	3.85	181.97	1.63	244.00	2.23	212.23
08/12/2012	2	320	3.34	178.01	1.92	175.28	2.84	203.61
09/12/2012	2	270	2.96	181.74	2.34	196.29	1.83	201.26
10/12/2012	2	270	3.03	172.97	2.49	193.61	2.36	202.17
11/12/2012	2	90	2.98	79.34	1.89	141.21	2.56	180.31
12/12/2012	4	90	3.10	57.83	2.52	79.54	3.42	68.78
13/12/2012	5	90	3.65	86.00	3.83	93.24	3.79	99.62
14/12/2012	1	90	3.22	73.52	3.50	62.05	4.21	67.46
15/12/2012	3	90	3.03	85.15	3.48	69.55	3.58	71.05
16/12/2012	4	90	4.21	63.43	3.83	61.13	4.24	61.21
17/12/2012	4	90	3.38	62.37	4.12	66.32	3.37	47.42
18/12/2012	3	90	4.68	57.82	4.15	58.77	4.18	51.74
19/12/2012	6	90	6.53	67.49	6.21	65.15	5.66	61.27
20/12/2012	4	90	6.13	69.64	5.96	66.52	5.57	65.83
21/12/2012	3	90	6.16	66.24	5.90	63.54	5.19	60.13
22/12/2012	5	90	5.60	63.66	6.59	60.63	5.70	55.37
23/12/2012	6	90	6.21	62.69	5.86	55.14	5.49	55.46
24/12/2012	4	90	5.90	67.08	6.96	63.94	5.96	62.65
25/12/2012	4	90	4.61	46.84	4.18	45.61	4.47	41.97
26/12/2012	3	320	5.93	31.08	4.76	0.72	6.29	58.25
27/12/2012	6	90	7.49	97.61	3.89	199.67	6.07	108.41
28/12/2012	3	90	3.63	91.21	4.42	137.11	4.38	95.10
29/12/2012	3	90	3.15	81.63	3.69	77.01	3.78	79.35
30/12/2012	2	90	3.54	76.33	2.52	88.67	2.88	78.78
31/12/2012	4	90	5.39	74.76	2.86	69.15	3.44	65.78

Appendix 4: Mesoscale Model Wind Direction Error and Bias Tables

Table 143. February 2010 Model Errors and Bias Quantification of Wind Speed

Configuration	ERA-Interim			NCEP-FNL			NCEP-CFS		
	RMSE	Bias	STDE	RMSE	Bias	STDE	RMSE	Bias	STDE
Coron Island	23.97	4.53	23.54	22.78	4.40	22.37	23.60	4.46	23.17
Cuyo Island	25.04	4.73	24.59	25.68	4.85	25.21	23.74	4.49	23.32
Puerto Princesa	3.27	0.62	3.21	1.51	0.29	1.48	0.21	0.04	0.21

Table 144. April 2010 Model Errors and Bias Quantification of Wind Speed

Configuration	ERA-Interim			NCEP-FNL			NCEP-CFS		
	RMSE	Bias	STDE	RMSE	Bias	STDE	RMSE	Bias	STDE
Coron Island	21.51	3.93	21.15	21.75	3.97	21.38	22.10	4.04	21.73
Cuyo Island	23.38	4.26	22.98	26.92	4.91	26.47	23.80	4.34	23.40
Puerto Princesa	2.84	0.52	2.80	2.99	0.55	2.94	0.14	0.03	0.14

Table 145. August 2010 Model Errors and Bias Quantification of Wind Speed

Configuration	ERA-Interim			NCEP-FNL			NCEP-CFS		
	RMSE	Bias	STDE	RMSE	Bias	STDE	RMSE	Bias	STDE
Coron Island	18.68	3.36	18.38	31.21	5.61	30.71	20.42	3.67	20.09
Cuyo Island	21.80	3.92	21.44	32.85	5.90	32.32	24.91	4.47	24.50
Puerto Princesa	9.30	1.67	9.15	8.68	1.56	8.54	5.43	0.97	5.33

Table 146. January 2011 Model Errors and Bias Quantification of Wind Speed

Configuration	ERA-Interim			NCEP-FNL			NCEP-CFS		
	RMSE	Bias	STDE	RMSE	Bias	STDE	RMSE	Bias	STDE
Coron Island	29.12	5.23	28.65	27.68	4.97	27.73	26.04	4.68	25.62
Cuyo Island	42.47	7.63	41.78	37.55	6.74	36.94	38.21	6.86	37.59
Puerto Princesa	11.02	1.98	10.84	5.80	1.04	5.71	7.69	1.38	7.57

Table 147. March 2011 Model Errors and Bias Quantification of Wind Speed

Configuration	ERA-Interim			NCEP-FNL			NCEP-CFS		
	RMSE	Bias	STDE	RMSE	Bias	STDE	RMSE	Bias	STDE
Coron Island	30.70	5.52	30.21	28.09	5.05	27.63	30.26	5.43	29.77
Cuyo Island	34.53	6.20	33.97	32.51	5.84	31.98	31.92	5.73	31.40
Puerto Princesa	8.27	1.48	8.13	5.99	1.08	5.90	6.72	1.21	6.61

Table 148. July 2011 Model Errors and Bias Quantification of Wind Speed

Configuration	ERA-Interim			NCEP-FNL			NCEP-CFS		
	RMSE	Bias	STDE	RMSE	Bias	STDE	RMSE	Bias	STDE
Coron Island	23.17	4.16	22.79	31.96	5.74	31.44	24.52	4.40	24.12
Cuyo Island	29.37	5.27	28.89	40.33	7.24	39.68	31.44	5.65	30.92
Puerto Princesa	9.93	1.78	9.77	9.51	1.71	9.35	5.37	0.96	5.28

Table 149. September 2011 Model Errors and Bias Quantification of Wind Speed

Configuration	ERA-Interim			NCEP-FNL			NCEP-CFS		
	RMSE	Bias	STDE	RMSE	Bias	STDE	RMSE	Bias	STDE
Coron Island	21.45	3.92	21.09	33.63	6.14	33.06	26.76	4.89	26.31
Cuyo Island	27.44	5.01	26.98	39.62	7.23	38.95	31.08	5.68	30.56
Puerto Princesa	9.15	1.67	9.00	8.68	1.58	8.53	3.94	0.72	3.88

Table 150. November 2011 Model Errors and Bias Quantification of Wind Speed

Configuration Location	ERA-Interim			NCEP-FNL			NCEP-CFS		
	RMSE	Bias	STDE	RMSE	Bias	STDE	RMSE	Bias	STDE
Coron Island	18.24	3.33	17.94	23.99	4.38	23.58	17.48	3.19	17.18
Cuyo Island	22.88	4.18	22.49	26.65	4.87	26.20	21.73	3.97	21.36
Puerto Princesa	6.50	1.19	6.39	6.13	1.12	6.02	2.52	0.46	2.48

Table 151. March 2012 Model Errors and Bias Quantification of Wind Speed

Configuration Location	ERA-Interim			NCEP-FNL			NCEP-CFS		
	RMSE	Bias	STDE	RMSE	Bias	STDE	RMSE	Bias	STDE
Coron Island	27.03	4.85	26.59	30.46	5.47	29.97	28.31	5.09	27.85
Cuyo Island	31.30	5.62	30.79	33.30	5.98	32.76	32.26	5.79	31.73
Puerto Princesa	4.24	0.76	4.17	4.06	0.73	3.99	3.95	0.71	3.89

Table 152. June 2012 Model Errors and Bias Quantification of Wind Speed

Configuration Location	ERA-Interim			NCEP-FNL			NCEP-CFS		
	RMSE	Bias	STDE	RMSE	Bias	STDE	RMSE	Bias	STDE
Coron Island	29.66	5.42	29.17	39.86	7.23	39.19	26.23	4.79	25.79
Cuyo Island	24.59	5.80	23.90	32.93	7.76	32.00	23.26	5.48	22.61
Puerto Princesa	13.77	2.51	13.54	14.72	2.69	14.47	9.46	1.73	9.30

Table 153. November 2012 Model Errors and Bias Quantification of Wind Speed

Configuration Location	ERA-Interim			NCEP-FNL			NCEP-CFS		
	RMSE	Bias	STDE	RMSE	Bias	STDE	RMSE	Bias	STDE
Coron Island	21.87	3.99	16.97	26.76	4.89	26.31	23.26	4.25	22.87
Cuyo Island	27.68	5.05	27.21	28.14	5.14	27.66	23.82	4.35	23.42
Puerto Princesa	4.79	0.87	4.71	4.25	0.78	4.18	2.78	0.51	2.74

Appendix 5: 7SEAS Sites Wind Speed and Wind Direction Charts

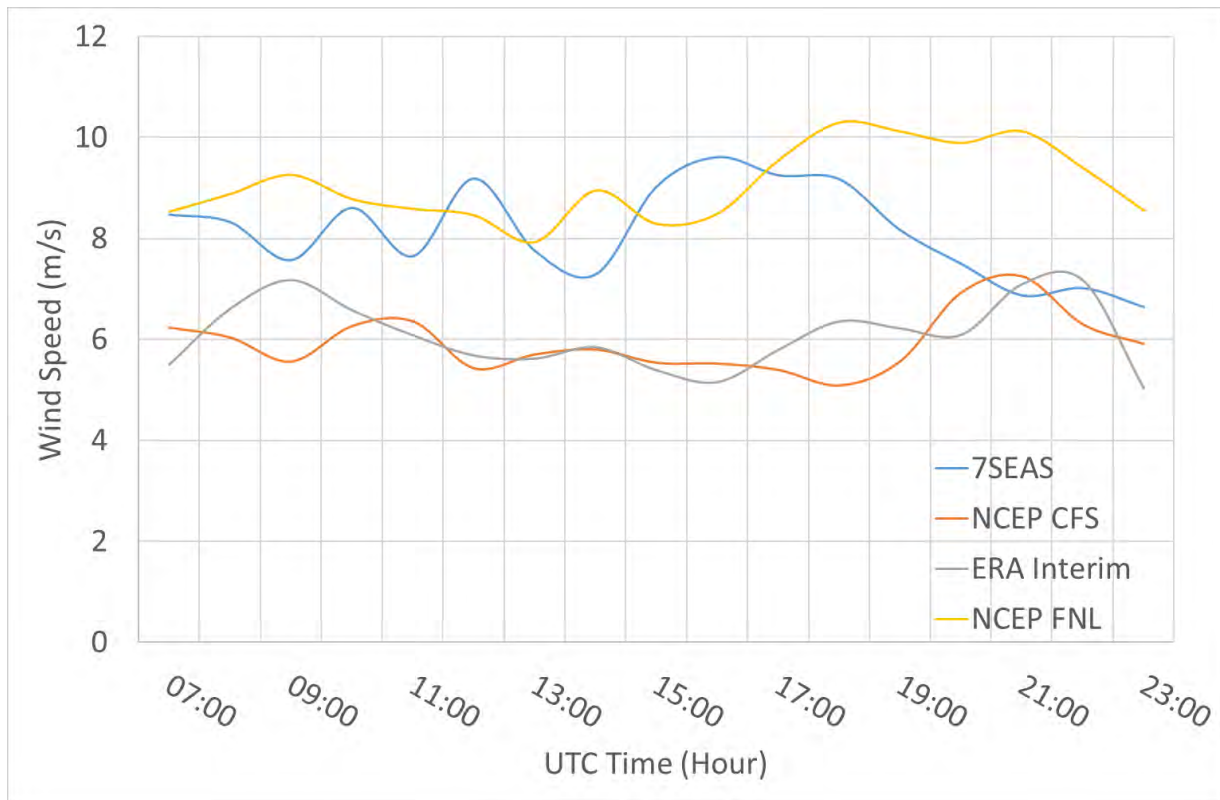


Figure 206. Wind speeds from WRF outputs and actual observations at Balabac Island on 15 September 2012

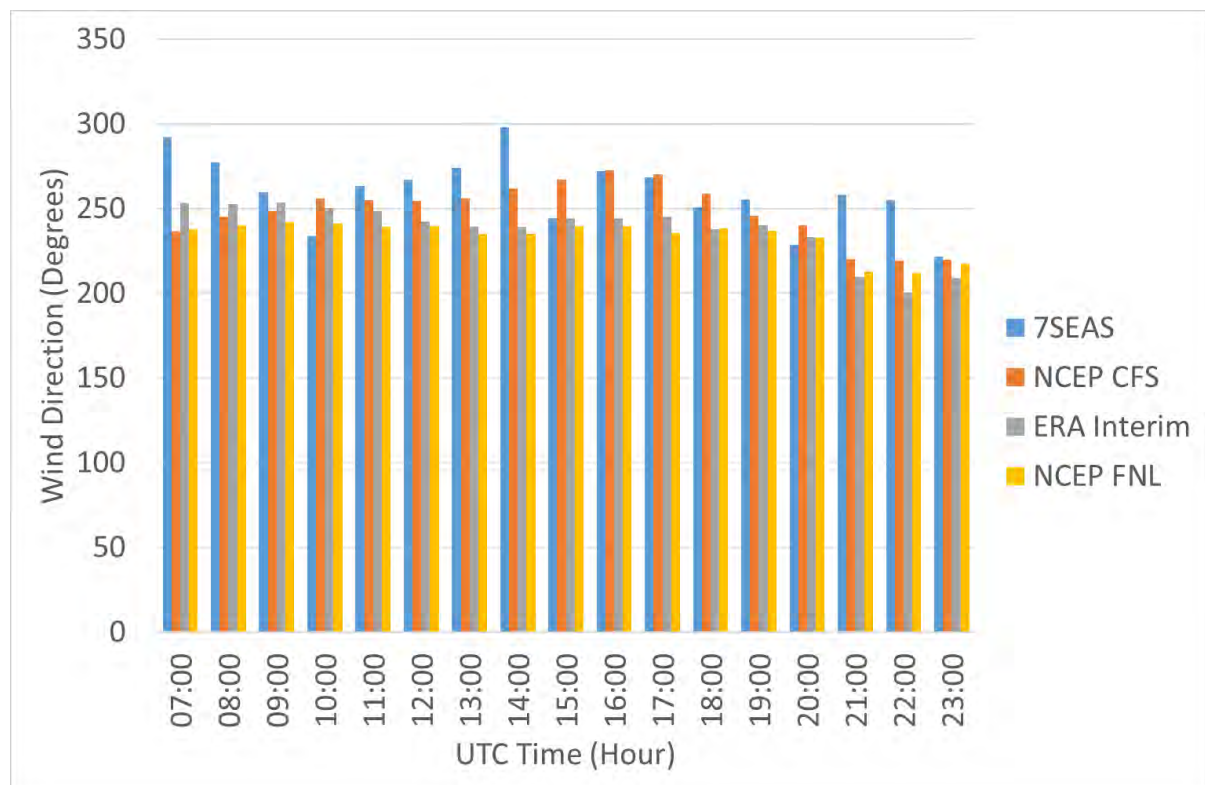


Figure 207. Wind direction values from WRF results and measurements for Balabac Island on 15 September 2012

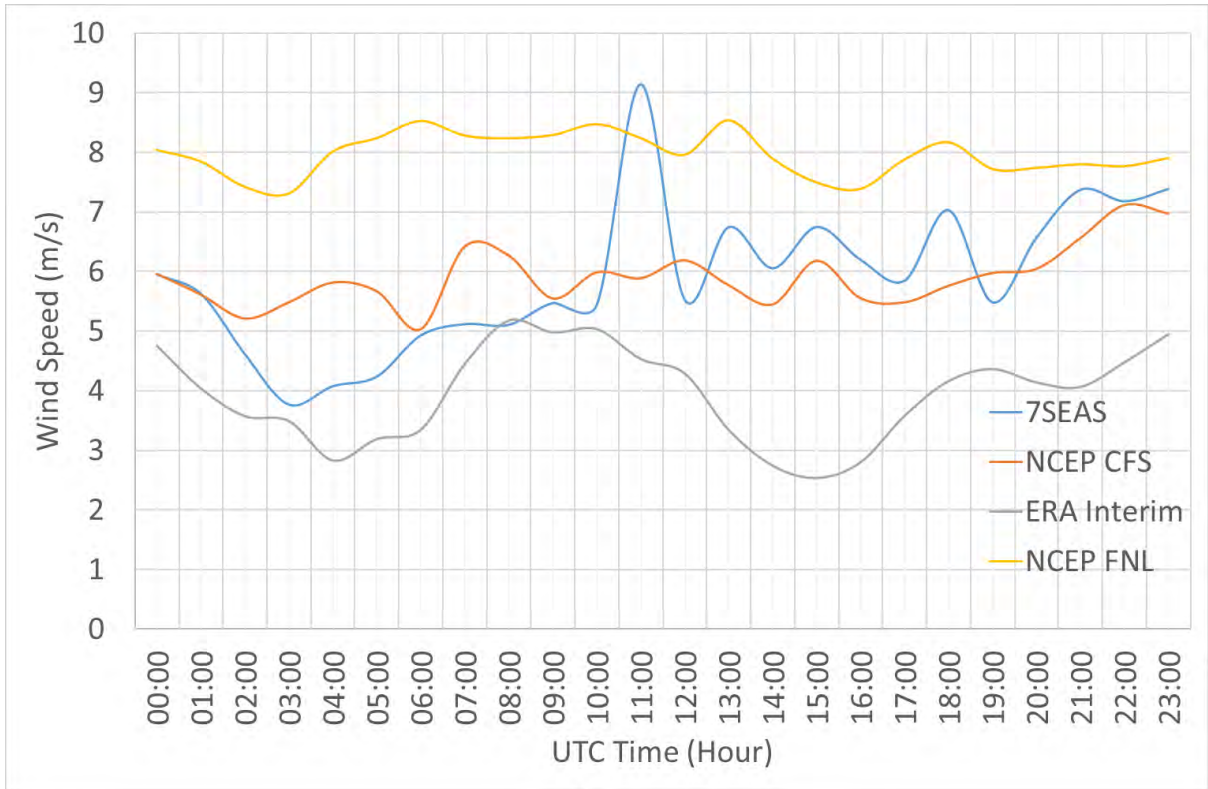


Figure 208. Wind speeds from WRF outputs and actual observations at Balabac Island on 16 September 2012

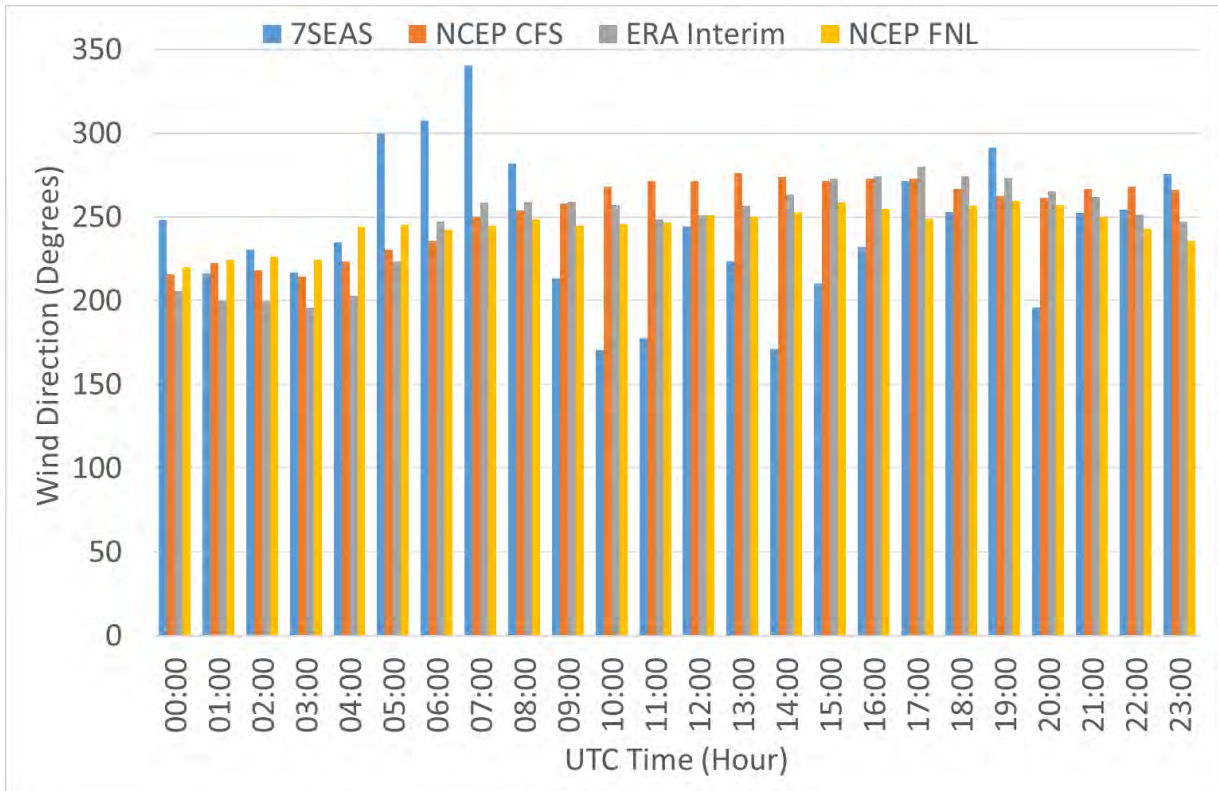


Figure 209. Wind direction values from WRF results and measurements for Balabac Island on 16 September 2012

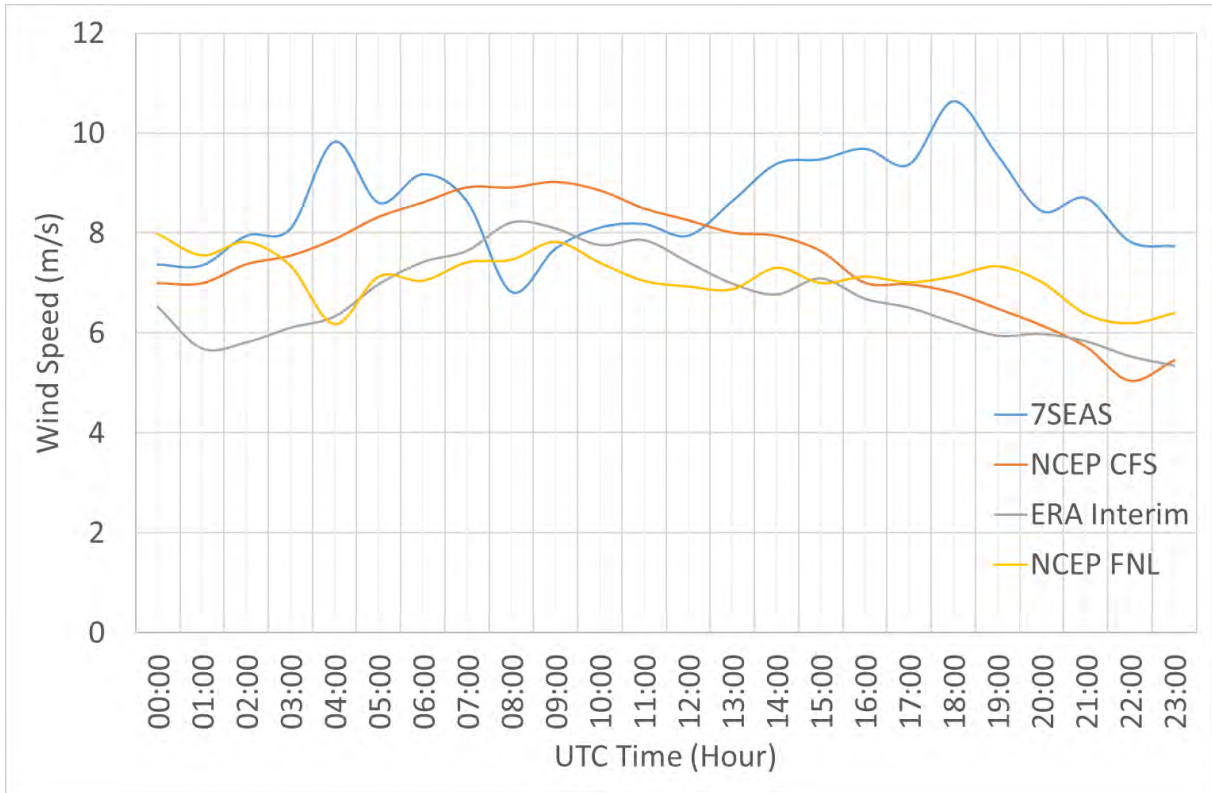


Figure 210. Wind speeds from WRF outputs and actual observations at Balabac Island on 17 September 2012

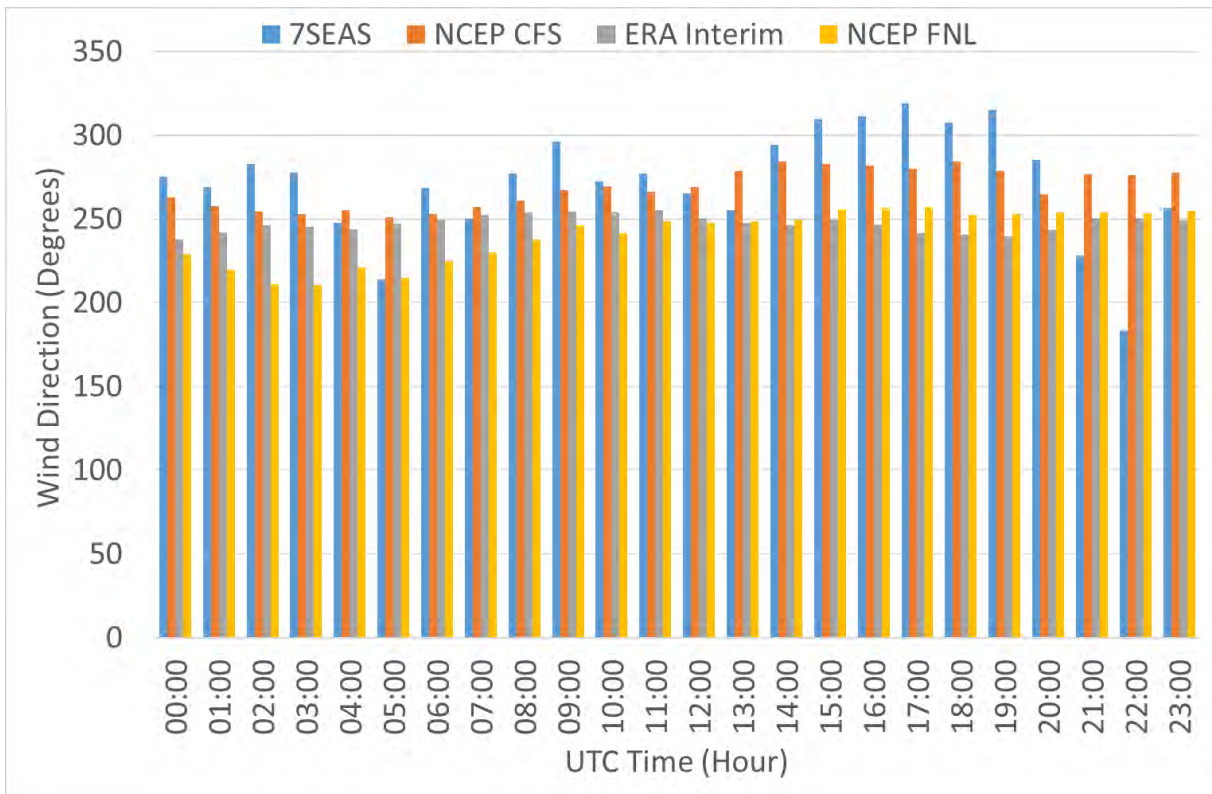


Figure 211. Wind direction values from WRF results and measurements for Balabac Island on 17 September 2012

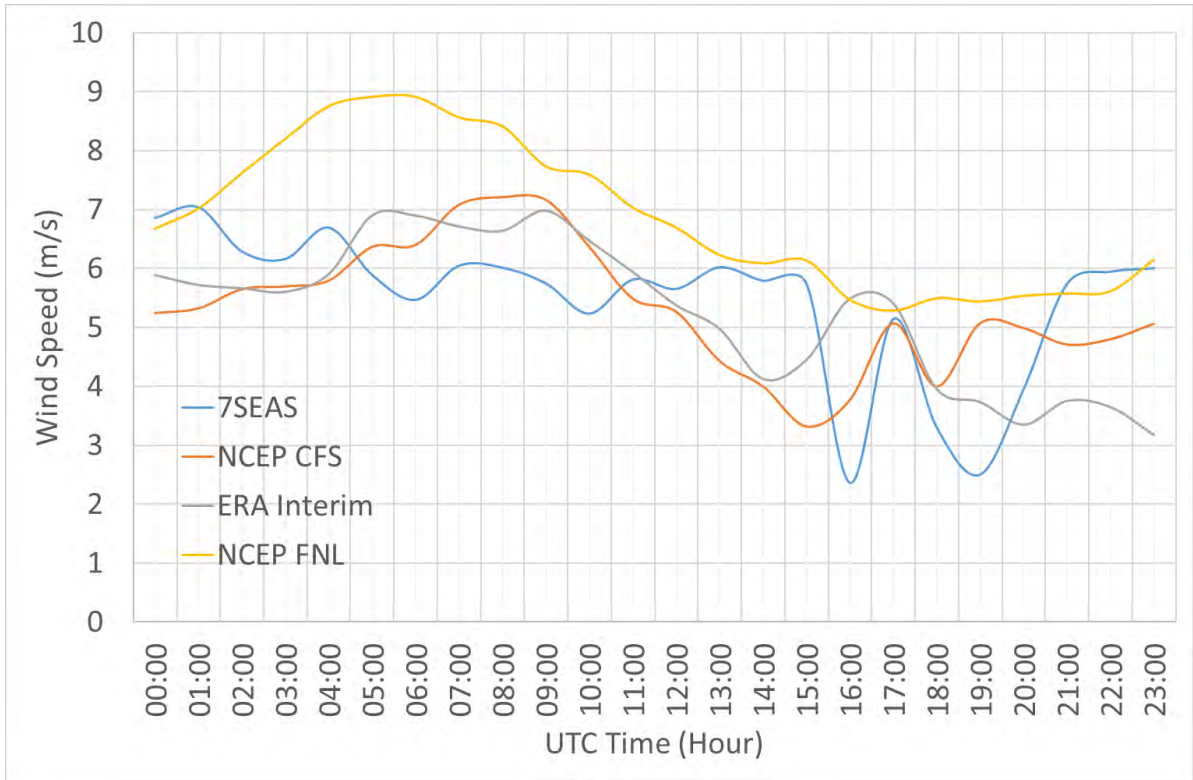


Figure 212. Wind speeds from WRF outputs and actual observations at Balabac Island on 18 September 2012

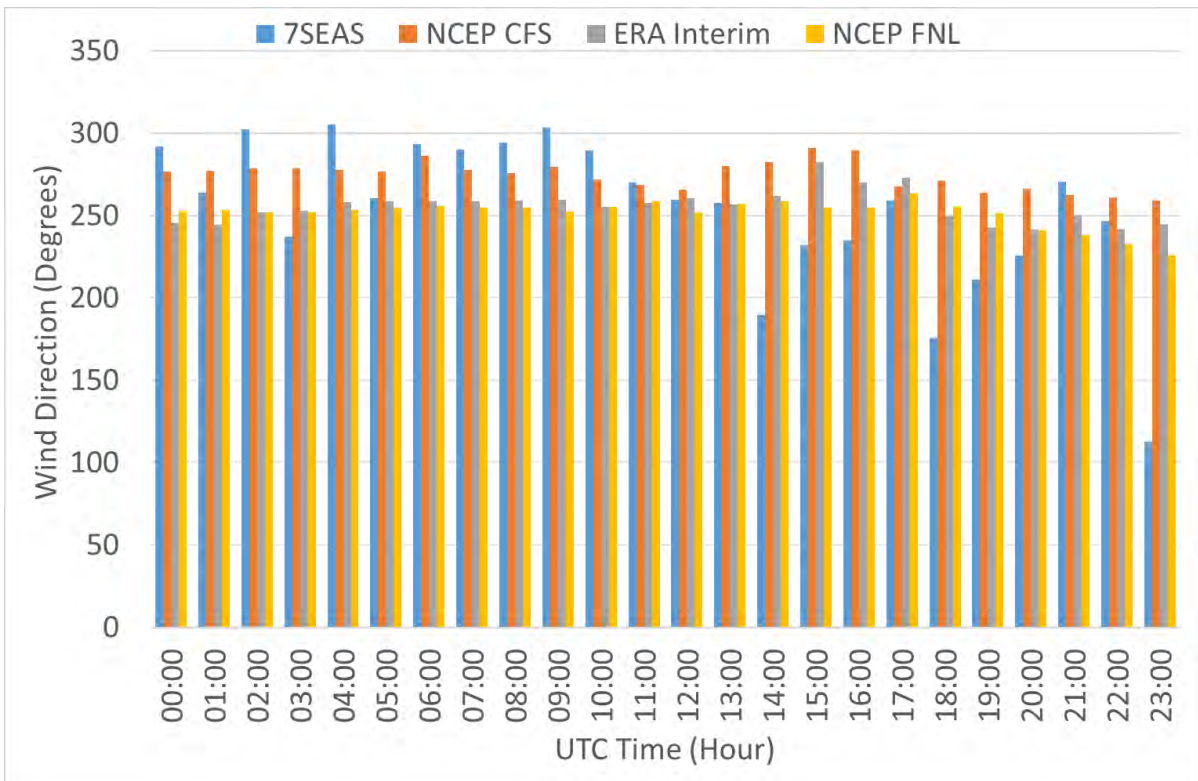


Figure 213. Wind direction values from WRF results and measurements for Balabac Island on 18 September 2012

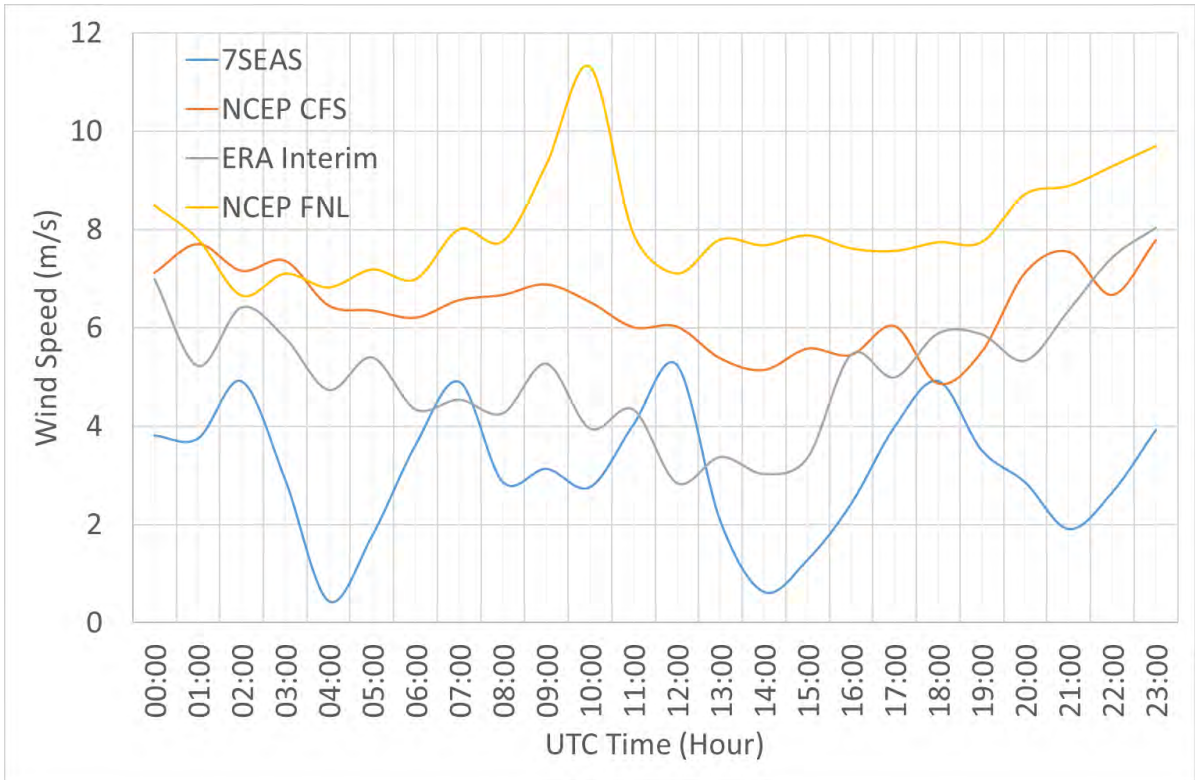


Figure 214. North Guntao Island wind speeds from WRF simulations and ship observations on 20 September 2011

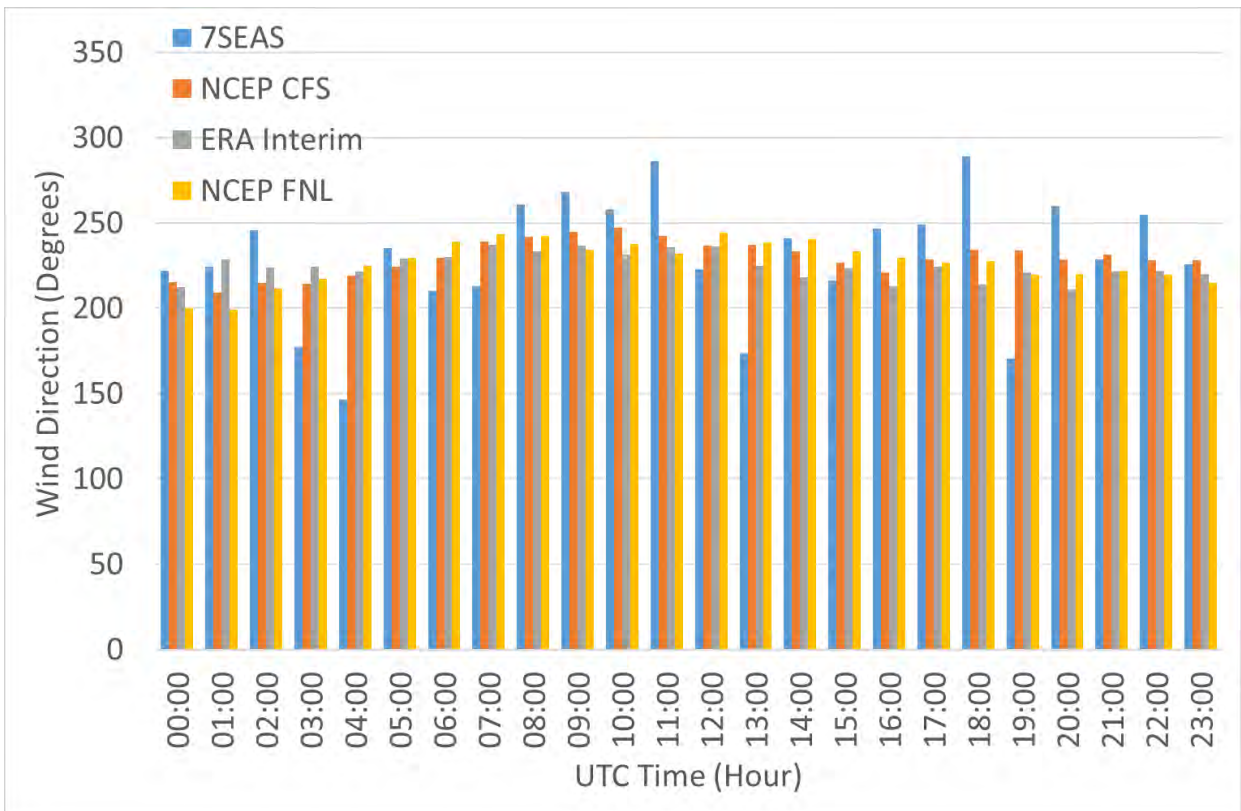


Figure 215. Wind direction values from ship measurements and WRF outputs for North Guntao Island on 20 September 2011

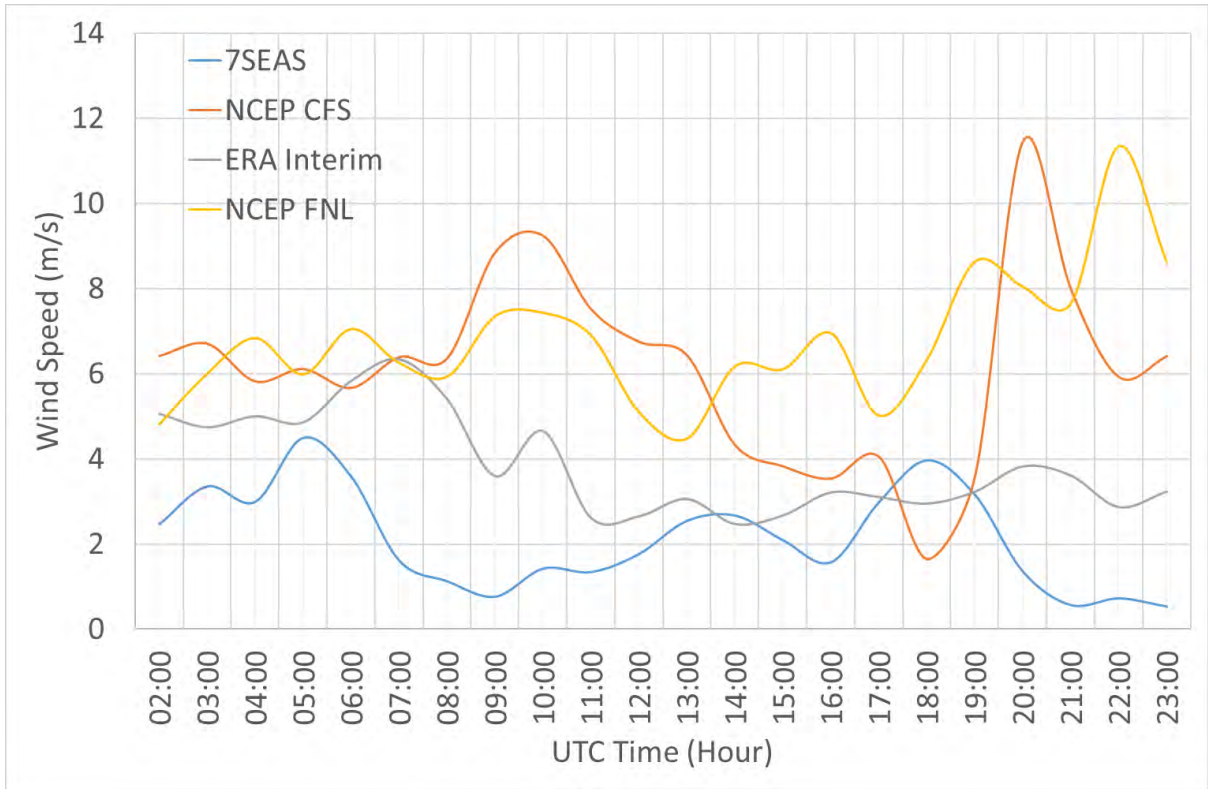


Figure 216. North Guntao Island wind speeds from WRF simulations and ship observations on 8 September 2012

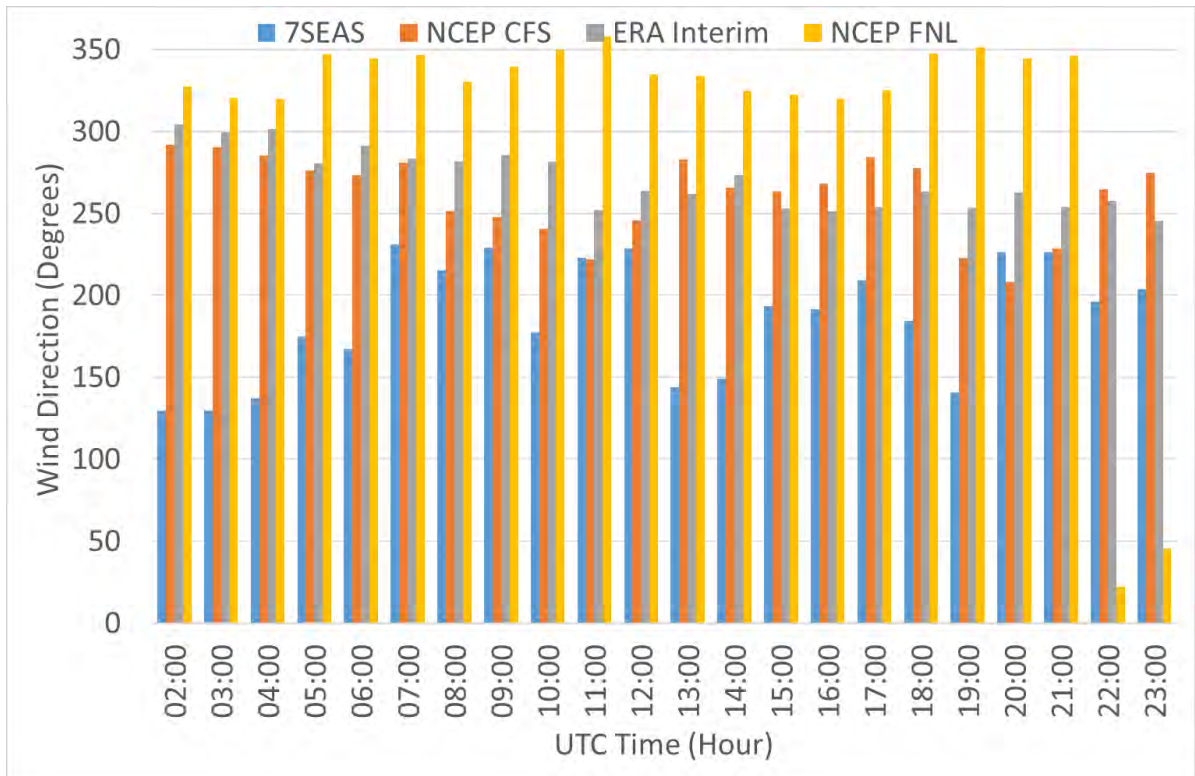


Figure 217. Wind direction values from ship measurements and WRF outputs for North Guntao Island on 8 September 2012

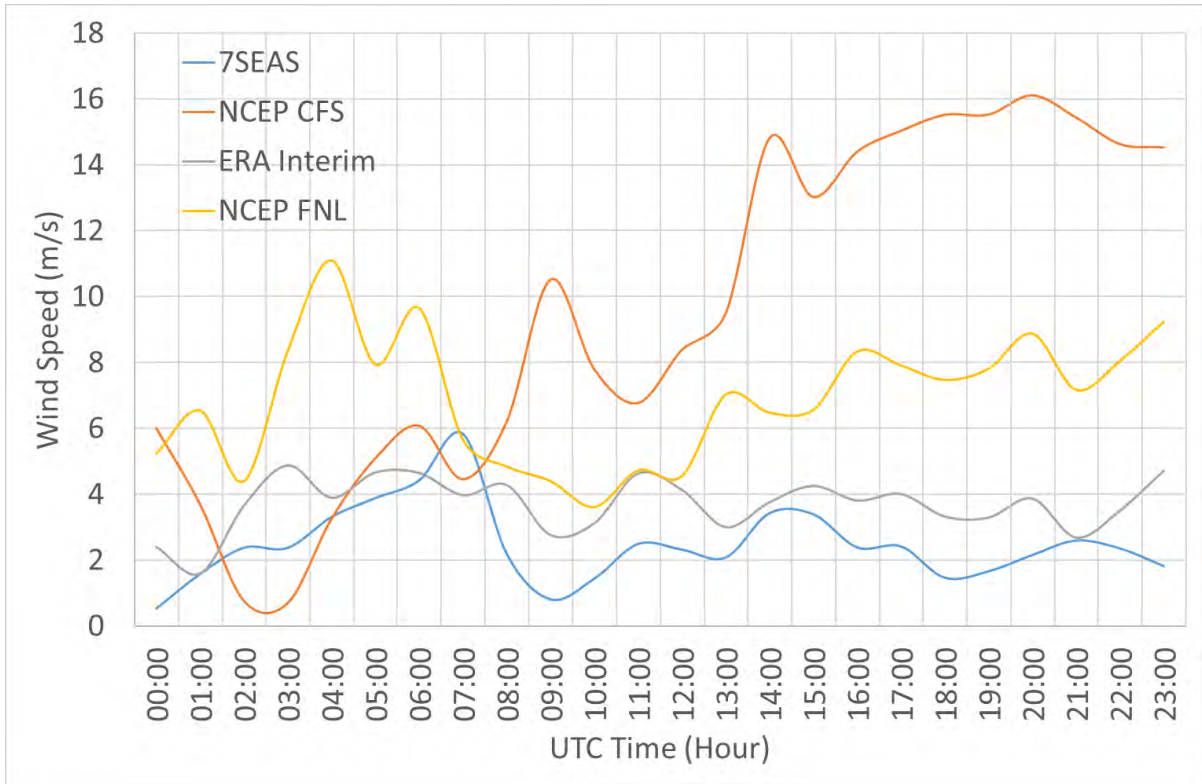


Figure 218. North Guntao Island wind speeds from WRF simulations and ship observations on 9 September 2012

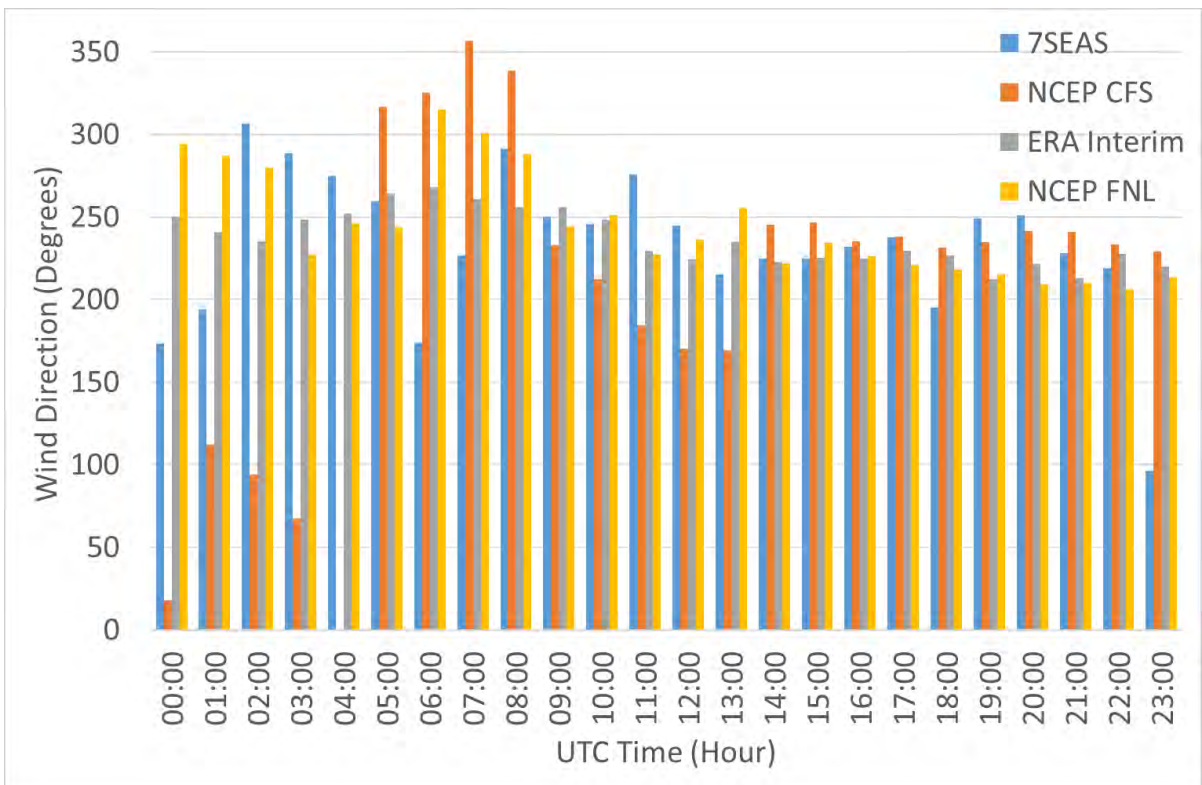


Figure 219. Wind direction values from ship measurements and WRF outputs for North Guntao Island on 9 September 2012

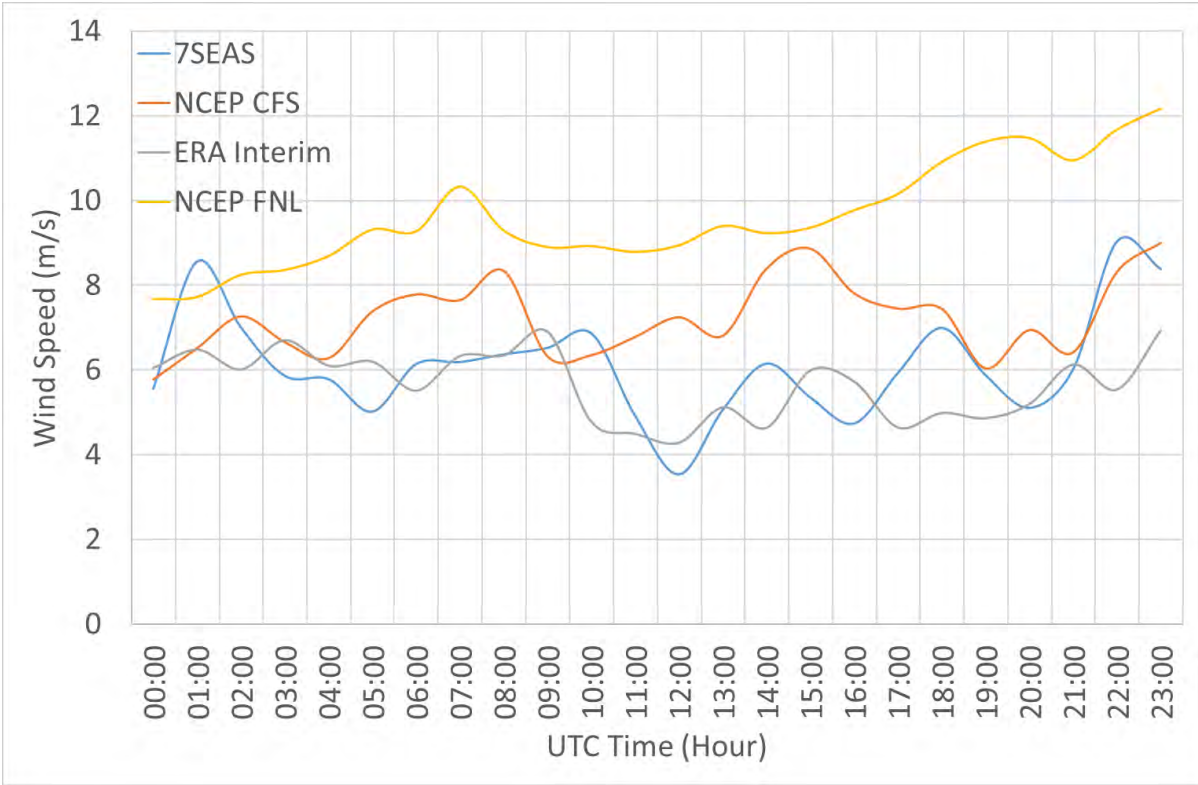


Figure 220. Simulated and observed wind speeds Notch Island on 21 September 2011

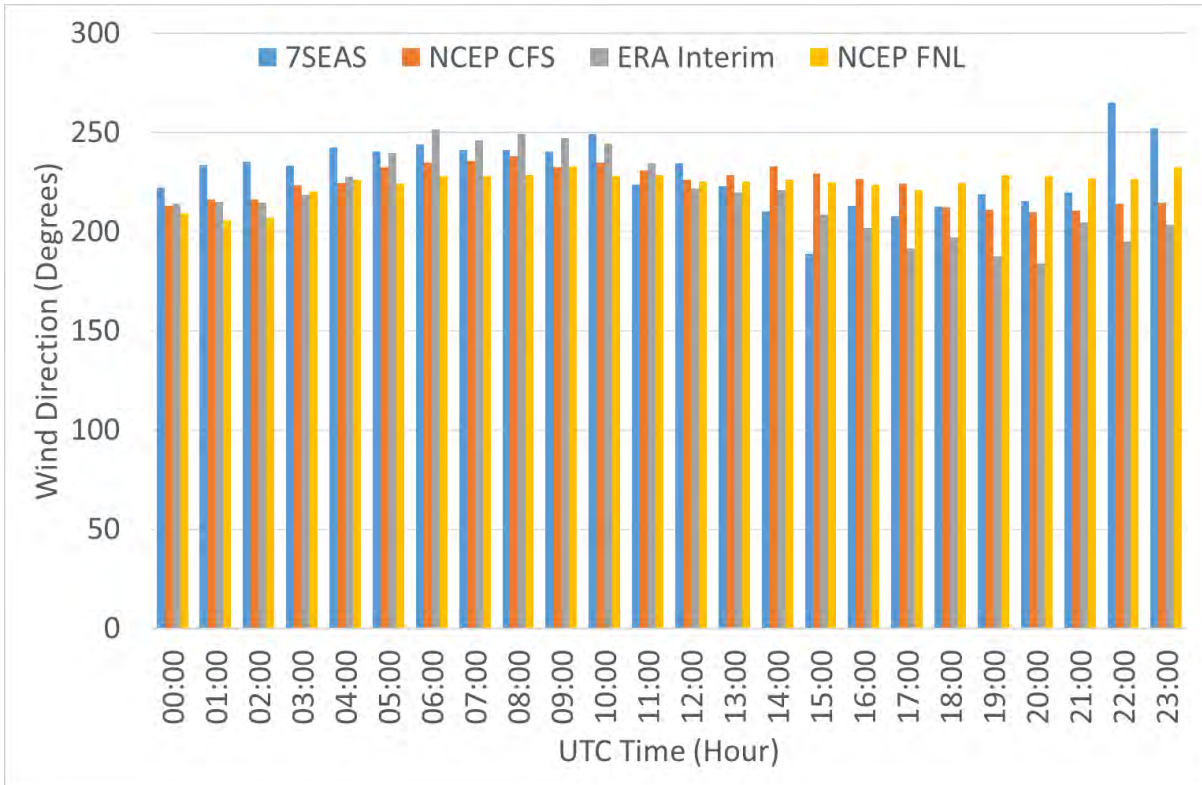


Figure 221. Model outputs and measured wind direction for Notch Island on 21 September 2011

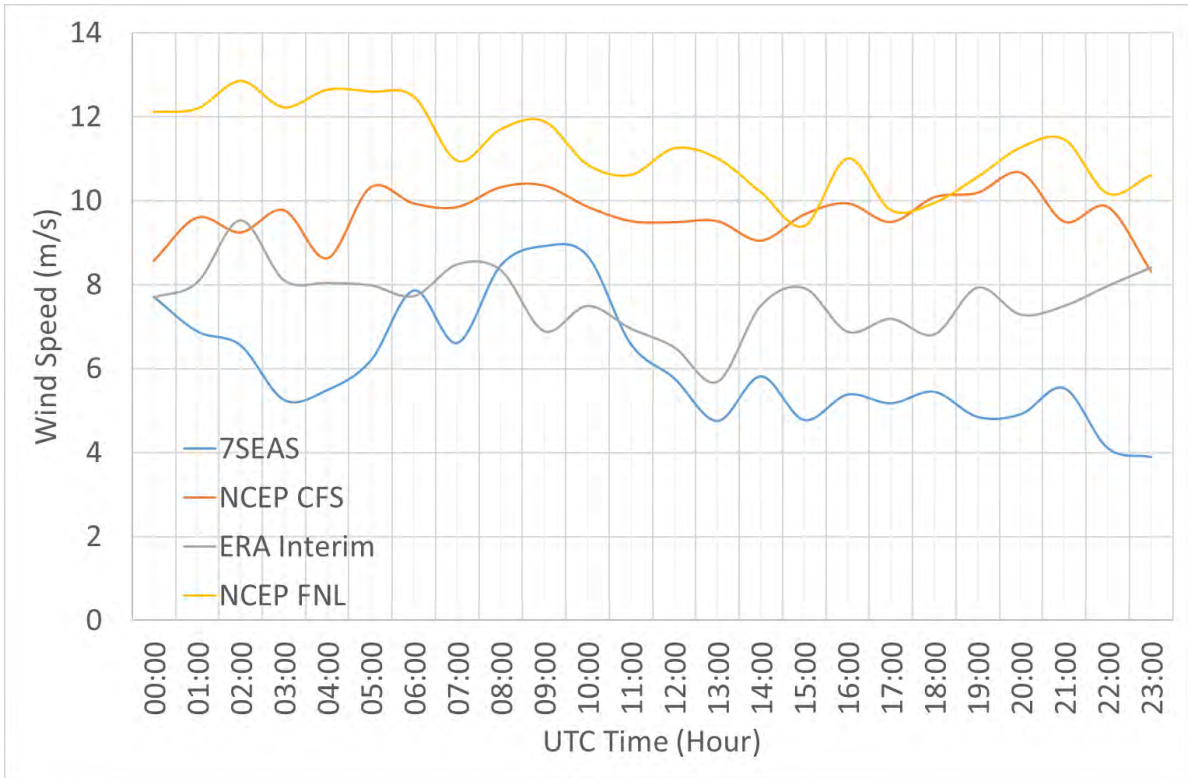


Figure 222. Simulated and observed wind speeds Notch Island on 22 September 2011

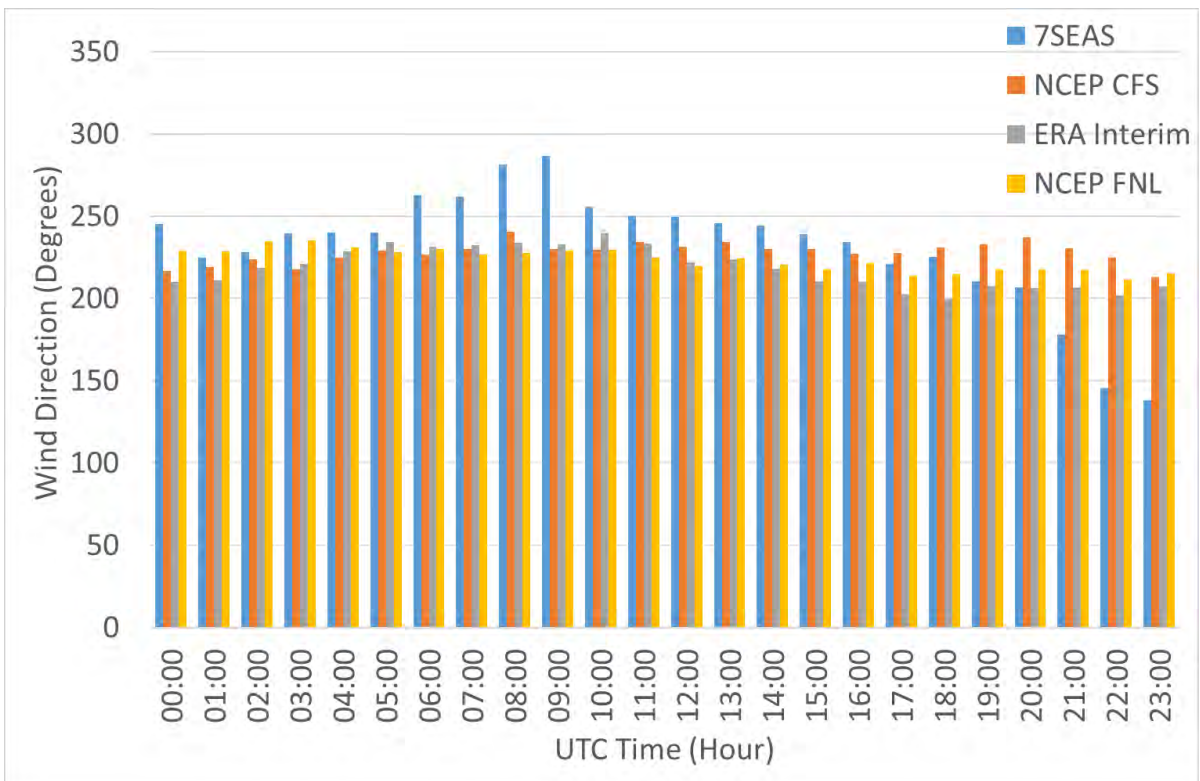


Figure 223. Model outputs and measured wind direction for Notch Island on 22 September 2011

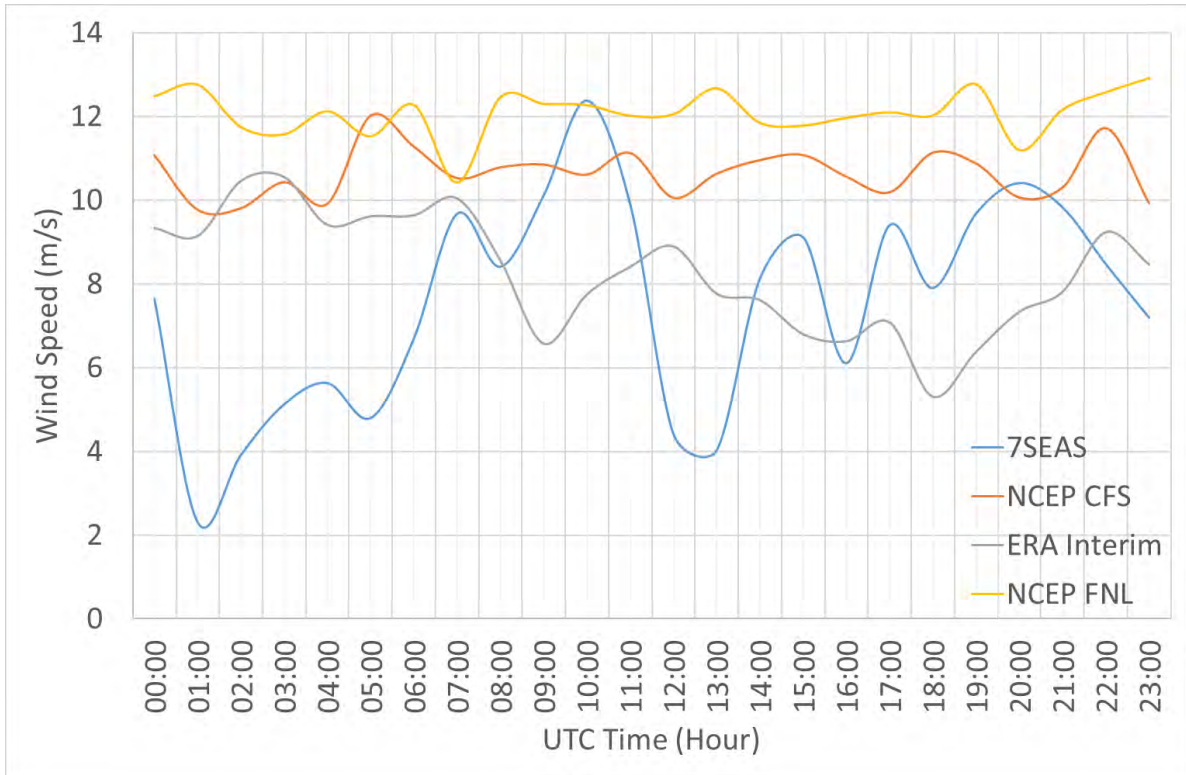


Figure 224. South Guntao Island wind speed measurements and model results for 23 September 2011

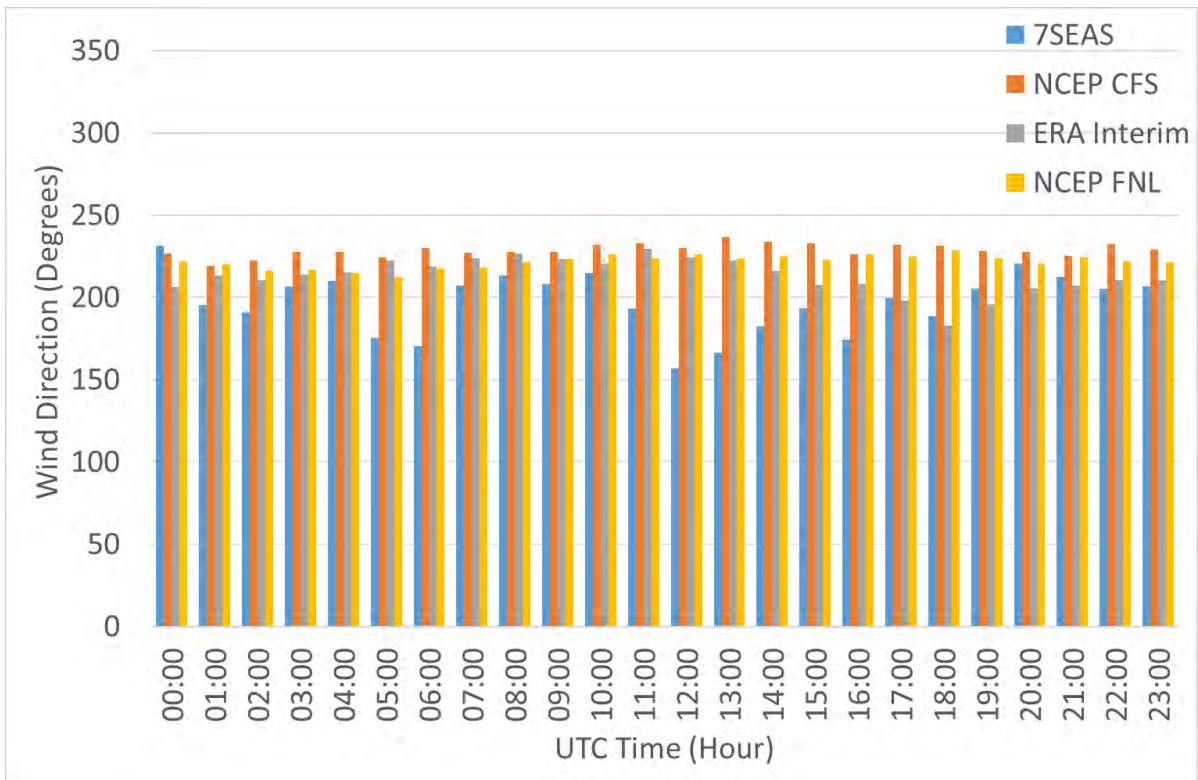


Figure 225. Modelled wind direction alongside measurements for South Guntao Island on 23 September 2011

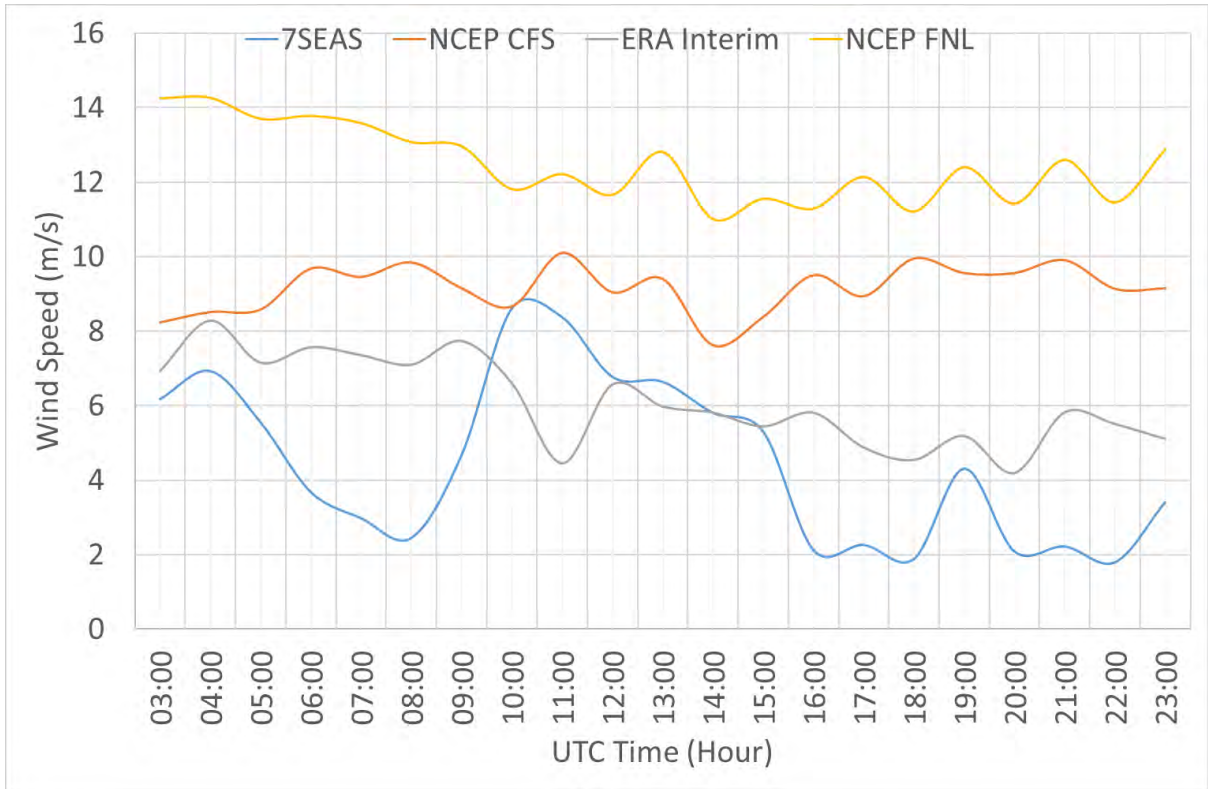


Figure 226. South Guntao Island wind speed measurements and model results for 11 September 2012

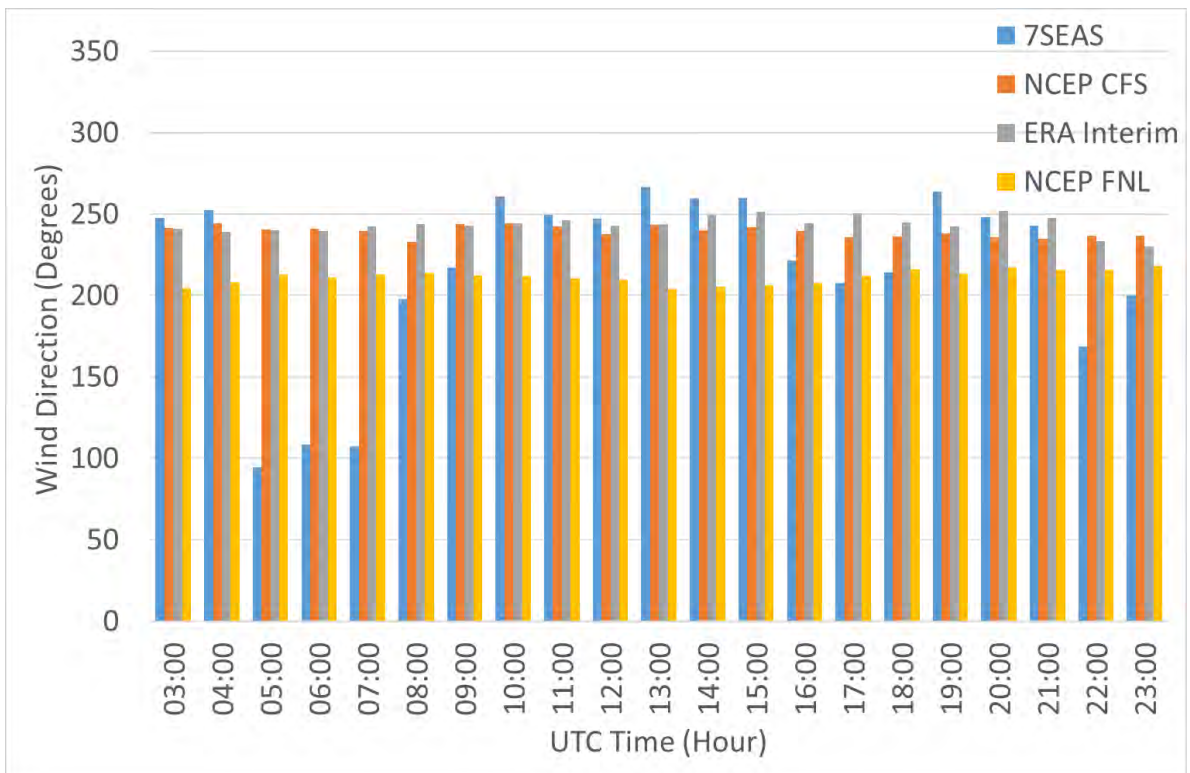


Figure 227. Modelled wind direction alongside measurements for South Guntao Island on 11 September 2012

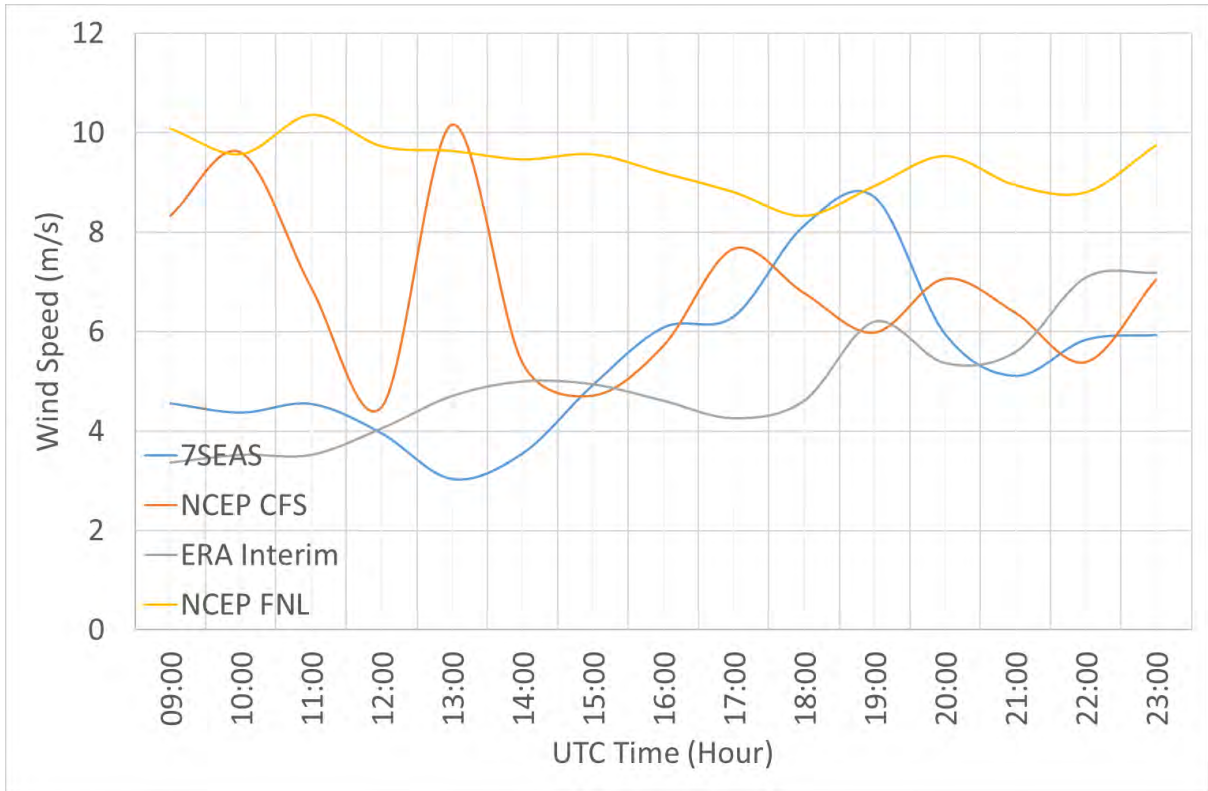


Figure 228. Tubbataha North Reef wind speeds on 21 September 2012

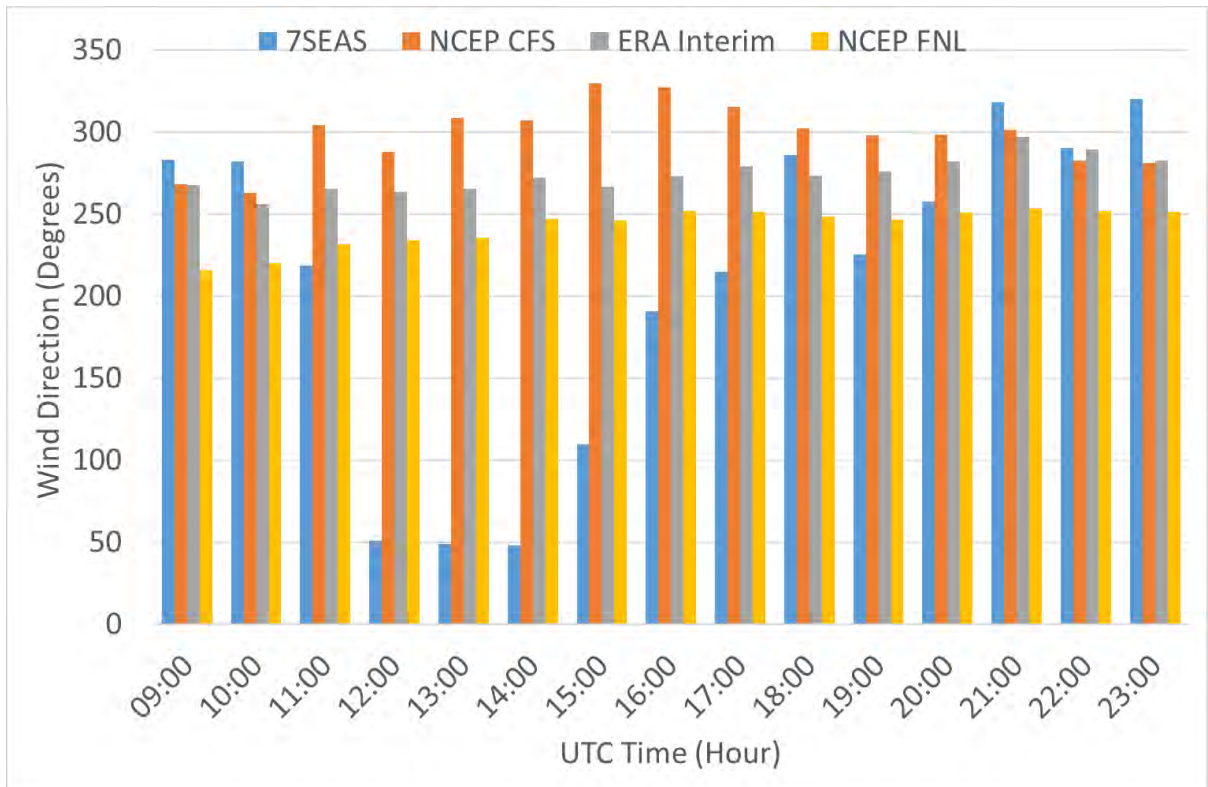


Figure 229. Wind directions for Tubbataha North Reef on 21 September 2012

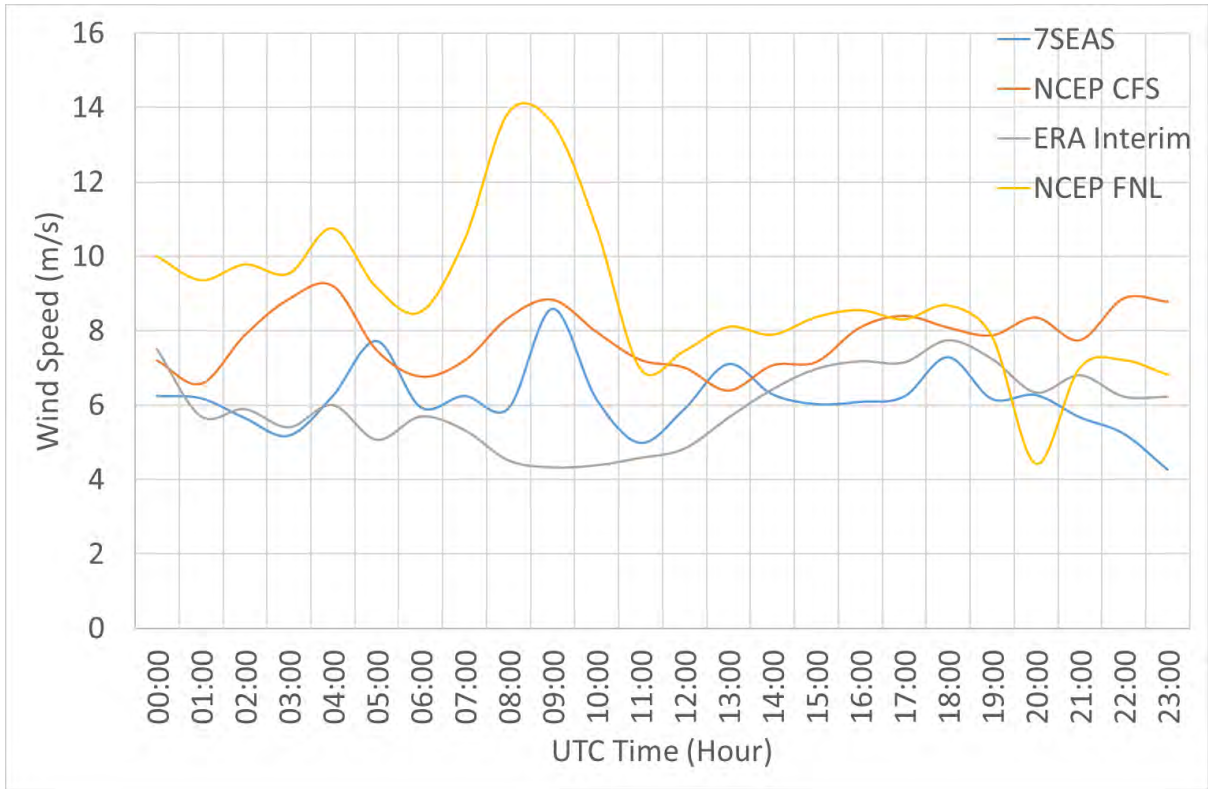


Figure 230. Tubbataha North Reef wind speeds on 22 September 2012

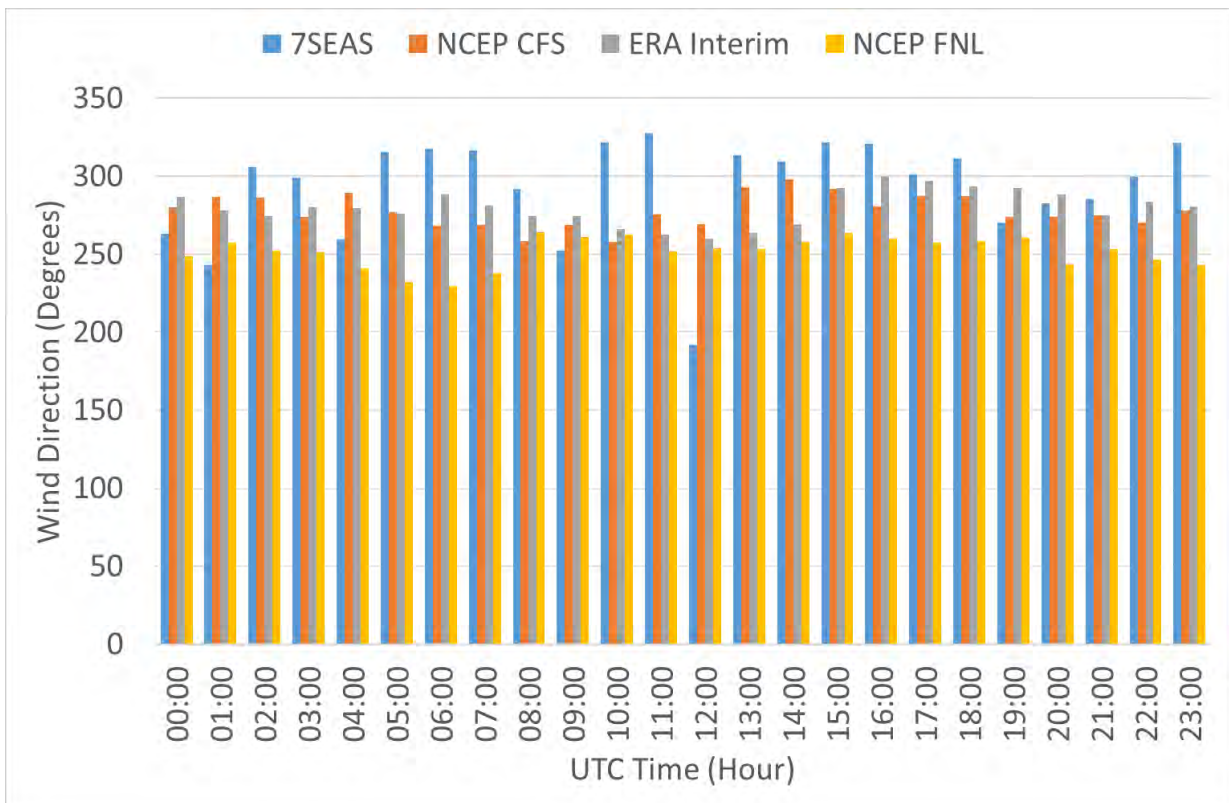


Figure 231. Wind directions for Tubbataha North Reef on 22 September 2012

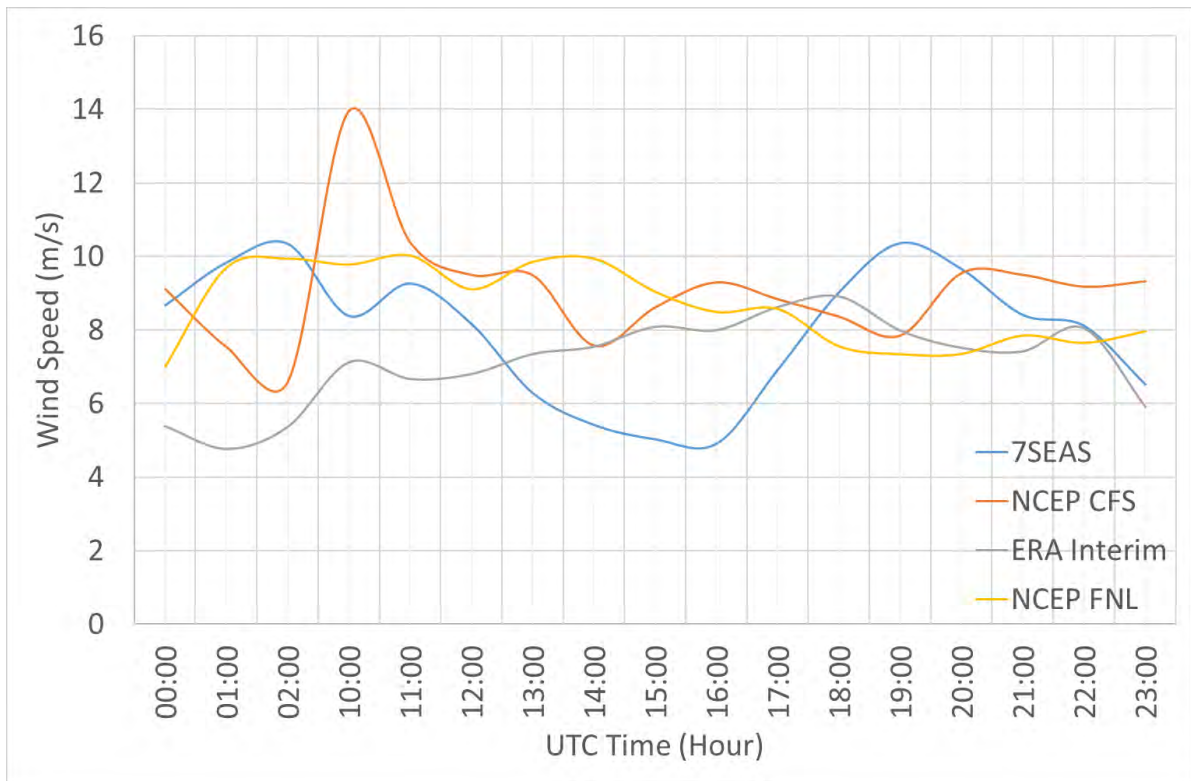


Figure 232. Tubtataha North Reef wind speeds on 23 September 2012

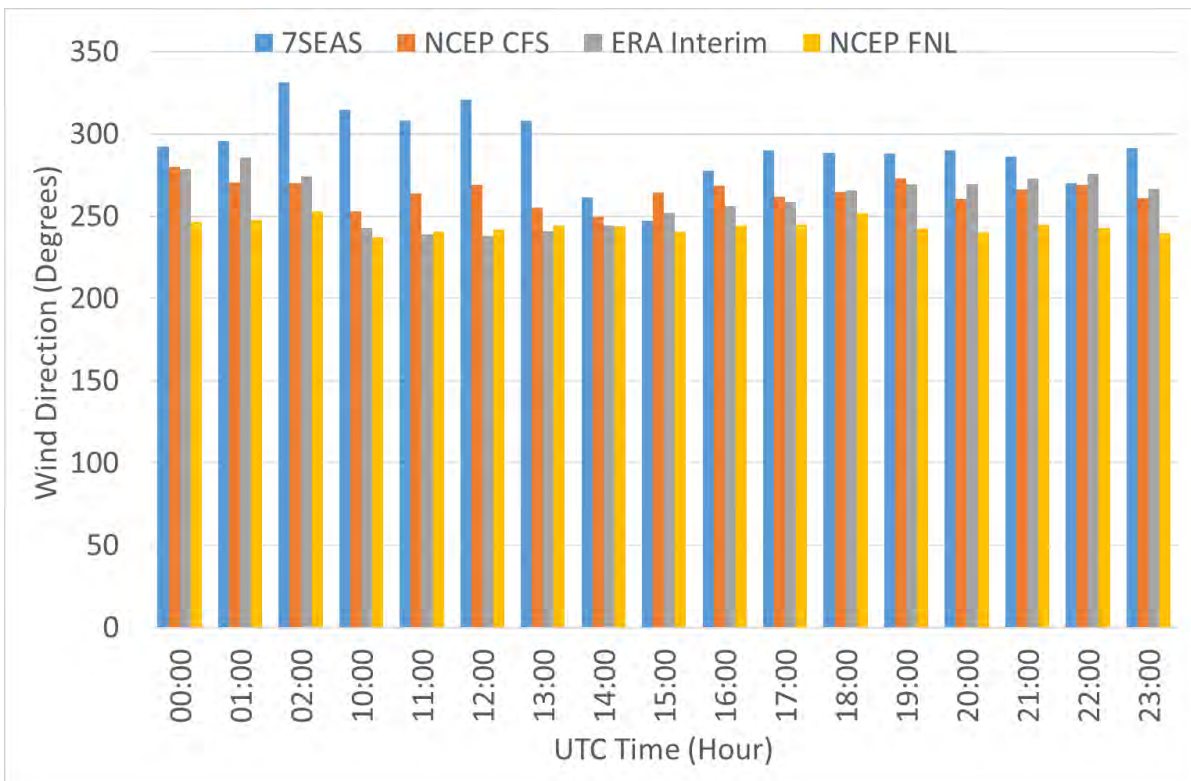


Figure 233. Wind directions for Tubtataha North Reef on 23 September 2012

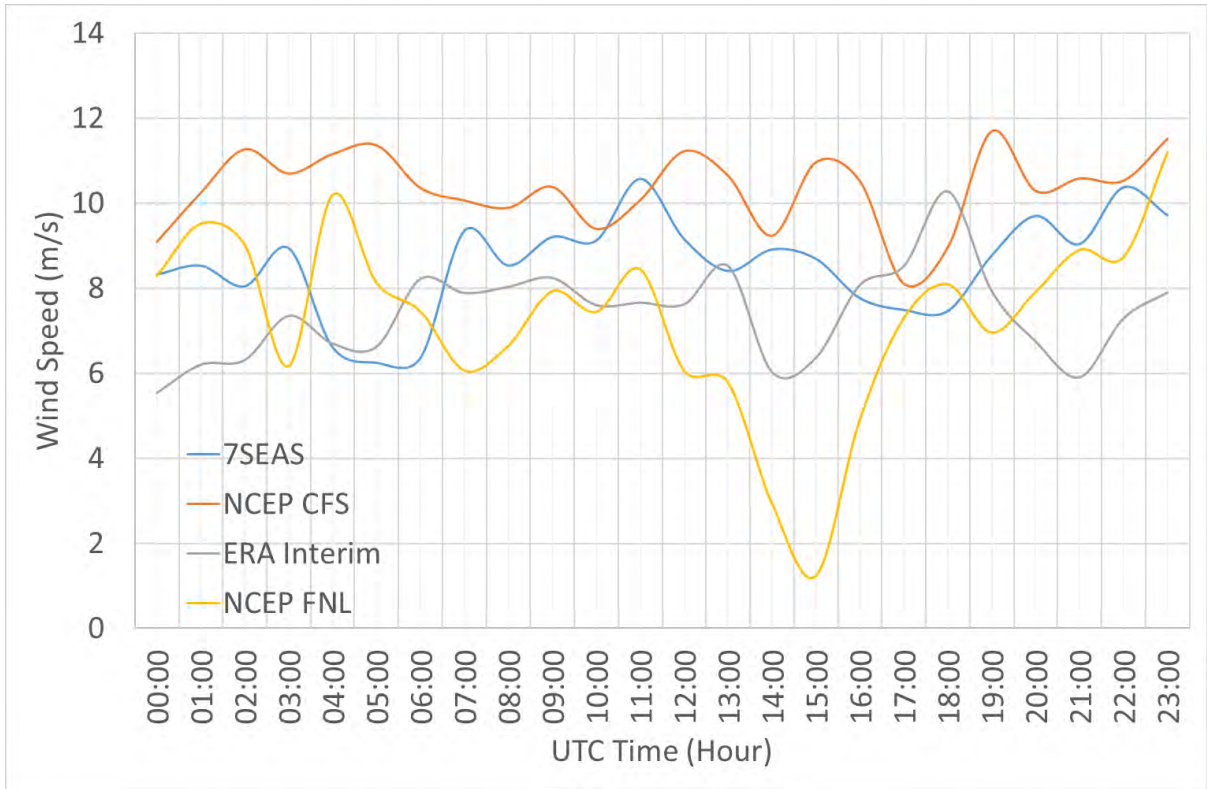


Figure 234. Tubbataha North Reef wind speeds on 24 September 2012

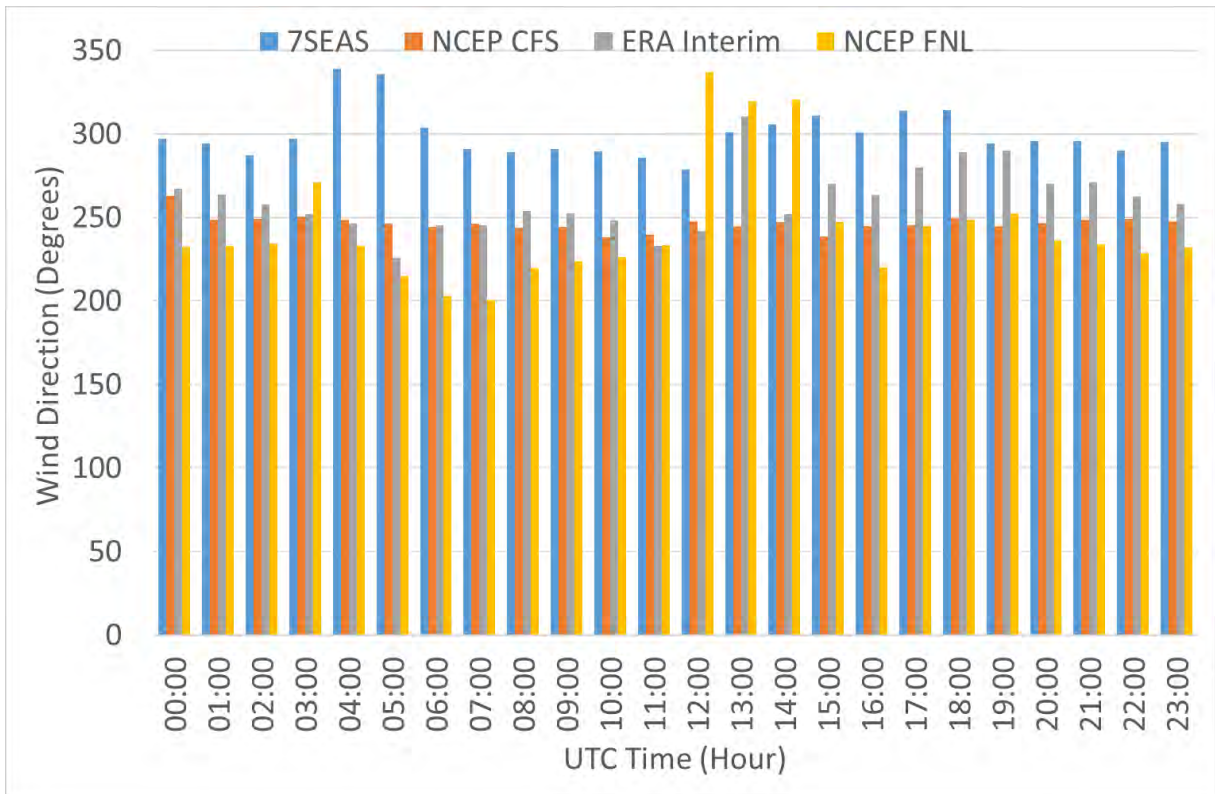


Figure 235. Wind directions for Tubbataha North Reef on 24 September 2012

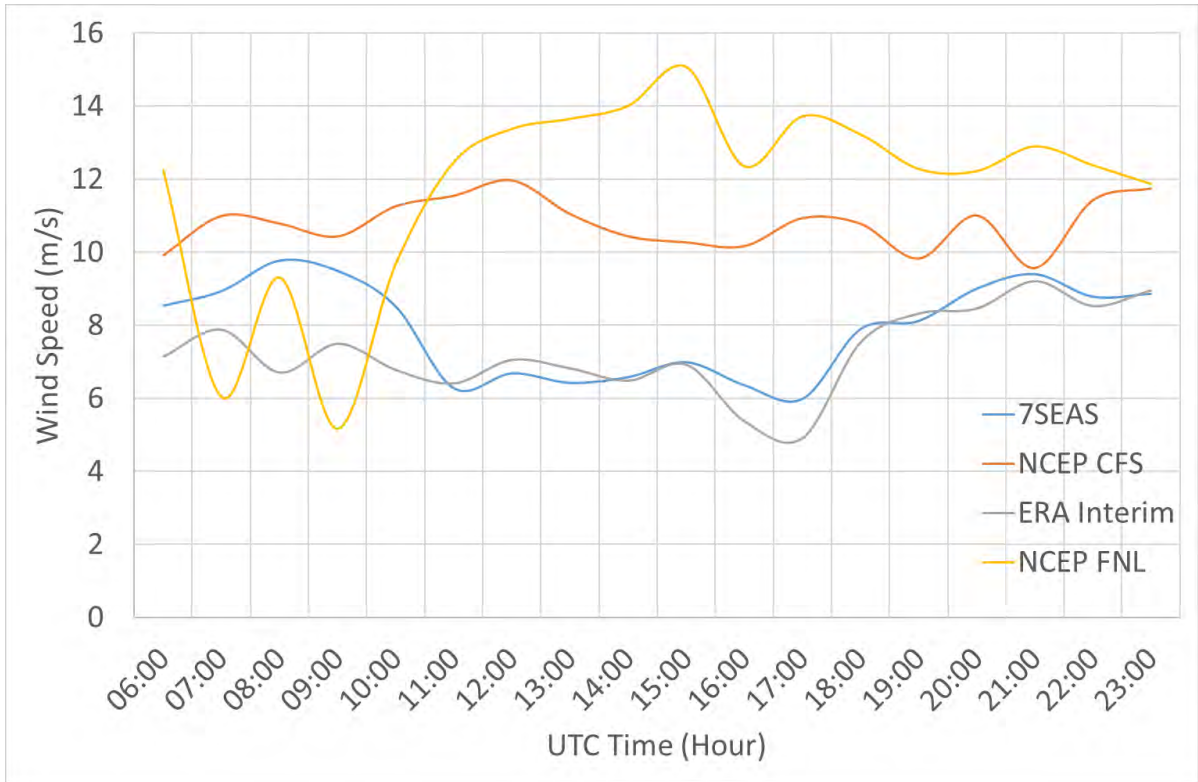


Figure 236. Wind speed comparison for Tubbatata South Reef on 25 September 2012

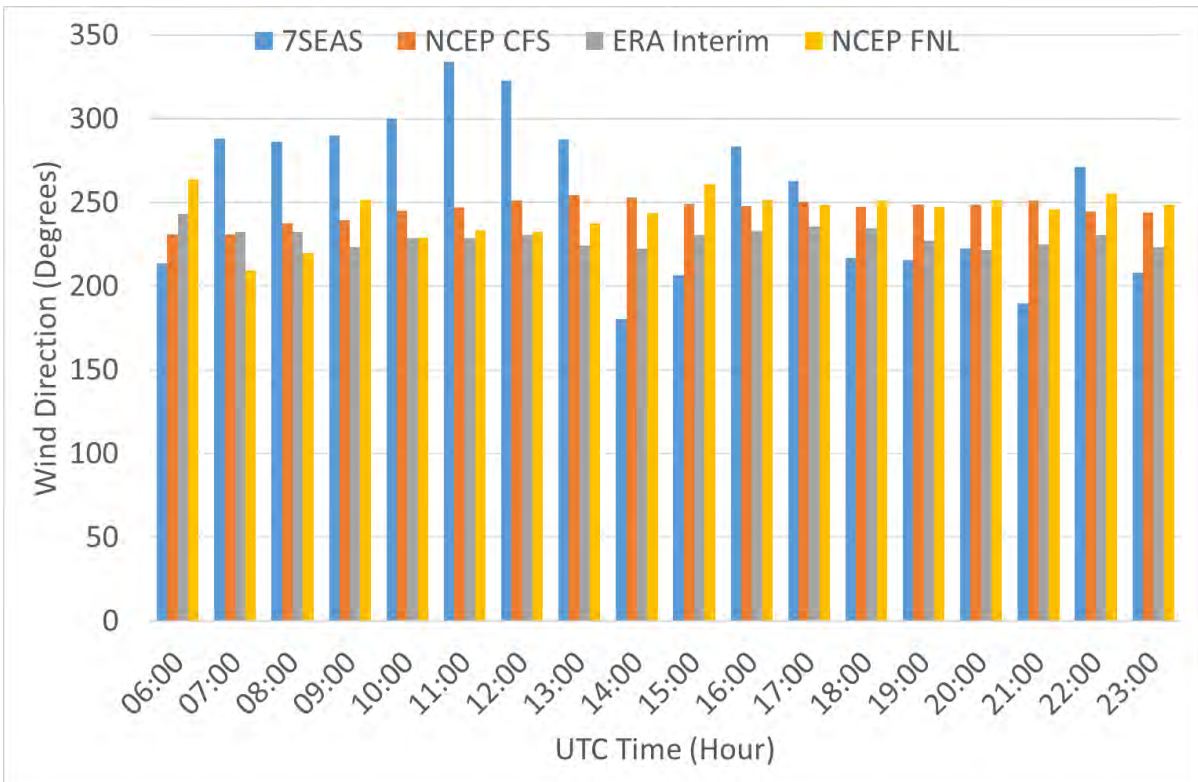


Figure 237. Comparison of wind direction for Tubbatata South Reef on 25 September 2012

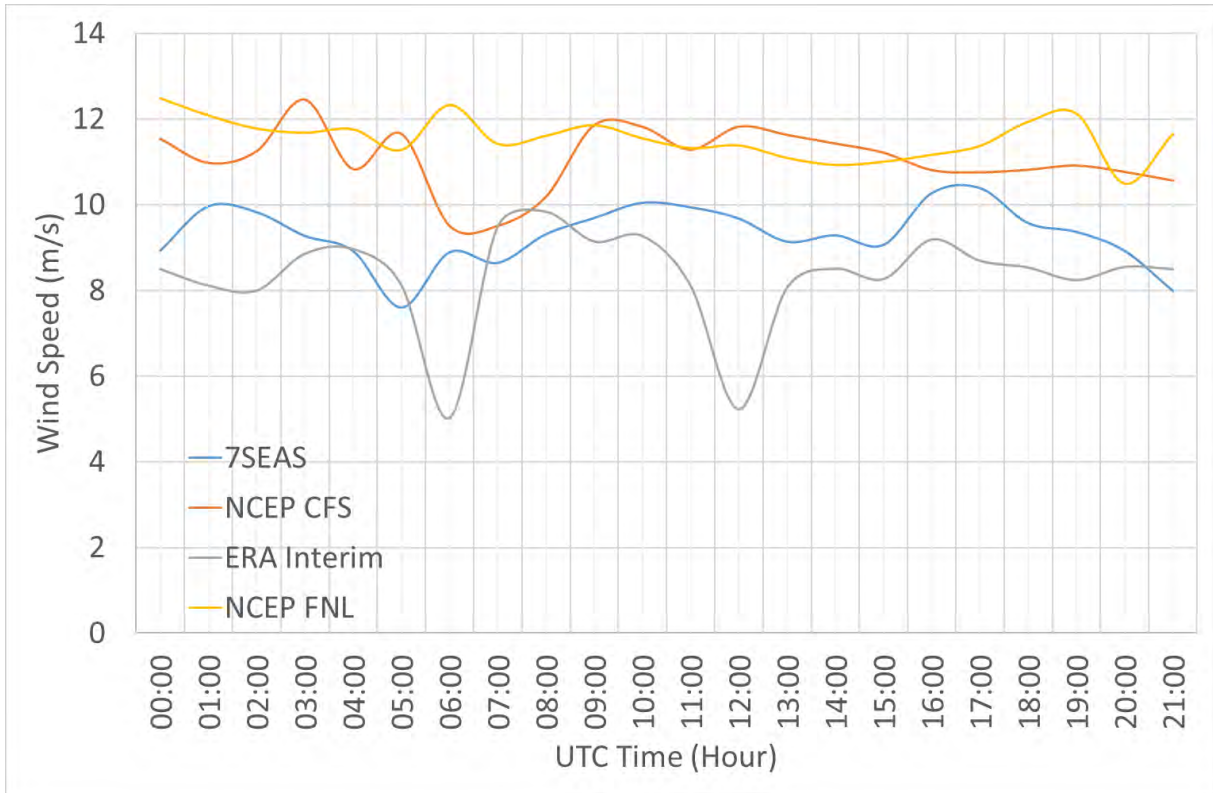


Figure 238. Wind speed comparison for Tubbatata South Reef on 26 September 2012

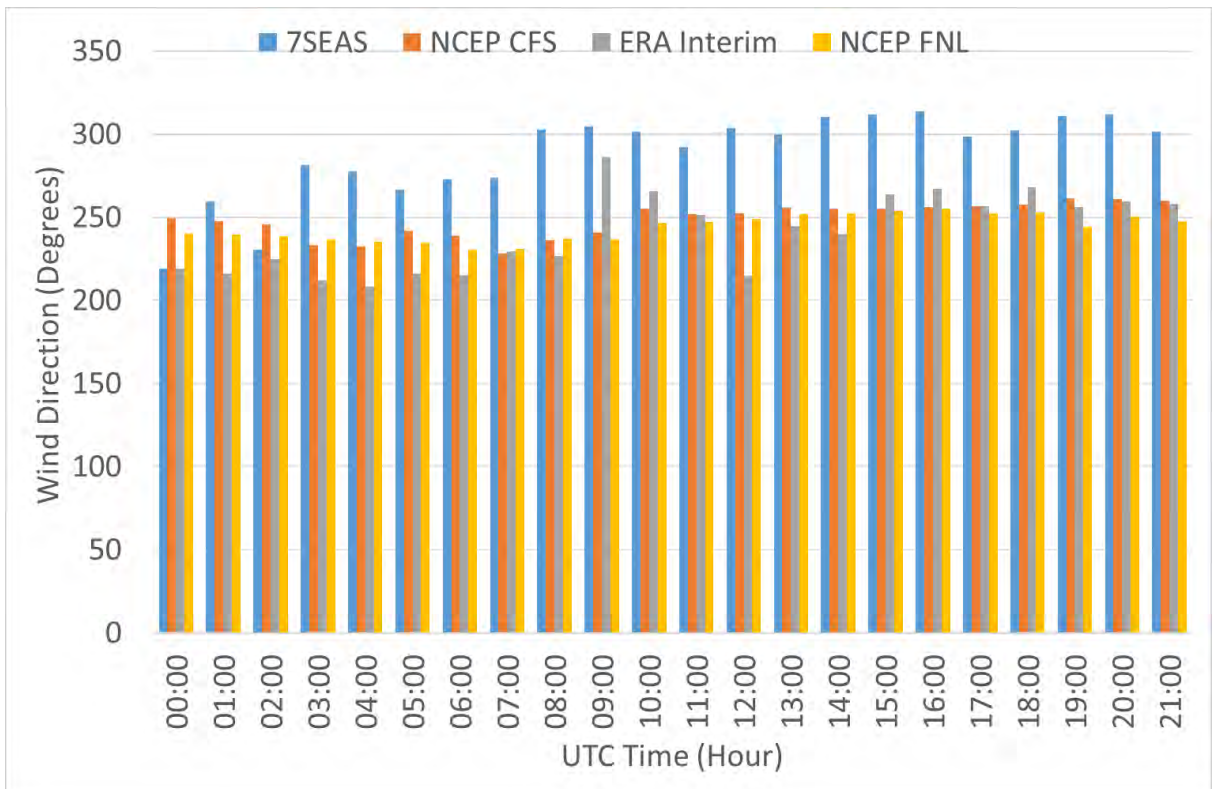


Figure 239. Comparison of wind direction for Tubbatata South Reef on 26 September 2012

Appendix 6: 7SEAS, Mesoscale Model, and Microscale Model Wind Velocity Data

Table 154. Balabac Island wind speed and wind direction values on
16 September 2012

Data Time	7SEAS		Mesoscale		Microscale	
	Wind Speed (m/s)	Wind Direction (°)	Wind Speed (m/s)	Wind Direction (°)	Wind Speed (m/s)	Wind Direction (°)
00:00	5.96	248.31	5.96	215.84	4.90	215.60
01:00	5.63	216.31	5.61	222.58	4.49	221.17
02:00	4.62	230.46	5.21	217.95	4.00	218.48
03:00	3.77	216.81	5.49	214.17	4.22	214.88
04:00	4.08	234.89	5.82	223.16	4.43	224.66
05:00	4.24	299.72	5.67	230.70	4.06	228.99
06:00	4.93	307.42	5.04	235.71	3.96	235.60
07:00	5.12	340.52	6.42	249.93	4.69	246.35
08:00	5.11	282.02	6.27	253.96	4.66	251.61
09:00	5.48	213.41	5.55	258.23	4.44	258.09
10:00	5.44	170.63	5.99	268.11	4.73	265.75
11:00	9.15	177.85	5.89	271.19	4.56	268.87
12:00	5.54	244.09	6.19	271.55	5.00	267.26
13:00	6.75	223.52	5.77	276.03	4.57	273.94
14:00	6.06	171.12	5.45	273.81	4.24	272.05
15:00	6.75	210.05	6.18	271.34	4.73	267.27
16:00	6.20	231.80	5.55	272.81	4.55	268.17
17:00	5.85	271.26	5.49	272.86	4.54	269.75
18:00	7.04	252.81	5.76	266.83	4.79	264.88
19:00	5.49	291.43	5.98	262.50	4.93	259.89
20:00	6.57	195.83	6.05	261.59	4.83	258.77
21:00	7.38	252.41	6.56	266.69	5.17	263.15
22:00	7.19	254.47	7.12	268.06	5.51	264.36
23:00	7.39	275.61	6.97	266.19	5.50	263.34

Table 155. Guntao Islands wind speed and wind direction values
on 24 September 2011

Data Time	7SEAS		Mesoscale		Microscale	
	Wind Speed (m/s)	Wind Direction (°)	Wind Speed (m/s)	Wind Direction (°)	Wind Speed (m/s)	Wind Direction (°)
00:00	6.71	224.91	8.12	210.34	5.06	210.31
01:00	6.80	206.04	7.90	211.07	6.31	210.66
02:00	5.92	207.47	8.11	209.77	5.11	196.11
03:00	5.01	215.31	7.78	214.67	3.85	211.42
04:00	4.63	208.30	7.10	222.37	3.48	222.20
05:00	4.45	200.40	7.20	227.82	3.77	224.80
06:00	4.66	212.39	7.47	228.05	4.14	225.06
07:00	4.82	205.46	7.52	223.25	5.18	220.08
08:00	4.75	181.11	8.14	219.64	3.83	218.09
09:00	4.76	220.16	5.76	219.30	3.54	220.36
10:00	5.67	198.25	6.32	217.04	4.45	216.52
11:00	6.00	218.22	5.27	214.85	2.98	204.96
12:00	5.42	217.47	3.61	176.80	4.15	198.44
13:00	5.45	210.51	4.35	192.28	3.19	199.30
14:00	5.41	220.62	4.33	192.58	3.95	200.75
15:00	6.72	219.22	4.10	168.31	3.41	175.87
16:00	6.78	187.60	4.46	164.84	3.47	173.19
17:00	6.44	202.60	4.08	171.09	4.42	185.10
18:00	5.04	181.19	4.76	174.53	4.35	188.70
19:00	3.25	176.78	4.88	186.09	4.94	193.90
20:00	3.59	182.33	6.03	199.30	4.15	200.88
21:00	3.63	197.28	6.73	207.57	2.71	195.83
22:00	4.63	190.15	6.69	200.56	5.87	200.89
23:00	4.85	201.43	5.64	187.20	5.11	196.11

Table 156. Notch Island wind speed and wind direction values on
21 September 2011

Data Time	7SEAS		Mesoscale		Microscale	
	Wind Speed (m/s)	Wind Direction (°)	Wind Speed (m/s)	Wind Direction (°)	Wind Speed (m/s)	Wind Direction (°)
00:00	5.56	222.08	6.05	214.14	6.41	213.79
01:00	8.57	233.70	6.48	214.87	5.94	211.54
02:00	7.01	235.19	6.01	214.61	6.12	209.86
03:00	5.86	233.00	6.70	218.48	6.04	209.93
04:00	5.79	242.32	6.10	227.79	5.51	214.52
05:00	5.02	240.41	6.20	239.65	5.32	230.27
06:00	6.14	244.04	5.51	251.34	4.38	231.45
07:00	6.19	241.08	6.33	245.87	2.68	226.78
08:00	6.37	241.12	6.34	248.95	7.70	241.76
09:00	6.53	240.26	6.90	247.13	4.30	240.74
10:00	6.87	249.05	4.77	244.10	5.08	240.51
11:00	4.92	223.63	4.49	234.21	3.60	242.22
12:00	3.54	234.42	4.28	221.51	3.21	235.02
13:00	5.06	222.99	5.12	219.64	2.78	227.31
14:00	6.15	210.03	4.64	221.03	3.87	221.77
15:00	5.35	188.46	5.99	208.41	3.87	221.77
16:00	4.74	212.98	5.73	201.77	6.39	203.96
17:00	5.94	207.84	4.64	191.30	7.01	206.77
18:00	7.00	212.61	4.99	196.82	6.18	197.03
19:00	5.88	218.70	4.86	187.62	6.35	188.96
20:00	5.11	215.16	5.20	183.77	7.49	205.26
21:00	6.03	219.50	6.13	204.75	7.04	208.97
22:00	9.04	264.95	5.54	195.16	6.70	199.85
23:00	8.39	251.91	6.94	203.29	6.70	207.99

Table 157. Tubbataha Reef wind speed and wind direction values
on 22 September 2012

Data Time	7SEAS		Mesoscale		Microscale	
	Wind Speed (m/s)	Wind Direction (°)	Wind Speed (m/s)	Wind Direction (°)	Wind Speed (m/s)	Wind Direction (°)
00:00	6.24	262.93	7.50	286.74	5.16	288.10
01:00	6.18	242.98	5.70	278.19	4.05	278.99
02:00	5.65	305.59	5.90	274.57	4.21	274.46
03:00	5.17	299.18	5.40	279.96	4.13	281.00
04:00	6.24	259.30	6.00	279.35	3.86	280.04
05:00	7.72	315.85	5.07	275.89	2.82	277.17
06:00	5.94	317.55	5.69	288.36	3.59	287.43
07:00	6.24	316.45	5.33	281.21	3.58	280.70
08:00	5.91	291.86	4.52	274.14	3.13	272.96
09:00	8.59	252.00	4.33	274.43	2.93	273.89
10:00	6.16	321.87	4.39	266.35	3.14	263.79
11:00	4.98	327.55	4.59	262.68	3.18	262.49
12:00	5.89	191.91	4.83	260.15	3.74	257.76
13:00	7.10	313.60	5.66	263.35	3.79	263.33
14:00	6.29	309.66	6.42	269.38	4.57	276.36
15:00	6.02	322.03	6.97	292.37	4.52	295.39
16:00	6.08	320.75	7.17	299.64	4.13	300.61
17:00	6.22	301.23	7.14	297.27	4.32	295.46
18:00	7.29	311.69	7.74	293.69	4.84	290.78
19:00	6.16	270.24	7.24	292.58	4.75	292.37
20:00	6.27	282.49	6.34	288.06	4.94	290.53
21:00	5.67	285.41	6.80	274.86	4.70	279.48
22:00	5.23	299.63	6.23	283.48	4.26	284.15
23:00	4.25	321.05	6.22	280.60	3.86	278.50

Appendix 7: WRF Configuration Files

The files containing the configuration settings of the WRF model are listed here. These are sample configurations that will require changes based on the dataset to be used for the model.

The `namelist.wps` contains the settings for domain, geographical data, and input dataset required for the WRF model simulations.

Listing `namelist.wps`:

```
&share
  wrf_core = 'ARW',
  max_dom = 3
  start_date = '2009-12-29_00:00:00', '2009-12-29_00:00:00', '2009-12-
29_00:00:00',
  end_date   = '2013-01-02_00:00:00', '2013-01-02_00:00:00', '2013-01-
02_00:00:00',
  interval_seconds = 21600
  io_form_geogrid = 2,
/

&geogrid
  parent_id      = 1, 1, 2,
  parent_grid_ratio = 1, 3, 3,
  i_parent_start = 1, 15, 20,
  j_parent_start = 1, 15, 32,
  e_we          = 90, 160, 154,
  e_sn          = 87, 178, 190,
  geog_data_res = '10m', '5m', '30s',
  dx = 27000,
  dy = 27000,
  map_proj = 'mercator',
  ref_lat  = 12.3,
  ref_lon  = 122.5,
  truelat1 = 12.3,
  truelat2 = 12.3,
  stand_lon = 122.5,
  geog_data_path = '../WPS_GEOG/'
/

&ungrib
  out_format = 'WPS',
  prefix = 'SFC',
/

&metgrid
  fg_name = 'SFC', 'PL'
  io_form_metgrid = 2,
/
```

The namelist.input contains the configuration needed to run the NWP system of the WRF model.

Listing namelist.input:

```
&time_control
run_days           = 32,
run_hours          = 0,
run_minutes        = 0,
run_seconds        = 0,
start_year         = 2010, 2010, 2010,
start_month        = 03, 03, 03,
start_day          = 31, 31, 31,
start_hour         = 00, 00, 00,
start_minute       = 00, 00, 00,
start_second       = 00, 00, 00,
end_year           = 2010, 2010, 2010,
end_month          = 05, 05, 05,
end_day            = 02, 02, 02,
end_hour           = 00, 00, 00,
end_minute         = 00, 00, 00,
end_second         = 00, 00, 00,
interval_seconds   = 21600
input_from_file    = .true.,.true.,.true.,
history_interval   = 60, 60, 60,
frames_per_outfile = 24, 24, 24,
restart            = .false.,
restart_interval    = 10800,
io_form_history     = 2
io_form_restart    = 2
io_form_input       = 2
io_form_boundary    = 2
debug_level        = 0
/

&domains
time_step           = 135,
time_step_fract_num = 0,
time_step_fract_den = 1,
max_dom             = 3,
e_we                = 90, 160, 154,
e_sn                = 87, 178, 190,
e_vert              = 50, 50, 50,
p_top_requested     = 5000,
eta_levels =
  1, 0.995, 0.9925, 0.990, 0.9875, 0.985, 0.9825, 0.980, 0.9775,
0.975, 0.9725, 0.970, 0.965, 0.960, 0.950, 0.940,0.930, 0.920,
0.910, 0.900, 0.890, 0.880, 0.870,
  0.840, 0.801, 0.761, 0.722, 0.652, 0.587, 0.527, 0.472, 0.421,
0.374,
  0.331, 0.291, 0.255, 0.222, 0.191, 0.163, 0.138, 0.115, 0.095,
0.077,
  0.061, 0.047, 0.035, 0.024, 0.015, 0.007, 0,
num_metgrid_levels = 38,
num_metgrid_soil_levels = 4,
dx                  = 27000, 9000, 3000,
```

```

dy = 27000, 9000, 3000,
grid_id = 1, 2, 3,
parent_id = 1, 1, 2,
i_parent_start = 1, 15, 20,
j_parent_start = 1, 15, 32,
parent_grid_ratio = 1, 3, 3,
parent_time_step_ratio = 1, 3, 3,
feedback = 1,
smooth_option = 0
nproc_x = 3
nproc_y = 8
/

&physics
mp_physics = 6, 6, 6,
ra_lw_physics = 1, 1, 1,
ra_sw_physics = 1, 1, 1,
radt = 45, 45, 45,
sf_sfclay_physics = 2, 2, 2,
sf_surface_physics = 2, 2, 2,
bl_pbl_physics = 2, 2, 2,
bldt = 0, 0, 0,
cu_physics = 1, 1, 1,
cudt = 0, 0, 0,
isfflx = 1,
ifsnow = 0,
icloud = 1,
surface_input_source = 1,
num_soil_layers = 4,
sf_urban_physics = 0, 0, 0,
/

&fdda
/

&dynamics
w_damping = 0,
diff_opt = 1, 1, 1,
km_opt = 4, 4, 4,
diff_6th_opt = 0, 0, 0,
diff_6th_factor = 0.12, 0.12, 0.12,
base_temp = 290.
damp_opt = 0,
zdamp = 5000., 5000., 5000.,
dampcoef = 0.2, 0.2, 0.2,
khdif = 0, 0, 0,
kvdif = 0, 0, 0,
epssm = 1, 1, 1,
non_hydrostatic = .true., .true., .true.,
moist_adv_opt = 1, 1, 1,
scalar_adv_opt = 1, 1, 1,
/

&bdy_control
spec_bdy_width = 10,
spec_zone = 1,

```

```
relax_zone           = 9,  
specified           = .true., .false., .false.,  
nested              = .false., .true., .true.,  
/  
  
&grib2  
/  
  
&namelist_quilt  
nio_tasks_per_group = 0,  
nio_groups = 1,  
/  


---


```

Appendix 8: Cray Job Submission Scripts

These scripts are the necessary files to submit job requests to run calculations to the Cray HPC systems used for running the WRF model.

The `geogrid.pbs` is the job request to run the `geogrid.exe`.

Listing `geogrid.pbs`:

```
#!/bin/bash --login

# PBS job name
#PBS -N geogrid
# PBS requested number of nodes
#PBS -l select=1
# PBS walltime to run job
#PBS -l walltime=1:00:00
# PBS budget code for job
#PBS -A e508-snuy

# Change to work directory
cd /WRF/WRFV3/WPS
# Turn off threading
export OMP_NUM_THREADS=1

# Launch the parallel run
pwd > cur_dir.txt
# aprun -n 8 ./geogrid >& log_geogrid.txt
```

The `ungrib.pbs` is for unpacking the input dataset to be used for the simulations. This module is done serially thus, the appropriate job request is shown in the listing that follows.

Listing `ungrib.pbs`

```
#!/bin/bash --login

# PBS job name
#PBS -N ungrib
# PBS requested number of nodes
#PBS -l select=serial=true:ncpus=1
# PBS walltime to run job
#PBS -l walltime=24:00:00
# PBS budget code for job
#PBS -A e508-snuy

# Change to work directory
cd /WRF/WRFV3/WPS

# Launch the parallel run
pwd > cur_dir.txt
# ./ungrib >& log_ungrib.txt
```

The metgrid.pbs is the job request to run the metgrid.exe.

Listing metgrid.pbs:

```
#!/bin/bash --login

# PBS job name
#PBS -N metgrid
# PBS requested number of nodes
#PBS -l select=1
# PBS walltime to run job
#PBS -l walltime=24:00:00
# PBS budget code for job
#PBS -A e508-snuy

# Change to work directory
cd /WRF/WRFV3/WPS
# Turn off threading
export OMP_NUM_THREADS=1

# Launch the parallel run
pwd > cur_dir.txt
# aprun -n 8 ./metgrid >& log_metgrid.txt
```

The realrun.pbs is the job request for initialising the domain and input data for the WRF model simulation.

Listing realrun.pbs:

```
#!/bin/bash --login

# PBS job name
#PBS -N runreal
# PBS requested number of nodes
#PBS -l select=1
# PBS walltime to run job
#PBS -l walltime=10:00:00
# PBS budget code for job
#PBS -A e508-snuy

# Change to working directory for job
cd /work/e508/e508/snuy/WRF/WRFV3/em_real
# Turn off threading
export OMP_NUM_THREADS=1

# Launch the parallel run
aprun -n 24 ./real.exe >& log_real.txt
```

The wrfrun.pbs is the job request to run the NWP module of the WRF model.

Listing wrfrun.pbs:

```
#!/bin/bash --login

# PBS job name
#PBS -N runWRFmod
# PBS requested number of nodes
#PBS -l select=1
# PBS walltime to run job
#PBS -l walltime=03:00:00
# PBS budget code for job
#PBS -A e508-snuy

# Change to working directory for job
cd /work/e508/e508/snuy/WRF/WRFV3/em_real
# Turn off threading
export OMP_NUM_THREADS=1

# Launch the parallel run
aprun -n 24 ./wrf.exe >& log_wrf.txt
```

Appendix 9: Scripts for Wind Mapping

These scripts are written with the NCL language. These have been used to extract specific datapoints at a particular location for validation with observations and for generating wind maps.

CCMP_wpd.ncl is used for generating the wind maps from the CCMP dataset.

Listing CCMP_wpd.ncl:

```
load "$NCARG_ROOT/lib/ncarg/nclscripts/csm/gsn_code.ncl"

begin

  cdf_file=addfile("CCMP_Wind_Analysis_climatology_V02.0_L3.5_RSS.nc", "r")

  lat = cdf_file->latitude
  lon = cdf_file->longitude
  climtime = cdf_file->time
  nclimtime = dimsizes(climtime)
  wsc = cdf_file->wspd(0, :, :)
  do iclimtime = 1, nclimtime-1
    wsctemp = cdf_file->wspd(iclimtime, :, :)
    wsc = wsc + wsctemp
  end do

  delete(wsctemp)
  wsc = wsc/12
  printVarSummary(wsc)
  printMinMax(wsc, False)

  wpd = wsc(:, :)
  wpd = 0.5*1.225*wpd^3
  printMinMax(wpd, False)
  wpd@long_name = "Climatological Wind Power Density"
  wpd@units = "W/m^2"
  delete(wsc)

; We generate plots, but what kind do we prefer?
; type = "x11"
; type = "pdf"
; type = "ps"
; type = "ncgm"
type = "png"
wks = gsn_open_wks(type, "dataonmap")

print(wpd!0)           ; Print the dimension names for the
print(wpd!1)           ; first two dimensions of wsc.
print(wpd@long_name)  ; Print "long_name" and "units"
print(wpd@units)      ; attributes of "wsc".
print(wsc&lat)         ; Print coordinate variables "lat"
print(wsc&lon)         ; and "lon".

res                    = True
res@gsnMaximize        = True
res@cnFillOn           = True
res@cnLinesOn          = False
res@tiMainString       = "Climatology Wind Data Average for 1988 - 2017"
```

```

plot = gsn_csm_contour_map(wks,wpd,res)

delete(plot)      ; Clean up.
delete(wpd)
delete(res)
end

```

The script `wind_speed_ERA-5.ncl` is used for the visualisation of ERA-5 winds dataset.

Listing `wind_speed_ERA-5.ncl`:

```

load "$NCARG_ROOT/lib/ncarg/nclscripts/csm/gsn_code.ncl"

begin

  cdf_file = addfile("ERA-5_Monthly_Ave_1979-2018_100m_Wind.nc","r")

  lat = cdf_file->latitude
  lon = cdf_file->longitude
  months = cdf_file->time
  nmonths = dimsizes(months)
  u_pck = cdf_file->u100(0,,:,)
  v_pck = cdf_file->v100(0,,:,)
  uwspd = short2flt(u_pck)
  vwspd = short2flt(v_pck)
  do imonths = 1,nmonths-1
    u_pck = cdf_file->u100(imonths,,:,)
    v_pck = cdf_file->v100(imonths,,:,)
    utemp = short2flt(u_pck)
    vtemp = short2flt(v_pck)
    uwspd = abs(uwspd) + abs(utemp)
    vwspd = abs(vwspd) + abs(vtemp)
  end do

  delete(utemp)
  delete(vtemp)
  uwspd = uwspd/nmonths
  vwspd = vwspd/nmonths
  wsc = sqrt(uwspd^2 + vwspd^2)
  printVarSummary(wsc)
  printMinMax(wsc,False)

; We generate plots, but what kind do we prefer?
  type = "x11"
; type = "pdf"
; type = "ps"
; type = "ncgm"
; type = "png"
  wks = gsn_open_wks(type,"dataonmap")

  print(wsc(20:50,70:90))      ; Print subset of "wind speed
                              ; climatology" variable.

  print(wsc!0)                ; Print the dimension names for the
  print(wsc!1)                ; first two dimensions of wsc.
  print(wsc@long_name)       ; Print "long_name" and "units"

```



```

    print(wsc@units)                ; attributes of "wsc".
;   print(wsc&lat)                  ; Print coordinate variables "lat"
;   print(wsc&lon)                  ; and "lon".

    res                            = True
    res@gsnMaximize = True
    res@cnFillOn      = True
    res@cnLinesOn     = False
    res@tiMainString = "Climatology Wind Data Average for 1979 - 2018"

    plot = gsn_csm_contour_map(wks,wsc,res)

;   res@mpLimitMode      = "Corners"
;   res@mpLeftCornerLonF = lon(70)
;   res@mpRightCornerLonF = lon(90)
;   res@mpLeftCornerLatF = lat(20)
;   res@mpRightCornerLatF = lat(50)

;   plot = gsn_csm_contour_map(wks,wsc,res)

    delete(plot)      ; Clean up.
    delete(wsc)
    delete(res)
end

```

The WindSat_wpd.ncl script is used for producing wind maps using the WindSat dataset.

Listing WindSat_wps.ncl:

```

load "$NCARG_ROOT/lib/ncarg/nclscripts/csm/gsn_code.ncl"

begin

    cdf_file = addfile("ws_v07r01_198801_201903.nc4.nc","r")

    lat = cdf_file->latitude
    lon = cdf_file->longitude
    climtime = cdf_file->climatology_time
    nclimtime = dimsizes(climtime)
    wsc = cdf_file->wind_speed_climatology(0,,:,)
    do iclimtime = 1,nclimtime-1
        wsctemp = cdf_file->wind_speed_climatology(iclimtime,,:,)
        wsc = wsc + wsctemp
    end do

    delete(wsctemp)

    wsc = wsc/12
    printVarSummary(wsc)
    printMinMax(wsc,False)

    chkWSC = ndtooned(wsc(:,,:))
    indLt = ind(chkWSC.lt.0.0)
    chkWSC(indLt) = -999
    wsc(:,,:) = onedtond(chkWSC, dimsizes(wsc))
    printMinMax(wsc,False)
    delete(chkWSC)

```

```

wpd = wsc(:, :)
wpd = 0.5*1.225*wpd^3
printMinMax(wpd, False)
wpd@long_name = "Climatological Wind Power Density"
wpd@units = "W/m^2"
delete(wsc)

; We generate plots, but what kind do we prefer?
; type = "x11"
; type = "pdf"
; type = "ps"
; type = "ncgm"
type = "png"
wks = gsn_open_wks(type, "dataonmap")

print(wpd!0) ; Print the dimension names for the
print(wpd!1) ; first two dimensions of wsc.
print(wpd@long_name) ; Print "long_name" and "units"
print(wpd@units) ; attributes of "wsc".
; print(wsc&lat) ; Print coordinate variables "lat"
; print(wsc&lon) ; and "lon".

res = True
res@gsnMaximize = True
res@cnFillOn = True
res@cnLinesOn = False
res@tiMainString = "Climatology Wind Power Density Average for 1988 - 2007"

;-----
; Values below are some of the areas of interests:
; South China Sea: 90,150,50,130
; Indian Subcontinent: 60,90,90,120
; South America and Carribbean: 240,340,60,120

res@mpLimitMode = "Corners" ; Tropics band values
res@mpCenterLonF = 100
res@mpLeftCornerLonF = lon(90) ; 170
res@mpRightCornerLonF = lon(170) ; 190
res@mpLeftCornerLatF = lat(50) ; 50
res@mpRightCornerLatF = lat(130) ; 130

;-----
; Code below is for mapping the African and American continents
; Africa: 350, 20, 80, 40, 40
; Americas: 240, 10, 90, 40, 30

; res@pmTickMarkDisplayMode = "Always"
; res@mpLimitMode = "Angles"
; res@mpCenterLonF = 240
; res@mpLeftAngleF = 10
; res@mpRightAngleF = 90
; res@mpTopAngleF = 40
; res@mpBottomAngleF = 30
; res@mpPerimOn = True

plot = gsn_csm_contour_map(wks, wpd, res)

delete(plot) ; Clean up.

```

```

delete(wpd)
delete(res)
end

```

The script for generating wind maps from the WRF outputs is the wrf_EtaLevels_color.ncl.

Listing wrf_EtaLevels_color.ncl:

```

load "$NCARG_ROOT/lib/ncarg/nclscripts/csm/gsn_code.ncl"
load "$NCARG_ROOT/lib/ncarg/nclscripts/csm/gsn_csm.ncl"
load "$NCARG_ROOT/lib/ncarg/nclscripts/wrf/WRFUserARW.ncl"

begin
;
; The WRF ARW input file.
; This needs to have a ".nc" appended, so just do it.
a = addfile("./wrfout_d03_2011-01-25_00:00:00.nc","r")

; We generate plots, but what kind do we prefer?
; type = "x11"
type = "pdf"
; type = "ps"
; type = "ncgm"
wks = gsn_open_wks(type,"plt_EtaLevels")

; Set some Basic Plot options
res = True
res@MainTitle = "REAL-TIME WRF"
; res@cnFillPalette = "gsltod"

pltres = True
; pltres@cnFillPalette = "gsltod"
mpres = True
; mpres@cnFillPalette = "gsltod"
mpres@mpGeophysicalLineColor = "Black"
mpres@mpGeophysicalLineThicknessF = 4.0
; mpres0 = True
; mpres0@mpGeophysicalLineColor = "Black"
; mpres0@mpNationalLineColor = "Black"
; mpres0@mpUSStateLineColor = "Black"

;;;;;;;;;;;;;
;;;;;;;;;;;;;

; What times and how many time steps are in the data set?
times = wrf_user_getvar(a,"times",-1) ; get all times in the file
ntimes = dimsizes(times) ; number of times in the file

;;;;;;;;;;;;;

do it = 0,ntimes-1,2 ; TIME LOOP

print("Working on time: " + times(it) )
res@TimeLabel = times(it) ; Set Valid time to use on plots

```

```

;;;;;;;;;;;;;;;;;;;;;;;;;;;;;;;;;;;;;;;;;;;;;;;;;;;;;;;;;;;;;;;;;;;;;;;;;;;;;;;;
; First get the variables we will need

; th = wrf_user_getvar(a,"theta",it) ; theta
; qv = wrf_user_getvar(a,"QVAPOR",it) ; Qvstring
; qv = qv*1000.
; qv@units = "g/kg"

u = wrf_user_getvar(a,"ua",it) ; u averaged to mass points
v = wrf_user_getvar(a,"va",it) ; v averaged to mass points
spd = (u*u + v*v)^(0.5) ; speed in m/sec
spd@description = "Wind Speed"
spd@units = "m/s"
; u = u*1.94386 ; winds now in kts
; v = v*1.94386 ; winds now in kts
; u@units = "kts"
; v@units = "kts"

;;;;;;;;;;;;;;;;;;;;;;;;;;;;;;;;;;;;;;;;;;;;;;;;;;;;;;;;;;;;;;;;;;;;;;;;;;;;;;;;

; dimsv = dimsizes(th) ; Get levels
; do level = 0,dimsv(0)-1,5 ; LOOP OVER LEVELS
level = 3
display_level = level + 1

res@PlotLevelID = "Eta Level " + display_level

; Theta
; opts = res
; opts@cnLineColor = "Red"
; opts@ContourParameters = (/ 5.0 /)
; opts@gsnContourLineThicknessesScale = 2.0
; contour = wrf_contour(a,wks,th(level,,:),opts)
; plot = wrf_map_overlays(a,wks,(/contour/),pltres,mpres0)
; delete(opts)

; Qv
; opts = res
; opts@cnLineColor = "Blue"
; opts@cnFillOn = True
; contour = wrf_contour(a,wks,qv(level,,:),opts)
; plot = wrf_map_overlays(a,wks,(/contour/),pltres,mpres)
; delete(opts)

; Wind Vectors and Speed
opts = res
opts@ContourParameters = (/ 2., 10., 1. /)
;opts@cnMonoFillColor = True
opts@cnFillOn = True
opts@cnFillColors =
(/"gray100","gray90","gray80","gray70","gray60","gray50","gray40","gray30",
"gray20","gray10","gray0"/)
opts@cnFillOpacityF = 0.7
; opts@cnFillPalette = "gsltod"
;opts@cnMonoFillPattern = False
;opts@cnFillPattern = 1
;opts@cnFillPatterns = (/2,5,12/)
contour = wrf_contour(a,wks,spd(level,,:),opts)
delete(opts)

```

```

opts = res
opts@FieldTitle      = "Wind"          ; Overwrite Field Title
opts@NumVectors      = 35             ; wind barb density
vector = wrf_vector(a,wks,u(level, :, :),v(level, :, :),opts)
delete(opts)

plot = wrf_map_overlays(a,wks,(/contour, vector/),pltres,mpres)

; end do          ; END OF LEVEL LOOP

;;;;;;;;;;;;;

end do          ; END OF TIME LOOP

end

```

The `Coron_daily_10m_winds.ncl` is a script for extracting wind data at a location for validation with daily averaged wind observations. It is a sample for all the three onshore sites that had been compared with PAGASA data.

Listing `Coron_daily_10m_winds.ncl`:

```

#####
load "$NCARG_ROOT/lib/ncarg/nclscripts/csm/gsn_code.ncl"
load "$NCARG_ROOT/lib/ncarg/nclscripts/csm/contributed.ncl"
load "$NCARG_ROOT/lib/ncarg/nclscripts/csm/wind_rose.ncl"
load "$NCARG_ROOT/lib/ncarg/nclscripts/wrf/WRFUserARW.ncl"

begin

  dataDir = "./"
  dataFiles = systemfunc("ls -l "+dataDir+ "wrfout_d03*")
  nFiles = dimsizes(dataFiles)
  header = (/Wind Speed; Wind Direction; StdDev;/)
  write_table("Coron_Mar_2010_cfs.txt", "w", [/header/], "%s")

  do nday = 0, nFiles-1
    f = addfile(dataFiles(nday)+".nc", "r")

    uvm10 = wrf_user_getvar(f,"uvmet10",-1)
    u10 = uvm10(0, :, :, :)
    v10 = uvm10(1, :, :, :)

    ; Pick one grid point
    loc = wrf_user_ll_to_ij(f, 120.2033, 11.9983, True)
    mx = loc(0) - 1
    ny = loc(1) - 1

    lat1 = f->XLAT(0,ny,mx)
    lon1 = f->XLONG(0,ny,mx)
    res = True

    wspd1= ndtooned( sqrt(u10(:,ny,mx)^2 + v10(:,ny,mx)^2) )
    wdir1= ndtooned(atan2(u10(:,ny,mx),v10(:,ny,mx))/0.01745329 +180. )

    wAve = avg(wspd1)
    wDir=ndtooned(atan2(avg(u10(:,ny,mx)),avg(v10(:,ny,mx)))/0.01745329
+180.)

```

```

        wStd = stddev(wspd1)

        dataOut=sprintf("%f; ", wAve)+sprintf("%f; ", wDir)+sprintf("%f",
wStd)
        write_table("Coron_Mar_2010_cfs.txt", "a", [/dataOut/], "%s")

    end do

end

```

The Balabac_hourly_10m_winds.ncl is a script for extracting wind data at a location for validation with hourly averaged wind observations. It is a sample for all the four offshore sites that had been compared with 7SEAS wind measurements.

Listing Balabac_hourly_10m_winds.ncl:

```

;#####
load "$NCARG_ROOT/lib/ncarg/nclscripts/csm/gsn_code.ncl"
load "$NCARG_ROOT/lib/ncarg/nclscripts/csm/contributed.ncl"
load "$NCARG_ROOT/lib/ncarg/nclscripts/csm/wind_rose.ncl"
load "$NCARG_ROOT/lib/ncarg/nclscripts/wrf/WRFUserARW.ncl"

begin

    dataDir = "./"
    dataFiles = systemfunc("ls "+dataDir+ "wrfout_d03*")
    nFiles = dimsizes(dataFiles)
    header = (/ "Time; Wind Speed; Wind Direction;"/)
    write_table("Balabac_Sep_2012_cfs.txt", "w", [/header/], "%s")

    do nDay = 0, nFiles-1
        f = addfile(dataFiles(nDay)+".nc", "r")
        times = wrf_user_getvar(f,"times",-1)
        uvml0 = wrf_user_getvar(f,"uvmet10",-1)
        u10 = uvml0(0,:,:,)
        v10 = uvml0(1,:,:,)

        ; Pick one grid point
        loc = wrf_user_ll_to_ij(f, 116.937, 7.8646, True)
        mx = loc(0) - 1
        ny = loc(1) - 1
        lat1 = f->XLAT(0,ny,mx)
        lon1 = f->XLONG(0,ny,mx)
        wspd1= ndtooned( sqrt(u10(:,ny,mx)^2 + v10(:,ny,mx)^2) )
        wdir1= ndtooned( atan2(u10(:,ny,mx),v10(:,ny,mx))/0.01745329 +180. )

        dataOut = times + "; " + sprintf("%f; ", wspd1) + sprintf("%f; ",
wdir1)
        write_table("Balabac_Sep_2012_cfs.txt", "a", [/dataOut/], "%s")
    end do

end

```

Appendix 10: WindSim Pre-processing and Post-processing Scripts

The area to be extracted from the WRF results that are to be converted into .xyz files can be defined using the `get_domain.ncl`. The listed script is for the Balabac Island location but it can be used for other areas by changing the coordinates of the domain. The output values are necessary for the header definition of the .xyz file.

Listing `get_domain.ncl`:

```
load "$NCARG_ROOT/lib/ncarg/nclscripts/csm/gsn_code.ncl"
load "$NCARG_ROOT/lib/ncarg/nclscripts/csm/contributed.ncl"
load "$NCARG_ROOT/lib/ncarg/nclscripts/wrf/WRFUserARW.ncl"

begin
;
; The WRF ARW input file.
; This needs to have a ".nc" appended, so just do it.
  a = addfile("./wrfout_d03_2012-09-15_00:00:00.nc","r")

  glon2d = a->XLAT(0,::)
  glat2d = a->XLONG(0,::)

  printMinMax(glat2d, 0)
  printMinMax(glon2d, 0)

  latS   = 7.75                ; Balabac Island convert to lat-lon
  latN   = 7.95
  lonW   = 116.80
  lonE   = 117.05

  opt = True
  loc  = wrf_user_ll_to_ij(a,(/lonW,lonE/),(/latS,latN/),opt)
  loc  = loc-1                ; To convert to NCL subscripts

;---The requested and calculated values should be close
  print("Requested min/max xlat = " + latS + "/" + latN)
  print("Calculated min/max xlat = " + glon2d(loc(1,0),loc(0,0)) + "/" + \
        glon2d(loc(1,1),loc(0,1)))

  print("Requested min/max xlon = " + lonW + "/" + lonE)
  print("Calculated min/max xlon = " + glat2d(loc(1,0),loc(0,0)) + "/" + \
        glat2d(loc(1,1),loc(0,1)))

;---Count number of x and y elements.
  nix = 0
  njy = 0

  do elem = loc(0,0),loc(0,1),1          ; Count x
    nix = nix + 1
  end do

  do elem = loc(1,0),loc(1,1),1          ; Count y
    njy = njy + 1
  end do

  print("Number of x = " + nix)
  print("Number of y = " + njy)
```

end

The Balabac_sfc_wrf_to_xyz.ncl reads the WRF output files and extracts the terrain height, wind velocity, pressure, and temperature at 0 m and 10 m levels. These are written to a .xyz file created by the script.

Listing Balabac_sfc_wrf_to_xyz.ncl:

```
load "$NCARG_ROOT/lib/ncarg/nclscripts/csm/gsn_code.ncl"
load "$NCARG_ROOT/lib/ncarg/nclscripts/csm/contributed.ncl"
load "$NCARG_ROOT/lib/ncarg/nclscripts/wrf/WRFUserARW.ncl"

begin
;
; The WRF ARW input file.
; This needs to have a ".nc" appended, so just do it.
a = addfile("./wrfout_d03_2012-09-15_00:00:00.nc","r")

header = ("/10 6 18"/)

write_table("WindSim_out.txt", "w", [/header/], "%s")

glon2d = a->XLAT(0,::)
glat2d = a->XLONG(0,::)

printMinMax(glat2d, 0)
printMinMax(glon2d, 0)

printVarSummary(glat2d)
printVarSummary(glon2d)

latS = 7.75 ; Balabac Island lat-lon
latN = 7.95
lonW = 116.80
lonE = 117.05

opt = True
loc = wrf_user_ll_to_ij(a,(/lonW,lonE/),(/latS,latN/),opt)
loc = loc-1 ; To convert to NCL subscripts

;---Just for fun, pick a variable and take a subdomain of it.

times = wrf_user_getvar(a,"times",-1) ; get all times in the file
ntimes = dimsizes(times) ; number of times in the file

it = 7
print("Working on time: " + times(it) )

;;;;;;;;;;;;;
; First get the variables we will need

slp = wrf_user_getvar(a,"slp",it) ; surface pressure
tk2 = wrf_user_getvar(a,"T2",it) ; T at 2m in K
u10 = wrf_user_getvar(a,"U10",it) ; U at 10m
```



```

v10 = wrf_user_getvar(a,"V10",it)           ; V at 10m
z   = wrf_user_getvar(a, "z",it)           ; grid point height
ter = wrf_user_getvar(a, "ter",it)         ; surface terrain height

;;;;;;;;;;;;;
;;;Ground level
do jy = loc(1,0),loc(1,1),1
  do ix = loc(0,0),loc(0,1),1
    grd = wrf_user_ij_to_ll(a, ix, jy, opt)
    xy = latlon2utm((/grd(1), grd(0)/),2)
    height = 0.0
    ter_out = height + abs(ter(jy,ix))
    u_out = 0.0
    v_out = 0.0
    w_out = 0.0
    slp_out = slp(jy,ix)
    tc_out = tk2(jy,ix)

    dataOut = sprintf("%f ", xy(0)) + sprintf("%f ", xy(1)) +
sprintf("%f ", ter_out(:)) + sprintf("%f ", height) + sprintf("%f ",
u_out(:)) + sprintf("%f ", v_out(:)) + sprintf("%f ", w_out(:)) +
sprintf("%f ", slp_out(:)) + sprintf("%f ", tc_out(:))
    write_table("WindSim_out.txt", "a", [/dataOut/], "%s")

  end do
end do

;;;10m level
sthgt = wrf_user_getvar(a,"ter",it)
do jy = loc(1,0),loc(1,1),1
  print("j value is: " + jy)
  do ix = loc(0,0),loc(0,1),1
    print("i value is: " + ix)
    grd = wrf_user_ij_to_ll(a, ix, jy, opt)
    print("Longitude location is: " + grd(0))
    print("Latitude location is: " + grd(1))
    xy = latlon2utm((/grd(1), grd(0)/),2)
    print("UTM lat location is: " + xy(0))
    print("UTM lon location is: " + xy(1))
    sthgt_sub = sthgt(jy,ix)
    print("Terrain height is: " + sthgt_sub)

    height = 10.0
    ter_out = height + ter(jy,ix)
    if(sthgt_sub .gt. height) then
      u_out = 0.0
      v_out = 0.0
      w_out = 0.0
      slp_out = slp(jy,ix)
      tc_out = tk2(jy,ix)
    else
      u_out = u10(jy,ix)
      v_out = v10(jy,ix)
      w_out = 0
      slp_out = slp(jy,ix)
      tc_out = tk2(jy,ix)
    end if
    dataOut = sprintf("%f ", xy(0)) + sprintf("%f ", xy(1)) +
sprintf("%f ", ter_out(:)) + sprintf("%f ", height) + sprintf("%f ",
u_out(:)) + sprintf("%f ", v_out(:)) + sprintf("%f ", w_out(:)) +
sprintf("%f ", slp_out(:)) + sprintf("%f ", tc_out(:))
  end do
end do

```

```

        write_table("WindSim_out.txt", "a", [/dataOut/], "%s")
    end do
end do
end

```

The Balabac_ml_wrfout_to_xyz.ncl reads the WRF output files and extracts the terrain height, wind velocity, pressure, and temperature from 30 m and 2000 m levels. These are written to the .xyz file created by the Balabac_sfc_wrf_to_xyz.ncl script by appending the read data into it.

Listing Balabac_ml_wrfout_to_xyz.ncl:

```

load "$NCARG_ROOT/lib/ncarg/nclscripts/csm/gsn_code.ncl"
load "$NCARG_ROOT/lib/ncarg/nclscripts/csm/contributed.ncl"
load "$NCARG_ROOT/lib/ncarg/nclscripts/wrf/WRFUserARW.ncl"

begin
;
; The WRF ARW input file.
; This needs to have a ".nc" appended, so just do it.
a = addfile("./wrfout_d03_2012-09-15_00:00:00.nc", "r")

glon2d = a->XLAT(0, :, :)
glat2d = a->XLONG(0, :, :)

printMinMax(glat2d, 0)
printMinMax(glon2d, 0)

printVarSummary(glat2d)
printVarSummary(glon2d)

latS = 7.75 ; Balabac Island lat-lon
latN = 7.95
lonW = 116.80
lonE = 117.05

opt = True
loc = wrf_user_ll_to_ij(a, (/lonW, lonE/), (/latS, latN/), opt)
loc = loc-1 ; To convert to NCL subscripts

; The specific height levels that we want the data interpolated to.
height_levels = (/ 30., 50., 60., 80., 100., 120., 150., 200., 250., 300.,
400., 500., 750., 1000., 1500., 2000./) ; height levels to plot - in meter
nlevels = dimsizes(height_levels) ; number of height levels

;---The requested and calculated values should be close
print("Requested min/max xlon = " + latS + "/" + latN)
print("Calculated min/max xlon = " + glon2d(loc(1,0),loc(0,0)) + "/" + \
glon2d(loc(1,1),loc(0,1)))

print("Requested min/max xlat = " + lonW + "/" + lonE)
print("Calculated min/max xlat = " + glat2d(loc(1,0),loc(0,0)) + "/" + \
glat2d(loc(1,1),loc(0,1)))

;---Just for fun, pick a variable and take a subdomain of it.

```

```

times = wrf_user_getvar(a,"times",-1) ; get all times in the file
ntimes = dimsizes(times)           ; number of times in the file

it = 7
print("Working on time: " + times(it) )

;;;;;;;;;;;;;
; First get the variables we will need

slp = wrf_user_getvar(a,"slp",it)      ; surface pressure
tk2 = wrf_user_getvar(a,"T2",it)      ; surface temperature
u10 = wrf_user_getvar(a,"U10",it)     ; U-component of wind at 10m
v10 = wrf_user_getvar(a,"V10",it)     ; V-component of wind at 10m
tk = wrf_user_getvar(a,"tk",it)       ; T in K
u = wrf_user_getvar(a,"ua",it)        ; u averaged to mass points
v = wrf_user_getvar(a,"va",it)        ; v averaged to mass points
w = wrf_user_getvar(a,"wa",it)        ; w averaged to mass points
p = wrf_user_getvar(a, "pressure",it) ; pressure is our vertical
coordinate
z = wrf_user_getvar(a, "z",it)        ; grid point height
ter = wrf_user_getvar(a, "ter",it)    ; surface terrain height

;;;;;;;;;;;;;

sthgt = wrf_user_getvar(a,"ter",it)
do level = 0,nlevels-1                ; LOOP OVER LEVELS
do jy = loc(1,0),loc(1,1),1
print("j value is: " + jy)
do ix = loc(0,0),loc(0,1),1
print("i value is: " + ix)
grd = wrf_user_ij_to_ll(a, ix, jy, opt)
print("Longitude location is: " + grd(0))
print("Latitude location is: " + grd(1))
xy = latlon2utm(/grd(1), grd(0)/),2)
print("UTM lat location is: " + xy(0))
print("UTM lon location is: " + xy(1))
sthgt_sub = sthgt(jy,ix)
print("Terrain height is: " + sthgt_sub)

height = height_levels(level)

p_plane = wrf_user_intrp3d( p,z,"h",height,0.,False)
tc_plane = wrf_user_intrp3d(tk,z,"h",height,0.,False)
u_plane = wrf_user_intrp3d( u,z,"h",height,0.,False)
v_plane = wrf_user_intrp3d( v,z,"h",height,0.,False)
w_plane = wrf_user_intrp3d( w,z,"h",height,0.,False)

w_sample = w_plane(jy,ix)

ter_out = height + ter(jy,ix)
if(ismissing(w_sample)) then          ; Value is not available in
WRF output
    u_out = u10(jy,ix)
    v_out = v10(jy,ix)
    w_out = 0.0
    p_out = slp(jy,ix)
    tc_out = tk2(jy,ix)
else if(sthgt_sub .gt. height) then   ; Check if terrain
height is greater than altitude
    u_out = 0.0

```

```

        v_out = 0.0
        w_out = 0.0
        p_out = slp(jy,ix)
        tc_out = tk2(jy,ix)
    else                                     ; Get values at that level
        u_out = u_plane(jy,ix)
        v_out = v_plane(jy,ix)
        w_out = w_plane(jy,ix)
        p_out = p_plane(jy,ix)
        tc_out = tc_plane(jy,ix)
    end if
end if
    dataOut = sprintf("%f ", xy(0)) + sprintf("%f ", xy(1)) +
sprintf("%f ", ter_out(:)) + sprintf("%f ", height) + sprintf("%f ",
u_out(:)) + sprintf("%f ", v_out(:)) + sprintf("%f ", w_out(:)) + sprintf("%f
", p_out(:)) + sprintf("%f ", tc_out(:))
    write_table("WindSim_out.txt", "a", [/dataOut/], "%s")

    end do                                     ; END OF LEVEL LOOP
end do
end do

end

```

The plot_CFD.m is a Matlab script for making contour plots of the wind speeds from the WindSim results.

Listing plot_CFD.m:

```

clearvars;clc;fclose('all');
%% Load data
dtm_path = 'C:\Users\ID917614\Desktop\WindSim_Processing\';
load([dtm_path 'dtm.mat'])

%% root{1} = 'E:\01 Mesoscale data\03 Grizzly Bear\07 Results\01
Standalone\';
%% root{2} = 'E:\01 Mesoscale data\03 Grizzly Bear\07 Results\02 dTH\';
root = 'C:\Users\ID917614\Desktop\WindSim_Processing\';
s = [10 11];
% s = [1];

%% Measurements
Px = [495103,491842,495782,490843,497358,498655,491425];
Py = [5897228,5894806,5892225,5898490,5900855,5894977,5901646];
Mnames = {'2281','2282','2340','2368','2407','2408','WLS7'};

xmin = 488052.091;          % Balabac Island
ymin = 864323.297;
zp = 38;

%% Do plots
for r = 1:2
    for c = 1:length(s)
        caseT = num2str((s(c)-1)*30);
        if (s(c)-1)*30<10
            caseT = ['00' caseT];
        elseif (s(c)-1)*30<100

```

```

        caseT = ['0' caseT];
    end
    %% load([root{r} caseT '_red_phi.mat'])
    load([root '001_red_phi.mat'])
    %% Prepare plots
    nn = size(U);

    X_c = phi_coord(:, :, 1:nn(3), 1)+xmin;
    Y_c = phi_coord(:, :, 1:nn(3), 2)+ymin;
    Z_c = phi_coord(:, :, 1:nn(3), 3);

    H_c = NaN(nn(1), nn(2), nn(3));
    for k = 1:nn(3)
        H_c(:, :, k) = Z_c(:, :, k)+H;
    end

    %% Horz. plots
    Mc = NaN(nn(1), nn(2));
    TKEc = NaN(nn(1), nn(2));
    for i = 1:nn(1)
        for j = 1:nn(2)
            Mc(i, j) = spline(Z_c(i, j, :), M(i, j, :), zp);
            TKEc(i, j) = spline(Z_c(i, j, :), TKE(i, j, :), zp);
        end
    end

    end

    % speed
    pcolor(X_c(:, :, 1), Y_c(:, :, 1), Mc)
    shading interp
    colormap(jet(15))
    caxis([0 15])
    daspect([1 1 1])
    colorbar
    xlabel('x-coordinate')
    ylabel('y-coordinate')
    hold on
    contour(X_c(:, :, 1), Y_c(:, :, 1), H_c(:, :, 1), 15, '-k')
    plot(Px, Py, 'ok', 'MarkerFaceColor', 'k', 'MarkerSize', 5)
    for m = 1:length(Mnames)
        text(Px(m), Py(m), Mnames{m})
    end
    hold off
    % print(gcf, '-dtiff', [root{r} caseT '_Horz_speed.tiff']);
    print(gcf, '-dtiff', [root caseT '_Horz_speed.tiff']);

    % TKE
    pcolor(X_c(:, :, 1), Y_c(:, :, 1), TKEc)
    shading interp
    colormap(jet(15))
    caxis([0 1])
    daspect([1 1 1])
    colorbar
    xlabel('x-coordinate')
    ylabel('y-coordinate')
    hold on
    contour(X_c(:, :, 1), Y_c(:, :, 1), H_c(:, :, 1), 15, '-k')
    plot(Px, Py, 'ok', 'MarkerFaceColor', 'k')
    for m = 1:length(Mnames)
        text(Px(m), Py(m), Mnames{m})
    end
    hold off

```

```

print(gcf, '-dtiff',[root caseT '_Horz_TKE.tiff']);

%% Vertical plots

for m = 1:length(Mnames)
    [~,is]= min(abs(X_c(:,1,1)-Px(m)));
    [~,js]= min(abs(Y_c(1,:,1)-Py(m)));

    %NS

pcolor(squeeze(Y_c(is,:,:)),squeeze(H_c(is,:,:)),squeeze(M(is,:,:)))
    shading interp
    colormap(jet(15))
    caxis([0 15])
    colorbar
    xlabel('y-coordinate')
    ylabel('Height')
    title(Mnames{m})
    hold on
    plot(Py(m),zp+H_c(is,js,1),'ok','MarkerFaceColor','k')
    hold off
    print(gcf, '-dtiff',[root caseT '_' Mnames{m} '_M_NS.tiff']);

pcolor(squeeze(Y_c(is,:,:)),squeeze(H_c(is,:,:)),squeeze(TKE(is,:,:)))
    shading interp
    colormap(jet(15))
    caxis([0 1])
    colorbar
    xlabel('y-coordinate')
    ylabel('Height')
    title(Mnames{m})
    hold on
    plot(Py(m),zp+H_c(is,js,1),'ok','MarkerFaceColor','k')
    hold off
    print(gcf, '-dtiff',[root caseT '_' Mnames{m} '_TKE_NS.tiff']);

pcolor(squeeze(Y_c(is,:,:)),squeeze(H_c(is,:,:)),squeeze(TEM(is,:,:)))
    shading interp
    colormap(jet(15))
    colorbar
    xlabel('y-coordinate')
    ylabel('Height')
    title(Mnames{m})
    hold on
    plot(Py(m),zp+H_c(is,js,1),'ok','MarkerFaceColor','k')
    hold off
    print(gcf, '-dtiff',[root caseT '_' Mnames{m} '_TEM_NS.tiff']);

%
pcolor(squeeze(Y_c(is,:,:)),squeeze(H_c(is,:,:)),squeeze(EDR(is,:,:)))
%     shading interp
%     colormap(jet(15))
%     print(gcf, '-dtiff',[root{r} caseT '_' Mnames{m}
'_EDR_NS.tiff']);

%WE

pcolor(squeeze(X_c(:,js,:)),squeeze(H_c(:,js,:)),squeeze(M(:,js,:)))

```

```

        shading interp
        colormap(jet(15))
        caxis([0 15])
        colorbar
        xlabel('x-coordinate')
        ylabel('Height')
        title(Mnames{m})
        hold on
        plot(Px(m),zp+H_c(is,js,1),'ok','MarkerFaceColor','k')
        hold off
        print(gcf, '-dtiff',[root caseT '_' Mnames{m} '_M_WE.tiff']);

pcolor(squeeze(X_c(:,js,:)),squeeze(H_c(:,js,:)),squeeze(TKE(:,js,:)))
    shading interp
    colormap(jet(15))
    caxis([0 1])
    colorbar
    xlabel('x-coordinate')
    ylabel('Height')
    title(Mnames{m})
    hold on
    plot(Px(m),zp+H_c(is,js,1),'ok','MarkerFaceColor','k')
    hold off
    print(gcf, '-dtiff',[root caseT '_' Mnames{m} '_TKE_WE.tiff']);

pcolor(squeeze(X_c(:,js,:)),squeeze(H_c(:,js,:)),squeeze(TEM(:,js,:)))
    shading interp
    colormap(jet(15))
    colorbar
    xlabel('x-coordinate')
    ylabel('Height')
    title(Mnames{m})
    hold on
    plot(Px(m),zp+H_c(is,js,1),'ok','MarkerFaceColor','k')
    hold off
    print(gcf, '-dtiff',[root caseT '_' Mnames{m} '_TEM_WE.tiff']);

%
pcolor(squeeze(X_c(:,js,:)),squeeze(H_c(:,js,:)),squeeze(EDR(:,js,:)))
%     shading interp
%     colormap(jet(15))
%         print(gcf, '-dtiff',[root{r} caseT '_' Mnames{m}
'_EDR_WE.tiff']);
    end
end
end
end

```

APPLICATION OF NUMERICAL WEATHER PREDICTION MODEL FOR OFFSHORE WIND RESOURCE ASSESSMENT IN THE PHILIPPINES

S.N. Uy¹ and A. Alaswad²

1. School of Engineering and the Built Environment, Birmingham City University, Birmingham, UK; email: sherdon.uy@mail.bcu.ac.uk
2. School of Engineering and the Built Environment, Birmingham City University, Birmingham, UK; email: abed.alaswad@mail.bcu.ac.uk

ABSTRACT

Due to the Philippines' need to power its numerous islands with minimal environmental impact, offshore wind energy is a promising sustainable energy resource for the country. Presently, there are limited offshore wind observations in the country with available data insufficient for determining the wind potential over its waters. Alternatively, using numerical wind prediction, an initial offshore wind resource assessment can be carried out.

In this study, wind simulations over the Western waters of Palawan Island, Philippines were carried out using the Weather Research and Forecasting (WRF) Model. Different input operational and reanalysis datasets were used, with varying planetary boundary layer (PBL) configurations, to test WRF's sensitivity and find suitable settings for the studied area. Model results were compared with the 2010 and 2011 Puerto Princesa station readings operated by the weather bureau.

The study finds that WRF results are in line with the daily wind speed trends and wind direction. However, the obtained model performs better using ERA-Interim dataset for high wind speed conditions while NCEP CFSR dataset allows for better accuracy on low wind speeds. The resultant model has been concluded to be useful in guiding the process of seeking suitable locations for offshore wind projects in the Philippines.

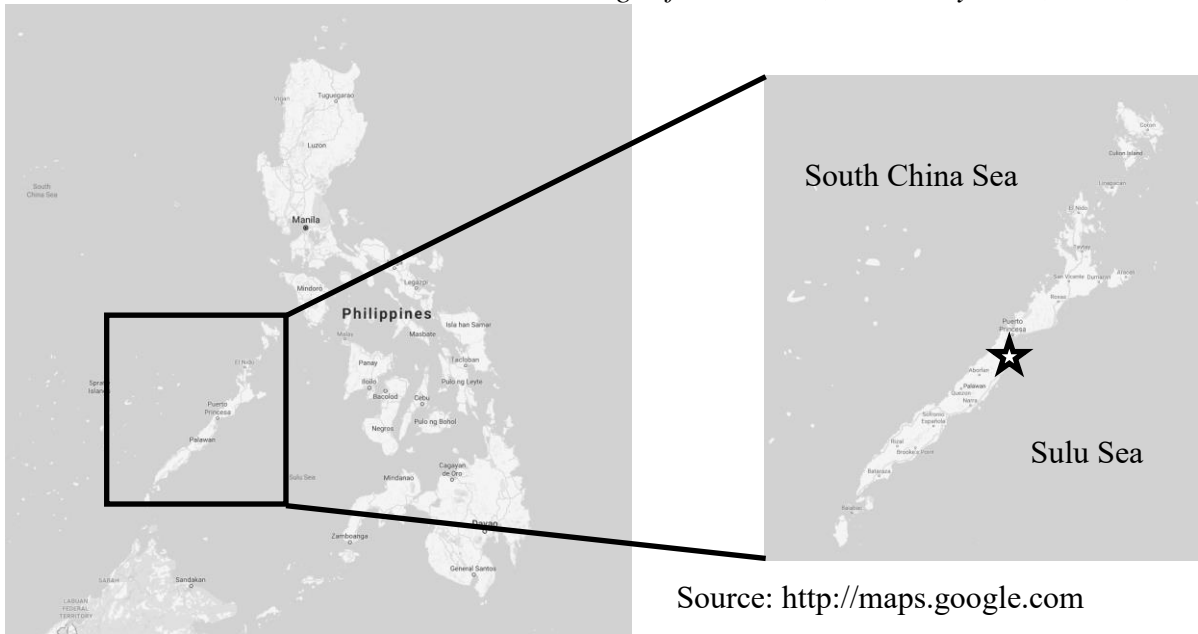
Keywords: Offshore Wind, Wind Resource Assessment, Numerical Weather Prediction

INTRODUCTION

Wind resource in offshore locations have greater available energy for exploitation in comparison with sites found on land [1]. It is this potential that research on offshore wind energy are being undertaken in different parts of the world. The Philippines has the potential to generate power from offshore wind but a thorough wind resource assessment (WRA) must be made for wind energy prospecting [2]. WRA is essential for any wind energy development in order to minimise risks in investments [3]. This study aims to use numerical weather prediction (NWP) method in making a WRA for offshore regions around Palawan Island, Philippines. Results of the study demonstrate how NWP can be used for offshore WRA on the different islands in the country. This will help in guiding offshore wind projects in the Philippines for the stakeholders on wind energy.

OBSERVED DATA AND STUDY SITE

This study is focused on generating a WRA for Palawan, Philippines using NWP method. Palawan Island is located at the western part of the Philippines and it is in between the South China Sea and Sulu Sea. This island is a province of the Philippines where the capital is called Puerto Princesa. Figure 1 shows the location of the island within the Philippine archipelago. It is a popular tourist destination for its beaches and underground river. There are several fishing ports around the island since fishing is one of its major industry. An offshore platform is also located at the west side of this island for gas production. It has been selected as the study site since the island has shown that it has a good wind resource [2]. Another reason for studying the waters around Palawan Island is because the South China Sea has been found to be rich in wind resources [1].



Source: <http://maps.google.com>

Figure 1. Map of Philippines and Palawan Island. The weather station is located within Puerto Princesa which is marked by the star symbol.

The study used 2010 and 2011 weather station observation at Puerto Princesa for validation of the NWP. This station is maintained by the Philippine Atmospheric, Geophysical, and Astronomical Services Administration (PAGASA) which is the official weather bureau of the country. The wind observations are done at 10 m above ground level using a cup anemometer and a wind vane. The site for this station is beside the city’s airport where the immediate vicinity is surrounded by suburban area. This location is a small peninsula that is facing the Sulu Sea and the city proper is towards North.

MODEL CONFIGURATION AND DESIGN

For this work, the Weather Research and Forecasting (WRF) Model is used to make offshore wind fields around the Palawan Island. The model is configured using three different settings found to perform well in other studies in the Philippines [4, 5] and Thailand [6] in order to compare each one with observed data. Reanalysis data and operational data from the National Centres for Environmental Prediction (NCEP) and European Centre for Medium-Range Weather Forecasts (ECMWF) have been used as input data for WRF. The specific datasets used are the European Reanalysis-Interim (ERA-Interim), NCEP Climate Forecasts System Reanalysis (NCEP_CFSR), and the NCEP Final Operational Global Analysis Data (FNL). For the planetary boundary layer (PBL) parameter, there are also three different ones used for comparison. PBL used for the simulations are Mellor-Yamada-Janjic (MYJ), Asymmetric Convective Model ver. 2 (ACM2), and Yonsei University (YSU) along with their prescribed surface layer parameters namely, Eta similarity and revised Mesoscale Model ver. 5 (MM5). In addition, the microphysics scheme settings utilised WRF single-moment 3-class (WSM3) and 6-class (WSM6) options. These settings are summarised in Table 1.

Table 1. WRF Configuration Settings

Parameters	Authors	Dado and Takahashi [4]	Cruz and Narisma [5]	Chancham, Waewsak, and Gagnon [6]
Input Data		ERA-Interim	NCEP-FNL	NCEP-CFSR
Planetary Boundary Layer		MYJ	ACM2	YSU
Surface Layer		Eta Similarity	Revised MM5	Revised MM5
Microphysics Scheme		WSM6	WSM6	WSM3

Although studies reported in [4, 5] are focused on rainfall, similar configurations have been used for wind in other studies [6, 7]. Slight modifications have been made to the referred studies in order to limit the comparison between input data and PBL. The first modification involved enabling the cumulus parameterization scheme for [4]. The second one is using NCEP-CFSR dataset as input for [6]. Model setting differences have been narrowed to these two parameters as previous studies have shown that wind

simulations in WRF is highly sensitive with them [7, 8]. These minor changes are similar with the configuration used for other offshore wind research in the South China Sea [9]. Differences with the microphysics scheme has been maintained according to the respective settings of the prior works as these pertain to the precipitation in the model and not essential for this study. The surface layer option had to vary because the PBL parameter selected dictates the compatible surface layer setting. Other model parameters are kept the same in the three model configurations selected for this study. Radiation schemes use the Rapid Radiative Transfer Model (RRTM) for long wave and Dudhia for short wave. The same land use and land cover parameter using the 30 arcsec US Geological Survey (USGS) data have been set and the Noah land surface model has been activated for all simulation runs [4, 5, 6]. The Kain-Fritsch cumulus parametrisation scheme has been utilised for all but has been disabled at the third domain since the model explicitly calculates this parameter for fine resolutions.

There are three domains setup for this simulation in WRF where Domain 1 has 27 km x 27 km resolution, Domain 2 has 9 km x 9km, and Domain 3 has 3 km x 3 km resolution with all domains having an hourly time resolution. Palawan Island is contained within the third domain. The defined domains for the study site can be seen in Figure 2.

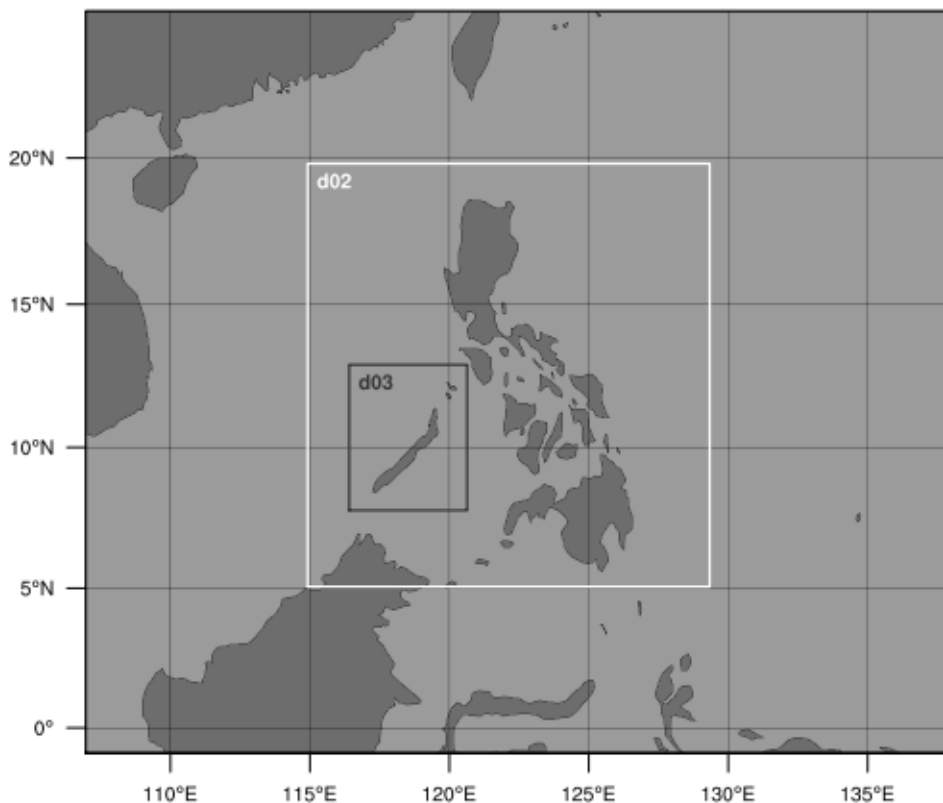


Figure 2. Domains configured for WRF. Palawan Island is within Domain 3 (d03).

Vertical resolution of the model has been increased to 50 vertical eta levels where the first 9 levels are within the 200 m height in order to enable WRF to perform better in accounting for the atmospheric dynamics within the boundary layer [10]. Two-way nesting has been enabled for all the model runs even for simulations that are configured as reported in [5] where one-way nesting was used in the study. Simulations were done on the Advanced Research Computing High End Resource (ARCHER) supercomputing facility where a Cray XC30 is used to provide high performance computing services.

SENSITIVITY TEST AND ANALYSIS

The WRF has been run on three different settings used in other studies which are summarised in Table 1. PAGASA weather station in Puerto Princesa is used for validating the results. Daily wind speed averages have been calculated from the model output since the obtained observation data are also daily averages. A scatter plot to compare the performance of each WRF configuration with measured data is made for validating the wind speeds [4, 11]. This chart shows the accuracy of simulation data in determining the wind speed observed values. It also presents the percentage error of the WRF simulations results in comparison

with the PAGASA wind data. The root-mean-square error (RMSE) of wind speeds are calculated in order to know how much the model results deviates from the measured data [5, 7, 12]. RMSE is determined using the following equation:

$$RMSE = \sqrt{\frac{1}{N} \sum_{i=1}^N (U^{sim} - U^{obs})^2} \quad (1)$$

where U^{sim} is the simulated wind speed and U^{obs} is the measured wind speed in m/s.

Wind direction are analysed with monthly averages in order to see the seasonal trends and determine the predominant wind direction which is essential for WRA of wind farms [13]. Wind maps at 80 m above ground level is generated to determine the areas with good wind resources.

RESULTS AND DISCUSSION

5.1. Wind speed results

Simulation runs on WRF has been done for the years of 2010 and 2011. The wind speeds in the simulation has been compared with the measured data from PAGASA [14]. The chart that shows this comparison is in Figure 3. In the succeeding discussion, WRF settings will be referred by the name of input dataset for readability and brevity but the complete settings are those in Table 1.

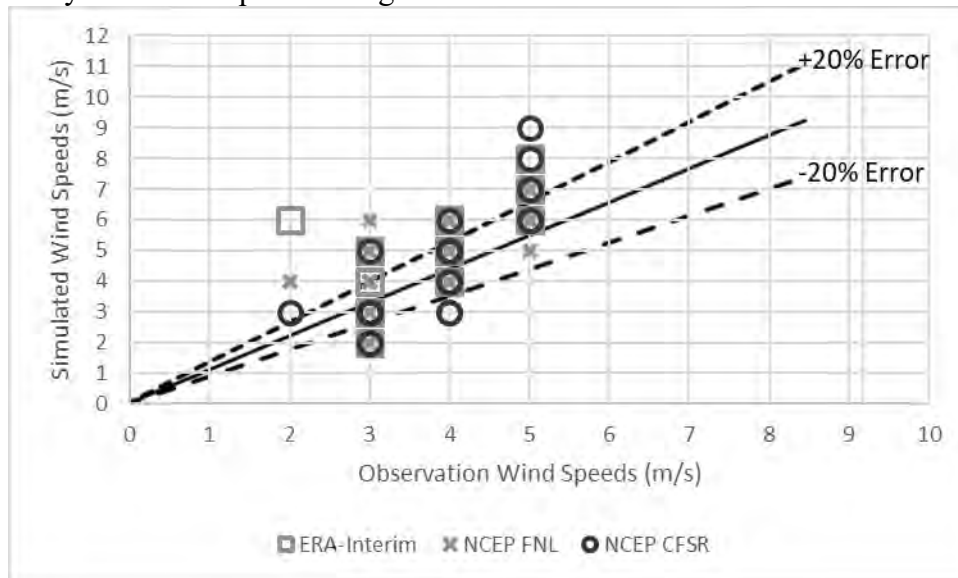


Figure 3. Scatter plot of different WRF model settings with PAGASA station data (January 2010).

All input data have a tendency to overestimate the wind speed in comparison with the observations. NCEP-CFSR and ERA-Interim have similar performance in simulating the winds. Comparing both reanalysis datasets with NCEP-FNL, the average winds of NCEP-FNL gives slightly better performance when accounting for the entire wind speed value range. But it is apparent in Figure 3 that low wind speeds is simulated better using NCEP-CFSR, while ERA-Interim yields better results in high wind speed regimes. This is found in line with studies reported in the literature [15, 16], while WRF simulates better with wind speeds that are greater than or equal to 4 m/s. This is apparent in the chart as wind speeds that are 2 m/s are overestimated by all input data and the model tends to equally overestimate or underestimate 3 m/s wind occurrences. Then, it begins to give more consistent wind speeds beginning at 4 m/s – 5 m/s. The ability of NCEP-FNL to simulate wind speeds better is also seen with the RMSE values. It ranges from 3.6 m/s to 4 m/s for monthly comparison while ERA-Interim and NCEP-CFSR can range from 5.7 m/s to 6 m/s.

5.2. Wind directions results

Monthly averages of wind direction show that NCEP-FNL modelling gives more accurate results than NCEP-CFSR and ERA-Interim models. As an example, Figure 4 shows the average monthly wind direction for January 2010 and 2011.

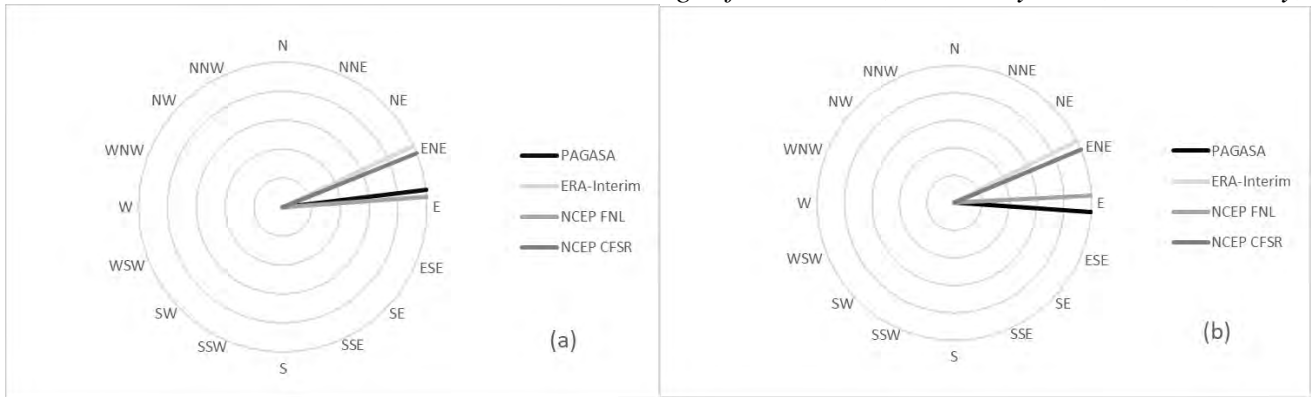


Figure 4. Comparison between WRF output and observation data of average monthly wind direction for January 2010 and 2011

From Figure 4, the January months have more winds coming from the East based on the observations which is better captured by NCEP-FNL. NCEP-CFSR and ERA-Interim show that the winds are coming from the East-Northeast which is the characteristic of the Northeast Monsoon from December to February in the Philippines. On seasonal and climate trends; reanalysis data, namely NCEP-CFSR and ERA-Interim, are useful for long-term trend analysis for wind farm projects [17]. NCEP-FNL is better with monthly wind direction means may be with its purpose as an operational analysis data, it is used for weather forecasting and diagnostics which are short-term events for the atmosphere [5]. From the results, the winds are greatly affected by monsoons and must be considered when planning offshore wind projects as they determine the predominant wind flow direction in the region.

5.3. Wind maps for January and May 2010 and 2011

Monthly wind maps have been produced from the simulations in order to see the offshore wind resource in the vicinity of Palawan Island. Some of these maps are shown in Figure 5. These are maps that show the time when the Northeast Monsoon is strong (January) and the month when the onset of Southwest Monsoon is beginning (May).

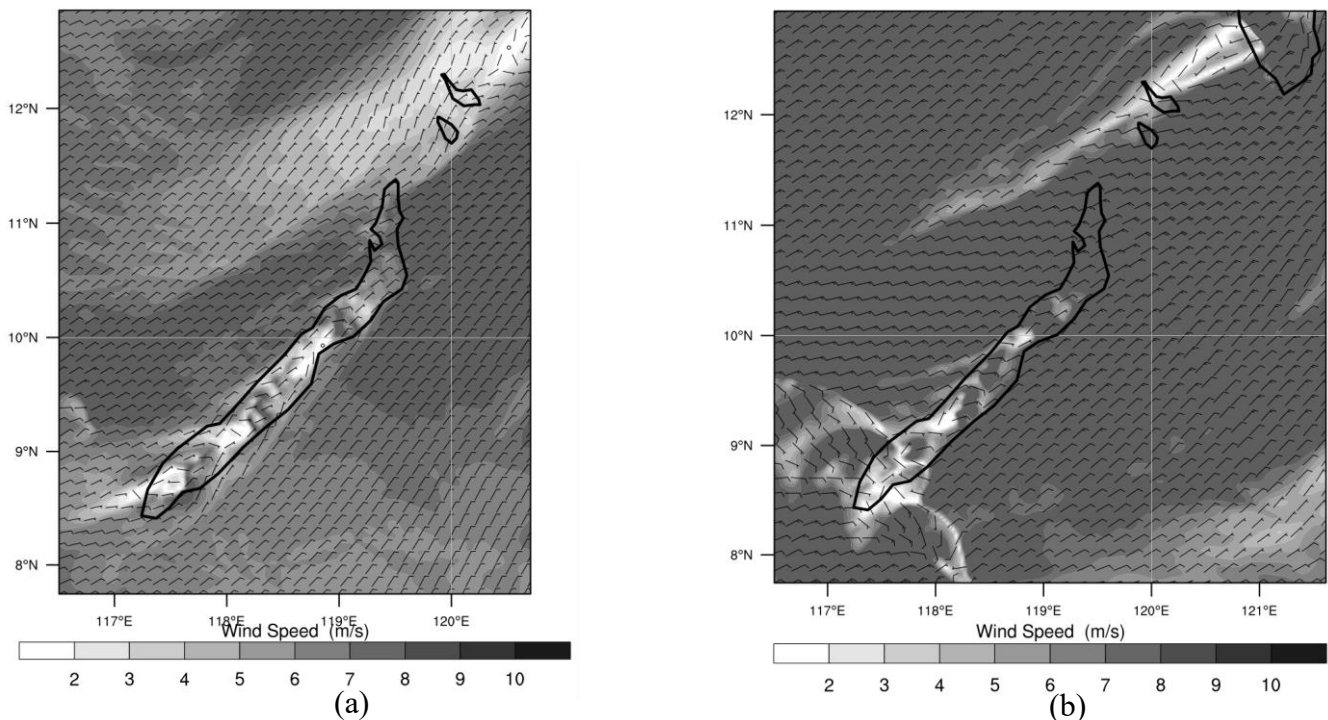


Figure 5. Wind maps for Palawan Island showing the available offshore wind resource around the island at 80 m: (a) January 2010, (b) January 2011

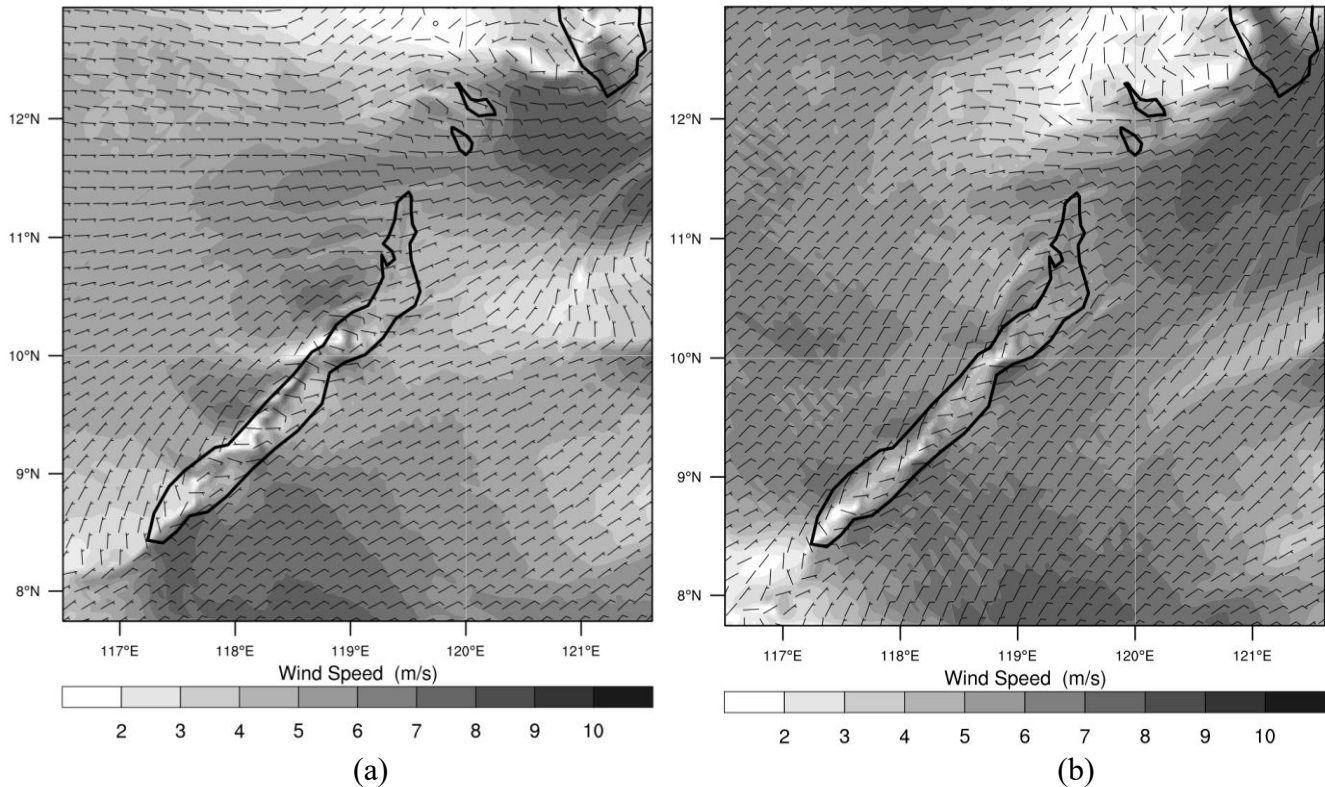


Figure 6. Wind maps for Palawan Island showing the available offshore wind resource around the island at 80 m: (a) May 2010, (b) May 2011

From Figures 5 and 6, it can be seen that the offshore winds at the 80 m level can range from 5 m/s to more than 10 m/s when considering the vicinity that is 100 km from the shore. Months of January are more productive for wind power generation than May since majority of the waters have wind speeds greater than 6 m/s during January. This suggests that the Northeast Monsoon is the season when wind energy can be a significant power source for the island. Looking at the northeast region in May, it is possible for winds to drop down between 5-6 m/s when comparing Figure 6(a) and Figure 6(b). This is indicative that the winds in northeast may be highly variable and could have a negative impact when operating offshore wind farms there. The area of Palawan that is facing the South China Sea can be a better site for offshore wind projects since the winds there are more consistent. There is only a small patch in the southern end that can have 4-6 m/s speeds at times that is depicted in Figure 5(b). For parts of the island that is facing Sulu Sea, the southern half of the island has potential for offshore wind power generation. Wind variability for the northern part that is covered by Sulu Sea may make wind projects there produce less power than other offshore areas surrounding Palawan.

CONCLUSION

WRF has been configured using three different numerical settings that have been found to be suitable for simulating winds. These have been tested by validating the simulation results with weather station observations made in 2010 and 2011. It is found that ERA-Interim performs well for high wind speed regimes while NCEP-CFSR is better on low wind speed conditions. NCEP-FNL is more capable in modelling the wind directions in comparison with ERA-Interim and NCEP-CFSR. WRF is a tool that can be used for the Philippines as the wind maps generated are able to determine the prevailing winds and show the areas that have offshore wind resource potential. Within 100 km from the coast, winds can range from 5 m/s to greater than 10 m/s at 80 m above the surface. The Northeast Monsoon brings with it stronger winds and has less wind variability which makes it the best time to operate wind farms within the study area. Most of the areas in the South China Sea as well as the southern part of Palawan are good offshore wind sites. With these results, further work is needed to improve the sensitivity tests including more weather stations and using longer observation periods for model validation. The use of computational fluid dynamics (CFD) model will also improve the generated wind maps.

ACKNOWLEDGEMENTS

The authors would like to thank Newton-Agham Fund programme and the Department of Science and Technology of the Philippine Government for sponsoring this work. The authors are thankful to PAGASA for providing the wind observation data used for validation. The authors wish to express their gratitude to EPCC for giving access and training in using the ARCHER supercomputing facility for this research.

REFERENCES

- [1] Y. Liu, D. Chen, Q. Yi, and S. Li, Wind Profiles and Wave Spectra for Potential Wind Farms in South China Sea. Part I: Wind Speed Profile Model, *Energies*, Vol. 10, pp. 1-24, 2017.
- [2] D. Elliott, Philippines Wind Energy Resource Atlas Development, *Business and Investment Forum for Renewable Energy and Energy Efficiency in Asia and Pacific Region*, Kuala Lumpur, 2000.
- [3] P. Jain, P. P. Calcetas, and B. An, *Guidelines for Wind Resource Assessment: Best Practices for Countries Initiating Wind Development*, Asian Development Bank, 2014.
- [4] J. M. B. Dado and H. G. Takahashi, Potential Impact of Sea Surface Temperature on Rainfall over the Western Philippines, *Progress in Earth and Planetary Science*, Vol. 4, pp. 1-12, 2017.
- [5] F. Cruz and G. Narisma, WRF Simulation of the Heavy Rainfall over Metropolitan Manila, Philippines during Tropical Cyclone Ketsana: A Sensitivity Study, *Meteorology and Atmospheric Physics*, Vol. 128, pp. 415-428, 2016.
- [6] C. Chancham, J. Waewsak, and Y. Gagnon, Offshore Wind Resource Assessment and Wind Power Plant Optimization in the Gulf of Thailand, *Energy*, Vol. 139, pp. 706-731, 2017.
- [7] D. Carvalho, A. Rocha, M. Gomez-Gesteira, and C. Silva Santos, WRF Wind Simulation and Wind Energy Production Estimates Forced by Different Reanalyses: Comparison with Observed Data for Portugal, *Applied Energy*, Vol. 117, pp. 116-126, 2014.
- [8] F. J. Santos-Alamillos, D. Pozo-Vazquez, J. A. Ruiz-Arias, V. Lara-Fanego, and J. Tovar-Pescador, Analysis of WRF Model Wind Estimate Sensitivity to Physics Parameterization Choice and Terrain Representation in Andalusia (Southern Spain), *Journal of Applied Meteorology and Climatology*, Vol. 52, pp. 1592-1609, 2013.
- [9] R. Chang, R. Zhu, M. Badger, C. B. Hasager, X. Xing, and Y. Jiang, Offshore Wind Resources Assessment from Multiple Data and WRF Modeling over South China Sea, *Remote Sensing*, Vol. 7, pp. 467-487, 2015.
- [10] I. Barstad, Offshore Validation of a 3 km ERA-Interim Downscaling – WRF Model's Performance on Static Stability, *Wind Energy*, Vol. 19, pp. 515-526, 2016.
- [11] J. Waewsak, M. Landry, and Y. Gagnon, Offshore Wind Power Potential of the Gulf of Thailand, *Renewable Energy*, Vol. 81, pp. 609-626, 2015.
- [12] M. Bilal, K. Solbakken, and Y. Birkelund, Wind Speed and Direction Predictions by WRF and WindSim Coupling over Nygardsfjell, *Journal of Physics: Conference Series*, Vol. 753, pp. 1-9, 2016.
- [13] K. Y. Oh, J. Y. Kim, J. K. Lee, M. S. Ryu, and J. S. Lee, An Assessment of Wind Energy Potential at the Demonstration Offshore Wind Farm in Korea *Energy*, Vol. 46, pp. 555-563, 2012.
- [14] Philippine Atmospheric, Geophysical, and Astronomical Services Administration (PAGASA), Daily Climatic Data (2010 – 2011).
- [15] D. Carvalho, A. Rocha, and M. Gomez-Gesteira, Ocean Surface Wind Simulation forced by Different Reanalyses: Comparison with Observed Data along the Iberian Peninsula Coast, *Ocean Modelling*, Vol. 56, pp. 31-42, 2012.
- [16] D. Carvalho, A. Rocha, M. Gomez-Gesteira, and C. Silva Santos, Offshore Winds and Wind Energy Production Estimates Derived from ASCAT, OSCAT, Numerical Weather Prediction Models and Buoys – A Comparative Study for the Iberian Peninsula Atlantic Coast, *Renewable Energy*, Vol. 102, pp. 433-444, 2017.
- [17] A. Silang, S. N. Uy, J. M. Dado, F. A. Cruz, G. Narisma, N. Libatique, and G. Tangonan, Wind Energy Projection for the Philippines Based on Climate Change Modeling, *Energy Procedia*, Vol. 52, pp. 26-37, 2014.



DEVELOPMENTS OF OFFSHORE WIND RESOURCE ASSESSMENT FOR LOW LATITUDE REGIONS

S.N. Uy¹ and A. Alaswad²

1. School of Engineering and the Built Environment, Birmingham City University, Birmingham, UK; email: sherdon.uy@mail.bcu.ac.uk
2. School of Engineering and the Built Environment, Birmingham City University, Birmingham, UK; email: abed.alaswad@mail.bcu.ac.uk

ABSTRACT

Vulnerability to fossil fuel prices and dependence on such fuels necessitates developing countries and small island nations in the low latitudes to foster their locally available renewable energy sources. There are vast bodies of water in this region that may have high wind energy potential thus, offshore wind energy can be a viable option for local power generation in these locations. However, offshore wind farm projects are significantly costly in terms of capital investment, on-site measurements for wind resource assessment (WRA), operations, and maintenance. Therefore, a meticulous WRA must be made before considering any offshore wind project to avoid unnecessary costs and failures.

This paper presents a review of offshore WRA methods, wind modelling techniques, and decision support systems that are applicable for small islands and nations within the tropical and subtropical region. More particularly, research in East Asia and the Southeast Asian region were reviewed to represent the subtropical and tropical conditions. The review finds that satellite observations and numerical wind modelling can be used for wind resource assessment, when actual measurements are absent, and able to support offshore wind farm project development decisions.

Keywords: Wind Energy, Offshore Wind Development, Wind Resource Assessment

1 INTRODUCTION

Winds over oceans and seas are much more stable and possess higher speeds in comparison with those over land [1]. This energy resource is immense for the entire world [2]. Thus, offshore wind energy is viewed as one potential power source that can help address the increasing demand for energy across the globe. A thorough wind resource assessment (WRA) must be made for any proposed site but the conventional method of operating wind masts is expensive for offshore locations [3]. WRA is required to enable strategic investments to be done for any wind energy project [4]. This work surveys the literature regarding the development in offshore wind energy resource assessment and efforts in applying them to various situations. It is essential to do a review of the literature so that an evaluation of the different techniques can be done to find the appropriate methods for the countries in low latitudes. Accurate and sufficient WRA data can help decision makers to determine the suitable locations for offshore wind farm development [5].

2 STATE OF OFFSHORE WIND ENERGY

Development for offshore wind turbines began in Europe with pilot projects starting in 1991 with a prototype deployment in Denmark [1]. Significant strides has been made since that initial offshore wind farm that by the middle of 2011, the total capacity in Europe reached 3,294 MW [6]. Wind farms located at offshore sites has been growing by 40% per annum for the entire world with Denmark and U.K. leading the effort having 1,271 MW and 4,494.4 MW in capacity by the end of 2014, respectively [7]. Germany is also spearheading the development with an installed capacity of 3476 MW in that same year [8]. These efforts have been in the North Sea but there are interests in developing offshore wind farms in the Adriatic Sea and Mediterranean Sea as well [7,9]. Other areas such as the Baltic Sea, Irish Sea, and the Atlantic Ocean have seen some developments as Finland, Sweden, Norway, Ireland, and Portugal have deployed and pushed wind farm projects of their own [8].

Across the Atlantic Ocean, the idea of offshore wind turbines has been brought about in a conference at Massachusetts back in 1972 [2]. However, offshore wind farm projects in Canada and U.S are mostly at the planning and evaluation phase [6]. There are four Canadian projects that are being evaluated where two have power production capacities of 414 MW and 300 MW situated in the Great Lakes [6, 10]. In the U.S., both the Atlantic Ocean and Great Lakes are being considered for offshore wind projects [6, 8]. The most promising is the Block Island project that has a 30 MW power production capability and commissioned in December 2016 [8, 11].

In East Asia, Japan began the research and development on offshore wind turbine technology in the region with two 600-kW turbines back in 2003 [12]. This initial effort had revitalised after the dangers of nuclear power became apparent in Fukushima for earthquake prone regions [8]. In fact, Japan has 49.6 MW offshore wind power and actively develops floating platforms for wind turbines [13]. Despite the recent progress in Japan, China is the leading investor in the technology for the Asia-Pacific region in terms of manufacturing and deployment [8, 11]. The country has surpassed Denmark in terms of total capacity installed with 1,627 MW in 2016 [11]. South Korea has started adopting the technology as well with a 5-MW installation in Cheju Island done in 2011 and 2012.

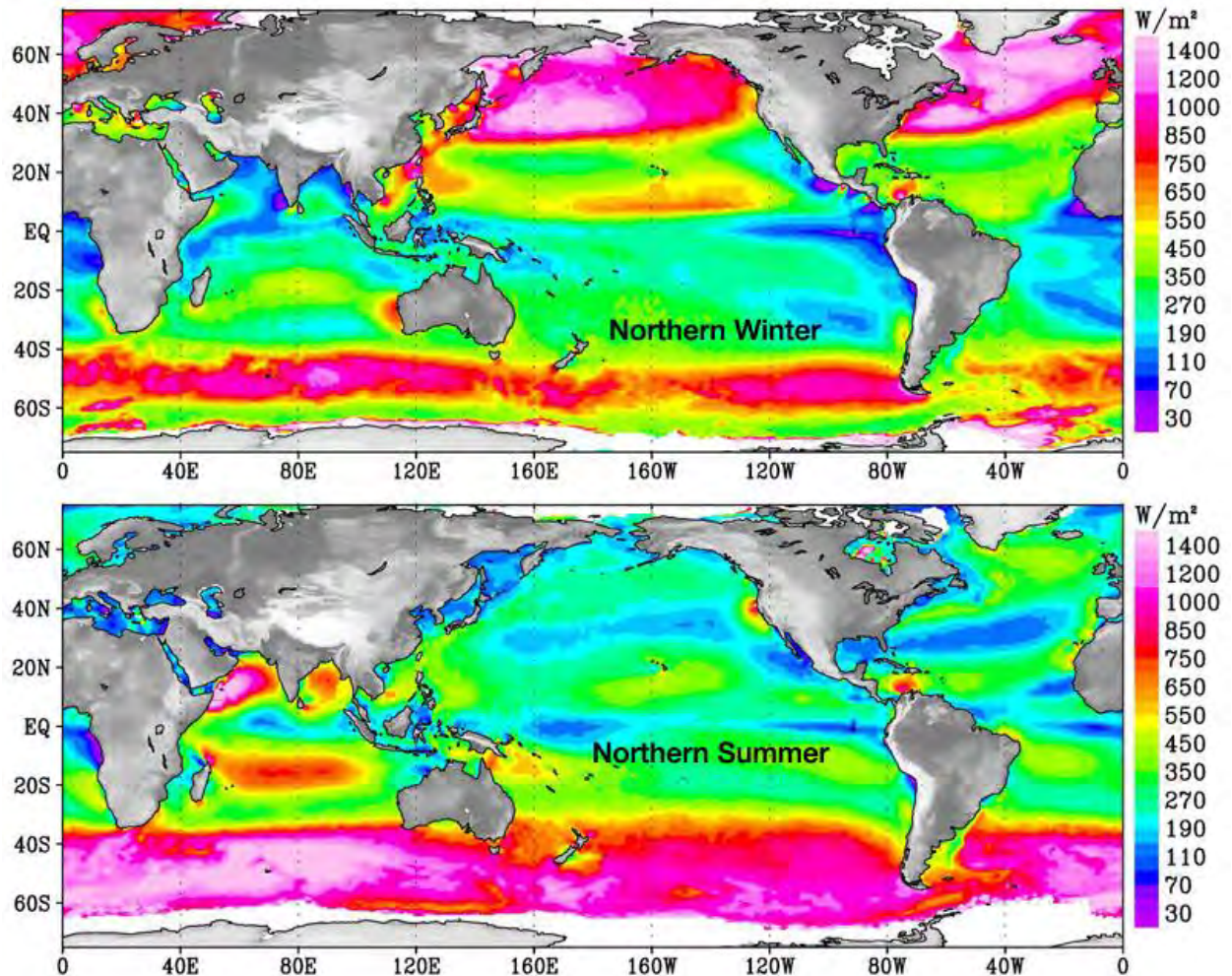
These developments show the viability of offshore wind energy for developed countries and have caught the attention of other nations, demonstrating that offshore wind power may supplant conventional fossil fuel power plants [14]. On the other side, interests are growing in different countries to determine the potential of offshore wind farms and their scales for local power generation [15].

3 GLOBAL OFFSHORE WIND RESOURCE

Many research have dealt with available offshore wind resource on the planet and they show that it is a promising option for high power production. These studies were possible because of the fast progress with regards to observations and computations [16]. In a study by Zheng and Pan [17], they found high wind speeds over open waters in 60% of a year and over $50\text{W}/\text{m}^2$ wind power density is available in 80% of a year in most ocean surfaces. Another work by the same authors investigated climate trends of the world's ocean wind speeds and found that there is a 3.35 cm/s increase every year from 1988 to 2011 [18]. Thus, offshore wind resource has an increasing trend going forward. Recent developments have even considered global offshore wind power prediction which is essential for wind farm operations. Such a research has been made by Sasaki [19] where he found that 5-day ahead wind power production forecasts are possible but notes that there is much to be done for reliable predictions. In addition to improving wind forecasting capabilities, Zheng et al. [20] suggests that grade division by wind turbine classes and production of a wind energy development index is necessary to aid in offshore wind project decisions. These efforts are indeed useful for the development of offshore wind farms for the different nations.

4 OFFSHORE WIND STUDIES IN LOW LATITUDE REGIONS

Many developing countries are found in the low latitude region and there are plenty of open waters in these locations. Offshore wind energy is a potential choice for power production in these areas but, unfortunately, there are very few research on the subject in these nations [21]. Rusu and Onea [21] investigated the marine energy resource of developing nations where they had compiled the wind power densities available at a given height above ground level from the different countries and this section will use a similar treatment. In selected regions where they analysed wind data, they found that Somalia has a wind power density of $1,073\text{W}/\text{m}^2$ while Vietnam has $695.5\text{W}/\text{m}^2$ for the 80 m height above the surface. These values are recommended for offshore wind development and may be a viable sustainable energy source for the future [21]. They also studied the areas close to Angola, Brazil, Guinea-Bissau, Madagascar, Mexico, Myanmar, Peru, Papua New Guinea, and Timor where wind resource reserves are moderate since it ranges from $67\text{W}/\text{m}^2$ - $315\text{W}/\text{m}^2$. These values are well above the global average wind power density determined by Zheng and Pan [17] which could be tapped for power generation by these countries in the future. Satellite observations has enabled initial WRA on oceans for different locations where wind map products such as in Figure 1 can be used for analysis [20].



(Source: <https://www.nasa.gov/topics/earth/features/quikscat-20080709.html> accessed 26 March 2018)

Figure 1. Wind power density in the winter and summer months for the Earth's ocean surface at 80m level from Quik Scatterometer (QuikSCAT) data analysis

But this remote sensing method has limits since each satellite scan can only cover a portion of the planet at a particular time so, its spatial and temporal resolution is not sufficient for a complete offshore WRA [20]. A careful evaluation is needed to better understand the wind energy reserves for each country thus, there have been efforts to do this that can be found in the literature.

Areas of Latin America facing the Atlantic were investigated by Pimenta, Kempton, and Garvine [22]; it has been reported that Brazil has $300 W/m^2 - 550 W/m^2$ wind power density between $19^{\circ}S - 23^{\circ}S$ latitude at 80 m level. Their results showed that offshore wind energy in Brazil is promising since the highly populated cities there are close to shore and may complement the hydro power [22]. On the other hand, Soler-Bientz et al. [23] studied the offshore wind at the Yucatan Peninsula in Mexico using wind observations at 10 m and 25 m above ground level and characterised the wind profile in the area for the initial work [23].

Similar works have been carried out in South Asia aiming to investigate the exclusive economic zone (EEZ) of India. Nagababu et al. [24] has seen that there is $437 W/m^2$ of wind power density at 80 m height in the Indian EEZ. Potentially, it could supply 41% of the nation's energy requirement for the fiscal year (2015-2016 [24]. Although India does invest on renewable energy and possess offshore wind energy it can tap, the country requires a policy to foster offshore wind farm development [25]. In that part of the world, even small island nation like Maldives has potential offshore wind resource with power densities ranging from $72 W/m^2$ to $104 W/m^2$ that could contribute in making the country self-sufficient for its energy needs [26].

Offshore wind research is more active within the South China Sea which is evident from the deployment of China [11]. The first operational offshore wind farm outside Europe is found in Donghai Bridge [13]. From

there, the Chinese planned for other offshore projects that are under construction or in commissioning phase [8], while other projects are being developed by Taiwan, Vietnam, and Thailand. A study by Chang et al. [27] involved analysing the wind resource around Hainan Island. Their results show that the surrounding waters of that island have 400 W/m^2 to 600 W/m^2 wind power density at 100 m height [27]. Further investigation in the area was done by Liu et al. [28] which dealt with a larger study domain that included East and South China Sea in order to cover the 29 wind farm sites under evaluation. They compared the performance of different vertical wind profile methods under various atmospheric stability conditions [28]. This work of Liu et al. [28] presents that a better understanding of atmospheric dynamics is needed to produce improved wind resource assessment in the region. A deeper comprehension of atmospheric dynamics in the region was reflected in a study for three offshore islands at the western part of Taiwan that was done by Hsieh and Dai [29]. In this study, they employed Hilbert-Huang transform and Fast Fourier transform in order to improve the statistical models used for characterising winds in terms of climate time scales in Taiwan and a tool for wind forecasting that is needed in reporting power production capacity outlook to the grid for operations [29]. A more comprehensive study on the wind resource at the western coast of Taiwan and the Penghu archipelago, which includes the three islands in the previous study, was done by Fang [30]. The results from that study yielded that the offshore area close to Taiwan's western coasts has a power density of approximately $1,000 \text{ W/m}^2$ and the offshore winds located in the region of Penghu can be greater than $1,400 \text{ W/m}^2$ for the heights between 100 m to 200 m [30]. These findings have been reinforced by the work of Chang, Yang, and Lai [31] in the western Taiwan offshore wind resource where the authors found that for the 100 m level, the area have $1,079 \text{ W/m}^2$ to $2,665 \text{ W/m}^2$ power density. In Southeast Asia, studies on Thailand offshore wind resource have been made for the Gulf of Thailand [32, 33]. One of the studies at Thaksin University have found that the Gulf of Thailand has $3,500 \text{ km}^2$ area that is appropriate for offshore wind development with a 15 TWh/year power production potential [32]. In another work by the same institution, a wind map for the Gulf of Thailand is generated and they made wind farm optimizations so that they were able to suggest priority development sites for offshore wind plants [33]. Vietnam is starting its offshore wind deployment in the region with a 99.2 MW wind farm in the Mekong Delta and other upcoming projects in the area are being planned [11].

With all these research on the low latitude region on offshore wind, it is apparent that it has great potential to be tapped for energy for countries located there. Offshore wind energy can supply the needed power demand of the cities situated there that could allow a sustainable manner for economic development [21]. But, as the literature shows, a meticulous wind resource assessment for offshore sites is necessary before proceeding on any offshore wind projects.

5 TECHNIQUES IN OFFSHORE WIND RESOURCE ASSESSMENT

Many of the methods for offshore wind resource assessment has been adopted from onshore wind project developments. The use of wind measurements and analysis as well as wind simulations are found in the literature when carrying out offshore wind resource assessments which are very much the same for onshore ones. In this section, the various techniques employed for offshore wind resource assessment are reviewed.

5.1 Wind Observations and Wind Map Products

Published works in the literature are using wind data over the oceans from buoys, meteorological masts, ship observations, and satellite-mounted scatterometer. Performing analysis on these observations enable the researchers to generate wind resource maps. One of the widely used technique for producing high quality wind resource maps is measure-correlate-predict (MCP) [4]. This was employed by Oh et al. [34] in determining the wind power potential at an offshore site in South Korea. They analysed the wind observations from a meteorological tower at sea in order to select the wind turbine class suited and the feasibility of the project based on the annual energy production (AEP) and capacity factor (CF) [34]. The use of wind observation masts was also done in the 2016 Adriatic Sea study of Schweizer et al. but they included wave data from buoys. Extending beyond the use of wind data on wind potential and wind project feasibility, they were able to study different wind farm design scenarios [9].

There are studies that use remote sensing techniques or reanalysis data when in situ measurements are not available or insufficient for the requirements of the work to produce wind maps or for wind profile analysis. Although these can serve as substitutes to actual ground measurement, validation of these data have been done and deemed necessary by researchers [35, 36]. These studies have been made to see the usability of such data in the absence of wind masts for offshore WRA and they found that they can serve as proxy data as long as the users know the limitations of such datasets [35, 36]. In the literature, global or regional scale wind resource assessment has been done using reanalysis wind data. One of such studies was made by Zheng et al. [16] over the South China Sea region where they classified the wind power based on the National Renewable Energy Laboratory (NREL) classification levels and segregated the temporal portion according to seasons [16].

The mentioned datasets in these section allowed many studies on offshore wind potential for different locations on the planet. But there are cases when high spatial and temporal resolutions are needed for WRA or there is lack of data to perform WRA. In such situations, researchers have used computer simulations of wind fields to address the requirements for fine resolution and wind data generation for analysis.

5.2 Wind Modelling

Usage of wind simulations for the study of offshore wind resource is being undertaken in many published research. In the paper of Ayotte [37], he noted that there has been constant development for high resolution calculations involving complex geometries on meteorological models. These improvements in meteorological models made numerical weather prediction (NWP) be utilisable for WRA as well. An example of WRA using wind simulations can be seen in Figure 2.

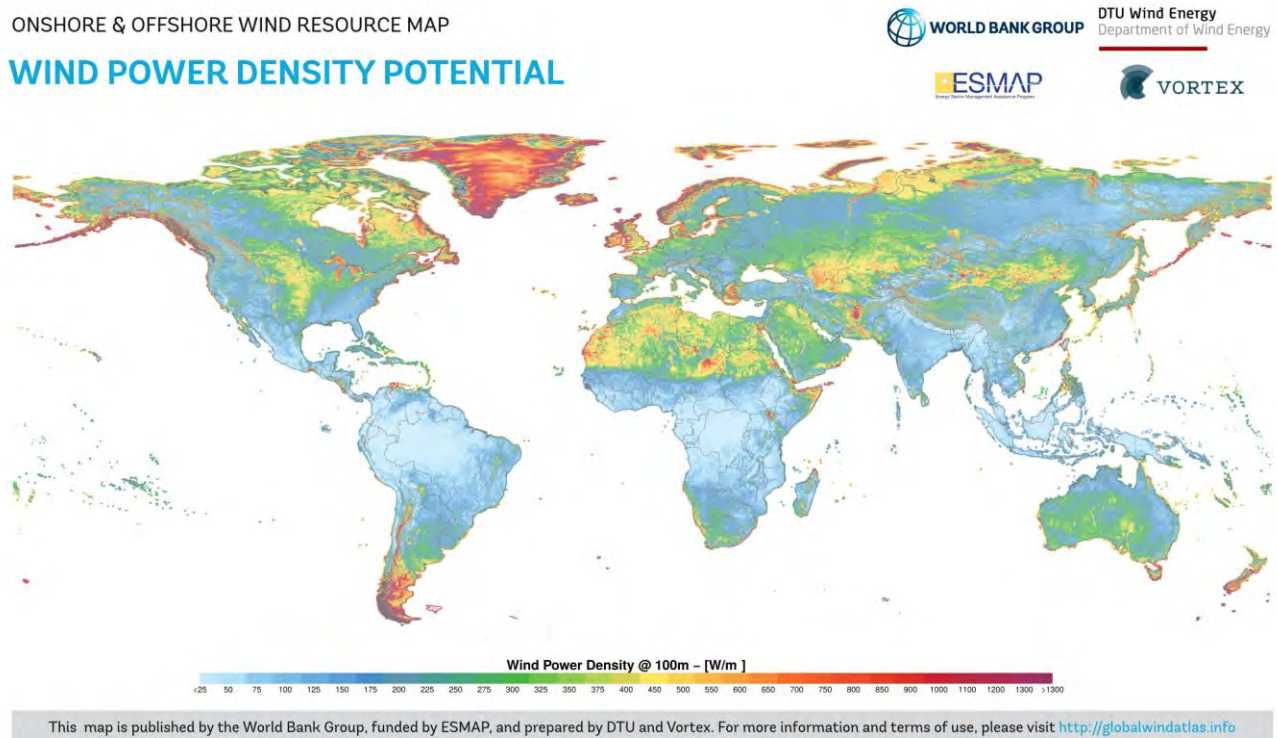


Figure 2. Global wind power index that includes open waters from coastline to 30 km distance of land masses at 100 m above ground level

A review on the role of NWP in WRA by Al-Yahyai et al. [38] stated that observations have coarse spatial resolutions that require high cost investments in equipment and operations. They also pointed out that different vertical levels for measurements and long observation periods are necessary before making wind analysis for assessment study therefore, NWP was found to address these problems since simulation cost would be the system used to run the computations and that can already yield high spatial resolution wind vectors with multiple atmospheric layers [38]. For these reasons, NWP has been utilised for offshore wind research in the literature.

Various studies have used NWP involving WRA for their research interest where they compare the simulation results with actual measurements or assimilate wind data to improve the model output. When wind observations are lacking, data obtained through remote sensing and reanalysis data were used for comparison or as model inputs for the NWP. In a similar manner, these have been found to be applicable to offshore WRA. One study made by Carvalho, Rocha, and Gomez-Gesteira [39] employed NWP to simulate the seas off the Iberian Peninsula coasts. They used different reanalysis data to drive the Weather Research and Forecast (WRF) model then, validated it with buoy wind data where results show that using European Reanalysis-Interim (ERA-Interim) as input gave adequate results for offshore WRA [39]. Continuing on this research, a more recent work from the group evaluated the performance of scatterometers and saw that WRF simulations have the best overall performance in the open seas when compared with the other datasets [40]. Such work has been done in the South China Sea also in order to determine the available wind resource in the region. Other examples in the literature include the study of Chang et al. [31] reported on WRF and assimilated satellite-based data into the model to determine the wind resource around Hainan Island. For the study in Taiwan, Fang [30] used the Mesoscale Model ver. 5 (MM5) in generating wind maps for open seas over the western side of the country. Offshore WRA for the Gulf of Thailand was simulated using WRF in the work of Chancham, Waewsak, and Gagnon [33].

It can be concluded that there has been extensive use of NWP in different parts of the world for offshore wind research. It has been useful for areas that lack in situ observations despite its limitations [40]. Even when wind mast data are available, NWP can complement the observed data for wind energy resource assessment [38].

6 DISCUSSION

Research in the literature have shown that offshore wind resource is available in low latitude countries even though they are not as rich as those found in the mid and high latitudes. These could still be tapped for energy that can make these countries capable of producing energy locally in a sustainable manner.

There are very few offshore wind projects in the area where only China has offshore wind farms that are operational while Taiwan and Vietnam are only beginning with their first offshore wind farm deployment. Studies in the low latitude region are mostly on assessing the available offshore wind resource of the various nations. As China is one of the leaders in adopting the technology, the South China Sea has become an active area for offshore wind projects and development. At present, other nations are doing their initial WRA for offshore locations within their waters.

Offshore WRA is a crucial step prior to any offshore wind project. Similar with onshore techniques, offshore wind resource assessments involve measure-correlate-predict, satellite and reanalysis data, wind mapping, and wind simulations. Since MCP is expensive, the other methods are suitable for initial assessment since developing nations have limited finances. These methods involve data analysis using observations from remote sensing, reanalysis, and wind modelling. All of these are suitable substitutes to actual wind measurements based on the results of different research found in the literature.

7 CONCLUSIONS

Offshore wind energy is a promising resource that low latitude countries can exploit for their local power production. The resource is available but an intensive WRA must be made before proceeding further in developing offshore wind projects. Wind maps can be generated using satellite observations, reanalysis data, and wind simulations but must be subjected to careful validation for their locality. WRA is a very important step for offshore wind development since these projects are very expensive and WRA enables the avoidance of risks involved with high cost investments. Even with the high cost of offshore wind development, the literature presents that offshore wind resource can be a viable energy source for low latitude nations and could allow them to become self-sufficient with their power requirements.

ACKNOWLEDGEMENTS

The authors would like to thank Newton-Agham Fund programme and the Department of Science and Technology of the Philippine Government for sponsoring this work.

REFERENCES

- [1] A. R. Henderson, C. Morgan, B. Smith, H. C. Sorensen, R. J. Barthelmie, and B. Boesmans, Offshore Wind Energy in Europe – A Review of the State-of-the-Art, *Wind Energy*, Vol. 6, pp. 35-52, 2003.
- [2] S. Butterfield, W. Musial, J. Jonkman, P. Sclavounos, and L. Wayman, Engineering Challenges for Floating Offshore Wind Turbines, *2005 Copenhagen Offshore Wind Conference*, Copenhagen, 2005.
- [3] C. L. Archer, B. A. Colle, L. D. Monache, M. J. Dvorak, J. Lundquist, B. H. Bailey, P. Beaucage, M. J. Churchfield, A. C. Fitch, B. Kosovic, S. Lee, P. J. Moriarty, H. Simao, R. J. A. M. Stevens, D. Veron, and J. Zack, Meteorology for Coastal/Offshore Wind Energy in the United States: Recommendations and Research Needs for the Next 10 Years, *Bulletin of the American Meteorological Society*, Vol. 95, pp. 515-519, 2014.
- [4] P. Jain, P. P. Calceas, and B. An, *Guidelines for Wind Resource Assessment: Best Practices for Countries Initiating Wind Development*, Asian Development Bank, 2014.
- [5] L. Niyomtham, C. Lertsathittanakorn, J. Waewsak, and Y. Gagnon, On the Wind Resource Assessment along the Western Coast of Thailand, *Energy Procedia*, Vol. 138, pp. 1190-1195, 2017.
- [6] X. Sun, D. Huang, and G. Wu, The Current State of Offshore Wind Energy Technology Development, *Energy*, Vol. 41, pp. 298-312, 2012.
- [7] E. I. Zountouridou, G. C. Kiokos, S. Chakalis, P. S. Georgilakis, and N. D. Hatziaegyriou, Offshore Floating Wind Parks in the Deep Waters of Mediterranean Sea, *Renewable and Sustainable Energy Reviews*, Vol. 51, pp. 433-448, 2015.
- [8] S. Rodrigues, C. Restrepo, E. Kontos, R. Teixeira Pinto, and P. Bauer, Trends of Offshore Wind Projects, *Renewable and Sustainable Energy Reviews*, Vol. 49, pp. 1114-1135, 2015.
- [9] J. A. Schweizer, Antonini, L. Govoni, G. Gottardi, R. Archetti, E. Supino, C. Berretta, C. Casadei, and C. Ozzi. Investigating the Potential and Feasibility of an Offshore Wind Farm in the Northern Adriatic Sea, *Applied Energy*, Vol. 177, pp. 449-463, 2016.
- [10] R. Perveen, N. Kishor, and S. R. Mohanty. Off-shore Wind Farm Development: Present Status and Challenges, *Renewable and Sustainable Energy Reviews*, Vol. 29, pp. 780-792, 2014.
- [11] Global Offshore Wind 2016 Report <http://www.gwec.net/wp-content/uploads/2017/05/Global-Offshore-2016-and-Beyond.pdf> [Accessed 12 March 16, 2018].
- [12] M. Esteban and D. Leary, Current Developments and Future Prospects of Offshore Wind and Ocean Energy, *Applied Energy*, Vol. 90, pp. 128-136, 2012.
- [13] Y. C. Tsai, Y. F. Huang, and J. T. Yang, Strategies for the Development of Offshore Wind Technology for Far-East Countries – A Point of View from Patent Analysis, *Renewable and Sustainable Energy Reviews*, Vol. 60, pp. 182-194, 2016.
- [14] B. Snyder, and M. J. Kaiser, Ecological and Economic Cost-Benefit of Offshore Wind Energy, *Renewable Energy*, Vol. 34, pp. 1567-1578, 2009.
- [15] K. Y. Oh, J. Y. Kim, J. K. Lee, M. S. Ryu, and J. S. Lee. An Assessment of Wind Energy Potential at the Demonstration Offshore Wind Farm in Korea, *Energy*, Vol. 46, pp. 555-563, 2012.
- [16] C. Zheng, C. Li, C. Gao, and M. Liu, A Seasonal Grade Division of the Global Offshore Wind Energy Resource, *Acta Oceanologica Sinica*, Vol. 36, pp. 109-114, 2017.
- [17] C. W. Zheng and J. Pan, Assessment of the Global Ocean Wind Energy Resource, *Renewable and Sustainable Energy Reviews*, Vol. 33, pp. 382-391, 2014.
- [18] C. W. Zheng, J. Pan, and C. Y. Li, Global Oceanic Wind Speed Trends, *Ocean and Coastal Management*, Vol. 129, pp. 15-24, 2016.
- [19] W. Sasaki, Predictability of Global Offshore Wind and Wave Power, *International Journal of Marine Energy*, Vol. 17, pp. 98-109, 2017.
- [20] C. W. Zheng, C. Y. Li, J. Pan, M. Y. Liu, and L. L. Xia, An Overview of Global Ocean Wind Energy Resource Evaluations, *Renewable and Sustainable Energy Reviews*, Vol. 53, pp. 1240-1251, 2016.
- [21] E. Rusu and F. Onea, Joint Evaluation of the Wave and Offshore Wind Energy Resources in the Developing Countries, *Energies*, Vol. 10, pp. 1-20, 2017.

- [22] F. Pimenta, W. Kempton, and R. Garvine, Combining Meteorological Stations and Satellite Data to Evaluate the Offshore Wind Power Resource of Southeastern Brazil, *Renewable Energy*, Vol. 33, pp. 2375-2387, 2008.
- [23] R. Soler-Bientz, S. Watson, D. Infield, and L. Ricalde-Cab, Preliminary Study of the Offshore Wind and Temperature Profiles at the North of the Yucatan Peninsula, *Energy Conversion and Management*, Vol. 52, pp. 2829-2843, 2011.
- [24] G. Nagababu, S. S. Kachhwaha, N. K. Naidu, and V. Savsani, Application of Reanalysis Data to Estimate Offshore Wind Potential in EEZ of India based on Marine Ecosystem Considerations, *Energy*, Vol. 118, pp. 622-631, 2017.
- [25] S. Mani and T. Dhingra, Offshore Wind Energy Policy for India – Key Factors to be Considered, *Energy Policy*, Vol. 56, pp. 672-683, 2013.
- [26] P. Contestabile, E. D. Lauro, P. Galli, C. Corselli, and D. Vicinanza, Offshore Wind and Wave Energy Assessment around Male and Magoodhoo Island (Maldives), *Sustainability*, Vol. 9, pp. 1-24, 2017.
- [27] R. Chang, R. Zhu, M. Badger, C. B. Hasager, X. Xing, and Y. Jiang, Offshore Wind Resources Assessment from Multiple Data and WRF Modeling over South China Sea, *Remote Sensing*, Vol. 7, pp. 467-487, 2015.
- [28] Y. Liu, D. Chen, Q. Yi, and S. Li, Wind Profiles and Wave Spectra for Potential Wind Farms in South China Sea. Part I: Wind Speed Profile Model, *Energies*, Vol. 10, pp. 1-24, 2017.
- [29] C. H. Hsieh and C. F. Dai, The Analysis of Offshore Islands Wind Characteristics in Taiwan by Hilbert-Huang Transform, *Journal of Wind Engineering and Industrial Aerodynamics*, Vol. 107-108, pp. 160-168, 2012.
- [30] H. F. Fang, Wind Energy Potential Assessment for the Offshore Areas of Taiwan West Coast and Penghu Archipelago, *Renewable Energy*, Vol. 67, pp. 237-241, 2014.
- [31] P. C. Chang, R. Y. Yang, and C. M. Lai, Potential of Offshore Wind Energy and Extreme Wind Speed Forecasting on the West Coast of Taiwan, *Energies*, Vol. 8, pp. 1685-1700, 2015.
- [32] J. Waewsak, M. Landry, and Y. Gagnon, Offshore Wind Power Potential of the Gulf of Thailand, *Renewable Energy*, Vol. 81, pp. 609-626, 2015.
- [33] C. Chancham, J. Waewsak, and Y. Gagnon, Offshore Wind Resource Assessment and Wind Power Plant Optimization in the Gulf of Thailand, *Energy*, Vol. 139, pp. 706-731, 2017.
- [34] K. Y. Oh, J. Y. Kim, J. K. Lee, M. S. Ryu, and J. S. Lee, An Assessment of Wind Energy Potential at the Demonstration Offshore Wind Farm in Korea *Energy*, Vol. 46, pp. 555-563, 2012.
- [35] D. Carvalho, A. Rocha, M. Gomez-Gesteira, I. Alvarez, and C. Silva Santos, Comparison between CCMP, QuikSCAT, and Buoy Winds along the Iberian Peninsula Coast, *Remote Sensing of Environment*, Vol. 137, pp. 173-183, 2013.
- [36] Alvarez, I., M. Gomez-Gesteira, M. de Castro, and D. Carvalho. "Comparison of Different Wind Products and Buoy Wind Data with Seasonality and Interannual Climate Variability in the Southern Bay of Biscay (2000-2009)." *Deep-Sea Research II* 106. 2014: 38-48.
- [37] K. Ayotte, Computational Modelling for Wind Energy Assessment, *Journal of Wind Engineering and Industrial Aerodynamics*, Vol. 96, pp. 1571-1590, 2008.
- [38] S. Al-Yahyai, Y. Charabi, and A. Gastli, Review of the Use of Numerical Weather Prediction (NWP) Models for Wind Energy Assessment, *Renewable and Sustainable Energy Reviews*, Vol. 14 pp. 3192-3198, 2010.
- [39] D. Carvalho, A. Rocha, and M. Gomez-Gesteira, Ocean Surface Wind Simulation forced by Different Reanalyses: Comparison with Observed Data along the Iberian Peninsula Coast, *Ocean Modelling*, Vol. 56, pp. 31-42, 2012.
- [40] D. Carvalho, A. Rocha, M. Gomez-Gesteira, and C. Silva Santos, Offshore Winds and Wind Energy Production Estimates Derived from ASCAT, OSCAT, Numerical Weather Prediction Models and Buoys – A Comparative Study for the Iberian Peninsula Atlantic Coast, *Renewable Energy*, Vol. 102, pp. 433-444, 2017.
-

Applying Mesoscale and Computational Fluid Dynamics Models for Offshore Wind Resource Assessment in the Philippines

S.N. Uy^{1,2*}, V. Chennam Vijay^{1,*}, N. Perera¹, A. Alaswad³, J. S. Reid⁴, and N.D. Lagrosas²

1. School of Engineering and the Built Environment, Birmingham City University, Birmingham, UK;
2. Manila Observatory, Quezon City, Philippines
3. School of Engineering Applied Science, Aston University, Birmingham, UK;
4. Marine Meteorology Division, Naval Research Laboratory, Monterey, CA, USA

*Corresponding author: Millennium Point Building, 1 Curzon Street, Birmingham City University, B4 7XG

Email: venkatesh.chennamvijay@bcu.ac.uk

ABSTRACT

Driven by the Philippines' need to provide electrical power to multiple islands with minimal environmental impact, offshore wind energy has been regarded as promising sustainable energy resource for the country. However, there are limited offshore wind observations in the country, which makes the available data insufficient for determining the wind potential over its waters. A proper offshore wind resource assessment must be carried out, with the support of offshore meteorological observations, prior to any wind farm development project. These offshore meteorological masts are itself expensive in terms of capital and operations, and in order to get a robust data, it requires long duration of continuous measurements for wind resource assessment.

In this study, wind simulations over the Western waters of Palawan Island, Philippines were carried out using the Weather Research and Forecasting (WRF) Model. Different input operational and reanalysis datasets were used, with varying planetary boundary layer (PBL) configurations, to test WRF's sensitivity for the studied area. Model results were compared with the data measured by the 7 Southeast Asian Studies (7SEAS) aerosol research cruise in September 2011 and September 2012.

The study finds that WRF results are in line with the hourly wind speed trends, and that the obtained model performs better using ERA-Interim dataset in most of the chosen sites. The resultant model has been concluded to be useful in guiding the process of seeking suitable locations for wind measurement campaigns that can be observed for further wind profiling for potential offshore wind projects in the Philippines.

Keywords: Offshore Wind, Wind Resource Assessment, Numerical Weather Prediction

INTRODUCTION

Developing countries are hugely dependent on fossil fuels as the primary source for energy [1,2]. However, the volatility for fossil fuel pricing pose an adverse impact to economies which highlights the use of renewable resources as a way to attain energy independence for many developing nations [3–6]. Wind resource is a renewable resource that have a greater availability in offshore locations in comparison with sites found on land [7,8]. The Philippines has the potential to generate power from offshore wind but a thorough wind resource assessment (WRA) must be made for wind energy mapping [9]. WRA is essential for any wind energy

development in order to minimise risks in investments [10]. This study aims to use the numerical weather prediction (NWP) method in making a preliminary WRA for offshore regions around the Palawan Island, Philippines. Since the study is a preliminary WRA, the wind speeds will be the focus for this paper. The offshore wind speed observations from the 7 Southeast Asian Studies (7SEAS) aerosol research cruise will be utilised for the modelling validation. The study's results demonstrate how NWP can be used for offshore WRA on other different islands in the country, helping to build a strategic view on the investment in the offshore wind resource in the Philippines.

STUDY AREA AND 7SEAS RESEARCH CRUISE

This study is focused on generating a preliminary WRA for Palawan, Philippines using NWP method. Palawan Province is located at the western part of the Philippines and it is in between the South China Sea and Sulu Sea. This island is a province of the Philippines where the capital is called Puerto Princesa. Figure 1 shows the location of the island within the Philippine archipelago. It is a popular tourist destination for its beaches and the underground river. There are several fishing ports around the island since fishing is one of its major industry. An offshore platform is also located at the west side of this island for gas production. For interests in tropical meteorology phenomena and aerosol transport, this island had been selected for the 7SEAS research cruise in 2011 and 2012 [11,12]. Upon reviewing the meteorological parameters measured on the research cruise, it has been deemed that the wind measurements can be used for preliminary offshore WRA around Palawan. The island has been selected as the study site due to its good wind potential, being near to the South China Sea which has been found to be rich in wind resources [9].

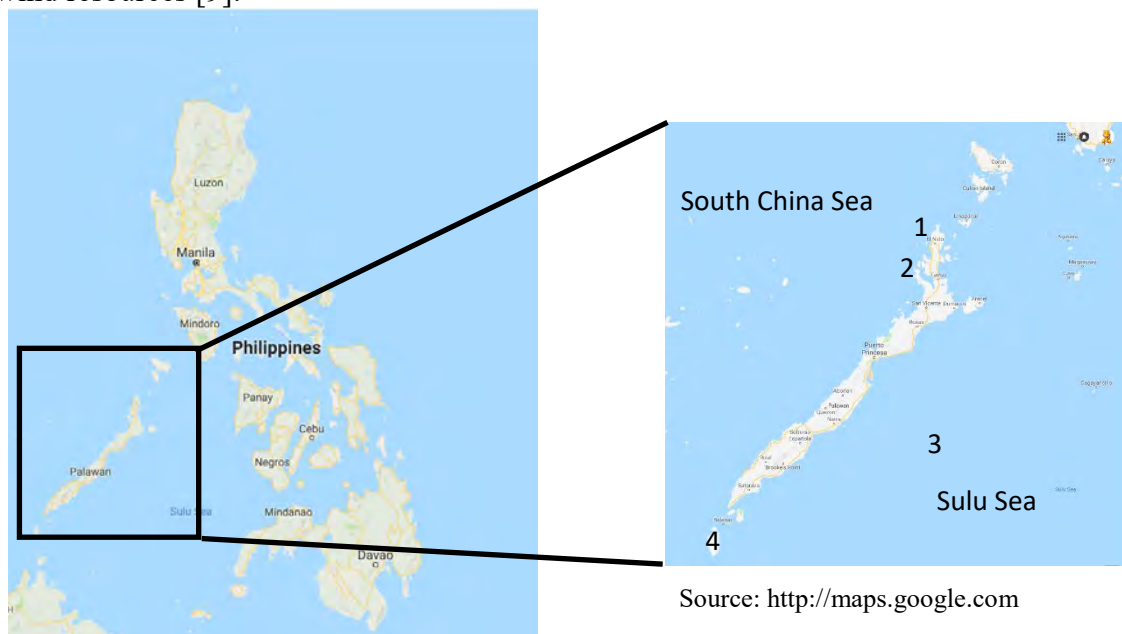


Figure 1. Map of Philippines and Palawan Island. The ship made observations at the locations marked by numbers on the zoomed in map. These sites are 1. Guntao Islands, 2. Notch Island, 3. Tubbataha Reef, and 4. Balabac Island

The study used the 2011 and 2012 wind observations aboard the ship for the aerosol research cruise that was part of the 7SEAS programme to validate the NWP. Four locations were selected for the model validation, namely the Guntao Islands, Notch Island, Balabac Island, and the Tubbataha Reef as shown in Figure 1. The 5-minute interval wind observations were recorded at 10 m above the sea level using a Campbell sonic anemometer [11]. The 2011 campaign took place in September which covered the Guntao Islands and Notch Island [11], while the 2012 campaign covered both the Balabac Island and Tubbataha Reef on September

also [12]. Guntao Islands and Notch Island are located at the northern part of Palawan Province that faces the South China Sea. Tubbataha Reef is situated Southeast of Palawan and within the Sulu Sea. Balabac Island is at the southern tip of Palawan and close to Borneo.

MODEL CONFIGURATION AND DESIGN

For this work, the Weather Research and Forecasting (WRF) Model ver. 3.8.1 in the Advanced Research WRF (ARW) mode is used to make offshore wind fields around the Palawan Island. The model is configured using three different settings found to perform well in other studies in the Philippines [13,14] and Thailand [15] in order to compare each one with observed data. Reanalysis data and operational data from the National Centres for Environmental Prediction (NCEP) and European Centre for Medium-Range Weather Forecasts (ECMWF) have been used as input data for WRF. The specific datasets used are the European Reanalysis-Interim (ERA-Interim), NCEP Climate Forecasts System Reanalysis (NCEP_CFSR), and the NCEP Final Operational Global Analysis Data (FNL). For the planetary boundary layer (PBL) parameter, there are also three different ones used for comparison. PBL used for the simulations are Mellor-Yamada-Janjic (MYJ), Asymmetric Convective Model ver. 2 (ACM2), and Yonsei University (YSU) along with their prescribed surface layer parameters namely, Eta similarity and revised Mesoscale Model ver. 5 (MM5). In addition, the microphysics scheme settings utilised WRF single-moment 3-class (WSM3) and 6-class (WSM6) options. These settings are summarised in Table 1.

Table 1. WRF Configuration Settings

Parameters \ Authors	Dado and Takahashi [13]	Cruz and Narisma [14]	Chancham, Waewsak, and Gagnon [15]
Input Data	ERA-Interim	NCEP-FNL	NCEP-CFSR
Planetary Boundary Layer	MYJ	ACM2	YSU
Surface Layer	Eta Similarity	Revised MM5	Revised MM5
Microphysics Scheme	WSM6	WSM6	WSM3

Although studies reported in [13,14] are focused on rainfall, similar configurations have been used for wind in other studies [15,16]. The input data for the configuration used by Chancham, Waewsak, and Gagnon [15] has been changed to utilise NCEP-CFSR dataset as input instead of NCEP Reanalysis II. Model setting differences have been narrowed to the input data and PBL as previous studies have shown that wind simulations in WRF are highly sensitive to them [16,17]. These minor changes are similar with the configuration used for other offshore wind research in the South China Sea [18]. Differences with the microphysics scheme has been maintained according to the respective settings of the prior works as these pertain to the precipitation in the model and not essential for this study. The surface layer option had to vary because the PBL parameter selected dictates the compatible surface layer setting. Other model parameters are kept the same in the three model configurations selected for this study. Radiation schemes use the Rapid Radiative Transfer Model (RRTM) for long waves and the Dudhia scheme for short waves. The same land use and land cover parameter using the 30 arcsec US Geological Survey (USGS) data have been set and the Noah land surface model has been activated for all simulation runs [13–15]. The Kain-Fritsch cumulus parametrisation scheme has been utilised for all, but has been disabled at the third domain since the model explicitly calculates this parameter for fine resolutions.

There are three domains setup for this simulation in WRF where Domain 1 has 27 km x 27 km resolution, Domain 2 has 9 km x 9km, and Domain 3 has 3 km x 3 km resolution with all domains having an hourly time resolution. Palawan Island is contained within the third domain. The defined domains for the study site can be seen in Figure 2.

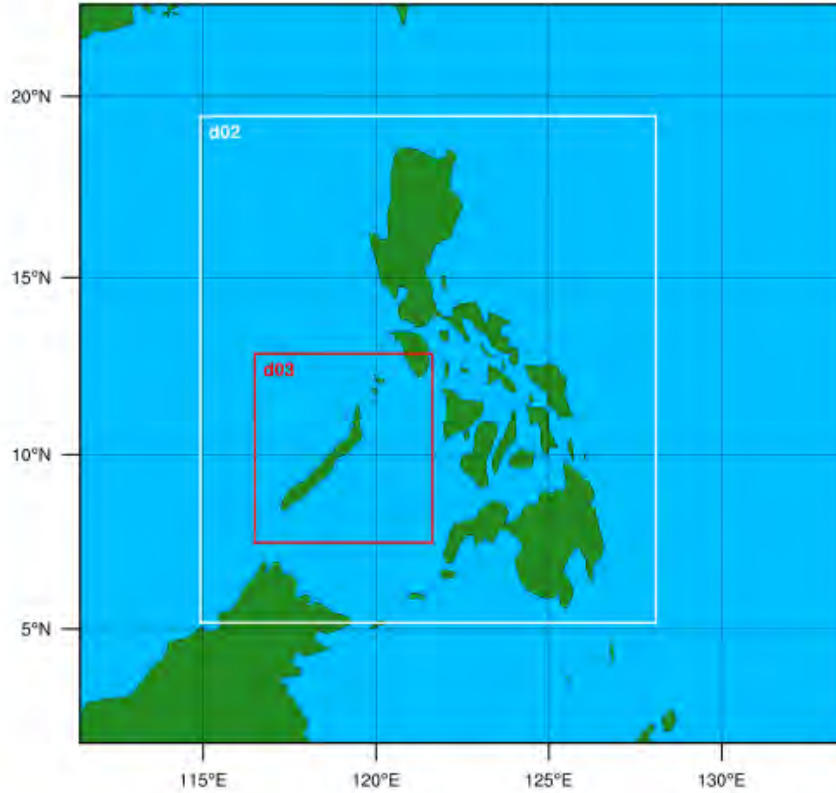


Figure 2. Domains configured for WRF. Palawan Island is within Domain 3 (d03).

Vertical resolution of the model has been increased to 50 vertical eta levels where the first 9 levels are within the 200 m height in order to enable WRF to perform better in accounting for the atmospheric dynamics within the boundary layer [19]. Two-way nesting has been enabled for all the model runs even for simulations that are configured as reported in [14] where one-way nesting was used in the study. Majority of the simulations were carried out on the Advanced Research Computing High End Resource (ARCHER) supercomputing facility where a Cray XC30 is used to provide high performance computing services. Some simulations were also done at the supercomputer of ECMWF which uses Cray XC40 multiprocessor supercomputer.

RESULTS AND DISCUSSION

The WRF has been run on three different settings as explained in Table 1. 7SEAS research cruise campaigns for September 2011 and 2012 in Guntao Islands, Notch Island, Tubbataha Reef and Balabac Island are used for validating the results. Hourly wind speed averages have been calculated from the 7SEAS wind data. Plots that compare the performance of each WRF configuration with the measured data is made for validating the wind speeds [13,20]. These charts show the accuracy of the simulation data in determining the wind values at a specific location. The root-mean-square error (RMSE) of wind speeds are calculated in order to know how much the model results deviate from the measured data [14,16,21]. RMSE is determined using the following equation:

$$RMSE = \sqrt{\frac{1}{N} \sum_{i=1}^N (U^{sim} - U^{obs})^2} \quad (1)$$

where U^{sim} is the simulated wind speed and U^{obs} is the measured wind speed in m/s.

An inter-comparison of the three WRF configuration with the 7SEAS aerosol measurement campaign around Palawan Island has been carried out. Wind observations made while the ship was stationary, facing open seas, and have contiguous data of at more than twelve hours were selected for the validation. For simplicity, the WRF configurations listed in Table 1 will be referred by their input data. Local times will be the reference despite the data being given in UTC since daytime and night time atmospheric phenomena affect the winds. Figure 3 presents the wind speeds off the coast of Balabac Island when the ship was anchored there. It is apparent from the figure that both NCEP-CFS and ERA-Interim reanalyses are underestimating the wind speeds while NCEP-FNL operational dataset is within the range in the afternoon until after midnight local time. As the winds die down before midnight and into the early morning, it shows that NCEP-FNL overestimates the wind speeds. Right before dawn, NCEP-CFS and ERA-Interim are capable of simulating the lower wind conditions measured at Balabac Island.

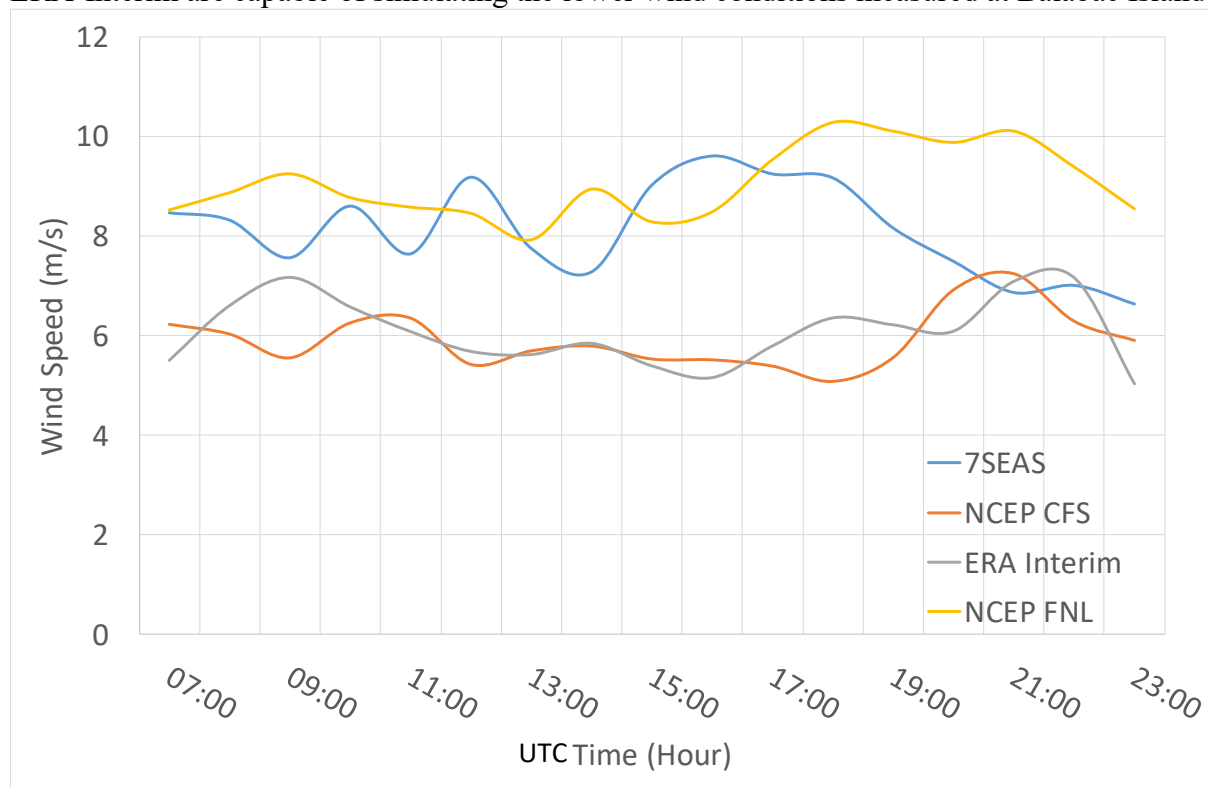


Figure 3. Wind speeds from WRF outputs and actual observations at Balabac Island on 15 September 2012

There has been two stationary observations points around Guntao Islands and Figure 4 is the graph for the North Guntao Island. Here, it is found that NCEP-CFS and NCEP-FNL are overestimating wind speeds. ERA-Interim results are closer to the wind speed data measured aboard the ship where even the late afternoon and evening trends are reflected by the model despite the low wind speeds.

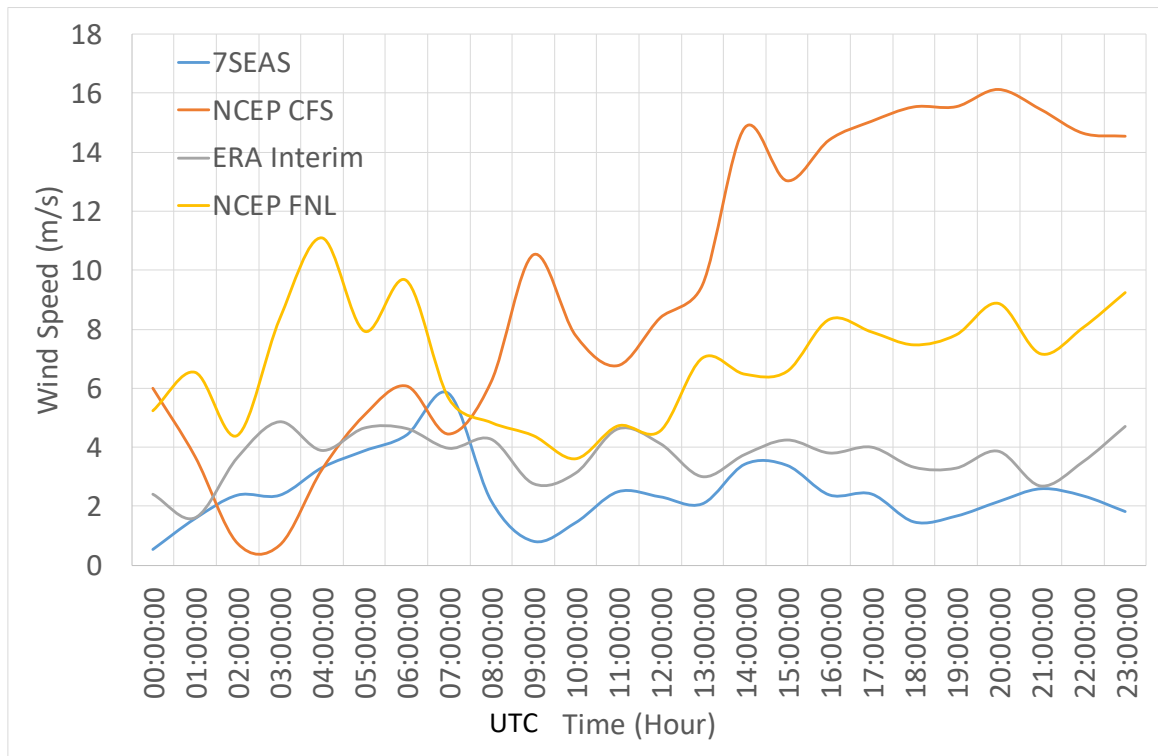


Figure 4. North Guntao Island wind speeds from WRF simulations and ship observations on 9 September 2012

At the Notch Island, it is shown in Figure 5 that ERA-Interim simulates the wind speeds better than NCEP-CFS and NCEP-FNL. Both NCEP-CFS and NCEP-FNL tend to overestimate the wind speeds while ERA-Interim show similar wind magnitudes as the recorded wind data. However, it can be noticed that ERA-Interim underestimates wind speed values after midnight while NCEP-CFS is able to track the wind speed trends in those times.

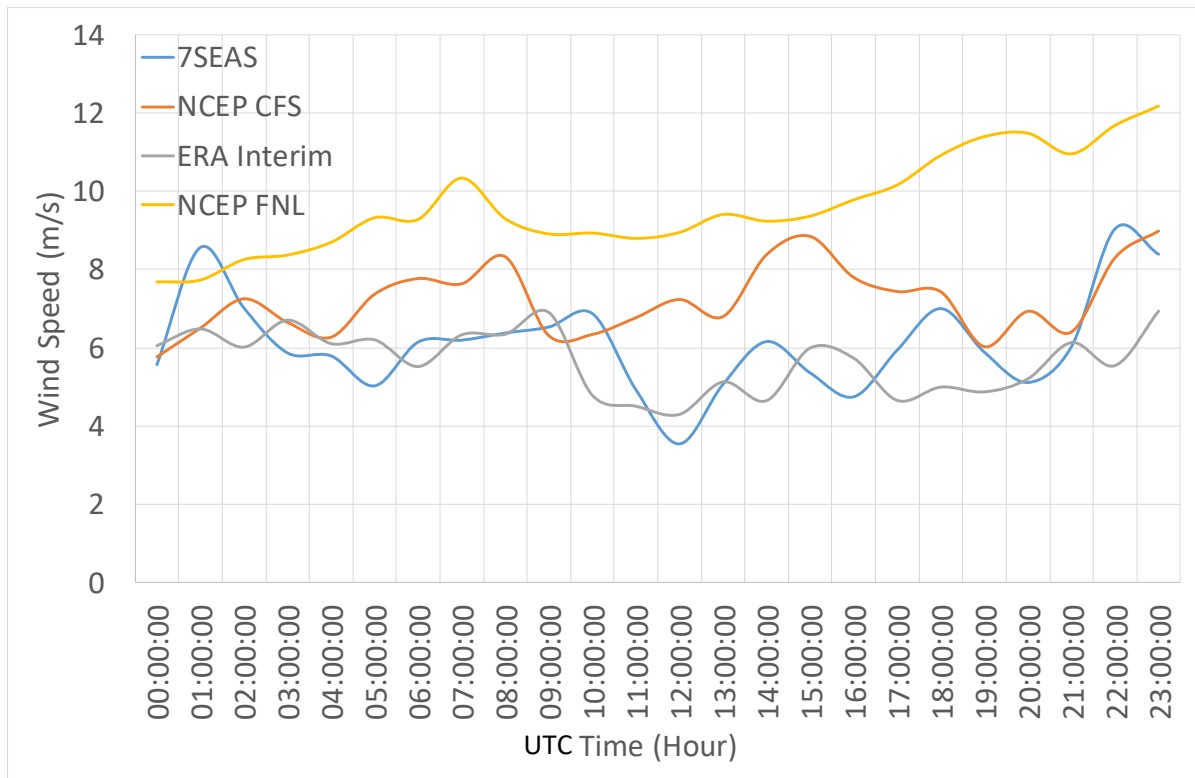


Figure 5. Simulated and observed wind speeds Notch Island on 21 September 2011

The second location for the Guntao Islands site is the South Guntao Island where the wind speed chart for that place is in Figure 6. Similar to the North Guntao Island, both NCEP-CFS and NCEP-FNL are overestimating the wind speeds. The ERA-Interim dataset shows better performance until the sudden drop in wind magnitude observed at night. This has been associated with the approaching typhoon named Nesat at the time [11]. It shows that WRF in ARW has limitations when simulating sudden changes in weather conditions due to extreme weather events which may be modelled better by WRF in operational mode [14].

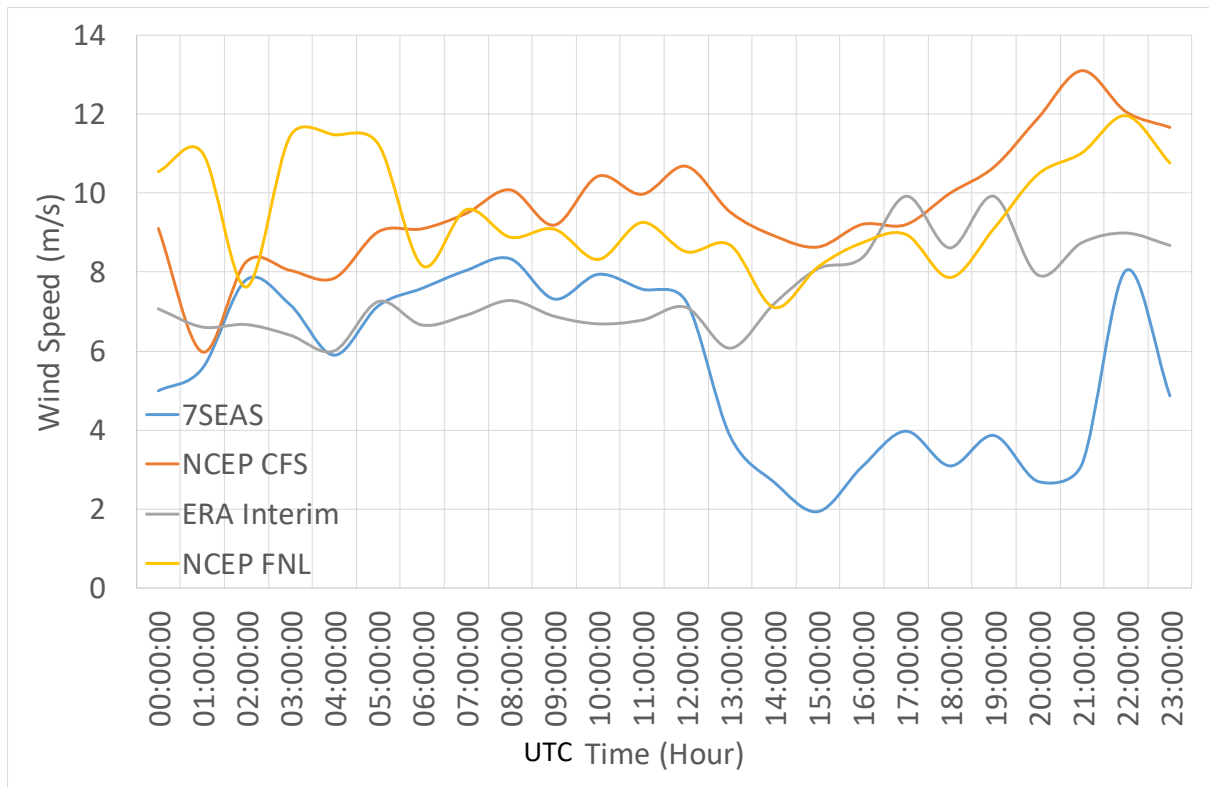


Figure 6. South Guntao Island wind speed measurements and model results for 25 September 2011

The last site to be discussed is the Tubbataha Reef which is located far from any coastline. At this location, two observation sites have been selected for analysis. The first site is the Tubbataha North Reef where a chart of the WRF simulation and ship observation wind speeds are in Figure 7. Here, it shows that NCEP-CFS and NCEP-FNL are overestimating the magnitudes with NCEP-CFS is showing closer results to the actual measurements. It can be found that the ERA-Interim is more capable of modelling the wind speeds among the three at this site although there is a slight underestimation between noon time until early evening and a slight overestimation late in the evening until the early morning of the following day.

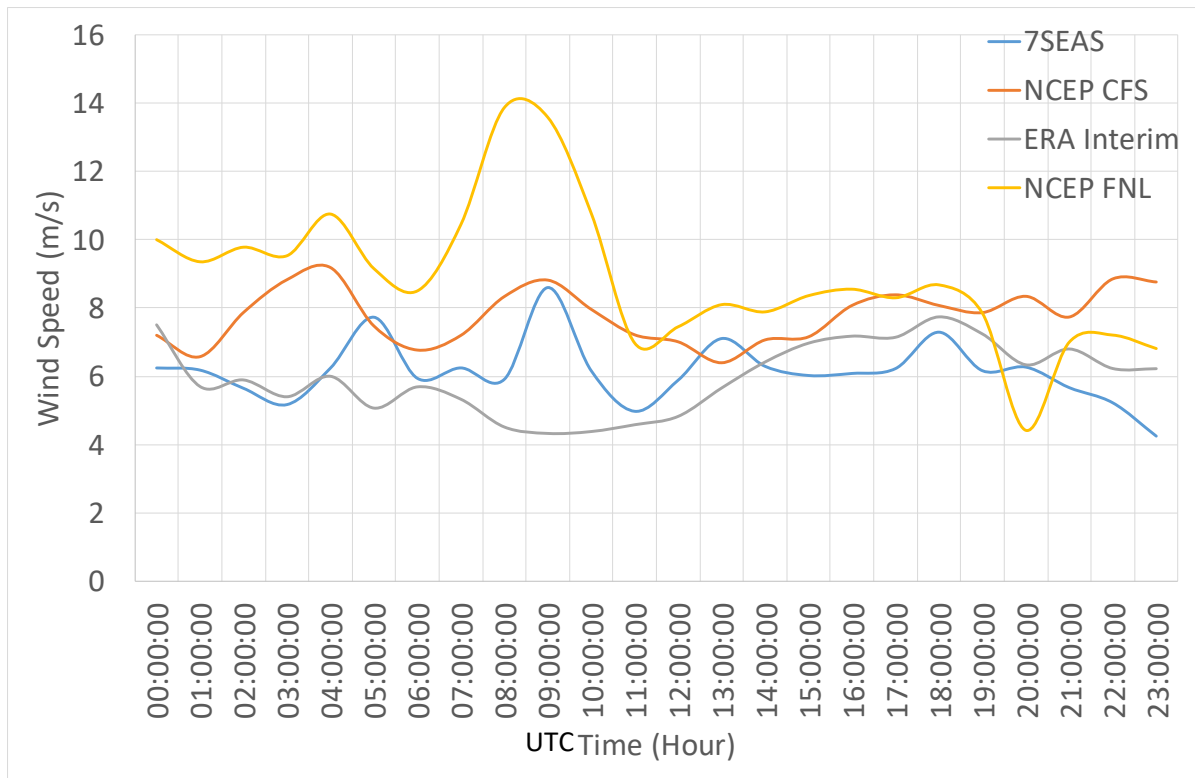


Figure 7. Tubbataha North Reef wind speeds on 22 September 2012

For the South Reef of Tubbataha, the ERA-Interim is able to model the wind speeds better than both the NCEP-CFS and NCEP-FNL as shown in Figure 8. Both the NCEP produced dataset have a tendency to overestimate the wind magnitude. Although ERA-Interim underestimates the wind values in the afternoon, it tracks the wind speeds well beginning at the early evening until the early morning of the following day.

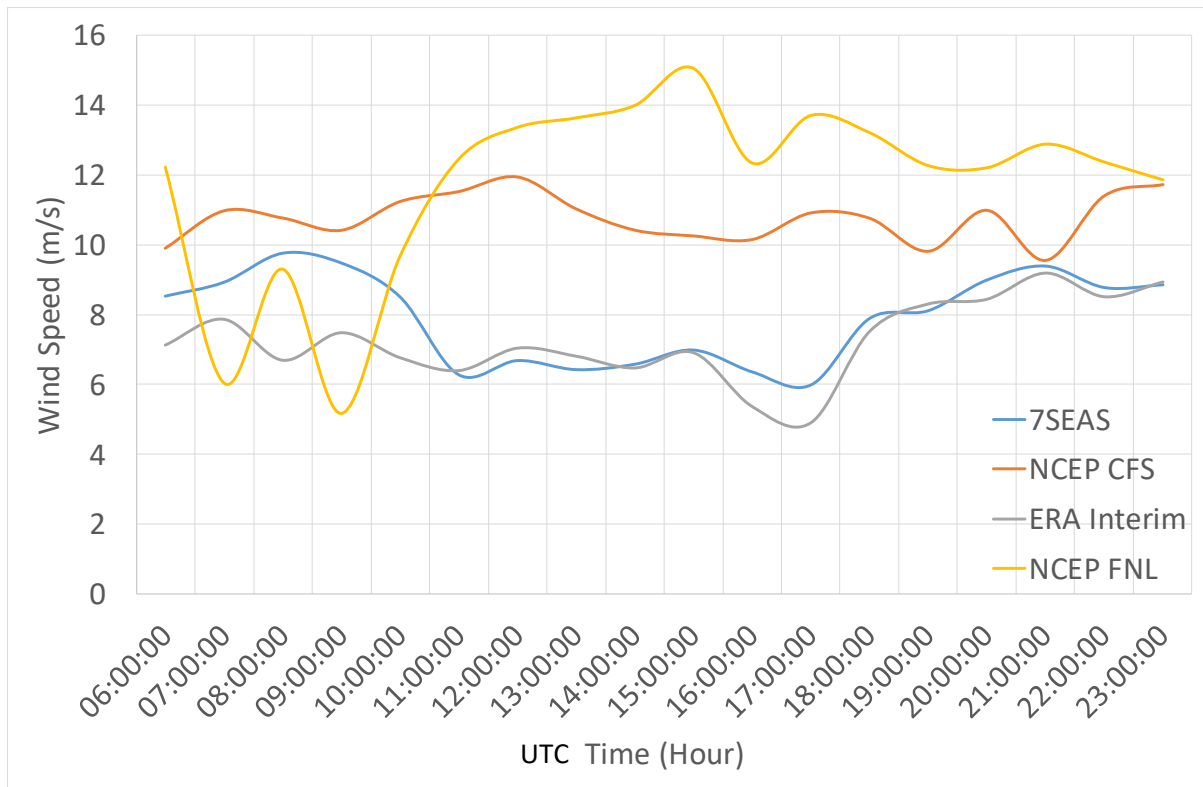


Figure 8. Wind speed comparison for Tubbataha South Reef on 25 September 2012

To quantify the performance of each WRF configuration, the RMSE has been calculated for the wind speed. These results are listed in Table 2 for comparison. For Balabac Island, NCEP-FNL has the least RMSE value of 1.53 for wind speed which makes the NCEP-FNL the suited input dataset for Balabac.. The RMSE values for Guntao Islands present that ERA-Interim is the best performing configuration for these islands. NCEP-CFS performed the worst among the three configurations in the Guntao Islands. Notch Island is where ERA-Interim yields the best wind speed simulations with an RMSE value of 1.26. It is noted that NCEP-CFS is a close second for this location because of the 1.75 RMSE value. The Tubbataha Reef area is also the region where ERA-Interim is capable of simulating the wind speeds better than NCEP-CFS and NCEP-FNL configuration settings. Overall, the ERA-Interim WRF configuration is the best setting for wind simulations on coastal and open waters surrounding Palawan Province with an average RMSE of 1.87 but a more extensive offshore observation is needed to make a better validation study and sensitivity test. The average RMSE of NCEP-CFS and NCEP-FNL are 3.90 and 3.87, respectively. This shows that both input datasets performs similarly for the Palawan Province. Nevertheless, these results suggest that the Balabac Island, South Guntao Island, and Tubbataha Reef have potential wind resource where offshore wind measurement campaigns can be deployed to build a better wind profile of the sites.

Table 2. RMSE values of wind speed for each WRF configuration settings

Configuration Location	NCEP CFS	ERA Interim	NCEP FNL
Balabac Island	2.56	2.42	1.53
North Guntao Island	8.89	1.58	4.84
Notch Island	1.75	1.26	3.81
South Guntao Island	4.93	3.43	4.57
Tubbataha North Reef	2.07	1.40	3.31
Tubbataha South Reef	3.22	1.12	5.18
Average	3.90	1.87	3.87

CONCLUSIONS

Offshore wind energy is a valuable resource that may enable developing countries, like the Philippines, to produce their power needs locally and avoid importation of fuels. Although actual wind measurements for long periods of time are necessary to any wind farm project development, offshore wind observation are expensive and time consuming. NWP methods like WRF modelling can be a tool for preliminary WRA that can be used to identify locations with promising wind potential for extensive offshore wind measurement campaigns. In this study, the Palawan Province is the focus on making a preliminary WRA based on WRF simulations that are validated by short-term offshore wind measurements by the 7SEAS research cruise campaign of 2011 and 2012. Particularly, the locations selected for this study are the Balabac Island, Guntao Islands, Notch Island, and Tubbataha Reef. There are three configuration settings used in the study to determine which one is the best performing for Palawan. Wind speed and wind direction chart comparison show that WRF can simulate the general wind flow around the coastal and open waters of Palawan Province. These are also reflected with the RMSE values calculated using the wind vectors obtained from the model results. The validation has shown that Balabac Island is modelled well by NCEP-FNL in terms of wind speed and by NCEP-CFS for wind direction. The Notch Island is simulated best by ERA-Interim for wind speeds and by NCEP-FNL for wind direction. These findings demonstrate that a combination of two input dataset WRF results can yield the best wind flow profiles in the absence of measurements. In general, the best performing WRF configuration is the one with ERA-Interim as the input data because of its lowest RMSE for both wind speed and direction at most sites in this study. From the results, preliminary WRA show that the Balabac Island, South Guntao Island, and Tubbataha Reef are promising offshore wind farm sites where wind measurement campaigns can be deployed for further wind profiling studies. These results may be improved using computational fluid dynamics (CFD) model like WindSim. CFD models have the capability to simulate grid resolutions that are less than 1km x 1km with high resolution terrain data. Such a tool can yield better wind profiles with smaller RMSE when compared to the observations thus, offering a better WRA for Palawan Province.

References

- [1] Van Kooten GC, Wong L. Economics of wind power when national grids are unreliable. *Energy Policy* 2010;38:1991–8. doi:10.1016/j.enpol.2009.11.080.
- [2] Chang Y, Li Y. Renewable energy and policy options in an integrated ASEAN electricity market: Quantitative assessments and policy implications. *Energy Policy* 2015;85:39–49. doi:10.1016/j.enpol.2015.05.011.

- [3] Pickard M. Global investment in renewable energy projects: How the whole world is jumping on the renewables bandwagon. *Renew Energy Focus* 2016;17:229–30. doi:10.1016/j.ref.2016.10.008.
- [4] Diesendorf M, Elliston B. The feasibility of 100 % renewable electricity systems : A response to critics ☆. *Renew Sustain Energy Rev* 2018;93:318–30. doi:10.1016/j.rser.2018.05.042.
- [5] Chattopadhyay M, Kumar Mitra S. Exploring asymmetric behavior pattern from Indian oil products prices using NARDL and GHSOM approaches. *Energy Policy* 2015;86:262–72. doi:10.1016/j.enpol.2015.06.035.
- [6] Ghassan HB, AlHajhoj HR. Long run dynamic volatilities between OPEC and non-OPEC crude oil prices. *Appl Energy* 2016;169:384–94. doi:10.1016/j.apenergy.2016.02.057.
- [7] Liu Y, Chen D, Yi Q, Li S. Wind profiles and wave spectra for potential wind farms in South China Sea. Part I: Wind speed profile model. *Energies* 2017;10. doi:10.3390/en10010125.
- [8] Henderson AR, Morgan C, Smith B, Sørensen HC, Barthelmie RJ, Boesmans B. Offshore wind energy in Europe - A review of the state-of-the-art. *Wind Energy* 2003. doi:10.1002/we.82.
- [9] Elliott D. Philippines Wind Energy Resource Atlas Development. *Bus. Invest. Forum Renew. Energy Energy Effic. Asia Pacific Reg.*, Kuala Lumpur: 2000, p. 1–10.
- [10] Jain P, Calcetas PP, An B. Guidelines for Wind Resource Assessment: Best Practices for Countries Initiating Wind Development. 2014.
- [11] Reid JS, Lagrosas ND, Jonsson HH, Reid EA, Sessions WR, Simpas JB, et al. Observations of the temporal variability in aerosol properties and their relationships to meteorology in the summer monsoonal South China Sea/East Sea: The scale-dependent role of monsoonal flows, the Madden-Julian Oscillation, tropical cyclones, squall l. *Atmos Chem Phys* 2015;15:1745–68. doi:10.5194/acp-15-1745-2015.
- [12] Reid JS, Lagrosas ND, Jonsson HH, Reid EA, Atwood SA, Boyd TJ, et al. Aerosol meteorology of Maritime Continent for the 2012 7SEAS southwest monsoon intensive study- Part 2: Philippine receptor observations of fine-scale aerosol behavior. *Atmos Chem Phys* 2016;16:14057–78. doi:10.5194/acp-16-14057-2016.
- [13] Dado JMB, Takahashi HG. Potential impact of sea surface temperature on rainfall over the western Philippines. *Prog Earth Planet Sci* 2017;4:23. doi:10.1186/s40645-017-0137-6.
- [14] Cruz FT, Narisma GT. WRF simulation of the heavy rainfall over Metropolitan Manila, Philippines during tropical cyclone Ketsana: a sensitivity study. *Meteorol Atmos Phys* 2016. doi:10.1007/s00703-015-0425-x.
- [15] Chancham C, Waewsak J, Gagnon Y. Offshore wind resource assessment and wind power plant optimization in the Gulf of Thailand. *Energy* 2017;139:706–31. doi:10.1016/j.energy.2017.08.026.
- [16] Carvalho D, Rocha A, Gómez-Gesteira M, Silva Santos C. WRF wind simulation and wind energy production estimates forced by different reanalyses: Comparison with observed data for Portugal. *Appl Energy* 2014;117:116–26. doi:10.1016/j.apenergy.2013.12.001.
- [17] Santos-Alamillos FJ, Zquez DPV, Ruiz-Arias JA, Lara-Fanego V, Tovar-Pescador J. Analysis of WRF model wind estimate sensitivity to physics parameterization choice and terrain representation in Andalusia (Southern Spain). *J Appl Meteorol Climatol* 2013;52:1592–609. doi:10.1175/JAMC-D-12-0204.1.
- [18] Chang R, Zhu R, Badger M, Hasager CB, Xing X, Jiang Y. Offshore wind resources assessment from multiple satellite data and WRF modeling over South China Sea. *Remote*

Sens 2015;7:467–87. doi:10.3390/rs70100467.

- [19] Barstad I. Offshore Validation of a 3 km ERA-Interim Downscaling - WRF Model's Performance on Static Stability. *Wind Energy* 2016;19:515–26. doi:10.1002/we.
- [20] Waewsak J, Landry M, Gagnon Y. Offshore wind power potential of the Gulf of Thailand. *Renew Energy* 2015;81:609–26. doi:10.1016/j.renene.2015.03.069.
- [21] Bilal M, Solbakken K, Birkelund Y. Wind speed and direction predictions by WRF and WindSim coupling over Nygårdstjønn. *J Phys Conf Ser* 2016;753:082018. doi:10.1088/1742-6596/753/8/082018.